ENERGY 2011

The First International Conference on Smart Grids, Green Communications and IT Energy-aware Technologies

May 22-27, 2011

Venice/Mestre, Italy

ENERGY 2011 Editors

Angelantonio Gnazzo, Telecom Italia - Torino, Italy

Ritwik Majumder, ABB AB / Corporate Research Center - Vasteras, Sweden

ENERGY 2011

Foreword

The First International Conference on Smart Grids, Green Communications and IT Energy-aware Technologies (ENERGY 2011), held between May 22 -27, 2011 in Venice, Italy, was an inaugural event considering Green approaches for Smart Grids and IT-aware technologies. It addressed fundamentals, technologies, hardware and software needed support, and applications and challenges.

There is a perceived need for a fundamental transformation in IP communications, energy-aware technologies and the way all energy sources are integrated. This is accelerated by the complexity of smart devices, the need for special interfaces for an easy and remote access, and the new achievements in energy production. Smart Grid technologies promote ways to enhance efficiency and reliability of the electric grid, while addressing increasing demand and incorporating more renewable and distributed electricity generation. The adoption of data centers, penetration of new energy resources, large dissemination of smart sensing and control devices, including smart home, and new vehicular energy approaches demand a new position for distributed communications, energy storage, and integration of various sources of energy.

We welcomed technical papers presenting research and practical results, position papers addressing the pros and cons of specific proposals, such as those being discussed in the standard forums or in industry consortia, survey papers addressing the key problems and solutions on any of the above topics short papers on work in progress, and panel proposals.

We take here the opportunity to warmly thank all the members of the ENERGY 2011 technical program committee as well as the numerous reviewers. The creation of such a broad and high quality conference program would not have been possible without their involvement. We also kindly thank all the authors that dedicated much of their time and efforts to contribute to ENERGY 2011. We truly believe that, thanks to all these efforts, the final conference program consisted of top quality contributions.

We hope that ENERGY 2011 was a successful international forum for the exchange of ideas and results between academia and industry and to promote further progress in energy-aware technologies.

We are certain that the participants found the event useful and communications very open. We also hope the attendees enjoyed the beautiful surroundings of Venice.

ENERGY 2011 Chairs
Stefan Mozar, CCM Consulting / CQ University - Sydney International Centre, Australia
Mehrdad (Mark) Ehsani, Texas A&M University - College Station, USA
Petre Dini, Concordia University, Canada / China Space Agency Center, China
Mardavij Roozbehani, Massachusetts Institute of Technology, USA
Dave Cavalcanti, Philips Research North America, USA
Marco Di Girolamo, Hewlett-Packard Company - Cernusco sul Naviglio, Italy
Thomas M. Overman, Boeing Energy Cyber Security, USA
Angelantonio Gnazzo, Telecom Italia - Torino, Italy

Dragan Obradovic, Siemens AG, Germany
Avi Mendelson, Microsoft Corporation, USA
Peter Müller, IBM-Zurich, Switzeland
Giorgio Nunzi, NEC Europe Ltd. - London, UK
Ritwik Majumder, ABB AB / Corporate Research Center - Vasteras, Sweden
Brian P. Gaucher, IBM Research Division - Yorktown Heights, USA
Gargi Bag, ABB Corporate Research, Sweden
Ken Christensen, University of South Florida, USA
Grzegorz Swirszcz, IBM Watson Laboratory, USA
Luciano Bertini, Fluminense Federal University, Brazil
Cathryn Peoples, University of Ulster, UK

ENERGY 2011

Committee

ENERGY Advisory Chairs

Stefan Mozar, CCM Consulting / CQ University - Sydney International Centre, Australia
Mehrdad (Mark) Ehsani, Texas A&M University - College Station, USA
Petre Dini, Concordia University, Canada / China Space Agency Center, China
Mardavij Roozbehani, Massachusetts Institute of Technology, USA

ENERGY Industry Liaison Chairs

Dave Cavalcanti, Philips Research North America, USA
Marco Di Girolamo, Hewlett-Packard Company - Cernusco sul Naviglio, Italy
Thomas M. Overman, Boeing Energy Cyber Security, USA
Angelantonio Gnazzo, Telecom Italia - Torino, Italy
Dragan Obradovic, Siemens AG, Germany
Avi Mendelson, Microsoft Corporation, USA

ENERGY Special Area Chairs on Nano-Grids

Peter Müller, IBM-Zurich, Switzeland

ENERGY Special Area Chairs on Efficient Energy Consumption

Giorgio Nunzi, NEC Europe Ltd. - London, UK

ENERGY Special Area Chairs on Smart Grids

Ritwik Majumder, ABB AB / Corporate Research Center - Vasteras, Sweden

ENERGY Special Area Chairs on IT-energy- aware, Planning

Brian P. Gaucher, IBM Research Division - Yorktown Heights, USA

ENERGY Special Area Chairs on Grid, Green Communication

Gargi Bag, ABB Corporate Research, Sweden
Ken Christensen, University of South Florida, USA

ENERGY Special Area Chairs on Vehicular

Grzegorz Swirszcz, IBM Watson Laboratory, USA

ENERGY Publicity Chairs

Luciano Bertini, Fluminense Federal University, Brazil
Cathryn Peoples, University of Ulster, UK

ENERGY 2011 Technical Program Committee

Amir Abtahi, Florida Atlantic University - Boca Raton, USA
Nizar Al-Holou, University of Detroit Mercy, USA
S. Massoud Amin, University of Minnesota, USA
Lachlan Andrew, Swinburne University of Technology - Melbourne, Australia
Cosimo Anglano, Universitá del Piemonte Orientale - Alessandria, Italy
Gargi Bag, ABB Corporate Research, Sweden
Luciano Bertini, Fluminense Federal University, Brazil
Vít Bršlica, University of Defence - Brno, Czech Republic
Michael Caramanis, Boston University, USA
Davide Careglio, Universitat Politècnica de Catalunya - Barcelona, Spain
Mari Carmen Domingo, Barcelona Tech University, Spain
Dave Cavalcanti, Philips Research North America, USA
Trishul Chilimbi, Microsoft Research, USA
Ken Christensen, University of South Florida, USA
Peter Corcoran, College of Engineering & Informatics, NUI Galway, Ireland
Stephen Dawson-Haggerty, University of California - Berkeley, USA
Stojan Denic, Toshiba Research Europe Limited - Bristol, UK
Marco Di Girolamo, Hewlett-Packard Company - Cernusco sul Naviglio, Italy
Mehrdad (Mark) Ehsani, Texas A&M University - College Station, USA
Janaka Ekanayake, Institute of Energy / Cardiff University, UK
Steffen Fries, Siemens Corporate Technology - Munich, Germany
Shravan Garlapati, Virginia Polytechnic Institute and State University, USA
Brian P. Gaucher, IBM Research Division - Yorktown Heights, USA
Jean-Patrick Gelas, Université Claude Bernard Lyon 1, France
Erol Gelenbe, Imperial College London, UK
Hamid Gharavi, National Institute of Standards and Technology, USA
Harald Gjermundrod, University of Nicosia, Cyprus
Angelantonio Gnazzo, Telecom Italia - Torino, Italy
Haibo He, University of Rhode Island - Kingston, USA
Daniel Hissel, University of Franche-Comté, France
Helmut Hlavacs, University of Vienna, Austria
Chun-Hsi Huang, University of Connecticut, USA
Dijiang Huang, Arizona State University, USA
Philip Johnson, University of Hawaii - Honolulu, USA
Aman Kansal, Microsoft, USA
Young-Chai Ko, Korea University, South Korea
Harald Kosch, University of Passau, Germany
Jean-Yves Le Boudec, EPFL, Switzerland
DongJin Lee, University of Auckland, New Zealand
Laurent Lefevre, INRIA, University of Lyon, France
Ralf Lehnert, Technische Universitaet - Dresden, Germany

Hua Lin, Virginia Tech, USA
Eugene Litvinov, ISO New England, USA
Jaime Lloret Mauri, Universidad Politécnica de Valencia, Spain
Ritwik Majumder, ABB AB / Corporate Research Center - Vasteras, Sweden
Moacyr Martucci, Universidade de São Paulo, Brazil
Nicholas F. Maxemchuk, Columbia University - New York, USA
Michele Mazzucco, University of Tartu, Estonia
Jean-Marc Menaud, Ecole des Mines de Nantes, France
Avi Mendelson, Microsoft Corporation, USA
George Michailidis, University of Michigan, USA
Nicolas Montavont , Institut Telecom / Telecom Bretagne, France
Daniel Mossé, University of Pittsburg, USA
Stefan Mozar, CCM Consulting / CQ University - Sydney International Centre, Australia
Peter Müller, IBM-Zurich, Switzeland
Giorgio Nunzi, NEC Europe Ltd. - London, UK
Dragan Obradovic, Siemens AG, Germany
Ariel Oleksiak, Poznan Supercomputing and Networking Center (PSNC), Poland
Thomas M. Overman, Boeing Energy Cyber Security, USA
Manish Parashar, Rutgers University, USA
Cathryn Peoples, University of Ulster, UK
Darren Robinson, Ecole Polytechnique Fédérale de Lausanne (EPFL), Switzerland
Mardavij Roozbehani, Massachusetts Institute of Technology, USA
Dirk Uwe Sauer, ISEA / RWTH - Aachen University, Germany
Nigel Schofield, University of Manchester, UK
Aline Senart, Accenture Technology Labs, Sophia Antipolis, France
Sandra Sendra Compte, Polytechnic University of Valencia, Spain
Mohammad Shahidehpour, IIT Armour College of Engineering / Illinois Institute of Technology, USA
Grzegorz Swirszcz, IBM Watson Laboratory , USA
Domenico Talia, Consiglio Nazionale delle Ricerche - Rende, Italy
Zhibin Tan, Wayne State University - Detroit, USA
Sekhar Tatikonda, Yale University - New Haven, USA
Bernard Tourancheau, INRIA, France
Tuan Anh Trinh, Budapest University of Technology and Economics, Hungary
Rod Tucker, University of Melbourne - Victoria, Australia
Jean-Philippe Vasseur, Cisco Systems, Inc., France
Stéphane Vialle, SUPELEC, France
Martina Zitterbart, University of Karlsruhe, Germany
Albert Zomaya, University of Sydney, Australia

Copyright Information

For your reference, this is the text governing the copyright release for material published by IARIA.

The copyright release is a transfer of publication rights, which allows IARIA and its partners to drive the dissemination of the published material. This allows IARIA to give articles increased visibility via distribution, inclusion in libraries, and arrangements for submission to indexes.

I, the undersigned, declare that the article is original, and that I represent the authors of this article in the copyright release matters. If this work has been done as work-for-hire, I have obtained all necessary clearances to execute a copyright release. I hereby irrevocably transfer exclusive copyright for this material to IARIA. I give IARIA permission or reproduce the work in any media format such as, but not limited to, print, digital, or electronic. I give IARIA permission to distribute the materials without restriction to any institutions or individuals. I give IARIA permission to submit the work for inclusion in article repositories as IARIA sees fit.

I, the undersigned, declare that to the best of my knowledge, the article is does not contain libelous or otherwise unlawful contents or invading the right of privacy or infringing on a proprietary right.

Following the copyright release, any circulated version of the article must bear the copyright notice and any header and footer information that IARIA applies to the published article.

IARIA grants royalty-free permission to the authors to disseminate the work, under the above provisions, for any academic, commercial, or industrial use. IARIA grants royalty-free permission to any individuals or institutions to make the article available electronically, online, or in print.

IARIA acknowledges that rights to any algorithm, process, procedure, apparatus, or articles of manufacture remain with the authors and their employers.

I, the undersigned, understand that IARIA will not be liable, in contract, tort (including, without limitation, negligence), pre-contract or other representations (other than fraudulent misrepresentations) or otherwise in connection with the publication of my work.

Exception to the above is made for work-for-hire performed while employed by the government. In that case, copyright to the material remains with the said government. The rightful owners (authors and government entity) grant unlimited and unrestricted permission to IARIA, IARIA's contractors, and IARIA's partners to further distribute the work.

Table of Contents

Modelling the Energy Efficiency of Microcell Base Stations

Margot Deruyck, Emmeric Tanghe, Wout Joseph and Luc Martens
Ghent University - IBBT, Departement of Information Technology (INTEC)
Gaston Crommenlaan 8 bus 201, 9050 Ghent, Belgium
Email: {margot.deruyck, emmeric.tanghe, wout.joseph, luc.martens}@intec.ugent.be

***Abstract*—The power consumption of wireless access networks will become a major issue in the coming years. Therefore, it is important to have a realistic idea about the power consumption of each element in those access networks. In this paper, an energy efficiency model for microcell base stations is proposed. Based on this model, the energy efficiency of microcell base stations is compared for various wireless technologies, namely mobile WiMAX, HSPA and LTE. The power consumption of microcell base stations is about 70-77% lower than for macrocell base stations but a macrocell base station is more energy-efficient than a microcell base station for the same bit rates. However, for the considered case and assuming our parameters are correct, a reduction in power consumption can be obtained by using microcell base stations to fill coverage holes.**

***Keywords*-energy efficiency, green wireless access networks, microcell base station, power consumption.**

I. INTRODUCTION

Looking at the complete life cycle (production, use and end-of-life) tells us that ICT is responsible for 4% of the worldwide primary energy consumption [1]. Without any precautions, this percentage will even double within the next 10 to 15 years. 9% of this ICT consumption is caused by radio access networks [2]. Within these networks, 10% of the energy is consumed by the user terminals, while 90% is caused by the base stations. These numbers indicate that the power consumption of wireless access networks is going to become an important issue in the next few years. To model and optimize the power consumption in those networks, the focus should therefore be on the base stations.

An operator's wireless access network has a hierarchical structure of different cell types. Three different cell types can be found: macrocell, microcell and picocell. A macrocell has the highest possible coverage range. A microcell has a smaller coverage range and is often used in densely populated urban areas. A picocell is much smaller than a microcell and is mostly used for indoor coverage in large office buildings, shopping centres or train stations. To determine the power consumption of the whole wireless access network, the power consumption of the macrocell, microcell and picocell base stations have to be modelled. In [3][4], an energy efficiency model for the macrocell base station is proposed. The aim of this study is to model and compare the energy efficiency between microcell and macrocell base stations for various wireless technologies. The same approach as in [3][4] is followed: the power consumption of a microcell base station is first modelled and related to the range to determine the energy efficiency. The wireless technologies considered are: mobile WiMAX (Worldwide Interoperability for Microwave Access) [5], HSPA (High Speed Packet Access) [6] and LTE (Long Term Evolution) [7].

Few work has been done about the energy efficiency of microcell base stations. The most valuable contribution to this topic can be found in [8] where the power consumption of different equipment is combined into three parameters. This makes it difficult to investigate the influence of the different components on the base station's power consumption, as well as the influence of possible dependencies between the components. Furthermore, only one wireless technology is considered, while our work shows that there are significant differences in energy efficiency between the wireless technologies.

The remainder of this paper is organized as follows. In Section II the power consumption of a microcell base station is modelled and related to the coverage. Section III describes some results obtained with the model proposed in Section II. Section IV presents our conclusions.

II. METHOD

In this section, a power consumption model for a microcell base station is proposed.

A. Energy-efficiency of a microcell base station

Just like for a macrocell base station, the power consumption PC_{area} per covered area of a microcell base station is defined as (in W/m^2) [3][4] :

$$PC_{area} = \frac{P_{el/micro}}{\pi \cdot R^2} \quad (1)$$

with $P_{el/micro}$ the power consumption (in Watt) and R the range (in meter) of the microcell base station. The next sections discuss how $P_{el/micro}$ and R are determined. The lower PC_{area}, the more energy-efficient the technology is.

1) Power consumption of a microcell base station: A base station is here defined as the equipment needed to communicate with the mobile stations and with the backhaul network. The microcell base station consists of several power consuming components, which are shown in Fig. 1.

 ISBN: 978-1-61208-136-6

The following components are found: the transceiver (responsible for sending and receiving of signals to the mobile stations and includes the signal generation), digital signal processing (responsible for system processing and coding), the power amplifier, the AC-DC converter or rectifier, and the air conditioning (if present). In contrary to a macrocell base station, a microcell base station supports only one sector and each component is therefore used once. This assumption is based on the confidential information retrieved from an operator.

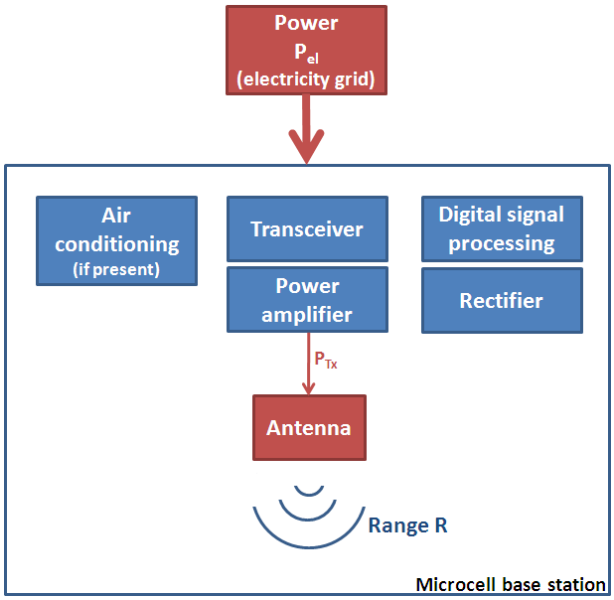

Figure 1. Block diagram of microcell base station equipment.

The power consumption of each component is constant (in Watt), expect for the air conditioning and the power amplifier. The air conditioning's power consumption depends on the internal and ambient temperature of the base station cabinet. Assuming an internal and ambient temperature of 25° C gives also a constant power consumption for the air conditioning. However, an air conditioning is not always necessary for a microcell base station. In this paper, the worst case for the power consumption, which includes the air conditioning, is investigated. The power consumption $P_{e/amp}$ of the power amplifier depends on the required input power P_{Tx} of the antenna and is determined as follows [9]:

$$P_{el/amp} = \frac{P_{Tx}}{\eta} \quad (2)$$

with P_{Tx} the input power of the antenna (in Watt) and η the efficiency of the power amplifier, which is the ratio of RF output power to the electrical input power [9]. The RF output power corresponds with P_{Tx} as indicated in Fig. 1.

Once the power consumption of each component is known, the power consumption $P_{el/micro}$ of the entire microcell base station can be determined (in Watt):

$$P_{el/micro} = P_{el/amp} + P_{el/trans} + P_{el/proc} + P_{el/rect} + P_{el/airco} \quad (3)$$

with $P_{el/amp}$, $P_{el/trans}$, $P_{el/proc}$, $P_{el/rect}$, $P_{el/airco}$ and $P_{el/link}$ the power consumption of, respectively, the power amplifier, the transceiver, the digital signal processing, the rectifier, and the air conditioning. Table I summarises the typical power consumption of the different components for the technologies considered. These values are retrieved from data sheets of various network equipment manufacturers and are very similar to those of the macrocell base station [3][4], except for the air conditioning. The air conditioning's cooling power is significant lower for the microcell base station, resulting in a lower power consumption for the microcell base station (60 W versus 225 W for the macrocell base station, based on confidential information from an operator).

Table I
POWER CONSUMPTION OF THE DIFFERENT COMPONENTS OF THE MICROCELL BASE STATION.

Equipment		Value
Digital signal processing	$P_{el/proc}$	100 W
Power amplifier	η	12%
Transceiver	$P_{el/trans}$	100 W
AC-DC converter	$P_{el/conv}$	100 W
Air conditioning	$P_{el/airco}$	60 W

2) Calculation of the range of a microcell base station: To determine the coverage of a microcell base station a link budget has to be determined. Table II-A2 summarises the link budget parameters for the coverage calculations of the microcell base stations. The same parameters as for the macrocell base stations are usable, however, some of these parameters will have a different value such as the input power of the antenna and the antenna gain. The typical input power of the antenna P_{Tx} for a microcell base station is 2 W or 6 W. In this investigation, we use P_{Tx} equal to 2 W, which corresponds with 33 dBm [8]. As mentioned above, a microcell base station has only one sector, therefore, an omnidirectional antenna is used. The antenna gain for this type of antennas and the base station considered varies from 4 to 6 dB depending on the technology. The other parameters remain the same because these parameters are either technology dependent (such as the frequency, bandwidth, etc.) or mobile station dependent (such as antenna gain of mobile station, feeder loss of the mobile station, etc.) or fixed assumptions (such as the yearly availability, fade margin). Note that the cell interference margin assumed might be too optimistic because the same cell interference margin is used for both the macrocell and the microcell base station just like in [8].

In Table III, the characteristics of the scenario considered are presented. A suburban area is assumed with a height of

Table II
LINK BUDGET TABLE FOR A MICROCELL BASE STATION FOR THE TECHNOLOGIES CONSIDERED.

Parameter	Mobile WiMAX	HSPA	LTE
Frequency [MHz]	2500	2100	2600
Maximum input power of base station P_{Tx} [dBm]	33	33	33
Effective input power of base station P_{Tx}^{TCH} [dBm]	33	13.8	33
Antenna gain of base station [dBi]	6	5	4
Antenna gain of mobile station [dBi]	2	0	0
Soft handover gain [dB]	0	1.5	0
Feeder loss of base station [dB]	0.5	0	2
Feeder loss of mobile station [dB]	0	0	0
Fade margin [dB]	10	10	10
Cell interference margin [dB]	2	2	2
Bandwidth [MHz]	5	5	5
Receiver SNR [dB]	[6, 8.5, 11.5 15, 19, 21][1]	[-3.1, 0.1, 3.4 6, 7.1, 9.6 15.6][2]	[-1.5, 3, 10.5 14, 19, 23 23, 29.4][3]
Number of used subcarriers	360	—	301
Number of total subcarriers	512	—	512
Noise figure of mobile station [dB]	7	9	8
Implementation loss of mobile station [dB]	2	0	0
Duplexing	TDD		
Building penetration loss [dB]	8.1	8.1	8.1

(1) [1/2 QPSK, 3/4 QPSK, 1/2 16-QAM, 3/4 16-QAM, 2/3 64-QAM, 3/4 64-QM]

(2) [1/4 QPSK, 1/2 QPSK, 3/4 QPSK, 3/4 8-QAM, 1/2 16-QAM, 3/4 16-QAM, 3/4 64-QAM]

(3) [1/3 QPSK, 1/2 QPSK, 2/3 QPSK, 1/2 16-QAM, 2/3 16-QAM, 4/5 16-QAM, 1/2 64-QAM, 2/3 64-QAM]

1.5 m for the mobile station and a coverage requirement of 90%. The antenna of the microcell base station is placed typically at a height of 6 m, which corresponds with the height of the roof-gutter of a three-storied house (i.e., 2 m per floor). The base stations are placed outdoor and for the mobile stations an indoor residential scenario is considered with a Wireless Network Interface Card (WNIC) for a laptop.

The Walfisch-Ikegami (W-I) model is used as propagation model for microcells [10]. The Erceg-model, which is used for macrocell base stations, is not suitable for microcell base station heights [11].

Table III
SCENARIO TABLE.

Parameter	Value
Area type	Suburban
Height of base station	6 m
Height of mobile station	1.5 m
Coverage requirement	90%
Path loss model	W-I
Shadowing margin	12.8 dB

III. RESULTS

In this section, some results obtained with the model from Section II are discussed.

A. Energy-efficiency of microcell base stations

In this section, the wireless technologies considered are compared for a bandwidth of 5 MHz. The parameters given in Tables I, II-A2 and III are used. Fig. 2 shows the power consumption PC_{area} per covered area (in W/m^2) as a function of the bit rate (in Mbps).

In general, Fig. 2 shows that each technology becomes less energy-efficient for higher bit rates as PC_{area} increases for increasing bit rates. The higher the bit rate, the higher the receiver SNR (Signal-to-Noise Ratio) as given in Table II-A2. Furthermore, a higher receiver SNR corresponds with a smaller range for the same power consumption P_{el} resulting in a higher value for PC_{area} (eq. (1)) and thus a lower energy efficiency.

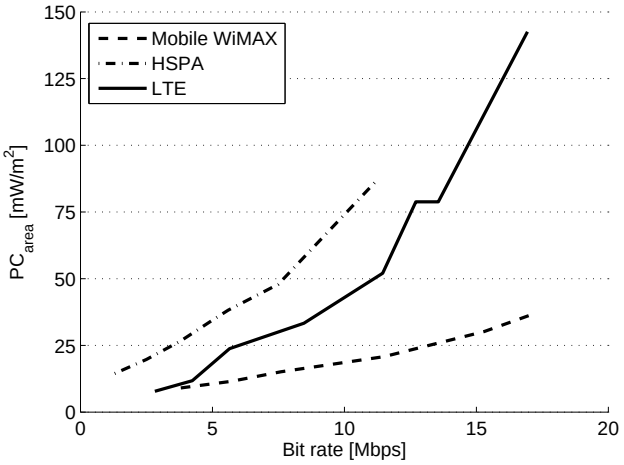

Figure 2. Energy efficiency of a microcell base station for different bit rates in 5 MHz channel.

A microcell base station consumes about 376.6 W for each technology (Table I). However, the range R differs between the technologies considered. For a bit rate of 10 Mbps, R equals to 76.0 m, 37.0 m and 48.0 m for mobile WiMAX, HSPA and LTE respectively. A higher R for the same P_{el} results in a lower PC_{area} and thus in a higher energy efficiency.

Fig. 2 shows that mobile WiMAX is the most energy-efficient technology for bit rates higher than 3.8 Mbps (lowest PC_{area} of 20.8 mW/m^2 at 10 Mbps versus 87.6 mW/m^2 and 52.0 mW/m^2 for HSPA and LTE respectively). For the bit rates considered, mobile WiMAX performs better than HSPA and LTE due to its higher antenna gain for both the base station and the mobile station (Table II-A2). Moreover, mobile WiMAX has a higher effective input power of the antenna P_{Tx}^{TCH} than HSPA. P_{Tx}^{TCH} is the power reserved by the base station for the traffic channels and is lower for HSPA because it uses a W-CDMA (Wideband Code Division Multiple Access) based multiple access technique, while mobile WiMAX uses OFDMA (Orthogonal Frequency Division Multiple Access).

The bit rates between 2.8 Mbps and 3.8 Mbps are only supported by HSPA and LTE. In this case, LTE is the most energy-efficient due to its higher P_{Tx}^{TCH} (PC_{area} of

2.8 mW/m^2 versus 19.7 mW/m^2 for a bit rate of 2.8 Mbps). Bit rates below the 2.8 Mbps are only supported by HSPA (PC_{area} = 14.5 mW/m^2 for 1.3 Mbps).

B. Energy-efficiency of microcell base stations versus macrocell base stations

In this section, the energy efficiency of a microcell base station is compared to that of a macrocell base station for the technologies considered and in a 5 MHz channel. For the macrocell base station, the same settings as in [4] are used. Fig. 3 presents the power consumption per covered (PC_{area}) as a function of the bit rate (in Mbps) for both the macrocell and the microcell base station.

Fig. 3 shows that, in general, the macrocell base stations are more energy-efficient than microcell base stations as PC_{area} is lower (about 82 to 93%). The power consumption P_{el} of the microcell base station is about 70.6% lower for mobile WiMAX and about 77.5% lower for HSPA and LTE compared to the corresponding macrocell base stations (Table IV). However, a macrocell base station has a significant higher range (297.0%, 346.3% and 498.4% for mobile WiMAX, LTE and HSPA respectively) resulting in a higher energy efficiency.

Furthermore, for the macrocell base station, it was found that HSPA is the most energy-efficient technology until a bit rate of 2.8 Mbps (which corresponds with the results for microcell base stations), LTE is the most energy-efficient for bit rates between 2.8 Mbps and 11.5 Mbps (versus 2.8 Mbps and 3.8 Mbps for microcell base stations) and mobile WiMAX is the most energy-efficient for bit rates higher than 11.5 Mbps (versus 3.8 Mbps for microcell base stations).

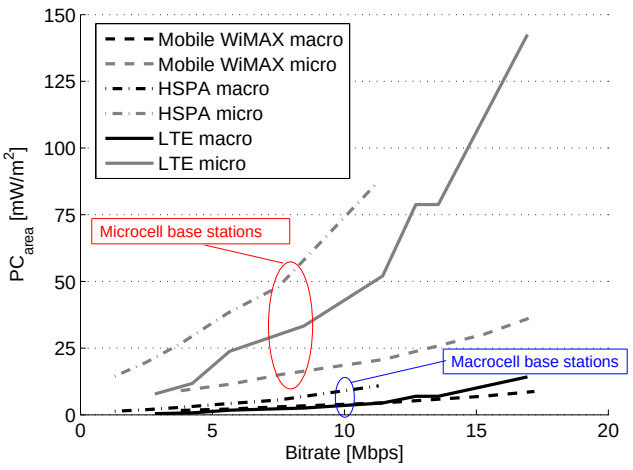

Figure 3. Comparison of the energy efficiency of a macrocell base station and a microcell base station for different bit rates in a 5 MHz channel.

Table IV
COMPARISON OF THE POWER CONSUMPTION P_{el} AND THE POWER CONSUMPTION PC_{area} PER COVERED AREA FOR MACROCELL AND MICROCELL BASE STATIONS IN A 5 MHZ CHANNEL AND A BIT RATE OF (APPROXIMATELY) 10 MBPS.

Technology	Macrocell			Microcell		
	P_{el} [W]	R [m]	PC_{area} [mW/m^2]	P_{el} [W]	R [m]	PC_{area} [mW/m^2]
Mobile WiMAX	1279.1	301.7	4.5	376.6	76.0	25.2
HSPA	1672.6	346.3	10.9	376.6	48.0	106.2
LTE	1672.6	221.4	4.4	376.6	37.0	63.1

C. Microcell base stations in realistic network deployments

Based on the results mentioned above, one might ask if it is interesting to use microcell base stations in real network deployments. The answer to that question is positive. Microcell base stations can be used to increase the capacity of a macrocell base station in a certain area. Furthermore, microcells can also be used to solve coverage holes. In this section, a simple example is given where a benefit can be obtained by using microcell base stations to solve coverage holes.

Fig. 4(a) shows the example considered. An operator has to cover an area of 4 km^2 for 100% with mobile WiMAX base stations. A bit rate of 3.8 Mbps is considered. Seven macrocell base stations are placed in the area and these sites have to be re-used. Five of these base stations have an input power P_{Tx} of 35 dBm (blue circles), which corresponds with a range of 499.0 m and a power consumption of 1279.1 W; the other two have a P_{Tx} of 31 dBm (red circles) resulting in a range of 399.0 m and a power consumption of 1234.5 W. The current situation has a power consumption of 8.9 kW:

$$P_{el,curr} = 5 \cdot 1279.1\ W + 2 \cdot 1234.5\ W = 8864.5\ W \quad (4)$$

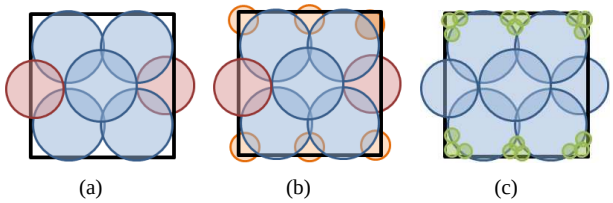

Figure 4. Possible solution to cover coverage holes: start situation (a), only macrocell base stations are used (b), and both macro- and microcell base stations are used (c).

In Fig. 4(b), the coverage holes are filled by using only macrocell base stations. Six macrocell base stations are introduced. Each macrocell base station added has a P_{Tx} of 18 dBm corresponding with a range of 193.0 m and a power consumption of 1206.5 W. The total power consumption $P_{el,1}$ to cover the area is in this case:

$$\begin{aligned} P_{el,1} &= 5 \cdot 1279.1\ W + 2 \cdot 1234.5\ W + 6 \cdot 1206.5\ W \\ &= 16104\ W \end{aligned} \quad (5)$$

The network in Fig. 4(b) consumes thus about 16.1 kW.

In Fig. 4(c), the coverage holes are filled by placing microcell base stations (green circles). 18 microcell base stations are needed to cover the area considered. Each of these base stations have a P_{Tx} of 33 dBm, which corresponds with a range of 115.0 m and a power consumption of 376.6 W. The total power consumption $P_{el,2}$ to cover the area is then approximately 15.6 kW:

$$\begin{aligned} P_{el,2} &= 5 \cdot 1279.1\ W + 2 \cdot 1234.5\ W + 18 \cdot 376.6\ W \\ &= 15643.0\ W \end{aligned} \quad (6)$$

The solution with both macrocell and microcell base stations consumes about 461 W less. This is a power consumption reduction of 3% than the solution where only macrocell base stations are considered. It is thus interesting to add microcell base stations in a realistic network deployment.

IV. Conclusion

In this paper, an energy efficiency model for microcell base stations is proposed. Based on this model, the energy efficiency of microcell base stations is compared for various bit rates and wireless technologies, namely mobile WiMAX, HSPA and LTE. Furthermore, the energy efficiency between a microcell and macrocell base station is investigated. The base stations were placed outdoor in a suburban environment and for the mobile stations an indoor scenario was considered with a WNIC for a laptop. A bandwidth of 5 MHz was assumed. For the parameters considered, a microcell base station has ranges from 40 m to 80 m for a power consumption of approximately 377 W.

Mobile WiMAX is the most energy-efficient technology for bit rates higher than 3.8 Mbps, LTE for bit rates between 2.8 Mbps and 3.8 Mbps and HSPA for bit rates lower than 2.8 Mbps. HSPA is the only technology which supports bit rates lower than 2.8 Mbps. Mobile WiMAX support only bit rates higher than 3.8 Mbps. The power consumption P_{el} of the microcell base station is 70.6% lower for mobile WiMAX and 77.5% lower for HSPA and LTE but a macrocell base station is more energy-efficient than a microcell base station due to the higher ranges of the macrocell base stations.

However, it is interesting to use microcell base stations in real network deployments. In this paper, a solution was presented to fill coverage holes by using only macrocell base stations and by using both macrocell and microcell base stations. The latter showed a reduction in power consumption compared to the solution with only macrocell base stations for the case considered and assuming our parameters are correct.

In the future, the power consumption model should be validated with measurements and will be added in the GRAND (Green Radio Access Network Design) tool, which is a deployment tool we developed for green wireless access networks.

Acknowledgment

The work described in this paper was carried out with support of the IBBT-project GreenICT.
W. Joseph is a Post-Doctoral Fellow of the FWO-V (Research Foundation Flanders).

References

[1] M. Pickavet, W. Vereecken, S. Demeyer, P. Audenaert, B. Vermeulen, C. Develder, D. Colle, B. Dhoedt, and P. Demeester, *Worldwide Energy Needs for ICT: the Rise of Power-Aware Networking*, 2008 IEEE ANTS Conference, Bombay, India, December 2008, pp. 1-3.

[2] G. Koutitas, and P. Demestichas, *A Review of Energy Efficiency in Telecommunication Networks*, 17th Telecommunications forum TELFOR 2009, Serbia, Belgrade, November 24-26, 2009, pp. 1-4.

[3] M. Deruyck, E. Tanghe, W. Joseph, W. Vereecken, M. Pickavet, B. Dhoedt, and L. Martens, *Towards a deployment tool for wireless access networks with minimal power consumption*, 21st Annual IEEE International Symposium on Personal, Indoor and Mobile Radio Communications (PIMRC), Istanbul, Turkey, September 26-29, 2010, pp. 294-299.

[4] M. Deruyck, E. Tanghe, W. Joseph, and L. Martens, *Modelling and Optimization of Power Consumption in Wireless Access Networks*, Elsevier Computer Communications special issue on European Wireless, *submitted*.

[5] IEEE Computer Society and the IEEE Microwave Theory and Techniques Society, *Part 16: Air Interface for Fixed and Mobile Broadband Wireless Access Systems: Amendment 2: Physical and Medium Access Control Layers for Combined Fixed and Mobile Operation in Licensed bands and Corrigendum 1*, February 2006.

[6] 3GPP, *3rd Generation Partnership Project: Technical Specification Group Radio Access Network: Physical layer aspects of UTRA High Speed Packet Access (Release 4), TR 25.848 v4.0.0*, March 2001.

[7] 3GPP, *LTE: 3rd Generation Partnership Project: Technical Specification Group Radio Access Network: Evolved Universal Terrestrial Radio Access (E-UTRA): User Equipment (UE) radio transmission and reception (TS 36.101 v9.1.0 Release 9)*, September 2009.

[8] F. Richter, G. Fettweis, M. Gruber, and O. Blume, *Micro Base Stations in Load Constrained Cellular Mobile Radio Networks*, 21st Annual IEEE International Symposium on Personal, Indoor and Mobile Radio Communications (PIMRC), Istanbul, Turkey, September 26-29, 2010, pp. 356-361.

[9] F. H. Raab, P. Asbeck, S. Cripps, P. B. Kenington, Z. B. Popovic, N. Pothecary, J. F. Sevic, and N. O. Sokal, *RF and Microwave Power Amplifier and Transmitter Technologies - Part 1*, High Frequency Electronics, May 2003, pp. 22-36.

 ISBN: 978-1-61208-136-6

[10] Commission of the European Communities and COST Telecommunications, *COST 231 Final report, Digital Mobile Radio: Cost 231 View On the Evolution Towards 3rd Generation Systems*, Brussels, 1999.

[11] V. Erceg, L. Greenstein, S. Tjandra, S. Parkoff, A. Gupta, B. Kulic, A. Julius, and R. Bianchi, *An Empirically Based Path Loss Model for Wireless Channels in Suburban Environments*, IEEE Journal on Selected Areas in Communications, vol. 7, no. 7, July 1999, pp. 1205-1211.

 ISBN: 978-1-61208-136-6

Energy-Aware Routing in the Cognitive Packet Network

Erol Gelenbe and Toktam Mahmoodi
Intelligent Systems & Networks Group
Department of Electrical & Electronic Engineering
Imperial College, SW7 2BT London UK
{e.gelenbe, t.mahmoodi}@imperial.ac.uk

***Abstract*—An energy aware routing protocol (EARP) is proposed to minimise a performance metric that combines the total consumed power in the network and the QoS that is specified for the flows. The algorithm uses source routing based on the functionalities provided by the Cognitive Packet Network (CPN), running autonomously at each input node to the network based on smart packets which gather relevant information throughout the network using reinforcement learning at each of the intermediate nodes. Measurements on an experimental test-bed that uses EARP are presented and they indicate that it offers a reduction in power consumption, as compared to a purely QoS driven approach, and also respects the requested QoS level.**

***Index Terms*—Energy Efficiency, Routing Protocol, Cognitive Packet Network**

I. INTRODUCTION

Energy efficient protocols have been extensively studied for wireless networks, because energy savings for battery powered nodes is crucial [1], [2]. However research on energy consumption is relatively new in wired networks even though the amount consumed on a day to day basis is a significant fraction of the total energy used for ICT systems. Surprisingly the total energy consumption for ICT and for air travel are comparable [3]. Since wired networks form the backbone of all of the world's ICT, the energy consumption in this area is bound to rise unless serious efforts are made to achieve significant savings in wired networks and computer systems. Thus recent research on wired energy aware network management includes [4][5][6][7][8].

The most thorough measurement studies that have been performed in [9] which quantify the energy consumed by many network devices, ranging from the core switches to wireless access points, and including different vendors. These measurements are carried out under various traffic and network configurations, together with an index associated with each network device so that the proportionality of power consumption to the device's traffic load can be evaluated. As investigated by [9], the ratio of the actual power consumed by a networking device on average to its maximum power consumption, varies widely across different device families. The impact of the hardware processing rate and traffic load on power consumption is also examined in [4]. Moreover, research work in [10] introduces a generic model for router power consumption.

However because there does not seem to be a single unified model that captures the power characteristics of a wide class of network devices, in the experiments we conducted in this paper, we use offline power measurements that have been conducted on our own experimental testbed's nodes, and which have been previously reported in [11]. In particular, we will rely on the measurements reported in Figure 1 for a single core router to relate router traffic rates in packets per second to the power consumed by each of our routers.

In this paper we propose an energy aware routing protocol (EARP) that not only attempts to minimise the total consumed power in the network but also respects the requested QoS by each incoming flow. EARP relies on the underlying Cognitive Packet Network (CPN) [12] for the information it requires, and uses it to minimise power consumption. CPN's smart packets are used to gather information about the power usage at the nodes, and EARP is run in a fully distributed manner using CPN's source routing scheme that is modified to include power consumption as a decision criterion.

The remainder of this paper is organised as follows. We first give a brief overview of CPN and its existing routing protocol. Section II elaborates the proposed energy-aware routing protocol. The implementation is summarised and then we detail some performance results in Section III. Conclusions and further work are discussed in Section IV.

A. Background

The Cognitive Packet Network (CPN) is an experimental protocol that allows a network with an arbitrary topology to observe its state in a distributed manner and exploit the data being gathered to improve different QoS metrics [13]. The CPN routing algorithm runs autonomously at each node using Reinforcement Learning with a recurrent Random Neural Network [14][15][16], and measurement results for this protocol are summarised in [17]. CPN makes use of three types of packets: smart packets (SP) for discovery, source routed dumb packets (DP) to carry payload, and acknowledgements (ACK) to bring back information that has been discovered by SPs. Conventional IP packets can also tunnel through CPN, so as to seamlessly operate mixed IP and CPN networks. The SPs are constantly generated by each of the source users of CPN as a fraction of the total number of DPs that are

 ISBN: 978-1-61208-136-6

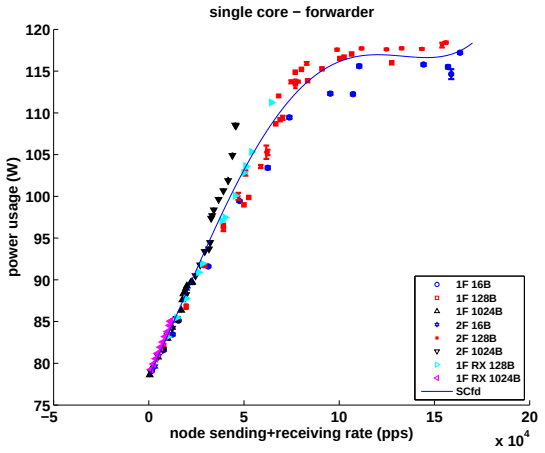

Figure 1. Power consumption as a function of packet rate for a single core router and for different packet sizes (16, 128, and 1024 Bytes) [11]

sent forward, in order to seek paths to the destination that minimise the desired QoS. In addition, they update the QoS information about different paths used by the source and hence allow it to make informed decisions. Since DPs are source routed, the choice of the path that is used to convey the DPs to the destination, is made at the source on the basis of the information it receives from ACKs sent back by the successful SPs. In previous work CPN has been proposed as a means to optimise energy consumption [5][6], and this paper is a continuation of this previous research. However here we will use a decision scheme that attempts to minimise the power consumed provided the overall end-to-end packet delay remains below a predetermined value.

II. Energy and QoS Aware Routing

At each node i, let us denote by T_i, the traffic this node carries in packets/sec (pps). Assuming that a flow l carries traffic of rate t_l pps, then T_i can be computed as,

$$T_i = \sum_{l \in F(i)} t_l \tag{1}$$

where $F(i)$ denotes the set of flows that use node i. Let $p_i(T)$ and $Q_i(T)$ the power consumption and QoS of node i when the traffic it carries is T, so that adding a new flow k to node i will result in a change of power consumption and QoS at that node.

Let $p_i(x)$ be the instantaneous power consumption at node i when it carries x packets per seconds, in watts, that include all aspects of packet processing, including storing packets, routing them, and forwarding them through appropriate link drivers. It is of course possible to detail these different elements of power expenditure. In modern routers $p_i(x)$ will increase with x, but because of the increasing use of multi-cores in processing elements, the increase may have a step-like behaviour.

Let us denote the *Power Cost* associated with the $k-th$ flow at node i by $M_i^k(t_k, T_i)$, and define it as a combination of the flow's own power consumption, and of the impact it has on other flows which are using the node:

$$M_i^k(t_k, T_i) = at_k \frac{p_i(T_i + t_k)}{T_i + t_k} + bT_i[\frac{p_i(T_i + t_k)}{T_i + t_k} - \frac{p_i(T_i)}{T_i}] \tag{2}$$

where $a,\ b \geq 0$. Here the first term is the power (watts) total used by the $k-th$ flow, multiplied by some constant a. The second term represents the increase in wattage for the other flows, multiplied by some constant b. Note that if $a = b = 1$ both of these elements have an equal weight, while if $b = 0$ then we are ignoring the effect on the other flows that are using the node. However this metric assumes that the $k-th$ flow is concerned with a form of payment of "wattage per packet" that may be paid. In fact, a flow may also be concerned just with the total wattage itself, in which case a more appropriate metric may be:

$$m_i^k(t_k, T_i) = cp_i(T_i + t_k) + d[p_i(T_i + t_k) - p_i(T_i)] \tag{3}$$

for $c,\ d \geq 0$. Note that for any quality of service function $Q_i^k(t_k, T_i)$ we can adopt similar forms as (2) and (3), but generally a simplified version of the latter may be adopted for quantities such as node delay and packet loss.

The power related cost functions for the k-th traffic flow of rate t_k on a path $\pi(i)$ originating at node i is written as:

$$M_{\pi(i)}^k(t_k, \overline{T_{\pi(i)}}) = \sum_{n \in \pi(i)} M_n^k(t_k, T_n), \tag{4}$$

or we can choose the simpler form:

$$m_{\pi(i)}^k(t_k, \overline{T_{\pi(i)}}) = \sum_{n \in \pi(i)} m_n^k(t_k, T_n), \tag{5}$$

Similarly, we would have the QoS criterion, such as loss, delay or some other metric:

$$Q_{\pi(i)}^k(t_k, \overline{T_{\pi(i)}}) = \sum_{n \in \pi(i)} Q_n^k(t_k, T_n) \tag{6}$$

where $\overline{T_{\pi(i)}} = (T_{n_1},\ \ldots\ , T_{n_{|\pi(i)|}})$ where $n_1 = i$, and the n_j, with $1 \leq j \leq |\pi(i)|$ are the successive nodes of path $\pi(i)$.

The main drawbacks of using the metric $M_{\pi(i)}^k(t_k)$ are twofold. (a) Because of the factor $t_k/(t_k + T_i)$, the first term may be quite small, and the second term may also be small because we compute a difference in energy consumption. Small values compounded with the effect of inevitable statistical fluctuations in measurements make this metric unattractive. (b) The need to measure three quantities at each node plus the traffic rate t_k can lead to excessive overhead and measurement delays. Thus it appears more attractive and much simpler to use $m_{\pi(i)}^k(t_k, \overline{T_{\pi(i)}})$ as the energy criterion to be optimised.

A. Reinforcement Learning in EARP

In CPN, each router stores a specific Random Neural Network (RNN) for each flow that is active at that node. Each RNN has as many neurons as there are outgoing links in the node. The arrival of an SP will trigger the interrogation of the RNN to determine the next hop for the SP; this is done by computing the current state of the RNN and selecting

 ISBN: 978-1-61208-136-6

the output port of the node that corresponds to the neuron of the RNN which is the most excited. On the other hand, the arrival of an ACK back from the destination of that flow, will trigger the execution of the reinforcement learning (RL) process [15]. Since EARP is expected to minimise the overall cost of power while satisfying the requested QoS, the goal G_i to be optimised will combine the power consumption with the QoS constraint. All quantities of interest for some flow k will relate to the forward path from any node i to the destination node of that flow. Thus the goal will take the form:

$$G_i = m^k_{\pi(i)}(t_k, \overline{T_{\pi(i)}}) \\ +\beta 1[Q^k_{\pi(i)}(t_k, \overline{T_{\pi(i)}}) - Q^k_o > 0](Q^k_{\pi(i)}(t_k, \overline{T_{\pi(i)}}))^\nu \quad (7)$$

where:

- $m^k_{\pi(i)}(t_k, \overline{T_{\pi(i)}})$ is the total power cost function on the path going from the $i-th$ node to the destination of flow k, with the corresponding traffic loads on each of the intermediate nodes,
- $1[X]$ is the function that takes the value 0 if X is true, and takes the value 1 if X is false.
- $\nu \geq 1$, and $\beta > 0$ is a constant meant to match the delay units with respect to power, while Q^k_o is the QoS value that *should not be exceeded* for flow k, e.g. the maximum tolerated path delay,
- $Q^k_{\pi(i)}(t_k, \overline{T_{\pi(i)}}))$ is the total QoS value measured from this node to the destination by the SPs.

CPN uses the reward function $R = G^{-1}$ as follows. If the R_θ are the successive measured values of the reward function R at some node, then the RNN weights are updated based on the threshold Θ_θ, which captures a historical sliding window average of the reward:

$$\Theta_\theta = \alpha\Theta_{\theta-1} + (1-\alpha)R_\theta, \quad (8)$$

where he constant value $0 \leq \alpha \leq 1$ tunes the responsiveness of the algorithm. Weights are increased or reduced or based on the difference between the current reward R_θ and the previous threshold $\Theta_{\theta-1}$; if R_θ is larger than $\Theta_{\theta-1}$ then this results in a significant increase in the excitatory weights from all neurons to that neuron, with a slight increase in the inhibitory weights leading to other neurons. Otherwise, if R_θ is smaller than $\Theta_{\theta-1}$, all excitatory weights leading to all neurons are moderately increased, except for the previous winner, and the inhibitory weights leading to the previous winning neuron are significantly increased, in order to "punish" it for not being successful. $\Theta_{\theta-1}$ is first computed, and then the network weights are updated as follows. In the following expression that, the neurons i, j, n correspond to output links of the node where the update is being conducted, and none of these output links can be identical to the link from which the connection (for which the updates are being carried out) has entered this particular node. Thus, if the node has N links, one of them is excluded because the input link for the connection cannot be re-used as the output link (i.e. packets cannot be sent back along the link through which they entered), j denotes the output link that was most recently used by the connection, and hence there are $N-2$ alternate output links to be considered:

$$\Theta_{\theta-1} \leq R_\theta : \begin{cases} w^+(i,j) & \leftarrow & w^+(i,j) + R_\theta, \\ w^-(i,n) & \leftarrow & w^-(i,n) + \frac{R_\theta}{N-2},\ \forall n \neq j, \end{cases}$$

$$\Theta_{\theta-1} > R_\theta : \begin{cases} w^-(i,j) & \leftarrow & w^-(i,j) + R_\theta, \\ w^+(i,n) & \leftarrow & w^+(i,n) + \frac{R_\theta}{N-2},\ \forall n \neq j. \end{cases} \quad (9)$$

III. EXPERIMENTS

Our experimental testbed consists of 46 nodes, which are Pentium IV-machines with up to fifteen Ethernet interfaces running Linux Kernel 2.6.15. These nodes are connected using a topology depicted in Figure 2, with full-duplex links at 10 Mbps Mega-bits-per-second). The topology we have selected resembles that of the Swiss Education and Research Network, and artificial delays are used to replicate the link-level delays of the real network. We further assume that all the nodes have the same power consumption characteristic as a function of traffic rate as in Figure 1 that was measured for the single core routers that are used in our network test-bed, and the function p_i, that relates traffic rate to power consumption in node i is approximated by a piecewise linear function. In the EARP, we have chosen a maximum value of acceptable end-to-end delay of $Q^k_o = 80$ms. The constants $\nu = 8$ and $\beta = 1$ so that the second term in (8) tends to become very large when the end-to-end delay approaches 80ms, so that this delay is never exceeded. All delays are expressed and measured in milliseconds. In Equation (8) $\alpha = 0.8$ that represents an "average sliding window" over the five past values of R_θ.

A. Experiments with three source-destination pairs and no background traffic

We first chose three source and destination nodes, as indicated in Figure 2, and set up three flows: from node 19 to 3, from node 30 to 2 and from node 33 to 14. The three flows have the same data rate, which was varied with four values 0.5, 1, 1.5 and 2 Mbps. There was no other traffic in the network in this first experiment.

All the experiments were based on UDP traffic, and packet size was fixed at 1024 bytes. Each experiment ran for 600 secs, and measurements were collected from each node every five seconds. Additional background traffic at a rate of 200 kbps (2% of the link capacity) was also set up to run alternately every other 100 seconds over all the links between nodes 45-24, 35-10, and 46-38 in both directions, so as to create a time varying power load as well as a time-varying power consumption pattern in the network.

With this configuration, we compare the performance of EARP with that of the CPN protocol which aims to minimise end-to-end delay. We thus measured the power consumption in all the nodes of the network and the round trip delay experienced by the active flows.

All three flows were first run at a data rate of 0.5 Mbps, which was then increased in steps of 0.5 Mbps for each successive round of the experiment simultaneously for all

 ISBN: 978-1-61208-136-6

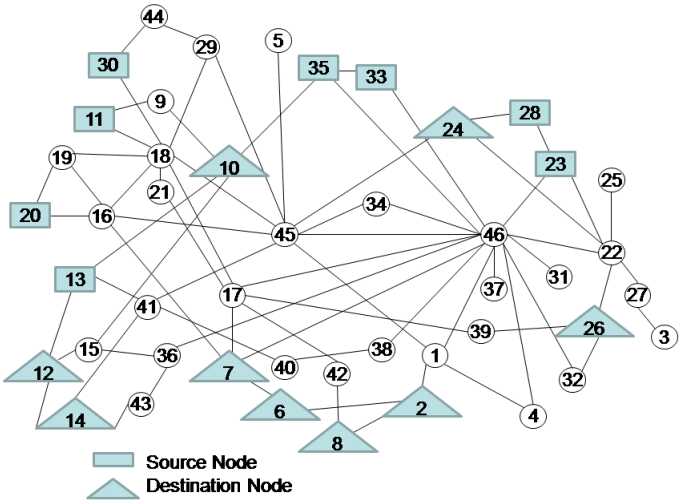

Figure 2. Network topology.

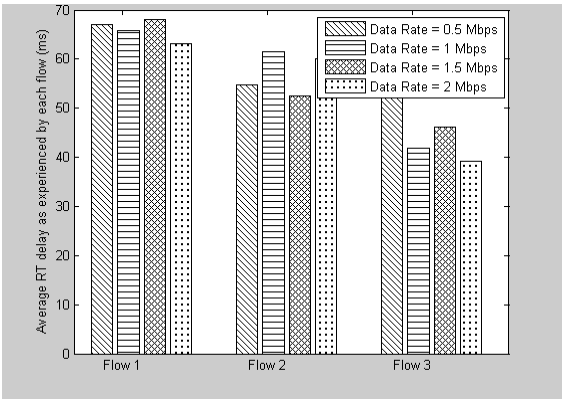

(a) Routing based on energy with delay constraint

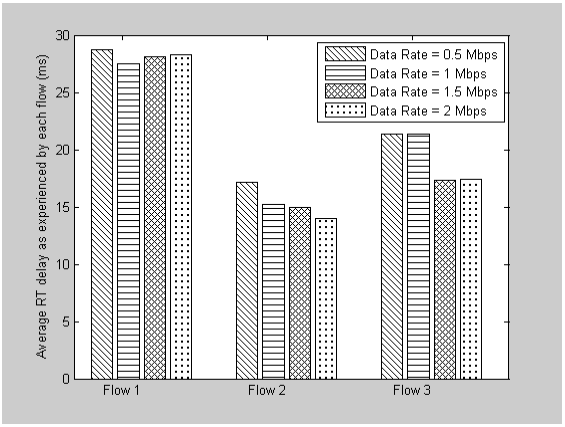

(b) Routing based on delay

Figure 3. Average round trip delay for the three flows with different traffic levels

three flows, up to the maximum value of 2 Mbs. Experiments were conducted separately with the EARP, and also with conventional CPN that was using delay only as the QoS goal.

On the other hand, as would be expected, EARP results in higher end-to-end delays as shown in Figure 3, mainly due to the longer paths taken by EARP to avoid nodes that carry more traffic and hence which consume more power per packet. To detail this point, the average length of the end-to-end paths used by each of the two schemes are plotted in Figure 4. It can be seen that the routes selected by CPN with delay minimisation are on average 40% shorter than those selected by EARP. Furthermore, Figure 3 also reveals that although delay may increase with EARP, each flows' round trip delay remains within the prescribed limit. This suggests that we could also modify EARP to include other QoS bounds, such as loss, a combination of loss and delay, and jitter.

B. Network-wide Energy Savings

We repeated the previous experiments with three flows, but also additional background traffic was added running throughout all the network links, in each direction at a constant rate of 200 kbps.

The resulting measured total power consumption over all nodes is shown in Figure 5 for routing based on energy, on delay and on shortest path, and for the different traffic rates on each connection. As expected, the routing based on energy (EARP) results in the lowest energy consumption, while routing based on shortest path which is insensitive to load conditions results in the highest energy consumption because energy consumption itself depends on load. Also as expected, we see that delay based routing provides a compromise since at low traffic levels it results in comparable energy consumption to EARP, while at high traffic loads it does not do as well as EARP.

Figure 6 compares the *average route length* in number of hops, averaged over all traffic levels for the three connections, for EARP on the one hand, and CPN that is based on using the number of hops as the QoS criterion. Note that the averages that are taken ar not "per packet", but rather per experiment. We see that EARP can result in significantly longer path lengths being taken, so that short path lengths obviously will not in general lead to lower overall energy consumption per path.

Figure 7 on the other hand examines the average round-trip delay experienced by packets, where again the average is taken over all the different traffic intensities and experiments for all of the three connections, where we compare EARP with the CPN protocol that attempts to minimise delay. We see that EARP can lead to significantly higher delays in its attempt to minimise energy consumption.

C. Experiments with nine connections

In a second set of experiments, we take nine (rather than three) source-destination pairs. Three flows are initially activated in the network, and then during the experiment three additional connections are launched, followed by three more. The three flows activated at the start of the experiment go from node 23 to 12, 30 to 14 and 33 to 2. Another three flows are

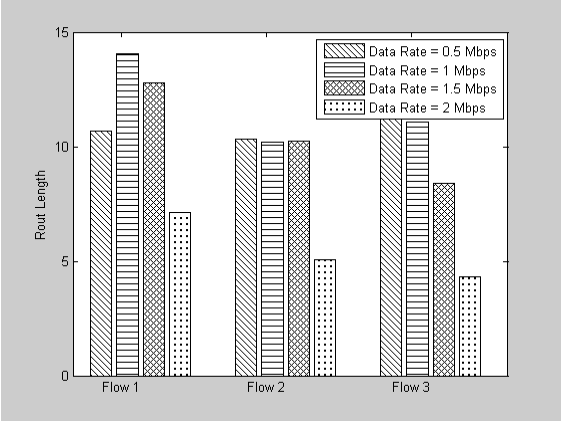

(a) Routing based on energy with delay constraint

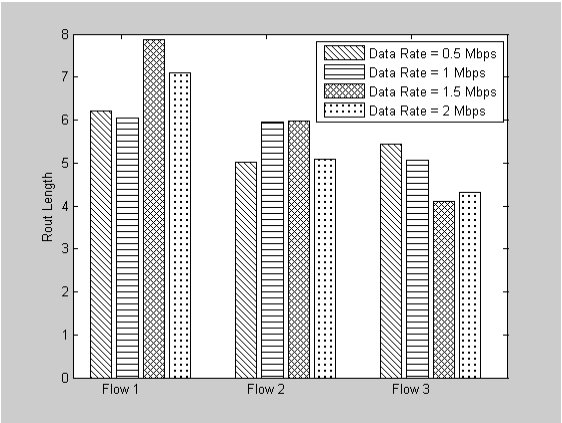

(b) Routing based on delay.

Figure 4. Average length of the end-to-end path taken by the three active flows.

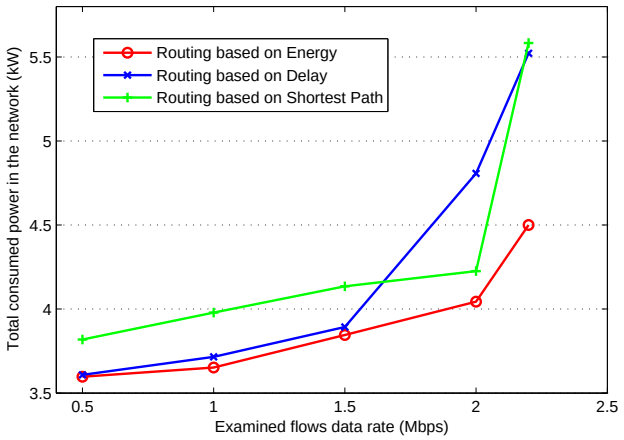

Figure 5. Experiment with three flows: total power consumption in the network vs. traffic rate all connections.

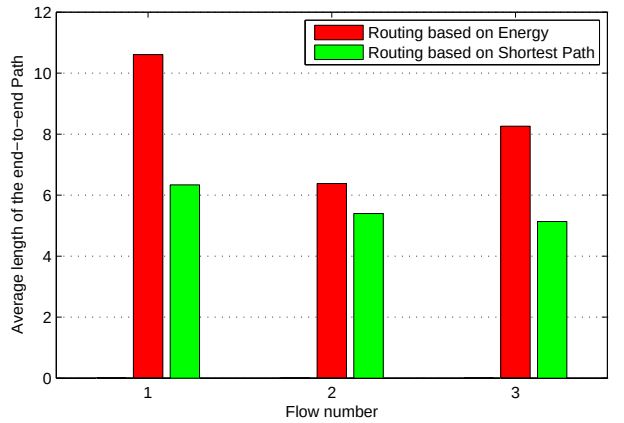

Figure 6. Experiment with three flows: average length of the paths taken by the connections.

initiated 100 secs later (from node 20 to 26, from node 28 to 10 and from node 35 to 7), and the finally three flows are activated 200 secs after the start from node 11 to 8, node 13 to 24 and node 29 to 6. Each flow's lifetime is 400 secs, and the total experiment lasts for 600 secs. All nine flows are first run at a data rate of 0.5 Mbps, and the data rate is then increased to 1, 1.5, 2, and 2.2 Mbps in successive steps. In addition we have 200 kbs of background traffic being conveyed in both directions over every link in the network.

The instantaneous power consumed by the network for flow rates of 1Mbps and 2Mbps is shown in Figure 8 during the first 400 secs of the experiment while all the nine flows are still active, as well as the step increases in power consumption at 100sec and 200secs, when three new flows are initiated each time. We observe the saving in power consumption when the EARP is used for both flows' rates 1 Mbps and 2 Mbps, as compared to shortest and delay based routing.

On the other hand, in Figure 9 we observe average values over the whole experiment (rather than instantaneous values) of power for five different data rates of the nine flows, and we see that using EARP always results in savings in power consumption. The irregularity in the curve for the power consumed using shortest path routing with CPN just indicates that CPN shortest path routing can actually use different paths, and these different paths can result in different levels of energy consumption that do not necessarily result in an overall increase when traffic rates increase on each flow.

IV. Conclusions

This paper introduces a novel energy-aware routing protocol (EARP) that is based on the autonomic network routing protocol CPN that was described in several other papers. EARP attempts to minimise the total power consumption of each flow in a packet network, while trying to keep the "damage" to the delay experienced by packets principal QoS metric to a value which is below an acceptable upper bound. We have implemented EARP on a large network test-bed, conducted measurements with different loads for long periods, and observed the network as the number of connections varies with time. In future work we plan to address QoS metrics which incorporate energy, as well as loss, jitter and delay.

 ISBN: 978-1-61208-136-6

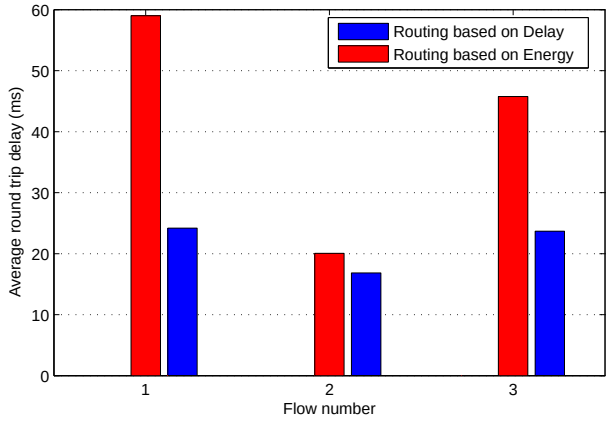

Figure 7. Experiments with three flows: average round trip packet delay for the three connections.

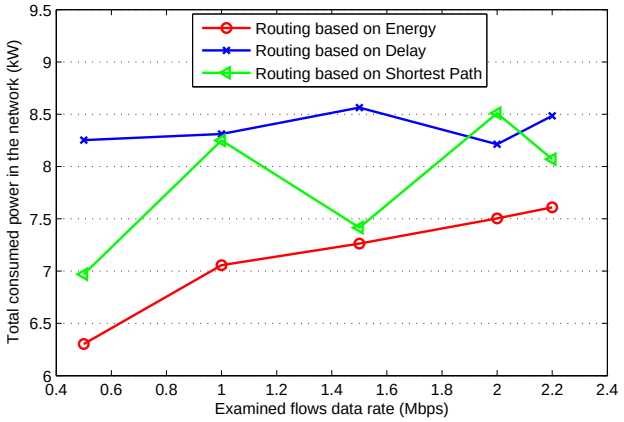

Figure 9. Scenario two: Total power consumption in the network vs. traffic rate of the connections

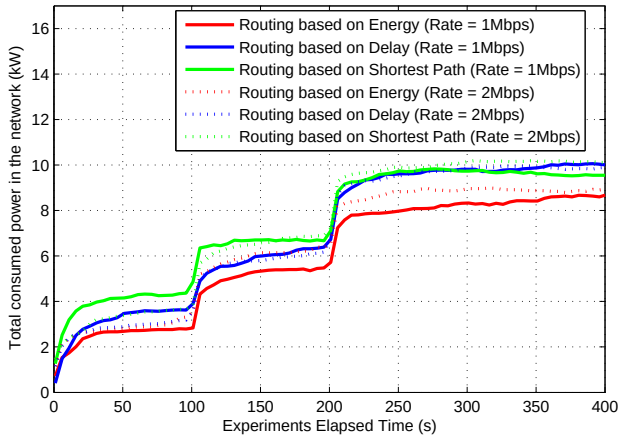

Figure 8. Scenario two: Total power consumption in the network Vs. the experiment's elapsed time.

REFERENCES

[1] S. Cui, R. Madan, A. Goldsmith, and S. Lall, "Joint routing, mac, and link layer optimization in sensor networks with energy constraints," in *IEEE International Conference on Communications (ICC '05)*, pp. 725–729, May 2005.

[2] E. Gelenbe and R. Lent, "Power-aware ad hoc cognitive packet networks," *Ad Hoc Networks*, vol. 2, no. 3, pp. 205–216, 2004.

[3] A. Berl, E. Gelenbe, M. D. Girolamo, G. Giuliani, H. de Meer, M. Q. Dang, and K. Pentikousis, "Energy-efficient cloud computing," *The Computer Journal*, vol. 53, no. 7, pp. 1045–1051, 2010.

[4] S. Nedevschi, L. Popa, G. Iannaccone, S. Ratnasamy, and D. Wetherall, "Reducing network energy consumption via sleeping and rate-adaptation," in *the 5th USENIX Symposium on Networked Systems Design and Implementation (NSDI '08)*, pp. 323–336, April 2008.

[5] E. Gelenbe and S. Silvestri, "Reducing power consumption in wired networks," in *the 24th International Symposium on Computer and Information Sciences (ISCIS '09)*, pp. 292–297, IEEE, September 2009.

[6] E. Gelenbe and S. Silvestri, "Optimisation of power consumption in wired packet networks," in *the 6th International ICST Conference on Heterogeneous Networking for Quality, Reliability, Security and Robustness (QSHINE '09)*, vol. 22 of *Lecture Notes of the Institute for Computer Sciences, Social Informatics and Telecommunications Engineering (LNICST)*, pp. 717–729, Springer, November 2009.

[7] C. Panarello, A. Lombardo, G. Schembra, L. Chiaraviglio, and M. Mellia, "Energy saving and network performance: a trade-off approach," in *the 1st International Conference on Energy-Efficient Computing and Networking (e-Energy '10)*, pp. 41–50, ACM, April 2010.

[8] A. Cianfrani, V. Eramo, M. Listanti, M. Marazza, and E. Vittorini, "An energy saving routing algorithm for a green ospf protocol," in *IEEE Conference on Computer Communications (INFOCOM '10), Workshops*, March 2010.

[9] P. Mahadevan, P. Sharma, S. Banerjee, and P. Ranganathan, "A power benchmarking framework for network devices," in *the 8th International IFIP-TC 6 Networking Conference (Networking '09)*, pp. 795–808, Springer-Verlag, May 2009.

[10] J. Chabarek, J. Sommers, P. Barford, C. Estan, D. Tsiang, and S. Wright, "Power awareness in network design and routing," in *the 27th Conference on Computer Communications (INFOCOM '08)*, pp. 457–465, IEEE, April 2008.

[11] R. Lent, "Simulating the power consumption of computer networks," in *the 15th IEEE International Workshop on Computer Aided Modeling, Analysis and Design of Communication Links and Networks (CAMAD '10)*, pp. 96–100, December 2010.

[12] E. Gelenbe, "Cognitive packet network," *U.S. Patent 6,804,201*, October 11 2004.

[13] E. Gelenbe, R. Lent, and A. Nunez, "Self-aware networks and qos," *Proceedings of the IEEE*, vol. 92, no. 9, pp. 1478–1489, 2004.

[14] E. Gelenbe, "Learning in the recurrent random neural network," *Neural Computation*, vol. 5, no. 1, pp. 154–164, 1993.

[15] E. Gelenbe, E. Şeref, and Z. Xu, "Simulation with learning agents," *Proceedings of the IEEE*, vol. 89, no. 2, pp. 148–157, 2001.

[16] U. Halici, "Reinforcement learning with internal expectation for the random neural network," *European Journal of Operational Research*, vol. 126, no. 2, pp. 288–307, 2000.

[17] E. Gelenbe, "Steps toward self-aware networks," *Communications of the ACM*, vol. 52, no. 7, pp. 66–75, 2009.

 ISBN: 978-1-61208-136-6

SmallCAN - A Reliable, Low-Power and Low-Cost Distributed Embedded System for Energy Efficient Building Automation

Harald Schrom, Tobias Michaels, Steffen Stein, Rolf Ernst
Institut für Datentechnik und Kommunikationsnetze
TU Braunschweig
Braunschweig, Germany
schrom|michaels|stein|ernst@ida.ing.tu-bs.de

***Abstract*—In this paper we propose a new reliable, low-power and low-cost platform for a building automation system, BAS, which is suitable to be used as a single platform for all appliances of a building. Furthermore today's platforms for building automation do not focus on low-energy consumption of the platform itself. The costs are also quite high and the installation has limited flexibility and needs extensive planning. The proposed platform features low-power consumption, has a reliable wired structure which is flexible, simply structured and can easily be extended. The low-power and low-cost approach targets the wide spreading of smart buildings to maximize global energy saving and to easily interface with a future smart grid. The SmallCAN platform has shown during evaluation in our demonstrator that it is able to fullfil all identified requirements of a modern building automation system.**

***Index Terms*—low-power; low-cost; building automation; embedded systems; smart grid; platform;**

I. Introduction

Nowadays up to 40 % of the overall european energy consumption is used by buildings [1]. Since resources in general and energy in particular are limited, different measures are researched to lower the total energy consumption of buildings.

Today's buildings are containing many energy consuming appliances like air conditioning, heating, lighting, fire detectors, burglar alarm etc. and also energy generating appliances start to enter the building sector for example solar panels or small combined heat and power units. Usually every single appliance is controlled separately. For example heatings often use a dedicated temperature sensor measuring the outside temperature and the temperature in the living room to control the heating.

The logic separation of appliances does not take advantage of a comprehensive control of all appliances regarding efficient energy usage. A trivial example would be to make the data of burglar alarm sensors available to the heating. The heating would then be able to check whether there are any open windows before starting to try raising the room temperature.

One can think about many other examples how the logic coupling of separate appliances of a building may boost the energy efficiency of the particular building. Consequently it is an obvious approach to use only one platform which controls every appliance of the building. This single platform would be aware of all the available data of the building and can control the building appliances as energy efficient as possible.

Furthermore a single platform will be able to easily provide comprehensive energy usage or energy generation data in real-time to the smart grid. A fast and broad reaction upon data provided by the smart grid is also an advantage of a single platform.

Another important parameter of a platform for building automation is often overseen: the energy consumption of the platform itself. Many of the current platforms are not energy efficient and do not scale well with respect to their own energy comsumption. Additionally the overall cost of the available platforms is quite high.

Therefore we propose a new platform for a building automations system which is able to control all appliances of a building by providing a reliable communication network, has a low power consumption and is designed of cheap standard components.

We will begin with identifying the needed requirements of a platform for building automation in the following section. In section III we will compare current platforms for building automation the identified requirements. Based on this comparison and the requirements identified in section II we propose a new platform which fulfils all of the mentioned requirements in sections IV to VII. We will then describe a demonstrator that we built to evaluate the new platform in section VIII. After that we finish with our conclusion.

II. Requirements

A platform for building automation which should be used to control all appliances of a building and provide/receive data to/from a smart grid has to fulfil several requirements to be beneficial for the energy efficiency and the general usability of the building. Several different platforms have been developed and/or proposed so far addressing the control of building appliances. A comprehensive and detailed overview of current platforms can be found in [2].

One of the main requirements of a single platform which may be used for all possible appliances is high reliability.

 ISBN: 978-1-61208-136-6

This is needed to ensure a safe and secure operation over several decades without causing dangerous conditions in case of errors. Furthermore appliances like burglar alarm systems or fire detectors rely on a reliable communication network.

Another important requirement is a low power consumption. The power consumption of the platform has to be as low as possible to guarantee maximum energy savings without spending to much energy in operating the platform itself. Otherwise buildings equipped with a building automation system may consume more energy in total, because operating the system uses more energy than it saves by efficient control of the building's appliances. This does also depend on the size of the building and the number of installed appliances, because a platform may scale bad with respect to power consumption. Therefore the overall energy consumption of a platform becomes a main factor for its success.

The overall cost of the platform, including component and installation cost is last but not least important to make the platform affordable for everyone to maximize the global energy saving by installing a building automation system in every building. Therefore a platform for building automation is in general cost sensitive.

In the next section current platforms for building automation will be compared against the identified requirements.

III. Differentiation of current building automation systems

The reliability of the used communication network is the main requirement for a platform which should be used for all appliances of a building. Recent research has proven that wireless systems do not fulfil this requirement since they tend to be easily disturbed. Especially the often used IEEE802.15.4 Standard mainly used in wireless sensor networks for building automations systems suffers heavily from IEEE802.11 data communication resulting in a packet loss rate of up to $100\ \%$, [3], [4], [5], [6]. However, the ease of installation and the flexibility make a wireless network an interesting option for appliances which do not require high reliability of the communication network like light switches or temperature sensors.

Power-line communication is another option, if the focus lies on ease of installation, especially for retro-fitting buildings, but power-line communication can be interrupted by devices without or defect noise suppression or by other devices injecting noise into the low-voltage grid like light dimmers or microwave ovens for example, [7], [8]. Up to $78\ \%$ packet loss was observed in low-thoughput power-line channels under adverse circumstances and even in optimal configuration there was still a remaining packet loss of $15\ \%$, [9]. Therefore power-line communication is similar to the wireless approach with respect to reliability of the communication network.

Platforms fulfilling the reliability requirement by using dedicated data-lines for a reliable communication network can be divided in platforms, which power the nodes over bus, also known as linkpower, and platforms where each node is powered by a separate power supply. The power consumption, which was identified as another important requirement, differs between these two principles. Platforms powering each node separately suffer from the fact that each node has to generate its own low voltage supply including the inherent power loss of the respective power supply. This leads to maximum power consumption per node of 4.6 W [10].

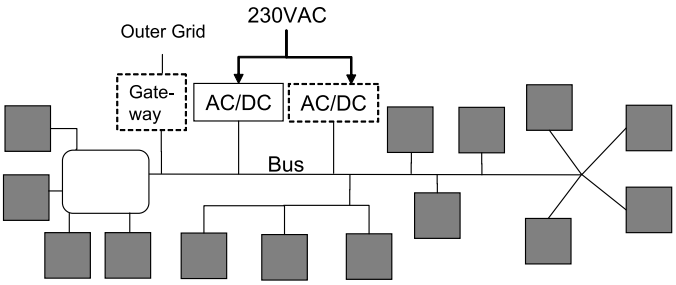

Fig. 1. SmallCAN System

Linkpowered platforms use one or more central power supplies which supply all nodes. This approach leads to a lower power consumption compared to separately powered nodes, because the power supply standby losses only occur once and not at every node. The operational losses can be further reduced by the use of a highly efficient and reliable power supply. Furthermore there is an inherent need to design energy efficient nodes to be able to supply as many nodes as possible. Typical nodes of such a platform for example are supplied by one central $24 - 30$ V power supply and consume about 0.6 W each [11], [12].

Other existing approaches such as I2C or one-wire bus are not designed for use in harsh building environment, not dealing with potential differences, voltage losses on long lines, auxiliary power for arbitrary sensors and actuators and high efficient throughput.

The different platforms also cause different installation costs. Direct digital control-based platforms for example usually require a star topology instead of an easier to install bus topology which raises the installation cost compared to systems using bus topologies. Platforms allowing a completely free topology cause the lowest installation costs, if only dedicated wiring platforms are considered, since no detailled planning is needed and the shortest path between two adjacent nodes can always be taken.

In the next section we will propose and describe a new reliable, low-power and cost-sensitive system for building automation, called SmallCAN, since no current platform for building automation fulfils all requirements satisfyingly.

IV. SmallCAN System Overview

We propose a system meeting the requirement for high availability and reliability by using dedicated wiring for data transmission together with a reliable communication protocol. Furthermore the topology of the wired bus medium is not restricted and completely decentralized to lower costs for planning and installation. The low-power requirement is met by powering all bus components with a single extra-low voltage power supply over the bus line. This reduces the losses which usually occur if every bus component needs to supply

itself. We also developed a sophisticated busnode layout with respect to power consumption to be able to deal with the restricted amount of power provided by the single power supply. To also satisfy the cost sensitiveness we use as many unified parts as possible in an exemplary implementation to proof that a cheap mass production of all system components is possible.

Thus we present a new distributed embedded system for the control of building appliances which is able to completely satisfy all of the identified requirements by implementing the above named design decisions. The system which we present in this paper is called SmallCAN, because the communication protocol is mainly derived from the CAN specification, [13]. Our system consists of:

- low-power bus-devices, which are build of a unified busnode and a function-specific device adapter
- dedicated bus wiring for communication and power supply of the bus-devices
- a central power supply
- an optional gateway interfacing the SmallCAN to smart grids or the internet for remote control

The bus-devices usually contain sensors, actuators or both and are used to operate the building appliances forming different applications such as room temperature or lighting control for example. The topology of the dedicated bus wiring connecting and supplying the bus nodes is completely free, see fig (1). Only one central power supply, backup power supply possible, is used to power all bus-devices via the bus.

The following sections will describe in-depth the SmallCAN system starting with the communication network.

V. COMMUNICATION

A. Physical Layer

The *SmallCAN communication network* uses a dedicated star quad cable for data transmission and power supply. Two wires are used for data transmission consisting of the data line itself and the associated ground wire. The dataline is driven to $23\ \mathrm{V}$ by the central power supply unit. $23\ \mathrm{V}$ is the idle level of the dataline which also complies to the recessive state of the bus. The busnodes are able to drive the voltage level of the dataline low with a single transistor. The low-level corresponds to the dominant state of the bus. With respect to the binary-physical-allocation the high-voltage-level, recessive state corresponds to 0 and the low-voltage-level, dominant state corresponds to 1. The used datarate is $9.6\ \mathrm{kbit/s}$. Several measures, described in the next subssection, have been taken to allow for an efficient system operation by reducing the required telegram and data rate. The comparatively low datarate allows for a long busline without the need of termination resistors or restricted stub lengths, because the datarate enables the voltage-level to settle before the next bit is transmitted. Therefore the bus lines can be arranged in a completely free topology. This hierarchy free topology enables adding nodes easily to an existing system. The physical layer is designed to operate up to $1000\ \mathrm{nodes}$ with an overall bus length of $1000\ \mathrm{m}$.

The remaining two wires of the dedicated star quad cable are used for the $30\ \mathrm{V}$ power supply of the busnodes. Due to the low-power design of the busnodes all nodes can be powered by the bus through a single power supply. This power supply is a high quality mains adapter regardless of high costs, because this is only needed once per system or segment. This central power supply should be highly efficient to ensure a low overall system power consumption. The availability of the system can be further improved by the optional use of a second redundant mains adapter to prevent this central unit from being a single point of failure. It is also possible to use battery buffering to be protected against mains flicker or temporal mains shutdown.

To maintain our target of a low-cost system, we decided to not galvanically insulate data and power supply ground which would otherwise lead to a higher component count and therefore to higher cost.

B. Protocol

The implemented multi-master *communication protocol* uses CSMA/CA for medium access which guarantees a very efficient use of the medium's datarate. It uses short telegrams with a fixed length. This fixed length can easily be handled in software by the busnodes. This is needed to achieve a simple software implementation of the protocol.

The developed protocol is in general very similar to the widely-known CAN specification which is used mainly in automotive environments[14]. SmallCAN inherits most of the properties of CAN to reach the same reliability. Therefore it is also easily possible to port the system to using a normal CAN-Bus, if needed.

A SmallCAN telegram consists of a unique $2\ \mathrm{byte}$ address which identifies the sender of the information and implies the priority. This is followed by 2 bytes containing payload and one CRC-byte for protection against transmission errors. The termination is done by positive or negative acknowledgement flags respectively and an inter-frame space to separate the telegrams. Each of the address, payload and CRC-bytes is accompanied by separate start and stop bits to allow for resynchronization of the receiving busnodes. These start and stop bits are also a replacement for bitstuffing which is used in CAN. Therefore frame errors can be recognized by missing or wrong positioned start or stop bits respectively.

This telegram structure leads to a constant and short telegram length of $69\ \mathrm{bit}$ including the minimum inter-frame space of $11\ \mathrm{bit}$. Every single data value is packed into the payload of only one telegram leading to low latencies with respect to measurement value or command transmission.

C. Communication Network Properties

The *availability* of the communication network is high due to the use of a dedicated, wired communication medium. The central, high reliable power supply powers all nodes via the bus wire. An additional power supply can be installed to compensate down times of the main power supply. These

 ISBN: 978-1-61208-136-6

power supplies can also be backed up by a USV to protect the system against local mains breakdowns.

The high *reliability* is also based on the wired communication and the CRC protection against transmission errors. The CRC allows the detection of corrupted data and the needed telegram acknowledgement bits make it possible to signal data corruption or loss by the receiving busnode, [15].

A wired communication network generally comes with low error rates and a continuous availability thus enabling low latencies. In combination with the CSMA/CA medium access, timing guarantees can be calculated for all running applications by doing a formal system analysis, [16]. Therefore applications with mixed criticality may also run on this system.

The wired connection with integrated powering of the nodes also enables easy *maintainability* because the status of every node can be polled every time. The bus integrated power supply has an advantage compared to battery powered or energy harvesting devices, because it allows the use of sensors and actuators without the restriction for extremely low-power operation between actions. Thus high sampling rates of sensors for example as well as safety and security related functions which require fast condition monitoring are possible.

The *robustness* of the system follows from the conceptual design being an independent system. For example there is no personal computer needed to operate the system which would be an unforeseeable maintenance factor.

The *network performance* is a result of a predictable timing behaviour. Retransmissions in case of communication errors are the main reason for timing problems in the system. The low bus latency during medium access - implied by a short data telegram length and supported by a lightweight fast software implementation - in combination with the low error rate on the wired medium reduces timing problems and supports mixed criticality as described above. The data rate of $9.6\,\mathrm{kbit/s}$ may seem low, but the efficient protocol leads to an effective telegram rate of up to $140\,\mathrm{telegrams/s}$. In BAS the telegram rate is more important than the sheer data rate since the transmitted data or commands usually fit into one telegram, making the data rate a negligible parameter compared to the telegram rate. Different measures may be taken to further reduce the required telegram rate for the respective applications and therefore use the available telegram rate more efficiently. Common measures include: Event driven message transmission, send-on-delta with sophisticated jitter suppression, traffic shaping and discarding outdated data prior to transmission.

The following sections will further describe the structure of the bus-devices regarding hard- and software.

VI. Bus-Device

A. Hardware

A *bus-device* consists of two parts, a unified busnode and a function-specific device adapter. The current busnode operates with $20\,\mathrm{V}$ to $30\,\mathrm{V}$. The average power consumption of the bus-node itself is $0.060\,\mathrm{W}$, the average power consumption of a complete bus-device including sensors, relays or other small actuator elements is $0.080\,\mathrm{W}$. A busnode contains nearly all of the electronic parts and the complete software for bus communication and the device functionality. The device adapter only implements a few components needed for the specialised bus-device function, for example to interface a special kind of sensor etc. The layout for a device-adapter can be deviated from a set of templates and therefore usually requires only small design efforts. At this stage the overall power consumption of every bus-device has to be limited and optimized by appropriate circuit design and power management for the sensors and actuators. For cost and reliability reasons the bus-devices use as few electronic components as possible. A significant amount of effort have been put into the optimization of the *busnode* with respect to power, cost and size. Only standard components are used which are available in high quantities for low prizes. The central part of the *busnode* is a PIC16F88-microcontroller which was chosen for its low-power consumption and its predictable structure with respect to timing. The only other active parts are a crystal and a voltage regulator. The bus driver circuit consists only of a MOSFET transistor and a resistive voltage divider.

Multiple measures have been taken to protect the nodes and the bus in case of errors, such as over-voltage protection, short circuit protection, and shut-off of the physical bus driver.

Primary common and cheap sensors and actuators are used to be integrated in device adapters (e.g. relays, humidity sensors, text displays). Sometimes it is necessary to interface modules and third party devices even though they are more expensive and less power efficient. This is done by standardized interfaces, such as RS232 or an ”0-10V” analog interface. Devices of other domain specific bus systems are interfaced as well to avoid the need for parallel bus cabling, especially for new installations. The local integration of such domain specific bus systems is done by a so called gateway device adapter, e.g. for DALI, MBUS and MP-BUS. These gateway device adapters are build similar to the normal bus-devices including their low complexity and power consumption. Standalone devices without dedicated bus connections have also to be controlled by specialized device adapters, e.g. gas heaters or electric meters. Because of the many possibilities of easy direct *interfacing* on device level, it is possible to use the presented system as a universal and holistic solution for all appliances of a building.

B. Software

The *software structure* consists run time kernel, an interface to local user functions and the user functions itself. The OS handles the bus communication protocol and standard functions such as I/O port operations and diagnostic functions. The implemented OS has a small code base and is well tested. The system also allows user functions which are in-system programmable over the bus. These user functions can be divided into two groups: hardware-related, hr, and non-hardware-related, nhr, functions. The hr function is used to control the hardware connected to the busnode or device adapter. The nhr function can be used to implement logic

 ISBN: 978-1-61208-136-6

functions without being allowed to access hardware, for example a controller coordinating the access to window blinds and window openers. Each busnode may contain one hr and one nhr function. The user functions are connected to the OS by an interface which routes all calls of the OS to the user functions.

C. Bus-Device Properties

A high availability of the hardware is reached by a robust design and the reliability of the components itself. The number of the used electronic parts was kept as low as possible to reduce the probability of hardware failures. Furthermore extra circuits to monitor power stages, etc, enable an online surveillance of the hardware status to support fast response times in case of severe hardware failures. Thus defective busnodes can be easily located and exchanged fast.

The OS was kept as simple and small as possible. It was tested under several different conditions and for a longer time period to make sure it works reliable.

The *costs* of the bus-device are low because of the few standard components and the small design effort for new device-adapters. Especially the unified busnode uses a small pcb which can be assembled by common SMEs.

As mentioned before the average power consumption of only 0.080 W per bus-device is at least an order of magnitude lower compared to the systems which are currently state of the art and also fulfil the reliability requirements.

It is now possible to derive the system properties from the detailled descriptions of the system components. This will be done in the following section.

VII. System Properties

By combining the described communication network with the bus-devices and the central power supply we get a system with the following general attributes:

- Highly available, because of the dedicated, wired communication network and the high availability of the bus-devices
- High reliability, because of the used robust protocol and thoroughly designed bus-devices
- Low-cost, since unified bus-nodes are used with a low component count and low part prizes
- Low-power, because of the central high efficient power supply and the careful considered part choice and layout of the bus-devices

The *robustness* of the system follows from the conceptual design of an independent system. The multi-master communication, the redundant power supply and the absence of a central controlling unit avoids a single point of failure. Especially there is no personal computer involved which would be an unpredictable maintenance factor. The high signal amplitudes were chosen to avoid problems with interferences. All signals leaving or entering the bus-devices are protected against damage by over-voltage etc.

Fig. 2. Demonstrator: Future Workspace

The *installation costs* are split into the initial installation of the wiring and the costs for later system extensions by adding new bus-devices. The free topology allows the freedom to install and expand the system at any time without any detailled planning. Especially there is no need to route dedicated cables between sensors and actuators, e.g. between light switches and lights, because all nodes are wired in the same manner. However the dedicated wiring makes retro-fitting of an existing building uncomfortable compared to systems using wireless or power-line communication.

In summary the overall system costs are quite low compared to the currently available systems. Furthermore the operation costs are kept low, because of the energy efficient design of the system itself. Talking about several decades of operation the energy consumption itself becomes one of the main factors for the overall costs.

The busnodes offer sufficient *performance* for intelligent distributed controls. This enables a full exploitation of the energy saving potential by enabling easy to configure rules and functions as well as more complex algorithms.

The *energy consumption* of the overall system is the sum of the used bus-devices, the loss on the communication lines and the loss at the high efficient main power supply. For a common system in a family home a simple system may contain 25 bus-devices up to 250 bus-devices in total for a high-comfort system covering all possible applicances. Inclusive all sensors and actuators, excluding the 230 V devices like lights, motors, etc., the simple system will need about 2.5 W. The high-comfort system will only need about 20 W.

In the next section we describe a demonstrator which is used to evaluate the presented system, before we conclude in the last section.

VIII. Demonstrator

To be able to test and evaluate the above presented SmallCAN system we decided to build a demonstrator. Therefore we became partner of a local architectural research project in Braunschweig called future:workspace [17].

The aim of this project is to transform a floor of a tower building belonging to TU Braunschweig into the perfect workspace of the future. This includes the energy efficient use

 ISBN: 978-1-61208-136-6

Fig. 3. Wirings looms and single wire

of several building appliances like air conditioning, heating, lighting, etc. Therefore we installed our SmallCAN system in one of the four offices of the future:workspace. About $100\ \mathrm{m}$ of bus-line and 93 busnodes were installed in total. The installed system consists of many sensors for room and outside temperature, temperatures inside the heating and air conditioning subsystems, humidity, brightness, windspeed, noiselevel, etc and also switches and other possibilities to interact with the system like LC-Displays for example. Furthermore several nodes controlling actuators of the appliances were installed like window blinds and electric window openers, lighting control, power socket relays, waterpumps, etc.

The other three offices of the future:workspace were equipped with a state of the art DDC system using Ethernet for communication between the busnodes. All four offices were configured to reach the same range of functions so that both systems can be directly compared in a real application environment.

Some advantages of the SmallCAN system were observed immediately. The star-topology wiring loom of the DDC system showed to be more complex and space-occupying compared to the single bus-line of SmallCAN, see fig 3. *Material usage* is an important factor in terms of environment protection and economical handling of materials. Additionally the fire load and cable conduits do affect the overall costs. Furthermore the overall power-consumption of the SmallCAN system is only $9\ \mathrm{W}$ including an optional ARM-based Linux-gateway for remote control over internet. The power consumption of the DDC system is currently monitored. The SmallCAN shows an average telegram rate of $8\ \mathrm{telegrams/s}$ in the current configuration which corresponds to an average busload of $5.7\ \%$ for a system consisting of 93 busnodes of the possible 1000 busnodes. Since the implemented control algorithms are way above average in the demonstrator, this shows that the choice of a low-datarate communication medium together with an efficient protocol and measures to keep the telegram rate low is working well. Further measurements to characterize SmallCAN like monitoring the packet loss rate and the busload with varying control algorithms are currently conducted and will be used to further improve the current platform or its successor. Smart power sockets, based on the SmallCAN platform, being able to measure and control the power usage of $230\ \mathrm{Volt}$ devices will be added in future to further increase the potential energy savings.

IX. Conclusion

The first test results of the presented SmallCAN system are promising and the system seems to fulfil all proposed requirements. It was proven that a platform for building automation which provides all necessary functions can be built with an exceptionally low-energy usage and without sacrificing system cost. Furthermore, due to the holistic approach to control every building appliance with one platform, comprehensive data can be sent and received to/from a smart grid. Future work will contain a more detailed comparison and analysis of the energy efficiency of the SmallCAN system and other BAS. Currently a model of the timing behaviour of the unified bus-nodes and the whole system is being build to be able to investigate the SmallCAN system by methods of formal analysis. Also porting the system to a more recent processor architecture is planned.

References

[1] *DIRECTIVE 2002/91/EC*, Official Journal of the European Communities, The European Parliament Std., 01 2003. [Online]. Available: http://www.eebd.org/filelibrary/docs/Directive_English_Version.pdf

[2] W. Kastner, G. Neugschwandtner, S. Soucek, and H. Newmann, "Communication systems for building automation and control," *Proceedings of the IEEE*, vol. 93, no. 6, pp. 1178 –1203, jun. 2005.

[3] A. Sikora and V. Groza, "Coexistence of ieee802.15.4 with other systems in the 2.4 ghz-ism-band," vol. 3, may. 2005, pp. 1786 –1791.

[4] S. Pollin, I. Tan, B. Hodge, C. Chun, and A. Bahai, "Harmful coexistence between 802.15.4 and 802.11: A measurement-based study," may. 2008, pp. 1 –6.

[5] M. Petrova, L. Wu, P. Mahonen, and J. Riihijarvi, "Interference measurements on performance degradation between colocated ieee 802.11g/n and ieee 802.15.4 networks," apr. 2007, pp. 93 –93.

[6] M. Z. n. Zamalloa and B. Krishnamachari, "An analysis of unreliability and asymmetry in low-power wireless links," *ACM Trans. Sen. Netw.*, vol. 3, June 2007. [Online]. Available: http://doi.acm.org/10.1145/1240226.1240227

[7] S. Bolognani, L. Peretti, L. Sgarbossa, and M. Zigliotto, "Improvements in power line communication reliability for electric drives by random pwm techniques," in *IEEE Industrial Electronics, IECON 2006 - 32nd Annual Conference on*, 2006, pp. 2307 –2312.

[8] F. Canete, J. Cortes, L. Diez, and J. Entrambasaguas, "Modeling and evaluation of the indoor power line transmission medium," *Communications Magazine, IEEE*, vol. 41, no. 4, pp. 41 – 47, 2003.

[9] Y.-J. Lin and H. Latchman, "On the effects of maximum transmission unit in power line communication networks," in *Power Line Communications and Its Applications, 2007. ISPLC '07. IEEE International Symposium on*, 2007, pp. 511 –516.

[10] *Busch-Powernet EIB Jalousie-/Serienaktor 6972 AG-102*, Busch-Jaeger Elektro GmbH, 2010.

[11] *HS485 D*, ELV AG, 2010.

[12] Siemens, *KNX bus*, 2010.

[13] *ISO 11898*, ISO Std.

[14] *CAN Specification Version 2.0b*, Robert Bosch GmbH Std.

[15] J. Wolf and R. I. Blakeney, "An exact evaluation of the probability of undetected error for certain shortened binary crc codes," in *21st Century Military Communications - What's Possible?*, vol. 1, October 1988, pp. 287 – 292.

[16] R. Henia, A. Hamann, M. Jersak, R. Racu, K. Richter, and R. Ernst, "System level performance analysis - the symta/s approach," *IEE Proceedings Computers and Digital Techniques*, vol. 152(2), pp. 148–166, 2005.

[17] C. Bremer, "future:workspace - moderne arbeitswelt an der tu braunschweig," *xia intelligente architektur, Zeitschrift für Architektur und Technik*, vol. 60, pp. 48–51, 2007.

 ISBN: 978-1-61208-136-6

ASIA: An Access Control, Session Invocation and Authorization Architecture for Home Energy Appliances in Smart Energy Grid Environments

Rainer Falk, Steffen Fries, Hans Joachim Hof
Siemens AG
Corporate Technology
Germany
{rainer.falk; steffen.fries; hans-joachim.hof}@siemens.com

Abstract—**With the advent of the smart energy grid – an energy transportation and distribution network being combined with an IT network for its monitoring and control – information security has gained tremendous importance for energy distribution and energy automation systems. Integrated security functionality is crucial to ensure a reliable and continuous operation of the smart energy grid. Further security related challenges arise from the integration of millions of smart homes into the smart grid. This paper gives an overview of the smart energy grid environment and its challenges. Many future use cases are centered around the smart home, using an ICT gateway. Approaches to protect the access and data exchange are described, preventing manipulation of ICT gateway operation. The paper presents ASIA – an Authentication, Session Invocation, and Authorization component to be used in the smart energy grid, to protect ICT gateways and to cope with problems like ICT gateway discovery and ICT gateway addressing.**

Keywords – Smart Grid, Information Security, Cyber Security, Authentication, Authorization, Energy Automation, Smart Home, Discovery

I. INTRODUCTION

Power generation, transmission, and distribution systems are characterized by the existence of two parallel infrastructures, the electrical grid carrying the energy, and the information and communication infrastructure used to automate, control and supervise the electrical grid. Especially the latter is becoming more and more one of the essential parts for power system operations as it is responsible not only for retrieving information from field equipment but most importantly for transmitting control commands. The power system as a critical infrastructure requires integrated protection against intentional attacks. A highly dependable management and operation of the information infrastructure is a prerequisite for a highly reliable energy network as the power system relies on the availability of the information infrastructure. Therefore the information infrastructure must be operated according to the same level of reliability as required for the stability of the power system infrastructure to prevent any type of outage. Integrated security functionality is therefore a central part of the energy control network.

Today's rather centralized approach for power generation has already and will continue to evolve into a decentralized power generation involving existing power plants, power plants producing renewable energy (like wind parks) down to households having their own micro power plants (e.g., solar cells). The importance of decentralized energy generation is expected to increase in the future due to the efforts to reduce the CO_2 footprint to fight global warming. Introducing decentralized energy generators into the current energy distribution network poses great challenges for energy automation (EA) in the smart grid scenario, especially secure communication between a control station (e.g., substation) and equipment of users (e.g., decentralized energy generators) must be addressed. Another trend in energy automation networks is the extended focus on the customer/user. From an architectural approach, users are expected to connect to the smart grid or more specific to the information and communication technology (ICT) infrastructure of the smart grid using an ICT gateway, which on the one hand provides metering data to the meter management service based on the locally measured and accumulated data. On the other hand, the ICT gateway also receives commands for load reductions to avoid power demand peaks. Additionally, an interface for the user to control certain home appliances or loads from remote location is needed. The ICT gateway may also be connected to a market place to sell locally generated energy or get price signals indicating a low price for energy, which can be coupled with profiles for dedicated energy con-

 ISBN: 978-1-61208-136-6

sumers. All these new services require a way for smart grid participants (e.g., distribution network provider, energy provider, marketplace, meter data management) to discover ICT gateways. Once discovered the secure connectivity to the user's home energy gateway provides the base for secure service provisioning and secure information exchange. Security comes in different flavors here, as at least authentication and authorization are required, to reliably control access to the ICT gateway and thus to secure energy appliances. Based on the required security level, integrity and privacy protection can leverage the initial security interaction. This supports also security requirements from different regulation bodies (examples are provided in [6] and [7]).

The remainder of this paper is organized as follows: Section II provides an overview of smart grid challenges with respect to security in general and describes in two subsections the end user and the utility perspective. Section III builds on that and describes security considerations to be obeyed when designing a secure access solution to home energy appliances. Section IV afterwards provides three different approaches to securely connect to the ICT gateway, whereby security is related to authentication and authorization of accessing peers. Section V concludes the paper.

II. Challenges and Smart Grid Perspectives

Current challenges for the power grid include the integration of fluctuating renewable energy sources, distributed power generation, short interval feedback on users on their energy usage, user indicated demand peaks, and the foreseeable need for the integration of electric vehicles, leading to an even higher energy demand of customers at peak times. A "smarter" grid can meet many of these challenges. With the move to a smart grid the importance of IT communication technologies in energy automation rises. With the availability of pervasive IT communication services, a variety of new use cases becomes possible enhancing the service to end customers and mitigates the impact of the challenges mentioned above.

Many use cases center around the Smart Home scenario. Smart Home in combination with the Smart Grid will allow people to understand how their household uses energy by smart metering, manage energy use better, e.g., through dynamic pricing or time of use pricing. Moreover, it enables them to sell locally generated energy on a market place, and reduce their carbon footprint. As the energy automation standard IEC 61850 (cf. [1]) is already used in the backend of energy automation networks, IEC 61850 is a good candidate to be used for communication between instances of the Smart Grid and the gateway of a Smart Home. The standard IEC 62351 (cf. [2] and [4]) defines security functions to protect IEC 61850 communication. The availability of an established security standard supports the approach to use IEC 61850 for communication between instances of the Smart Grid and the gateway of a Smart Home.

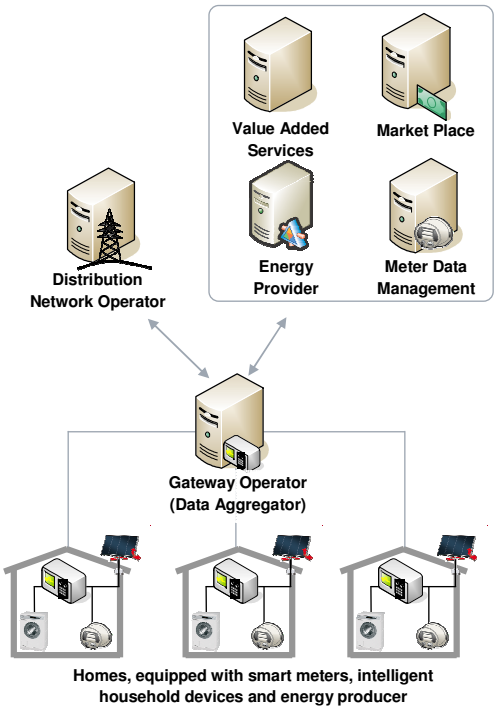

Figure 1. Connection of households to the smart grid

Figure 1 shows an example of a generic system architecture for a smart energy grid:

- Homes are equipped with smart meters, intelligent household devices, and energy producers.
- Home ICT gateways control the communication between these entities within a home and with the smart grid and thus define a security perimeter. The ICT gateway hides the complexity of the in-house network from the smart grid. Moreover, by acting as a gateway, it also protects the user's privacy, in terms of installed devices, network topology, and the generated data, when communicating with other smart grid entities. The ICT gateway may also act as a proxy for the appliances of the home. An example is a connection to the energy market place typically requiring communication in both direc-

 ISBN: 978-1-61208-136-6

tion, initiated by either the household or the market place.

- A gateway operator is responsible for administration of ICT gateways and provides connectivity for smart grid participants to the ICT gateways. As he controls the connectivity to the ICT gateway, he may also provide centralized authorization functions for the ICT gateway. This also applies to the user, when remotely controlling his household equipment.
- The distribution network operator is likely to communicate with the ICT gateways via the gateway operator, which hides the complexity of the ICT gateway management from the distribution network operator.
- The Meter Data Management processes the information received from the smart meters and provides the processed information to other market participants, e.g., for accounting.
- At the energy market, prosumers (resp. their ICT gateways) may buy and also sell energy. Hence the market offers a demand regulated price. An energy market alleviates the integration of distributed energy generators (e.g. solar cells).
- The smart grid information and communication infrastructure is also the enabler for other value added services. Remote serviceability of household equipment is just one example.

The functionality depicted can only be realized if two main challenges are solved: one is the addressability through external entities (e.g. the Distribution Network Operator) – the ICT gateways must be reachable by external entities. The second, after being reachable, access to the ICT gateways must be restricted to a distinct group of people, like the market place sending offers, a smart grid operator sending commands to the gateway, or the user accessing the gateway remotely in order to meet security and privacy requirements.

A. *Consumer Perspective: Smart Home*

Having an information and communication infrastructure like this at hand, the following use cases can be supported in the user environment:

1) *Energy-aware home appliances*

Currently, the price of energy for private consumers is mostly constant. From the perspective of a utility it would be beneficial to have dynamic pricing to influence the energy usage of customers; therefore it is likely that there will be dynamic pricing in the near future. On the customer side, new intelligent, energy-aware home appliances can optimize the costs for energy usage by starting and stopping energy extensive tasks (e.g., cloth or dish washing, charging an electric car) at appropriate times (e.g., start when energy is cheap). This requires that the current price of energy is known and there is some way to determine the price of energy for the duration of an operation. One way to implement such a system is an energy market, where energy-aware home appliances buy a certain amount of energy before they start an operation. Especially charging an electrical car during the night is an extremely flexible operation that requires much energy but has a large time window for execution, hence benefits from a good deal.

To integrate this functionality with the architecture presented above, the ICT gateway trades energy at the energy market. Accounting for any contract on the energy market includes the energy provider as well as the meter data management.

2) *Distributed power generation*

If energy is produced in a customer's home, e.g., by solar cells, the energy not needed at that point in time can be either stored or traded on an energy market. Especially if the energy market is on a large scale, selling the energy with dynamic pricing may be more attractive than fixed pricing. On the other hand, energy markets may be restricted to a smaller geographical area (e.g., city district). Thus, energy can be locally distributed, supporting self-containment of that area.

As for the scenario above, the ICT gateway is connected with external smart grid entities to trade energy. Accounting for contracts includes the distribution network provider as well as the smart meter management.

3) *Energy Management and User Awareness*

An application with integrated user interface in the home is used for communication with the utility, e.g., to get a diagram of current energy usage, to get current energy pricing, to get the personal energy usage history, to get energy saving tips and the like. The user interface may also be used to receive energy outage forecasts, for troubleshooting, or to dynamically select a desired energy mix.

Energy-aware home appliances may also offer a user interface that states the current price for one operation execution. E.g. a coffee machine may state the price per coffee pot or the washing machine may suggest a

 ISBN: 978-1-61208-136-6

different start time to save money resulting from a better tariff.

To implement this use case with the architecture presented above, the ICT gateway informs appliances about current energy prices, which it either gets at the energy market or directly from an energy provider (price signals as incentive for a special behavior).

B. Utility Operator Perspective

Further use cases are focused on keeping the distribution network stable and keeping costs for utilities low (e.g., because it is not necessary to buy additional energy at short notice). As IEC 61850 is already widespread in use in the distribution network, it is a natural candidate for the following use cases:

1) Reactive reduction of residential load

A utility has the ability to shut down a certain amount of residential load in the household of users to react on certain situations in the network (e.g., if too many consumers are active). In doing so, the utility avoids buying energy on short notice, which is very expensive (prices may go up to 100 Euros per kWh). The ability and permission to issue such switch-off commands can be based on special contracts between user and utility operator. As the ICT gateway provides a security perimeter, it hides the internal energy consumer network from the utility.

To implement this use case with the architecture presented above, the utility must only have a certain amount of energy (kilowatt hours), which can be unloaded in households as well as the communication addresses of the associated ICT gateways. ICT gateways may be addressed through the gateway operator that also ensures the connectivity of the ICT gateways. The utility sends a shutoff message via the gateway operator to a set of ICT gateways. Sending this shutoff message to many households must be finished in a short time to allow fast reactions. The shutoff message must be protected to avoid being misused by attackers. The ICT gateway takes the appropriate actions to meet the request of the utility, especially, it communicates with proper home appliances to be shut off.

2) Reduction of distributed power generation

The utility may not only tear down energy consumption, it may also instruct distributed power generators to not feed energy to the distribution network to fight situations when there is a low demand for energy. The signaling process is the same as in the previous use case. Again, the ability and permission to issue switch-off commands to residential power generators is expected to be based on special contracts between user and utility operator.

3) Demand Response

Another use case from a utility prospect is demand response: A utility can send price signals (either a rather high price if energy demand is too high or a low price if the energy demand is too low) without using the energy market to influence energy usage of intelligent home appliances. Price signals are especially interesting for energy intensive tasks that have a large time window for execution, e.g. charging of electric cars. Price signals can be sent for future time periods or as real time pricing information. The utility sends price signals via the gateway operator to the ICT gateways. The ICT gateway may either distribute the pricing information to the appropriate home appliances or act on the pricing information based on defined profiles.

III. Considerations for ICT Gateway Access

As described above, the secure discovery and access to a home energy gateway is a central functionality for a secure smart energy grid. Based on the described scenarios, the following entities may require secure access, via both local and remote communication, to an ICT gateway:

- Energy provider (including metering / billing)
- Distribution network operator
- Gateway operator
- Energy Market
- End user

Therefore an ICT gateway has to support remote access, allowing secure exchange of measurement, supervision and control data with the energy network. Secure access involves the following parts:

- Authentication: Mutual authentication between ICT gateway and accessing entity.
- Authorization: Determine access permissions. The decision whether a certain access is authorized, may be decided locally on the device or centrally by an authorization server. The access control enforcement takes place at the gateway itself.
- Secure Communication: Confidentiality and Integrity of the communication is protected, e.g., by us-

 ISBN: 978-1-61208-136-6

ing IPsec or SSL/TLS.

The following subsections discuss the different aspects for the realization of secure access to an ICT gateway and propose an appropriate solution.

A. Platform Security

It is expected that the ICT gateway itself supports certain security features. These may comprise:

- Secure credential store for storing user or service relate credentials. These may be issued by the gateway service provider or even the energy provider himself. A flexible approach for providing a secure credential store is the use of pluggable security modules, e.g. in form of a smart card. Similar to a mobile phone SIM card, the user can then simply change his energy provider by replacing the energy provider's security module.
- Self-integrity check to ensure that the system configuration has not been altered in an unauthorized way
- Tamper protection to detect if changes to the hardware have been made.

The latter feature is especially important if the ICT gateway provides information for billing, is part of a smart meter device, or is mounted in a place, which are publically accessible.

B. Network Connectivity

One requirement arising from these use cases is scalability. Security solutions for the Smart Grid must scale with millions of devices – Germany for example has more than 39 million households and each household is likely to have more than one device.

Users will connect their ICT gateways to already existing ICT networks, which are used for Internet access and services like Voice over IP (VoIP) or multimedia streaming. The user infrastructure typically involves a gateway connecting to the Internet (DSL box), which has a Network Address Translation (NAT) component as well as a firewall component integrated. Thus, accessibility of an ICT gateway connected to a user's home network is limited, as the ICT gateway is not addressable from outside. Hence, another requirement is NAT-traversal (the ability to address and reach a component behind a NAT device).

Multiple levels of hierarchy from a control station to a device in a household are a common solution to address scalability. This includes communication other than the point to point communication used today.

A solution that enables NAT-traversal is described below.

C. ICT Gateway Discovery

As shown in Figure 1, in smart grid scenario's new roles and/or components may be introduced. One example is the ICT gateway operator. This gateway operator is in charge of concentrating the communication from the home energy gateways up to the control center as well as providing an easy way to the control center to reach a high number of energy gateways at once. Moreover, a gateway operator can support the discovery of ICT gateways and most likely will also offer additional services based on this discovery like remote access for user's or remote management of the ICT gateways, e.g., to provide enhanced functionality or updates for installed software.

D. Permissions

The following permissions resp. kinds of access to the ICT gateway have to be distinguished:

- Change configuration
- Install applications
- Get status information
- Issue commands (e.g. shutoff command)

E. Access Authentication

Access to the home energy gateway should be limited to a distinct group of entities, which may comprise the distribution network operator, the gateway operator, and the user itself. Moreover, communication with the gateway should be performed in a secure manner. Both can be achieved as described in the following:

- Gateways possess a certificate, which was either provided by the vendor of the gateway or the gateway operator.
- Roles or components accessing the gateway also possess a public resolvable certificate and corresponding private key.
- Mutual authentication between gateway and accessing component/role based on credentials is performed.
- Home energy gateways are not always reachable from the Internet, i.e. they may not use a public IP address.
- The IP address may be resolved by the gateway

 ISBN: 978-1-61208-136-6

operator directly or by a network operator (in case of DSL at the users home) if requested by other smart grid entities

In the following options for the access decision points are discussed.

F. Local access control decision at the ICT gateway

To ensure a secure communication of roles/persons allowed to access the home gateway, an access control list (containing credentials, potentially role information, associated rights, etc.) has to be managed at the gateway directly. This may be done by either the user or the gateway operator. As the user has the choice of a preferred energy provider, service aggregator or other smart grid roles, there will be individual communication connections per user. Thus user-specific configuration has to be done at each home energy gateway. Dedicated roles can initiate a secure connection to every ICT gateway based on a device certificate installed at the gateway.

The advantage of this approach is a direct accessibility for different roles or components to the ICT gateway. The disadvantage is that user specific connection credentials have to be administered at each ICT gateway separately. Note that the gateway discovery and address resolution is neglected here. Deployment in existing home environments may not lead to the establishment of a communication channel through the existence of NAT and Firewall functionality. Thus, the approach of direct access is not feasible.

G. Centralized access control decision

An alternative to the decentralized handling of access control is a central, network-based functionality of a security provider, who authenticates and authorizes potential roles and components, that wish to access an ICT gateway. Such an approach is already known from telecommunication environments like the Generic Bootstrapping Architecture (GBA) of 3GPP networks. A further example can be given through server components in voice over IP (VoIP) networks, e.g., in SIP (Session Initiation Protocol, RFC 3261). The following section investigates in centralized access control.

IV. SOLUTIONS FOR CENTRALIZED ACCESS CONTROL

The proposed central security function provides **A**uthentication – **S**ession **I**nvocation – **A**uthorization. Hence the abbreviation ASIA is used further on for this component. ASIA would be typically combined with other functions needed, e.g., for ICT gateway address resolution or discovery. It is therefore expected that the ICT gateways register with the ASIA component to publish their IP addresses. This registration connection is kept online to allow access to the ICT gateway from remote and may also be used to communicate consumption data or to connect to value added services. As it is expected that the ICT gateway is operated in a home environment behind a DSL router, this permanent connection also keeps the NAT bindings as well as the opened communication ports in the DSL router. To achieve connectivity with an ICT gateway using ASIA different modes are described in the following subsections.

A. ASIA – Operation in Session Invocation Mode

In this mode, ASIA initiates a connection establishment with a requesting smart grid role/component.

Process:

- ASIA authenticates and authorizes the connecting smart grid role/component (energy provider, aggregator, meter data management, etc.)
- Accessing role/component provides a TAN (transaction number) for the ICT gateway to associate the ICT gateway in the direct connection later on. Alternatively, the TAN may be generated by ASIA and provided to the accessing role/component and the ICT gateway as part of a software token. This has the advantage that the software token may contain further information about security parameter of the connection to be established between the ICT gateway and the accessing role/component. Examples are the fingerprints of the used certificates for authentication at ASIA.
- ASIA sends the connection request from the role/component via the permanent connection to the ICT gateway including the connection parameter (address of role/component, TAN, software token, etc.) and optionally the requested command to be executed.
- The ICT gateway uses the received information to establish a direct connection to the requesting role/component. The distributed TAN can be used to associate the connection attempt with the initial request of the requesting role/component.
- After successful authentication the information exchange can be started.

 ISBN: 978-1-61208-136-6

Technical approach:

- If web-based services are already used in the system the authorization process may be realized using SAML and XML security (cf. [3]). This approach supports certificate based authorization as well as pre-shared key based authorization.
- An alternative to SAML may be the application of Kerberos for a purely symmetric infrastructure without the need for certificates.
- Authentication on the direct connection may be performed on transport layer, e.g., by applying TLS.

The following figure shows the general protocol flow for a session invocation.

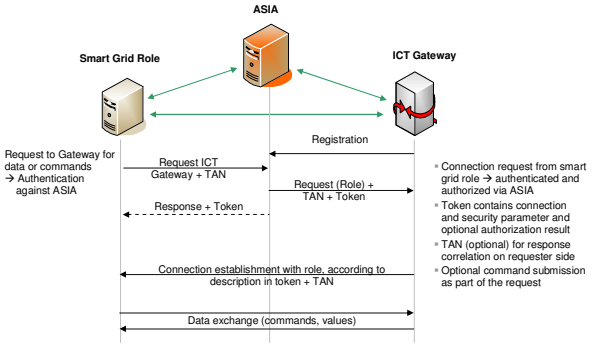

Figure 2. ASIA – Session Invocation Mode

The advantage of this approach is the flexibility and scalability in changing environments, especially when the communication relations change. The approach supports a central authentication and authorization component, which keeps the administrative effort low per gateway. This may influence the used gateway hardware. The central component is not involved in the actual data exchange. The disadvantage is that there is no option for a direct communication establishment between the requesting role/component and the ICT gateway, which stems from the user environment, because of the missing TAN.

B. ASIA – Operation in Redirect Mode

In this mode the ASIA server provides the address location information to the requestor after successful authentication. The requestor can then directly connect to the ICT gateway.

Process:

- The ASIA component authenticates the requesting smart grid role/component based upon certificates or pre-shared keys alternatively.
- According to the ASIA rule set, the address information will be provided to the requesting role/component. Here, it is also possible to include a software token as proof that the role/component has been authenticated and authorized at the ASIA server. This token may include further security parameter.

Technical approach:

Based on the described functionality, the ASIA server would resemble a Kerberos like KDC authenticating and authorizing the access to the ICT gateway. Note that this approach builds upon the general accessibility of the ICT gateway in terms of addressing and connection establishment, which may be limited due to the user's environment.

The following figure depicts the general call flow.

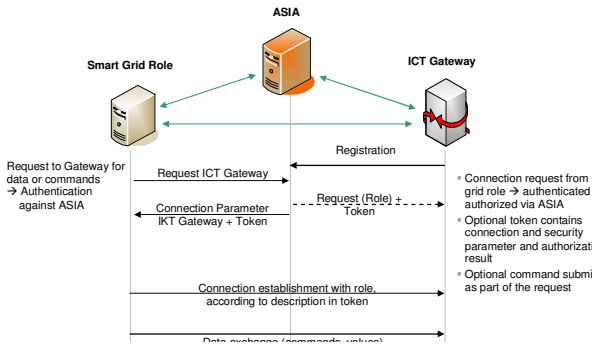

Figure 3. ASIA – Redirect Mode

The advantage of this approach is the flexibility to react on changing communication relations. Like the previous approach this solution allows for a central authentication and authorization component. The obvious disadvantage is the requirement to have direct accessibility to the ICT gateway from other components. In user environments with NAT and FW devices, this solution will fail, as the Firewall will block access to the ICT gateway. Moreover, if the user has a common DSL account the associated IP address is likely to change within 24 hours (at least in Germany).

C. ASIA – Operation in Proxy Mode

The ASIA server may act as proxy for restricting access to the ICT gateway.

Process:

- The ASIA component authenticates the requesting

 ISBN: 978-1-61208-136-6

role/component based upon certificates or pre-shared keys alternatively.

– Based on the permanent connection between the ICT gateway and the ASIA server, the connection attempt of the requesting role/component is forwarded to the ICT gateway.

– ASIA may provide information about the authentication and authorization state, in a software token.

– To achieve end-to-end security also in the case of a communication proxy, application layer security mechanisms may be used. An example is the application of XML signatures to achieve integrity protection.

Technical approach:

– ASIA simply connects both links and operates as a data proxy for the duration of the connection.

This approach may be realized by using the previously described approach, with the exception, that ASIA does deliver the own address instead of providing the ICT gateway address. It may be realized with the first approach letting the ASIA server connect to the requesting role/component. Thus, this approach is rather a configuration of the first two approaches with central access control.

The following figure shows the abstract call flow or the connection establishment.

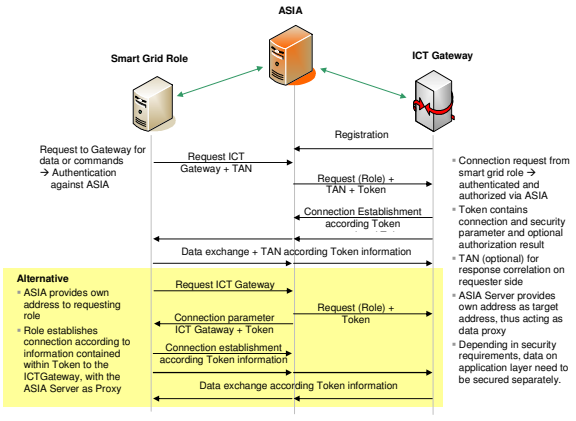

Figure 4. ASIA – Proxy Mode

The advantage of this approach is the flexibility to react on changing communication relations. A disadvantage is the missing end to end connection establishment. Moreover, as all traffic is processed though the ASIA server, dedicated hardware requirements may arise.

Generally, the ASIA functionality can also be used to deliver configuration information, which communication connections are allowed or normal and which not. This configuration information can also be used to enrich the effectiveness of IDS/IPS tools, by making them aware of the network configuration.

V. CONCLUSION

This paper provides an overview of smart grid environment and challenges. Many future use cases in the smart grid are centered on the smart home. An intelligent ICT gateway is the key to provide the intended services. Nevertheless, the base for the service provisioning is connectivity. This paper described approaches to protect access and data exchange, preventing manipulation of ICT gateway operation. It presented an ASIA (Authentication, Session Invocation, and Authorization) component to be used in the smart grid environments to protect access to energy appliances at a user's home from remote and to cope with basic problems like ICT gateway discovery and addressing. Three different modes of operation allow the ASIA component to be adapted to a very large range of smart grid communication network settings. The concept of ASIA was also introduced into the E-DeMa project (cf. [5]), which is one of six projects funded by the German Federal Ministry of Economics and Technologies (BMWi) in the national joint research initiative E-Energy.

REFERENCES

[1] ISO-IEC 61850, Part 1: Introduction and Overview, May 2003

[2] ISO-IEC 62351, Part 1: Data and communication security – Part 1: Introduction and overview, 2006

[3] XML Signature Syntax and Processing (second Edition), W3C Rec., June 2008, http://www.w3.org/TR/xmldsig-core/ last access March 2011

[4] Fries, S.; Hof, H-J; Seewald, M.: The Fifth International Conference on Internet and Web Applications and Services – ICIW 2010: "Enhancing IEC 62351 to Improve Security for Energy Automation in Smart Grid Environments", May 2010, ISBN 978-0-7695-4022-1, pp. 135-142

[5] E-DeMa Project - Development and Demonstration of Locally Networked Energy Systems to the E-Energy Marketplace of the Future, Project Webpage: http://www.e-dema.de, last access March 2011

[6] NERC, North American Reliability Corporation, Standards: http://www.nerc.com/page.php?cid=2|20, last access March 2011

[7] NIST IR 7628 Guidelines for Smart Grid Cyber Security, Vol. 1 Smart Grid Cyber Security Strategy, August 2010, Volume 1-3, http://csrc.nist.gov/publications/nistir/ir7628/ last access March 2011

 ISBN: 978-1-61208-136-6

Exploiting Demand Response in Web-based Energy-aware Smart Homes

Andreas Kamilaris
Department of Computer Science
Networks Research Laboratory
University of Cyprus
P.O. Box 20537, Nicosia, CY 1678, Cyprus
Email: kami@cs.ucy.ac.cy

Andreas Pitsillides
Department of Computer Science
Networks Research Laboratory
University of Cyprus
P.O. Box 20537, Nicosia, CY 1678, Cyprus
Email: andreas.pitsillides@ucy.ac.cy

***Abstract*—Energy conservation is a global issue with tremendous environmental implications. By 2030, the global energy demand will double. High demands and environmental concerns, force the transformation of electricity grids into smart grids, towards more rational utilization of energy. Residential smart metering transforms homes into energy-aware environments, allowing residents to make informed choices about electricity. Web-based smart homes employ Web principles to interconnect electrical appliances. The Web, as a highly ubiquitous platform, can be used to connect energy-aware smart homes to the smart grid. An important characteristic of the future grid is demand response, defined as real-time pricing, according to supply conditions. Energy-aware smart homes can exploit this capability to schedule electricity-related tasks for future execution. We investigate this possibility by deploying a Web-based, energy-aware smart home, adapted to demand response. An initial technical study denotes the feasibility of our approach and a small survey indicates the potential for saving energy and money.**

Keywords-Smart Home; Smart Meters; Electrical Appliances; Smart Grid; Demand Response; Web.

I. INTRODUCTION

Energy conservation is a big issue in the world with tremendous environmental, political and social implications. Predictions denote that by the year 2030, the global energy demand will double, rising up the energy-related green gas emissions by 55% [1].

This high energy demand cannot be accommodated by current electricity grids. Most of the electricity grids around the world have been designed many decades ago, to meet the energy requirements of the society at that time.

Increasing demand and environmental concerns, influenced initiatives towards more rational utilization of electrical energy. This goal can be achieved when the electric utilities are fully aware in real-time about the electrical consumption and the demands of their customers. The grid becomes intelligent when it manages to deliver electricity from suppliers to consumers using two-way digital communications and a smart metering system. This vision is believed to convert traditional electricity grids into modern *smart grids*.

Smart metering of electricity does not only affect the future development of the smart grid, but also motivates the rational management of the electrical consumption in houses and buildings. Buildings consume a large proportion of the total electrical energy [2]. This fact has a significant environmental impact, as more than 30% of all greenhouse gas emissions can be attributed to buildings.

Residential smart meters are devices that measure in real-time the energy consumption of a house, or even of various electrical devices and control their operation. These meters have gained popularity recently. For example, it is planned that every home in Britain will be equipped with such meters by 2020. Equipping home area networks (HAN) with smart meters, allows the enablement of *energy-aware smart homes*.

According to numerous studies such as [3], timely electrical consumption feedback through smart metering, is believed to reduce electrical consumption by a fraction of 5-15%.

However, further savings can be achieved, when energy-aware smart homes get connected to the smart grid. The Web is an appropriate platform for such a wide-scale interconnection.

In this work, we assume the existence of the smart grid and we develop an energy-aware smart home that can exploit the demand response functionality offered by the grid, through the Web. In such a way, home residents can save money, while electric utilities can save energy and be assured about the societal acceptance of the grid and its smooth operation.

The rest of the paper is organized as follows: Section II provides background information as well as related work, while Section III argues about the benefits of using the Web as an integration platform. Then, Section IV presents the system's implementation and Section V discusses the technical feasibility of our approach. Finally, Section VI investigates possible savings through a small case study and Section VII concludes the paper.

II. RELATED WORK

Our approach spans in two research domains: HAN equipped with residential smart meters and the smart grid.

In the following subsections, we present some background information regarding the smart grid and energy-aware home environments, along with significant related work in the fields.

A. Towards the Smart Grid

The smart grid is expected to provide advanced functionalities such as high power quality, immediate failure alarms,

 ISBN: 978-1-61208-136-6

reliability, security and improved customer service.

An important characteristic of the smart grid is real-time pricing, which is a smart energy pricing scheme that is set for a specific time period on an advance basis and which may change according to load demands or price changes in the market. Prices paid for electricity consumed during these periods are known to consumers a priori, letting them to vary their energy usage in response to these prices and manage their energy costs by shifting usage to a lower tariff period. This mechanism is mainly known as demand response (DR).

Many experts state that Plug-in Hybrid Electric Vehicles (PHEV) will be the grid's killer application. PHEV are hybrid vehicles with rechargeable batteries that can be restored to full charge when connected to an (external) electric power source.

For example, a study from the Pacific Northwest National Laboratory [4] states that even the existing grid in the United States, if optimally utilized, could provide enough power for PHEV to replace up to 73% of the nation's cars. However, if the charging times of PHEV are not properly managed, the load to the grid's distribution network will be highly increased. The smart grid can afford this issue by means of DR. Improved tariffs, adjusted to reflect the system's congestions, would promote proper scheduling of plug-in vehicle charging.

Pilot projects that implement the smart grid in an experimental basis have appeared lately. A popular pilot project is SmartGridCity [5], performed by Xcel Energy utility supplier in the area of Boulder, Colorado.

Masdar City [6] will be the world's first zero-carbon city, powered entirely by renewable energy sources. Pilot residences will be equipped with DR-enabled smart appliances. By receiving signals from the grid, they will customize the appliances' usage to reduce energy demand on the grid.

The interconnection of smart homes and the smart grid through the Internet, by means of Web services is proposed in [7]. It is stated that service-oriented architectures are well suited for the smart grid.

B. Energy-aware Smart Homes

Residential smart metering transforms home environments into energy-aware smart spaces. There exist two broad categories for household energy monitoring and control: whole-home and device-specific.

Whole-home approaches place one smart meter where the home connects to the power grid. Marchiori et al. [8] use circuit-level power measurements to separate aggregated data into device-level estimates, with 90% accuracy. ViridiScope [9] places inexpensive sensors near electrical appliances to estimate their power consumption with less than 10% error.

Traditional smart meters offer a house-level granularity, where only the whole-home energy consumption can be visualized. As the technology becomes more advanced, monitoring the energy consumption of each electrical appliance and controlling its operation, becomes possible. Device-specific techniques plug smart meters in individual electrical appliances.

Some device-specific smart meters offer even wireless networking capabilities, extending the residential smart metering infrastructure into a robust wireless network. As an example, Ploggs [10] incorporate wireless transceivers, based on the IEEE802.15.4 wireless standard.

ACme [11] is a high-fidelity AC metering network that uses wireless sensors, equipped with digital energy meters to provide accurate energy measurements of single devices. Energie Visible [12] employs smart meters to visualize in real-time the energy consumption of the appliances that are connected to the meters, in a Web interface. In the Energy Aware Smart Home [13], users can use their mobile phones as magic lenses to view the energy consumption of their appliances, by pointing out them with the phone's camera.

A big challenge for energy-aware smart homes, taking into account the existence of the smart grid, is to provide to the home environment visibility of grid conditions and dynamic prices, in order to take local decisions and intelligently control the usage of household electrical appliances, to save energy and money. Studies that specifically examine the implications of demand response functionality of the smart grid in energy-aware smart homes are still lacking, to our knowledge.

III. The Web as an Integration Platform

We believe the Web is an appropriate platform for bridging energy-aware smart homes and the smart grid. By means of the Web, smart homes can be fully synchronized with the grid.

The Web is highly ubiquitous and it scales particularly well. Almost every house has Internet connectivity today, while technological advancements in mobile telecommunications such as 3G and WiMAX, permit the Internet to penetrate in the mobile world.

A. The Web and the Smart Grid

We identify many benefits in using the Web as an integration platform for the smart grid.

A cloud-based smart grid strategy constitutes a cost-efficient practice for enhancing grid's functionality incrementally as energy demands arise. New capabilities can be implemented in parallel with existing operations and systems, while the impact on ongoing operations is minimized.

Existing systems can be securely integrated with new components and further be connected to users and customers, by means of the Web. The Web is a scalable framework for incorporating third-party and partner techniques.

Most importantly, utilization of the Web would promote the Web service model, minimizing expenses for additional infrastructure and overall implementation time. Web services are core parts of cloud computing, providing a wealth of proven methods for systems integration.

B. Web-based Smart Homes

Designing smart homes based on the Web principles is a recent practice. In the Web Home application framework [14], we reused central principles of the modern Web architecture to integrate physical devices to the Web and build an interoperable smart home that supports multiple home residents concurrently. By using the Web as application layer, flexible

 ISBN: 978-1-61208-136-6

applications on top of heterogeneous embedded devices can be built with a few lines of code, facilitating home automation.

Web-based smart homes build upon the notion of the *Web of Things* [15], which is about employing well-accepted Web practices to interconnect the quickly expanding ecosystem of embedded devices, built into future household appliances.

REpresentational State Transfer (REST) [16] is proposed for Web-based interaction with household appliances as it is a lightweight architectural style that defines how to use HTTP as an application protocol. REST advocates in providing Web services modeled as *resources*. Resources can be manipulated by the methods specified in the HTTP standard, under a uniform interface. REST guarantees interoperability and a smooth transition from the Web to home environments.

Enabling home appliances to the Web, permits the extension of Web mashups into *physical mashups* [17]. Physical mashups take advantage of real-world services offered by physical devices and combine them using the same tools and techniques of classic Web mashups. In this way, physical devices can be blended with Web content and services, without much effort.

A future cloud-based smart grid strategy would allow the seamless integration of the grid with Web-based, energy-aware smart homes. As an example, what follows is a shell script that implements a physical mashup, combining electrical appliances and Web services provided by an electric utility.

We assume in this example that the utility exposes, as a RESTful Web service, information about its real-time tariffs. This script checks the current home tariff and starts charging automatically a hybrid electric vehicle as soon as the tariff falls below some defined limit.

```
function check {
   if [ $? -le LOW_TARIFF ] ; then
       curl -d "State=ON"
            -X PUT [HomeAddress]/PHEV/Switch/
   fi
}
curl -s -X GET [UtilityAddress]/Tariff/Home/ $1
check;
```

Through the Web, residents can pull easily the data they need from an open API offered by their electric utility, and use them right away in their own applications, in any programming language that supports HTTP.

As a more general example, a reliable Web-based weather forecast service can be combined with smart appliances, e.g., to turn off the electric heating automatically, in case the temperature is about to increase in the next few hours.

These simple examples indicate that advanced home automation, high flexibility and energy conservation can be achieved, when using the Web as a platform.

IV. Developing a Web-based Energy-aware Smart Home

We extended our Web Home framework [14] to support interaction with residential smart meters and consequently with the electrical appliances of a smart home.

We utilized Plogg residential meters to create a wireless smart metering network inside the house. We exploit the fact that wireless sensor networks can provide a reliable and extensible solution for real-world deployments. Each Plogg is associated with some specific appliance, in order to monitor its electricity footprint and control its operation.

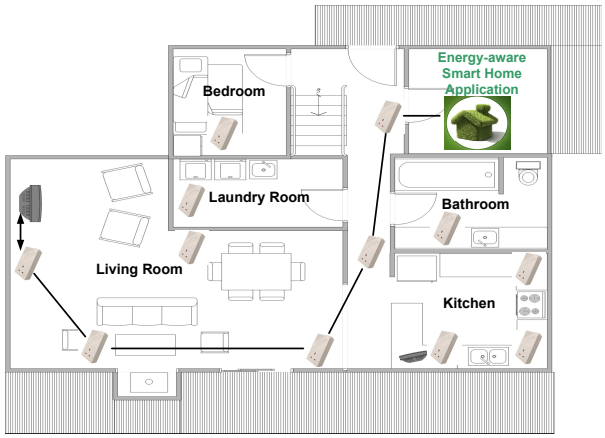

Fig. 1. A typical energy-aware smart home.

In Figure 1, a typical deployment of Ploggs inside an energy-aware smart home is shown. These smart meters use their multihop communication abilities to inform the resident about his electricity footprint. In the figure, five hops are needed from the meter that acts as the base station, to reach the meter which monitors and controls the television. Plogg discovery is automatic, based on the ZigBee specifications.

We exposed the functionality of the Web Home framework as a RESTful interface and we developed a client application in JavaScript, using the Google Web Toolkit (GWT). The client application offers a Web-based, interactive graphical user interface (GUI), in order to help residents to visualize their energy-aware home environment and fully manage their electrical appliances through the Web.

Detailed, real-time consumption data from each electrical appliance and the aggregation of historical data about energy into graphs, facilitate the extraction of informed knowledge about the home's energy performance, encouraging the habitant towards more rational usage of electricity.

In Figure 2, a typical snapshot of the client application can be observed, where the electricity footprint of each appliance is depicted in a pie chart. Through detailed energy monitoring, electricity-wasting actions can be avoided and energy-inefficient devices can be managed better or be replaced.

Through the Web, each appliance can be individually controlled. For example, the resident from his work may switch off the television he forgot on, when he hastily left the house.

Furthermore, our application enables the resident to associate the energy consumption of his electrical appliances with the actual tariffs from his electric utility, translating kilowatt hours (kWh) into money. Based on these tariffs, the electricity cost consumed by each appliance is automatically calculated.

 ISBN: 978-1-61208-136-6

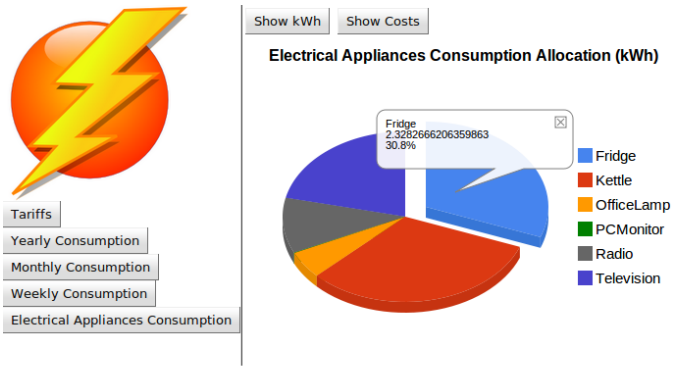

Fig. 2. Detailed electrical appliances' consumption allocation.

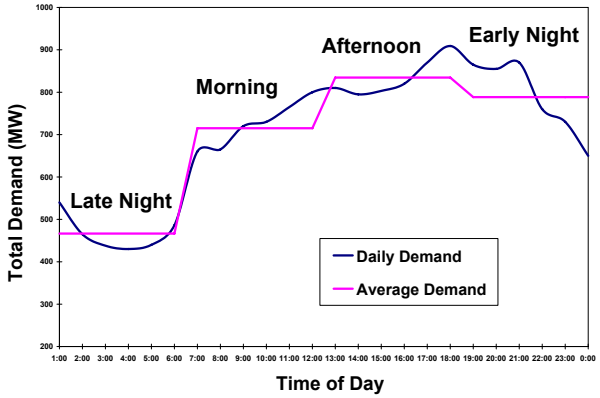

Fig. 3. Total electricity demand in a typical winter day.

A. *Exploiting Demand Response*

As we previously noted, a significant feature of the grid is DR. DR would assist in offering dynamic tariffs, according to supply conditions. Dynamic tariffs can be received in real-time, when utilities provide Web APIs to automatically disseminate them to the homes of the consumers. Since not many countries provide yet such capabilities, we also let the resident define himself the existing local tariffs.

The DR capability would allow users to cut their energy bills by telling low priority devices to harness energy only when it is cheapest. We included a task scheduling mechanism adapted to DR from electric utilities, following the physical mashup paradigm. The residents are able to program actions to be executed automatically in low-tariff hours. A low tariff is specified as a lower percentage from the basic tariff, which is offered by the utility. As an example, the resident can program the electric water heater to heat water for a shower, when the tariff is 10% less than normally.

The resident is able to further adjust the task scheduling procedure, according to his own preferences. He can define a maximum amount of waiting time, in case tariff does not fall below the specified limit in that time window. In this case, the task can start right after. The resident can also specify the execution of a task to be performed in morning, afternoon or night time. Finally, he can set the duration of each task, forcing the application to switch the corresponding electrical appliance off, as soon as the task completes.

A DR-based task scheduler can have a psychological factor. Energy-aware smart homes and the introduction of the smart grid in the residents' daily lives, can engage them in more sustainable lifestyles and energy-efficient practices [18]. The potential for saving energy and money can cultivate informed, actively involved and environmentally-aware consumers.

V. Technical Feasibility Study

In this section, we examine the feasibility of our approach from a technical perspective.

We have deployed inside an experimental smart home of around 100 m^2, a wireless network of Ploggs. The typical structure of the house is shown in Figure 1. Our application has been installed on a laptop inside the storeroom.

Since our country does not yet support the smart grid, we simulated its operation through the Web. We developed a Web server that simulates DR functionality for the Electricity Authority of Cyprus (EAC) [19], which is the only utility in the country. A RESTful Web service informs customers in real-time about the utility's current tariffs using RSS Web feeds.

These tariffs, although simulated, aim to reflect the actual energy loads and demands in our country. Figure 3 presents the total electricity demand in Cyprus, at a typical winter day. We assume that the power plants of EAC are able to operate in four different modes for generating electric power. These modes reflect the average electricity demands when dividing a winter day into morning, afternoon, early night and late night. These four modes can be observed in the figure.

To produce real-time tariffs, correlated to electricity demand patterns, we used the simple equation shown in (1):

$$Tariff = \alpha \cdot BasicTariff \cdot (\frac{InstantDemand}{AverageDemand}) \quad (1)$$

where α is a coefficient used to weight the prices according to differences in demands. Using this equation with $\alpha = 1$, we produce real-time tariffs that give incentives to consumers to utilize their electrical appliances not in peak hours. These tariffs fluctuate around the (current) basic home tariff, which is offered by EAC (20,07 cent/kWh), as shown in Figure 4.

To test the performance of our system, we considered a typical real-life scenario. Most washing machines allow a user to define a preferred operation mode and start the washing in a future time. We programmed such a washing machine through the task scheduling mechanism, to start the washing when the tariff from the electric utility is 5% less than its normal price. According to Figure 4, this would happen at 4:00, 7:00, 14:00 and 23:00 in a typical winter day. We also set some parameters such as the duration of the task to be one hour and 30 minutes and the maximum waiting time to be eight hours. We measured the execution times of this task, placing the washing machine and its corresponding Plogg, in different hops from our application (base station).

 ISBN: 978-1-61208-136-6

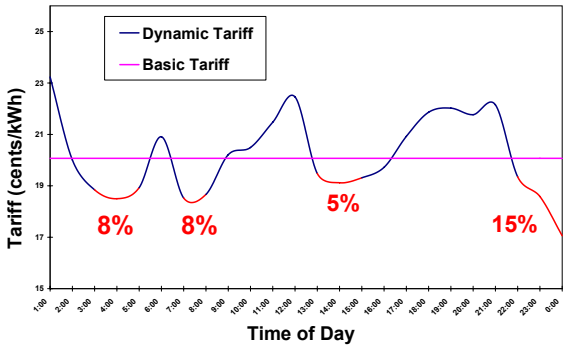

Fig. 4. Real-time tariffs based on electricity demand.

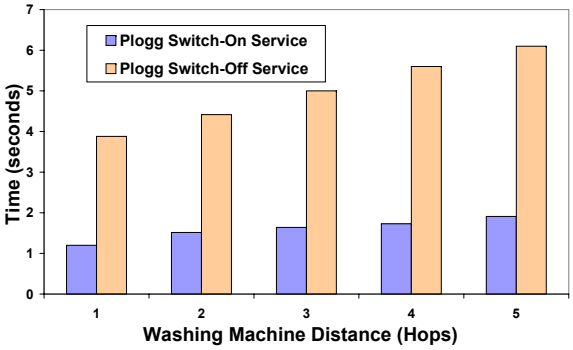

Fig. 5. Task scheduling performance.

Figure 5 illustrates the results of this experiment. In all five multihop scenarios, we created the task at 12:00, it started executing exactly at 14:00 and it finished execution at 15:30. Less than two seconds are needed, from the time the application is informed about the tariff change, until the washing machine starts working, even in five-hop distance. Switching off the device needs a bit longer, approximately 4-6 seconds. This difference is due to the specific operation of the Ploggs' firmware. Since the task scheduling mechanism will operate for control scenarios with low workload, our results in regard to task execution times, are considered satisfactory.

VI. Potential Savings

Connecting energy-aware smart homes to the smart grid, creates a new potential for saving energy and money. We attempt to estimate this potential, considering that household appliances account for 50-90% of the residential consumption.

We define home devices into three broad categories. *Permanent devices*, which should never be turned off such as a fridge, *on-demand devices*, which are utilized by home residents spontaneously, in order to accomplish a momentary task such as a toaster and *schedulable devices*, which are devices that are supposed to accomplish some specific task but their operation is not momentarily urgent and can be postponed for a future time such as a dishwasher.

We are mostly interested in schedulable devices as they are devices that can be programmed to operate during low-tariff periods of the day. These devices can fully harness the DR feature of the smart grid. Therefore, electric utilities can save energy by better managing their load conditions and residents can save money by using electricity when it is cheapest.

A. A Survey for Schedulable Devices

We performed a small-scale, telephone-based survey to identify schedulable electrical appliances. We discussed with twenty housewives and we posed to them the following question: "if your electric utility offered cheaper tariffs at some hours of the day, which tasks, handled by your electrical appliances would you schedule for these hours?". We also asked them about the duration of each task per day, translated into operational time of the relevant appliance and also the monthly frequency, in which they perform this task.

Their responses are listed in Table I. We used average values for task duration and monthly frequency. These values depend on many parameters such as weather conditions (electric water heater), number of family members (electric iron, washing machine), mentalities and habits of each society (electric oven, dishwasher) etc. Surely, these values are not absolute but just indicative, in order to facilitate our purpose of roughly estimating possible savings through our approach.

Observing the table, we can notice that some devices can be categorized both as schedulable and on demand (hair dryer, electric mixer, electric oven). Eight housewives commented that they were willing to use such devices according to low-tariff periods, in case this would save them significant money.

B. Calculations for Money Savings

After identifying home schedulable devices, we located some popular products for each device type and we recorded their energy consumption in kilowatt-hours (kWh). We computed the average values to derive typical consumption figures.

For our calculations, we used the typical home tariff offered by EAC (20,07 cent/kWh). In the last three columns of Table I, we can view possible savings for schedulable devices, when home tariff falls 10%, 20% or even 30%.

Devices such as the electric mixer do not contribute in money savings and there is no need to schedule them for future time. However, devices such as the washing machine and the electric oven could contribute more effectively, allowing monthly savings of more than €1 each, when tariff falls 10% and more than €4, in case tariff falls 30%.

If we apply our optimized policy for all electrical appliances, monthly savings can be summed around €6 in 10% tariff reduction and up to €19 in case of 30% reduction. Considering the fact that the average monthly cost for electricity in houses around Cyprus is €175, possible saving of €19 gives 10,85% reduction in the bill of a typical home.

A survey from Parks Associates [20] remarks that over 80% of US households would pay up to $100 for cost-saving equipment if it chopped at least 10% off their monthly electricity bills. This survey indicates a possible acceptance of our approach by home residents. This is only valid under certain conditions such as effective tariff reductions by utilities.

 ISBN: 978-1-61208-136-6

TABLE I
A LIST OF SCHEDULABLE ELECTRICAL APPLIANCES AND POSSIBLE SAVINGS.

Device	Consumption (kWh)	Duration	Monthly Frequency	Tariff Reduction in €		
				10%	20%	30%
Hair Dryer	2.1 (1.5 - 2.5)	35 minutes	25	0,63	1,27	1,9
Electric Mixer	1.3 (0.8 - 1.5)	20 minutes	8	0,07	0,14	0,22
Electric Iron	2.8 (2.4 - 3.0)	2 hours	8	0,93	1,85	2,78
Electric Oven	2.7 (2.5 - 3.0)	60 minutes	26	1,45	2,91	4,36
Electric Water Heater	3.0	30 minutes	20	0,62	1,24	1,86
Dishwasher	1.5 (1.3 - 2.0)	40 minutes	22	0,46	0,91	1,37
Washing Machine	2.6 (2.0 - 3.0)	1 hour 40 minutes	16	1,44	2,87	4,31
Clothes Dryer	3.6 (3.0 - 4.3)	50 minutes	11	0,68	1,37	2,05
Total Possible Savings				**6,28**	**12,56**	**18,84**
Plug-in Hybrid Electric Vehicle	3.3	8 hours	10	5,46	10,93	16,39

As we remarked before, an example killer application of the smart grid might be PHEV. It would be essential for the healthy operation of the grid to force residents to charge their PHEV in low-demand periods of the day, e.g., during the night. The last row of Table I shows possible savings when a typical PHEV exploits real-time pricing. We assume that a typical PHEV needs approximately eight hours of charging in 3.3 kWh and provides driving range on batteries up to 150 miles. Therefore, it would need charging every 3-4 days to adequately support the needs of a family. In this case, monthly savings can be more than € 10 when the tariff is reduced by 20%.

VII. CONCLUSION AND FUTURE WORK

Demand response is a promising capability of the smart grid. Energy-aware smart homes can exploit this functionality, using the Web as an integration platform. This seamless interconnection has the potential for significant energy and money savings, both for the electric utilities and the customers, allowing Web-enabled smart appliances to schedule their execution for low-demand and respectively low-tariff periods.

Few people predicted the revolutionary advancements the Internet has brought to the world. Even fewer have predicted that the Web would affect so many aspects of our lives. Energy-aware smart homes and the smart grid, represent the extension of this trend to power consumption.

In the future, we plan to perform a small-scale deployment of our Web-based, energy-aware home infrastructure in real houses around Cyprus. In cooperation with EAC, we will try to simulate the DR feature of the grid in realistic conditions. In this way, we will be able to extract more precise estimations about energy and money savings and to assess the overall influence of the smart grid in the society.

VIII. ACKNOWLEDGMENTS

This work was supported by the Electricity Authority of Cyprus. We would like to thank Mr Antonis Valanides, the director of the IT Department, for his valuable advice.

REFERENCES

[1] International Energy Agency. World Energy Outlook 2007. 2007.

[2] Europa Press Release. Communication from the European Commission. Energy Efficiency: Delivering the 20% target. November 2008.

[3] Sarah Darby. The effectiveness of feedback on energy consumption A review for defra of the literature on metering, billing and direct displays. *Environmental Change Institute, University of Oxford*, 2006.

[4] Pacific Northwest National Laboratory. Mileage from megawatts, May 2011. Online at: http://www.pnl.gov/news/release.aspx?id=204.

[5] Xcel Energy. SmartGridCity Project, May 2011. Online at: http://smartgridcity.xcelenergy.com/.

[6] Masdar City, May 2011. Online at: http://www.masdarcity.ae/en/.

[7] Cor Warmer, Koen Kok, Stamatis Karnouskos, Anke Weidlich, David Nestle, Patrick Selzam, Jan Ringelstein, Aris Dimeas, and Stefan Drenkard. Web services for integration of smart houses in the smart grid. In *Grid-Interop Conference*, Denver, November 2009.

[8] Alan Marchiori and Qi Han. Using Circuit-Level Power Measurements in Household Energy Management Systems. In *First ACM Workshop On Embedded Sensing Systems For Energy-Efficiency In Buildings (BuildSys)*, pages 7–12, Berkeley, California.

[9] Younghun Kim, Thomas Schmid, Zainul M. Charbiwala, and Mani B. Srivastava. ViridiScope: design and implementation of a fine grained power monitoring system for homes. In *Ubicomp '09: Proceedings of the 11th international conference on Ubiquitous computing*, pages 245–254, New York, NY, USA, 2009. ACM.

[10] Energy Optimizers Ltd. Plogg Smart Meters, May 2011. Online at: http://www.plogginternational.com/.

[11] Xiaofan Jiang, Stephen Dawson-Haggerty, Prabal Dutta, and David Culler. Design and implementation of a high-fidelity AC metering network. In *Proc. of the 2009 International Conference on Information Processing in Sensor Networks (IPSN)*, pages 253–264, Washington, DC, USA, 2009.

[12] Dominique Guinard and Robert Unteregger. Energie Visible, May 2011. Online at: http://www.webofthings.com/energievisible/.

[13] Marco Jahn, Marc Jentsch, Christian R. Prause, Ferry Pramudianto, Amro Al-Akkad, and Rene Reiners. The Energy Aware Smart Home. *In the 5th International Conference on Future Information Technology (FutureTech)*, pages 1–8, May 2010.

[14] Andreas Kamilaris, Vlad Trifa, and Andreas Pitsillides. The Smart Home meets the Web of Things. *International Journal of Ad Hoc and Ubiquitous Computing (IJAHUC), Special issue on The Smart Digital Home (To appear)*, 2011. Online at: http://seacorn.cs.ucy.ac.cy/papers/files/KamilarisIJAHUC10.pdf.

[15] Erik Wilde. Putting things to REST. Technical Report UCB iSchool Report 2007-015, School of Information, UC Berkeley, 2007.

[16] Roy Thomas Fielding. *Architectural Styles and the Design of Network-based Software Architectures*. PhD thesis, University of California, Irvine, California, 2000.

[17] Dominique Guinard and Vlad Trifa. Towards the Web of Things: Web Mashups for Embedded Devices. In *Workshop on Mashups, Enterprise Mashups and Lightweight Composition on the Web, in Proc. of WWW Conference*, Madrid, Spain, 2009.

[18] W. Fred Van Raaij and Theo Verhallen. A behavioral model of residential energy use. *Journal of Economic Psychology*, 3(1):39–63, 1983.

[19] Electricity Authority of Cyprus, May 2011. Online at: http://www.eac.com.cy/.

[20] Parks Associates. 50% of U.S. households are interested in home energy monitoring, May 2011. Online at: http://www.parksassociates.com/blog/article/50–of-u-s–households-are-interested-in-home-energy-monitoring-7.

 ISBN: 978-1-61208-136-6

Upgrading a Medium Size Enterprise Power System with Wind and Solar Sources: Design, Financial and Environmental Perspectives

Thair S MAHMOUD, Daryoush HABIBI, Octavian BASS
School of Engineering
Edith Cowan University
Joondalup, Australia
E-mail: {t.mahmoud, d.habibi, o.bass}@ecu.edu.au

***Abstract*—Efficient generation and distribution are crucial for economic power production. In this paper we discuss the planning and design of upgrading a medium size enterprise power system by installing Distributed Energy Resources (DERs), with particular emphasis on economic viability and environmental benefits. The planning for this project considers both conventional grid and $SmartGrid$ connections. Project planning, installation challenges and governmental support of renewable energy projects in Australia are discussed. It is found that upgrading a medium size enterprise power system with DERs can yield reasonable levels of energy cost savings and greenhouse gas mitigation with both conventional grid and $SmartGrid$ connections, but that $SmartGrid$ connection can deliver better outcomes.**

***Index Terms*—medium size enterprise power systems, solar and wind energies integration with smartgrid, economic and environmental analyses of energy projects**

I. INTRODUCTION

Concerns over catastrophic climate change, increased industrialisation, CO_2 emissions and fuel price rises are creating incentives for reliable, safe and environment-friendly energy sources. To help achieve a clean and secure electric power industry, the current power grid has been modernised to accept a range of renewable energy sources [1]. These are expected to become more competitive with conventional generators. As a part of the international trend towards restructuring electricity grids, many developed countries are establishing new investment support policies. They are also developing legislation for commercializing "Green Energy". As new clean-energy markets have been emerging around the world, opportunities exist for economic development, jobs creation and energy diversification benefits [2]. Thus, there is a need to develop efficient clean-energy regulations to direct companies, so that socio-economic benefits are maximised [3]. Regulators are initiating new programs for energy efficiency, renewable energy capacity generation, and reliability improvements [4]. Liberalizing power markets will also become more important because of the advantages of pooling large generation stations, sharing spinning reserves and using the most efficient energy resources [5].

The Australian Government has initiated major funding support plans to promote commercialization of renewable energy [6]. Australia is considered one of the most favourable nations for investment in energy resource development because of low political and regulatory risks [7]. Foreign investment is welcomed by the Australian Government and no mandatory local equity or local content requirements are imposed on energy resources development [8]. The Office of the Renewable Energy Regulator (ORER) in Australia administers the Renewable Energy (Electricity) Act 2000 (the Act), the Renewable Energy (Electricity) Charge Act 2000, the Renewable Energy (Electricity) (Small-scale Technology Shortfall Charge) Act 2010 and the Renewable Energy (Electricity) Regulations 2001 (the regulations) to increase renewable electricity generation from Australia's renewable energy sources by encouraging the generation of an additional 45,000 GWh of renewable energy per year by 2020 [9]. The Australian Government has established the Renewable Energy Target (RET) scheme to ensure that 20 per cent of Australia's electricity supply will come from renewable sources by 2020. The plan is to make the amount of energy coming from sources like solar, wind, wave and geothermal sources be around the same as all of Australia's current household electricity use [10].

The Australian Government has assisted consumers with the cost of installing solar panels on Australian homes and connecting them to the utility grid for energy commercialisation purposes $(SmartGrid)$ [6]. Although photovoltaic cells are still too expensive to compete effectively with the conventional power generators, the solar-cell market in Australia is expanding rapidly. Australia has a long history of using wind power for pumping water, and now it is been used widely for renewable power generation. Solar and wind systems are appropriate in Australia because of environmental concerns with conventional energy generation, usually based on burning coal, and a reluctance to adopt nuclear power or build more hydro electricity dams [11]. Solar and wind energies are popular because they are widely distributed, climate-benign, and have clean-attributes that no other major energy source can currently match. This paper is investigating the economic and environmental impacts of integrating solar and wind energies to upgrade medium size enterprise power systems for current grid and smartgrid connections.

 ISBN: 978-1-61208-136-6

II. Government schemes for emissions reduction and promotion of renewable energy source uptake

The Australian Government has taken on responsibility for reducing the carbon pollution in all its states and territories. Its main target is reducing Australian's carbon footprint by nearly one third to one half. They have also started to develop new policies and rules which are needed to help Australian businesses and households to reduce their carbon pollution [12].

A. Emissions reduction and investing in clean energies

Given that Australia has a very large ecological footprint, which is dominated by carbon dioxide emissions from fossil funds, it is appropriate that Australia to be very active in responding to climate change. This indicates major research and initiative project funding for energy balance and emissions reduction, for example the Low Emission Technology Demonstration Fund (LETDF) to support the Australian firms to commercialize low emissions technologies [13]. Carbon Pollution Reduction Scheme (CPRS) would introduce a price on carbon pollution and ensure that all businesses take this into account when they developing their business plan. Concurrently, the Australian Government is developing, commercialising, and investing on clean energy technologies [12]. These will be crucial for Australia's efforts to reduce its carbon pollution emissions. These technologies will also be important to the rest of the world as they also need to reduce their carbon pollution. Australia's RET goal will be met from renewable sources such as wind, solar and geothermal power by 2020. The Initiative will create more jobs in clean industries by giving investors the confidence to back low emissions technologies such as solar power, energy from 'hot rocks' in the earth's crust, and carbon capture and storage.

B. *SmartGrid* in Australia

In the state of New South Wales, the city of Newcastle is currently starting the first commercial-scale *SmartGrid* project. The governmental initiatives for such projects will help Australians save energy, commercialize renewable energy grid connection and tackle climate change. The aim is to optimise energy participation from local generation to the public grid. *SmartGrid* will involve soft computing and distributed control systems implementation to perform demand prediction, smart renewable energy participation and distribution generation management. New market schemes and economic energy generation can be performed from applying smart infrastructure on the energy grid. It is a substantial foundation for developing smart energy markets, and it allows public, private and business sectors to interconnect the small scale, on-site generators e.g., diesel and renewable energy resources, to participate in these markets.

III. Planning for Project Development

A main problem for project development is the availability of installation space. A sufficient share for renewable energy supply requires a high number of generation units located within new or existing facilities or at more remote installation sites. There is still an alternative solution for solving installation space problem, which is increasing utility grid share in such a way, it fits with utilizing all the available space in the project land, then supplying the rest from utility grid. *SmartGrid* connection is another planning consideration. Since *SmartGrid* is a foundation for commercializing energy suppliers, it will be a key solution for solving the installation space problem. *SmartGrid* will allow the private sector to feed energy into the public grid. The energy consumers will be able to get the energy back from the *SmartGrid* from different substations in different locations covered by *SmartGrid* connection. Selling and buying energy to and from the grid from different locations will add other expenses, which will be economically analysed and added to the project cost as it is explained in the Economic Analyses section in this paper. Figure 1shows the proposed planning strategy for adding renewable energy sources to an existing microgrid.

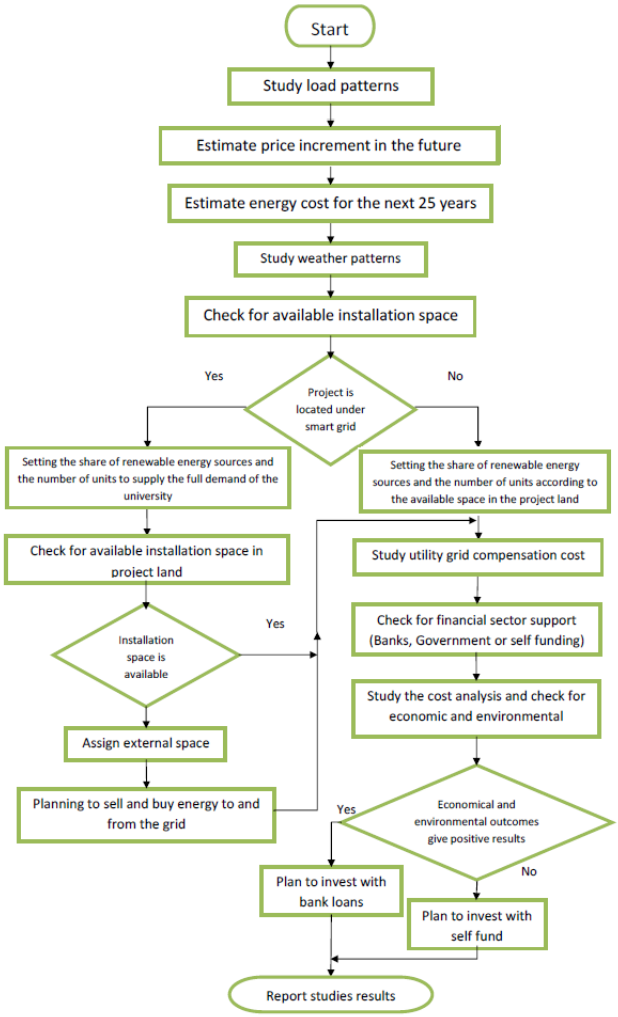

Figure 1. Project developement planning flowchart

IV. A CASE STUDY

As a case study, ECU's Microgrid at its Joondalup campus was selected for project development planning. The average climate from minimum to maximum values and safety considerations are considered in the studies. The city of Joondalup is located in one of the worlds five Mediterranean climate zones.

The geographical information for this city:
Country: Australia
State: Western Australia
City: Joondalup
Latitude: 31.44 °S
Longitude: 115.45 °E
Elevation / Altitude: 25 m
Average solar irradiation: 5.35 kWh/m²/day
Average wind speed: 12.24 km/h

The above details are helpful in detailing the installation challenges and solutions with solar panels and wind turbines. For maximum output, solar-electric (photovoltaic; PV) modules or solar thermal collectors need to be located where they receive the most sunshine. Ideally, hills, trees, buildings, or other obstructions should not shade a system site at any time during the year, so identifying the best place is complex.

Based on the university's energy demand readings, the highest amount of demand per hour occurs on summer's afternoons, reaching 1704 kWh, while the lowest energy occurs on winter nights or holidays, (284 kWh). To cover the demand in the university, a specific number of solar panels and wind turbines are needed. As the highest demands are always during the day time, more emphasis would be placed on solar panels rather than wind turbines.

A. Solar panel installation

According to the provided information about the climate in the city of Joondalup and generation efficiency of different brands of solar panel, generation outcomes were estimated. For best generation outcomes, the installation angles of the solar panel have to be adjusted according to the location of the project, and the angle of the sun during winter and summer seasons. To optimize the installation of solar panel in the city of Joondalup, the angle is adjusted to 23^o, facing north, (Fig 2).

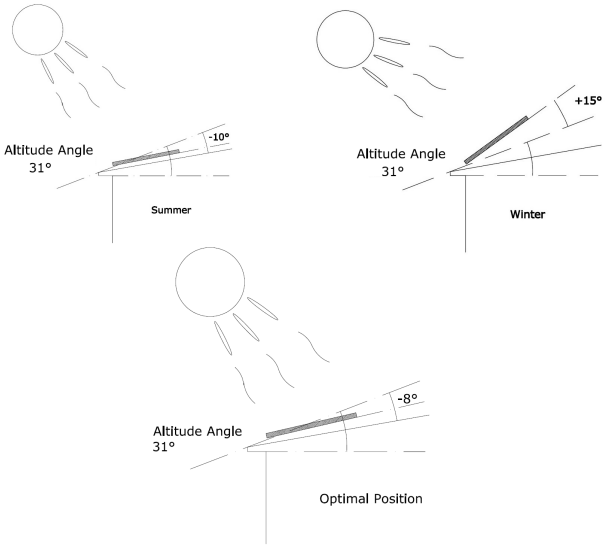

Figure 2. Summer, Winter and Optimal Angles for Solar Panel Installation

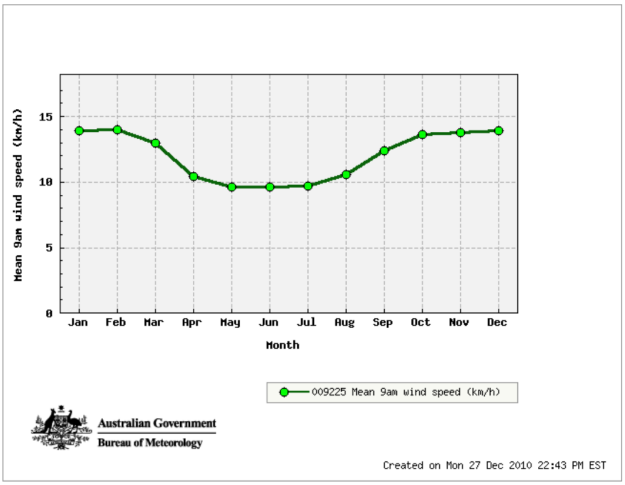

Figure 3. Average Monthly Wind Speed in the City of Perth

From the installation and sun angle challenges, the average lost generation for solar panel was estimated to be about 10% of the overall annual generation capacity. For the selected solar panel unit, the average daily solar panel output is estimated at 936 Wh, while the monthly average of minimum and maximum daily solar panel output is 439 and 1447 Wh respectively. The average annual solar panel output is 341 kWh. For 25 years, the total solar panel output will be about 8.525 MWh. Based on these calculations, this unit is considered appropriate for ECU's microgrid energy supply.

B. Wind turbine installation

In wind energy, useful energy contribution (work) is calculated by summing the amount of generated power over time taking into account variation in wind and operational conditions. The relationship between the size of the wind turbine and the generation outcomes may vary depending on the threshold point for wind speed and the amount of available wind speed annually. From the climate study results, it has been shown that wind speed drops to zero regularly from midnight till sunrise. The average wind speed is 12.24 km/h while minimum and maximum (monthly average) wind speeds are 9.36 km/h and 15.84 km/h respectively. The minimum wind speed to activate generation in the nominated unit is 9 km/h. For a secure power supply design, utility supply will cover the missing hours of generation availability for solar panels and wind turbines. The wind speed readings were collected from City of Perth station, which is located about 20 km south from the project location.

As a conservative estimation, the average monthly 9 am wind speed for the city of Perth since 1993 is illustrated in Fig. 3.

From the climate study, the safe estimated average of

 ISBN: 978-1-61208-136-6

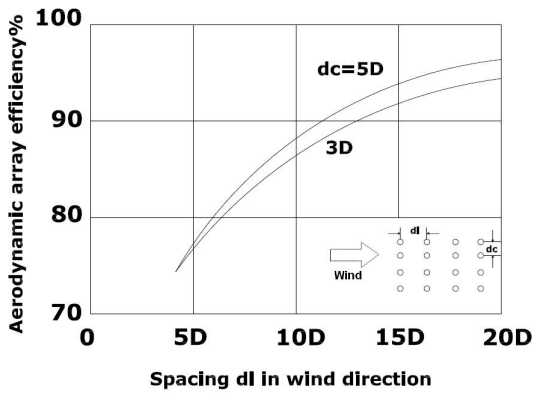

Figure 4. Aerodynamic array efficiency as a function of rotor distance in the wind direction [14], whre D is the wind turbine rotor diameter, dl is the space length between the two installed wind turbines in project land, and dc is the space width between the two installed wind turbines in project land.

missing wind generation hours varied between 20 hours in winter season and zero hours per day in summer season. For wind turbine, the technical layout and design of wind park installations are important. When installing several wind turbine concentrated in an array, the major challenge which arises is the spacing. The relationship between rotor distance and aerodynamic array efficiency is illustrated in Figure 4. A minimum clearance between the wind turbines must be guaranteed, otherwise power losses will be so high that the wind park will operate uneconomically.

This influences the required space needed for this project at Joondalup, where space can be limiting. However, for the $SmartGrid$ connection, an off-campus location is used and land cost becomes a factor.

V. Economic Analyses

Economic analyses for installing DERs for this project were conducted for conventional grid and $SmartGrid$ connections.

A. Conventional grid connection

For this project, a satellite image for the project's land has been added to identify available installation space. For this project, it has been found that the available installation space for the wind turbine is 17000 m² as shown in Figure 5. Adding to that, sufficient installation space has been allocated for solar panel installation.

From the climate study, and the characteristics of the project land, it has been estimated that solar panels and wind turbines can share the supply of 37% of the full electricity demand in the university. The 37% generation is set to be 85% from solar panels and 15% for wind turbines. Figure 6 is showing the assigned energy supply shares of the installed DERs.

From the current 2,000 kWh maximum daily demand, and the assigned 85% of the solar panel participation in the 37% share of DERs supply to the project, 735 kWh is required to be generated from solar panels. This can be obtained by

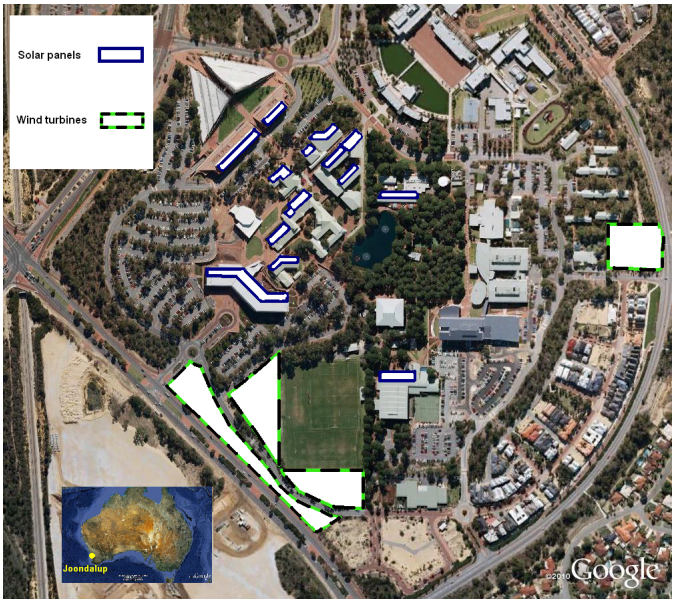

Figure 5. Satellite Image for the project plan

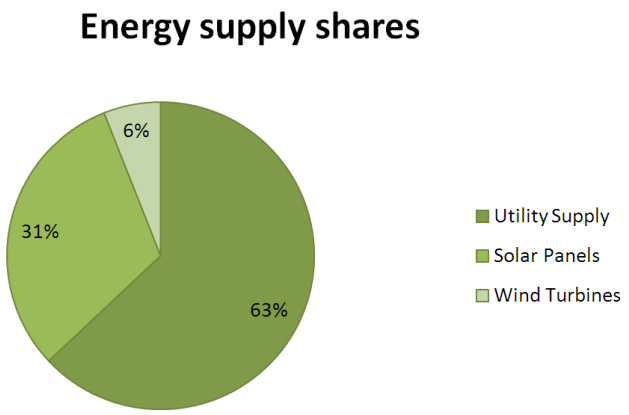

Figure 6. Proposed energy supply shares for ECU power system for the conventional grid connection

installing 3964 units of the in-market selected units "*Sharp NUS5E3E 185 W mono*". Each single unit required 1318 x 994 x 46 mm for installation space. Thus, for the needed number of solar panels, 5193.2 m² is required. For Wind turbine, the nominated generation unit is "WinPower 48V DC/240V 2000Watt", which has a 4 m rotor diameter. The required installation space is 300 m² for each wind turbine, allowing for the 56 wind turbines for this project. So, for both solar panel and wind turbine installation area, about 21,193 m² will meet the required installation space.

Other calculation assumptions for the missing generation hours due to clouds and low speed wind have to be considered under generation capacity for the installed renewable energy sources. The average calculated missing hours of generation are summarised in Table I.

These have to be compensated by utility grid supply and Tables II and III show the amount of non operating hours and the energy compensation needed from the utility grid

Energy Source\Time mode	Day time (8:00-17:00)	Night time (17:00-800)	Total missing hours
Wind turbine	3 hours	7 hours	10 hours
Solar panel	2 hours	13 hours	15 hours

Table I
THE DAILY AVERAGE OF MISSING GENERATION HOURS

Time mode\parameters	Daily consumption	Assigned share	Missing operation	Utility compensation
Day time (8:00-17:00)	12311 kW	3816 kW	2 hours	848 kW
Night time (17:00-8:00)	7566 kW	2346 kW	13 hours	2033 kW

Table II
CONVENTIONAL GRID SOLAR PANEL MISSING OPERATING HOURS AND UTILITY COMPENSATION

Time mode\parameters	Daily consumption	Assigned share	Missing operation	Utility compensation
Day time (8:00-17:00)	12311 kW	739 kW	3 hours	246 kW
Night time (17:00-8:00)	7566 kW	454 kW	7 hours	212 kW

Table III
CONVENTIONAL GRID WIND TURBINE MISSING OPERATING HOURS AND UTILITY COMPENSATION

under conventional grid connection. The average total daily utility compensation is 3,125 kW. Since the total annual energy consumption is 6,082,854 kW, the average daily consumption is about 16,666 kWh. Thus, the average daily utility compensation for the non-operating hours is 18.1% adding to that the actual 63% utility supply for the university. Then, the actual utility for the project will be 81.5% and the renewable energy participation will be 19% of the total needed generation. Table IV shows the details of the missing operation hours of the installed solar panels and wind turbines.

Additional weather studies have been applied to show the generation outcomes and the amount of non-operating hours shares. Figure 7 shows the shares of the proposed number of generation units and the non operating hours for renewable energy sources under conventional grid connection.

Time mode\Generation unit	Solar panel	Wind turbine	Total
Day time	734 kW	195 kW	929 kW
Night time	2029 kW	167 kW	2196 kW
Total	2763 kW	362 kW	3125 kW

Table IV
AMOUNT OF NON-OPERATING HOURS ENERGY

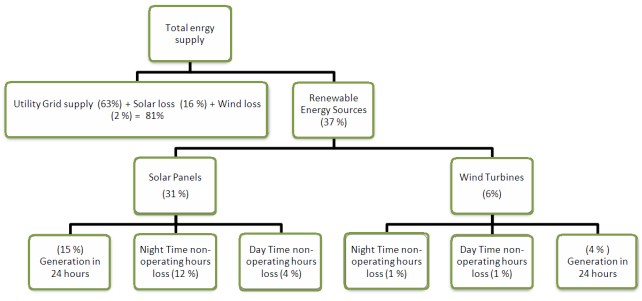

Figure 7. Energy supply shares for the proposed project under conventional grid connection

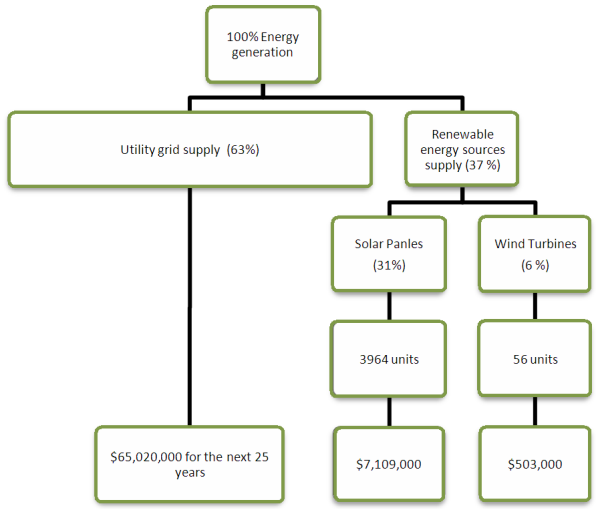

Figure 8. The distribution of generation shares for utility and renewable sources under conventional grid connection

Generation unit\details	Capital costs	Operating costs	Total
Solar panel	$3,554,559	$3,554,559	$7,109,118
Wind turbine	$251,563	$251,563	$503,126
Total	$3,806,122	$3,806,122	$7,612,244

Table V
CONVENTIONAL GRID CONNECTION RENEWABLE ENERGY SOURCES INSTALLATION COST[14]

For solar panel, the estimated generation price for 25 years from this unit was found to be between 0.0288-0.0354 $/kWH according to "$SharpNUS5E3E185Wmono$". For wind turbine, the equivalent is about 0.07$/kWh generation price over 25 years. The utility energy prices may increase for the next 3 years by 10% and may increase by another 90% by the next 25 years. The estimated cost that ECU is currently paying is about $2,140,594 a year. Thus, for the next 25 years with energy price increment, it is expected that ECU is willing to pay about $80,272,000 over 25 years if all assumptions are realised. For these calculations, load expansion will not be considered for generation capacity installation.

From the calculations of the renewable energy generation shares, it is expected that ECU will have to pay $65,020,000 in the next 25 years. Figure 8 shows the proposed generation shares of the renewable energy sources and utility grid supply for the proposed project.

Thus, the total generated energy by solar panels and wind turbines for this project will cost $7,612,244 for the next 25 years. The total cost savings will be $7,639,494. Table V details the estimated cost of installing and operating the DERs for the investigated project.

Note that, capital costs include the modules costs, while the

 ISBN: 978-1-61208-136-6

Generation unit\details	Capital costs	Operating costs	Total
Solar panel	$7,568,000	$7,568,000	$15,136,000
Wind turbines	$1,349,000	$1,349,000	$2,698,947
Total	$8,917,00	$8,917,00	$17,834,000

Table VI
$SmartGrid$ CONNECTION RENEWABLE ENERGY SOURCES INSTALLATION COST[14]

operating costs include converters, installation, maintenance, engineering consultation and insurance costs. Investigating the financial support from the finance sectors, the Australian Government promotes funding one third of the project budget, which will save about $2,537,414. The current loan rates are 7.1% for fixed annual interest. For the specified project, that all funding is borrowed except for Australian Government funding support, ECU will need to invest about $5,074,828 on this project. To refund this amount after 25 years, it required to pay extra $5,762,724 according to current Australian banks loan rates. Figure 11

From the above calculations , it has been conducted that: from the economic analyses point of view, this project will save about $4,414,189 including the $2,537,414 of Australian Government support. These calculations were to evaluate the investment values in 25 years time in case of loan funded scenario. In case of self funded scenario, the project will save about $10,176,910 including the Australian Government funding support, ignoring the opportunity costs for other uses of ECU funds.

B. $SmartGrid$ connection

Future $SmartGrid$ will have fair solutions for installation area problems. For this case study, this project can be implemented on a remote area covered by $SmartGrid$ power lines. $SmartGrid$ will allow private sectors to feed-in the energy to the public grid. The energy consumers will be able to have the energy back from the grid to supply their loads from wherever it is covered by $SmartGrid$. The difference in prices for selling and buying to and from the grid from different locations will be added to the project cost. Since installation space problem can be solved by $SmartGrid$, the full capacity generation will be supplied by renewable energy sources for the specified project rather than having a nett reliance on the utility grid supply. Thus, it is assigned to have the 2,000kWh from the renewable energy sources (70% for solar panel and 30% for wind turbine).

Due to missing operation hours of the renewable energy sources as shown in table I, utility grid compensation is considered under economic analyses to compensate for the missing operation hours. From the current 2,000 kWh maximum daily demand and the 70% solar panel with 30% of wind turbine generation share, it is required to install 7568 units of the above nominated solar panel type and 300 units of the nominated wind turbine type (Figure 9).

Table VIillustrates the renewable energy source installation costs for the $SmartGrid$ connection case.

Figure 10 shows the proposed energy supply shares and the non operating hours for the assigned renewable energy sources.

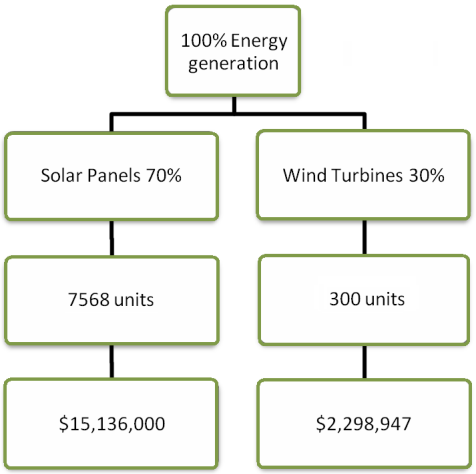

Figure 9. The distribution of generation shares for utility and renewable sources under $SmartGrid$ connection

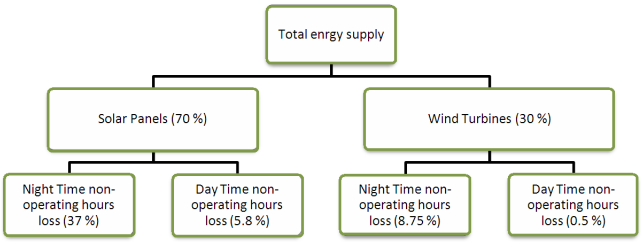

Figure 10. Energy supply shares for the proposed project under $SmartGrid$ connection

Table VII and VIII show the non operating hours details and the amount of energy to be compensated from the utility grid for $SmartGrid$ connection case. From tables VII and VIII it has been estimated that the estimated utility grid compensation for the missing operating hours of renewable energy sources is about: 7728 kW per day (24 hours). The utility compensation price for the 25 years is expected to be: $21,155,400. Thus, price difference of selling and buying to and from the grid, may cost an extra $11,085,962. The needed installation space for this project may cost $7, 500, 000 as well assuming that this location will have the same climate characteristics as those estimated for Joondalup, according to current Australian land prices. The total project cost may reach to $64,518,551 including the Australian Government support in case of fully loaned project. Thus, the project may save up to $15,753,751 in case of fully loan funded project, while it may save up to $32,277,190 including the Australian Government support a self funded project, ignoring the opportunity for cost associated with alternative uses of ECU's funds.

Time mode\parameters	Daily consumption	Assigned share	Missing operation	Utility compensation
Day time (8:00-17:00)	12311 kW	8618 kW	2 hours	1915 kW
Night time (17:00-8:00)	7566 kW	5296 kW	13 hours	4590 kW

Table VII
$Smartgrid$ SOLAR PANELS MISSING OPERATING HOURS AND UTILITY COMPENSATION

 ISBN: 978-1-61208-136-6

Time mode\parameters	Daily consumption	Assigned share	Missing operation	Utility compensation
Day time (8:00-17:00)	12311 kW	3693 kW	3 hours	1231 kW
Night time (17:00-8:00)	7566 kW	2270 kW	7 hours	1059 kW

Table VIII
$Smartgrid$ WIND TURBINE MISSING OPERATING HOURS AND UTILITY COMPENSATION

Generation unit\Values	Daily generation	CO_2emission/MWh	CO_2mitigation/MWh
Wind turbine	579 kW	9 kg (21.7 lb)	242.86 kg (555.84 lb)
Solar panel	2567 kW	282 kg (623.7 lb)	1834.64 (1840.62 lb)
Total	3146 kW	291 kg (645.5 lb)	2077.5 kg (2396.46 lb)

Table IX
THE AMOUNT OF MITIGATED CO_2 BY RENEWABLE ENERGY SOURCES UNDER CONVENTIONAL GRID CONNECTION

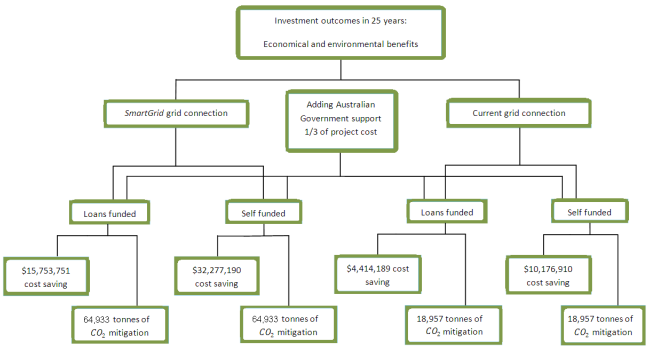

Figure 11. Investment economic and environmental benefits

VI. ENVIRONMENTAL ANALYSES

Solar panels are generating power with no noise and very low rate of emissions including those involved in manufacturing, transporting and installing the panels. The main environmental effects caused by wind turbine generation are: audible sound, infrasonic sound, disco effect, shadow impact, ice throw, visual interference with natural scenery, harm to bird-life, effects on other fauna, space consumption, offshore utilisation and social acceptance [15]. However, photovoltaic power plants emit 110 kg (243 lb) CO_2/MWh, while wind turbine plants are emitting 17 kg (37.5 lb) CO_2/MWh. By comparison: modern gas and steam turbine power plants emit 435 kg (960 lb) CO_2/MWh, while coal-fired power plants to emit 900 kg (1980 lb) CO_2/MWh [15]. From this project, tables IX and X show the amount of daily generation and CO_2 mitigation by solar panels and wind turbines for conventional grid and $Smartgrid$ connections.

Evaluating the importance of this project for the next 25 years, it is expected that this project will save 18,957 tonnes of CO_2 emission for conventional grid connection, and 64,933 tonnes of CO_2 for $SmartGrid$ connection. This average value is based on CO_2 release from modern gas and steam turbine and coal-fired power plants. Figure 11 provides the estimated investment benefits for this project under self funded and loan funded cases for conventional grid and $SmartGrid$ connection.

VII. CONCLUSIONS

Upgrading ECU's power grid with DERs installation has been described and costed this paper. There are great challenges in installing the estimated amount of DERs in terms of allocating suitable installation space and investigating the non operating hours of DERs based on the weather patterns at the project location. Economic and environmental impacts were investigated for this problem in this paper. The economic analyses have shown that the project may achieve different amount of profits including the Australian Government fund support under different connection modes: conventional grid or $SmartGrid$, and may vary according to the sponsored fund from financial sectors. The calculations showed that for best economic and environmental benefits, it is more beneficial to implement this project with $SmartGrid$ connection. From these calculated results, it is noticed that it is encouraging to invest on upgrading medium size enterprise power system projects with these friendly conditions.

Generation unit\Values	Daily generation	CO_2emission/MWh	CO_2mitigation/MWh
Wind turbine	3673 kW	63 kg (21.7 lb)	2390 kg (555.84 lb)
Solar panel	8476 kW	933 kg (623.7 lb)	4726 kg (1840.62 lb)
Total	12149 kW	996 kg (645.5 lb)	7116 kg (2396.46 lb)

Table X
THE AMOUNT OF MITIGATED CO_2 BY RENEWABLE ENERGY SOURCES UNDER $SmartGrid$ CONNECTION

REFERENCES

[1] B. Roberts, "Capturing grid power," *Power and Energy Magazine, IEEE*, vol. 7, no. 4, pp. 32–41, 2009.
[2] C. W. Joel Makower, Ron Pernick, "Clean energy trends 2009," *available on http://www.cleanedge.com/reports*.
[3] S. Honkapuro, "Business impacts and incentives of regulation for dsos and smart grids," in *Electricity Distribution - Part 2, 2009. CIRED 2009. The 20th International Conference and Exhibition on*, pp. 1–10, 2009.
[4] D. Novosel, "Emerging technologies in support of smart grids," in *Power and Energy Society General Meeting - Conversion and Delivery of Electrical Energy in the 21st Century, 2008 IEEE*, pp. 1–2, 2008.
[5] D. R. C. U. M. W. W. Breuer, D. Povh, "Prospects of smart grid technologies for a sustainable and secure power supply," tech. rep., World Energy Council, 2007.
[6] Australian-Governmentl, "Smart grid, smart city," *available on http://www.climatechange.gov.au/government/programs-and-rebates/smartgrid.aspx*.
[7] O. of-the Renewable-Energy-Regulator, "Legislation," *available on http://www.orer.gov.au/legislation/index.html*.
[8] Australian-Government, "Securing australia's energy future," *available on http://www.efa.com.au/Library/CthEnergyWhitePaper.pdf*.
[9] D. of-Climate-Change-and Energy-Efficiency, "Renewable energy target," *available on http://www.climatechange.gov.au/government/initiatives/renewable-target.aspx*.
[10] WAtoday, "renewable-energy-tariffs-announced," *available on http://www.watoday.com.au/wa-news/renewable-energy-tariffs-announced-20100527-wgnn.html*.
[11] P. Hu, R. Karki, and R. Billinton, "Reliability evaluation of generating systems containing wind power and energy storage," *Generation, Transmission and Distribution, IET*, vol. 3, no. 8, pp. 783–791, 2009.
[12] Australian-Government, "Reducing australia's emission," *available on http://www.climatechange.gov.au/government/reduce.aspx*.
[13] D. of-Resources-Energy-and Tourism, "Low emissions technology demonstration fund," *available on http://www.ret.gov.au/energy*.
[14] E. Hau, *Wind Turbines: Fundamentals, Technologies, Application, Economics*. Berlin: Springer, 2006.
[15] A. S.-A. W. Martin Kaltschmitt, Wolfgang Streicher, "Renewable energy: Technology, economics and environment," 2007.

A Review of Energy Efficiency Initiatives in Post-Secondary Educational Institutes

David F. Motta Cabrera
University of Calgary
Calgary, Canada
Email: dfmottac@ucalgary.ca

Hamidreza Zareipour
University of Calgary
Calgary, Canada
Email: h.zareipour@ucalgary.ca

***Abstract*—In this paper, a review of the steps taken by some of the higher educational institutes around the world to increase their energy efficiency is presented. The paper also provided an overview of the state-of-the-art in managing energy consumption in computers. With the growing number of computers being employed in higher educational institutes, this paper discuses and present an example on how power management in computer labs and IT centres can help educational institutes improve their energy efficiency and carbon footprint.**

***Index Terms*—Energy efficiency, computer power management, educational institutes.**

I. Introduction

The warming of the climate system is one the first main challenges of the twenty-first century. It has been argued that most of the observed increase in global average temperatures since the mid twentieth century is very likely due to the observed increase in anthropogenic greenhouse gas concentrations [1]. Thus, rising up to the challenge of climate change demands an effort from society to reduce greenhouse gasses (GHG) emissions using new ideas and tools to achieve sustainable development.

Universities constitute a suitable target for environmentally friendly initiatives. Universities and colleges are usually attended by young people who consider environmental issues important to their lives [2] and are ready to accept changes. Due to the rising utility costs that dwarf the annual rate of inflation, post secondary education institutions are open to new sustainability programs that tackle the ever-escalating energy expenses [3]. The size of the potential target audience also is an important reason for focusing in such educational institutions. In Canada and the United States alone, there were approximately 20 million students enrolled in 2007 [4] [5]. This is roughly the equivalent to the population of the whole Scandinavian Peninsula as of 2010 [6]. One way to reduce global GHG emissions is improving energy efficiency of small and extremely ubiquitous office equipment, such as computers, as the number of personal computers is expected to reach 2 billion by 2014 [7]. A significant portion of those billions of computers is located in post secondary educational institutes. Assuming that there is 1 computer per 10 students, as it is the case at the University of Calgary, Canada, there will be more than 2 million energy-hungry computers in North American universities and colleges alone. On average, and when kept on for the whole year, a desktop computer with a LCD monitor uses approximately 475 kWh a year [8]. Two million computers will consume approximately 950 MWh a year, producing close to 665,000 metric tons of CO2 [9]; this is roughly the same amount of CO2 emissions from 130,000 typical passenger vehicles [10]. Even a reduction of only 10% will have the same impact as taking 13,000 vehicles off the streets. Thus, there is a significant potential untapped for reducing GHG by improving current usage strategies of computers in higher education institutes.

In the present paper, efforts on improving carbon footprint of higher educational institutes are reviewed. The review is focused mainly on what universities are doing to increase the efficiency of buildings. This paper also reviews the approaches to reduce energy consumption including behaviour-oriented energy conservation programs, student-led initiatives and various retrofits to increase energy efficiency in university buildings. This paper also discusses a power management-based strategy for saving energy consumed by computers in post-secondary educational institutions. The results of preliminary ad hoc power management schemes provide incentive for using data mining and artificial intelligence-based strategies for power management in universities' computers.

The remainder of this paper is organized as follows: in Section II literature on energy approaches in higher educational institutes is reviewed, including approaches to reducing energy consumption such as behaviour-oriented energy conservation programs, student-led initiatives and various retrofits to increase energy efficiency in university buildings. Section III includes a review on available literature on computer-related energy consumption as well as studies on the impact of power management schemes in computers. Section IV presents the current state of affairs in the University of Calgary's computer labs as well as some preliminary results on estimated savings using power management. Section V includes the conclusions of the paper.

II. Energy efficiency improvements in higher education institutes

Universities across the world are being faced with highly increasing utility costs, which serve as a motivation for boosting up their efforts to save money. Currently, those efforts are headed towards developing new sustainability programs

 ISBN: 978-1-61208-136-6

to tackle the escalating energy expenses; however the goal of these projects is not only the containment of utility costs but also a reduction of the environmental footprint [11] [12] as can be inferred from the signing of the "President's Climate Commitment" by over 600 US college and university presidents [13].

The continuously growing energy budgets are forcing many university presidents to make hard decisions on how to keep the institution financially afloat. Options include cutbacks in building maintenance and postponing the building of new classrooms and laboratories, as well as postponing the update of existing facilities [14]. Fortunately, there are other approaches making their headways across universities. If an institution wants to reduce utility expenses, it can do so by adhering to LEED standards, establishing programs to reduce transportation cost, promoting energy conservation schemes among staff members, faculty members and students and also making sure that any new building is energy efficient.

Designing and constructing energy efficient buildings have the potential to reduce or eliminate negative environmental impacts. Once the building is constructed, operating costs are reduced, worker productivity and comfort are increased, all of which result in an enhancement of the building marketability [15]. All of these propositions mean that the construction of an energy efficient building has environmental, economic and social benefits for building owners, occupants and the general population.

Sustainability involves improving the environmental, economic and social impacts of resource use. The most common target when developing a strategy to fight climate change is the reduction of greenhouse gas (GHG) emissions. This requires much more than just technological change; it demands behavioural change and adaption from the community and long-term commitment.

Any university aiming to reduce GHG emission must take into account the fact that a behaviour-oriented energy conservation program, in addition to various system upgrades is essential to a comprehensive energy reduction effort. Any kind of measure is insufficient to reduce energy consumption by itself if the building's occupants are not actively engaged in the process [16].

One of the universities to implement such behaviour-oriented energy conservation programs is the University of Michigan (UM), an institution encompassing over 200 buildings, with over 41,000 students and 20,000 faculty and staff members. Since the late 1980s, UM has made efforts to reduce rising energy costs focusing on building modifications and retrofitting measures. In 2006, UM officially decided that it was necessary to go beyond the technological approach of the last 25 years. A pilot study was planned and conducted to examine the behavioural aspects of energy consumption among faculty, staff and students. The purpose of the study was to determine energy consuming practices and attitudes on campus and thus help university administrators to establish more effective policies [14]. The findings of the pilot study at the UM showed that a significant proportion of the faculty, staff and students were unaware of UM efforts to reduce energy consumption on campus. These poor results concluded that UM should launch a publicity campaign aimed letting everyone know of the concerted efforts of the university to reduce energy consumption in buildings by establishing clear energy reduction targets. Finally, the pilot study led to a more comprehensive understanding of how attitudes may affect energy conservation behaviour at a large educational institution and can also serve as a model for using behavioural research into energy consumption reducing efforts in universities around the globe.

In the fiscal year 2005/2006, the University of Calgary (UofC), emitted 214,733 metric tones of CO2 caused by its buildings operations. By identifying the best options in energy supply, energy conversion and distribution, and by using state of the art technology for energy sustainability for buildings, the UofC planned to have reduced 15% in utility budget costs by March 2009 [17]. Since 1995, the Energy Performance Initiative has been responsible for the use of lighting controls, variable air conditioning, occupant awareness dashboards and lighting retrofits. These upgrades resulted in the reduction of 8,100 metric tones of CO2 per year over the past 14 years. The medium term objective of this project is to meet the Kyoto Protocol target of reducing gas emissions 6% below 1990 levels and also to achieve LEED accreditation. The backbone of this project is the implementation of a cogeneration plant, which produces electrical power and thermal energy from a single energy source: in this case, natural gas. This would result in an increase of gas consumption by 20%, being the extra fuel required to run the turbine engine, and the reduction of electrical energy purchases by 50%. Although the UofC is among the top universities in Canada implementing sustainability measures, more emphasis must be placed on bringing the community together to work for this project. This should not be a project just for professors and students, but also for staff and even visitors, because all the efforts might lead to a poor results if there is no sufficient cooperation between the 40,000 people that currently work, live and study and the UofC.

The University of British Columbia (UBC), Vancouver, Canada, implemented the three-year project ECOTrek from 2003 to 2006. The main objective was to reduce energy consumption, water use and GHG emissions by retrofitting 300 academic buildings. The project resulted in reductions in energy consumption of 20%, water use reduction of 30%, a reduction of 15% in GHG emission and savings of 2.6 million dollars annually [18]. These results were achieved by using a Building Management System to automate 90% of the academic campus HVAC systems, to match performance to the exact occupancy of any given building. However, more work still must be done to show people what the university is doing and what they can do to help.

At the Polytechnic University of Catalonia (UPC), in Spain, a plan for sustainability in 2015 was drafted to achieve a change in mentality and behaviour of the academic community. This means putting more effort in social commitment

 ISBN: 978-1-61208-136-6

TABLE I
SOME OF INSTITUTIONS OF HIGHER EDUCATION IN THE USA WITH GREENHOUSE REDUCTION TARGETS

Institution	Commitment	Date of Commitment
Bowdoin College	11% below 2002 levels by 2010	January 2006
College of the Atlantic	Zero emission, effective immediately	October 2006
Cornell University	7% below 1990 levels by 2008	April 2001
Michigan State University	6% below 1998-2001 baseline by 2010	November 2006
Tufts University	7% below 1990 levels by 2012	April 1999
UNC at Chapel Hill	10% below 2005 levels by 2015; 20% by 2030	June 2006
Williams College	10% below 1990-91 levels by 2020	January 2007
Yale University	10% below 1990 levels by 2020	October 2005

Source: Association for the Advancement of Sustainability in Higher Education [20], [21]

to reduce UPC's carbon footprint instead of achieving high amounts of resources to retrofit a large number of buildings. The plan also includes the effort to secure money for research to identify the main factors that determine the inefficient consumption of energy in campus[19]. The UPS's Plan puts more focus on people instead of technology, which is a different paradigm from that of the aforementioned universities. Although there are no clear results of this plan yet, it will be interesting to follow because it might give a hint on what more can be done without spending millions of dollars on new technology.

Another adopter of a GHG reduction policy is Yale University, in the United States, which in 2003 set a goal of reducing its GHG emissions by 10% below 1990 levels by 2020. Yale's intention is to avoid falling into the trap of overreaching system modifications and instead focus on specific projects with a smaller number of participants and a less ambitious set of goals, which is often more successful [22]. In order to have a successful strategy to attain sustainability goals, Yale's GHG reduction target is part of a five step process: development of a vision, development of quantifiable goals, leadership endorsement, implementation and an institutional evolution towards a sustainable campus. Yale has identified that almost 90% of its GHG emissions come from purchased electricity and the two on-campus power plants, and plans to reduce these emissions by focusing on efficiency upgrades and renewable energy projects, instead of purchasing carbon offsets [20]. As of 2008, Yale had reduced is GHG emissions by 7% below 2005 levels, and has achieved LEED accreditation in 10 buildings. Although the project in Yale looks promising; it seems to rely too heavily on technology instead of people involvement in a project, which is something critical for any successful sustainability project.

The University of New Hampshire (UNH), in the United States, is among the pioneers in reducing energy consumption in educational institutes in America. For more than 35 years it has cultivated a sustainability outlook in its students integrating sustainability into the spirit of an institution of higher learning in order to cultivate a critical and creative global sustainability outlook in students, staff and faculty members [23]. The UNH approach to reduce GHG emissions is to calculate them by using a greenhouse gas inventory tool, developed by the UNH and marketed as the "Clear Air-Cool Planet Campus Carbon Calculator". This translates to a decrease of GHG emissions, and an increase in monetary savings for the campus.

The most ambitious project the UNH has taken so far to reduce its carbon footprint was the 2006 installation of a landfill gas pipeline to fuel the on-campus cogeneration heat and power plant, thus making heating/cooling and electricity no longer the largest contributor of emissions. With an initial $28 million investment, the plant has an anticipated payback time of 20 years and resulted in 21% emission reduction in the academic year 2006-2007 compared to the academic year 2005-2006. Another novel step the UNH has taken is to solicit everyone in the university community to come up with new ideas for projects, discuss targets and timelines. The UNH plan incorporates both state-of-the-art measures to reduce GHG emissions, but it also relies heavily on people and their actions [24].

Table I lists the USA institutions of higher education that were early adopters of greenhouse reduction targets, their commitments and dates of commitments.

There is also a variety of student-led initiatives to reduce energy consumption and fighting climate change in universities around the world, ranging from the use of renewable energy [25] to reducing GHG emissions using energy efficient equipment and energy efficient buildings [26]. The most common type of student-led initiative is focused on awareness-raising, providing students with real options for taking personal action to reduce their impact on the environment. Usually the core of these awareness-raising campaigns is a weeklong series of events to send a message to the student body about the importance of sustainability. Another type of student-led initiative is residence buildings competitions to reduce electricity consumption. This initiative proved to be the most compelling for students; the winning campus was able to incorporate 46% of students living on campus and achieved a reduction electricity consumption of 4%. An additional benefit of this competition is that it provided a new impetus to install energy meters in residences and a high level of institutional involvement was achieved at the participating universities [27]. Students are key players on campuses and have a unique perspective that is helpful to any type of discussion around campus climate solutions, this discussion should have in mind that the best option for encouraging young leadership in creating climate solutions on campuses is a shared power relationship, since the student body will implement many of the initiatives in residences and in their student union.

 ISBN: 978-1-61208-136-6

III. Current energy consumption in computers and related work

Since the introduction of the personal computer in the 1980, the growth in the market for this particular device has been remarkable. It was only until 1992 when the Environmental Protection Agency launched the Energy Star program, that computers among other electronic product and appliances started being tested and labeled for energy efficiency [28].

In order to improve energy efficiency, Energy Star labeled computers and electronic devices use power management (PM) schemes, in which products enter a low power state after a certain period of inactivity, saving energy. In computers, the period of inactivity that triggers a transition to a low power state can be customized by the user. Since PM parameters are customizable, a user can potentially drive energy savings down to zero.

The University of California, in Berkeley, conducted an after-hours survey in office, education and health-care buildings with the objective of collecting power data on a 1,453 desktop computers during 4 hours [29]. The results indicated a mean turn off rate of 36%, that varied from building to building. A mere 6% of the computers had a PM scheme in place. As for LCD monitors the average turn off rate was 32% with a 75% PM-on rate, however, the monitors needed a signal from the PC to enter a low power mode. The study reports that university buildings have the highest monitor PM rate, 87% but at the same time, monitor turn off rates were the lowest, 13%, in university buildings. The lack of an automated collection of data is responsible for making the study look like a snapshot of the problem. It is desirable to have a more extensive set of data over the time, which will show possible seasonalities.

The relationship between the user and the PM rates were studied by the Lawrence Berkeley National Laboratory. In this study, the information was collected using after-hours audits in non occupied commercial buildings, since they have relatively fixed schedules. The audit consisted in physical inspection of the power cord of the computer [30]. Not surprisingly it was found that PM influences energy use to a great extent, and also that the relationship between user behaviour and on/off modes is very straightforward. If somebody is using the device, it is on, otherwise, it is off. Background network activity may keep a computer from entering a low power mode, and if the computer enters a low power mode, it may fail to interact correctly with the network. In this case, the PM is disabled.

A PM scheme has to wait for a certain period of time of inactivity. The average PM delay time was found to be 15 minutes. Four scenarios were evaluated in [30]: as-found, computers always on but with PM in place, computer turned off after hours without PM in place, and finally, computers turned off after hours and with PM in place during the day. It was also found that PM rate depends on corporate culture which varies in different types of industry. Total energy consumption by a computer was calculated under each scenario. The first one constitutes 100% of consumption over a year. The second scenario, consumed only 52% over the same period, the third scenario consumed even less, 20% and finally, the fourth and most aggressive scenario takes consumption down to 17%. The same calculations were done for a LCD monitor under each scenario. Again, the first one constitutes 100% of consumption over a year. The second scenario, consumed only 22% over the same period, the third scenario consumed even less, 21% and finally, the fourth and most aggressive scenario takes consumption down to 17%.

These results must be taken cautiously, since they are based on a commercial building with more strict hours of operation, compared to a post secondary education institute where classes can go until 10 p.m. However, they provide a good argument to increase the implementation of PM successfully to attain energy savings. Weekends and evenings make up 75% of the week. In the average office space with a 35 hour work week, a computer that is on 7 hours is in active use only for 3 hours [31], the remaining time, it is idle and wasting energy.

In another study, the Lawrence Berkeley National Laboratory analyzed the relationship between consumption of energy and power on 14 desktop computers [32]. Computers and monitors have many levels of activity. A computer can be on-idle, which means that it is not running any process and thus the processor can be stop. Another mode of operation is on-active, when the computer is performing calculations. Hibernate is not a mode itself, but a process in which the computer saves the current state of the system into the hard drive, and then, the computer shuts itself down. Energy consumption was measured for every power mode using a power line meter. For desktop computers, it was found that they consume on average 3W when turned off, and an average of 9W when in sleep mode. Also, the average recovery time from sleep mode was close to 10 seconds. For monitors, it was found that their consumption is 2W on average both for when turned off and in sleep mode, and also, monitors require 2 seconds recovery time.

As mentioned before, any PM scheme requires time to enter a sleep state and also to recover itself from it. This amount of time will obviously have an impact on energy consumption. A study was conducted on this subject and it found - via surveys and field measurements - the relationship between the delay time and the average rate of PM [33]. The lower rate of use and the shorter delay time will result in a higher rate of PM operating during idling. For a time delay of 5 minutes, the PM rate was 76.3%, whereas for a delay of 60 minutes, the PM rate was 19.6%.

IV. Strategies for saving energy in computer labs: the example of the University of Calgary

The University of Calgary, Canada, with over 30,000 undergraduate and graduate students it is currently ranked as one of Canada's most sustainable universities by the College Sustainability Report Card 2011 [34]. The Information and Communication Technology, ICT Building at the University of Calgary has three Windows-based computer labs totalling 64 desktop computers. Each computer has the same make, the CPU consumes 50W idle, 2.9 W in sleep state and 0.7W

 ISBN: 978-1-61208-136-6

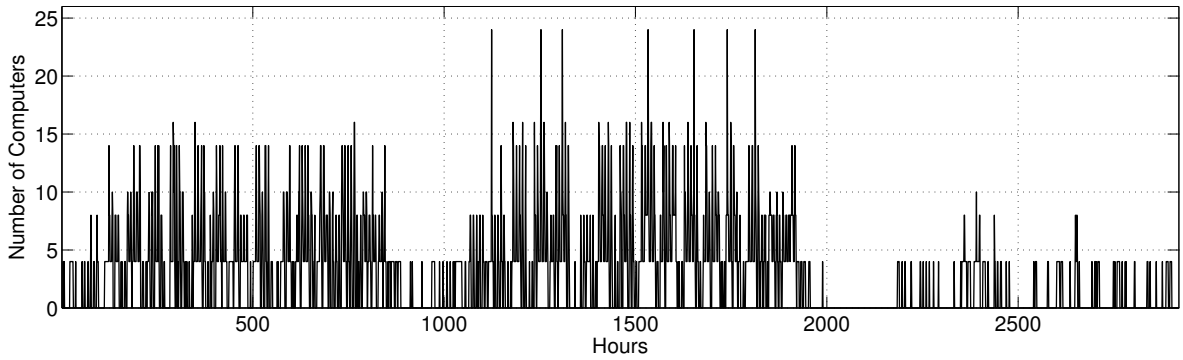

Fig. 1. ICT217 Computer Lab Usage September 2008 - August 2009

when it is off. As for the LCD monitors, they consume 22 W when used, and their consumption goes down to 0.4 W when in stand-by mode. Currently, the computers inside ICT building are never turned off as part of the IT policy in place. The rationale behind this is that the computers must be on so that they have immediate access to the latest security updates. Also, as part of the security policies of the U of C, every time a user logs in and logs out of a computer located inside a computer lab, a timestamp is recorded.

The timestamps recorded for those three labs from September 1st 2008 to August 31st 2009 were analyzed. Using the timestamps, the number of working computers in each minute of a full year was obtained, as shown in Fig. 1. Seasonalities are very clear, there are peaks and valleys and long periods of no computer use. Peaks are related to examination periods. Valleys are related to special periods such as the beginning of the semester, a no classes 1-week period and December holidays. After the Academic Year ends, the Spring/Summer term begins. During this particular period, computer usage drops dramatically since most of the undergraduate students are on vacation. Most of the usage thus can be attributed to graduate students. It is clear that using even a simple power management scheme would results in significant savings for the U of C. Three simple strategies are proposed based on common sense of the behaviour of computer labs over an extended period of time.

Under Strategy 1, all the computers inside the lab are kept on from 06:00 to 24:00, during the remaining 6 hours the computer would be in a deep sleep state. Strategy 2 is takes into account the fact that the computer usage patterns are not the same during weekdays and weekends. During the weekdays, computer labs are controlled using Strategy 1; however during the weekends, a new strategy is used. On Sundays, only 50% of the computers are kept on from 10:00 to 18:00; all the computers in the lab remain in the deep sleep state for the time remaining. On Saturdays, 50% of the computers are kept on from 06:00 to 18:00; after that time all the computers in the lab remain in deep sleep state.

Strategy 3 takes into account different patterns during the week and also seasons. During Fall and Winter it is expected that the number of computers in use will be higher than the number of computer in use during Spring and Summer. Strategy 2 is implemented during September 1st and April 30st. From May 1st until August 31st a new strategy is used. From Mondays to Saturdays, only 50% of the computers are kept on from 07:00 to 19:00; all the computers in the lab remain in the deep sleep state for the rest of the time. During Sundays, 50% of the computers are kept on from 10:00 to 18:00; all the computers in the lab remain in the deep sleep state for the rest of the time. Each strategy is simulated over the same 365 days period for each computer lab and then compared with the current 24/7 PM policy in place. Table II provides a comparison between all of them for each computer lab. It is easy to see that as the complexity of the strategies increase, so does energy efficiency for the computer labs.

	ICT217	ICT318	ICT320
Current Policy	11,355 (100%)	11,270 (100%)	7,590 (100%)
PM Strategy 1	8,740 (77%)	8,670 (77%)	5,850 (77%)
PM Strategy 2	7,100 (62.5%)	7,040 (62.5%)	4,760 (62.5%)
PM Strategy 3	5,700 (50%)	5,640 (50%)	3,830 (50%)

TABLE II
COMPARISON OF ENERGY CONSUMPTION (IN KWH) OF THE THREE SIMPLE PM SCENARIOS WITH THE CURRENT PM POLICY

The analysis of the gathered data shows that data mining and machine learning approaches can potentially generate PM schedules that improve efficiency computer labs significantly. Those approaches are under investigation and will be reported in future publications. It is important to ensure that sophisticated PM strategies are feasible. There is a need for balancing energy savings with the comfort level for students and acceptable security measures for IT operators.

V. CONCLUSION

This paper presented an overview of the ongoing efforts in some higher education institutes with regard to energy efficiency and conservation. The available reports point that while technological improvements and retrofits can potentially improve energy efficiency is such institutes, awareness programs to engage the students, faculty and staff in those programs

 ISBN: 978-1-61208-136-6

are key in obtaining acceptable results. Also reviewed in this paper is the potential for energy conservation in computer labs in higher educational institutes. With more than 20,000,000 in North America, and the typical one computer for each 10 student norm, the potential for energy conservation in computer labs and IT centres is significant.

An example of three simple power management schemes based on the data from typical computer labs at the University of Calgary was reported in this paper. The results show that with very naive solutions, energy consumption and emissions in computer labs can be cut by up to 50%, from an estimated 8 metric tons per computer lab during a year. Extrapolating the results, just by changing the current power management schemes in the computer labs, the UofC would stop emitting 495 metric tons of CO2 which has the same effect as taking approximately 95 cars off the streets. This would result in a smaller carbon footprint for the UofC, a boost for its sustainability credentials and a reduction in utility costs.

ACKNOWLEDGMENT

This work is partially supported by NSERC Canada and the Institute for Sustainable Energy, Environment and Economy (ISEEE) of the University of Calgary.

REFERENCES

[1] Intergovernmental, *Climate Change 2007 - The Physical Science Basis: Working Group I Contribution to the Fourth Assessment Report of the IPCC*, S. Solomon, D. Qin, M. Manning, Z. Chen, M. Marquis, K. B. Averyt, M. Tignor, and H. L. Miller, Eds. Cambridge, UK and New York, NY, USA: Cambridge University Press, September 2007. [Online]. Available: http://www.ipcc.ch/ipccreports/ar4-wg1.htm

[2] *Seeking a smaller footprint*, vol. 42, Business Officer, Jul./Aug. 2008.

[3] A. Strandbu and O. Krange, "Youth and the environmental movement - symbolic inclusions and exclusions," *The Sociological Review*, vol. 51, no. 2, pp. 177–198, 2003.

[4] Statistics Canada. (2009) University enrolments by registration status and sex, by province (Both sexes). [Online]. Available: http://www40.statcan.gc.ca/l01/cst01/educ53a-eng.htm

[5] National Center for Education Statistics. (2008, Aug.) Fall Enrollment in Colleges and Universities. U.S. Department of Education. [Online]. Available: http://nces.ed.gov/fastfacts/display.asp?id=98

[6] U.S. Central Inteligence Agency. (2010) The World Factbook 2010. [Online]. Available: https://www.cia.gov/library/publications/the-world-factbook/index.html

[7] G. Shiffler. (2008, Apr.) Forecast: PC Installed Base, Worldwide, 2004-2012. Gartner.

[8] EnergyStar. (2011, Jan.) Computer Desktops and Integrated Computers Voltage 115 List. [Online]. Available: http://www.downloads.energystar.gov/bi/qplist/computers_prod_list.pdf

[9] eGRID2007 Version 1.1. (2010, Mar.) U.S. annual non-baseload CO2 output emission rate, year 2005 data. U.S. Environmental Protection Agency. [Online]. Available: http://www.epa.gov/greenpower/pubs/calcmeth.htm

[10] Office of Transportation and Air Quality. (2005, Feb.) Greenhouse gas emissions from a typical passenger vehicle. U.S. Environmental Protection Agency. [Online]. Available: http://www.epa.gov/oms/climate/420f05004.htm

[11] A. Parker, ""creating a "green" campus"," *BioScience*, vol. 57, no. 4, p. 321, Apr. 2007.

[12] A. Rappaport, "Campus Greening: Behind the Headlines," *Environment: Science and Policy for Sustainable Development*, vol. 50, no. 1, pp. 6–17, Jan./Feb. 2008.

[13] American College & University Presidents' Climate Commitment. (2010, Oct.) Signatory List by Institution Name. [Accessed 21-March-2011]. [Online]. Available: http://www.presidentsclimatecommitment.org/signatories/list

[14] R. Marans and J. Edelstein, "The human dimension of energy conservation and sustainability: A case study of the University of Michigan's energy conservation program," *International Journal of Sustainability in Higher Education*, vol. 11, no. 1, pp. 6–18, 2010.

[15] U.S Green Building Council. (2005, Oct.) LEED for New Construction & Major Renovations Version 2.2. [Online]. Available: http://www.usgbc.org/ShowFile.aspx?DocumentID=1095

[16] F. Siero, A. Bakker, G. Dekker, and M. Van der Burg, "Changing organizational energy consumption behaviour through comparative feedback," *Journal of Environmental Psychology*, vol. 16, no. 3, pp. 235 – 246, 1996.

[17] Office of Sustainabiltiy, "University of Calgary 2007 Campus Sustainability Assessment," 2007.

[18] University of British Columbia. (2006) ecotrek. [Accessed 21-March-2011]. [Online]. Available: http://www.ecotrek.ubc.ca/index.htm

[19] Universitat Politecnica de Catalonia. (2006) Plan UPC Sostenible 2015. [Accessed 21-March-2011]. [Online]. Available: http://www.upc.edu/sostenible2015/upc-sostenible-2015/pla_upc_sostenible_2015_esp.pdf

[20] J. Rauch and J. Newman, "Institutionalizing a greenhouse gas emission reduction target at Yale," *International Journal of Sustainability in Higher Education*, vol. 10, no. 4, pp. 390–400, 2009.

[21] Association for the Advancement of Sustainability in Higher Education. (2010) Campus Global Warming Commitments. [Accessed 21-March-2011]. [Online]. Available: http://www.aashe.org/resources/campus-global-warming-commitments

[22] L. Sharp, "Green campuses: the road from little victories to systemic transformation," *International Journal of Sustainability in Higher Education*, vol. 3, no. 2, pp. 128–145, 2002.

[23] J. Aber, K. Tom, and M. Bruce, *The sustainable learning community : one university's journey to the future*. Durham, New Hampshire and Hannover, New Hampshire, USA: University of New Hampshire Press, June 2009.

[24] S. Cleaves, B. Pasinella, J. Andrews, and C. Wake, "Climate Action Planning at the University of New Hampshire," *International Journal of Sustainability in Higher Education*, vol. 10, no. 3, pp. 250–265, 2009.

[25] K. Marcell, J. Agyeman, and A. Rappaport, "Cooling the campus: experiences from a pilot study to reduce electricity use at Tufts University, USA, using social marking methods," *International Journal of Sustainability in Higher Education*, vol. 5, no. 2, pp. 169–189, 2004.

[26] S. Kahler, "The ripple effect: how one dorm room can affect a university's energy use," *International Journal of Sustainability in Higher Education*, vol. 4, no. 3, pp. 220–238, 2003.

[27] A. Helferty and A. Clarke, "Student-led campus climate change initiatives in Canada," *International Journal of Sustainability in Higher Education*, vol. 10, no. 3, pp. 287–300, 2009.

[28] EnergyStar. (2003, Aug.) Energy star - the power to protect the environment through energy efficiency. U.S. Environmental Protection Agency. [Accessed 21-March-2011]. [Online]. Available: http://www.energystar.gov/ia/partners/downloads/energy_star_report_aug_2003.pdf

[29] C. A. Webber, J. A. Roberson, M. C. McWhinney, R. E. Brown, M. J. Pinckard, and J. F. Busch. (2004, May) After-hours Power Status of Office Equipment and Energy Use of Miscellaneous Plug-Load Equipment. Ernest Orlando Lawrence Berkeley National Laboratory. [Accessed 21-March-2011]. [Online]. Available: http://enduse.lbl.gov/info/LBNL-53729_REV.pdf

[30] ——, "After-hours power status of office equipment in the USA," *Energy*, vol. 31, no. 14, pp. 2823 – 2838, 2006.

[31] K. Kawamoto, J. G. Koomey, B. Nordman, R. E. Brown, M. A. Piette, M. Ting, and A. K. Meier, "Electricity used by office equipment and network equipment in the US," *Energy*, vol. 27, no. 3, pp. 255 – 269, 2002.

[32] C. A. Webber, J. A. Roberson, M. C. McWhinney, R. E. Brown, G. K. Homan, J. G. Koomey, A. Mahajan, and B. Nordman. (2002, Jul.) Energy Use and Power Levels in New Monitors and Personal Computers. Ernest Orlando Lawrence Berkeley National Laboratory. [Accessed 21-March-2011]. [Online]. Available: http://enduse.lbl.gov/info/lbnl-48581.pdf

[33] K. Kawamoto, Y. Shimoda, and M. Mizuno, "Energy saving potential of office equipment power management," *Energy and Buildings*, vol. 36, no. 9, pp. 915 – 923, 2004.

[34] *University of Calgary earns an A- for sustainability*, UToday, Oct. 2010, [Accessed 21-March-2011]. [Online]. Available: http://ucalgary.ca/news/utoday/october28-2010/greenscene

 ISBN: 978-1-61208-136-6

Using Multitasking and SSD Disks for Optimising Computing Cluster Energy-Efficiency

Tapio Niemi
Helsinki Institute of Physics, Technology Programme
CERN, CH-1211 Geneva 23, Switzerland
tapio.niemi@cern.ch

Jukka Kommeri
Helsinki Institute of Physics, Technology Programme
CERN, CH-1211 Geneva 23, Switzerland
kommeri@cern.ch

Ari-Pekka Hameri
HEC, University of Lausanne, CH-1015 Lausanne, Switzerland
ari-pekka.hameri@unil.ch

***Abstract*—We tested how solid-state drives (SSD) and multitasking, i.e., running more than one task per CPU core, affect performance and energy consumption in I/O intensive data analysis jobs in high-energy physics (HEP) computing. Our motivation for the study comes from the LHC experiment at CERN producing up to 15 petabytes of data annually. The data is analysed by a huge grid computing infrastructure containing more than 100 000 CPU cores over 140 computing centres in different countries.**

Our tests indicated that in I/O intensive HEP computing multitasking, mixing heterogeneous tasks, and using SSD disks can clearly improve throughput and lower energy consumption. The throughput improved around 120% and energy consumption decreased around 50% compared to a conventional one task per CPU core setting with a hard disk system.

***Keywords*-energy-efficiency; multitasking; solid-state disk (SDD); scientific computing.**

I. INTRODUCTION

Energy consumption has become one of the main costs of computing and several methods to improve the situation has been suggested. The focus of the research in this field has been in hardware and infrastructure aspects, probably because of most of the computing centres focus on high-performance computing trying to optimise processing time of individual computing jobs. Jobs can have strict deadlines or require massive parallelism. Instead, in so called high-throughput computing the aim is slightly different, since individual tasks are not time critical and the aim is to optimise the total throughput over a longer period of time. This opens new possibilities for system optimisation, too. In the current work, our focus is closer to high-throughput computing than high-performance computing.

In modern multi-core servers, I/O access easily becomes a bottleneck. While prices of solid-state drives (SSD) are coming down and their capacity becoming larger, they can be used to alleviate this problem. SSD disks clearly have several benefits over conventional hard disks but it is not clear how much better they are in different application areas [1]. In this paper, we study applicability of SSD disks in data analysis needed in high-energy physics (HEP). Our focus is on a typical grid computing problem: How to optimise processing a large set of data intensive tasks for both energy consumption and throughput. By energy consumption we mean how much electricity is needed to process a task or a job, while throughput means how many similar tasks can be processed in a time unit. A computer or method is more energy-efficient than another one if it uses less energy for processing the same set of similar jobs.

In data and computing intensive sciences, such as high energy-physics, optimised and energy-efficient solutions are important. For example, the Worldwide LHC Computing Grid (WLCG[1]) being used for analysing the data that the Large Hadron Collier of CERN will produce, includes hundreds of terabytes of storage and tens of thousands CPU cores. In this scale, even a small system optimisation can offer noticeably energy and cost savings and performance improvements. Since high-energy physics computing has many special characteristics, common industry practices are not always the best but the methods must be tested and optimised especially for HEP computing. The main characteristics in this sense are: jobs contain large sets of similar tasks, data-intensive computing, processing times of individual tasks are not important but the aim is to optimise the total processing time of a set of hundreds or thousands of jobs each containing up to thousands of tasks, no preceding conditions among tasks, and little intercommunication between jobs or their tasks, i.e., high parallelisms. In spite of this special nature, optimising HEP computing and clusters has mostly focused on similar infrastructure issues as HPC computing in general such as cooling and purchasing energy-efficient hardware.

The paper has been organised as follows. After introduction, we review the related work in Section II. Our methodology is described in Section III. Then, the test environment and tests are explained in Section IV and their results given in Section V. Finally, conclusions and future work are given in Section VI.

[1] http://lcg.web.cern.ch/lcg/public

 ISBN: 978-1-61208-136-6

II. Related work

Generally, we can say that optimisation of scientific computing facilities has mostly focused on hardware and infrastructure issues, not so much on operational methods such as workload management and even less on operating system or application software optimisation. These methods mostly try to decrease energy consumption and keep computing power constant, while our aim is to increase utilisation rate of CPUs and I/O and in this way increase throughput, which decreases average power consumed by a computing job.

Scheduling is a widely studied topic but most of the work focuses on finding optimal schedules when jobs have preceding constrains and/or strict time limitations. Optimising total throughput or energy efficiency in high throughput computing has received less research interest. Instead some works suggest clearly opposite approaches: For example, Koole and Righter [2] suggest a scheduling model in which tasks are replicated to several computers.

Goes et al. [3] have studied scheduling of irregular I/O intensive parallel jobs. They note that CPU load alone is not enough but all other system resources (memory, network, storage) must be taken into account in scheduling decisions. Wang et al. [4] have studied optimal scheduling methods in a case of identical jobs and different computers. They aimed to maximise the throughput and minimise the total load. They give an on-line algorithm to solve the problem. There are also some studies on energy-aware scheduling. For example Bunde [5] has studied power aware scheduling methods for minimising energy consumption and not reducing system performance by applying dynamic voltage scaling technologies. However, none of these works directly aims at maximising throughput and minimising energy consumption.

Another group of studies focuses on the server level. These studies have more technology oriented approach than ours. A detailed overview on techniques that can be used to reduce energy consumption of computer systems was given by Venkatachalam and Franz [6]. Other work in this group includes, for example, Li et al. [7], who studied performance guaranteed control algorithms for energy management of disk and main memory. Ge et al. [8] studied methods based on Dynamic Voltage Scaling technology of microprocessors and created a software framework to implement and evaluate their method. Finally, Essary and Amer [9] have studied how disk arm movements can be optimised and in this way save energy, while Zhu et al. [10] proposed a disk array energy management system.

There is some recent research directly related to SSD disks. Rizvi and Chung have studied an application of solid-state drives (SSD) in large databases [11]. They showed that SSDs can improve both read and write throughput of the database mostly because of low latency of SSD disk in random data access. Schmidt et al. [12] studied XML database systems with SSD disks. In addition to performance, they also focused on energy-efficiency. Narayanan et al. [13] have analysed whether SSD disks are beneficial for server usage. They developed a tool for analysing storage workload and determining the best storage solution. They found out that SSD disks are much more energy-efficient than conventional hard disks but their current price does not make them a cost-efficient solution yet. Kim et al. [14] studied different disk scheduling methods for SSD disk. They noticed that common Linux disk schedulers are optimised more for hard disks than SSD disks. To improve the situating they proposed two new schedulers optimised for SSD disks. Chen et al. [1] studied performance of SSD disks. Their tests confirmed many commonly understood properties of SSDs but they also noticed many challenges in their performance. Generally, there is little work studying SSD disks in high-throughput computing, although modern multi-core servers obviously could benefit from faster disk access. In our current work, we aim at showing that this hypothesis is valid.

III. Methodology

Generally, HEP computing consists of two kinds of computing jobs: 1) simulation jobs modelling collisions in particle colliders and 2) analysis of data collected by detectors. In LHC computing there are two kinds of sources of these jobs: 1) centralised production teams that send up to millions of similar long simulation jobs, and 2) thousands of individual scientists sending analysis jobs in a non-controlled way. In analysis jobs data storage and transfer becomes a challenge. The data storage of the LHC experiments follows a so called tier model, in which the data is replicated from tier-0 via tier-1 and tier-2 centres to final users. Because of relatively slow data access over the Internet, the data is stored locally before analysis. Often it is beneficial to first copy a relevant piece of data to the local disk of the computing node, since the cluster file system is easily slower in a heavy use than the local disk. This is beneficial especially if the same data is iteratively analysed by only changing some parameters. Our study is the most relevant in this kind of use case.

Our earlier work showed that multitasking improves efficiency in HEP data analysis [15] but it also easily makes disk access a bottleneck. Since SSD disks are clearly faster than hard disk, they can be used to partially remove this bottleneck. In the current study, our aim was to test whether SSD disks can be used for improving throughput lowering energy consumption in HEP data analysis. As explained above, we assume having a large set of independent tasks, and we are interested in the total processing time of this set. By the total processing time we mean the total time from the submission of the first task of the set to the computing cluster to the end of processing of the last task of the same set. Our aim is to minimise both the amount of electricity and time needed to process the set. Minimising the processing time is equal to maximising the throughput.

We can present our research problem in a form of the following three hypotheses: Throughput can be improved and electricity consumption reduced in data intensive HEP computing compared to the common single task per CPU core processing with conventional hard disks by:

 ISBN: 978-1-61208-136-6

1) multitasking, i.e., processing more than one task per CPU core in parallel,
2) using SSD disks, and
3) mixing heterogeneous tasks while multitasking.

IV. TESTS

The test applications were real HEP analysis and simulation applications based on the CMSSW framework [16]. We used simulation jobs that ranged from CPU intensive to memory intensive. Our test method was to execute a job, i.e., a large set of tasks and measure the time and electricity consumed during the test run. The tests were run with different disks and configurations of the workload management system.

Our experiment system comprised of one front-end computer running the workload management system, one computing node (a Dell PowerEdge R410 server), 1 Gb local area network, and an electricity meter. The computing node was equipped with two Intel Xeon E5520 quad core 2.27 GHz processors and 16 GB DDR3 memory. The same hardware was used with both a normal magnetic disk and a solid state drive. In our tests only one drive was connected at a time. As a normal magnetic disk we used Seagate Barracuda ES.2 that came with the server. As a solid state drive we had an Intel's X25-M second generation 80GB drive. Both the hard disk and SSD disk were connected through the on-board SATA second generation connector. We used Rocks 5.3 with Linux Kernel 2.6.18 and Ext3 file system. Both disks used the CFQ (Completely Fair Queuing) scheduler, the default I/O scheduler of the Linux kernel. The electricity consumption of the computing nodes was measured with the Watts Up Pro electricity meter. The accuracy of the meter is around +-1%. We used Sun Grid Engine (SGE) workload management system [17] of Sun Microsystems that is also commonly used in grid computing clusters.

Our test applications were:

- *CPU intensive* jobs ran CMSSW [16] including event generation with Pythia6 [18] and full detector simulation with Geant4 [19]. The Pythia program is a standard tool for the generation of high-energy collisions using monte carlo methods. We had two versions of CPU intensive jobs: long and medium. The only difference between them is the run time.
- *Memory intensive* jobs are similar to CPU intensive ones but their memory requirement has been made larger by modifying the configuration file.
- *Data analysis* job is a data analysis application of the CMSSW framework [20]. Input data for the test was from the CRAFT (CMS Running At Four Tesla) experiment that used cosmic ray data recorded with CMS detector at the LHC during 2008 [21]. This detector was used in the similar way to current LHC experiments and the data was very close to the final data analysis. The analysis software reads the input file (94 MB or 360 MB), performs the analysis, and writes a small summary file (<10kB) on the local disk. The I/O traffic of one analysis job is shown in Figure 1.

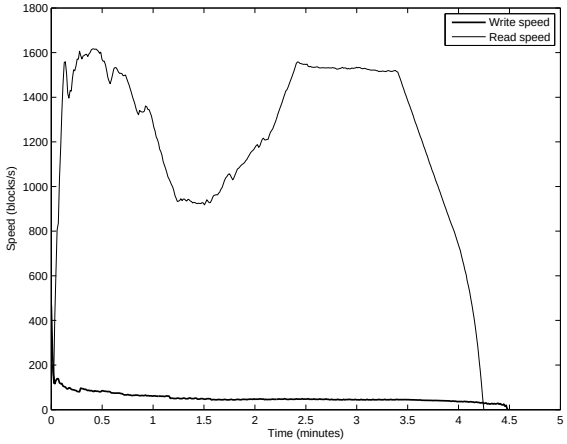

Fig. 1. I/O usage of a HEP analysis job

A summary of test application can be seen in Table I. The output files of all applications are very small, less than 10 kB.

TABLE I
SUMMARY OF HEP TEST APPLICATIONS

Program	Input file	Max mem	Run time
MEM intensive	-	859MB	449s
CPU medium	-	532MB	463s
CPU long	-	548MB	757s
data analysis heavy	360MB	368MB	99s
data analysis light	94MB	271MB	46s

The test applications were combined into three different test sets containing from 3 to 7 applications: 1) I/O intensive set (50 $\times$ 3 data analysis applications), 2) CPU intensive set (50 $\times$ 2 memory and 2 CPU intensive applications), and 3) Mixed set (50 $\times$ 3 data analysis, 2 memory, and 2 CPU applications). Each of these test sets were run 50 times to get results stable enough. Then these sets of 50 runs were run 3 times each and the final results were averages of these runs. The input data was different for each run to eliminate the effect of the disk cache. Additionally the disk cache was cleared between the test sets to provide a similar environment for all test sets. Since differences in averages among the different test sets were relatively high and standard deviation inside the sets low, this test setting gave us large enough sample size to look for statistically significant results.

V. RESULTS

First, we tested the effect of multitasking with different numbers of parallel homogeneous tasks in a core. Figure 2 shows how throughput and energy consumption develops when the number of tasks increases in a computing node. This result clearly shows that Hypothesis 1 is valid. The reason for improvements is not straightforward, since intuitively the result could be partially opposite: if disk access is the bottleneck, overloading it should slow down processing times. However, it

 ISBN: 978-1-61208-136-6

seems to be that this overloading improves disk performance. We assume two possible reasons: 1) Overloading keeps the bottleneck busy and eliminates the total I/O waiting time in the system, and/or 2) overloading improves the efficiency of disk caches since it is more likely that some other task has already fetched the required data.

Figure 3 shows the effect of multitasking with HDD and SSD disks. The figure clearly indicates that the best performance can be achieved using SSD and multitasking together.

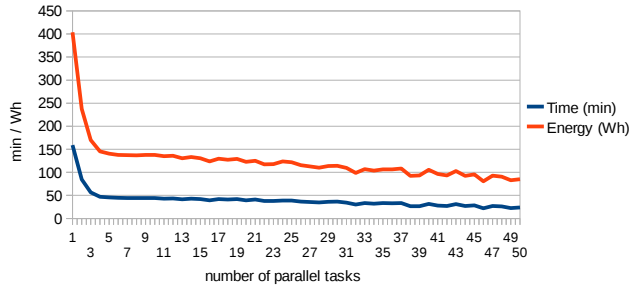

Fig. 2. Processing time of I/O jobs with different amount of parallelism using SSD

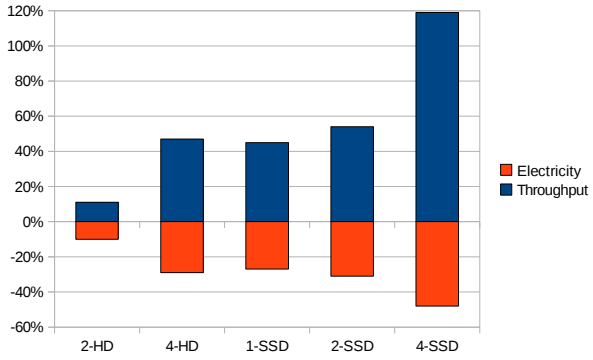

Fig. 3. Improvements of multitasking and SSD compared to 1 task/core with a hard disk

Next we compared the difference between an SSD and a hard disk with different HEP applications. The used scheduling method was two jobs per CPU core. Our earlier research [22], [15] indicates this setting is good in practical cases. It does not usually use too much memory and it is still clearly more efficient than the default scheduling settings of SGE, i.e., job slots being equal to the number of CPU cores. Figure 4 shows run times and electricity consumption of our three test sets in cases of an SSD disk and a hard disk. The numbers are averages of three independent runs. We can see that the differences between the SSD and the hard disk were clear in the I/O test set and smaller in other sets. Improvements of using an SSD disk compared to a conventional hard disk are shown in Table II and illustrated in Figure 5.

In all cases using SSD disks decreased electricity consumption per job but improvements heavily depended on the use-case. With I/O intensive jobs, throughput was 38% better and the energy consumption per job was 25% lower when using the SSD disk instead of the hard disk. The reason for this is much higher read speed and shorter access time of the SSD disk. The higher throughput caused higher CPU utilisation level and the computer using more power (average 174 W instead of 166 W with HD) but much shorter processing time lowered the total electricity consumption by 25%. Generally, the CPU power consumption dominates the disk consumption. In the case of the mixed workload, improvements both in energy efficiency and throughput were small, around 1-2%, but still statistically significant even in our small sample. In the case of pure CPU intensive workload using the SSD disk decreased energy consumption by 2% compared to the hard disk, also throughput was slightly improved but the improvement was not statistically significant.

The test results validate Hypothesis 2 by indicating that in I/O intensive HEP computing an SSD disk clearly outperformed a hard disk both in energy-efficiency and throughput. With the mixed workload the difference was less significant, since mixing I/O and CPU intensive tasks makes the disk speed less important. However, the SSD disk never decreased performance.

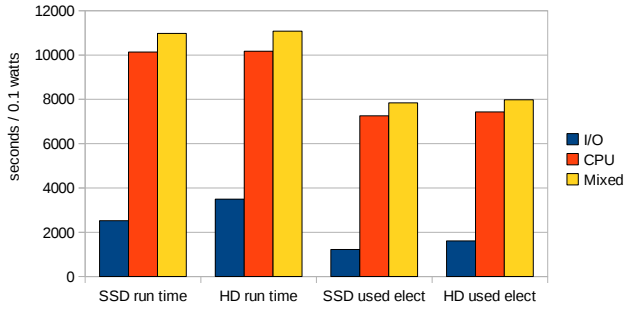

Fig. 4. Processing times and electricity consumption of different test sets

Finally, we tested the effect of mixing I/O and CPU intensive jobs when using the same disk. The second last rows of both disks in Table II show the results when the jobs were mixed while the last rows show the combined numbers of both I/O and CPU intensive job sets. This corresponds to a case in which all I/O jobs are scheduled to be processed before all CPU jobs. The results indicated that mixing jobs using different resources clearly improved both throughput and energy-efficiency. In this test case the hard disk gave better improvements but the SSD disk was still absolutely better. The results validate Hypothesis 3.

VI. Conclusions and Future Work

Our tests showed that throughput can be improved and energy consumption reduced using multitasking together with an SSD disk. However, the results depended highly on the used application. The best performance was achieved by combining

 ISBN: 978-1-61208-136-6

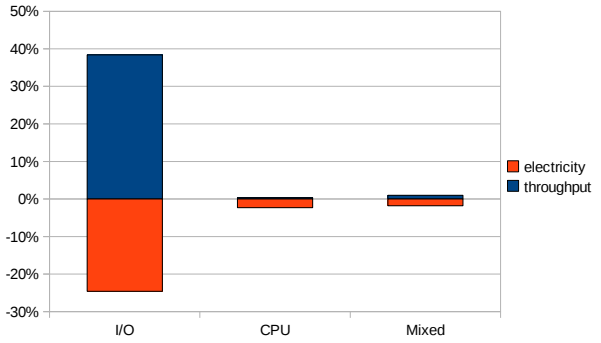

Fig. 5. Improvements of SSD compared to conventional HD (2 task/core setting)

TABLE II
COMPARISON BETWEEN HD AND SSD (2 TASK/CORE) SETTING

Disk	Test	jobs/h	%	Wh/job	%	Avg W
HD	I/O	51.6		3.2		166
HD	CPU	17.7		14.9		263
HD	Mixed	16.3		16.0		259
HD	I/O+CPU	13.2		18.1		238
SSD	I/O	71.4	38	2.4	-25	174
SSD	CPU	17.8	0.34	14.5	-2.3	258
SSD	Mixed	16.4	0.98	15.7	-1.8	257
SSD	I/O+CPU	14.2	7.8	17.0	-6.3	241

multitasking and mixing different workloads such as I/O intensive analysis and CPU intensive simulation. This improved the total throughput and decreased the energy consumption in both disk solutions.

Our tests showed that multitasking with SSDs can clearly lower energy consumption and increase throughput in I/O intensive computing compared to the hard disk. In the case of the mixed or CPU intensive workload the difference was less significant. When processing two tasks per CPU core and using an SSD disk, in I/O intensive physics data analysis throughput was 38% higher and energy consumption 25% lower compared to a hard disk, while in CPU intensive computing the disk solution makes only a couple of percentages difference. When increasing multitasking, the results got even better, but then the risk of over using memory becomes higher. The aim of our study was not to explain why multitasking improves performance but we can assume that the reason is better total utilisation of resources: the disk access is an obvious bottleneck in data analysis and processing several tasks in parallel keeps the bottleneck busy, since all the time some task is performing a disk operation. Another reason may be a better utilisation of the disk cache. Multitasking, of course, increases the processing time of an individual task, since there is often a queue for the disk access but the total processing time of a set of tasks, i.e., a job, becomes shorter.

Today SSD disks are still significantly more expensive per gigabyte than hard disks (the cheapest SSDs around $2.5/GB, HDs $0.15/GB), and therefore they may not improve total cost-efficiency if lots of storage space is needed. In some cases, a small SSD disk may be enough in a computing node and thus it can be a cost-efficient solution if using it removes an I/O bottleneck and in this way dramatically improves utilisation rates of other components. In 2010, a small (80GB) SSD disk costs around $250 and a small hard disk (160GB) around $50. This difference is only around 10% of the total price of the server but, according to our study, it can give up to 38% more performance in data intensive computing. This means reducing energy cost by 25% per computing job and makes it also possible to save in hardware, infrastructure, and personnel costs. Further, SSD disk storage is still around 10 times cheaper than RAM memory and in many applications a non permanent RAM disk is not a working solution. Although SSD market is fairly new, the price per performance keeps improving and the role of the price of SSD in total cost of the computing node becomes less important.

Our future work will include studying how different disks, disk schedulers, and task scheduling methods affect performance and energy-efficiency of HEP computing applications. We are also developing a simulator to determine an optimum amount of multitasking for different computing tasks and methods profiling analysis jobs.

ACKNOWLEDGEMENTS

We would like to thank Magnus Ehrnrooth's Foundation for a grant for the test hardware and Matti Kortelainen of the Helsinki Institute of Physics for helping with physics applications.

REFERENCES

[1] F. Chen, D. A. Koufaty, and X. Zhang, "Understanding intrinsic characteristics and system implications of flash memory based solid state drives," in *SIGMETRICS '09: Proceedings of the eleventh international joint conference on Measurement and modeling of computer systems*. New York, NY, USA: ACM, 2009, pp. 181–192.

[2] G. Koole and R. Righter, "Resource allocation in grid computing," *J. Scheduling*, vol. 11, no. 3, pp. 163–173, 2008.

[3] L. F. Ges and et al., "Anthillsched: A scheduling strategy for irregular and iterative i/o-intensive parallel jobs," in *Job Scheduling Strategies for Parallel Processing - JSSPP 2005*. Springer, 2005.

[4] C.-M. Wang, X.-W. Huang, and C.-C. Hsu, "Bi-objective optimization: An online algorithm for job assignment," in *GPC 2009, Geneva, Switzerland*, 2009, pp. 223–234.

[5] D. P. Bunde, "Power-aware scheduling for makespan and flow," in *SPAA '06: Proceedings of the 18th annual ACM symposium on Parallelism in algorithms and architectures*. New York, NY, USA: ACM, 2006, pp. 190–196.

[6] V. Venkatachalam and M. Franz, "Power reduction techniques for microprocessor systems," *ACM Comput. Surv.*, vol. 37, no. 3, pp. 195–237, 2005.

[7] X. Li, Z. Li, Y. Zhou, and S. Adve, "Performance directed energy management for main memory and disks," *Trans. Storage*, vol. 1, no. 3, pp. 346–380, 2005.

[8] R. Ge, X. Feng, and K. W. Cameron, "Performance-constrained distributed dvs scheduling for scientific applications on power-aware clusters," in *SC '05: Proceedings of the 2005 ACM/IEEE conference on Supercomputing*. Washington, DC, USA: IEEE Computer Society, 2005, p. 34.

[9] D. Essary and A. Amer, "Predictive data grouping: Defining the bounds of energy and latency reduction through predictive data grouping and replication," *Trans. Storage*, vol. 4, no. 1, pp. 1–23, 2008.

 ISBN: 978-1-61208-136-6

[10] Q. Zhu, Z. Chen, L. Tan, Y. Zhou, K. Keeton, and J. Wilkes, "Hibernator: helping disk arrays sleep through the winter," in *SOSP '05, 20th ACM symposium on Operating systems principles*. New York, NY, USA: ACM, 2005, pp. 177–190.

[11] S. S. Rizvi and T.-S. Chung, "Flash memory ssd based data management for data warehouses and data marts," *Convergence Information Technology, International Conference on*, vol. 0, pp. 858–860, 2009.

[12] K. Schmidt, Y. Ou, and T. Härder, "The promise of solid state disks: increasing efficiency and reducing cost of dbms processing," in *C3S2E '09: Proceedings of the 2nd Canadian Conference on Computer Science and Software Engineering*. New York, NY, USA: ACM, 2009, pp. 35–41.

[13] D. Narayanan, E. Thereska, A. Donnelly, S. Elnikety, and A. Rowstron, "Migrating server storage to ssds: analysis of tradeoffs," in *EuroSys '09: Proceedings of the 4th ACM European conference on Computer systems*. New York, NY, USA: ACM, 2009, pp. 145–158.

[14] J. Kim, Y. Oh, E. Kim, J. Choi, D. Lee, and S. H. Noh, "Disk schedulers for solid state drivers," in *EMSOFT '09: Proceedings of the seventh ACM international conference on Embedded software*. New York, NY, USA: ACM, 2009, pp. 295–304.

[15] T. Niemi, J. Kommeri, and H. Ari-Pekka, "Energy-efficient scheduling of grid computing clusters," in *Proceedings of the 17th Annual International Conference on Advanced Computing and Communications (ADCOM 2009), Bengaluru, India*, 2009.

[16] F. Fabozzi, C. D. Jones, B. Hegner, and L. Lista, "Physics analysis tools for the CMS experiment at LHC," *IEEE Trans. Nucl. Sci.*, vol. 55, pp. 3539–3543, 2008.

[17] *BEGINNER'S GUIDE TO SUNTM GRID ENGINE 6.2 Installation and Configuration*, Sun Microsystems, 2008.

[18] T. Sjostrand, S. Mrenna, and P. Z. Skands, "PYTHIA 6.4 Physics and Manual," *JHEP*, vol. 05, p. 026, 2006. [Online]. Available: http://www.slac.stanford.edu/spires/find/hep/www?key=6566170{\&}FORMAT=WWWBRIEFBIBTEX

[19] S. Agostinelli *et al.*, "GEANT4: A simulation toolkit," *Nucl. Instrum. Meth.*, vol. A506, pp. 250–303, 2003.

[20] CMS_Experiment, *CMSSW Application Framework*, https://twiki.cern.ch/twiki/bin/view/CMS/WorkBookCMSSWFramework.

[21] D. Acosta and T. Camporesi, "Cosmic success," *CMS Times*, November 2008.

[22] T. Niemi, J. Kommeri, K. Happonen, J. Klem, and A.-P. Hameri, "Improving energy-efficiency of grid computing clusters," in *Advances in Grid and Pervasive Computing, 4th International Conference, GPC 2009, Geneva, Switzerland*, 2009, pp. 110–118.

 ISBN: 978-1-61208-136-6

Integrated Renewable Energy Infrastructure - Challenges And Opportunities

Dr Mirek Piechowski
Group Leader – Meinhardt Building Science Group
Meinhardt Australia Pty Ltd
Melbourne, Australia
E-mail: mirek.piechowski@meinhardtgroup.com
Executive Director – Centre for GeoExchange and
Renewable Energy Infrastructure (CGREI)
centre.grei@gmail.com

Anila Weerakkody
Environmental Engineer
Meinhardt Australia Pty Ltd
Melbourne, Australia
E-mail: anila.weerakkody@meinhardtgroup.com

Abstract—**Traditional approach to the sustainable built environment focuses on the passive design and energy efficient heating and cooling technologies. Most of the green building rating systems reward buildings with integrated renewable energy power generation, such as building integrated photovoltaic (BIPV) or wind power. Experience indicates that while such initiatives can be justified by achieving the desired rating outcome or a demonstration of the owner's commitment to sustainability, rarely they can be justified from the commercial point of view. In many cases such initiatives begin to be seen as a cynical attempt at scoring points rather than demonstrating efficient design or environmental sustainability. While renewable energy generation is undoubtedly the right way for the future, the commercially viable strategies for integrating them with the built environment receive much less attention. It seems that the renewable energy sector and the built environment sector have not yet developed a framework for the integration of the two, both on the technical, commercial and legal levels. Smart grids can provide partial solution to such integration. The proposed renewable energy infrastructure consists of the distributed sources of renewable, or low emissions, power generation and also include thermal storage component designed to offset adverse effect of thermal, and electrical, demand fluctuations of buildings due to ambient temperature variations. The paper provides examples of integration of GeoExchange infrastructure with different sources of distributed, renewable energy generation. The paper also discusses some of the key commercial and technical challenges related to the integrated renewable energy infrastructure. The paper discusses some of the opportunities and challenges of integrated approach to the development of precinct scale sustainable built environment and its supporting renewable energy infrastructure. It also proposes a two-tier sustainability rating system which aims to encourage integration of renewable energy resources with urban design.**

Keywords- Reknewable energy; district energy; sustainable precincts; green building;rating schemes.

I. PROGRESS ON CLIMATE CHANGE POLICY TO DATE IN AUSTRALIA AND THE ROLE OF THE BUILDING SECTOR

Renewed awareness on climate change driven by global protocols and climate change summits are driving governments to set standards for environmental governance. The Australian federal government has currently committed to a 25% reduction in Green House Gas (GHG) emissions from 2000 levels by 2020 [1]. In order to deliver these targets the government has proposed options for the implementation of a carbon price in Australia and renewable energy targets where the federal government aims to deliver 20 per cent of Australia's electricity supply from renewable sources by 2020 [1].

As energy use by buildings (residential and commercial) accounts for approximately 20 per cent of Australia's greenhouse gas emissions [2], the introduction of stricter energy efficiency standards mandated through the Building Code of Australia (BCA) 2010, proposed new mandatory disclosure provisions and fiscal incentives such as the Green Building Fund and Renewable Energy Bonus Scheme aim to reduce GHG emissions from the building sector. Furthermore, sustainability agendas and environmental stewardship is now embedded in many corporate policies, which then influence decisions to incorporate sustainability principles into new development and buildings.

Using building environmental assessment methods such as Green Star, BCA (Building Code of Australia) FirstRate, NABERS (National Australian Built Environment Rating System) and LEED (Leadership in Energy and Environmental Design) provides third-party verification that a building was designed and built using strategies aimed at improving performance across environmental metrics: water efficiency, CO_2 emissions reduction, improved indoor environmental quality and materials stewardship. In this context there is an opportunity for environmental rating systems to encourage and promote renewable energy and other sustainability infrastructure as an integral part of the sustainable built environment.

The aim of this paper is to discuss and develop the idea of district level sustainability infrastructure as a driver for full integration of renewable energy resources with urban design. In creating a discourse around this concept the paper is structured as follows: Section 2 argues that large scale sustainable infrastructure such as renewable energy, co/tri-generation and recycled water should be provided at a district network level such that individual buildings can tap into these resources rather than the building itself having to provide these costly and complex systems and services to meet its sustainability objectives or green building rating

 ISBN: 978-1-61208-136-6

system criteria. This is illustrated by examining the provision of GeoExchange Infrastructure (GXI) as a means of precinct, or subdivision, scale integration of renewable energy storage, generation and distribution with the built environment. Section 3 presents the case study of vicurban@officer to illustrate the financial viability of coupling district level sustainable infrastructure with individual high performance passive building design. Section 4 discusses the potential for resource sharing between buildings connected to a district infrastructure network. Section 5 presents an argument for a two tired green building rating system; where the buildings passive design elements are assessed separately to its large scale active sustainable systems such as renewable energy and recycled water which, have a strong correlation to the urban infrastructure. Finally Section 6 examines the role of the local government in driving these sustainable district level infrastructure networks.

II. RETHINKING OWNERSHIP AND PROVISION OF SUSTAINABLE AND REKNEWABLE BUIDING SYSTEMS AND SERVICES

The stakeholders involved in the design, construction, operation and use of sustainable buildings are the building developer and operators, owners and occupants, local councils, planning and regulatory agencies, the local community and the commonwealth government. All these stakeholders interact with the building on different levels. Starting at the level of commonwealth government, the sustainable features of the building and its reduction in resource use contribute to the overarching commonwealth resource minimisation targets and environmental objectives. To the local government or planning and regulatory body, the building represents progress made in the community in recognising and promoting environmentally sustainable design as the resource use within that community is reduced. At the level of local government the availability of sustainable infrastructure and the level of urban environmental governance within the local community both complement and drive the sustainable aspects of the building. For the developer/operator the sustainability of the building presents a marketing opportunity; to raise the developer's community profile, showcase the developments sustainability credentials and increase return on investment. However the implementation of individual building scale sustainable services which, is required for higher levels of "environmental performance" such as renewable energy systems, co-gen, tri-gen, and grey/blackwater treatment systems often involve a high cost premium. This can sometimes be a deterrent in the desire to pursue sustainable design especially adopting voluntary green building rating scheme assessment. For the owner/occupiers the sustainability of the building represents potential operational energy savings and an improved indoor environmental quality. It may also be a means to promote their corporate ethos and environmental policies. However the owner/developer must also pay for the higher cost associated with the large scale sustainable building services and systems. These usually include recycled water, renewable energy and sustainable transport and are typically delivered at the site level and have a strong correlation to the local urban context, community and landscape. Opportunity exists for the provision of this infrastructure at the local government/precinct/district level by supplying reticulated, recycled water, district energy systems and the provision of sustainable transport options, routes and links. A building when placed in a certain location and community will play a role within that community's socio-economic and environmental context. The idea of sustainable development should extend beyond the realm of individual buildings. Building based sustainable services should be incorporated into the wider urban infrastructure network, involve other parties such as the community, adjacent buildings and councils which, are all stakeholders in their immediate built environment. The building should be seen as part of an integrated precinct or neighborhood resource and energy system. This concept is illustrated in Figure 1.

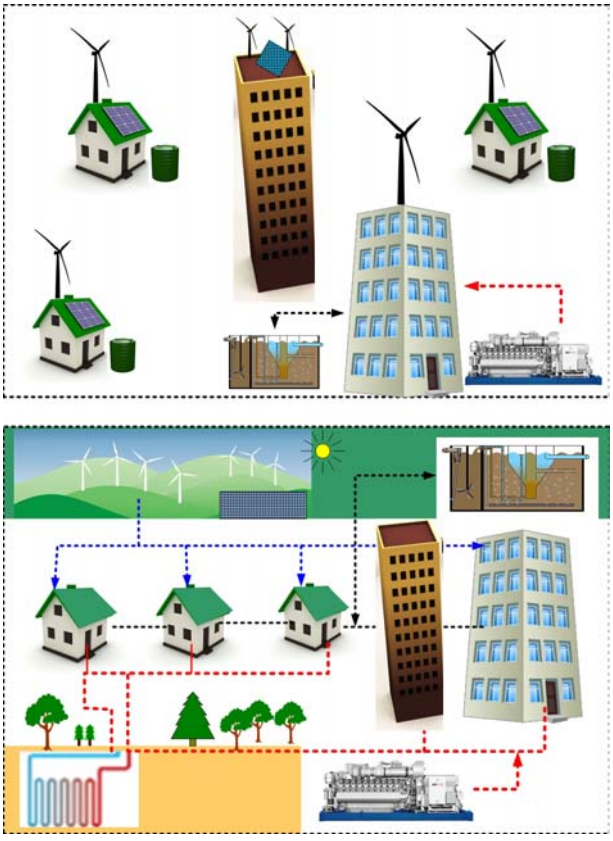

Figure 1. Buildings with individual sustainable and reknewable sevices (top) and buildngs integrated with district based sustainable infrastructure (bottom)

 ISBN: 978-1-61208-136-6

A. GeoExchage infrastructure (GXI)

Examples of sustainable district infrastructure systems which, feed into individual buildings and developments within a neighborhood or precinct include geoexchange systems. GXI is an example of a renewable energy storage system utilising large thermal capacity and inertia of the ground. Due to its large thermal capacity and inertia the ground temperature at a certain depth is almost constant throughout the year. Similarly thermal storage effects can be achieved with bodies of water, lakes, groundwater aquifers and ponds. GXI can provide both heat sink and source at the same time, particularly in temperate climates. A heating system combined with GXI will source up to 75% of heating energy from solar energy accumulated in the ground. GXI networks can also be integrated with, and supplemented by waste-to-energy plants, wood biomass, combined heat and power (co/tri-generation) systems and solar thermal systems. Waste heat generated from building services and equipment, especially in neighborhoods which, have an industrial component can be fed into and distributed through a GXI network. In summer where there is a need for cooling, this waste heat can be directed to an absorption chiller which uses low temperature heat to generate chilled/cold water. The GXI network aims to provide a more or less constant water temperature which, can be used for heating or cooling in heat pump systems. Similarly, renewable energy infrastructure such as extents of thermal solar collector panels established at district and neighborhood level can feed into the individual buildings that comprise of the energy precinct. Solar thermal systems can also be integrated into GXI to provide solar cooling through absorption chillers, etc. The building is no longer a stand-alone element in the built environment but an entity integrated with its landscape and neighborhood infrastructure. Figure 2 and Figure 3 illustrate an example of an integrated GXI system.

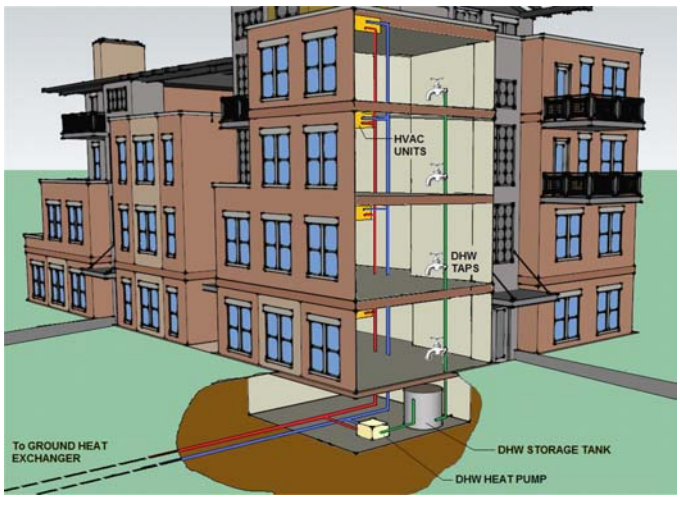

Figure 2. Example of geoexchange system for space conditioning and domestic hot water

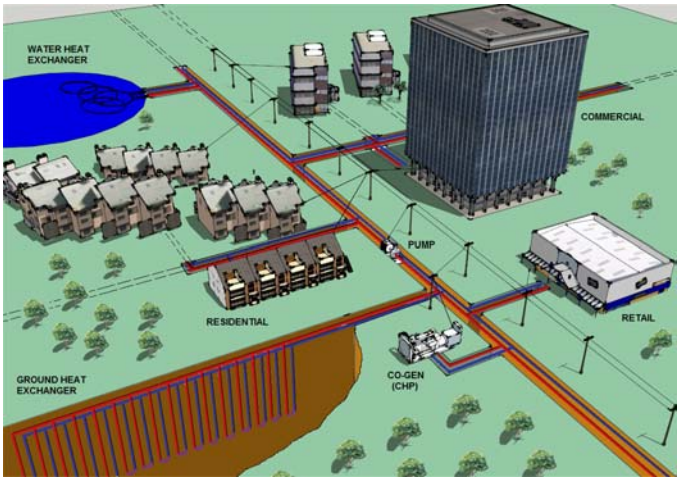

Figure 3. Example of geoexchange system integrated with co-gen

GXI lends itself to be a perfect coplement to the smart grid infrastructure. While smart grid is focusing on IT and active supply and demand management, GXI provides natural thermal energy storage component. Coupling the electricity demand for comfort heating and cooling with natural thermal storage, independent of ambient temperature variations provides a means of demand management. Lower and flatter demand characteristic is an inherent feature of GXI, as compared with the traditional air source air conditioning systems.

III. CASE STUDY IN SUSTAINABLE INTERATED DISTRICT INFRASTRUCTURE-VICURBAN@OFFICER

VicUrban@Officer is one of 16 projects selected worldwide by the Clinton Climate Initiative (CCI). It is a 32ha mixed-use site built around the Officer Train station, south-east of Melbourne, Australia. Figure 4 below shows a masterplan of the entire development. Stage 1 of the development is the precinct discussed in this case study. It is a mixed used precinct consisting of residential, commercial, retail and community buildings. It is anticipated that the residential gross floor area (GFA) will be in the order of 130,000m^2, retail up to 40,000m^2 and commercial approximately 50,000m^2. Alternative and renewable energy solutions are being considered for the precinct as part of an integrated district based energy strategy. GXI is one the alternatives being considered.

Figure 5 shows an energy and cost performance comparison between using conventional air source heat pumps for heating and cooling for the residential component of stage 1 and a water source heat pumps coupled to a GXI network. The analysis was done based on a minimum code compliant dwelling (BCA First Rate (FR) 6 Star) as a base line and then compared against better performing design (FR8 and better than 50% FR6 and FR8). Figure 5 illustrates the cost saving produced when a dwelling is designed to better than code compliant standards and coupled to GXI system. It also highlights the impact of

 ISBN: 978-1-61208-136-6

building passive design on the estimated size of GXI. It clearly demonstrates how best practice passive design, such as glazing, insulation, shading, building form and orientation impact on the viability of GXI.

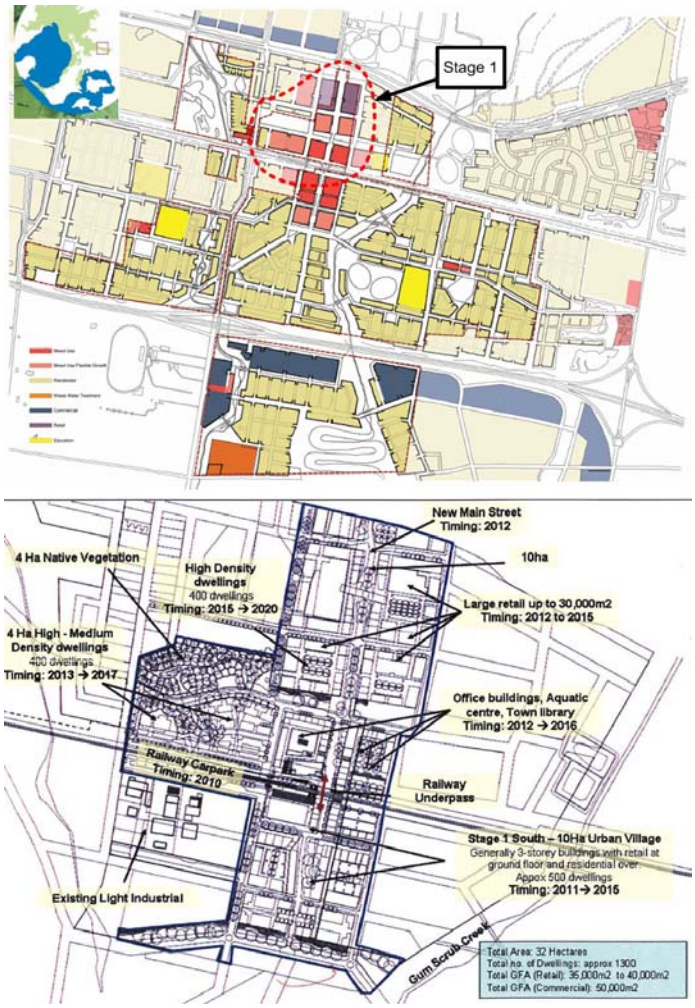

Figure 4. vicurban@officer MASTERPLAN

Main Street – comparison between air source AC and GeoExchange

	FR 6*	FR 8*	50% FR 6*	50% FR 8*
No. Loops	416	272	208	136
MD reduction, kW	648	424	324	212
Cost, $'000	$4,156	$2,719	$2,078	$1,359

Inner South – comparison between air source AC and GeoExchange

	FR 6*	FR 8*	50% FR 6*	50% FR 8*
No. Loops	1,392	911	696	455
MD reduction, kW	2,171	1,420	1,085	710
Cost, $'000	$13,923	$9,108	$6,962	$4,554

Figure 5. vicurban@officer sample calcualtiopns for Geoexchange at Officer

IV. INFRASTRUCTURE CONTEXT FOR SUSTAINABLE BUILDINGS-OPPORTUNITY FOR RESOURCE SHARING THROUGH SUSTAINABLE DISTRICT LEVEL INFRASTRUCTURE NETWORKS

The rating systems as well as local and regional regulation do not address resource sharing in building design and operation. In instances where commercial buildings are located adjacent to each other it is possible to share resources; especially renewable resources. For example; if a building harvests rainwater, generates waste heat or produces solar hot water that far exceeds its own demand, there is no concession or credit driven by regulation or the green building rating system, which, promotes the supply and distribution of this excess to nearby and adjacent buildings that may not have the production capabilities or systems. This will reduce the overall municipal potable water and electricity demand. Although such schemes may be eligible for innovation points under Green Star and LEED; subject to the judgment of assessors, they need stronger policy driven support mechanisms to be adopted by developers. Developers should be encouraged to contribute to infrastructure schemes that extend beyond the buildings site boundaries and incorporate nearby buildings and communities. In order to make these schemes viable and cost affective to the developer, cost of additional reticulation and connection infrastructure would need to be supported by concessions and mutually beneficial commercial funding models.

V. THE DICHOTOMY OF THE GREEN BUILDING RATING SYSTEM

There exists a dichotomy in green building design, construction and operation where different building design and operational elements are delineated at building level and site level. Therefore, in order to encourage and promote renewable energy and other sustainability infrastructure as an integral part of the sustainable built environment and sustainable building construction and operation we propose a two-tier green building rating system. The building level sustainability features such as the fabric, shading, massing and services are assessed separately to the larger site level features such as renewable energy, recycled water, sustainable transport and local ecology.

The objectives of the fist tier should be the assessment of the building level sustainable features based on matrices such as water use reduction, energy consumption minimisation, thermal comfort and the provision of a healthy indoor environment. The objectives of the second tier assess the interaction and integration of the site level sustainable infrastructure with the building function and operation. This would refer to the availability of district energy, renewable energy options and recycled water supply and reticulation etc which, the building could tap into, as well as the availability of sustainable transport routes and how the building caters for the use of these facilities through allocation of bike

 ISBN: 978-1-61208-136-6

storage, etc. The objectives of the second tier assessment is to build social awareness of community infrastructure and its role in achieving sustainable community outcomes, increase equity in sustainable infrastructure and encourage economic activity through access to this infrastructure. The provision of building level sustainability features is the responsibility of the developer/owner whereas the provision of the site level sustainable infrastructure should also involve the local planning authority and local government agencies as they are all stakeholders in the buildings use and operation. The site level sustainability features should be assessed in relation to the availability and provision of such sustainable infrastructure within the surrounding landscape and local community.

In green building design it is important to look beyond the building supplying the entire infrastructure required for it to operate sustainably but examine a sustainable building within a community which provides sustainable infrastructure such as a recycled water network, district heating etc. To achieve this, provision of district level sustainable infrastructure must be mandated by strong environmental commitments from governments and be supported by the local government policy and planning processors. A two-tiered system provides for better social inclusion and equity as sustainable infrastructure is made available and accessible to all. A two tiered system also makes green building construction and operation more feasible as the large-scale sustainable infrastructure is provided at the community level and the cost shared by all stakeholders and not merely the developer/owner.

VI. The Role of Government Stakeholders in Driving Sustainable Infrastructure

Planning authorities must integrate sustainable infrastructure with their urban renewal and redevelopment plans. Zoning laws and requirements should encourage symbiotic or related developments and industries to be sited in the same areas with an intention for resource sharing and building resource networks. In this way, through careful land-use planning and the design of individual buildings and developments the sharing of utilities and resources can be facilitated. Strategies to develop sustainable infrastructure could include support for distributed generation, waste heat utilisation, financial incentives to locate developments near energy and waste heat sources, establishment of district heating zones, establishment of wastewater reuse zones, local level investment in GXI, wind and solar technologies and financial and technical assistance for building level alternative technologies. Consequently the availability of the types of sustainable infrastructure will mean it will be easier for the buildings to meet their green building rating system objectives. Availability of this sustainable infrastructure will also shape building design and the systems installed.

Local authorities have a key role to play in the provision of sustainable infrastructure. They are also at the level of government that has direct interaction and access to the community and are responsible for educating local communities and disseminating knowledge on sustainability, they are also in charge of current supply and maintenance of infrastructure. Local authorities are also aware of local issues and the infrastructure and sustainability needs particular to a community. Local issues on sustainability may vary from wider overarching commonwealth policies on sustainability. Different environmental segment may have regional and local priorities. Therefore local government is well placed to drive sustainable infrastructure and the subsequently encourage and facilitate green building development and adoption of green building rating tools. However, local government needs the support of overarching commonwealth and state legislature which will set a blueprint for sustainable development.

While the technological aspect of GXI and integrated infrastructure is reasonably well understood, its commercial and legal framework is much less understood. Before GXI, and similar concepts, become the reality some pressing questions in relation to the ownership, revenue generation and allocation among potentially diverse stakeholders have to be addressed. GXI technology provides solution to some key challenges facing energy generation and distribution at the precinct level, such as reduction of maximum demand and energy use, reduction of volatility of demand and integration of renewable energy resources. However, prospective GXI operators will have to develop commercial models which redistribute costs and benefits in an equitable manner among its key stakeholders.

VII. Conclusion

Often green building design and adoption of green building rating systems is seen as having an increased cost component over conventional design which can be a deterrent for builders and developers to pursue these options. The increased costs usually arise from installation of larger scale sustainable building systems and services such as grey/blackwater treatment systems, sewer mining, cogeneration, tri-generation and renewable energy systems. If this type of infrastructure could be provided at a community and local level it would free up capital for other less costly elements of the sustainable building design such as through building form, orientation, passive ventilation strategy, daylight strategy, exposed mass, shading devices, high performance glazing and insulation.

There needs to be planning and policy instruments that implement sustainable infrastructure at regional, local and community neighborhoods such that buildings can be slotted into this context of sustainable infrastructure. The building therefore only needs to be designed with the focus on the environmental performance of its façade, fabric and equipment in mind, the larger scale sustainable infrastructure such as wastewater treatment, renewable energy generation is provided at the local level. In the long run this will enable building design with better environmental performance since

 ISBN: 978-1-61208-136-6

the burden of high cost infrastructure has been removed freeing up capital for lower cost passive and active solutions.

REFERENCES

[1] Australian Government Department of Climate Change and Energy Efficicency

http://www.climatechange.gov.au/en/government/reduce.aspx Accessed 17/02/2011

[2] Australian Government Department of Climate Change and Energy Efficicency http://www.climatechange.gov.au/what-you-need-to-know/buildings.aspx, Accessed 17/02/2011

[3] F. Butera, "Towards the Rekenewable Built Environment-Urban Energy Transition," Edited by Peter Droege, from fossil fuels to reknewable power. University of Newcastle, NSW, Australia; World Council for Renewable EnergyChapter 14, pp. 329–364, March 2008.

[4] S. Lehmann, Sustainability on the urban scale; green Urabism-New models for urban growth and neighbourhoods, Edited by Peter Droege, University of Newcastle, NSW, Australia; World Council for Renewable Energy Chapter 18, pp. 409–430, March 2008.

[5] S Sayce, L Ellison and P Parnell. Understanding investment drivers forUK sustainable property. Building Research & Information (2007) 35(6), pp 629–643

[6] I.G. Theaker and R. J. Cole, The role of local governments in fostering 'green' buildings:a case study, Building Research & Information (2001) 29(5), pp 394–408

[7] I. C. Mell, Can green infrastructure promote urban sustainability, Proceedings of the Institution of Civil Engineers,Engineering Sustainability 162, March 2009 Issue ES1,pp 23–34

[8] V. Novotny., J. Ahern,.and P.Brown., Planning and Design For Sustainable And Resilient Cities: Theories, Strategies, And Best Practices For Green Infrastructure, Water Centric Sustainable Communities; Planning, Retrofitting and building the next urban Environment.2010 John Wiley and Sons inc. pp 135-176

[9] J Engel-Yan, C. Kennedy, S. Saiz, and K Pressnail, Toward sustainable neighbourhoods: the need to consider infrastructure interactions. Can. J. Civ. Eng. 32: pp 45–57 (2005)

 ISBN: 978-1-61208-136-6

Consumer Energy Management System: Contract Optimization using Forecasted Demand

Chi-Cheng Chuang, Jimi Y. C. Wen
Networks and Multimedia Institute
Institute for Information Industry
Taipei, TAIWAN
polon@nmi.iii.org.tw, jimi@nmi.iii.org.tw

Ray-I Chang
Dept of Eng. Science and Ocean Eng.
National Taiwan University
Taipei, TAIWAN
rayichang@ntu.edu.tw

***Abstract*—Smart grid initiative is gaining traction around the world, enabling more complexity in the utility contracts designed to revolutionize our society towards more energy efficient and effective. Consumer energy management system (EMS) is important in assisting how consumers participate in the smart grid with the increasing complexity of utility contracts. A web-based EMS was presented in this paper with two novel design features: i) a maximum demand load forecasting ii) maximum contracted demand (MCD) contract optimization. A maximum demand load forecasting based on space-specific regression models of simple latent variables, temperature, number of workdays and employees, was proposed. These regression models were accurate with a mean average percentage error of 4∼8% and robust to different space size of similar nature. The use of simple latent variables enables consumers to input parameters easily through the proposed EMS web-based interface. The Particle Swarm Optimization (PSO) algorithm is especially suitable in dealing with utility contract's interdependent and discontinuous structure. A MCD contract optimization based on the PSO algorithm was then proposed and showed significant savings in the studied cases of 10∼30% improvement over the current MCD contracts and a 5∼12.5% improvement over using the average maximum demand load. The results showed promising potential of the two proposed features in future consumer EMS.**

Keywords-Energy Management System, Load Forecasting, Contract Optimization, Particle Swarm Optimization.

I. INTRODUCTION

The world is gradually marching towards a severe energy crisis, what with an ever-increasing demand of energy overstepping its supply. The total installed electricity generating capacity of a system is typically 20 to 30% greater than the predicted peak load in order to provide reserves for maintenance and contingencies [1]. This surplus capacity can be used to pump and store water in elevated reservoirs to be released through hydraulic turbine generators during peak periods. There is loss with any mechanical systems' transfer of energy, so the ideal case is to facilitate the equilibrium in consumption and generations via economical approaches rather than pure physical/mechanical approaches, i.e., effectiveness vs efficiency. Information communication technology (ICT) plays a necessity in the realization of many different programs that aid more effective use of energy [2], [3], e.g., demand response, time of use, peak leveling, etc.

Most industrial and commercial electricity consumers sign a maximum contracted demand (MCD) contract with the electric utilities company, Taiwan Power Company (TPC), in Taiwan. A MCD contract is an agreement between the consumers and the utilities on the maximum demand load that the consumer plans to use for a given time period, if the consumers use more than the agreement load, they are charged a high penalty. The detail of such a contract is described in Section IV and [4]. This type of contract is advantageous in two ways: i) Knowledge of these MCD contracts allow the utilities a better estimate on demand, therefore the utilities can plan more effective electricity generation and transmission infrastructure. ii) The consumers reduce their electricity cost if they use their electricity more effectively under the agreed maximum demand load while not necessarily decreasing their overall electricity consumption, i.e., equivalent production.

Energy management systems (EMS) [1] play a important role for the consumer to manage either energy consumption or cost. An EMS should give recommendations or control energy consumption given the data it collects via sensors, interface or the internet. In this paper, an EMS is proposed with two main contributions: i) an accurate, robust maximum load forecasting and ii) a flexible and scalable MDC contract optimization feature. The proposed EMS has other features such as appliance monitoring, short term load forecasting. These features are out of the scope of this paper, due the length limitation.

This paper is structured as follows: Section II discusses the background, and the implementation for the proposed EMS. In Section III, a proposed maximum demand load forecasting module is formulated and discussed. The output of the forecasted value is then used as a input to the optimization module. Section IV discusses the methodol-

[1] In this paper, the term EMS is referring to consumer side energy management and not utility side EMS. This term is also used as home energy management system (HEMS) or building energy management system (BEMS).

 ISBN: 978-1-61208-136-6

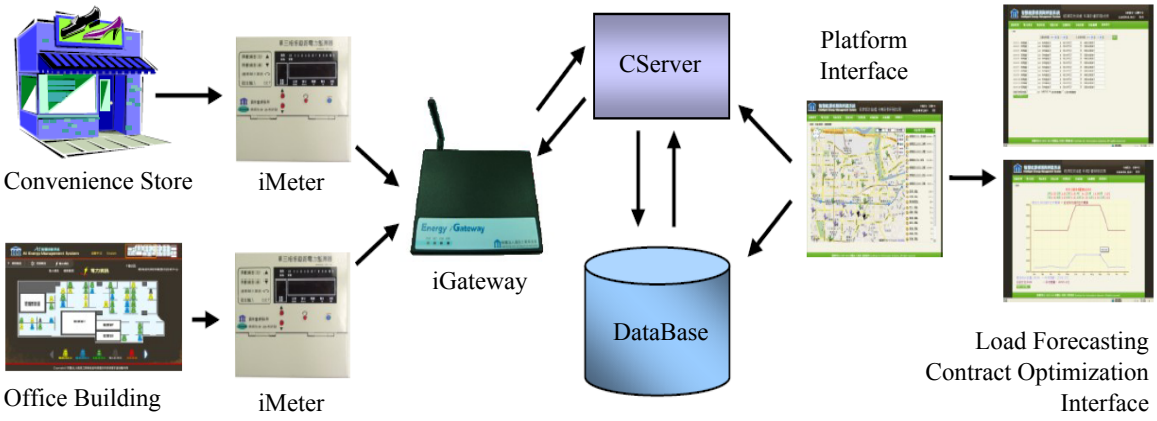

Figure 1: Overview of the proposed energy management system in this paper.

ogy, implementation and experimental analysis for a MCD contract optimization using the particle swarm optimization method. Section V concludes the paper.

II. WEB-BASED ENERGY MANAGEMENT SYSTEM

There has been an increase in interest in the research of EMS. An EMS is applied to many different applications, e.g., residential [5], [6], commercial [7], [8] or industrial [9]. An EMS may have one or more of the following features [10]:

- **Data Collection**: to collect real-time interval data from interval meters, sensors, directly from utilities, or other sources from the internet.
- **Reporting and Monitoring**: to automate energy and emissions auditing, to track and display real-time and historical data, includes various benchmarking tools, seeing exactly when and how energy is used, combined with anomaly recognition that can identify savings opportunities.
- **Engagement**: to connect consumers' daily choices with energy consumption, that can be used to offer advice to the occupants, or provide a forum for feedback on sustainability initiatives.

The proposed EMS in this paper presents consumers a way to optimize their MCD contract. System implementation is shown in Fig. 1 and described briefly in the following:

- **Deployment**: The EMS is deployed in 6 convenient stores, a 5000 m^2 office, a 500 m^2 office and 1 university lab. A total of nine spaces.
- **iMeter**: Meters that can measure 4 three-phase power or 12 single-phase power, and the data can transfered via RS-485 ModBus or Zigbee 1.0.
- **iGateway**: A gateway that converts the protocol stack of the iMeter to that of the server and database.
- **Server & DataBase**: Each running on an ASUS RS300-E6 Series servers featuring the Intel 3420 PCH chipset, Intel Xeon 3400 Series Processors, and 4GB memory.
- **Interface**: Web-based user interface. Initial page uses googlemap API to mark each of the deployment locations. Input interface for historical data for forecasting and contractual parameters for optimization.

The EMS features, maximum demand load forecasting and MCD contract optimization presented are shown in the following sections.

III. MAXIMUM DEMAND LOAD FORECASTING

Accurate models for maximum demand load forecasting are essential to MCD contract optimization. Load forecasts can be divided into three categories: short-term forecasts, which are usually from one hour to one week, medium term forecasts, which are usually from a week to a year, and long-term forecasts, which are longer than a year [11]. The problem definition in this paper is more suited using medium term forecasting. Load forecasting methods can be divide into [12]: i) Causal and econometric forecasting methods, identifying the underlying factors that might influence the variable, which is being forecast. ii) Time-series methods that uses historical data as the basis of estimating future outcomes. iii) Artificial intelligence methods such as artificial neural networks, support vector machines, etc.

A. Implementation

Due to the MCD contract structure, the maximum demand load is needed for MCD contract optimization and was forecasted in this paper as an example. For other types of contract optimization, different type of demand can be forecasted using similar method. A causal forecasting method is chosen for this implementation. The proposed maximum demand load model was formulated as follows:

$$D_i = \alpha K_i + \beta L_i + \gamma M_i + \epsilon \quad (1)$$

where the following variables are defined:

 ISBN: 978-1-61208-136-6

- D_i **maximum load**: The maximum demand load in a non-overlapping 15 minute period starting on the hour. The maximum load can be collected from past bills or utility database.
- K_i **temperature**: Apart from time factors, weather conditions are the most influential variables. Temperature is the most important weather factor with humidity second [13]. The historic or forecasted temperature data can be collected from the Central Weather Bureau database.
- L_i **workdays**: The number of workdays can affect a commercial site of their demand and can be provided by the consumer.
- M_i **employees**: The number of employees can affect the demand, i.e., more employees more demand, and can be provided by the consumer.
- α, β, γ: the regression coefficient for average monthly temperature, number of workdays in a month and numbers of employees respectively.
- ϵ: a constant.

The regression coefficients and constant can be estimated using historical data. The maximum demand, D_i can then be forecasted from latent variables, P_i, L_i and M_i. Pre-configured global and space-specific maximum demand load models were estimate by the EMS and are suitable for any similar type of commercial space and can be used by the consumer. Specific site training is then optional for the consumer, therefore making easier to use for the consumers. Although model coefficients may be needed to be re-estimated specifically for different types type, i.e., convenient stores with the use of fridge and freezers should have a different model than an office that composes of mainly PCs or an industrial space with heavy machinery.

B. Analysis

Both the global and space-specific regression models were tested for their accuracy and robustness. The accuracy (monthly error over one year) is tested with Mean Absolute Percentage Error (MAPE) defined as:

$$\text{MAPE} = \frac{\sum_{i=1}^{12} |(\hat{E}_i - E_i)/E_i|}{12}. \quad (2)$$

The robustness was tested with a *leave one out* method, where the partitioning of the estimation data and forecasting data can be seen in Table I. Table I also includes the MAPE of forecasting of the three models. It can be seen that a global regression model performs poorly in forecasting with a MAPE=55%, while space-specific models for office and convenient stores have a MAPE of 4% and 8% respectively.

A closer look of the forecasted maximum demand load of for both the global and the space-specific regression models can be seen in Fig. 2(a) and (b) for an office and a convenient store respectively. It can be seen that the maximum demand load is underestimated using global regression model for convenient stores and overestimated for offices.

Table I: FORECASTING PERFORMANCE OF DIFFERENT MODELS FOR DIFFERENT SPACES.

Regression model	Estimation	Forecasting	MAPE
Global	8	1	0.55
Office Space-specific	2	1	0.04
Convenient store Space-specific	5	1	0.08

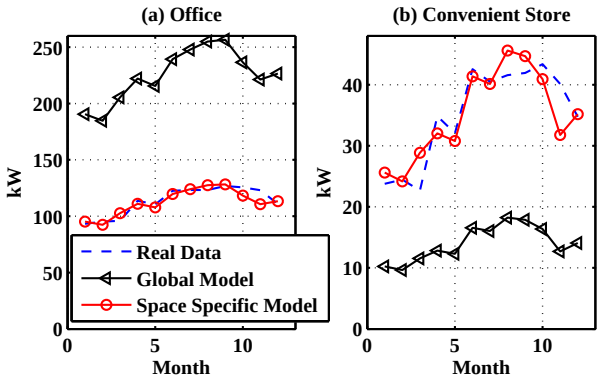

Figure 2: Detail of forecasted maximum demand load values of different models for different spaces.

This is because the latent variables defined in (1) cannot account for different type of appliances used in the space. However forecasting using space-specific regression model, the proposed latent variables can sufficiently forecast the maximum demand load. The forecasted maximum demand load is then used in the contract capacity optimization, describe in Section IV.

IV. MCD CONTRACT OPTIMIZATION

The deregulation and privatization of utility companies has led to dramatic changes in business models, an increased focus on efficiency of operations, and increased focus on reliability of service [14]. Contract optimization of tariff selection was as early as 1992 by Birch et al. [15]. Contracts are becoming more complex [2], therefore requiring more intelligent approaches to contracts from the point of view for all parties: generation [16] , distribution [17], consumer [18].

For problems over real-valued search-spaces, where the classic way of optimization is to derive the gradient of the function to be optimized and then employ gradient descent or a quasi-Newton method. However most utility contracts are not continuous as can be seen in Section IV-A. Another approach towards optimization problems use evolutionary algorithms. These methods do not use the gradient or Hessian matrix so their advantage is that the function to be optimized need not be continuous or differentiable and it can also have constraints [19]. In such cases, algorithmic procedures that take full advantage of modern computer

 ISBN: 978-1-61208-136-6

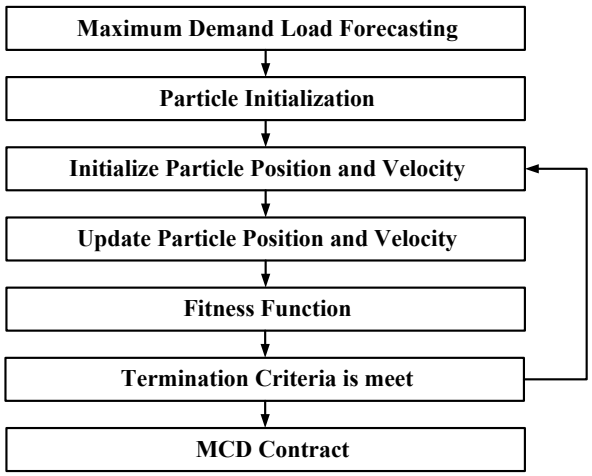

Figure 3: Procedure of MCD contract optimization

systems can be implemented to solve the underlying optimization problems numerically [20]. Popular evolutionary algorithms optimizers for real-valued search-spaces include particle swarm optimization (PSO), differential evolution and evolution strategies . Particle Swarm Optimization was used by Chen et al. to effective optimal demand contract in Taiwan for following advantages [21]: i) fewer parameters to adjust and easier implementation compared to GA, ii) more effective memory capability compare to GA iii) more efficient in maintaining the diversity. The implementation of PSO as illustrated in Fig. 3 on the MCD contract is discussed in the next section.

A. Implementation

Many different type of contracts or programs are offered by utilities, the proposed approach can be implemented for many type contract in a form that can be expressed as the fitness function of the PSO. Here an optimization of TPC's bi-period MCD contract is illustrated. Some notation are define as below:

- T_i^{periods} (kW): The consumers' MCD, a threshold for the $i-$th month determined according to the agreement between the consumers and the utilities for different periods: **peak**, **non**-summer and **off**-peak period.[2]
- $R_{\text{period}}^{\text{season}}$ ($TWD/kW): The rate charged by TPC for **sum**mer and **non**-summer seasons and different maximum contracted demand: **peak**, **non**-summer and **off**-peak.
- D_i^{period} (kW): Consumers' maximum demand load during **peak** or **off**-peak periods for the $i-$th month.
- E_i^{period}: Excess in consumer MCD during **peak** or **off**-peak periods for the $i-$th month.
- P_i^{period}: Penalty paid by consumer corresponding to the given E_i^{period} **peak** or **off**-peak periods for the $i-$th month.

[2]In typical scenarios, only the peak period MCD is selected. MCDs for other periods are only needed in atypical scenarios when these period demands are expected to be greater than the peak MCD.

The fitness function of the PSO is defined as the total cost for the MCD contract:

$$c_i^{\text{total}} = \sum_{i=1}^{12} c_i^{\text{adjust}} + c_i^{\text{basic}} + c_i^{\text{penalty}}, \tag{3}$$

where the adjustment charge for changing the MCD threshold is

$$c_i^{\text{adjust}} = 1670 \max\{(T_i^{peak} - T_{i-1}^{peak}), 0\}, \tag{4}$$

i.e a penalty is only charged for an increase in the MCD. For summer seasons June to September (i=6:9), the basic charge is:

$$c_i^{\text{basic}} = \quad R_{\text{peak}}^{\text{sum}} T_i^{\text{peak}} + R_{\text{off}}^{\text{sum}} \Gamma_i \tag{5}$$

where

$$\Gamma_i = \max\{[(T_i^{\text{off}}) - \frac{T_i^{\text{peak}} + T_i^{\text{sum}}}{2}], 0\} \tag{6}$$

and for other months (i=1:5,10:12), the basic charge is

$$c_i^{\text{basic}} = \quad R_{\text{peak}}^{\text{non}} T_i^{\text{peak}} + R_{\text{non}}^{\text{non}} T_i^{\text{non}} + R_{\text{off}}^{\text{non}} \Gamma_i. \tag{7}$$

The penalty for excess demand is the sum of two the penalty for the peak-period and off-peak period, i.e.,

$$c_i^{\text{penalty}} = \quad P_i^{\text{peak}} + P_i^{\text{off}}. \tag{8}$$

The excess in MCD is defined for the peak period:

$$E_i^{\text{peak}} \quad = \quad \begin{cases} D_i^{\text{peak}} - T_i^{\text{peak}} & \text{if } i = 6:9 \\ D_i^{\text{peak}} - T_i^{\text{peak}} - T_i^{\text{non}} & \text{otherwise} \end{cases} \tag{9}$$

and the off-peak period:

$$E_i^{\text{off}} \quad = \quad D_i^{\text{off}} - (T_i^{\text{peak}} + T_i^{\text{non}} + T_i^{\text{off}}). \tag{10}$$

The penalty for peak time excess demand can then be found for summer period $i = 6:9$ and if $E_i^{peak}/T_i^{peak} \leq 0.1$:

$$P_i^{\text{peak}} = 2R_{peak}^{sum} E_i^{peak} \tag{11}$$

otherwise, if $E_i^{peak}/T_i^{peak} > 0.1$:

$$P_i^{\text{peak}} = R_{peak}^{sum}[0.2T_i^{peak} + 3(E_i^{peak} - 0.1T_i^{peak})]. \tag{12}$$

For the non-summer period $i = 1:5,10:12$ and if $E_i^{peak}/T_i^{peak} \leq 0.1$

$$P_i^{\text{peak}} = 2R_{peak}^{non} E_i^{peak} \tag{13}$$

otherwise if $E_i^{peak}/T_i^{peak} > 0.1$:

$$P_i^{\text{peak}} = R_{peak}^{non}[0.2T_i^{reg} + 3(E_i^{peak} - 0.1T_i^{peak})]. \tag{14}$$

An additional penalty is charged when off-peak period excess is greater than peak period excess, i.e., $E_i^{off} - E_i^{peak} > 0$, and is defined for summer period $i = 6:9$ and if $(E_i^{off} - E_i^{peak})/(T_i^{peak} + T_i^{non} + T_i^{off}) \leq 0.1$

$$P_i^{\text{off}} = 2R_{off}^{sum}(E_i^{off} - E_i^{peak}) \tag{15}$$

 ISBN: 978-1-61208-136-6

Table II: PRICE OF MCD CONTRACTS IN $TWD

Scenario	Current	Average Load	PSO	Savings from current	Savings from average load
Office	$ 401	$ 290	$ 288	28 %	6 %
School	$ 482	$ 449	$ 444	10 %	5 %
Building	$ 3,790	$ 2,978	$ 2,800	26 %	6 %
Store	$ 500	$ 400	$ 350	30 %	12.5 %

otherwise

$$P_i^{\text{off}} = R_{off}^{sum}[-0.1(T_i^{peak} + T_i^{non} + T_i^{off}) + \\ +3(E_i^{peak} - 0.1(T_i^{peak} + T_i^{non}))] \quad (16)$$

and non-summer period $i = 1 : 5, 10 : 12$ and if $(E_i^{off} - E_i^{peak})/(T_i^{regular} + T_i^{non} + T_i^{off}) \leq 0.1$

$$P_i^{\text{off}} = 2R_{off}^{non}(E_i^{off} - E_i^{peak}), \quad (17)$$

otherwise

$$P_i^{\text{off}} = R_{off}^{non}[-0.1(T_i^{peak} + T_i^{non} + T_i^{off}) \\ +3(E_i^{peak} - 0.1 * (T_i^{peak} + T_i^{non}))]. \quad (18)$$

It can be seen from (3)-(18) that the parameters to be optimized are interdependent and discontinuous. Therefore using a PSO approach is advantageous compare to classic gradient-based optimization methods.

B. Analysis

Using a the above defined fitness function a PSO was carried out. It can be seen that in Table. II, current peak MCD contracts are usually set too high without the computation of maximum demand load forecasting and MCD contract optimization modules. It can also be seen that, using the a 'naive' optimization using the average forecasted maximum demand load is setting the MCD too low. The proposed optimization gives a 10∼30% improvement over the the current MCD contracts and a 5∼12.5% improvement over MCD contracts using the average maximum demand load. It is also noted that under the current contract strucutre, the penalty is really high for adjustment of the MCD as seen by the constant 1690 TWD per every kW increase. This is due to the cost of increasing the limit of the physical infrastructure of current power system being too high and inflexible. However as the smart grid infrastructures advance [3], intermittent and adaptive power systems may lower the cost of varying this limit, thus allowing a more dynamic MCD structure, which can be easily adapted to by the proposed MCD contract optimization module.

V. CONCLUSIONS AND FUTURE WORK

A web-based EMS was presented in this paper with two novel design features: i) maximum demand load forecasting and ii) MCD contract optimization. A maximum demand load forecasting based on space-specific regression models of simple latent variables, temperature, number of workdays and employees, was presented. These space-specific regression models were accurate and robust to different space size of similar nature. The simple latent variables allow consumers to input their parameters easily through the web-based interface. A MCD contract optimization based on PSO was then proposed and showed significant savings. PSO is especially suited and flexible in dealing with utility contract's interdependent and discontinuous structure, and has the potential to be implemented in a distributed computing approach naturally [20]. This allows the scalability of web-based EMS to become a platform based service in the future assisting many people in the time of increasing utility contract complexity as smart grid advances. The next step in our research is to improve the robustness of contract optimization given load forecasting errors.

REFERENCES

[1] P. Kiameh, *Power Generation Handbook: Selection, Applications, Operation, Maintenance*. McGraw-Hill Professional, 2002.

[2] I. E. A. IEA, *The Power to Choose: Demand Response in Liberalised Electricity Markets*. OECD Publishing, 2003.

[3] C. W. Gellings, *The Smart Grid: Enabling Energy Efficiency and Demand Response*. CRC Press, 2009.

[4] Taipower, "Tariff book," Taiwan Power Company, Tech. Rep., 2008.

[5] D. M. Han and J. H. Lim, "Design and implementation of smart home energy management systems based on zigbee," *Consumer Electronics, IEEE Transactions on*, vol. 56, no. 3, pp. 1417 –1425, 2010.

[6] V. Sundramoorthy, G. Cooper, N. Linge, and Q. Liu, "The challenges and design concerns for the domestication of energy monitoring systems," *Pervasive Computing, IEEE*, vol. 10, no. 1, pp. 20–27, 2011.

[7] J. Van Gorp, "Enterprising energy management," *Power and Energy Magazine, IEEE*, vol. 2, no. 1, pp. 59 – 63, 2004.

[8] R. Brewer and P. Johnson, "Wattdepot: An open source software ecosystem for enterprise-scale energy data collection, storage, analysis, and visualization," in *IEEE Int. Conf. on Smart Grid Communications*, 2010, pp. 91 –95.

[9] T. Y. Wu, S. S. Shieh, S. S. Jang, and C. Liu, "Optimal energy management integration for a petrochemical plant under considerations of uncertain power supplies," *Power Systems, IEEE Transactions on*, vol. 20, no. 3, pp. 1431 – 1439, 2005.

 ISBN: 978-1-61208-136-6

[10] R. Aldrich and J. Parello, *IP-Enabled Energy Management: A Proven Strategy for Administering Energy as a Service*. Sybex, 2010.

[11] E. A. Feinberg and D. Genethliou, *Applied Mathematics for Restructured Electric Power Systems: Optimization, Control, and Computational Intelligence*. Springer, 2005, ch. 12, pp. 269–286.

[12] A. K. Palit and D. Popovic, *Computational Intelligence in Time Series Forecasting: Theory and Engineering Applications*, M. J. Grimble and M. A. Johnson, Eds. Springer, 2005.

[13] R. Weron, *Modeling and Forecasting Electricity Loads and Prices: A Statistical Approach*, R. Weron, Ed. Wiley, 2006.

[14] J. Momoh, *Economic Market Design and Planning for Electric Power Systems*. Wiley-IEEE Press, 2009, ch. 10, pp. 237–273.

[15] A. Birch and C. Ozveren, "An adaptive classification for tariff selection," in *Proc. Int. Conf. Metering Apparatus and Tariffs for Electricity Supply*, Nov. 1992, pp. 53 –57.

[16] Y. Ma, C. Jiang, Z. Hou, and C. Wang, "The formulation of the optimal strategies for the electricity producers based on the particle swarm optimization algorithm," *Power Systems, IEEE Transactions on*, vol. 21, no. 4, pp. 1663 –1671, 2006.

[17] P. Bajpai, S. Punna, and S. Singh, "Swarm intelligence-based strategic bidding in competitive electricity markets," *Generation, Transmission Distribution, IET*, vol. 2, no. 2, pp. 175 –184, 2008.

[18] T. Y. Lee and C. L. Chen, "Wind-photovoltaic capacity coordination for a time-of-use rate industrial user," *Renewable Power Generation, IET*, vol. 3, no. 2, pp. 152 –167, 2009.

[19] X. Yu and M. Gen, *Introduction to Evolutionary Algorithms*. Springer, 2010.

[20] E. Konstantinos, *Particle Swarm Optimization and Intelligence: Advances and Applications*. Information Science Publishing, 2010, ch. 2, pp. 25–41.

[21] J. C. Chen, J. C. Hwang, J. S. Pan, and Y. C. Huang, "PSO algorithm applications in optimal demand decision," in *proc. IEEE Int. Power Electronics and Motion Control Conf.*, May 2009, pp. 2561 –2565.

 ISBN: 978-1-61208-136-6

Monitoring IT Power Consumption in a Research Center: Seven Facts

Antonio Vetro', Luca Ardito, Maurizio Morisio
Dipartimento di Automatica e Informatica
Politecnico di Torino
Torino, Italy
e-mail: name.surname@polito.it

Giuseppe Procaccianti
Dipartimento di Automatica e Informatica
Politecnico di Torino
Torino, Italy
e-mail: name.surname@studenti.polito.it

***Abstract*—We analyze the power consumption of several IT devices placed in a research center affiliated to our University. The data collection lasted about one year and the analysis let us identify: i) the average instant power consumption of each type of device ii) trends of the instant power consumption curves iii) usage profiles and their power consumption iv) energy savings obtained from a different use of resources. Our main finding is that software and usage typology could affect power consumption more than hardware.**

Keywords—Green Computing, IT Energy Management, Electricity Meter, Data Analysis

I. INTRODUCTION AND RELATED WORK

Over the years, the use of Information Technology has exploded and IT has also contributed to environmental issues: the total electricity consumption by servers, computers, monitors, data communication equipment, etc. is increasing steadily [5]. According to [3], the ICT sector is responsible for a value between 2% and 10% of the worldwide energy consumption. Therefore, it is necessary to improve awareness in the IT industry with regard to environmental problems, and this aspect should be considered by the academic point of view [6]: in fact, "turning on research universities into living laboratories of the greener future" [8], will permit to quickly develop best practices and to make them available to industry and society in general. As an example we cite the work of Chiaraviglio et al. [1]: they applied a fully automatic measurement that is able to scale and track the number of devices powered on in real time. This technique has been applied at our same university, Politecnico di Torino. They created PoliSave, a software to turn on/off a PC by connecting directly to a website. PoliSave is being extended to all PC in the Campus, with the goal of saving about 250,000 € per year from the University energy bill. The study we present here is instead focused on the analysis of power consumption data, and it is designed to find out usage patterns of IT devices' energy consumption and to identify situations in which there is a waste of energy. Pinckard and Busch [2] also collected data on devices, focusing on the after-hours power state of networked devices in office buildings: they showed that most of devices are left powered on during night, concluding that this is the first cause of energy waste. Usage analysis is a crucial step to optimize the energy consumption: this task is even more necessary within data centers where the number of computers is large. In this field, Bein et al. [4] tried to improve the energy efficiency of data centers: they studied the cost of storing vast amounts of data on the servers in a data center and they proposed a cost measure together with an algorithm that minimizes such cost.

In our analysis the number of pc is lower, but we observe data from a real case. The paper is structured as follows: in the following section, the context of our work, including instrumentation and research questions, is described, section III presents results and, finally, section IV provides conclusions and future work.

II. CONTEXT OF THE ANALYSIS

One of the strategic goals of Politecnico di Torino is the green footprint cutting and related costs reduction. Managers know that whenever a change is needed, the first step is to figure out the current scenario in a quantitative way, that means to measure [7]. Starting from the indicators, it is then possible to find solutions, improve results and solve problems. Therefore, several measures should be present on the dashboard of the *green power manager*, one of them is the electrical power consumption of devices: for this reason, our University decided to install in several departments sensors to monitor the power consumption of rooms, lighting and conditioning systems, data elaboration centers and single IT devices such as servers, printers, switches. We were involved in the measurement process of such data in a research center affiliate to Politecnico di Torino, the Istituto Superiore Mario Boella (ISMB), and we present in this paper data collected and some facts found.

A. Instrumentation

The measurement of power consumption was done through a power monitoring system provided by an industrial partner. The system is composed by sensors inserted between the monitored devices and the electrical plugs to which they are plugged in. For entire sections of lighting and conditioning systems, instead, the sensor is applied directly on the conductor through a pincer. Both type of sensors can compute active and reactive power, voltage, current intensity, cos φ, with a desired sampling time (we selected ten minutes). Data collected by sensors are sent to a bridge through ZigBee, then the bridge forwards the data via Ethernet/Internet to the central servers. Data are then accessible on a web portal and can be exported to be analyzed. We monitor the active power consumption on the following devices of the ISMB research center:

 ISBN: 978-1-61208-136-6

- Three distinct servers:
  - Server 1 (from 22nd April 2010 to 23rd November 2010)
  - Server 2 (from 22nd April 2010 to 23rd November 2010)
  - Server 3 (from 7th May 2010 to 23rd November 2010)
- A printer (from 5th March 2010 to 23rd November 2010)
- The conditioning system "CED1", that is cooling the room where Server 1 and 2 are located (from 23rd November 2009 to 23rd November 2010)
- The lighting system in Server 3 Room (from 24th November 2009 to 23rd November 2010)

We list in Table I the characteristics of the three servers. Server 1 and Server 2 are both used as web servers: they host web sites of research projects, where researchers share documents and files. Server 3 instead is used both as web server and to perform graphical operations. The printer is HP Laserjet P3005dn , with an operational power supply of 600W and standby consumption of 9W. Unfortunately we do not have information on the conditioning and lighting system. Finally, we define "instant power consumption" the average power consumption consumed in the sampling unit time (ten minutes).

B. *Research questions*

Eight different research questions drive data analysis. Firstly we have a group of questions (*Overview*) that is very general, and aims at discovering what is the actual average instant power consumption of the equipment in the ISMB research center, that we suppose being the typical equipment of similar centers. Overview questions are listed below:

1. What is the average instant power consumption of the servers in the last year?
2. What is the average instant power consumption of the printer in the last year?
3. What is the average instant power consumption of the other equipment (light, conditioning)?

After that, we focus our analysis on the power consumption of servers, because we can reduce their consumption only understanding how and how much they consume. The first question that is raised up is whether the power consumption of the three servers is the same or not:

4. Are there differences between the servers instant power consumptions?

Assuming, from the exploratory data analysis, that the power consumption in the studied context is not following any well-known distribution, we answer question 5 performing the Wilcoxon Two Sample test [9]. The difference we try to find with this question is an inter-server difference: the next step is to explore the aspects related to the progress of the single servers' power consumptions. Initially, we investigate whether the power consumption is homogeneous or variant:

5. Are there any peaks in instant power consumption or is it homogeneous? If so, how long do they last? Are they relevant, in terms of power values?

We answer to this question in a qualitative way, i.e. plotting for each server 2 different graphs: the power consumption over time and the estimated probability density. The first plot let us identify the presence of peaks and trends in the observed time window, whilst the latter permits to see if power consumption accumulated by peaks is relevant, looking to the frequency of the values associated to the peaks. Peaks represent a rapid growth or decrease, or deviations from a normal behavior. However, a server could have several behaviors in terms of power consumption, associated for example to a different load or a particular software or hardware configuration. Therefore the scope of the next question is to understand the existence of different power consumption "behaviors", that we call "profiles".

6. Can we identify different usage profiles (e.g. active/standby)?

We perform a cluster analysis to answer question 7. We use the K-Means algorithm [10] and the bivariate plots, obtained through normalization and rescaling of the variables (watt-time couples). The selected clustering algorithm aims to group and find aggregations of data around certain values called "centers", which could point out different power consumption "profiles" and relationships between the variables (for instance, a typical profile in common computers is the standby profile).

TABLE I. SERVERS' TECHNICAL CHARACTERISTICS

	Server 1	**Server 2**	**Server 3**
Type	Dell PE r300	Dell PE1950 III	Dell Precision T5400
RAM	8 GB DDR 2	4 GB	4 GB
Proc	Quad Core Xeon X5460 3.16 GHz 64 bits	Quad Core Xeon E5410 2.33GHZ 32 bits	Dual Core Xeon 5200 2.49 GHz 64 bits
Power supply	400 W	670 W	875 W
Operating system	Windows Server 2003 R2 Enterprise X64	Ubuntu 2.6.24-19-server	i)Windows Server 2008 ii)Ubuntu 10.04 Server iii)Windows XP
Energy certification	NO	NO	Energy Star 4.0

 ISBN: 978-1-61208-136-6

The plots let us visualize and verify the clusters found. If profiles are found, it is also important to verify if they correspond to daily/nightly activities, relating, for each server, the progress of power consumption with time tables of human activities in ISMB. Hence, we plot, for each server, the power consumption in a whole day, selecting for each week of the last 3 months a random day between Tuesday, Wednesday and Thursday (we avoid week ends, Mondays and Fridays because typically in these days human activities are not representative of the typical work-day). Observing the 12 plots obtained and interviewing people working in the center, we are able to identify the time range in which the majority of activities on all the 3 servers is carried out, that is between 9 a.m. and 8 p.m. At this point, it is possible to divide data in daily and nightly consumption, and then compare the two subsets, using Wilcoxon Two Sample test, since data is not normally distributed.

Moreover, we are interested in pointing out the power consumption of each profile, in order to understand how much energy is saved/lost by applying the configurations and conditions that determine the different power profiles. This is done by tagging each observation with the profile it belongs to and then summing up the cumulated consumption. Therefore, the research question is:

7. How much total energy did servers consume in the last year in the different profiles?

Finally, the same question is replicated to the printer, that has two well-known profiles: an active profile when it is printing, and a stand-by profile when it is not.

8. How much energy can we save by turning off the printer when it doesn't work?

All questions are about power, and related data are expressed in Watt (W), exception given for RQ 7-8 that measure energy (KWh).

C. Threats to validity

The first threat of this research is an external threat: the analysis is performed on specific machines, thus generalizing these results is not possible. However, it can be possible to look at this equipment as representative of a category of equipments with similar characteristics.

Further, a derived internal threat is that the information on the technical characteristics of the IT equipment (printer, servers) and on their usage (massive, constant, etc) could be not enough to deeply motivate all the curves of the power consumption analyzed and determine with precision the impact on the measures. Therefore, the causes that we derive from the observation, can be biased.

Finally, we also identify a conclusion threat determined by the sampling time (ten minutes): as a consequence we have average values even for instant power consumption measures, and we could miss some fluctuations.

III. Analysis Results

A. Overview(RQ1 to RQ3)

We provide on Table II two descriptive statistics about RQ1 to RQ4: the average instant power consumption and the index of dispersion that quantifies how much data is sparse around the mean.

B. Servers (RQ4 to RQ7)

RQ4: Are there differences between the servers instant power consumptions?

We observe in Table III that power consumptions of Server 1 is very different from the consumptions of Server 2 and 3. However, Server 2 and 3, even if similar in mean values (difference is only 8 Watts), have statistically different mean power consumptions.

RQ5: Are there any peaks in instant power consumption or is it homogeneous? If so, how long do they last? Are they relevant, in terms of power values?

Looking to the time plots, we observe for Server 1 (Figure 1) many high spikes (that reach values that are more than the 50% of the mean), two low spikes and frequent switches between low and high values. However, the index of dispersion (see Table II) is reduced, that means that the time duration of the peaks is short. For Server 2 (Figure 2), data is more concentrated around the mean value, and the peaks (3 low spikes and a dozen of high peaks) lasts for short periods of time (but longer than Server 1, as the index of dispersion suggests).

TABLE II. Average instant power consumption of selected devices

RQ	Device	Average Instant Power Consumption	Index of dispersion (var/mean)
1	Server 1	108.02 W	0.55
1	Server 2	145.12 W	2.3
1	Server 3	139.63 W	22.44
2	Printer	13.46 W	199.95
3	Light (Server 3)	107.76 W	877.56
4	Conditioning (Server 1+2)	2713.77 W	880.12

TABLE III. Result of Wilcoxon test on servers instant power consumptions

Comparison	95% Difference Confidence Interval	P- val	Different?
Server 1 vs Server 2	{ -37.78 , -37.68 }	< 2.2e-16	YES
Server 1 vs Server 3	{ -47.57 , -47.36 }	< 2.2e-16	YES
Server 2 vs Server3	{ -8.43 , -8.33 }	< 2.2e-16	YES

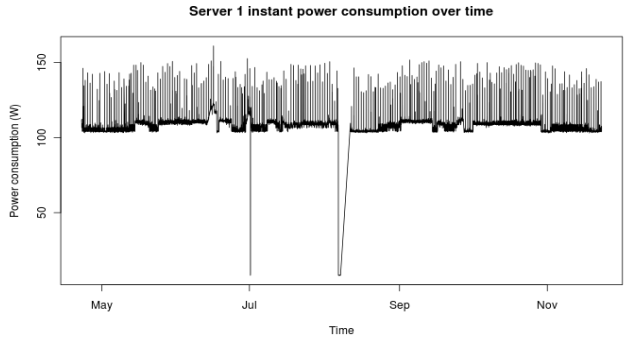

Figure 1. Instant power consumption over time (Server 1)

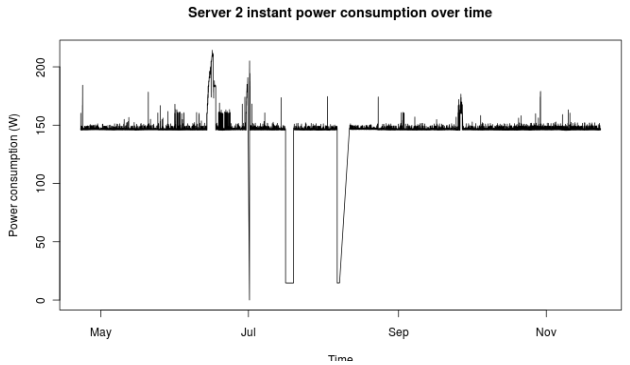

Figure 2. Instant power consumption over time (Server 1)

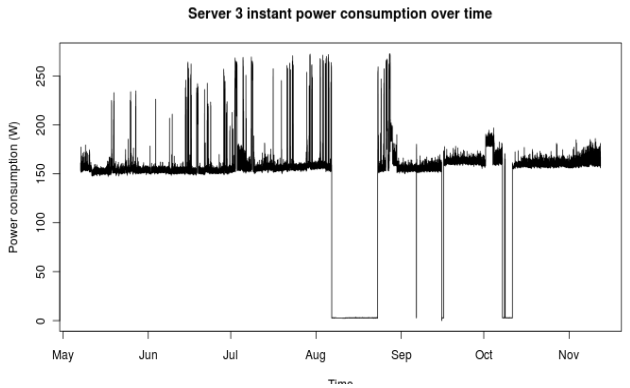

Figure 3. Instant power consumption over time (Server 3)

Finally, for Server 3 (Figure 3) the situation is yet different: it has a higher consumption and many high peaks until the end of August, then lower power consumption and peaks starting from September 2010. The change in the curve has a motivation: the server was used to perform continuous intensive tasks as image processing, parallel coding and massive video/audio streaming until end of August. Then, it was used as a normal web server, as Server 1 and Server 2.

The variability of data has also the same behavior: higher until September, then reduced. Moreover, there is a very long period (about 20 days) of zero power consumption (it was powered down), followed by 4 other smaller periods of zero consumption.

Plotting instead the probability density estimation of the servers' power consumptions, we can see around which values data is concentrated, and so if peaks are relevant both in terms of power consumption and duration. Server 1 (Figure 4) has 3 main concentrations of data: the highest is around the mean value (~108 W), then there is a similar peak at about 112 W and a lower one in their middle, finally two very low peaks at the two extremes of the graph. We conclude that peaks of Server 1 are relevant in terms of duration, but not in terms of variation from the mean value. The probability function of Server 2 (Figure 5) is totally different: data is concentrated around the mean value, and the distribution is very similar to a normal distribution with very low variance. The higher index of dispersion is due to the small peak toward the 10W and the other one on the right of the mean. We observe that peaks for Server 2 are irrelevant in terms of duration, but some are quite far from the mean. Finally, we observe Server 3 in Figure 6: except the peak around the mean, the 2 big peaks (~0 W and ~160 W) have high probabilities, whilst the small peak on the right is quite far from the mean. As a consequence, spikes of Server 3 are relevant both for time length and power consumption. This concludes the answer of RQ6.

RQ7: Can we identify different usage profiles (e.g. active/standby)?

We obtain from the K-Means algorithm 5 clusters for Server 1, 4 clusters for Server 2 and 4 Clusters for Server 3. The centers of the clusters are the following, in increasing order of power (W) :

- Server 1: 8.36, 105.23, 106.97, 109.44, 110.47
- Server 2: 14.64, 146.44, 146.68, 149.22
- Server 3: 2.80, 154.51, 160.56, 246.81

We can surely identify a “low power profile” for all the servers (the lowest-value center). Instead active profiles could be more than one, especially for Server 1 (data varies from 105 to 110 W) and Server 3 (where the difference is clear, since values go from 154 to 246 W). For this reason, we perform a further cluster analysis (Figure 7), focused just on the active profile, that allow us to gain more information. We find the following centers:

- Server 1: 104.93, 105.21, 105.92, 109.76, 111.10, 138.61
- Server 2: 146.46 , 146.63, 185.10
- Server 3 : 154.27, 160.64, 245.87

 ISBN: 978-1-61208-136-6

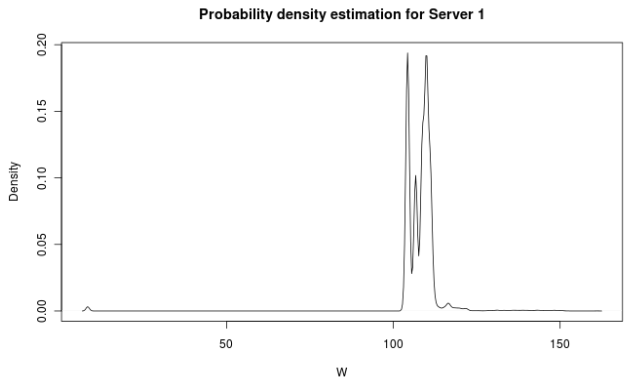

Figure 4. Probability density function estimation (Server 1)

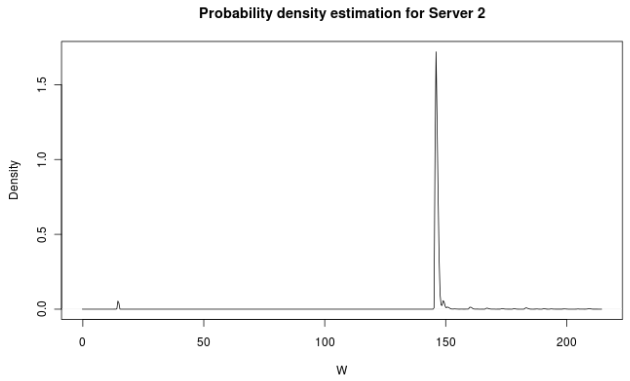

Figure 5. Probability density function estimation (Server 2)

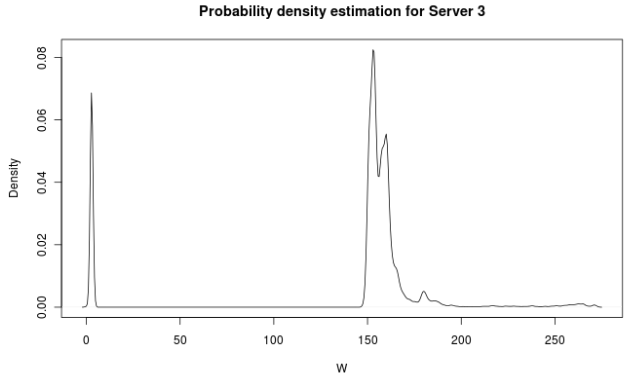

Figure 6. Probability density function estimation (Server 3)

Reducing to significant values, we can identify for all the servers at least two different high power profiles and a low power profile: we show values in Table IV . Subsequently, we investigate whether the two high power profiles are related to the day/night human activities. Even if the Wilcoxon statistical tests (Table V) verifies the difference between daily and nightly power consumption with the standard level of confidence of 95%, this difference is in practice negligible, since it's in the order of µW for Server 1 and Server 2 and it is less then 1 W for Server 3.

RQ8: How much total energy did servers consume in the last year in the different profiles?

The estimated cumulated energy consumption of servers in the different power profiles is shown in column "kWh" of Table VI, whilst the column "%" shows the percentage of each cumulated power with respect to the total.

C. *Printer (RQ8)*

RQ9: How much energy can we save by turning off the printer when it doesn't work?

This is the overall data of the energy consumption of the printer in the Active – Standby profiles:

- Active: 11.93 kWh
- Standby: 21.29 kWh

The difference is important indeed, 2/3 of energy are used (wasted) in the standby mode.

TABLE IV. SERVERS' POWER CONSUMPTION PROFILES OBTAINED THROUGH CLUSTERING OF DATA

Servers	High power profile 1 (W)	High Power Profile 2 (W)	Low Power Profile (W)
Server 1	~138	~105	~8
Server 2	~185	~146	~14
Server 3	~245	~160	~3

TABLE V. SERVERS' POWER CONSUMPTION COMPARISON BETWEEN DAY AND NIGHT

Server	95% Diff C.I. Between Day/Night (W)	P- val	Different?
Server 1	{-1.00 e-05, -1.80 e-05}	0.05	YES
Server 2	{3.86 e-05 , 4.22 e-05}	0.01	YES
Server3	{ 0.625 , 0.937 }	< 2.2e-16	YES

TABLE VI. CUMULATIVE POWER CONSUMPTION BY PROFILES

Servers	High power profile 1		High Power profile 2		Low power profile	
	kWh	%	kWh	%	kWh	%
Server 1	20.37	3.75	523.05	96.21	0.22	0.04
Server 2	33.57	4.62	692.2	95.17	1.57	0.22
Server 3	89.09	13.82	554.25	85.98	1.29	0.2

 ISBN: 978-1-61208-136-6

IV. CONCLUSIONS AND FUTURE WORK

We analyzed the power consumption in the last months of the equipment in the research center ISMB, affiliated to our University. We monitored at high level data about conditioning and lighting systems and general devices and we conducted a more detailed analysis on the servers and the printer. We draw from the statistical analysis and the answers of the research questions the following facts, and related further questions for future work.

Servers

Fact 1. We found differences between the power consumptions of the three servers (RQ4), likely determined by software usage, not by hardware equipment. In fact, despite Server 1 has a more powerful hardware equipment (CPU, memory), it has the lowest power consumption.

Fact 2. The power consumption of servers is not homogeneous over time (RQ5).

There are several peaks. Peaks are determined by software usage: as a matter of fact, Server 3 consumes up to 75% more when it is used for graphical operations.

Fact 3. Servers have different power consumption profiles (RQ7). This is determined by software usage.

Fact 4. Conditioning and lighting for servers consume more than computation (especially conditioning, that consumes approximately ten times more) (RQ3).

Fact 5. Low power profile (or Stand-by) for servers is useless (< 1%) (RQ7).

Fact 6. There is no substantial difference between day and night servers' power consumption (RQ7).

Printer

Fact 7. The printer consumed more energy in standby mode than in active mode (RQ9).

Indeed, in our analysis, with a mechanism able to turn off the printer when it doesn't work, 21 kWh would have been saved in the period March-November 2010, which is the 64% of the printer's total power consumption in that time range. Or, alternatively, shutting down the printer during night, it is possible to save the standby power consumption (13 W, despite the 9W declared in the technical sheet), that means to save 47.45 KWh per year.

Even if this analysis is very initial, and specific to few machines that may not be representative of the whole population, we believe it points out some simple checks that every energy manager should do as a first step to reduce energy consumption: consumption of conditioners and lighting, consumptions of printers in idle mode, consumption of servers both over day and night. Moreover, data we have presented could be compared to other analysis on equipment with similar characteristics.

Future work will be devoted to understand more the reasons of the behaviors observed. Notably to investigate deeper the motivations of the differences of servers power consumptions, and to verify them experimentally by setting up different configurations/conditions in the machines to evaluate their impact on power consumption. Secondly, we will repeat the same analysis on the Data Elaboration Center of our university, and we will compare it with the data presented in this paper. We think that the research questions that drove this analysis could be adopted and answered by other researchers in different universities and centers: building up a common benchmark of power consumption, it is possible to identify common and efficient solutions that can be then exported in industry and society.

ACKNOWLEDGMENTS

Authors thank Antonino Fiume for his precious help in the handling with the monitoring system youmeter [11], and Maurizio Molinaro for his help in collecting information at ISMB.

REFERENCES

[1] L. Chiaraviglio and M. Mellia, "PoliSave: Efficient Power Management of Campus PCs", Telecommunications and Computer Networks (SoftCOM), 2010 International Conference on, Publication Year: 2010, Page(s): 82 - 87

[2] J. A. Roberson, C. Webber, M. McWhinney, R. Brown, M. Pinckard, and J. Busch, "After-hours Power Status of Office Equipment and Energy use of Miscellaneous Plug-load Equipment", Report LBNL-53729-Revised, LBNL, Berkeley, CA, Pubblication Year: 2004

[3] SMART 2020 Report, “Enabling the low carbon economy in the information age”, http://www.theclimategroup.org

[4] D. Bein, W. Bein, and S. Phoha, "Efficient Data Centers, Cloud Computing in the Future of Distributed Computing", Information Technology: New Generations (ITNG), 2010 Seventh International Conference on, Publication Year: 2010, Page(s): 70 - 75

[5] S.Herat, "Sustainable Management of Electronic Waste (e-Waste)", CLEAN – Soil, Air, Water, Volume 35, Issue 4, Publication Year: 2007, Page(s) 305–310

[6] Y. Wati and K. Chulmo, "The Green IT Practices of Nokia, Samsung, Sony, and Sony Ericsson: Content Analysis Approach", 43rd Hawaii International Conference on System Sciences (HICSS), Publication Year: 2010, Page(s): 1 - 10

[7] T. DeMarco, "Controlling software projects: management, measurement & estimation", ISBN: 0917072324, Publisher: Prentice Hall, Publication Year: 1986

[8] D. Estrin, "Participatory sensing: applications and architecture [Internet Predictions]", IEEE Internet Computing, Volume 14, Issue 1, Pubblication Year: 2010, Page(s) 12-42

[9] L. Sachs, "Applied Statistics - A Handbook of techniques", ISBN: 0387909761, Publisher: Springer, Publication Year: 1978

[10] P.Tan, M. Steinbach, and K. Vipin, "Introduction to Data Mining", ISBN: 0321321367, Publisher: Addison-Wesley, Publication Year: 2005

[11] https://www.youmeter.it/youmeter/ , last access 7th March 2011

 ISBN: 978-1-61208-136-6

Optimal Scheduling of Smart Homes Energy Consumption with Microgrid

Di Zhang and Lazaros G. Papageorgiou
Department of Chemical Engineering
University College London
London WC1E 7JE, U.K.
e-mail: l.papageorgiou@ucl.ac.uk

Nouri J. Samsatli and Nilay Shah
Centre for Process System Engineering
Imperial College
London SW7 2BY, U.K.
e-mail: n.samsatli@imperial.ac.uk

Abstract—**Microgrid is taken as the future Smart Grid, and can work as a local energy provider to domestic buildings and reduce energy expenses. To further lower the cost, a Smart Homes idea is suggested. Smart Homes of the future will include automation systems and could provide lower energy consumption costs and comfortable and secure living environment to end users. If the energy consumption tasks across multiple homes can be scheduled based on the users' requirement, the energy cost and peak demand could be reduced. In this paper the optimal scheduling of smart homes' energy consumption is presented using mixed-integer linear programming. In order to minimize a one-day forecasted energy consumption cost, operation and electricity consumption tasks are scheduled based on different electricity tariffs, electricity task time window and forecasted renewable energy output. A case study of thirty homes with their own microgrid indicates the possibility of cost saving and asset utilization increase.**

Keywords: planning/scheduling; smart homes; microgrid; mixed-integer linear programming; optimization

I. INTRODUCTION

The future electricity distribution system will be meshed and intelligent and better known as Smart Grid, which includes advanced digital meters, distribution automation, communication systems and distributed energy resources. The desired Smart Grid functionalities include self-healing, optimizing asset utilization and minimizing operations and maintenance expenses [1]. As Smart Grid of the future, microgrid is considered to enable widespread inclusion of renewable resources, distributed storage and demand response programs in distribution [2].

Several studies have considered how to design the capacity of a microgrid system to minimize the annual cost [3]–[5]. A computer program that optimizes the equipment arrangement of each building linked to a fuel cell network and the path of the hot-water piping network under the cost minimization objective has also been developed [6]. Energy management systems and optimal scheduling of microgrid have been produced to generate an optimum operation plan for a microgrid [7]–[9]. Hawkes and Leach [10] presented a linear programming cost minimization model for the high level system design and corresponding unit commitment of generators and storages within a microgrid. Compared with centralized generation, the sensitivity analysis of results to variations in energy prices indicates a microgrid can offer an economic proposition. This model can provide both the optimized capacities of candidate technologies as well as the operating schedule.

This paper considers a residential building with its own microgrid, distributed energy resources and automation system. The idea of the smart home originated from the concept of home automation, which provides some common benefits to the end users, which include lower energy costs, provision of comfort and security and provision of home-based health care and assistance to elderly or disabled users [11]. Several works have been proposed to achieve the energy conservation and management perspectives [12]–[16] but these scheduling optimization models only consider operation scheduling based on the given energy profile. Derin and Ferrante [17] described a model that concerns both operation scheduling and electricity consumption tasks order scheduling. However, their results indicate relatively a high computation time to schedule only three electricity consumption tasks.

Scheduling tasks subject to limited resources is a well known problem in many areas of the process industry and of other fields [18]–[22] but there are differences for the scheduling of electrical appliances. In this work, the objective is to minimize the total one-day-ahead expense of the Smart Homes' energy consumption, including the operation and energy cost. Both operation of the distributed energy generation technologies and domestic electrical appliances are scheduled based on the electricity price at each time interval, the renewable energy output forecast, subject to constraints on the starting and ending time for each appliance.

The rest of this paper is organized as follows: the mathematical model is shown in Section II, the case study is presented in Section III, the optimal results are given in Section IV, and the discussion and conclusions are given in Section V.

II. MATHEMATICAL MODEL

The smart homes power consumption scheduling problem is formed as a mixed integer linear programming model. The daily power consumption tasks are scheduled based on their given operation time window (earliest starting time and latest ending time), and the objective is to minimize the daily power cost and shave the power consumption peak. It assumes the smart building system has its own microgrid and some decentralized resources (such as wind generator,

 ISBN: 978-1-61208-136-6

CHP generator, boiler, thermal storage and electrical storage) to provide the basic electricity and also it has a grid connection to obtain electricity during peak hours or sell electricity to the grid when there is surplus electricity generation. Since this model only provides the optimal scheduling for one day, equipment capacity selection is not considered and all the equipment capacities are given. The electricity price profile from the grid is given and may vary according to time of day. The model also assumes the weather forecast can provide 24 hour wind speed data.

A list of the notation used in the MILP model is given below:

Indices

i	tasks
j	homes in the smart building
t	time interval

Parameters

a_t	electricity price at time t (£/kWh$_e$)
A	wind generator blade area (m^2)
C_i	power consumption capacity of task i
C_{CHP}	CHP generator capacity (kW$_e$)
C_{WIND}	wind generator capacity (kW$_e$)
C_B	boiler capacity (kW$_{th}$)
C_{ELE}	electrical storage capacity (kWh$_e$)
C_{THS}	thermal storage capacity (kWh$_{th}$)
CH_{ELE}	electrical storage charge limit (kW$_e$)
CH_{THS}	thermal storage charge limit (kW$_{th}$)
DI_{ELE}	electrical storage discharge limit (kW$_e$)
DI_{THS}	thermal storage discharge limit (kW$_{th}$)
$E_{j,i}$	latest ending time of task i in home j
H_t	head demand at time t (kW$_{th}$)
m_{ELE}	cost per unit input (maintenance) for electrical storage unit (£/kWh$_e$)
m_{THS}	cost per unit input (maintenance) for thermal storage unit (£/kWh$_{th}$)
m_{WIND}	wind generator maintenance cost (£/kWh$_e$)
n_E	electricity selling price (£/kWh$_e$)
n_G	price of natural gas (£/kWh)
$P_{j,i}$	processing time of task i in home j
$S_{j,i}$	earliest starting time of task i in home j
v_t	wind speed (m/s)
wi_t	output from wind generator at time t (kW$_e$)
α	CHP generator electrical efficiency
β	boiler efficiency
γ	CHP heat-to-power ratio
δ	Time interval duration (hour)
ρ	air density (kg/m^3)
η_{ELE}	electrical storage charge/discharge efficiency
η_{THS}	thermal storage charge/discharge efficiency
η_W	wind generator efficiency

Positive Variables

Ex_t	electricity exported to the grid at time t (kW$_e$)
f_t	thermal storage discharge rate at time t (kW$_{th}$)
g_t	thermal storage charge rate at time t (kW$_{th}$)
In_t	electricity imported from the grid at time t (kW$_e$)
ISe	initial state of electrical storage (kWh$_e$)
ISt	initial state of thermal storage (kWh$_{th}$)
Q	daily electricity cost of a home (£)
Se_t	electricity in storage at time t (kWh$_e$)
St_t	heat in storage at time t (kWh$_{th}$)
wc_t	output from CHP generator at time t (kW$_e$)
x_t	output from boiler at time t (kW$_{th}$)
y_t	electrical storage discharge rate at time t (kW$_e$)
z_t	electrical storage charge rate at time t (kW$_e$)

Binary Variables

$Te_{j,i,t}$	1 if task i in home j ends at time t, 0 otherwise
$Ts_{j,i,t}$	1 if task i in home j starts at time t, 0 otherwise
$w_{j,i,t}$	1 if task i in home j is done at time t, 0 otherwise

The constraints imposed on the optimization are:

A. *Capacity constraints:*

The output from each equipment should not be over its designed capacity,

CHP generator:

$$wc_t \le C_{CHP} \quad \forall 1 \le t \le T \tag{1}$$

Boiler:

$$x_t \le C_B \quad \forall 1 \le t \le T \tag{2}$$

Electrical storage:

$$Se_t \le C_{ELE} \quad \forall 1 \le t \le T \tag{3}$$

Thermal storage:

$$St_t \le C_{THS} \quad \forall 1 \le t \le T \tag{4}$$

B. *Energy storage constraints*

Electricity stored in the electrical storage at time t is equal to the amount stored at $t - 1$ plus the electricity charged minus the electricity discharged.

$$Se_t = Se_{t-1} + z_t \eta_{ELE} \delta - y_t \delta / \eta_{ELE} \quad \forall 1 \le t \le T \tag{5}$$

Electricity stored must return to the initial state at the end of the day (no nett accumulation over the whole day),

$$Se_0 = Se_T = ISe \tag{6}$$

The rates of discharge or charge of electricity cannot exceed the electrical storage discharge and charge limits:

$$y_t \le DI_{ELE} \quad \forall 1 \le t \le T \tag{7}$$

$$z_t \le CH_{ELE} \quad \forall 1 \le t \le T \tag{8}$$

 ISBN: 978-1-61208-136-6

Heat stored in the thermal storage at time t is equal to the amount stored at $t-1$ plus the heat charged minus the heat discharged.

$$St_t = St_{t-1} + g_t \eta_{THS} \delta - f_t \delta / \eta_{THS} \quad \forall 1 \le t \le T \tag{9}$$

Stored heat must return to the initial state at the end of the day,

$$St_0 = St_T = ISt \tag{10}$$

The rates of discharge and charge of heat cannot exceed the thermal storage discharge and charge limits:

$$f_t \le DI_{THS} \quad \forall 1 \le t \le T \tag{11}$$

$$g_t \le CH_{THS} \quad \forall 1 \le t \le T \tag{12}$$

C. Wind generator ouput

The electricity output from the wind generators is calculated from the wind power generation equation:

$$wi_t = 0.5 \rho A v_t^{\,3} \eta_W \quad \forall t \tag{13}$$

D. Energy balances

The electricity consumed during each time period is supplied by the wind generator, CHP generator, electricity received from the electrical storage and grid minus electricity sent to the electrical storage and grid.

$$\sum_j \sum_i w_{j,i,t} C_i = wi_t + wc_t + y_t - z_t + In_t - Ex_t \quad \forall 1 \le t \le T \tag{14}$$

The heat consumed during each time period is supplied by the CHP generator, boiler, heat received from the thermal storage minus heat sent to the electrical storage.

$$H_t = wc_t \gamma + x_t + f_t - g_t \quad \forall 1 \le t \le T \tag{15}$$

E. Starting time and finishing time

The starting time of each task cannot be earlier than the given earliest starting time,

$$\sum_{t \ge S_{j,i}} Ts_{j,i,t} = 1 \quad \forall j,i \tag{16}$$

The finishing time of each task cannot be later than the latest ending time,

$$\sum_{t \le E_{j,i}} Te_{j,i,t} = 1 \quad \forall j,i \tag{17}$$

If a task starts at time t, it must end at time t plus its processing time, $P_{j,i}$,

$$Ts_{j,i,t} = Te_{j,i,t+P_{j,i}} \quad \forall j,i,1 \le t \le T - P_{j,i} \tag{18}$$

All tasks must operate continuously from their starting time to their ending time.

$$w_{j,i,t} = w_{j,i,t-1} + Ts_{j,i,t} - Te_{j,i,t} \quad \forall j,i,1 \le t \le T \tag{19}$$

F. Objective function

The objective function is to minimize the total daily electricity cost, which includes: the operation and maintenance cost of the CHP generator, wind generator, electrical storage and thermal storage; the cost of electricity purchased from the grid; the revenue from electricity sold to the grid. Since the equipment capacities are fixed, their capital costs are independent of the schedule and are therefore not considered.

$$Q = \sum_t [(wc_t n_G / \alpha + wi_t m_{WIND} + In_t a_t - Ex_t n_E + x_t n_G / \beta + y_t m_{ELE} + f_t m_{THS}) \delta] \tag{20}$$

III. CASE STUDY

The case study building system has 30 homes with the following energy suppliers:

- one CHP generator with a capacity of 40kW$_e$ its electrical efficiency is 35%, heat to power ratio is 1.3, and natural gas cost is 2.7p/kWh;
- one wind farm with a capacity of 10kW$_e$ and a maintenance cost of 0.5p/kWh$_e$;
- one boiler with capacity of 85kW$_{th}$ and natural gas cost is 2.7p/kWh;
- one electrical storage unit with a capacity of 10kW$_e$h; the charge/discharge efficiency is 95%, discharge limit and charge limit are both 10kW$_e$, and the maintenance cost is 0.5p/kWh$_e$;
- one thermal storage unit with a capacity of 20kW$_{th}$h; the charge/discharge efficiency is 98%, discharge limit and charge limit are both 20kW$_{th}$, and the maintenance cost is 0.1p/kWh$_{th}$;
- a grid connection (allowing import and export of electricity when operating parallel to the grid); the electricity price at different times is collected from Balancing Mechanism Reporting System [23] and shown in Fig.1 and when electricity is sold to the grid, it is 1p/kWh$_e$;

Each time interval is half an hour, so in total there are 48 time intervals. The total heat demand profile is generated for a building with floor area of 2500m^2 on a sample winter day using CHP Sizer Version 2 Software [24]. For the electricity demand, each home has 12 basic tasks that consume electricity as shown in Table I. These tasks are available to

 ISBN: 978-1-61208-136-6

be scheduled according to the given earliest starting time, latest finishing time, their respective processing times and power requirements [25].

In this case study, there are 10 identical wind generators, with an efficiency of 47%. The blade diameter is 1.6m and the wind speed is generated from a Weibull distribution using MATLAB with a mean velocity of 7m/s. The cut-in and cut-out wind speeds are respectively 5m/s and 25m/s, and the nominal wind speed is 12m/s. The wind generators do not produce any power when the wind speed is under the cut-in speed or above the cut-out speed. When the wind speed is above the nominal wind speed, the power output is at the maximum output, which is equal to the output produced at the nominal wind speed. Between cut-in and nominal wind speed, the wind generator power output varies according to equation 13.

IV. RESULTS

A. *Results with earliest starting time*

The starting time of the case study is from 8am and the ending time is 8am the next morning. The earliest starting case (a scheduling heuristic) means all the domestic electricity appliances are turned on at their given earliest starting time. It is similar to common living habits: for example, the washing machine would be turned on as soon as people want to do some washing, most probably when people leave home for work in the morning. The optimal heat balance resulting from this case is shown in Fig. 2 and the optimal electricity balance is shown in Fig. 3. Equipment operation time from each technique is scheduled accordingly to minimize the total operation cost. The electrical storage is used to store electricity when there is excess electricity; it is mainly for utilizing the wind generator output more efficiently. There is no excess electricity sold to the utility grid. With the earliest starting time schedule, the peak hours are mainly during the evening when occupants are back from work. During this time, about 51% of the total electricity is imported from the utility grid. The total cost is £144.6.

B. *Results with time window*

When a time window is allowed, the domestic tasks as well as the equipment operation time are scheduled in order to minimize the total electricity cost (equation 20). Tasks, such as interior lighting and fridge, have fixed electricity consumption time period and have no other alternatives. But tasks with flexible operation time can be scattered as much as possible to avoid electricity consumption peak and utilize electricity generated from local generators as much as possible. But when electricity is cheaper from grid, it will be imported instead of generating from generators. The optimal heat balance is shown in Fig. 4 and the optimal electricity balance is shown in Fig. 5. There are only two peak periods: early in the morning and in the evening. The other time periods have a flat electricity consumption. Only 30% of the total electricity is bought from the utility grid, electricity being mainly provided by the local distributed resources, and there is no electricity sold back to the utility grid. The total cost is £117.5, which is 18.7% lower than the earliest starting time case. The solution was obtained using CPLEX 11.0.1 in GAMS 22.7 on a PC with an Intel Core 2 Duo, 2.99 GHz CPU and 3.25GB of RAM. The model involved 36,770 equations with 53,510 continuous and 52,920 discrete variables. This case required 7.5 CPU s to solve.

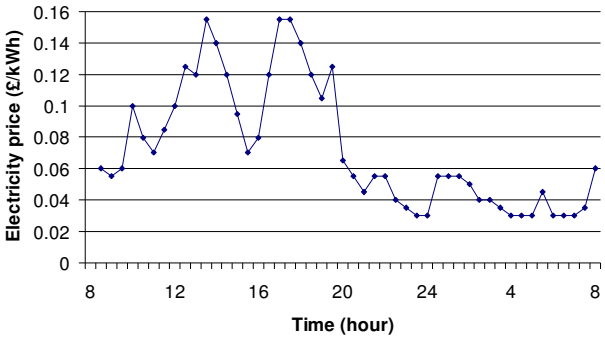

Figure 1. Electricity tariff (Jan 10th , 2010)

TABLE I. ELECTRICITY CONSUMPTION TASK

	Task	Power (kW)	Earliest starting time (hour)	latest Finishing time (hour)	Duration (hour)
1	Dish Washer	1	9	17	3
2	Washing machine	1	9	12	1.5
3	Spin Dryer	3	13	18	1
4	Cooker Hob	3	8	9	0.5
5	Cooker Oven	5	18	19	0.5
6	Cooker Microwave	1.7	8	9	0.5
7	Interior lighting	0.84	18	24	6
8	Laptop	0.1	18	24	2
9	Desktop	0.3	18	24	3
10	Vacuum cleaner	1.2	9	17	0.5
11	Fridge	0.3	0	24	24
12	Electrical car	3.5	18	8	3

 ISBN: 978-1-61208-136-6

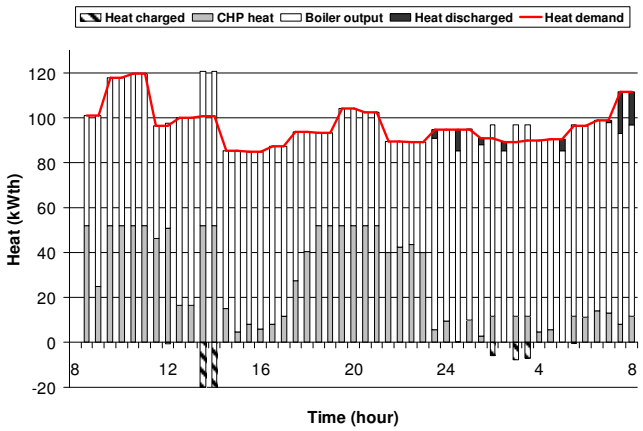

Figure 2. Heat balance with the earliest starting time

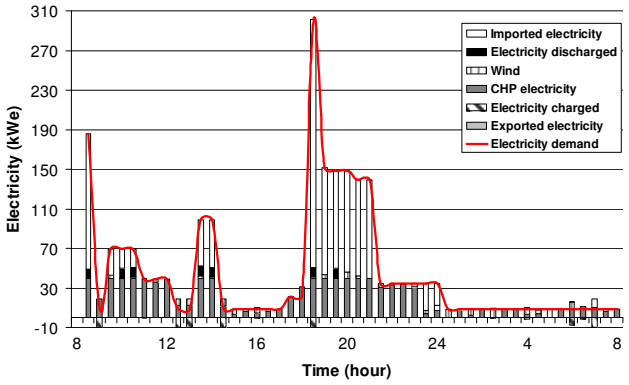

Figure 3. Electricity balance with the earliest starting time

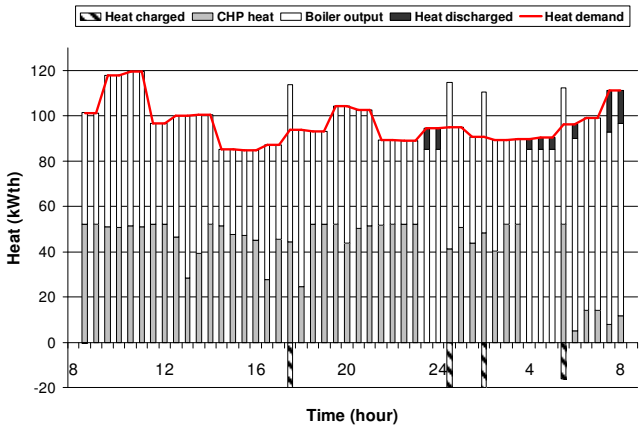

Figure 4. Heat balance with time window

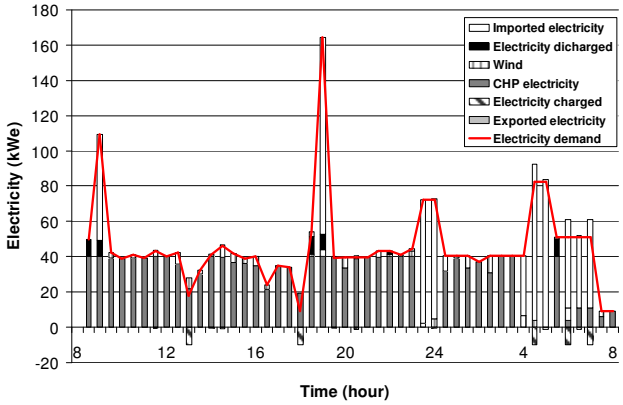

Figure 5. Electricity balance with time window

V. DISCUSSION AND CONCLUSIONS

In the case study, twelve domestic tasks from thirty homes are scheduled. Compared with the case where the tasks all start at their earliest possible starting time, the electricity consumption peak was decreased from 290kW to 165kW and the electricity consumption pattern became flatter. This peak shaving has the benefit of releasing the burden on the central grid and reducing the expense of up-grading the current grid infrastructure to fulfill increasing energy demand. The peak shaving also depends on the family living habits: for instance, they may prefer doing the washing during night time and would specify their own time window for the task. On the other hand, when the domestic task scheduling is implemented in real life, it could also affect people's behaviour.

Given the fixed heat demand profile used in these case studies, scheduling the tasks results in a more balanced heat supply than the earliest starting time case. This can be seen in Fig. 4, which shows that the CHP is providing more heat more steadily than in the earliest starting time case

The tasks shown are assumed to have constant power consumption over the processing time but this is not always realistic: e.g., washing machines have different power consumption during different stages of each program. Future scheduling models will need to account for tasks with time-varying power consumption.

The smart homes energy consumption scheduling problem is formulated as a mixed integer linear programming model. According to the case study for a winter day, it could provide 18.7% savings compared with the earliest starting time case (our current living habit). With the objective function, the tasks can be scheduled to coincide with the cheapest electricity price while keeping their operation within the desired time window. There are further benefits more when power is supplied by the wind generator. The power output from the wind generator is not constant and varies from hour to hour according to the weather conditions and other constraints. But when a weather forecast can be used to predict the power output during the next 24 hours, or even longer, the domestic tasks

 ISBN: 978-1-61208-136-6

can be scheduled to use the output of the wind generators when it is available, providing further savings for the customers. The scheduling formulation also increases the asset utilization, e.g., in the case study, the CHP generator was be used more efficiently and became the main supplier of electricity and heat.

In the area of Smart Grids, it is considered that there is two-way communication between the power supplier and the customers. The power will be distributed according to the demand and supply. Traditional methods provide the customers only peak price hours while the Smart Grid could provide real-time electricity pricing. The process of price recalculating is similar to real-time traffic monitoring, aiming for a balance between supply and demand. This model considers the problem from the point of view of the customers, with a fixed electricity price profile. In the future, it might be possible to include this model as part of a full Smart Grid model where the electricity price is determined as part of the optimization, along with the scheduling of tasks.

ACKNOWLEDGMENT

D.Z. would like to thank the Centre for Process System Engineering, Imperial College for financial support.

REFERENCES

[1] R. E. Brown, "Impact of smart grid on distribution system design," in Proc. 2008 IEEE Power and Energy Society General Meeting, pp. 1-4.

[2] J. Mitra and S. Suryanarayanan, "System analytics for smart microgrids," in Proc. 2010 IEEE Power & Energy Society General Meeting, Minneapolis, MN, Jul 2010.

[3] C. Marnay, G. Venkatarmanan, M. Stadler, AS. Siddiqui, R. Firestone and B. Chandran, "Optimal technology selection and operation of commercial-building microgrids," IEEE Transactions on Power Systems 2008; 23(3), pp. 975–982.

[4] H. Asano, H. Watanabe and S. Bando, "Methodology to Design the Capacity of a Microgrid," System of Systems Engineering, IEEE International Conference on 16-18 April 2007, 1 – 6, San Antonio, TX

[5] Y. Zhang, M. Mao, M. Ding, and L. Chang, "Study of Energy Management System for Distributed Generation Systems," Electric Utility Deregulation and Restructuring and Power Technologies, 2008, Third International Conference on 6-9 April, 2465 – 2469, Nanjuing.

[6] S. Obara, "Equipment arrangement planning of a fuel cell energy network optimized for cost minimization," Renewable Energy vol.32 (3), 2007, pp. 382-406.

[7] A. Bagherian and S.M.M. Tafreshi, "A developed energy management system for a microgrid in the competitive electricity market," PowerTech, 2009 IEEE Bucharest, June 28 -July 2 2009, 1 – 6, Bucharest.

[8] F.A. Mohameda and H.N. Koivob, "System modelling and online optimal management of MicroGrid using Mesh Adaptive Direct Search," International Journal of Electrical Power & Energy Systems, vol.32 (5), June 2010, pp. 398-407.

[9] H. Morais, P. Kadar, P. Faria, Z.A. Vale and H.M. Khodr, "Optimal scheduling of a renewable micro-grid in an isolated load area using mixed-integer linear programming," Renewable Energy, vol.35, 2010, pp. 151-156.

[10] A.D. Hawkes and M.A. Leach, "Modelling high level system design and unit commitment for a microgrid," Applied Energy, vol.86, 2009, pp. 1253-1265.

[11] M.A.A. Pesdrasa, T.D. Spooner and I.F. MacGill, "Coordinated Scheduling of Residential Distributed Energy Resources to optimize Smart Home Energy Services," IEEE Trans. on smart grid, vol. 1, September 2010, pp. 134-143.

[12] C.H. Lien, Y.W. Bai and M.B. Lin, "Remote-controllable power outlet system for home power management," IEEE Trans. Consumer Electronics, vol. 53, Nov. 2007, pp. 1654-1641.

[13] E. Sierra, A. Hossian, P. Britos, D. Rodrigurez and R. Garcia-Martinez, "Fuzzy control for improving energy management within indoor builing environments", in Proc. Electronics, Robotics and. Automotive Mechanics Conference on September 25-28 2007, pp. 412-416.

[14] S. Rojchaya and M. Konghirun, "Development of energy management and warning system for resident: An energy saving solution," in 6th Internation Conference on Electrical Engineering/Electronics, Computer, Telecommunication and Information Technology, vol. 1, May 2009, pp. 426–429.

[15] C.Y. Chen, Y.P. Tsoul, S.C.Liao and C.T. Lin, "Implementing the design of smart home and achieving energy conservation," in Proc. 7th IEEE internationl Conference. Industrial Informatices, June 23-26, 2009, pp. 273-276.

[16] E.Willias, S. Matthews, M. Breton and T. Brandy, "Use of a computer-based system to measure and manage energy consumption in the home," in Proc. IEEE International Symposium on Electronnics and Environment, May 8-11, 2006, pp. 167-172.

[17] O. Derin and A. Ferrante, "Scheduling energy consumption with local renewable micro-generation and dynamic electricity prices," In CPSWEEK/GREEMBED 2010: Proceedings of the First Workshop on Green and Smart Embedded System Technology: Infrastructures, Methods and Tools, Stockholm, Sweden, April 2010

[18] J.M. Pinto and I.E. Grossmann, "Assignment and Sequencing Models for the Scheduling of Process Systems," Ann. Oper. Res., vol. 81, 1998, pp. 433–466.

[19] J. Kallrath, "Planning and Scheduling in the Process Industry," OR Spectrum, vol. 24, 2004, pp. 219–250.

[20] C.A. Floudas and X. Lin, "Continuous-Time versus Discrete-Time Approaches for Scheduling of Chemical Processes: A Review," Comput. Chem. Eng., vol. 28, 2004, pp. 2109–2129.

[21] N. Shah, C.C. Pantelides and R.W.H. Sargent, "A General Algorithm for Short-Term Scheduling of Batch Operations. 2. Computational Issues," Comput. Chem. Eng., vol 17, 1993, pp. 229–244.

[22] C.L. Chen, C.L. Liu, X.D. Feng and H.H. Shao, " Optimal short-term scheduling of Multiproduct single-stage batch plants with parallel lines, " Ind. Eng. Chem. Res., vol 41, 2002, pp. 1249-1260.

[23] Balancing Mechanism Reporting System. http://www.bmreports.com. Last assessed Feb 11, 2011.

[24] Action Energy, CHP Sizer Version 2. The Carbon Trust: London, UK; 2004.

[25] Electropaedia. http://www.mpoweruk.com/electricity_demand.htm. Last assessed Feb 11, 2011.

 ISBN: 978-1-61208-136-6

Smard Grid Software Applications for Distribution Network Load Forecasting

Eugene A. Feinberg, Jun Fei
Stony Brook University
Stony Brook, NY 11794, USA
Eugene.Feinberg@sunysb.edu
Jun.Fei@stonybrook.edu

Janos T. Hajagos, Richard J. Rossin
Long Island Power Authority
Hicksville, NY 11801, USA
Janos.Hajagos@us.ngrid.com
Richard.Rossin@us.ngrid.com

***Abstract* — This paper describes three software applications for distribution network load forecasting in a Smart Grid environment: (i) short-term feeder load forecasting, (ii) short-term substation transformer load forecasting and transformer rating, and (iii) next-year load pocket forecasting. The short-term feeder load forecasting allows a utility to reduce the possibility of feeder overloading. The substation transformer load forecasting and transformer rating application achieves similar goals at the distribution substation level. The load pocket forecasting software allows a utility to estimate load trends at different locations (called load pockets), to estimate next-year peaks, to calculate weather normalized factors, and to estimate the probability distribution of the next-year peak load. The use of these software applications significantly improved the efficiency and reliability of the distribution network.**

Keywords: load forecasting, feeder, transformer, load pocket, SmartGrid

I. INTRODUCTION

One of the important aspects of emerging Smart Grid technologies is measuring, transmitting, storing and processing electric power system data, such as voltage, current, phase angle, etc., and using this information for system control and management. In particular, operators of traditional distribution networks often do not have complete information about certain parts of the network such as three-phase measurements at substations and feeders, measurements along feeders, and so on. In many cases, certain SCADA data are monitored, but not stored.

This paper describes particular applications that demonstrate how measuring, storing and processing substation and feeder load measurements can help improve the distribution network efficiency and reliability. The monitored data have been used to develop transformer and feeder load models and apply these models to load forecasting in the distribution network. In particular, this paper describes three applications: (i) short term (from one hour up to seven days) feeder load forecasting, (ii) short-term substation transformer load forecasting and transformer rating, and (iii) next-year load pocket forecasting and Weather Normalization Factor (WNF) computations.

The goal of the first application, the short-term feeder load forecasting, is to provide the system operators with advanced warnings on potential normal feeder overloading. Once such overloading signal is received, the operators can take several measures to avoid the undesired event. These measures include load switching, feeder reconfiguration, load reductions, and voltage control. In future Smart Grid applications, load reductions can be implemented by time-differentiated pricing.

The second application combines load forecasting with transformer rating. Both load and temperature forecasts are used as inputs to the transformer rating software. Again, the transformer rating results can be used by operators for switching and load reduction decisions to protect transformers.

The third application deals with area planning. The goal is to compute Weather Normalization Factors for various areas served by a utility. The WNF is a ratio of the normal annual load to the observed annual peak load for a particular area (also called load pocket). Different load pockets may have different WNFs. This is typically for two reasons: (i) different weather conditions in different areas, and (ii) different load mixtures (industrial, commercial, residential; small houses, large houses, apartment buildings, and so on) in different areas. WNFs play an important role in area planning and capital budgeting.

Electric load forecasting is a useful tool needed and used by most electric utility companies to make some important decisions including decisions on purchasing and generation of electric power, load switching, and area planning. By the forecasting horizon load forecasting can be divided into three types: short-term (one hour up to a week), medium-term (a month up to three years), and long-term (over three years) [1].

In the literature majority of the works on load forecasting can be classified into four categories by the modeling and forecasting method used, namely statistical, intelligent systems, neural networks and fuzzy logic [2]. A more complete literature review was presented in [3, chapter 12].

In a Smart Grid environment, the importance of forecasting increases because of the growing complexity of challenges and the availability of more data inputs from a data-rich smart grid environment [4]. Additional data inputs include AMI loads, price information, and additional information from the grid.

The sequel of the paper is organized as follows. In Section II we provide a brief description of the model. In Section III we discuss the software for short-term feeder load forecasting. Section IV focuses on short-term substation transformer load forecasting and transformer rating. In Section V we introduce the next-year load pocket forecasting

 ISBN: 978-1-61208-136-6

software. Discussions and conclusions are made in Section VI.

II. MODEL DESCRIPTION

The model, one version of which is described in [3], uses calendar information, weather information, and some additional information. We modified the model structure by adding an additive term. In mathematical terms the model is presented as

$$y_t=F_t(d_t, h_t, w_t, p_t) \\ =L_0(d_t, h_t)+L_1(d_t, h_t)\cdot f(w_t, p_t) + e_t, \quad (1)$$

where y_t is the actual load at time t;

L_0 is the weather-independent component;

L_1 is the normalized load, also independent of weather;

f is weather normalized factor;

d_t is the day of the week, 1, 2, …, 7;

h_t is the hour of the day, 0, 1, …, 23;

w_t are weather parameters including the temperature and humidity;

p_t are other factors including electricity prices, sunrise and sunset times;

e_t is a random error.

Similar to other statistical method, the model parameters are estimated using the historical data. The hourly weather information including ambient temperature and humidity measurements is provided by the NCDC (National Climatic Data Center). The hourly historical load data are extracted from the utility database. The applications need historical hourly load observations for at least one year.

To optimally estimate the parameters, we use the least square method and minimize the total squared residues, i.e.,

$$\min \Sigma_t[y_t - F_t(d_t, h_t, w_t, p_t)]^2. \quad (2)$$

Problem (2) is an unconstrained nonlinear optimization problem. Due to the excessive number of parameters and the mixture of discrete and continuous parameters in the model traditional methods such as trust region method, Newton-Raphson method, quasi-Newton method, double dogleg method, conjugate gradient method, and Levenberg-Marquardt (LM) method are not very efficient. Instead we found a convenient form of the function F, as in (1) above, and developed a recursive algorithm that estimates the parameters.

We used Mean Absolute Percentage Error (MAPE), Mean Absolute Deviation (MAD) and regression R^2 to measure the goodness-of-fit of the model. The definition of MAPE and MAD are

$$\text{MAPE}=\frac{1}{N}\sum_t \frac{|y_t - F_t|}{y_t}, \quad (3)$$

$$\text{MAD}=\frac{1}{N}\sum_t |y_t - F_t|, \quad (4)$$

where N is the number of observations used in the model.

The algorithm converges quickly, mostly in less than 10 steps. Figures 1-3 show the model Mean Absolute Percentage Error (MAPE), Mean Absolute Deviation (MAD), and model R-squared at different iteration steps. Figure 4 shows the scatter plot between the model result and actual load for a load pocket.

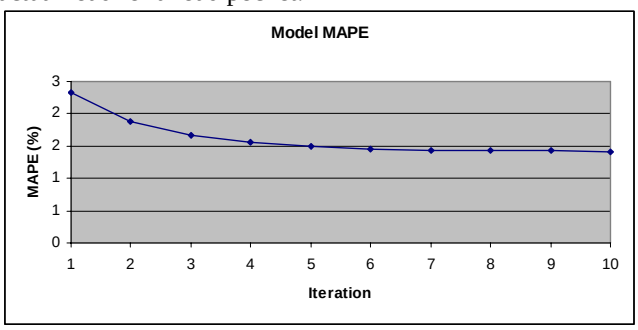

Figure 1. Model MAPE at different iteration steps

The model in (1) is relatively simple, robust and reliable. It can be easily used for different levels of forecasting: system level for an entire utility, substation/transformer level (load pocket), feeder level or even customer level load forecasting. It has been rigorously tested and used for years.

We remark that the installation of Advanced Meter Infrastructure (AMI) provides the possibility to use the AMI data to advance load models and improve load forecasts. We are currently investigating this approach.

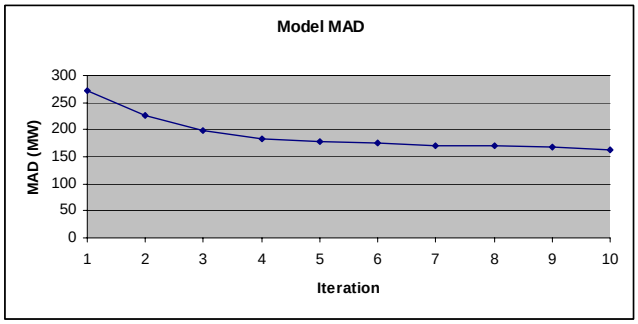

Figure 2. Model MAD at different iteration steps

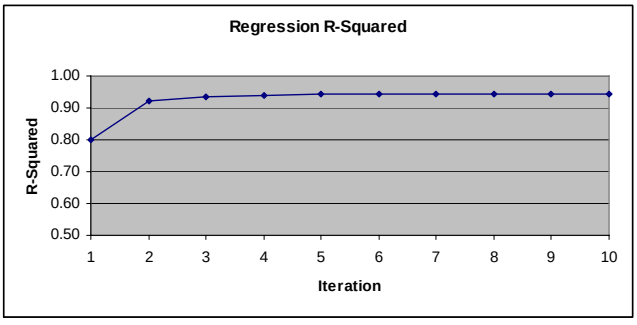

Figure 3. Regression R^2 at different iteration steps

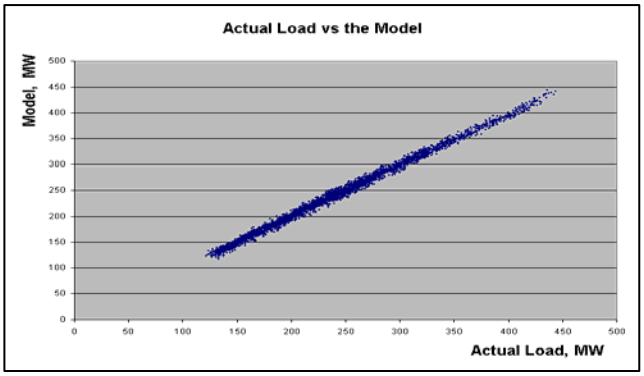

Figure 4. Scatter plot between model result and actual load

III. SHORT-TERM FEEDER LOAD FORECASTING

The goal of short-term feeder load forecasting is to provide the system operators with advanced warnings on potential normal feeder overloading. Once such an overloading warning is received, the operators can take several actions to avoid the overloading. These actions include load switching, feeder reconfiguration, load reductions, and voltage control. In future Smart Grid applications, load reductions can be implemented by time-differentiated pricing.

Our model can be easily adapted to provide feeder level load forecasting with a few additional procedures specially designed for feeder level load modeling and forecasting. These procedures include iterative filters during model training, periodic model updating, adaptive procedure and conservative adjustment.

The iterative filters are used to detect and exclude outliers in the training dataset. At each iteration step the Mean Absolute Percentage Error (MAPE) for the model is computed. The inclusion/exclusion criterion is to exclude all points with absolute percentage error greater than a certain threshold.

Periodic model updating is to use the most recent observations to replace the oldest observations in the original training dataset and build the model again on a periodic basis, say every two weeks.

Adaptive procedure uses the adaptive filtration technique to fit a simple linear regression between the actual load and the model result and then fine-tune the model result to reflect the most recent load pattern.

Conservative adjustment is implemented after the adaptive procedure by adding the underestimated amount at midnight (12AM) to the next day's forecasts. For example, if at midnight yesterday the actual load was 235 Amps but the forecast was 230 Amps, then 5 Amps will be added to the next day's forecasts. If the forecast was actually higher than the actual no adjustment is needed.

Another consideration in the implementation of feeder load forecasting is the heavy computation because sometimes there may be more than 1,000 feeders. The software was tested on actual feeders during summer peak times. It took at most 20 minutes to finish all calculations for about 140 feeders. The Mean Absolute Percentage Error (MAPE) was around 6%.

Figure 5 shows the actual and forecast loads (in Amps) for a feeder during June 1-July 9, 2010 in a Northeastern part of the USA.

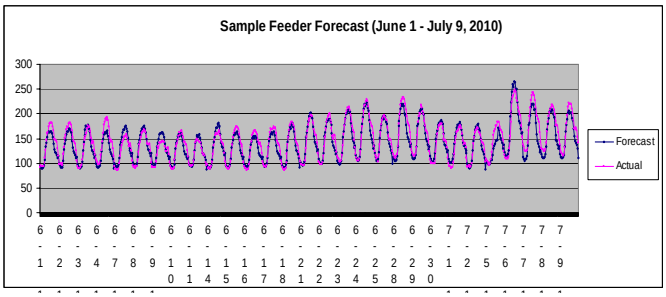

Figure 5. Actual and forecast loads for a sample feeder

IV. SHORT-TERM SUBSTATION TRANSFORMER LOAD FORECASTING AND TRANSFORMER RATING

Transformers are expensive assets to a utility. Overloading or overheating will generally reduce the useful life of a transformer. For this reason, it is important for a utility to make sure that their transformers are not overloaded or overheated. EPRI's PTLoad software can be used to determine a transformer's condition based on loading and temperature.

A developed application of short-term load forecasting to a transformer is shown in Figure 6. In the diagram load forecasts produced by load forecasting software are used as inputs to PTLOAD. PTLOAD calculates the transformer ratings and then the load forecasts as well as the transformer ratings are delivered to some internet based applications. For transformer level load forecasting, the accuracy of the one-day-ahead forecasts is around 4.5%.

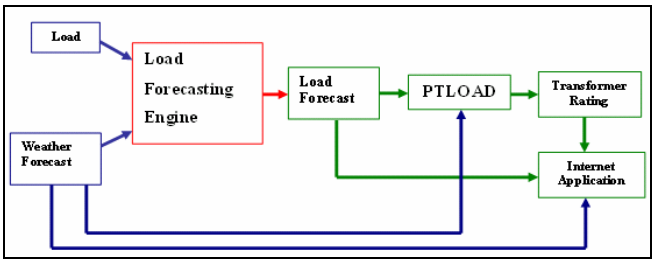

Figure 6. Application of short-term load forecasting

V. LOAD POCKET FORECASTING SOFTWARE

Load pockets refer to the aggregate of several close geographic areas [5]. It usually consists of a few substations or transformers. The concept provides flexibility in modeling regional loads. Our load pocket forecasting software makes the next year peak load forecasting.

For each load pocket, the software computes the model described in (1). In addition to the model performance graphs shown in Figures 1-4, it also estimates the weather normalized loads. Based on the historical weather data and the current model, the software simulates the current load

 ISBN: 978-1-61208-136-6

model on the historical weather data. A screenshot is shown in Figure 7. The user can select which of the past years to use to calculate the design-day parameters. The software analyzes and forecasts two types of peaks. The first type is the pocket peak, which is the maximal hourly load during the year. The second type is the system peak, which is the pocket load during the hour when the system experienced its peak.

One of the software inputs is the historical system peak dates and hours. Other inputs include historical hourly loads of distribution transformers and weather measurements, including temperature and humidity.

The software estimates historical peak days for load pockets (Figure 7). These are called pocket peak days and hours. The software then calculates the design-day parameters. For each load pocket, the design-day parameters are calculated for pocket peak days and for system peak days. Different load pockets may have different design days. An example of design-day parameters is presented in Tables II and III.

Once design-day parameters are calculated, the system calculates the ratio of the estimated load on the design day to the actual peak load. This ratio is known as the Weather Normalization Factor (WNF). The WNFs are useful in explaining what part of the annual load pocket peak is attributed to the specific weather conditions for that particular year. In addition, the software calculates weather-normalized trends as shown in Figures 8 and 9.

The software also contains a probability distribution calculator of the peak load for the next year (Figure 10). The user has two input parameters: the peak load value and the probability. The user can get the probability that the load will not exceed a particular value or get the value that the peak load will not exceed with a given probability. This peak distribution analysis is available for both pocket and system peak data. The software is used by area planners to compute WNFs and next year capital expenditure allocation.

Pocket Peak Dates
2010 Design Day

HH	DATE	LOAD	STRING	TEMP	DP	THI	THI DAILYMAX	THI DAILYMAX TIME	THI_4	THI_24	TEMP DAILYMAX	TEMP DAILY TIME
14	8/28/73	291	1	95	73	85	85	14	83	77	95	
14	6/10/74	275	1	90	72	82	82	12	82	74	94	
15	8/1/75	290	1	93	72	83	83	15	83	77	93	
16	8/25/76	262	0	87	70	80	80	16	78	71	89	
15	7/19/77	295	3	93	68	83	83	14	82	77	95	
14	8/17/78	269	2	88	74	81	82	12	81	78	89	
15	8/1/79	270	2	86	75	81	81	15	80	77	86	
15	8/27/80	285	1	92	64	81	81	13	81	75	92	
16	7/9/81	295	2	95	70	84	84	15	84	78	95	
15	7/26/82	264	1	91	63	80	80	15	80	74	91	
16	7/15/83	278	0	94	66	83	83	16	81	74	94	
13	6/11/84	273	3	89	71	81	81	13	80	75	89	
15	9/6/85	272	3	90	69	81	81	15	80	77	90	
17	7/7/86	282	1	95	68	84	84	18	83	74	95	
16	7/21/87	276	1	93	64	82	82	16	81	75	93	
15	8/12/88	283	4	87	76	81	82	13	82	78	88	

Go Back | Export | Get WNF

Figure 7. Pocket Peak Dates (2010 Design Day)

Figure 7 shows pocket peak dates, the dates on which the pocket attained the maximal load during that year. Also shown are peak hours and weather parameters during those hours.

Pocket WNFs using 2010 Design Day

2010 Design Day

TEMP	92
TEMP_DAILYMAX	92
TEMP_DAILYMAX_HOUR	14
STRING	2
THI	82
THI_DAILYMAX	83
THI_4	82
THI_24	77

Get Peak Distribution | Export | Go Back

LOADS AND WNFS AT POCKET PEAK DAYS

YEAR	DESIGN DAY LOAD	PEAK LOAD	WNF	Date	Hour
2001	331.3	345.3	0.9558	8/8/2002	16
2002	343.8	326.8	0.9913	7/29/2003	17
2003	348.2	341.8	1.0153	6/26/2004	17
2004	354.5	312.6	1.1006	8/4/2005	16
2005	304.6	296.2	1.0265	8/3/2006	16
2006	318.3	328.2	0.9353	8/3/2007	15
2007	292.7	285.5	1.0227	8/8/2008	17
2008	288.1	275.8	1.0444	6/10/2008	16

TRENDS

Year	Trend
2001 - 2002	1.0377
2002 - 2003	1.0128
2003 - 2004	1.0181
2004 - 2005	0.8592
2005 - 2006	1.045
2006 - 2007	0.9196
2007 - 2008	0.9843
2008 - 2009	0.9023

Figure 8. Normal Weather and Pocket WNFs

Figure 8 shows the WNFs calculated using the pocket peak dates and the year-to-year trends. A user may modify the last trend based on personal judgment.

 ISBN: 978-1-61208-136-6

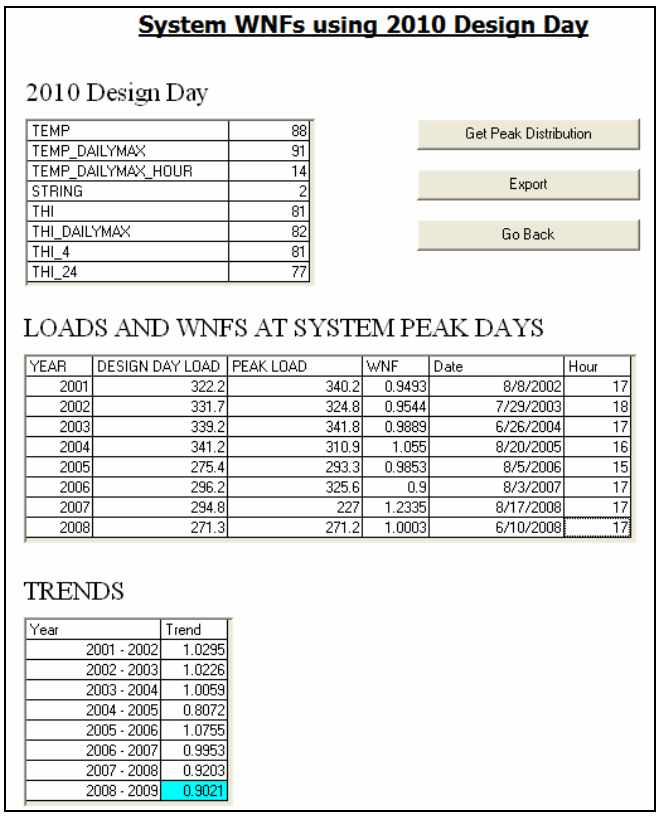

Figure 9. Normal Weather and System WNFs

Figure 9 is similar to Figure 8, but the WNFs are calculated using the system peak dates. Again, a user may modify the last trend.

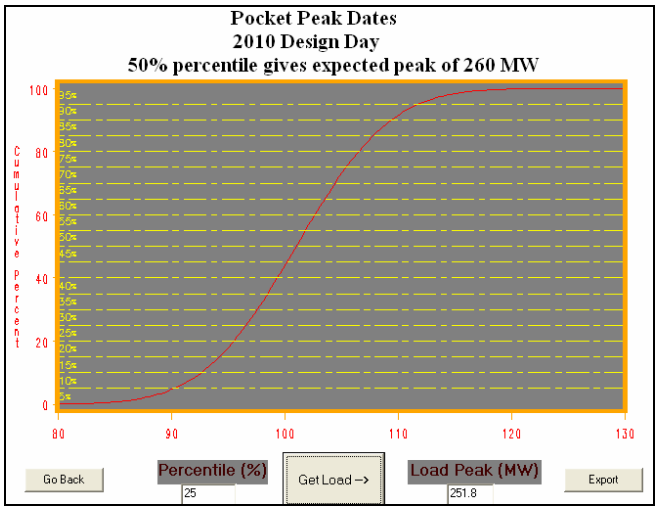

Figure 10. Peak Distribution Screenshot

Figure 10 shows the calculator for peak load distribution. A user can find the load value by entering the percentile (%), or find the percentile (%) by entering a load value. The 50th percentile corresponds to the expected peak.

VI. Discussions and Conclusions

This paper discusses three applications of distribution network load forecasting in the Smart Grid environment, where the SCADA data are stored, processed and the results of analysis are used to improve the system reliability and efficiency. The short-term feeder load forecasting enables operators to take appropriate measures in case of the potential overloading. These measures include load switching, feeder reconfiguration, load reduction and voltage control. The use of the application improves the reliability of the distribution network.

The substation transformer load forecasting and transformer rating application computes the transformer rating by combining load forecasts and temperatures and provides operators with warning of potential transformer overloading/overheating. The use of the application protects transformers from being overloaded or overheated.

The load pocket forecasting software allows a utility to estimate load trends at different load pockets, to estimate next-year peaks, to calculate weather normalized factors, and to estimate the probability distribution of next-year peak load. The use of this software improves the decision-making capabilities of area planning and capital budgeting and the reliability of service to the customers.

References

[1] H. L. Willis, Spatial Electric Load Forecasting, New York, Marcel Dekker, 1996.

[2] A. D. P. Lotufo and C. R. Minussi, Electric power systems load forecasting: a survey, presented at the IEEE Power Tech Conference, Budapest, Hungary, 1999.

[3] E. A. Feinberg and D. Genethliou, Applied Mathematics for Restructured Electric Power Systems: Optimization, Control, and Computational Intelligence (J.H. Chow, F.F. Wu, and J.J. Momoh eds), Spinger, pp. 269-285, 2005.

[4] How Does Forecasting Enhance Smart Grid Benefits?, SAS Institute, White Paper no 104501_S52140.0510, 2010

[5] E. A. Feinberg, D. Genethliou, J. T. Hajagos, B. G. Irrgang, and R. R. Rossin, Load Pocket Forecasting Software, Proceedings of 2004 IEEE Power Systems Conference & Exposition, New York, October 10-13, 2004

 ISBN: 978-1-61208-136-6

Non-intrusive Appliance Monitoring Now: Effective Data, Generative Modelling and LETE

Chi-Cheng Chuang, Today J. T. Sung, Gu-Yuan Lin, Jimi Y. C. Wen
Networks and Multimedia Institute
Institute for Information Industry
Taipei, TAIWAN
polon, today, guyuan, jimi @nmi.iii.org.tw

Ray-I Chang
Dept of Eng. Science and Ocean Eng.
National Taiwan University
Taipei, TAIWAN
rayichang@ntu.edu.tw

***Abstract*—Monitoring energy consumption at appliance level is a necessary condition for many energy efficient applications. In this paper, we have identified non-intrusive load monitoring (NILM) as a transitional technology, and competing NILM methods must be evaluated not only on performance, but also economical feasibility and user usability of now. Since in the event of maturing an IoT infrastructure, there would be no need for NILM. In this paper, we proposed a NILM for now, a complete solution with novel features: i) pre-processing for effective data, thus more accurate and faster training for user. ii) generative modelling for appliance configuration states, thus without the need for exhaustive training, and iii) LETE algorithm for a simple stateful enhancement. Experiments show the proposed methodology perform well even under only the most simplistic assumptions.**

***Keywords-Energy Management System, Non-Intrusive Load Monitoring, Appliance Monitoring.*;**

I. INTRODUCTION

In an effort to become a smarter energy world, the movement towards smart grid infrastructure along with the advances in information communication technologies, there is a need for consumer energy management system. Energy management on the consumer side can be monitoring, planning, control consumer's energy consumption. To reduce waste in energy consumption, building occupants and facilities managers need to better understand how buildings use energy, broken down over space and time through appliance monitoring [1]. Today, however, energy usage statistics are usually available only in the *aggregate* and monthly time resolution or sometimes in 15 minute intervals with the advance metering infrastructure. *Disaggregated* energy usage statistics are more useful than *aggregated* when implementing new efficient energy services, e.g., bill disaggregation, high bill resolution, incentive plan based on individual appliances, bad user usage or appliance operation diagnostics [2].

This ideal paradigm of smarter energy aligns with the developments towards the Internet of Things (IoT) [3], i.e., all things or significant appliances will be connected to the internet with the capability to upload energy usage statistics. There are few obstacles against the disruptive technology of IoT: i) legacy systems, i) cost of communication devices and iii) infrastructure including network protocols to service applications. For *now*, the cost of adding additional sensors to appliance individually is not feasible, economically, for most appliances especially at home. Thus there exists a window of opportunity, before we reach the confirmation stage of IoT for smarter energy applications, to develop a transition technology, viz. the disaggregation of energy usage consumption using algorithms, devices, deployments methods, etc. This dis-aggregating of energy usage is non-intrusive load monitoring (NILM).

There are several approaches on formulating this NILM problem by making different assumptions on the signal properties, environment, application scenario, etc. Here we first make the distinction between NILM and appliance recognition type approaches. These approaches aim to recognize which unknown appliance is operating and does not aim to do disaggregation. Disaggregation is important to reduce cost using less sensors and communication devices. Aggregated load can be analyzed on the transient state or power line noise or the steady-state. Steady-state can also be divided into enveloped-based or harmonic-based. However methods that analyze on the transient or harmonics or noise require a much higher sampling rate from 1 kHz to even 1 MHz, which require either one or both of the following support which are not quite yet the state of the art: i) higher communication bandwidth infrastructure to transmit larger data, ii) additional micro controller chip on the meters to perform more complex NILM. When such a support is ready, NILM is probably not needed.

In additional to monitoring from appliance load, it is also possible other modes of (ambient) signals, such as light, acoustic, vibration, motion, RIFD tags electro-magnetic interference, etc. The assumption for using these multi-modal sensors, is that these ambient sensors are already in everyday house-hold or commercial buildings for various *ubiquitous computing* applications. We do not believe this assumption is a viable candidate as a transitional technology before the full maturation of IoT. Since i) the sensing, computation, network structure required for such ubiquitous sensing is

 ISBN: 978-1-61208-136-6

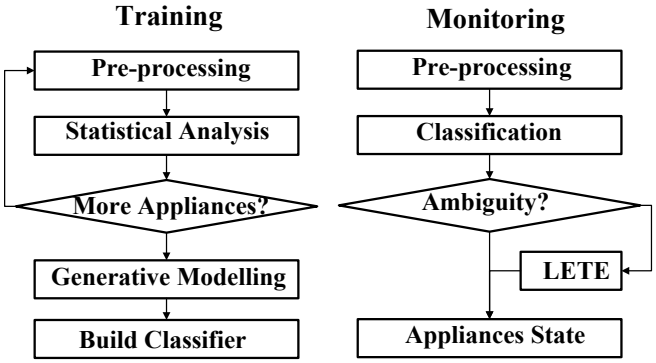

Figure 1: Overview of the proposed methodology for the training stage and the monitoring stage.

essentially a mature IoT infrastructures. Furthermore ii) under such assumptions, appliance of significance would need to be controlled or automated intelligently therefore communication device for the downlink is a necessary condition as well as the uplink. Some methods leverage the knowledge of an given environment, e.g., Jiang et al. proposed to disaggregate specific appliance load under a tree structure [1]. This requires domain experts to customize sensor deployment with specific load distributions, which would not be economically-feasible for most users. Schoofs proposed a niche solution to leverage networked business equipment through LAN network [4].

To attract users to NILM, methodologies should be inexpensive, simple, ready to use and provide the services that are demanded. This paper is structured as follows: in Section II, we present a total solution with the following contributions: i) pre-processing effective data, ii) generative appliance model for simpler training and iii) least effort transition enhancement (LETE) for more accurate and stateful monitoring. Experiments and related work are discussed in Section III and Section IV. We conclude in Section V.

II. Methodology

In this section, we discuss the methodology of the proposed NILM solution as can be seen in Fig. 1(a) and (b) for the training and monitoring stage respectively. In the training stage, the energy usage statistics, namely the load, is pre-processed before the statistical modelling is carried out. An individual appliance model is next computed for all appliances. Finally a statistical generative appliance configuration model is formed using a naïve Bayesian classifier. Pre-processing is also done during the monitoring stage. Classification of the appliance configuration states (ACS) is done next. A Least Effort Transition Enhancement (LETE) algorithm is proposed to solve 'ambiguity' after the classifier.

A. Pre-processing: Effective Data

The objective of pre-processing in the training stage is to train only on 'enough' steady-state load while bypassing transient load, therefore making the training data more effective. The objective of pre-processing in the monitoring is to only classify when there is a transition in steady state there making it more effective, i.e., transients and same steady-states are not classified in monitoring. Computation is not wasted and less messy classified data will be post-processed.

The aggregate load, l_t, can be modelled as a non-stationary signal, and can be decomposed into sequences of transient and steady states. When the aggregated load reaches steady-state conditions, we can assume the load to be a weak stationary process. We assume that the load has reach its steady-state when a large enough window of load data is stationary. We first define an adaptive window, $w_{t-\Omega t+1}(l_t)$, on a sequence of load at time $t \in \mathcal{N}$:

$$w_{t-\Omega t+1}(l_t) = [l_{t-\Omega t+1}, l_{t-\Omega t+2}, \ldots, l_{t-1}, l_t], \quad (1)$$

and the finite sample distribution, W_t, for the load within the window at at time t:

$$l_\tau \sim W_t \quad \forall \tau \in \mathcal{N} : \quad t - \Omega_t + 1 \leq \tau \geq t. \quad (2)$$

We form the following hypotheses that the current load value distribution and the test statistics as:

$$H_t^0 : \quad l_t \sim W_t = W_{t-1}, \quad \frac{|l_t - \mu(W_{t-1})|}{\sqrt{\text{Var}(W_{t-1})}} \leq \alpha \quad (3)$$

where α represent the confidence interval. The logic of the adaptive window Ω_t is then defined as for $t > \omega_{min}$:

$$\Omega_t = \begin{cases} \omega_{\text{min}} + 1 & H_{t-1}^0 \text{ is rejected} \\ \Omega_{t-1} + 1 & H_{t-1}^0 \text{ is accepted} \end{cases}, \quad (4)$$

where ω_{min} denotes the implementation parameter for minimum training window. In the training stage, when $\Omega_{t'}$ is greater than a specified training window ω_{train}, then the load values $w_{t'-\Omega t'+1}(l_{t'})$ are used to train the individual appliance statistical model. In the monitoring stage, when $\Omega_{t'}$ is greater than a specified monitoring window ω_{mon}, then the load values $\mu(w_{t'-\Omega t'+1}(l_{t'}))$ are used for classifier as input.

B. Generative Models

The main objective here is to train each appliance once only, which we define as non-exhaustive training, i.e., without the need to train all the different combinations. This can increase the user-acceptability greatly by decreasing the training effort on the user. We propose a statistical model, $y_t^n(s^n) \sim Y^n(s^n)$, for the apparent power of $n-$th appliance with 3 operation states $s^n = \{0, 1, 2\}$.[1] The statistical model of steady-state appliance load can be written as:

$$y_t^n(s^n) \sim Y^n(s^n) = \begin{cases} 0 & s^n = 0 \\ x_t^n \sim X^n & s^n = 1 \\ x_t'^n \sim X'^n & s^n = 2, \end{cases} \quad (5)$$

[1]The proposed method can be generalized for higher dimension feature space and similarly for appliance with more than 3-states.

 ISBN: 978-1-61208-136-6

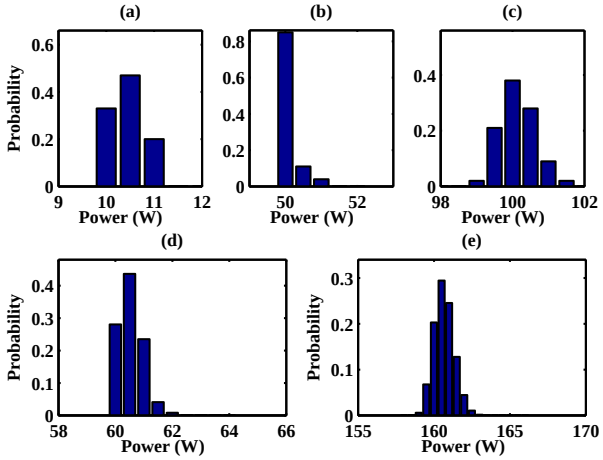

Figure 2: Load distribution of (a) appliance 1, (b) appliance 2 (c) appliance 3, state 2, (d) appliance 1 and appliance 2 and (e) appliance 1 and appliance 2 and appliance 3.

Distribution X^n can be trained by either forming an empirical distribution or some common probability distribution[2] and their parameters can be estimated. We now define a vector, the appliance configuration state (ACS), $\mathbf{s}$, for N total appliances:

$$\mathbf{s} = [s^1, s^2, \ldots, s^N]^{\mathrm{T}} \tag{6}$$

then the total aggregated load can be written as:

$$l_t(\mathbf{s}) = \sum_{n=1}^{N} y_t^n(s^n). \tag{7}$$

Assuming each appliance load is independent with respect to ACS, the distribution of the total aggregate load for a given ACS can be written as:

$$L(\mathbf{s}) = \Upsilon_{n=1}^{N} Y^n(s^n), \tag{8}$$

where Υ denotes the cumulative convolution operator. For example if

$$\mathbf{s} = [1\ 1\ 2\ 0\ 0\ \ldots\ 0]^{\mathrm{T}}, \tag{9}$$

total load can be written as

$$l_t(\mathbf{s}) = x_t^1 +_t^2 +x_t^{'3} + 0 + \ldots + 0, \tag{10}$$

thus the distribution of the the total load for this ACS can be written as:

$$L(\mathbf{s}) = X^1 * X^2 * X^{'3}, \tag{11}$$

where $*$ denotes the convolution operator. An illustration of (11) can be seen in Fig. 2. The load distribution of appliance 1, 2 and 3 are shown in Fig. 2(a), (b) and (c) respectively. The load distribution of the ACS, $\mathbf{s} = [1\ 1\ 0\ 0\ \ldots\ 0]^{\mathrm{T}}$ is next shown in Fig. 2(d) as the convolution on load distribution appliance 1 (Fig. 2(a)) and 2 (Fig. 2(b)). The load distribution of the ACS, $\mathbf{s} = [1\ 1\ 2\ 0\ \ldots\ 0]^{\mathrm{T}}$ is then shown in Fig. 2(e) as the convolution on the load distribution of the ACS, $\mathbf{s} = [1\ 1\ 0\ 0 \ldots\ 0]^{\mathrm{T}}$ (Fig. 2(d))and appliance 3 Fig. 2(c)). Therefore, in the proposed method, only N training on each individual appliance is required, different combinations are generated by convolution of individual distributions, instead of total combination of 2^n or more for exhaustive training. In the monitoring stage, each steady state value can be evaluated in a simple Bayesian sense i.e.

$$\max_{\mathbf{s}} \{p[L(\mathbf{s})|\mu(w_{t'-\Omega t'+1}(l_{t'}))]\}. \tag{12}$$

C. Least effort transition enhancement

We proposed an heuristic module: Least Effort Transition Enhancement (LETE). When there are more than one candidate ACS that score a relatively significant likelihood in the generative model, e.g.,

$$\underset{\star=c_1,c_2}{\mathrm{diff}}\ p[L(\mathbf{s}^\star)|\mu(w_{t'-\Omega t'+1}(l_{t'}))] < p_\sigma \tag{13}$$

The rational behind this is: it is less likely to have a sudden transition of many appliance at once, i.e., many switching on and off of appliances. Thus the hypothesis is that the *less* the effort in the transition from the previous ACS to the candidate ACS, the *more likely* the candidate ACS. Let us define the ACS transition, $\Delta\mathbf{s}^c$, for candidate, $c \in \mathcal{C}$, with respect to the previous ACS as

$$\Delta\mathbf{s}^c = \mathbf{s}_{t-1} \oplus \mathbf{s}_t^c, \tag{14}$$

where $\oplus$ denotes the XOR or exclusive disjunction operator. The estimated effort can then be calculated as

$$\min_{c\in\mathcal{C}} \{\epsilon\Delta\mathbf{s}\}, \tag{15}$$

where $\epsilon = [1\ 1\ \ldots\ 1]$. Other weights can be chosen that reflect the effort more realistically, e.g., switching off the fridge is less likely than the TV. This module is heuristic because we do not formulate a probability model for an given ACS transition, i.e., we can only minimize effort but cannot maximize posterior probability. The weights are also chosen heuristically, without the need for training. Training would defeat the purpose of advantages of the training only N-times on each individual appliance using generative modelling.

III. Experiments

In this section, we discuss the experiment setup and results. Load data are collected by a power meter EZ-RP-15 [3]at 1 Hz sampling rate and transmitted via the Zigbee protocol and processed by a PC. Each individual appliance model is found during the training stage. The three different appliance sets and the total number of reference ACS transitions collected are shown in Table I. A reference script for different ACS are generated randomly for all the

[2]i.e., a Gaussian distribution, a Rayliegh distribution, etc.

[3]www.joseph-tech.com.tw

Table I: APPLIANCE SETS FOR TESTING. NUMBER (#) OF s DENOTES THE NUMBER OF DIFFERENT STATES TESTED.

Set / # of s	appliances
1 / (70)	Desk lamp (24W), adjustable lamp (170W), tungsten light bulb (100W), tungsten light bulb (160W), fan (50W), Halogen light bulb (250W)
2 / (71)	Desk lamp (24W), fan (40W), tungsten light bulb (40W), tungsten light bulb (60 W), tungsten light bulb (200W), Halogen light bulb (230W), LCD monitor (12W)
3 / (101)	Refrigerator (120W), laptop (40W), tungsten light bulb (100W), tungsten light bulb (180W), Halogen light bulb (400W), Halogen light bulb (500W), computer server (230W)

appliances except for the computer server and refrigerator, where we manually placed, to better reflected actual practise in everyday life. The computer server is on for the first two-thirds and the refrigerator is on for last two-thirds of the total configurations. This script is carried out and the load is measured and stored. The performance is evaluated using word recognition rate (WRR) [5]:

$$\text{WRR} = \frac{M_R - E_I - E_D - E_S}{M_R}, \qquad (16)$$

where M_R is total number of reference ACS, E_S is the number of substituted appliance states in classified ACS, E_D is the number of appliance states from the reference ACS deleted in the classified ACS, and E_I is the number of appliance states inserted in the classified ACS not appearing in the reference ACS.

We first test the performance of with and without pre-processing for different waiting times. The waiting time for without preprocessing is the training time, but with pre-processing the waiting time is the sum of the training time and transient bypassing time. It can be seen that in Fig. 3(a) with pre-processing, the performance is greatly improved for shorter waiting times. For a 90 % WRR, the waiting time is reduced approximately from 90 seconds to 30 seconds with pre-processing and for a 95 % WRR, the waiting time is reduced approximately from 2 minutes toward 1 minute. For waiting times over 3 minutes, the two methods are the same, i.e., the effect transients on the appliance model is negligible.

We next test the performance of LETE for $p_\sigma = 0.1$ and $p_\sigma = 0.5$. It can be seen in Fig. 3(a) that LETE with $p_\sigma = 0.1$ does not make a significant difference in appliance set 1 or in appliance set 2, where LETE correctly corrects one substation error. In the case of relatively constant load appliances sets, 1 and 2, LETE with $p_\sigma = 0.5$ mistakenly corrects too many ACS of a lower likelihood. Since $p_\sigma = 0.5$ allows the difference of likelihood of competing candidate ACS up to 0.5, which might allow LETE to mistakenly determine the transition of the higher likelihood of the candidate ACS to be of *too much effort*. However for a more load varying appliance set 3, LETE with $p_\sigma = 0.5$ outperforms

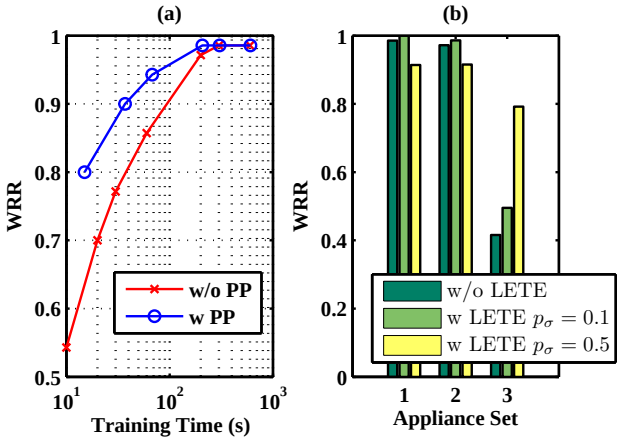

Figure 3: (a) WRR for different waiting times for with and without pre-processing on appliance set 1. (b) WRR for different appliance sets with and without LETE.

LETE with $p_\sigma = 0.1$ and without LETE greatly. Since LETE with $p_\sigma = 0.5$ allows higher likelihood discrepancies, it allows the hypothesis of least effort to work more. Thus this resulted a more stateful classifier, which can handle load varying appliances better. There is a performance tradeoff for the selection of p_σ, depending on the assumption of appliances being monitored.

IV. RELATED WORK

Recent interests in industry show towards improving building energy monitoring. Several startups, such as Tendril and EnergyHub, etc., provide detailed power measurements of selected individual loads. While this approach is useful in observing a few loads at high fidelity, it is neither practical nor cost-effective when full coverage of many appliances is desired.

An appliance recognition approach distinguishs the difference between a variety of appliances by individual appliance properties. Ito et al. [6] proposed several feature parameters, such as average, peak, crest factor, form factor, etc., to characterize the power waveform of individual appliance. They applied nearest neighbors method to recognize which appliance was in use. Kato et al. applied one-class SVM to classify appliance state based on individual current and voltage [7]. However they do not solve problem of one meter to monitoring multiple appliances problem.

The original work on NILM was done by George W. Hart [8], grouped appliance events in the real/reactive power space and built a finite state machine to infer the operating status of appliances according to the power difference between two steady-state periods. Laughman et al. discuss the two limiting assumptions used in Hart's method [9]: i) different loads of interest must exhibit unique signatures. ii) load composition is determined by steady-state power consumption only. Assumption 1 typically hold for homes or small offices, however as there are more appliance in a

 ISBN: 978-1-61208-136-6

total load it gets harder to satisfy assumption i). Laughman et al. then proposed to use higher harmonics in the aggregate current signal to distinguish loads with overlapping clusters in the real/reactive signature space [9]. Lee et al. proposed to use signature correlations in harmonic content to estimate appliances with variable speed drive [10]. This relaxes assumption ii) described by laughman et al. Kushiro et al. attached sensors to a distribution board and employed wavelet transform on current waveform to obtain frequency domain features and utilized pattern matching method to identify the operating status of those target appliances which performed well in recognizing the operating status of appliances with irregular load [11]. Patel et al. measured the electrical noise delivered via power lines to detect the states change of appliances [12]. Such noise is generated by the fast switching of relatively high currents. They employed Fast Fourier Transform (FFT) on the measured noise to separate the component of frequencies and adopt SVM to classify the appliance's state. These frequency/harmonic approaches require higher sampling rate which would require additional hardware to process inside the meter or increase the communication bandwidth greatly.

Jiang et. al proposed a method based on the assumption that the fundamental structure of residential and commercial electrical power flow can be modelled as a load tree. It branches through several levels transformers, bus bars, panels, breakers, power strips, receptacles to individual appliances and within those appliances to various subsystems [1]. Jung and Sawides proposed a method for estimating the power consumption breakdown per appliance inside a home assuming simple ON/OFF appliance state information is available [13]. Schoofs et al. presented NetBem, a novel energy monitoring technique ad hoc to office buildings, capturing the contribution of networked business equipment to a power load through the LAN [4]. The above method are based on the assumption of extra information based on domain knowledge sensor deployment, which would restrict the universality of methods to be used in the real world.

Gupta et al. and Rowe et al. both relied on the fact that most modern consumer electronics and fluorescent lighting employ switch mode power supplies which continuously generate high frequency electromagnetic interference during operation that propagates throughout a homes power wiring which can be measured via electromagnetic sensors [14] [15]. Kim et al. proposed ViridiScope, a finegrained power monitoring system that uses ambient signals from magnetic, light, and acoustic sensors placed near appliances to estimate power consumption [16]. Schoofs et al. proposed a system to automate electricity data annotation leveraging cheap wireless sensor nodes. Characteristic sensory stimuli captured by sensor nodes placed next to appliances are translated into appliance operating state and correlated to the electricity data, autonomously generating the annotation of electricity data with appliance activity [4]. These approaches are base on different mode of sensors which is still far from commercialization.

We now discuss two similar approaches to our work, namely i) super-second sampling so no additional hardware is needed in existing meters or increased communication requirements. ii) non-exhaustive training, i.e., appliance configuration are generated instead of trained, for better user acceptance. Marchiori et al. proposed two methods for NILM, i) a heuristic approach which process individual appliance models into peak points in a feature space and then generated appliance configuration models in a simple vector addition sense therefore uncertainty is measured by distance not probability, and ii) a Bayesian approach which require training of randomly generated different configurations, therefore a semi-exhausitive training is needed. In our proposed non-heuristic generative modelling, the uncertainty based on probability. Ruzzelli et al. presented a plug-and-play tool identify consumption of individual appliances using a neural network (NN). Although a NN require much more training effort than a simple statistical appliance model proposed in our work, Ruzzelli et al. championed NN over a simpler Bayesian type of classifier to incorporate different state or parameter variations. In our work, the proposed LETE improves a simple Bayesian classifier by giving it a *sense of states*. It is to the knowledge of the authors, this work is also the first to study the acceleration of training.

V. Conclusion and Future Work

Monitoring energy consumption at appliance level is a necessary condition for many energy efficient applications. In this paper, we have identified non-intrusive load monitoring (NILM) as a transitional technology, and competing NILM methods must be evaluated not only on performance, but also economical feasibility and user usability of now. Since in the event of maturing an IoT infrastructure, there would be no need for NILM. In this paper, we proposed a NILM for now, a complete solution with novel features: i) pre-processing for effective data, thus more accurate and faster training for user. ii) generative modelling for appliance configuration states, thus without the need for exhaustive training, and iii) LETE algorithm for a simple stateful enhancement. Experiments show the proposed methodology perform well even under only the most simplistic assumptions. The next step in our research is to convert appliance configuration states into human activities, therefore enabling value-added services for energy efficiency, comfort and convenience.

References

[1] X. Jiang, M. Van Ly, J. Taneja, P. Dutta, and D. Culler, "Experiences with a high-fidelity wireless building energy auditing network," in *Proc. SenSys '09*, ser. SenSys '09. New York, NY, USA: ACM, 2009, pp. 113–126.

[2] S. Drenker and A. Kader, "Nonintrusive monitoring of electric loads," *IEEE Computer Applications in Power*, vol. 12, no. 4, pp. 47 –51, Oct. 1999.

 ISBN: 978-1-61208-136-6

[3] C. Floerkemeier, M. Langheinrich, E. Fleisch, F. Mattern, and S. Sarma, Eds., *The Internet of Things*, ser. Lecture Notes in Computer Science. Springer, 2008, vol. 4952.

[4] A. Schoofs, A. Sintoni, A. G. Ruzzelli, and G. M. P. O'Hare, "Netbem: business equipment energy monitoring through network auditing," in *Proc. BuildSys '10*, ser. BuildSys '10. New York, NY, USA: ACM, 2010, pp. 49–54.

[5] I. McCowan, D. Moore, J. Dines, D. Gatica-Perez, M. Flynn, P. Wellner, and H. Bourlard, "On the use of information retrieval measures for speech recognition evaluation," IDIAP Research Institute, Tech. Rep., March 2005.

[6] M. Ito, R. Uda, S. Ichimura, K. Tago, T. Hoshi, and Y. Matsushita, "A method of appliance detection based on features of power waveform," in *Int. Sym. on Applications and the Internet*, 2004, pp. 291–294.

[7] T. Kato, H. Cho, D. Lee, T. Toyomura, and T. Yamazaki, "Appliance Recognition from Electric Current Signals for Information-Energy Integrated Network in Home Environments," *Ambient Assistive Health and Wellness Management in the Heart of the City*, vol. 5597, pp. 150–157, June 2009.

[8] G. Hart, "Nonintrusive appliance load monitoring," in *Proc. of the IEEE*, vol. 80, no. 12, Dec. 1992, pp. 1870 –1891.

[9] C. Laughman, K. Lee, R. Cox, S. Shaw, S. Leeb, L. Norford, and P. Armstrong, "Power signature analysis," *Power and Energy Magazine, IEEE*, vol. 1, no. 2, pp. 56 – 63, 2003.

[10] K. Lee, S. Leeb, L. Norford, P. Armstrong, J. Holloway, and S. Shaw, "Estimation of variable-speed-drive power consumption from harmonic content," *Energy Conversion, IEEE Transactions on*, vol. 20, no. 3, pp. 566 – 574, 2005.

[11] N. Kushiro, M. Katsukura, M. Nakata, and Y. Ito, "Non-intrusive human behavior monitoring sensor for health care system," in *Proceedings of the Symposium on Human Interface 2009 on Human Interface and the Management of Information.* Berlin, Heidelberg: Springer-Verlag, 2009, pp. 549–558.

[12] S. N. Patel, T. Robertson, J. A. Kientz, M. S. Reynolds, and G. D. Abowd, "At the flick of a switch: detecting and classifying unique electrical events on the residential power line," in *Proc. UbiComp '07*, ser. UbiComp '07. Berlin, Heidelberg: Springer-Verlag, 2007, pp. 271–288.

[13] D. Jung and A. Savvides, "Estimating building consumption breakdowns using on/off state sensing and incremental sub-meter deployment," in *Proc. SenSys '10*, ser. SenSys '10. New York, NY, USA: ACM, 2010, pp. 225–238.

[14] S. Gupta, M. S. Reynolds, and S. N. Patel, "Electrisense: single-point sensing using emi for electrical event detection and classification in the home," in *Proc. Ubicomp '10*. New York, NY, USA: ACM, 2010, pp. 139–148.

[15] A. Rowe, M. Berges, and R. Rajkumar, "Contactless sensing of appliance state transitions through variations in electromagnetic fields," in *Proc. BuildSys '10*, ser. BuildSys '10. New York, NY, USA: ACM, 2010, pp. 19–24.

[16] Y. Kim, T. Schmid, Z. M. Charbiwala, and M. B. Srivastava, "Viridiscope: design and implementation of a fine grained power monitoring system for homes," in *Proc. Ubicomp '09*, ser. Ubicomp '09. New York, NY, USA: ACM, 2009, pp. 245–254.

 ISBN: 978-1-61208-136-6

Energy Coupling Control of Telecommunication Network and Power Grid

Heiko Lehmann, Christoph Lange and Andreas Gladisch
Deutsche Telekom Laboratories
Ernst-Reuter-Platz 7
10587 Berlin, Germany
[H-Lehmann, Christoph.Lange, Andreas.Gladisch]@telekom.de

***Abstract*—In this paper, we present a control architecture that allows to operate the energy storage facilities integrated into the wide area telecommunication network as mediators between the optimality criteria of the *Smart Grid* and the energy consumption modeling of the telecommunication network itself. Different control modes are discussed.**

***Keywords*—Green ICT, Smart Grid, energy storage facilities, telecommunication network**

I. INTRODUCTION

In this paper, it will be argued that the storage facilities for electrical energy which have been integrated into the national carrier networks as a power reserve for blackouts with system-wide coverage may serve as a crucial link between the telecommunication network domain and the emerging *Smart Power Grid* (for an – albeit not rigorous – definition and basic discussion see [1]).

Consider the following three-part reasoning, first seen from the energy domain point of view:

- The success of the so-called *Smart Grid* will hinge on its capability to incorporate renewable energy sources on a large scale.
- The renewable energy sources (mainly wind and solar energy) come with a high volatility – time and place of their availability will, as a rule, not coincide with the demand.
- Hence, technically efficient and controllable energy storage topologies with a system-wide coverage have to be set up.
- (Also, concurrent transmission network capabilities have to be created. For the argument of the present paper, this aspect shall be disregarded.)

On the other hand, the national carrier telecommunication networks such as e.g. *Deutsche Telekom* (DT) in Germany are heavy consumers of electrical energy (German landline operation of DT alone consumes around 2 TWh per year). As the traffic load of network services increases in near-exponential fashion (e.g. [2]), to curb the energy consumption in all layers of the ICT (information and communication technology) domain is a paramount task for the ICT industry, summed up in the term *Green ICT*. The reasoning given above is now met by the ICT domain point of view:

- Emergency electricity provisioning has historically been integrated into the telecommunication network at each of the major technology sites (approximately 9.000 in the case of DT) and further real estate sites.
- Whereas at a share of these sites performance is individually measured with a high temporal resolution, others are provisioned according to suitable standard load profiles.
- The actual technology is a lead-acid storage battery with a summed-up capacity of ca. 22 MAh. This value is, at closer inspection, a nonlinear function of the discharge current.
- As per current operation, the default charge level is 100%.

The conclusion is fairly simply to draw: provided the option of remote management is given for the storage batteries, their charge levels can now be regarded as control entities with two competing control paradigms:

A. *Telecommunication Consumption Modelling*

The storage capacity is used to cap peak loads of the telecommunication network energy demand and shift them to off-peak times. As the spot market prices of electrical energy (day-ahead trading) are strongly correlated to the aggregate load profile, even minor shifts of peak loads result in reductions of the overall power bill. Further optimization dimensions are the transmission fees which are a strongly nonlinear function of site-specific performance values and controllable variations of the standard load profile. This is a purely Telco-internal optimization scenario.

B. Smart Grid *Stabilization Services*

Alternatively, the buffer control can be operated according to the necessities of the utilities: positive and negative control energy options could be realized, or, storage elements may be operated as parts of virtual power plants. The remuneration in this control paradigm is external and is derived from the economical value of the *Smart Grid* stabilization.

Both paradigms may, however, be combined. With a common value scale (e.g. currency units), a joint cost function can be constructed comprising the values of *Smart Grid* stabilization services *and* power purchase bill reductions. The mathematics of complex optimization allows, then, to identify the optimal operation of the storage elements with respect to the two domains *"Smart Grid"* and *"Green ICT"*.

This work reports first findings on the presented control mechanisms derived from research at Deutsche Telekom

 ISBN: 978-1-61208-136-6

Laboratories and discusses the possible further developments.

The paper is organized as follows: in the first section, the joint control architecture of the coupled domains *"Smart Grid"* and *"Green ICT"* is developed and discussed. In the second section, partial optimization scenarios for the operation of the energy buffers are developed and recent R&D work (at DT) is scanned for relevant input. A synthesis is subsequently developed. Finally, an outlook is given.

II. JOINT CONTROL ARCHITECTURE AND CONTROL PARAMETERS

In Figure 1, the layer coupling as described above is schematically depicted. In the topmost layer, the network structure of energy consumption in the telecommunication domain is shown. The energy buffer elements integrated in this network constitute the mediating middle layer, whereas the bottom layer represents the power grid.

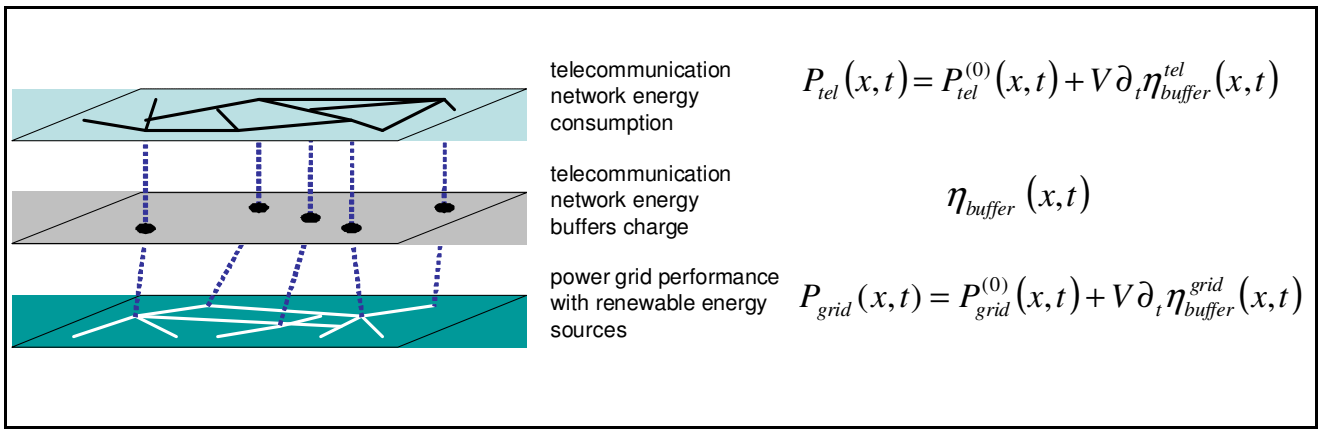

Figure 1: Telecommunication and electrical power network coupled by energy buffer elements.

The coupling function η is a capacity measured in Ah. Its first temporal derivative gives a current which describes charging and discharging of the buffers. Multiplied by the voltage a positive or negative performance is expressed which might be operated to modify the performance balance in the top and bottom layer. Several observations are due:

- In the telecommunication network no energy is generated. Therefore, $\partial_t \eta_{\text{buffer}}^{\text{tel}} \leq 0$ at all times.
- A cyclical recharging boundary condition is implemented: $\eta(t) = \eta(t+T)$ with T = 24 h as the starting point.
- Discharge current limitations are derived from the battery technology: $|\partial_t \eta_{\text{buffer}}| \leq I^*$ in order to preserve the nominal capacity and ensure the life expectancy of the battery.
- Note also the basic dimensioning $P_{\text{tel}} \approx 0.02 \times P_{\text{grid}}$.

Let us now shortly discuss Figure 1. In the top layer, the buffered performance of the telecommunication network as presented to the grid is expressed as the sum of the unmediated consumption $P_{\text{tel}}^{(0)}$ and the buffer performance. The latter is always negative as energy can – in this layer – only be taken out of the buffers. $\partial_t \eta_{\text{buffer}}^{\text{tel}}$ presents thus a means to react to price variations as it dissolves the rigid coupling between consumption and grid-based provisioning.

In the mediating middle layer, the buffer charge $\eta_{\text{buffer}} = \eta_{\text{buffer}}^{\text{tel}} + \eta_{\text{buffer}}^{\text{grid}}$ is here modeled to consist of two parts – one mediating the telecommunication network consumption and one interacting with the grid itself. The latter describes the purchase of buffer energy in off-peak hours ($\partial_t \eta_{\text{buffer}}^{\text{grid}} \geq 0$) as well as technoeconomical operations typical for the *Smart Grid*. The most important of these are:

- Positive control energy: Buffer energy is fed into the grid in order to counteract under-provisioning ($\partial_t \eta_{\text{buffer}}^{\text{grid}} < 0$). The corresponding economics is usually a traded option over a specified amount of energy with defined performance. The use of distributed medium-sized buffers prevents the costly use of control power plants, e.g. gas turbines and is very efficient with respect to transport costs.
- Negative control energy: Buffer capacity is offered to be charged with surplus energy which threatens to destabilize the transmission grid. The typical situation is a high feed of wind energy in night hours not met by comparable consumption. Again, options to charge buffers are traded as a reassurance against grid destabilization. As above, the system-wide coverage of buffers allows to act in the lower hierarchy layers of the grid, thus transferring – and effectively curbing – risks from the high-voltage grid to medium-and low-voltage parts.
- Virtual power plants: Physically the same effect as the positive control energy discussed above, the coupling of buffer performance into a cloud of generation facilities constitutes a virtual power plant. The mode of operations, however, will be different: option trading with rare actual events is replaced by regular operation. Lifecycle considerations have, thus, to be taken into account.

 ISBN: 978-1-61208-136-6

III. BUFFER OPERATION CONTROL

In this section, first approaches to the control paradigms presented above are reviewed and discussed. Before embarking on the full systemic case, let us consider the decoupled regimes $\eta_{buffer}^{y} = 0$, where $y = \{tel, grid\}$, respectively.

A. *Telecommunication Consumption Modelling*

Following the reasoning given in the introduction, research activities at T-Labs, the central R&D department of Deutsche Telekom Group, have been set up to investigate the use of buffers in the pure y = tel mode discussed above. Starting point is an energy provisioning mode where the bulk of energy is secured by long-term base and peak contracts. This results in a rectangular function which has to be shaped by day-ahead trading on the stock exchange to the actual demand function. Only this latter part of the overall provisioning is subject to the buffer mediation as discussed in this paper since for long-term effects the buffer size is not sufficient.

In a detailed analysis of historical data (consumption data and stock exchange prices of the years 2008 and 2009), the feasibility of buffer operation to model the Telco network consumption has been studied. Two effects have been shown to dominate the optimization:

- Balancing group management: The stock exchange price curve (see Figure 2) gives clear indication at what times purchase should be avoided and at what times encouraged.

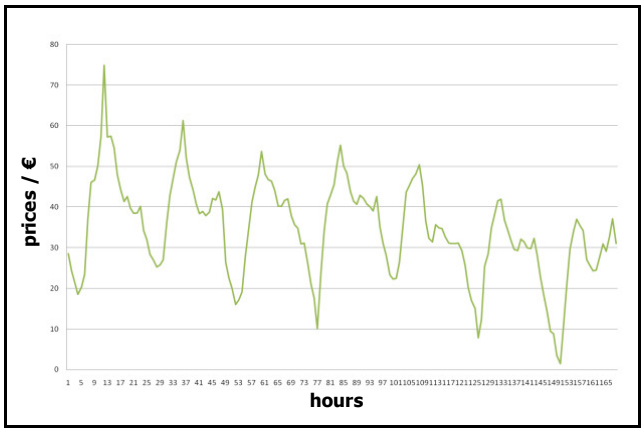

Figure 2: Exemplary stock exchange prices over a week, beginning with Monday. Night times, especially at the weekend lead to zero, even negative prices.

- Transmission fee optimization: transmission fees are built on the basis of the maximal current integrated over any 15 minutes in the course of a year. Uncontrolled buffer recharging, e.g. after a maintenance operation or an actual black-out incidence, leads to high transmission bills. This effect cannot be studied in the aggregate model developed in the initial analytics approach since the consumption sites have individual characteristics and have to be modeled individually.

In a first evaluation, perfect a priori knowledge about stock exchange prices has been assumed (given by the historical data). Also, operational issues of the battery management have been neglected (lifecycle issues, current limitations etc.). Then, the optimal buffer operation has been determined by linear optimization. The result is given in Figure 3 [3] .

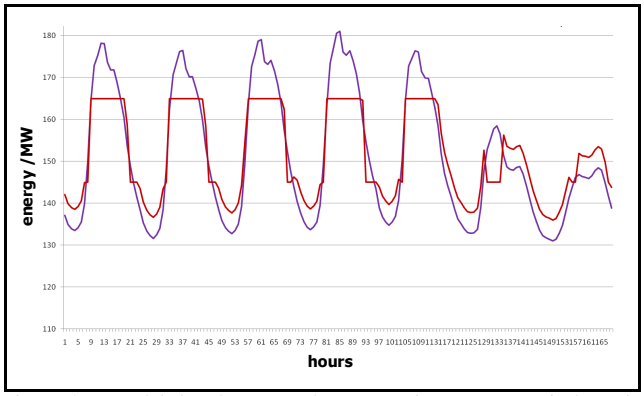

Figure 3: Modeled Telco network consumption over a typical week beginning with Monday: The red curve shows how the load peaks are capped by buffer energy.

Figure 3 shows how the load peaks of the Telco network consumption can be capped by $\partial_t \eta_{buffer}^{tel}$: Charging at night and weekend times enables the aggregate buffer (note again: this is a model pathology) to substitute the peak loads over the working week.

B. Smart Grid *Stabilization Services*

In this subsection the pure y = grid mode – as introduced in the beginning of section III – and the related use of the buffers is elaborated on.

In *Smart Grid* environments several types of energy have to be integrated and handled within an overall electricity grid: Besides the energy generated by conventional power plants like coal-burning power plants or nuclear power plants renewable energies have to be included. Typical renewable energy sources are wind, sun and tides, but also for example biomass. Renewable energy is highly volatile with respect to time t and location x of its occurrence in a power grid – and the amount of renewable energy generation is thus a function of time t and location x. Wind energy is typically generated in certain regions – e.g. in maritime regions by using on-shore facilities and in off-shore wind parks, where strong wind activity is observed. The wind occurrence and intensity has a statistical nature [4] leading to a high variation in wind output with respect to time and locality. Solar energy is best generated in regions with long periods and high probability of sunshine. These areas may be preferably desert-like regions which are – in general – different from regions with high wind output. Tidal energy sources depend on tidal flows in the sea. They are expected to be better predictable with respect to temporal occurrence [4], but this type of energy is restricted to sea shores with significant tidal activity. Some

 ISBN: 978-1-61208-136-6

congruence between the wind and tidal energy source locations may be argued, but also in these cases there may be significant discrepancies since high wind capacity is not only observed in maritime and off-shore regions, but also in central country parts [4]. Another renewable energy source is bioenergy for future energy supply where a major challenges lies in its sustainable and efficient use and generation [5].

The time periods of interest are expected to range from short times, like diurnal or weekly periodicity, up to yearly and seasonal variability: An example would be the more strong wind activity in maritime regions during autumn and spring compared to typical summer winds – where instead the solar energy generation is expected to have a peak value with respect to historical observations.

The associated overall generated power $P_{\text{grid}}^{(0)}$ may be modeled as a function of time t and location x:

$$P_{\text{grid}}^{(0)}(x,t) = P_{\text{coal}}(x,t) + P_{\text{nucl}}(x,t) + P_{\text{wind}}(x,t) + P_{\text{sun}}(x,t) + P_{\text{tide}}(x,t)$$

Since the renewable energy sources generate a highly volatile power, the remaining conventional power plants will have to be able to provide a varying electricity demand – depending on the wind, sun and tide activity: Considering an exemplary case of a power consumer with approximately constant power draw – like, for example, current telecommunication networks within certain limits are – the electricity demand remaining for the coal-burning and nuclear power plants will vary and there is a need of energy storage to accommodate this in an efficient way.

Energy storage facilities are installed in electricity grids: As an example there are the pumped storage plants in mountainous regions which are able to store energy in mechanical form and convert them back to electricity on demand. However, the high volatility of renewable energy with respect to time and location will require, first, energy storage facilities which are able to handle requests in short times for storing and providing energy as well as, second, distributed storage facilities with sufficient capacity in a certain region to accommodate the location dependency of renewable energy generation. During times of generation of high amounts of renewable energy it will be necessary to store considerable amounts, but being able to deliver it during times of low activity of renewable energy sources. Central storage facilities, connected to e.g. geographical characteristics – like pumped storage plants are – may be not sufficient, since in that case possibly long distances would have to be bridged and the transmission loss would decrease the energy efficiency. Here a clear argument for de-centralized storage facilities is observed, since transmission losses can be minimized by distributed storage energy facilities. In conclusion of this paragraph it can be stated that current energy storage facilities are not flexible enough to handle the future grid requirements and hence more suitable solutions are necessary allowing for a more economical grid operation.

For the future it is expected that the share of renewable energies in the overall energy mix will increase targeting at a reduced greenhouse gas emission. For example in Germany there is the target established to have 35 % of the gross energy consumption generated by renewable energy sources by 2020 [5]. After that time, Germany targets at 50 % by 2030, 65 % by 2040 and 80 % by 2050 of gross energy consumption generated from renewable energy sources [5]. With respect to the longer term future, like e.g. looking at 2050 it is expected that wind energy will play a key role in electricity generation [5].

Before this background it will be necessary to establish concepts like those elaborated on in this paper to allow for an efficient and reliable energy supply by future electricity grids. The energy storage elements of the telecommunications network are distributed all over the country and have a certain capacity – which is usually much lower than the grid would require to accommodate the whole amount of variations. However, the distributed energy storage facilities may help to stabilize the grid and ensure its economical operation in cases of small variations of the provided grid power with respect to the power demand.

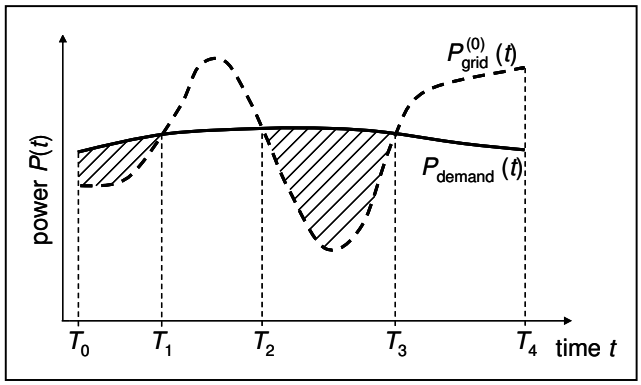

Figure 4: Exemplary and principle curves of the the power demand $P_{\text{demand}}(t)$ and of the grid-provided power $P_{\text{grid}}^{(0)}(t)$ over time t at a constant location x.

Figure 4 shows the principal behaviour of the generated power $P_{\text{grid}}(t)$ by the grid and the power $P_{\text{demand}}(t)$ demanded by the consumers as exemplary functions of time t, i.e. for a certain location (x = const.). The electricity demand $P_{\text{demand}}(t)$ is assumed to be nearly constant over time. Two cases concerning the buffer usage can be distinguished: Energy stored in the buffers is fed into the grid in order to counteract under-provisioning ($\partial_t \eta_{\text{buffer}}^{\text{grid}} < 0$) or the grid produces more power than demanded by the consumers and this surplus energy amount is stored in the buffers ($\partial_t \eta_{\text{buffer}}^{\text{grid}} > 0$). In Figure 4 this is illustrated: There are shaded areas – between T_0 and T_1 as well as between T_2 and T_3 – where $P_{\text{grid}}(t) < P_{\text{demand}}(t)$ ($\partial_t \eta_{\text{buffer}}^{\text{grid}} < 0$): In this case the grid generates less power than demanded by the power consumer, for example since there is low wind energy output. Then the difference power $P_{\text{demand}}(t) - P_{\text{grid}}(t)$ has to be provided by the energy storage facilities of the network, i.e. the batteries which had to be previously charged appropriately. During times, where $P_{\text{grid}}(t) > P_{\text{demand}}(t)$ ($\partial_t \eta_{\text{buffer}}^{\text{grid}} > 0$) – i.e. between T_1 and T_2 as well as between T_3 and T_4 – the batteries may serve as buffers and store the power generated, but not used by the

power consumers at that particular time period. These amounts of energy than may be used at later points in time, when the first case applies.

C. Synthesis

Let us now sketch the combined control of Telco network energy consumption modeling and *Smart Grid* stabilization services. In the modeling language developed above in section II, a unifying cost function has now to be developed. In continuation of earlier work where the essential coupling mechanisms between layers have been modeled qualitatively [6], here, a more analytical approach is sought. To this end, the performance modeling of Figure 1 has to be set in relation to real costs.

Consider the performance-related costs as a functional (in arbitrary dimensionless units) of the overall buffer charge $\eta_{\text{buffer}}(t)$:

$$C[\eta_{\text{buffer}}] = \int \mathrm{d}t\, \pi_{\text{bm}}^{(0)}(t)\, \eta'^{2}_{\text{buffer}}(t) + \pi_{\text{c}} \eta_{\text{buffer}}(t). \qquad (1)$$

Here, the first rhs term describes the costs of the balancing group management: the stock exchange price function $\pi_{\text{bm}}^{(0)}(t)$ weights the charging and discharging performance, respectively. As discussed above, a further dependence of the costs on the charge and discharge currents exists (transmission fees) whence a quadratic dependence on the currents follows.

In the oversimplified model presented here, the positive control energy (see discussion above) may be regarded as subsumed in the balancing group management, since the corresponding option prices will strongly correlate with the stock exchange prices, so that $\pi_{\text{bm}}^{(0)}(t)$ may be understood as incorporating both.

The negative control energy costs, however, have to be modeled separately. This is done in the second term in eqn. 1: If π_{c} is a constant option price for providing negative control energy, the costs are directly proportional to the available buffer. It has to be stressed again at this point, that this model is not designed for mathematical accuracy but for highlighting the leading effects in the presented control problem. The Euler equation for the optimization problem (1) follows immediately to

$$\frac{\mathrm{d}}{\mathrm{d}t}\left[2\eta'_{\text{buffer}}(t)\pi_{\text{bm}}^{(0)}(t)\right] = \pi_{\text{c}} \qquad . \qquad (2)$$

Figure 5 shows the principal effects of the optimization problem (2): The higher the option price π_{c}, the more favourable it is to discharge the buffers since this creates capacity for accommodating the surplus energy (see above). In Figure 5, $\pi_{\text{bm}}^{(0)}$ has been modeled as a Gaussian centered at midday – in the rough modeling presented here, this mimics the realistic curve in Figure 2.

Obviously, a realistic negative control energy option price would reflect the higher risk of network instabilities due to overfeeding in the night hours. Also, correlations between stock exchange prices $\pi_{\text{bm}}^{(0)}$ and the aggregate load profiles which will also strongly influence both control energy prices have been neglected here.

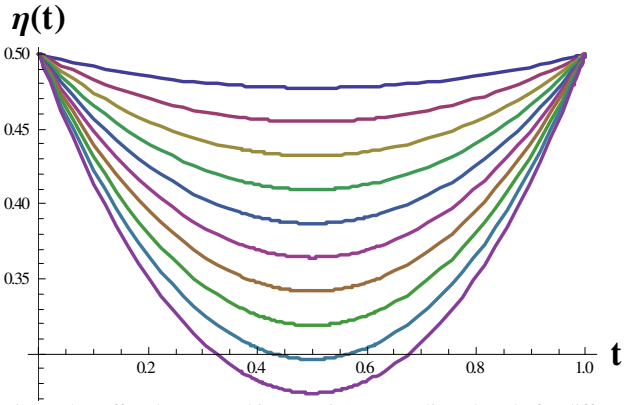

Figure 5: Buffer charge η (arbitrary units) over a diurnal cycle for different values of negative control energy option prices (increasing values from top to bottom).

In current R&D work at Deutsche Telekom Laboratories, a detailed spatio-temporally resolved model is developed in order to realistically gauge the effects presented here qualitatively.

IV. Conclusions and Outlook

In conclusion of the presented joint control approach of Telco network consumption modeling and *Smart Grid* effects, several principal findings can be stated:

- First, the gross demand and supply of electrical energy are coupled by prices – be that the stock exchange prices for day-ahead provisioning or the hedging prices for control energy of either sign.
- Further, a system-wide buffer structure integrated into the Telco network may be used in two different modes: either to model proprietarily the Telco consumption characteristics by load-shifting, or, to mediate performance surpluses and deficits of the *Smart Grid* itself.
- Thus, with integrated prices as a unifying basis, a cost functional can be derived for combining the different control requirements on the operation of the buffer charges integrated into the Telco network.

With respect to the behaviour of the combined control strategy, interesting options open up:

- There is mutual competition and enhancement of cost effects: Whereas negative control energy and balancing group management both act towards buffer discharge, positive control energy and Telco network consumption modeling compete. Here, a more refined model is needed to derive the optimal control strategy.
- Current initiatives for load-adaptive mode in the Telco network operation (see section III B and e.g. [6]) will amplify the presented effects: Whereas today the Telco network energy consumption varies little over time (see Figure 4), load-adaptive mode will correlate it more strongly with the general

 ISBN: 978-1-61208-136-6

demand curve and, thus, the price curve. The buffering effects are expected to increase in scale for such a scenario.

- Furthermore, load-adaptive mode of the Telco network operation, turns the initially unresponsive $P_{tel}^{(0)}(t)$ into a controllable entity. Thus, new options for stabilizing the *Smart Grid* arise.

For a working real-time control strategy, the stochastic character of prices and the renewable energy grid feed has to be taken into account. Furthermore, the model has to be broken down to the individual operation of the different buffer elements.

The principal argument of the presented work is that the energy elements integrated into the telecommunication carrier network may serve as a catalyst in *Smart Grid* evolution scenarios. As imperfect as sites and technology of today's energy buffers may be, they provide a relevant starting point by their system-wide coverage.

REFERENCES

[1] IEEE Standard 2030 Guide for Smart Grid Interoperability of Energy Technology and Information Technology operation with the Electric Power System (EPS) and End-Use Applications and Loads, doc.: IEEE 802.15-09-0658-00.

[2] Cisco Visual Networking Index: Forecast and Methodology, 2009–2014. Cisco Systems, 2010, Available: http://www.cisco.com/en/US/solutions/collateral/ns341/ns525/ns537/ns705/ns827/white_paper_c11-481360.pdf

[3] Deutsche Telekom Laboratories, Internal Project Report ,*Smart Sub-Grid,* July 2010.

[4] J. Cox, "Impact of Intermittency: How wind variablity could change the shape of the British and Irish electricity markets", Pöyry Energy Consulting report, July 2009.

[5] German Federal Ministry of Economics and Technology (BMWi) and German Federal Ministry for the Environment, Nature Conservation and Nuclear Safety (BMU) (eds.), "Energy Concept for an Environmentally Sound, Reliable and Affordable Energy Supply", Berlin, September 28, 2010.

[6] C. Lange, A. Gladisch, "Energy Efficiency Limits of Load Adaptive Networks", Proc. Optical Fiber Communication Conference and Exposition (OFC). San Diego (CA, USA), March 21–25, 2010, paper OWY2.

[7] H. Lehmann, A. Gladisch and U. Bub, "Energy-Aware End-to-End ICT Production", Proc. Going Green CARE INNOVATION 2010, Vienna, *Austrian Society for Systems Engineering and Automation* eds., November 8–11, 2010

 ISBN: 978-1-61208-136-6

An Overview of Smart Grids in Brazil

Opportunities, Needs and Pilot Initiatives

Cesare Quinteiro Pica, Daniella Vieira, Gabriel Dettogni
Reference Centers of Innovative Technologies – CERTI
Florianopolis-SC, Brazil
e-mail: cqp@certi.org.br, dpv@certi.org.br, gdt@certi.org.br

Abstract—**With the Smart Grid boom, vendors and investors are already looking for the opportunities in this area. Some of the greatest possibilities might be constructed in Latin America, especially in Brazil. This article aims to present an overview about Smart Grid developments in Brazil. Furthermore, four cases are described to show the challenges that confront energy companies in constructing and implementing the base for an efficient and real Smart Grid.**

Keywords: Smart Grid; Research and development; Pilot Initiatives; Regulatory demands.

I. CURRENT SCENARIO OF SMART GRIDS IN BRAZIL

Latin America is also a region of the world that is showing significant Smart Grid activity. In many Latin American countries, utilities have undertaken pilot projects in Smart Grids. Since 2008, there has been a growing interest in smart energy technologies among Latin American countries, with Brazil leading the way. Currently, the concept of Smart Grid is the subject with the greatest emphasis in the Brazilian energy sector [1].

Brazil is identified as a country that recently has had and continues to have huge economic growth and, hence, the need for expansion and modernization of the electric power system, in order to cope with the increased energy demand. According with the Brazilian National Energy Plan for 2008-2017, the government set a goal to build 54 gigawatts of installed capacity to attend the increase of the consumption expected in 60 percent [2].

In 2010, almost all Brazilian electric utilities began studying Smart Grid in order to prepare themselves and to strategically direct their investments in new infrastructure and Research and Development (R&D) projects towards the modernization of the Brazilian electric system.

The following issues might be considered as motivating factors for Smart Grid implementation in Brazil: (i) reduction of non-technical losses; (ii) increase of the operational efficiency; (iii) expansion and automatization of the electric power system with standardized smart technologies; (iii) improvement of the system reliability and power quality, especially for industries and high-tech based companies.

This paper aims to present an overview of Smart Grids in Brazil and is organized as follow. In Section 2, information about investments for R&D activities is provided. In Section 3, some initiatives and challenges for the implementation of Smart Grid are presented. In Section 4, the most important Brazilian pilot projects are detailed. Finally, in Section 5, some final highlights of opportunities for Smart grid development in Brazil are presented.

II. INVESTMENTS FOR RESEARCH AND DEVELOPMENT

Due to a Brazilian law [3], all public service concessionaires of electric power distribution must invest approximately 1% of their operating revenues in research and development programs that could be conducted by universities, research centers and innovative companies.

Most of the investment in addressing these issues is being made by energy companies (Generation, Transmission and Distribution). These initiatives are: (i) Research and Development Program; (ii) Energy Efficiency Program, that are coordinated by the energy companies which support practical actions; and (iii) Government Fund, that support the modernization of the Brazilian electric power system and other development projects. The data shown in Table 1 represents how much companies must invest in each of the three initiatives.

TABLE 1. INVESTMENTS IN EACH INITIATIVE

	Research and Development	**Energy Efficiency**	**Government Fund**
Distribution	0.2%	0.5%	0.3%
Transmission	0.4%	-	0.6%
Generation	0.4%	-	0.6%

For this reason, the Brazilian Electricity Regulatory Agency (ANEEL) improved the segment's R&D Program with the objective of encouraging the constant search for innovation and to confront the technological challenges of the electrical sector.

A report prepared by the Brazilian Development Bank (BNDES) shows that overall investments in energy infrastructure will increase by 7.4% per year until 2013 [4]. Between 2010 and 2013, Brazil will invest around US$60 billion in the electric system, solely taking into account

 ISBN: 978-1-61208-136-6

projects that already have been granted or have had authorization given by the government.

Other investments are being launched by private companies. Large companies such as IBM, Silver Springs Networks and GE are already making investments in this sector in Brazil. The Brazilian market for Smart Grids is seen as a potential for many countries and there should be great opportunities for business development, especially due Brazil hosting the World Cup of 2014 and Olympic Games of 2016.

III. INITIATIVES AND CHALLENDGES

The Brazilian Ministry of Mines and Energy (MME) has recently established a work group responsible for studying and planning the deployment of a Smart Grid in the country. The members of the work group, besides the MME, are representatives from the Energy Research Company (EPE), the Electric Energy Research Center (CEPEL), the ANEEL and the Operator of the National Electric System (ONS). The work group is expected to complete its work during the first half of 2011. This group has to review the technical studies and prepare an analysis with recommendations on measures that should be adopted, focusing principally on: (i) the consolidation of Smart Grid programs in Brazil; (ii) the adequacy of regulations and standards for distributors of electricity; (iii) the identification of resources for funding and promoting incentives for the production of equipment in the country; and (iv) the regulation of potential new players in the market, including consumers and distributed generation providers [5].

At the moment the main challenges related to the implementation of Smart Grid architecture in a Brazilian context are: size of matrix energy in Brazil, remote areas like Amazon and rural areas, reliability standards, illegal connections and regulation of the sector.

In Brazil Smart Grid is being implemented mostly through large scale adoption of electronic meters, as a strategy for distribution companies to increase operational efficiency through remote meter readings, and to reduce energy commercial losses. As an example, in 2009, the city of Rio de Janeiro's total energy losses were about 21% which corresponds to 5TWh. Of this total, around 15% refers to commercial losses. In 2009, energy commercial losses in the whole country represented approximately US$5 billion in economic losses for distribution companies [6].

In 2009, the ANEEL opened a public hearing on Smart Metering and also approved a regulation allowing the use of Power Line Communication (PLC) throughout the country. The agency ANEEL announced plans for replacing around 65 million electromechanical energy meters, nowadays installed in residential and commercial buildings in Brazil, with new Smart Meters. In the near future, Smart Metering will enable the registration of the energy generated by residential consumer units by means of solar panels and residential wind turbines, for example.

Another important challenge in Brazil is that there are not yet specific policies and regulations for free markets tariffs. The agency will invest in efforts to define the regulations that permit differentiated tariffs by time, which will enable consumers to manage their consumption.

IV. PILOT PROJECTS IN BRAZILIAN COMPANIES

Despite many financial and regulatory barriers, several national companies are already working on pilot projects. In this section we highlight four cases that were constructed by pioneer companies within Smart Grid. They are: CEMIG, AES Eletropaulo, COPEL and CELESC.

Figure 1. Some smart grids initiatives in Brazil.

Case 1: Cities of the Future in Minas Gerais (CEMIG)

The *Companhia Energética de Minas Gerais* (CEMIG) [7] has been working to construct the innovative solution to automate the infrastructure of energy distribution. In this model, the concept of the Smart Grid architecture contribute to modelling the integration of technical and commercial systems, providing an approach focused on client, on service quality, on ambiental sustainability and on energy market.

For this reason, CEMIG adopted projects that are integrated with the categories of Smart Grid architecture. The main projects in course are Distribution´s automatization and City of the Future.

In 2009, the project City of the Future was started. The project has the objective to validate products, services and innovative solutions applied to Smart Grid architecture, in an appropriate and representative scale for the company.

The city that was chosen to start the implementation of this program is Sete Lagoas, located near Belo Horizonte. This is a municipality with a big diversity of economic activities in the industrial, agriculture and service sectors with a population of over 200,000 inhabitants and more than 80,000 customers. Another point is that the location had the capacity to integrate experiments with consumers of telecommunication systems.

The project City of the Future includes actions that cover all business processes focusing most notably in the following areas: (i) automation of consumers' measurement, (ii) automation of substations, (iii) automation of energy distribution grid, (iv) telecommunications systems, (v) operational computer systems, and (vi) management and integration of distributed generation. In 2010, the R&D projects started and the first step for implementation was realized.

 ISBN: 978-1-61208-136-6

For CEMIG, the principal difficulty in constructing Smart Grid architecture is that the rules for implementation were not defined for ANEEL. For this reason, the process to obtain financial resources has been difficult. However, the adopted practices for the implementation and the expected results are strategic for all stakeholders with emphasis for the company and governmental entities.

The project City of the Future has as expected result: serve as a model for implementation of new real time tariffs and billing; reduce the energy costs and losses; improve efficiency of the power grid; optimize the management and control; improve quality of the services and promote R&D.

Case 2: Smart Grid in Sao Paulo (AES Eletropaulo)

Since 2007, AES Eletropaulo [8] has been conducting initiatives related to the comprehension and dissemination of Smart Grid concepts. In 2010, the company invested R&D resources in a pilot project to develop a smart distribution system integrating communications solutions, advanced equipment and information systems. At this stage, the project aims to monitor the electrical system and automate the process of power distribution.

The Smart Grid pilot project is being implanted over a circuit that has 4.4 kilometers of overhead and underground cables which make up distribution grid, in Ipiranga, São Paulo. This region has 2,000 units consumption of low and medium voltage, in residential, commercial and industrial segments. In this region, electronic meters were installed to monitor the customers' energy consumption, as well as monitor the energy balance in 39 secondary circuits and allow the remote execution of various services, such as power reading, cutting and reconnection.

AES Eletropaulo started doing experiments that involve communication between electronic meters, substations, toggle switches and other equipment, as well as integration between the company systems. The company intends to analyse the information, obtained from the measurement system, and integrate it with the automation and operation systems of the concessionaire.

To put the project into practice, various features of the intelligent grids' concept are being tested and among them is "self-healing" (a tool that reduces recovery time from a failure in the electrical system). In the case of power failure, a voltage sensor detects the interruption and sends information to the distribution management system of the company, which will automatically identify an alternative to restore the power supply. If it was not feasible, the system will send an alert to the specific distributor's operations center, which will trigger a team to meet directly at the site identified.

AES Eletropaulo has continuing investing in R&D initiatives and organizes a multidisciplinary committee to coordinate and analyze the activities.

Case 3: Companhia Paranaense de Energia (COPEL)

The COPEL [9] plans to invest more than $ 330 million in projects that are related to Smart Grids concepts until 2014. The main view is to transform Curitiba into a digital city. The investments are directed towards infrastructure, including installation of electrical networks and adaptation of modern systems to energy transfer. Some projects are already being implemented, while others remain in the preparation and study stage.

The technology platform, based on the Smart Grid concepts, is been tested in Fazenda do Rio Grande, in Metropolitan Region of Curitiba, covering 100 million consumers.

The COPEL's program is being formulated in coordination with other public services, under the coordination of the State Secretariat of Urban Development. The planned actions are intended to expand and modernize the electric system.

Projects intend to spread the Smart Grid by 2020 to reduce the rates of equivalent duration of interruption per customer (DEC) and equivalent frequency of interruption per customer (FEC) [10]. The priority is to improve the supply. In addition, technical losses tend to fall from 6.5% to 4% and the commercial 1.5% to 0.5%.

Over the next few years, COPEL will automate all operational keys and automatic reclosers installed that supply the 650,000 consumer units. This action will reduce the number of interruptions and shorten the time needed to restore services. The company also expects to build 700 km of new compact power grids.

The idea for new projects incorporates sensing, monitoring, information technology and telecommunications for the best network performance. In the next step of implementation the system will be able to identify early failures and be able to reestablish itself, therefore improving performance. COPEL sees that the system itself, supplied by data and information collected by geoprocessing techniques, will identify the items that are being repaired, define the process of isolation and restore power within minutes.

Another initiative related to Smart Grids concepts, in 2010, was the launch of the first electric taxi at the Afonso Pena airport, in São José dos Pinhais, COPEL installed the first electric fueling station. The station that recharges the batteries will also be used within the project site for studies on vehicle performance and the impacts of its use on the electrical system. Today the charging time of this car is 8 hours, but they expected to improve that performance.

Case 4: Micro Grid of Sustainable Energy (CELESC)

The CELESC [11] company is developing R&D pilot projects with the objective to build structures to accommodate the Smart Grid architecture. Accordingly, the projects are reported: (i) Demand Response in Florianópolis, (ii) Measurement system in Blumenau and (iii) Planning District Distribution Network and Generation of Sustainable Energy.

To be approved by ANEEL, the project Demand Response in Florianópolis, Santa Catarina, has the objective to improve load factor of distribution systems, through the technology used for demand response. The project will

 ISBN: 978-1-61208-136-6

install load control devices in 10,000 consumer units and smart meters in 3,500 consumer units. The company hopes to avoid the occurrence of blackouts and shutdowns, especially in critical times during the summer. The demand management and the most efficient use of the power system will reduce the costs.

CELESC launched the Project Measurement system in Blumenau that aims to serve 3,670 consumers in the municipality. The project uses PLC (Power Line Communications) technology to send and receive information through the power energy distribution grid. The project implementation consists of three steps: replace the mechanical meters for electronic meters, install a new communication system between each meter and the Blumenau´s substation and install a control center in headquarters in Florianopolis.

Information regarding consumption will be obtained remotely. The installed meters are connected to a communication module, called transponder, which sends signals with information about electricity consumption. These signals are sent through a distribution network, before they reach the CELESC's substation. In this place, special equipment receives and retransmits the signals to a central control, which analyses the collected data.

The automated measurement system introduces many facilities and benefits for consumers, such as: automatic metering reading; remote connection and disconnection modules in meters and automatic restart after the cut-off; lifting load curve of consumption; automatic record of power failure, with date and time of occurrence; monitoring the voltage on the grid.

A project will be started in 2011, Planning District Distribution Network and Generation of Sustainable Energy aims to achieve integration planning for alternative sources of generation energy (renewable, waste and sewage) in a distribution district. This project will be applied in Sapiens Park [12], in Florianopolis, with the purpose to be sustainable in generation and consumption.

Sustainable Energy district networks are defined as local electrical systems (consisting of generators, loads, storage and distribution) but with different features as well as been sustainable. These systems provide connection to the current energy system in CELESC. The project will elaborate on the methodology for developing these networks and devised a test case. This project must justify the deployment of district networks in different environments of interest, promoting, for example: (i) energy efficiency and quality, supported by local management and operation of the system; (ii) opportunity in the market for Smart Grids and offering new services and rates; (iii) convergence of energy and environmental solutions.

The results can be applied in different environments/districts that seek quality and energy and environmental sustainability. Moreover, it is noteworthy that the solutions studied in the project can be implemented to modernize the electrical system, even if initially these solutions are not grouped in the form of district networks.

V. CONCLUSIONS

In Brazil, the concept of Smart Grid has become the subject with greatest emphasis in the energy sector. The focus for now remains on Smart Meters. Very soon other smart solutions are expected to emerge on the national landscape with very positive forecasts for distributed generation, communication infrastructure and IT applications.

The Brazilian market for Smart Grids is seen as a potential market for many countries. Moreover, even with many financial and regulatory barriers, several national companies are already working on pilot projects to increase the national energy capacity and define models for future deployment of Smart Grid in Brazil.

Regarding the barriers for Smart Grid implementation in Brazil, most of them are the same as other countries. They are principally: (i) Market uncertainty and lack of policies on market structure and rules; (ii) Low public awareness and engagement; (iii) Interoperability and scalability assurance, (iv) Revenue uncertainty due to lack of regulatory definitions. In addition to these barriers, it is worth mentioning other particular issues in Brazil: (i) The electric power grid in Brazil is very large and it requires a huge amount of investment; (ii) More than 70% of the Brazilian energy matrix is hydropower and for this reason, another kind of renewable system is not easily accepted; (iii) In Brazil there are large and low density rural and remote areas and (iv) The electric energy and the telecom agencies are not aligned in relation to the roadmap for Smart Grid development in Brazil [5].

As described in this article, the companies have initiatives that explore the reality of Smart Grid. CEMIG are exploring a defiant idea of constructing a pilot in a city. AES Eletropaulo was the first to implement and integrate the Smart Metering in their systems. COPEL has worked to implement electrical vehicles and contributed to transform Curitiba into a digital city. And CELESC has been investing in new R&D projects that involve demand response.

Therefore, it is understood that there is a great opportunity to R&D and do business in Brazil, a country that is prominent in the global economic environment, with opportunities for investors in both the energy sector, and Smart Grids.

ACKNOWLEDGEMENT

We had the pleasure to write this paper with the important contribution of:

- Mr. Ricardo Van Erven, Director of Technology and Service, at AES Eletropaulo. He related the company's experiences about pioneering projects in Smart Grid presented in *Case 2: Smart Grid in Sao Paulo*.
- Mr. Daniel Senna Guimarães, at CEMIG, who discussed the challenges involved in implementing the project presented in *Case 1: Cities of the Future in Minas Gerais*.

 ISBN: 978-1-61208-136-6

REFERENCES

[1] Smart Grid Spotlight: Brazil. <http://www.itsyoursmartgrid.com/blog/2009_12_4_brazil.jsp>. March, 2011.

[2] International Energy Outlook 2010. <http://www.eia.doe.gov/oiaf/ieo/electricity.html>. March, 2011.

[3] Brazilian Electricity Regulatory Agency. Law Nº 12.212. <http://www.aneel.gov.br/area.cfm?idArea=546&idPerfil=6>. March, 2011.

[4] PUGA, Fernando Pimentel. *Visão do Desenvolvimento*. Brazilian Development Bank. <http://www.bndes.gov.br/SiteBNDES/export/sites/default/bndes_pt/Galerias/Arquivos/conhecimento/visao/Visao_81.pdf>. March, 2011.

[5] ECOEE Energia Eficiente. Smart grid: moving from theory to practice and in the fast lane in Brazil & Latin America. Report of the III Smart Grid Latin American Forum. Sept. 2010.

[6] Brazilian Electricity Regulatory Agency. <http://www.aneel.gov.br/areaPerfil.cfm?idPerfil=13>. March, 2011.

[7] *Companhia Energética de Minas Gerais.* (CEMIG). <http://www.cemig.com.br/sites/en/Pages/default.aspx>. March, 2011.

[8] AES Eletropaulo. <http://www.aeseletropaulo.com.br>. March, 2011.

[9] *Companhia Paranaense de Energia* (COPEL) < http://www.copel.com/hpcopel/english/>. March, 2011.

[10] DEC and FEC. <http://www.aneel.gov.br/cedoc/prt1978046.pdf>. March, 2011.

[11] *Centrais Elétricas de Santa Catarina* (CELESC). <http://www.celesc.com.br/>. March, 2011.

[12] Sapiens Parque in Santa Catarina. <http://www.sapiensparque.com.br>. March, 2011.

 ISBN: 978-1-61208-136-6

Smart Beijing: Correlation of Urban Electrical Energy Consumption with Urban Environmental Sensing for Optimizing Distribution Planning

Yong Ding, Takashi Miyaki, Till Riedel, Michael Beigl
Department of Informatics, TecO
Karlsruhe Institute of Technology (KIT)
Karlsruhe, Germany
Email: {firstname.lastname}@kit.edu

Wenzhu Zhang, Lin Zhang
Department of Electronic Engineering
Tsinghua University
Beijing, China
Email: {zhwz, linzhang}@tsinghua.edu.cn

***Abstract*—This paper focuses on consumer-side activities and investigates the environmental impact of the electrical energy consumer (transportation, buildings, street lighting, etc.), in order to improve the operational efficiency of the city as a whole. To achieve the goal we propose a two-layer approach which consists of a sensing layer and an application layer. To begin, circumstances within the city of Beijing are identified which have a large temporal impact on environmental conditions. A taxi-based vehicular ad hoc network is proposed as a low-cost and efficient approach for urban sensing using information collection methods of "Internet of Things" to capture various environmental parameters (air quality, noise pollution, traffic levels, water quality, etc.) in a distributed manner in real time. Using this data and correlation analysis techniques, global machine learning approaches will be trained to recognize important city events and dynamics which will affect electrical power consumption and create anomolies in pollution levels in specific locations, such as sporting events, rallies and fairs. This event-driven situational information could then indicate a predictive relationship with electrical energy consumption information, which can be exploited in the application layer. Besides, we introduce a middleware above the application layer to proactively plan a certain information management system around the Common Information Model and other information standards, in order to deal with lack of stable integration of the standards. Utilities could then get intelligence and values as expected from the data that will be collected from our system.**

Keywords-urban sensing; electrical energy consumption; two-layer approach; middleware; correlation analysis.

I. INTRODUCTION

Population growth, as well as a growing middle class, has caused an explosion in the number of vehicles on roads, resulting in traffic jams, environmental pollution and a series of other social problems. The urban electrical energy development has also been greatly impacted by these growth spurts as well [4], [6]. In the 21st century, development of low-carbon economy, construction of an ecological civilization and achievement of sustainable development are the general consensus of scientific community. Within the generalized Smart Grid concept, Smart City is in full swing in the development, especially for metropolises, megacities and cities in emerging economies. Though cities are major consumers of energy and generators of pollution, they can be active participants of Smart Grid and turning to be "prosumers" utilizing an urban environmental sensing network, which is a remote information sensing application in prospects of the entire city's resources.

The Internet of Things has the potential to broaden the Digital City concept [7] by adding more rich content, the result of which is a new concept called a Smart City. The Smart City concept emphasizes the inclusion of urban information for use in intelligent control and handling. If a Digital City is analogous to the information society which mainly relies on personal computing, a Smart City is then a reflection of a networked society which relies on pervasive computing with intelligent devices. Authors in [9] present a simulator based on software agents that attempts to create the dynamic behavior of a smart city, in order to analyze and investigate the system complexity of the future smart grid infrastructure. Through mobile cellular networks [2], a real-time urban monitoring system is constructed for evaluating the urban dynamics, and the visualizations of combined data realize several information layers on top of a map of Rome. Within the vision of smart cities, Copenhagen uses the Copenhagen Wheel [10] to achieve real-time environmental sensing and improve the cycling experience through the powers of crowd sourcing, Lisbon introduces a map-based service platform [11] that allows access to real-time information about the state of taxi transportation as well as predictions regarding its future state based on a naive Bayesian classifier.

Although several current Smart City activities have shown interdependencies between inter-personal interactions and their urban environment through a mobile platform [1], [3], such as the in daily life existing sensing infrastructure of mobile phones, they are still not directly involving some actuation technology in terms of energy reduction or efficiency. The presented work is going to investigate the impact of end-user behavior on the entire energy consumption, and the environmental impact of the urban energy consumer (transportation, buildings, street lighting, etc.), through

1) Developing complex machine learning approaches for

 ISBN: 978-1-61208-136-6

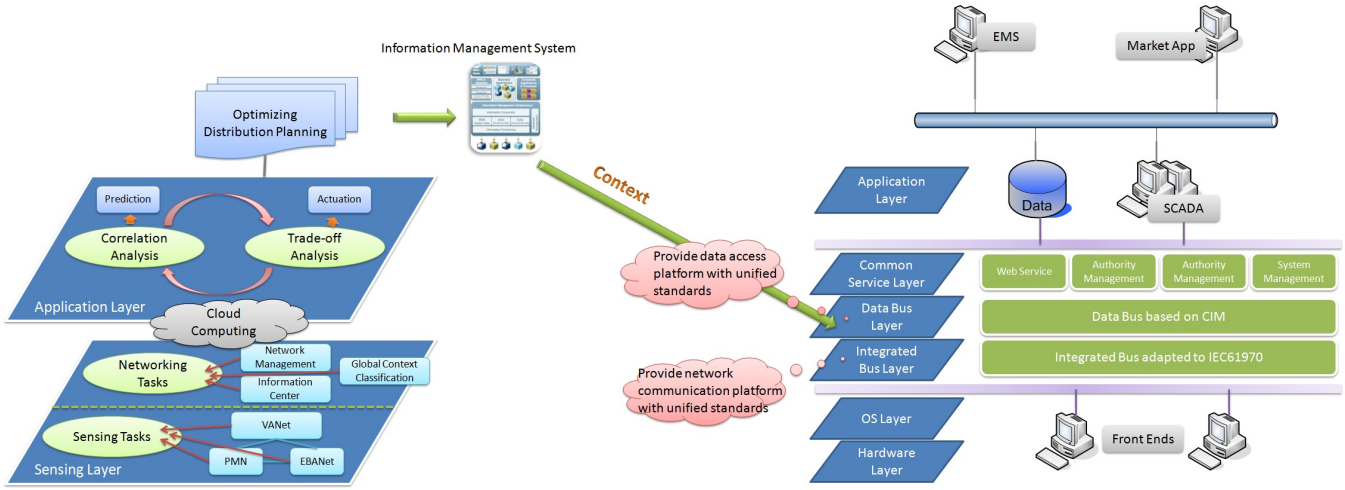

Figure 1. System architecture of two-layer approach with middleware to interface with CIM (Common Information Model)

distributed, city-wide situation recognition;

2) Defining abstraction levels of urban situational information;
3) Analyzing the influence of urban situational information on energy consumption and environmental quality levels.

Being able to recognize large-scale crowd and population level activities will enable prediction of the immediate future developments in energy consumption levels as well as active locations, which could be characterized as one proactive and interactive measure of electricity price reduction.

However, to achieve the goal of recognition of city events and dynamics, such as sporting events, rallies and fairs that will affect electrical power consumption and create new issues of pollution in specific locations, a dynamical, low-cost and energy efficient sensing platform is required. A taxi-based VANet (vehicular ad hoc network) as the main platform for a large city-scale sensing is to be presented, which is complemented with a PMN (Participatory Monitoring Network) using flash disks or mobile phones for a small-scale sensing with a finer granularity. Based on this metropolitan sensing network, an event-driven prediction process of the immediate future developments in energy consumption levels and highly active locations is then to be constructed in an application layer. Furthermore, a high level ODP (Optimizing Distribution Planning) is going to be introduced as a middleware over the application layer, which could give electric power industry standards such as CIM (Common Information Model) a proper context through an IMS (Information Management System), since today the UML-based CIM is broadly applied for system and business process integration by utilities worldwide (see Figure 1 right part), and related information exchange between systems.

II. System Architecture

As described in Section I, a two-layer approach presented in Figure 1 (left part) is employed to realize an application framework based on the urban sensing for supporting the optimization of the energy consumption.

- The metropolitan sensing network based mainly on VANet consisting of city taxis, collects and processes the urban sensing data in distributed manner. The integration of wireless environmental sensing terminals in city taxis realizes a unique information collection by incorporating these vehicles in the IoT (Internet of Things), capturing environmental and taxi-based information in real time.
- An application layer is established on the sensing layer as one framework, which combines the IoT technology with Smart City requirements. This will enable intelligent decision making, control and services based on a networked solution leveraging situational recognition technology, the IoT and distributed intelligent systems.

Through correlation analysis IV, such as a multivariate linear regression analysis [8], [13] among the non-urban structural factors, based on global situation recognition in the sensing layer, immediate future energy development is then predictable in the application layer. In electric power transmission and distribution, the CIM that is defined in UML, provides a common language to describe exactly what data is being exchanged among a utility's business systems. The major motivation for this exchange has been to support system planning functions including transmission planning, maintenance scheduling, and operations planning. So above this application layer, a local model of ODP is proposed as middleware to interface with CIM. The local ODP will give the CIM a proper context as input through a certain information management system, which could let the utility

 ISBN: 978-1-61208-136-6

adjust the activated transmission planning in real-time in view of the predicted immediate future energy development, in order to optimize the urban electrical energy distribution in real-time, thereby reducing the electricity price.

III. Sensing Layer

For the purpose of a metropolitan sensing, a model of distributed urban sensing is proposed, in which each mobile sensor node is responsible for the distributed processing task with respect to the coverage zone of the neighboring nodes, including local recognition processing. This sensing layer enables besides the urban sensing and networking tasks, the global situation recognition for city events as well, which could alternatively accomplished through a social network service like Twitter or Facebook.

The main platform of this mobile sensing network, which has already been done, is a VANet that uses every participating taxi as a wireless node to gather and transmit data based on IEEE802.15.4c, because 802.11p that is the standardized MAC layer of VANet fails to provide reliable broadcast support in a congested highway.

Some units in a city are more important for energy consumption and must be monitored with a finer granularity than the rest of the system. Examples of these are government buildings, tourist attractions and university campuses. Therefore, a small-scale sensing is being developed, which will be accomplished with a PMN using flash disks or mobile phones.

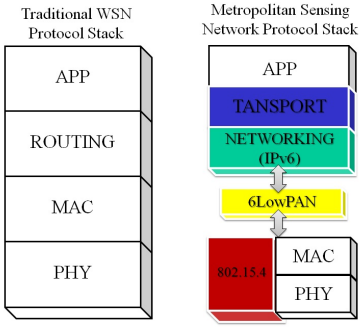

Figure 2. Comparison of protocol stack between traditional WSN and our metropolitan sensing network

A. Protocol Stack

This main metropolitan sensing network has a large number of sensor nodes which work in a distributed manner, so that the low cost design and energy efficiency protocols are the main features of this network. Differing from the conventional sensor networks whose protocol stack is composed of four layers, we designed a six-layer protocol stack, see Figure 2. The MAC and PHY layer are compliant to IEEE 802.15.4. We replace the ROUTE layer with IP layer which is running IPv6 protocol. Moreover, the node can be accessed via Internet directly from client computers. In order to transport IPv6 data packets over a low-power 802.15.4 radio, an adaptive layer is added between IP and MAC layer.

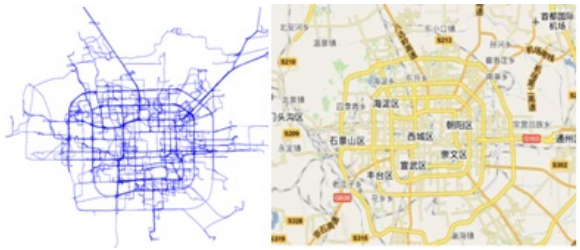

Figure 3. Coverage of the city by taxis; (left) the accumulated traces of ten taxis in one day (7 am - 9 pm)

B. First Dataset

Through analyzing the GPS traces of over 20,000 taxis of Beijing, an interesting fact is revealed that quite a few taxis could offer excellent spacial coverage of the city, at the cost of a long round trip time, see Figure 3. For the delay-tolerant applications, such as air quality monitoring, carbon emission surveillance etc. using taxis as data collector and data carrier will be a most low-cost and efficient way to get a better understanding of the dynamics of a city.

IV. Application Layer

Situation classification and prediction based on the urban sensing are proposed for detecting city events and dynamics, to improve prediction of temporal and spatial energy consumption characteristics. This situational information is event-driven, and cannot be statistical derived, as opposed to other information sources such as weather forecasting which currently factor into such models. In order to make this correlation clearly, we will proceed with the following three research topics:

- Developing machine learning approaches: for urban pattern (situation) recognition or classification, the sensing data is assumed to be temporally dynamical, so HMM (Hidden Markov Models) or other classification algorithms based on time series are going to be considered. Due to the complexity of the city scene, we are going to decompose the scene into many relatively homogenous objects. The various statistical characteristics of these homogenous objects in the scene are then subjected to an object-oriented classification, such as traditional statistical classification combined with fuzzy logic classification.
- Researching the optimal abstraction levels of situational information [12]: 1) raw sensor data of for instance, taxi-based sensor nodes; 2) low level contexts, such as states of taxis, like taxi location; 3) high level contexts, are the city activities and dynamics, such as infrastructure changes at the edge of Inner City,

 ISBN: 978-1-61208-136-6

waterfront development, household services activities, etc.

- Researching the influence of urban situational information on energy consumption: the benefits of context (situation) prediction for enabling spatially fine-grained evaluation and control of power consumption in an industrial application have been discussed in [5]. For the urban scenario, we will investigate the use of a multivariate linear regression analysis among the non-urban structural factors that have a significant impact on the power demand, such as the location of the residence relative to the city center, availability of private car in the household, etc.

Correlation Analysis: through the data of air quality (CO, CO_2, SO_2, NO_x ...), location data of taxis, etc. collected by the deployed urban sensing network, the global situation classification system will recognize important city events and dynamics which are energy relevant. For instance, during the Football World Cup, many fans will get off work earlier in order to drive home before the game start. This action will surely change the city's activities and dynamics, which leads directly to the immediate distribution change of urban energy consumption. However, this change could not be in view of the previous statistical consideration of the urban energy distribution. The sudden surge of air pollution which is transport-conditional and the trajectory of the taxis could become the crucial situation contexts that correlate directly with the urban energy consumption in residential areas. Therefore, here mentioned correlation should be actually deduced not directly from the sensed urban data, but from some extracted situational information of the sensed urban environment as described before.

V. Conclusion and Future Work

This work began by identifying the need for energy correlation analysis with urban environmental sensing. A two-layer architecture was proposed that comprises a sensing layer and an application layer. The already realized metropolitan sensing network based on VANet collects and processes the urban sensing data in a distributed manner, which not only enhances the information processing capacity, but also has the capability of network layer.

An application layer was introduced as one of the next research steps, which enables an application framework based on the urban sensing for support of intelligent decision making, control and services. Through the proposed middleware ODP, utilities could get more intelligence and value from the data that will be collected from existing USI (Urban Sensing Infrastructure) and other "smart grid" devices, like AMI (Advanced Metering Infrastructure). Although the main concepts have been presented here, a full evaluation of the system is yet to be completed. The main aspect which is being explored is the parameterization of the correlation between event-based situational information and electrical energy consumption data to introduce this as a metric for further optimizing urban energy distribution by means of non-statistical energy consumption prediction.

References

[1] J. Burke, D. Estrin, M. Hansen, A. Parker, N. Ramanathan, S. Reddy, and M. B. Srivastava. Participatory sensing. In *Proceedings of World Sensor Web Workshop, ACM SenSys*, Boulder, Colorado, October 2006.

[2] F. Calabrese, C. Ratti, M. Colonna, P. Lovisolo, and D. Parata. Real-time urban monitoring using cell phones: a case study in rome. In *IEEE Transactions on Intelligent Transportation Systems*, volume 12, pages 141–151, 2011.

[3] A. T. Campbell, S. B. Eisenman, N. D. Lane, E. Miluzzo, and R. A. Peterson. People-centric urban sensing. In *Proceedings of the 2nd ACM/IEEE Annual International Workshop on Wireless Internet (WICON '06)*, number 18, Boston, MA, Aug. 2-5 2006.

[4] P. Crompton and Y. R. Wu. Energy consumption in china: past trends and future directions. *Energy Economics*, 27:195–208, 2005.

[5] Y. Ding, H. R. Schmidtke, and M. Beigl. Beyond context-awareness: Context prediction in an industrial application. In *Proceedings of the 12th ACM international conference adjunct papers on Ubiquitous computing (Ubicomp '10)*, pages 401–402, Copenhagen, Denmark, September 26-29 2010. ACM Press.

[6] Energy Information Administration. International energy outlook 2010. http://www.eia.doe.gov/oiaf/ieo/world.html, 2010.

[7] T. Ishida and K. Isbister. *Digital Cities: Technologies, Experiences, and Future Perspectives*, volume 1765, pages 1-17. Lecture Notes in Computer Science, Springer, 2000.

[8] O. Karkacier, Z. G. Goktolga, and A. Cicek. A regression analysis of the effect of energy use in agriculture. *Energy Policy*, 34(18):3796–3800, 2006.

[9] S. Karnouskos and T. N. de Holanda. Simulation of a smart grid city with software agents. In *Third UKSim European Symposium on Computer Modeling and Simulation, EMS '09*, pages 424–429, Washington, DC, USA, 2009.

[10] C. Outram, C. Ratti, and A. Biderman. The copenhagen wheel: An innovative electric bicycle system that harnesses the power of real-time information and crowd sourcing. In *Ecologic Vehicles Renewable Energies*, 2010.

[11] S. Phithakkutnukoon, M. Veloso, C. Bento, A. Biderman, and C. Ratti. Taxi-aware map: Identifying and predicting vacant taxis in the city. In *First International Joint Conference on Ambient Intelligence (AmI-10)*, pages 86–95, 2010.

[12] S. Sigg, S. Haseloff, and K. David. A study on context prediction and adaptivity. In *Proceedings of the International Workshop on Context Modeling and Management for Smart Environments (CMMSE '07)*, pages 717–722, 2007.

[13] F. S. Westphal and R. Lamberts. Regression analysis of electric energy consumption of commercial buildings in Brazil. In *Proceedings of Building Simulation*, pages 1543–1550, 2007.

 ISBN: 978-1-61208-136-6

Synchronisation Challenges within Future Smart Grid Infrastructure

Jonathan Shannon, Hugh Melvin, Ronan O hOgartaigh, Antonio Ruzzelli
College of Engineering and Informatics, NUI Galway Ireland
ESB Networks, Ireland
CLARITY, University College Dublin, Ireland
shannon.jonathan@gmail.com, hugh.melvin@nuigalway.ie, ronan.ohogartaigh@esb.ie, ruzzelli@ucd.ie

***Abstract*— Synchronisation of computer systems is a challenging task when the systems communicate across a dynamic and variable latency network but becomes especially challenging when the network contains wireless communication links. The success of the evolving smart grid project will depend hugely on Information and Communication Technologies to revolutionise the traditional power grid and will place various demands on current synchronisation techniques. Utilisation of wireless communication systems within the smart grid infrastructure seems inevitable, thus, if the project is to reach its full potential then some of the shortfalls of current synchronisation techniques over wireless must be remedied. This paper reviews the vital role of synchronisation within current and future smart grid infrastructures and outlines some proposals to remedy the shortfalls of current time synchronisation techniques. In particular, we focus on improving the implementation of the Network Time Protocol over 802.11 networks along with an optimisation technique to reduce the energy usage of a common Wireless Sensor Network synchronisation protocol.**

Keywords-802.11, NTP, PTP, Synchronisation, WSN.

I. INTRODUCTION

The current grid is a real-time system whereby generation must always match demand. In any real-time system, time is a critical factor and when the system is distributed, synchronisation of its various elements is essential. Current grid infrastructures employ synchronisation techniques to permit such functions as fault detection, protection testing, load balancing, scheduling and analysis. Supervisory Control And Data Acquisition (SCADA) [1] systems play a very significant role in grid operation and through the use of synchronised time also permit logging of data which, can prove useful in determining the events leading up to and during disturbance events. In distributed power generation, geographically distributed generators supply power to the grid and synchroscopes ensure that they do so safely by synchronising frequency and phase.

In recent years, more advanced ICT (Information and Communication Technologies) systems based on synchronisation techniques have evolved. These include fault detection systems such as the Fault Location Acquisition Reporter (FLAR) [2] system developed by the Bonneville Power Administration (BPA) in the US and PMUs (Phasor Measurement Units) [2] that utilise precisely synchronised phasor measurements to produce an instantaneous picture of the entire state of the grid in real time.

Looking to the future and the evolving Smart-Grid/Smart-Networks project, the role that time, timing and phase synchronisation will play will greatly expand. Smart grid will rely on advanced ICT technologies to revolutionise the traditional electricity grid. Smart grid will by definition significantly increase the complexity of the current grid's static design by transforming it into a much more dynamic network where the distinction between producer and consumer will often be blurred. The composite elements of this complex system will place significant demands on current synchronisation technologies in order to meet its full potential.

The remainder of this paper is structured as follows. Section II outlines the role of synchronisation techniques within the traditional grid. Section III highlights some of the possible synchronisation requirements of future smart grid systems. Section IV details some of the synchronisation techniques employed in current ICT systems and highlights the challenges of deploying these techniques over wireless communication links. Section V outlines some solutions to meet these challenges. Section VI concludes the paper.

II. ROLE OF SYNCHRONISATION IN CURRENT GRID INFRSTRUCTURE

Current grids operate using a demand-response scheme whereby electrical energy is generated in response to real-time demand. SCADA systems play a key role, performing four distinct functions, namely, data acquisition, data communication, data presentation and control. In relation to data logging, data collected using a SCADA system must be time stamped in order to determine the correct sequence of events. This is performed by Remote Telemetry Units (RTU) which, timestamp sensor data, typically to within a few milliseconds of global time.

A. Advanced Grid Synchronisation Topics

In recent years, the role of time synchronisation within grid infrastructures has evolved. One particular advanced application of synchronisation is transmission cable fault detection. In the case of a cable fault, manual inspection can be impractical, time consuming and costly. Some impedance based automatic fault location systems are prone to error. When a power cable is damaged an electromagnetic noise burst is propagated out which, can be detected and timestamped by fault detection units at substations on each end of the cable. Subsequent analysis of the reception times can deduce the position of the fault based on signal Time of Arrival (TOA). This system is only effective if the devices on each end are synchronised to within a microsecond or better. Synchronisation of this granularity allows the location of the fault to be determined to within 300 meters. The Fault Location Acquisition Reporter (FLAR) developed by BPA in US is

 ISBN: 978-1-61208-136-6

based on this scheme. The FLAR system has fault detection units located at numerous substations, each synchronised using GPS.

Another example is Phasor Measurement Unit (PMU) technology. A PMU is a device which, provides phasor information associated with a particular point on the power grid. This information describes the magnitude and phase angle of a sinusoidal waveform. If a number of PMUs are placed at various locations within the power grid and synchronised to within a microsecond of each other they can provide precise real-time information regarding the state of the grid. This proves invaluable for monitoring grid activity. PMUs employed in this manner are referred to as synchrophasors and form an integral part of a fully functional phasor network. A complete phasor network consists of dispersed PMUs together with Phasor Data Concentrators (PDC) to aggregate PMU data and a SCADA system to monitor the accumulated data. In a typical deployment PMUs are synchronised through the use of integrated GPS receivers. Each PMU sample is time stamped and transmitted to a PDU using a standard protocol. The PDU correlates samples from multiple PMUs based on time stamps and forms a measurement set for that particular segment of the grid. The PDU then provides a direct output to a SCADA system which, provides a real-time visualisation of that grid segment.

Finally, many line protection systems are based on precisely synchronised data for correct operation. Loss of synch can cause inadvertent (false positive, false negative) operation. For example, a utility might incorporate dedicated fiber links between grid sensing devices and a central aggregator. The propagation time of data via these links would be constant and known allowing data to be time stamped solely at the aggregator. If these links were to be replaced by leased lines incorporating deferent communication technologies and subject to varying traffic loads then time stamping solely at the aggregator would most likely be problematic.

III. SMART GRID

The smart grid project aims to revolutionise the current grid infrastructure in order to reduce inefficient energy consumption, to facilitate the move towards renewable energy, and to better utilise the grid's capacity so as to accommodate growing electricity demand. A key driver for this will be through integration of ICT into the electricity grid, from generators through transmission right down to consumers. The current grid is based largely on one-directional power flows in a demand-response scheme. The system is designed to handle peak demand by adding additional and less efficient "peaking" capacity, thus adding to the overall cost. A smart grid system will use a variety of technologies to monitor and better control consumer demand, possibly incentivised through real-time pricing structures. A core objective is to level the current peak demand curve thus reducing total costs and ensuring that additional grid capacity is used to its full potential. The extent to which, consumers will be motivated to control/minimise energy usage either due to environmental concerns or (more likely) economic cost remains to be seen and will dictate the success or otherwise of demand side management (DSM) strategies.

It must of course be borne in mind that the smart grid is not an end in itself, but a means to an end, and if there are other approaches which, meet the goals of increased fuel security (from local renewable resources) and reduced emissions (from decreased usage of fossil fuels) these should also be considered e.g., reconductoring transmission lines in High Temperature Low Sag (HTLS) Conductor to provide an extra 50% capacity. Additionally, smart grid can only operate where there is an existing Grid, and where this Grid has the capacity or "headroom" to operate as flexibly as smart grid system dynamics require.

As such, a smart grid system may facilitate generation from independent suppliers utilising different generation techniques, renewable or otherwise. These might include Combined Heat and Power (CHP), solar/wind/ocean energy, micro-generation as well as more futuristic sources such as Vehicle to Grid (V2G). Smart Metering at each consumer premises has a key role to play in this.

Technologies incorporated within the core of the grid will thus include HTLS conductors for efficient electricity transmission, storage units to house generated surplus energy and advanced PMU-based power flow monitoring for real-time grid activity monitoring. Within such a smart grid system the scale and complexity of SCADA systems will increase in orders of magnitude from current systems. Such SCADA systems may operate at a macro grid level or localised within micro-grids. Already, we have seen large strides in Energy Management Systems (EMSs) for end customers that seek to minimise/manage energy use. Currently, these communicate internally via a Home Area Network (HAN) with a multiplicity of devices to manage demand. In future, these will also be integrated within smart grid as they have an important role to play, leading to a merging of smart building, smart metering within the smart grid umbrella. We briefly describe both smart metering and smart buildings in later sections.

The evolution of smart grid systems will also extend to the transport sector. For many reasons, electric vehicles will be a key driver of DSM at customer level by incentivising charging in valley periods. Looking further to the future, vehicle-to-grid (V2G) systems may materialise allowing vehicles to take on the role of both an energy consumer and supplier within the grid.

While a wide variety of technologies will be essential to make a smart grid system a reality, one fundamental aspect will be the synchronisation technologies employed to glue the system together. A smart grid system will effectively be a large real-time distributed system and as such time and frequency will play a key role in its correct operation. Synchronisation of various elements of the system will be vital for effective monitoring and control of energy flow from suppliers to consumers, see Fig. 1.

 ISBN: 978-1-61208-136-6

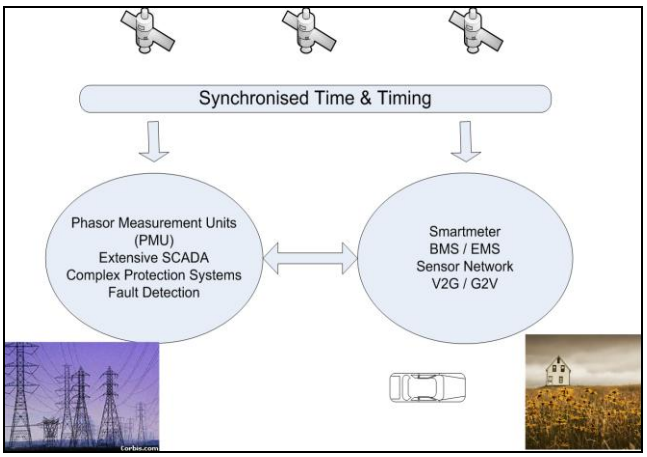

Figure 1- Synchronisation of Grid Elements

A. *Smart Metering*

An effective smart grid system can only be realised by means of precise real-time monitoring and control of power usage down to the end-consumer. Real-time monitoring of power usage permits accurate analysis of daily demand and allows for construction of an efficient energy plan based on real-time pricing. Recent years have seen the wide scale deployment of so-called smart meter trials in numerous countries across the globe. In contrast to traditional meters a smart meter provides a more comprehensive report of power consumption in addition to bi-directional communication capabilities. In a future scenario, smart meters could provide real-time data to a Home Area Network (HAN) that manages an internal Energy Management System; the HAN in turn will communicate externally with the smart grid. As such, meters must be synchronised to Universal Coordinate Time (UTC). HAN communication methods that have been used include Power Line Communication (PLC), Wired LAN, Wi-Fi and licensed radio networks. Undoubtedly, smart metering will play a key role in the development of future smart grid. One might envisage a multiplicity of smart meters within a commercial or industrial building each monitoring the activity of a power intensive system, for instance, a heating or air conditioning system. Each of these smart meters would be synchronised to a global time reference for use by the consumer's EMS. Analysis by the EMS would provide a means to construct a schedule to better optimise, from a cost perspective, the operation of these systems. Such a system would also permit DSM incentivised schemes including automatic load shedding in low frequency situations brought about by sudden loss of generation. Such notifications to the HAN will likely use both broadcasting and unicasting techniques, the former to reach multiple aggregated consumers where low priority loads could be removed at short notice, and the latter to manage larger individual loads.

A more elaborate scheme within a building might integrate networks of sensing devices to provide in-depth analysis of individual systems. For instance, sensing devices capable of measuring temperature, airflows could be dispersed around a building and networked together to form a Wireless Sensor Network (WSN). Data collected from sensors within a WSN needs to be time stamped effectively. Thus, use of WSN synchronisation techniques such as the Reference Broadcast Synchronization (RBS) algorithm [3] or the Flooding Time Synchronization Protocol (FTSP) [4] will be essential though the extent of synchronisation required is application dependent.

B. *Smart Buildings*

As described, both smart building and smart metering technologies are essential in the evolution of smart grid. Smart building is a term used to describe a building automation system with advanced automatic systems for controlling heating, cooling, lighting, security and various other functions. A smart building home controller may take the form of a PC with the required hardware and software to communicate with and monitor the systems. Communication between different devices might also be facilitated through emerging standards such as BACnet [5] or KNX [6]. As described, HAN communication between a home controller and various automated systems might be performed using a Power Line Communication protocol or some wireless protocol such as ZigBee or Wi-Fi. Coordination of the automatic systems within a smart building will typically be performed by defining various operating modes via the home controller. An operating mode may define the lighting, heating, air-conditioning and security requirements for a particular time of the day which, is subsequently activated automatically at that time by the synchronised home controller. The use of smart meters together with building automation systems would provide a means to better define operating modes that would meet an individual's desired demand profile.

C. *Electric Vehicles*

Electric vehicles (EVs) have a key role to play in smart grid by facilitating national strategies for reducing reliance on fossil fuel energy and moving to renewable electricity based on wind/ocean/biomass etc. Besides the environmental benefits, the use of indigenous sources of energy will eliminate external dependence, however, it will require a large initial investment and the benefits may not be observed for many years. Currently the main disadvantages of EVs are the low energy density and lengthy recharging time of their batteries, issues which, are likely to be remedied in future years. While it is largely agreed that EVs have a key strategic role to play in reducing fossil fuel dependency and fostering DSM (through off peak charging tariffs), it also appears possible that they may also take on the role of suppliers through vehicle-to-grid (V2G) technologies. Similar to the situation described above with smartmetering/smartbuildings, a V2G system will communicate via HAN to the grid and would allow EVs to provide electricity to the grid during critical events or during peak hours, thus helping to reduce need for traditional spinning reserve and inefficient peaking plant. A V2G system could also act as the main supplier to a residence in the event of an outage.. Ireland has a very ambitious target for electric vehicle penetration with a strategy to achieve 10% all-electric vehicles by 2020 with 3,500 charge points by 2011 underway [7].

 ISBN: 978-1-61208-136-6

IV. SYNCHRONISATION OVER ICT

The future scenario of a smart grid facilitated through smart metering and smart buildings will place huge demands on the supporting ICT infrastructure. As detailed, the current scale of SCADA will increase in orders of magnitude and such SCADA, operating at macro or micro scale will be IP based. For example, the SCADA system operated by ESB Networks, the Irish Distribution System Operator for the whole country currently communicates with < 1000 Medium/Low voltage sub stations connected largely through dedicated radio and roughly 1000 pole mounted devices with third part GPRS connectivity. Contrast this with possible future smart grid deployment that will see at a minimum each consumer smart meter and HAN connected. In addition to this, it is likely as outlined that via a the consumer's HAN, multiple devices such as secondary smart meters, vehicles, and various appliances will be connected, To facilitate this scenario, each node will have its own IP address to facilitate management within the HAN and also outside as they interact with smart grid. As such, the scale of the required infrastructure for a small country with just over 1m homes represents a huge step in SCADA scope. Realistically, a hierarchical network of SCADA systems will be deployed to distinguish between critical infrastructure i.e., substations and less critical. For example, in an Irish context, there are approximately 12,000 MV/LV substations of 200kVA and over. Moving to IP will ease some complexity but has already raised serious security and privacy concerns. Within the high, medium and low voltage grid, where power flows will be much more dynamic, the architecture of monitoring, control and protection systems will all have to be redesigned to meet the changing requirements.

Synchronisation of various elements of a smart grid system will be vital for effective monitoring and control of energy flow from suppliers to consumers. Smart grid will thus most likely incorporate the synchronisation techniques utilised by current ICT systems. The motivation for sync can be attributed to the imperfections in current computer system clocks which, typically utilise inexpensive quartz crystals as their frequency standard. While systems such as Oven Crystals and Global Navigation Satellite Systems (GNSS) (GPS, Glonass and Galileo) act as a very reliable and accurate source of time, they are not a practical or cost effective time sync solution in many scenarios As such the use of a software based synchronisation protocol is favored.

A. NTP & PTP

At present NTP (Network Time protocol) [8] and PTP (Precision Time protocol) [9] are the de-facto synchronisation protocols utilised over wired networks. NTP is designed for dynamic and variable latency packet switched wide area networks and can attain low-millisecond accuracies if well managed. PTP can attain microsecond accuracies over LANs, thus, meeting the precision requirements of applications that NTP cannot, but at the cost of requiring a tightly managed network and specialised time stamping hardware.

B. Synchronisation Errors

NTP and PTP use pair-wise synchronisation to synchronise the clocks of computer systems whereby a host wishing to be synchronised sends a time request to a reference node and records the transmission time t1. The reference node replies with the reception time of the request message and transmission time of the reply message, t2 and t3 respectively. The host node records the reception time of the reply message t4 and uses the four timestamps to calculate the propagation time and, thus, determine its clock offset from the reference. (1).

$$\theta = \frac{t2+t3-t1-t4}{2} \quad (1)$$

This technique operates on the assumption that the each-way message delays between a sender and receiver are symmetric. If this is not the case, which, in reality is often true, then the calculation of a clock's offset from its reference will be inaccurate. The different sources of synchronisation errors can be attributed to the different components of a synchronisation message's latency. These components can be categorised as the send time, access time, propagation time and receive time. The send time represents the time taken for a host to construct a synchronisation message and transfer it to the network interface. The access time corresponds to the delay incurred by the network interface while waiting to gain access to the communication medium. The propagation time is simply the time taken for the message to travel to the receiver once it has left the sender while the receive time represents the time taken for the receiver's network interface to receive the message from the communication medium, decode it and notify the host application that it has arrived. It is important to note that, with pair-wise synchronisation, the magnitude of a message's delay is not the factor which, results in a clock error but rather the difference between the delays of a request message and a response message.

NTP and PTP use different techniques to mitigate the effects of non-deterministic delays on time estimation. NTP references multiple time sources and utilises a suite of statistical algorithms to deduce the most probable clock offset. Conversely, PTP takes advantage of the fact that its operating environment is managed and employs PTP-aware internetwork nodes and hardware time stamping to increase precision. While these techniques prove very effective it is important to note that both NTP and PTP were designed to operate within the wired domain, and as such, wireless links pose greater challenges.

C. Wireless Issues

A wireless network utilizes a shared medium that must be allocated to individual nodes in a protocol-dependent fashion. Depending on the technique used and the traffic load at a particular time, transmission of packets between two particular nodes may be subject to large contention delays. The most accepted and widely implemented set of standards for wireless communication over LANs is defined by IEEE 802.11. The basic 802.11 specification defines both the physical and data link layers for communication across a wireless network. Access to the wireless medium as defined by the 802.11 MAC layer is controlled by the distributed coordination function (DCF) which, controls access by using a CSMA/CA (carrier sense multiple access with collision avoidance) mechanism. It

 ISBN: 978-1-61208-136-6

operates by first checking that the medium is clear using carrier sensing functions and if so begins transmission. If the medium is in use the station backs off for a random time interval to avoid a collision. In the case of an 802.11 network, all nodes including the access point conform to the same access rules. Since the access point (AP) carries out extra work, an NTP host operating over an 802.11 network with competing nodes can experience significant asymmetric round-trip delays and, thus, accumulate significant clock errors. In relation to a smart building with time sensitive devices running NTP implementations and communicating via the building's Wi-Fi LAN this would prove problematic.

D. Wireless Sensor Networks

As mentioned in section III, WSNs will most likely form a significant segment of smart grid, particularly at the consumer side. The greatest issue concerning WSNs is their limited energy supply. Thus, techniques to ensure optimal use of power consuming sensor components by synchronization algorithms will be required.

V. CONTRIBUTION

To summarise previous sections, future smart grid systems will be highly complex and dynamic and will require a comprehensive ICT support infrastructure for stringent monitoring and control of demand in real-time. These systems will require various degrees of synchronisation from generation down to the consumer premises. Within the latter, communication between nodes may be over wired or wireless networks. Wi-Fi is currently the most popular form of wireless communication due to ease of operation and installation. However, as described, contention delays can severely decrease the accuracies achievable by current time protocols and as such solutions must be found. In addition to this, the use of WSNs within smart grid systems will require that energy saving techniques are incorporated into WSN synchronization protocols to prolong battery life whilst maintaining adequate synchronisation levels.

A. Synchronisation over 802.11

One solution to asymmetry being implemented by the authors entails the use of 802.11 acknowledgement frames (ACKs) and special probe frames to deduce and eliminate the non-deterministic medium access times at the host and access point. Unlike many data link layer protocols, 802.11 incorporates positive acknowledgements. All transmitted frames must be acknowledged by the receiving party via an acknowledgement frame or the transmission is considered a failure. The transmission of data and reception of an acknowledgement is an atomic operation and must be completed fully or not at all.

As illustrated in Fig. 2, if the sender of a time message records the reception time of its corresponding ACK frame that sender could largely eliminate the non-deterministic send time, and more importantly, the medium access time of that message. The result would be the elimination of the effects of traffic contention and sender delays in the upload direction of the time message. While this method would be beneficial to some degree it would not address the larger issue of non-deterministic delays in the download direction. Larger download delays can be attributed to the fact that users in general download more data than they upload and more importantly, an access point must compete with all other wireless nodes equally. To estimate download delays the sender could send a special probe request frame to the access point that would initiate a corresponding response frame. The reception times of the request frame's acknowledgement and the response frame could then be used to estimate the send and access delays at the AP at that point in time, thus, reducing asymmetry errors.

Another possible solution being explored is improving synchronisation accuracy by real-time analysis of network related data. Analysis of past data can help to quickly identify network trends and make predictions about the state of the network. Both statistical techniques and more elaborate methods such as artificial neural networks are being investigated. A statistical approach might involve analysing network related data and forming a probability model to infer the most probable behavior of the network at a particular point in time. In addition, analysis of the correlation between a time packet's round trip delay and the corresponding estimated offset could be used to identify and correct for probable asymmetric delays. An artificial neural network could provide an even more effective solution by recognising patterns in the network and using this to improve NTP performance.

At an abstracted level, both approaches can be viewed as a module that can be linked to some synchronisation protocol and used to mitigate the asymmetric effects of wireless contention. For instance, an intermediate MAC to NTP interface module could provide one or both of the above techniques depending on the condition of the wireless network. (Fig. 3).

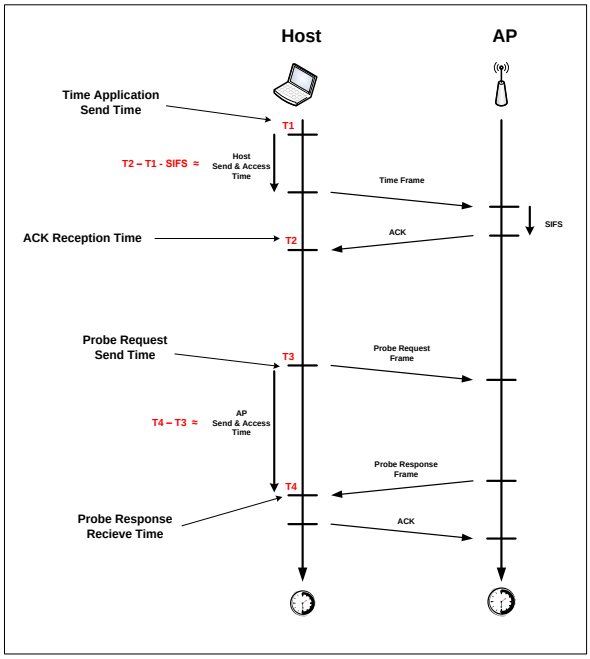

Figure 2. Determination of send and MAC delays

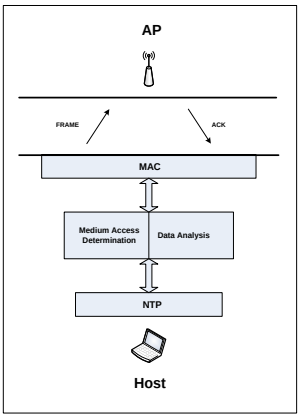

Figure 3. MAC to NTP interface module

B. Energy Conservation in WSN

At present FTSP is the de facto synchronisation protocol used in WSNs. To retain the precision requirements of a WSN application, FTSP nodes must broadcast messages at a predetermined periodic interval, the value of which, is influenced by the nodes operating environment and to a lesser extent their clock characteristics. These periodic transmissions allow nodes to determine their clock skew relative to an elected root node. In most cases this transmission interval is not optimal resulting in needless radio transmissions and, thus, energy wastage.

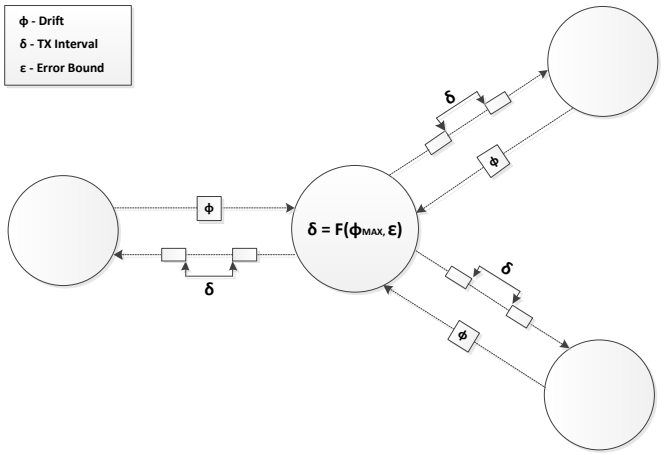

Figure 4. Dynamic FTSP

A solution the authors are currently implementing is to have an FTSP node alter its transmission interval based on the overall precision requirements of the WSN application and the rate of change of skew of neighboring nodes. A node's transmission interval would therefore be dictated by its most unstable neighboring node. This technique will result in a significant reduction in transmissions particularly in a variable operating environment (Fig. 4) and allow an administrator to customise the synch level for the application domain.

VI. CONCLUSIONS

This paper has explored the vital role that synchronisation currently plays in electrical grids and has highlighted the importance of synchronisation in the evolving smart grid project. It is certain that future smart grid systems will rely heavily on current ICT technologies and synchronisation techniques. This paper has briefly outlined two research projects to improve synchronisation performance over wireless networks. The first focuses on NTP performance over Wifi whereas the second has developed a novel extension to the FTSP protocol for sensor networks that will deliver quality synchronization at reduced energy cost.

ACKNOWLEDGMENT

Our research is funded by IRCSET (The Irish Research Council for Science, Engineering & Technology) and is being undertaken in collaboration with the Performance Engineering Lab (PEL) (http://pel.it.nuigalway.ie/). We also wish to acknowledge the assistance and contributions from ESB Networks, the Irish Distribution System Operator in realising this paper.

REFERENCES

[1] Daneels, A. and Salter, W., "What is SCADA?", (ICALEPCS), 1999.
[2] Martin, K. E., "*Precise Timing in Electric Power Systems,"* IEEE International Frequency Control Symposium (IEEE), pp. 15-22, 1993.
[3] Elson, J., Girod, L. and Estrin, D., "*Fine-Grained Network Time Synchronization using Reference Broadcasts,"* The Fifth Symposium on Operating Systems Design and Implementation (OSDI), pp. 147–163, 2002.
[4] Maróti, M., Kusy, B., Simon, G. and Ákos Lédeczi, "*The Flooding Time Synchronization Protocol*," Proceedings of the 2nd international conference on Embedded networked sensor systems (SenSys), pp. 39-49, 2004.
[5] www.bacnet.org (last accessed – 18 Mar, 2011)
[6] www.knx.org (last accessed – 18 Mar, 2011)
[7] www.esb.ie/main/press/press-release399.jsp (last accessed – 18 Mar, 2011)
[8] Network Time Protocol (NTP). http://www.faqs.org/rfcs/rfc1305.html (last accessed – 18 Mar, 2011)
[9] IEEE-1588 - Standard for a Precision Clock Synchronization Protocol for Networked Measurement and Control Systems.
[10] Mills, D. L., "*Internet time synchronization: the network time protocol*," IEEE Trans. Communications, vol. 39, no. 10, pp. 1482–1493,1991.
[11] Allan, D. W., Ashby, N. and Hodge, C. C., "*The Science of Timekeeping*, Technical report", Hewlett Packard Application Note 1287, 1997.
[12] Römer, K., Blum, P. and Meier, L., "*Time Synchronization and Calibration in Wireless Sensor Networks"*, In: Stojmenovic, I. (ed.) Wireless Sensor Networks, Wiley and Sons, Chichester, 2005.
[13] ITU-T G.810, "*Definitions and Terminology for Synchronisation Networks"*, International Telecommunication Union, 1996.
[14] Melvin, H., O Flaithearta, P., Shannon, J. and Beloqui Yuste, L., **"***Time Synchronisation at Application Level: Potential Benefits, Challenges and Solutions"*, Intl. Telecom Synchronisation Forum (ITSF), 2009.
[15] Shannon, J. and Melvin, H., *"Synchronisation Challenges for Wireless Networks*", Digital Technologies (DT), 2009.

 ISBN: 978-1-61208-136-6

Synchronization Issues for Smart Grids

Peter M. Corcoran, *Fellow IEEE,*
College of Engineering & Informatics,
National University of Ireland Galway
Galway, Ireland
e-mail: peter.corcoran@nuigalway.ie

Hugh Melvin,
College of Engineering & Informatics,
National University of Ireland Galway
Galway, Ireland
e-mail: hugh.melvin@nuigalway.ie

***Abstract*—The loss of time synchronization across a Smart Grid due to local A/D and D/A conversion processes between the digital domain and the analogue control domain is considered. It is shown that a local calibration can be implemented to enable a determination of clock skew in individual analog sub-systems. Given this information two correction strategies are explained, one based entirely on network-side modification of the control signal data stream. A second approach is based on modification of the control signal on individual client sub-systems allows use of a multi-cast control signal and facilitates both local and global synchronization of the control signals.**

Keywords- smart grid; synchronization; analog control; clock skew, standards IEEE 1588, IEC 61850

I. INTRODUCTION

Smart Grid is the integration of communications networks with the power grid in order to create an electricity communications superhighway extending from generation nodes right through transmission and distribution into end user premises. Such a Smart Grid has two distinct features; firstly it allows flexible and real-time decision making based on real-time pricing; furthermore, it is capable of monitoring its own health at all times, alerting operators immediately when problems arise and automatically taking corrective actions that enable the grid to fail gracefully and prevent a local failure from cascading out of control.

One can think of Smart Grid as a system of systems, each with its own architecture [1]. Some of the key infrastructure requirements are reliable distribution of information and time synchronization among network elements in order to correlate different network events. Time management and clock synchronization requirement in Smart Grid varies from system to system.

PSRC (Power System Relaying Committee) [2] working group H7 is defining IEEE1588 standard profile for power system applications to be called IEEE C37.238 [4]. The purpose of that standard is to facilitate adoption of IEEE1588-2008 for power system applications requiring high precision time synchronization. The profile specifies a well-defined subset of IEEE1588-2008 mechanisms and settings aimed at enabling device interoperability, robust response to network failures, and deterministic control of delivered time quality.

This set of PTPv2 parameters and options allows IEEE1588-2008 based time synchronization to be used in mission critical power system protection, control, automation and data communication applications.

The world of precise synchronization is standardized by the IEEE 1588 document [3] also known as the Precision Time Protocol (PTP) facilitates both time and timing synchronization. In recent years, it has become highly relevant to network providers who are migrating from circuit switched SDH/SONET networks to IP Based Next Generation Networks. Such providers need a replacement mechanism to transfer timing (and also time) within their networks Many application domains such as industrial automation, measuring, telecommunication, substation automation or audio/video transmission require a precise synchronization across their equipments to ensure a correct and safe execution. The main IEEE 1588 standard defines the basic rules and protocol elements to achieve precise synchronization, while profiles refine the main standard by adapting it to a specific application domain. Three profiles are currently under definition. The first one is the power systems profile driven by the IEEE Power Systems Relaying Committee (PSRC), the second one is the audio/video bridging of IEEE 802.1, while a third one addresses the telecom applications.

Another important standard is IEC 61850. This has been substantially developed for substations but is seen as a key standard for all field equipment operating under both real-time and non-real time applications. The use of IEC 61850 for wide-area communication is already discussed in IEC 61850-90-1 (Draft technical report) in the context of communication between substations.

Much of this work relies on the use of Network Time Protocol (NTP) to provide the underlying time synchronization for real-time systems [5]. Now NTP provides a well tested method to enable reasonably accurate time synchronization across TCP/IP networking infrastructure. It can be further refined using hardware extensions and taking advantage of the ubiquitous GPS 1pps signal to refine local time synchronization to the microsecond level.

However, returning to our earlier comment that the Smart Grid is a “system of systems” we can see that the above standards take a uniquely “digital” view of the Smart Grid,

 ISBN: 978-1-61208-136-6

conveniently ignoring that the underlying electricity which is carried by the grid is actually an "analog system" and must ultimately be monitored and controlled in the analog domain. Once we realize that Smart Grid relies on imposing a digital management, monitoring and control layer onto the underlying analog grid it becomes clear that we need to extend our considerations on synchronization beyond the digital domain.

In this paper we will outline some other fields where we have studied time synchronization, outlining the fundamental problem of moving from digital to analog signals and how the D/A process can introduce its own synchronization issues.

II. THE ANALOG SYNCHRONIZATION PROBLEM

NTP based techniques use a range of mechanisms to cleverly keep two networked digital systems in close time synchronization. However, if we step back a little from this, we realize that each local system has its own local clock and in a sense these digital techniques are simply providing us with a measurement of the clock skew between these two systems. The underlying problem, however, is that each networked system must in turn take input from a further series of analog monitoring sub-systems and/or drive a further series of analog control sub-systems as part of its role in monitoring/controlling the local power grid.

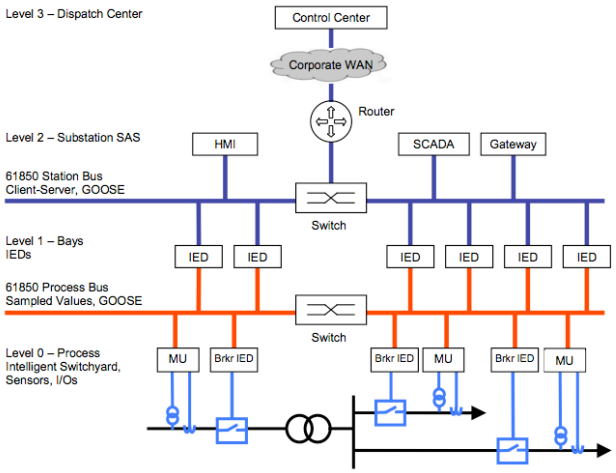

Fig 1: *Architecture of IEC 61850 Substation Automation System with Station Bus and Process Bus [8]*

Typically each of these individual sub-systems will have its own local clock hardware. Granted that it may take a signal from master clock derived from the original networked control system but while such master clock signals can provide microsecond levels of accuracy, peripheral clocks can be subject to buffering delays and jitter. More significantly, intelligent electronic devices (IEDs) within the substation infrastructure may connect to peripheral controllers or monitoring units over a local control bus such as CAN or SPI [9]. Such secondary control networks do not support 1588 synchronization and may use asynchronous or semi-synchronous timing mechanisms.

In addition the 1588 standard only considers the synchronization of digital clocks, yet many embedded systems will have separate clocking subsystems for their analog circuitry. In particular the D/A functionality of many embedded sub-systems may rely on individual timing circuits or crystals. In ***Fig 1(a)*** we show a typical IEC 61850 architecture from ref [8].

In summary, the underlying problem is that even when there is precise synchronization of the top-level monitoring or control signals carried by the Smart Grid local timing offsets or accumulated delays may still exist due to mismatch between the analog and digital sub-systems in local monitoring or control nodes.

III. ANALOG SYNCHRONIZATION IN AN AUDIO SYSTEM

The analog synchronization problem can be best understood by considering a simplified substation architecture. In ***Fig 2(a)*** we illustrate a legacy Electric Substation architecture. Real-time digital control data is streamed over a network connection from a control center and this data is written into a memory buffer by the main *substation controller*. It will then be processed and used to manage/control local *substation processes*. Similarly local *status monitoring* is performed and relayed back to the *substation controller*. Note that in this configuration both monitoring and control processes are directly wired to the main *substation controller* and thus synchronization of the monitoring and control data is trivial at the substation level. Synchronization between local substations and the main electric grid control center can be easily achieved using IEC 61850/IEEE 1588 compatible network protocols.

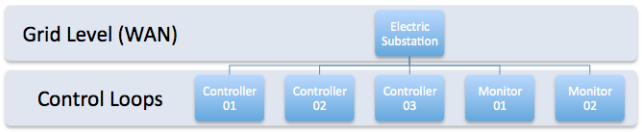

Fig 2(a): Legacy Electric Substation Architecture.

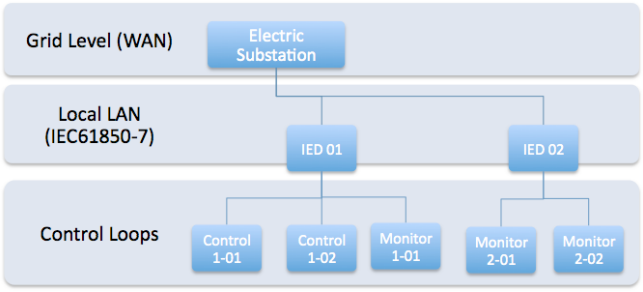

Fig 2(b): Next generation Electric Substation Architecture.

 ISBN: 978-1-61208-136-6

By contrast ***Fig 2(b)*** illustrates a next generation *distributed substation architecture* where two *intelligent electronic devices* (IED) are networked to the main *substation controller*. Now the embedded subsystems of such networked IEDs can be tightly synchronized using purely software techniques [3]. However the *analogue* control and monitoring subsystems of such client devices can introduces unspecified temporal drift. In normal operation, output analogue data is produced at a fixed rate, which is typically dependant on an internal (local) clock signal. As this signal is derived from some form of electronic oscillator it is subject to variations due to both manufacturing and environmental factors. Thus it is unlikely that two analogue subsystems can be exactly matched. Some local synchronization could be achieved using a local master clock for analogue subsystems but there are inherent difficulties in synchronizing between local, hard-wired environments.

To place this in context, even if the two networked IEDs illustrated in ***Fig 2(b)*** were resynchronized at the start of every control cycle – say every 3 minutes – a drift of 0.01% or 1 in 10,000 between two control channels will produce an inter-channel delay of 18mS which is more than sufficient to produce a significant phase difference and induce unwanted sub-harmonics onto the powerline.

IV. CLOCK SKEW IN ANALOG SUBSYSTEMS

A. Client-Side Callibration

Now it is well known that the local clock skew of the control and monitoring subsystems on each networked client IED can be accurately determined [6], [7].

In the field of digital multimedia it is known to determine a local clock skew rate and modify the received multimedia stream in a manner, which does not affect the quality of the rendered analog signal [7]. For a practical embodiment the client device or sub-system must be able to:

(i) perform real-time interrupt-driven analysis of its output signal in order to measure real-time clock skew;

(ii) at the same time it must decode the digital control signal and may also need to de-interleave the received control stream; and finally,

(iii) in order to increase, or decrease the size of a received audio data packet to compensate for the determined clock skew the client device should perform an analysis of each received audio packet to determine where, and how, to insert (or remove) audio samples.

All of these methods must be further implemented in real-time placing a high computational load on the client device typically requiring a powerful, high-end processing unit with significant power requirements. Furthermore, in a complex system architecture such as Smart-Grid there should be a uniform approach to such client-side recalibration of digital signals.

Also worth noting is that problems will occur in higher-level control algorithms if some sub-systems are accurately calibrated and others are not. Thus, even if local calibration were adopted as a solution, it would still be necessary to inform the external Smart-Grid of the local calibration status.

B. Network-Side Callibration

The alternative approach is to pass the calibration problem back to a server, or a network-side service. This approach is actually quite sensible in the context of Smart-Grid applications as it simplifies the requirements at the client-side (i.e. at the local substation level) and enables a uniform services model to be developed at the network level.

In such implementations the local client should initially register with the network service, providing technical details of the various analogue sub-systems integrated into the local grid infrastructure. Then from time-to-time the network service would send out calibration requests to these subsystems during slack periods. Each client device can perform a local clock skew measurement. Typically a control sequence would be provided which should be implemented by the local analogue sub-systems, which returns time-stamped messages at the start and after the completion of each digital control sequence. It is thus possible to determine the likely time deviations of individual systems from their ideal. Or in cases involving a sensing sub-system a fixed length dataset is recorded and returned to the central service with start and end-timestamps derived from a local time-synchronized clock.

The recording and statistical analysis of these data can be better performed and managed by a centralized network service. Further, it is more practical for network-level control algorithms to access such centralized data. It also offers a method of monitoring and determining local sub-systems that may require maintenance or replacement. If data is recorded over a period of time then degradation in performance or sub-systems accuracy will be easy to track.

These data are analysed as part of the network service and are statistically analysed to determine a long term clock skew rate which will be applied to each individual monitoring or controlling client sub-system. Also, these clock skew measurements should typically be initiated from the network-side and, typically, a more intensive calibration regime would be applied when a device is initially connected to the Smart Grid until a reliable clock skew rate is determined for it. Certain methods and techniques employed by NTP may be advantageously adapted for this purpose.

 ISBN: 978-1-61208-136-6

IV. CORRECTION STRATEGIES

Now that we have developed a strategy for determining the clock skew of individual analog monitoring or control subsystems we can consider a number of correctional approaches. As per our earlier discussion it makes sense to implement most of the corrections on the network-side rather than on the local system. This makes sense because correction of multiple local clock skews will be most important where Smart Grid algorithms are implemented across a section of the power grid, spanning multiple local substations. Similarly it is when local data is gathered to a central location that the correction of individual clock skews are most important so that individual monitoring data sets can be compared across a common timebase.

Because of the real-time nature of most Smart-Grid control applications it is important that correction strategies for measured signals and for applied digital control signals are simplified where possible. Thus in this preliminary consideration we will only look at correction strategies where individual bits of data can be dropped without significantly affecting the measured or applied signals.

A. A First Approach: Stripping of Signal Data

When the server is requested to initiate multiple new control signals spread across multiple control sub-systems it will need to prepare the data for digital streaming. The raw digital control data can typically be pre-encoded, or optionally passed through a codec which may be implemented as a hardware subsystem. The encoded signal data is next packetized and this process may also incorporate an interleaving step wherein the data from a single control sequence is spread over multiple data packets. This minimizes the effects of packet loss on the signal at the client. The precise implementation of each of these steps of encoding, packetization and interleaving will depend on the format of the digital data stream. Data formats may be optimized to facilitate packet de-interleaving, stream re-assembly and stream decoding.

Fig 4

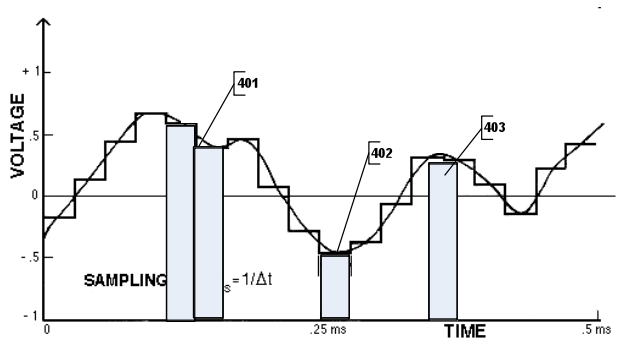

Fig 4: *Examples of Redundant Signal Samples (RSS).*

In our approach an additional step is now added to this chain of server-side processes. By employing the predetermined clock skew rates for each networked client device. This step performs additional stream processing to adjust the signal data for each individual client subsystem. The precise form of stream processing is, to some extent, dependent on the underlying control signal format. However we can identify two generalized techniques, which cover most applications where frequency spectrum characteristics must be preserved:

(i) an appropriate number of redundant signal samples are either removed or added to each analog channel; alternatively, as shown in figure 4;

(ii) where the underlying digital format requires close phase synchronization in addition to overall time synchronization, then redundant analog samples which should be added to (or removed from) the signal data are marked separately from the signal data and are conveyed to individual client sub-systems by means of a parallel data channel, or in the form of a packet header

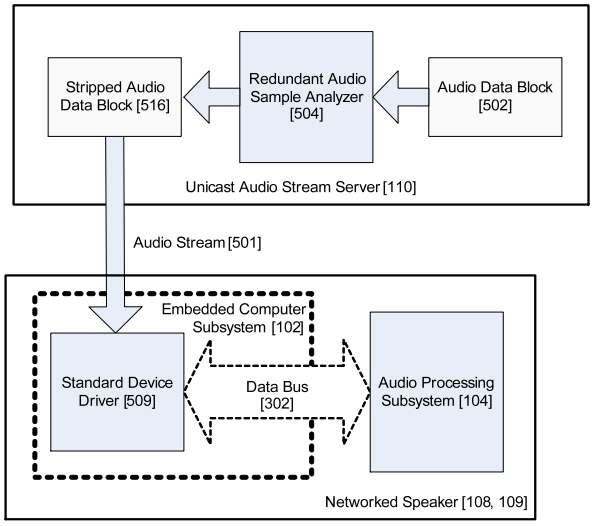

Fig 5: *Server-Side Stripping of Media Stream*

Hereafter we refer to method (i) as "stripping" and method (ii) as "marking". Now the preferred method of stream processing in a simple embodiment of the present invention is method (i) as it allows all of the stream processing to be achieved on the server side and, in turn, does not require any client side modifications. This embodiment is illustrated in ***Fig 5***.

For clarity the steps of encoding, packetization and interleaving are omitted. Thus, according to method (i) an signal data block is analyzed by a redundant signal sample analyzer which determines, based on the clock skew of the receiving subsystem, how many, redundant analog samples need to be removed to achieve clock skew compensation for the receiving subsystem. This process generates a stripped analog data block that may be optionally encoded prior to being packetized and broadcast over the network. As the

 ISBN: 978-1-61208-136-6

required clock skew compensation has been entirely performed on the server no modifications are required on the client devices.

B. A Second Approach: Marking of Signal Data

However there are potential disadvantages to this method, particularly where an algorithm needs to be applied across multiple local sub-systems. For example, the present implementation can be simply extended to multiple sub-stations each with more than one local analogue control (or monitoring) sub-system, as illustrated in ***Fig 7***. Thus multiple control sub-systems located in different sub-stations can simultaneously apply the same synchronized control algorithm data, each control group being locally synchronized within the sub-station environment, and globally synchronized with multiple sub-stations at diverse geographic locations. Each local control group obtains the signal data from the same multi-cast control data stream so that network bandwidth requirements are optimized. Evidently the "stripping" method of signal synchronization will not be suitable for such more widely-deployed control algorithms.

Thus method (ii), although being more complex to implement and requiring a combined client-server processing can have advantages over method (i). This marking method is illustrated in ***Fig 6***. The server must obtain clock skew rates for each networked analog sub-system and provide a "marked" list of redundant analog samples customized for each in the main control data. Typically there will be overlap between these "marked" lists and this data may be optionally organized in a set of difference tables to reduce network bandwidth requirements.

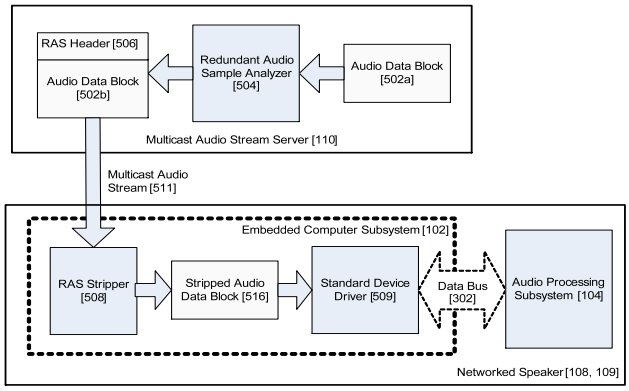

Fig 6: *Server-Side marking combined with Client-Side Stripping of the Control Signal Stream*

The operation of this embodiment is illustrated for a single client in ***Fig 6***. A control signal data block is analyzed as before by a redundant signal sample analyzer which determines, based on the clock skew of the receiving device which, and how many, redundant signal samples need to be removed from the digital signal block, for each receiving client sub-system, in order to achieve clock skew compensation for the receiving sub-system. In this embodiment these samples cannot be simply stripped from the signal stream as each client device will have a unique clock skew and require a different set of samples to be stripped. Accordingly the stripping operation must be performed separately on each client and the required "marking" data for each client is recorded within an RSS Header or otherwise communicated to the clients. The original audio data block remains in an unaltered form. This signal data is next packetized into a multicast stream which can be received by a plurality of networked client sub-systems.

When a signal data block (or payload) is received at the client the relevant list of "marked" audio samples is extracted or reconstructed, as appropriate, from the RSS Header by an RSS stripper, which may be implemented in either hardware or software or some combination thereof. The RSS stripper then determines from said list if audio samples should be inserted or removed at the "marked" locations. According to our preferred embodiment samples are either removed or simply duplicated, as appropriate. This has the advantage that only the location of a redundant audio sample needs to be recorded in the RSS header. The resulting stripped data block is next passed to the standard device driver for the analog subsystem and written over the data bus into the analogue output of the control subsystem. In this case the stripping operation occurs on the client, rather than on the server.

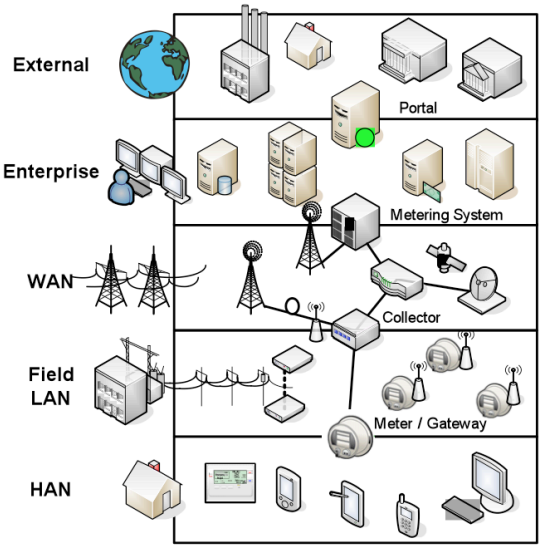

Fig 7: *Enterprise systems view of Smart-Grid*

V. CONCLUSIONS

We have outlined some issues in achieving accurately synchronized real-time control over the Smart-Grid. These are caused by differences in the behaviors of local D/A and A/D monitoring and control sub-systems.

 ISBN: 978-1-61208-136-6

Given the availability of calibration data we then examined two different approaches to modifying algorithm control sequences. The first is implemented entirely on the network-side and requires no modification to local subsystems. Our second approach relies on some client-side intelligence where individual analog subsystems can identify corrections to their data stream and modify a multi-cast control sequence accordingly. This approach has to benefit of allowing local corrections within a substation environment and a more global synchronization correction across multiple substations.

Compensation techniques can be applied at the local substation level, but we have noted that these are best developed and driven from a network control center, rather than being implemented within the local system components. It was also observed that centralized gathering and management of calibration data would enable long-term monitoring of Smart-Grid systems and provide indications of a need to service or replace components. The importance of this approach can be understood by considering the Enterprise level view of the smart-grid infrastructure shown in ***Fig 7*** above. While it would be possible to manage all timing aspects of the control cycle locally, our argument is that a local controller can only be aware of local issues. Some straightforward logic quickly makes it apparent why it may be sensible to have a higher-level management of these subtle local timing aberrations.

Consider a particular IED that is standard equipment across a power grid. Each device will behave slightly differently and while it could be compensated for at the local substation level it is not possible to consider the possible side effects of several dozen or even hundreds of these IEDs at a grid level, unless their control and calibration patterns are managed centrally. However this remains a topic for future investigation and further discussion.

ACKNOWLEDGMENT

I would like to acknowledge the contribution of *Alex Cucos* in assisting with the prototyping and technical evaluation of certain elements of the research work presented in this paper.

REFERENCES

[1] Don Von Dollen, Report to NIST on the Smart Grid Interoperability Standards Roadmap, June 2009

[2] www.pes-psrc.org

[3] Standard IEEE 1588, "Standard for a Precision Clock Synchronization Protocol for Networked Measurement and Control Systems", 2008.

[4] IEEE PSRC, IEEE 1588 Profile for Power system Application (work in progress)

[5] www.ntp.org

[6] H. Melvin and P. Corcoran, "Playback synchronization techniques for networked home appliances," in Proc. of IEEE International Conference on Consumer Electronics, pp. 1-2, 2007.

[7] A. Cucos and P.M. Corcoran, "Synchronizing multi-channel speakers over a network, United States Patent 7,805,210.

[8] J. McGhee and Maciej Goraj, Smart High Voltage Substation based on IEC 61850 Process Bus and IEEE 1588 Time Synchronization.

[9] M. Roman-Barri, I. Cairo-Molins, A. Sumper, & A. Sudria-Andreu, , "Experience on the implementation of a microgrid project in Barcelona," Innovative Smart Grid Technologies Conference Europe (ISGT Europe), 2010

 ISBN: 978-1-61208-136-6

Developing Methods for the Detection of High Impedance Faults in Distribution Power Grids

Tomasz Nowicki
IBM Watson Research Center
1101 Kitchawan Road
Yorktown Heights NY 10598, USA
Email: tnowicki@us.ibm.com

Grzegorz Świrszcz
IBM Watson Research Center
1101 Kitchawan Road
Yorktown Heights NY 10598, USA
Email: swirszcz@us.ibm.com

Mark Yao
IBM Watson Research Center
1101 Kitchawan Road
Yorktown Heights NY 10598, USA
Email: markyao@us.ibm.com

***Abstract*—High Impedance Faults are known to be extremely hard to detect. At the same time the efficient detection of them is very important to electric power providers. One of the challenges belonging to a Smart Grid paradigm is how to use new data not available before to improve methodology of High Impedance Fault detection. In the paper we describe our experiences, insights and lessons learnt from actual field experiments. A series of experiments was conducted that simulated most common High Impedance Faults. The data was recorded at 256 samples per cycle at 4 stations located at different places on a feeder. We describe the experiments, the process of acquiring the data and how we used it. Also, we discuss challenges we encountered and what we have learned in the process.**

***Keywords*-High Impedance Fault; PMU; sensors; time series; experiments;**

I. Introduction

”High Impedance Faults (HIFs) on distribution systems create unique challenges for the protection engineer. HIFs that occur do not produce enough fault current to be detectable by conventional overcurrent relays or fuses.” [10]. The difficulty in detecting High Impedance Faults is due mainly to two facts. Firstly they generate weak signal, very often resembling a change in the load caused by a legitimate usage. Secondly many diverse phenomena with very diverse physical properties are classified as HIFs. A downed line on a non-conducting surface (continuous flow), tree branch tapping on a wire (erratic, random series of faults depending on a wind of a high frequency), cracked insulator that causes HIF whenever water fills the cracks due to humidity (very weak flow, semi random nature, low frequency) are very different events all falling into the category of HIFs.

At the same time HIFs pose a threat to human life, to the equipment and can lead to high costs for the provider if not detected in time. Thus developing methods of detection of HIFs is an item of high priority. Many years of experience show that it is practically impossible to detect HIFs using conventional methods and on the level of substations. Therefore HIF detection fits perfectly as an essential component into the Smart Grid paradigm.

Currently HIFs are often detected using methods like breakers tripping, readout from meters at the substation (human) or a phone call from someone who noticed a fault. Needless to say, accuracy of those methods is highly insufficient and not acceptable in a modern power grid. The concept of Smart Grid provides an access to data that was not available neither in such quantity (number of measurement points, sampling rates), nor quality (accuracy of in situ sensors, resolution, time stamps, cross validation) nor in data management (transmission, preprocessing). This data can be used for HIF detection. As with every new paradigm this leads to new challenges. There is no sufficient textbook knowledge about how to use readouts of multiple sensors on the level of multiple samples per cycle to detect faults. Industrial standards how to use such new data are not yet established and the users are not yet trained. There are several approaches to model HIFs using neural networks, wavelets, Fourier transforms [2], [9], [3], [6], [8], [7] none of these models being satisfactory nor becoming a standard. Often such models are only partially validated by simulations and not field experiments. In general HIFs are not yet sufficiently well understood and characterized neither from theoretical nor practical point of view. Advances in physics and establishing technological methodology and procedures require experiments and HIF detection is not an exception.

We had a unique opportunity to actually be able to perform a series of field experiments that provided us with real (not simulated) data. In this paper we describe our experiences, insights and the lessons we have learnt.

The paper is organized as follows. In Section II we describe the setup of the experiments we performed, the equipment used and how the data was recorded. In Section III we discuss the outcomes of the experiments. Finally, in Section IV we present our insights and conclusions from the work we did.

II. Experiments

The experiments were performed thanks to a collaboration with a customer of IBM - a major electric energy provider. In this section we present an overview of what was done

 ISBN: 978-1-61208-136-6

Figure 1. Experiment site and 4 recording stations.

focusing on the general setup, equipment used, experiments performed and data collection and transmission.

A. Experiment setup

The experiments were performed on a lateral that was under construction and its end was in a remote location that could be easily secured. That way safety measures were met and generated faults did not cause interruption in the delivery of the electric power. The main feeder was leading to a residential area, thanks to which the requirement of having HIFs generated on top of a real load was met.

The feeder had a standard 4-wire configuration with grounded neutral wire. A wire was connected to phase B that was used to generate various types of faults. Due to security reasons experiments could not be 100% realistic - for example throwing a powered wire on the ground would pose too much danger for the crew. What was done instead - there was a switch installed on phase B before the wire used for the experiments. All the time except for when the trials were done the switch was in an ”off” position. The wire was secured in a position like on a block of concrete or on wet grass. Then the switch would be moved to ”on” position and the fault would be generated. See IV for insights and remarks related to the influence of that aspect of a setup on the data.

There were four recording stations named 101, 102, 103 and 104 (see Fig. 1) located on the main feeder.

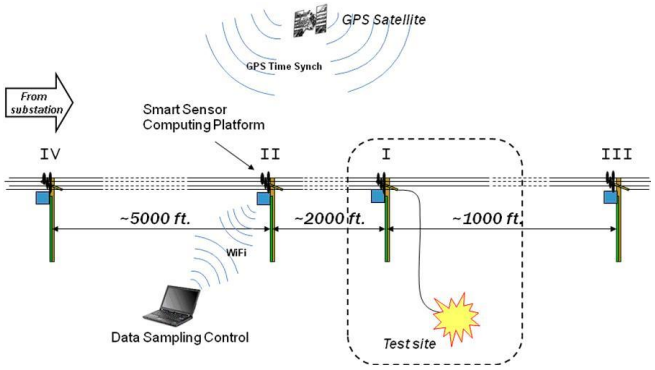

Figure 2. Experiment setup.

Station 101 was located downstream from the experiment site, stations 102, 103 and 104 were upstream. The distances from the experiment site to recording substations were

experiment site $\leftrightarrow$ station $101 = 2.38$ miles,
experiment site $\leftrightarrow$ station $102 = 2.07$ miles,
experiment site $\leftrightarrow$ station $103 = 3.66$ miles,
experiment site $\leftrightarrow$ station $104 = 5.44$ miles.

The signal was sampled 256*60 times per second. On each of four wires both current and voltage were recorded making a total of 8 channels recorded per station.

B. Equipment used

Each of four sampling stations selected along the distribution feeder had following hardware equipments and devices installed on the electric pole:

- Four pre-calibrated Lindsey Current & Voltage sensor for 3 line phase plus neutral line.
- Sensor wire terminator and power supply (for RTU) with enclosure.
- Intelligent RTU with following components in a weather proof enclosure.

Key hardware components and their functions within each intelligent RTU were

- **High speed A/D board** A 16-Bit Analog I/O board was selected for its compatibility with underlying system board and for its high speed data sampling rate to meet experiment requirement. This I/O board can provide 250,000 samples per second maximum sampling rate and, most importantly, 1024-sample FIFO for reduced interrupt overhead.
- **GPS** A GPS card was used to provide high resolution reference-time signal to synchronize all distributed RTU in time. Time synchronization was a critical data collection requirement to allow accurate time coordination for later data analysis and modeling. In the

 ISBN: 978-1-61208-136-6

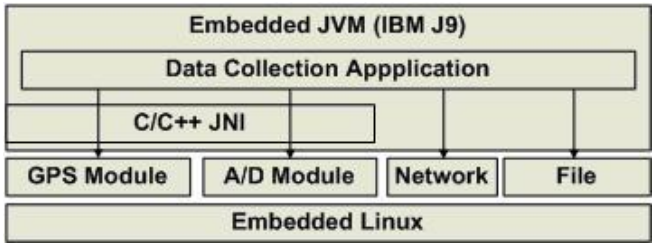

Figure 3. Data Collection Application.

experiment, the resolution of time stamp for the data record was set to micro-second.

- **Wifi Card** At the time of setting up the experiment there was no wide area communication link between RTU and workstation that would configure and control the RTU and the test site. Once the RTU was mounted at pole top, the communication interface available to control and configure the RTU was through either wired serial line communication with system terminal program or through Wifi communication through socket-based application program. The capability of control/configuration of RTU at runtime was critical to the experiment. For example, we turned on the data collection process through Wifi network at each RTU location only when the experiment had been ready to be conducted so the data storage would not overflow.
- **Storage card** An 8 GB USB storage card was used as a local storage for all data collected during the experiment time. Given the rate of data collection (256x60x8 samples/per second), the storage had a capacity to accommodate 4-5 hour time window of experiment.

The RTU system was an ultra-low power, high-performance, single board computer based on the 520 MHz PXA270 processor. The PXA270 was an implementation of the Intel XScal micro architecture, combined with a comprehensive set of integrated peripherals, including interrupt controller, real time clock and various serial/USB interfaces, and network interfaces. Fig. 3 displays the software stack installed for each of 4 intelligent RTUs. The data collection application was implemented in JAVA programming language. Once the experiment setting was ready, the application initialized and configured A/D board and on timer (through GPS module) based on pre-loaded configuration file, started the data collection process through hardware interrupt setting and serialized the data with pre-defined format to storage files. The application could be started, stopped and reconfigured through local Wifi communication interface.

C. Experiments performed

Experiments were performed in 9 categories corresponding to 9 most common types of High Impedance Faults.

1) Concrete Drops
2a) Sand Drops (Dry Sand)
2b) Sand Drops (Wet Sand)
3) Asphalt Drops
4) Grass/Soil Drops (note: grass and soil were very wet)
5) Capacitor Switching (Operate capacitor to see switching transient)
6) Tree Taps
7) Axial Pinhole Insulator (salt water sprayed into pinhole drilled in the insulator)
8) Dirty Insulator (Observations: No obvious activity, no sound)

It should be noted that Experiment 5) consisted of switching capacitor banks on and off, therefore it was not a simulation of a HIF but of a legitimate activity that is know to be a source of false positives.

In each of the categories 10 trials were planned to be performed, but in numerous cases less trials were done because of observed phenomena of the sort of:

Too high current flow that was causing breakers to trip (in case of wet soil and grass).
Difficulty in conducting the experiment and safety issues (in cases of Tree Tap, Axial Pinhole Insulator).
No observed activity (Dirty Insulator).
High repeatability (Capacitor switching).

Every trial was described by (manually) recording:

TRIAL NO: (*for example* 1)
Start Time: (*for example* 9:59:19)
Finish Time: (*for example* 9:59:30)
Arcing Visible: Y/N
Observations: (*for example* Small arc on surface)

D. Data recording and transmission

RTUs were recording the data in a custom-designed format (see Table I). The data for each channel was recorded in an interleaved way. This format was used for recording purposes. For working with the data we designed a format basing on .wav standard. Pure .wav format was not sufficient for our purposes as it does not contain information about timestamps containing information about when the data was recorded. We used a format DataStream that consisted of .wav files and a text file .cfg containing metadata such as time of the beginning of recording, time of recording end, Station ID, Phase, Current/Voltage and possible comments and remarks. Each DataStream could be built of one or multiple .wav files.

One of the main challenges we were facing was the proper synchronization of the equipment. For most part the use of GPS was the solution, but there still remained an issue of mapping the experiments happening to timestamps recorded in the data (see IV). We used a two-way approach. Our first source of data were manually made notes by an engineer. We used his handwatch that was synchronized with GPS

 ISBN: 978-1-61208-136-6

Table I
RTU RECORDING FORMAT

Block	Field	Size	Comment
Header block	sample_station_id	4 byte	Data collection station unit id
	sample_size	2 bytes	Data sample unit size, in number of bytes, for each data sampling. 2 bytes for this project
	sample_edian	2 bytes	1 for little and 0 for big endian
	chan_start_num	2 bytes	Starting data channel number
	chan_end_num	2 bytes	Ending data channel number
	chan_scan_rate	4 bytes	Data channel scan rate in Hz. Each scan converts all channel data specified by start and end channel number
	chan_time_interval	4 bytes	Time interval between each channel data in micro-seconds (default 4 micro-sec)
	time_stamp_sec	4 bytes	Time stamp in sec when first data scan happened
	time_stamp_usec	4 bytes	Time stamp in micro-seconds for when first data scan happened
Data block	<start_chan_data> ... <end_chan_data> <start_chan_data> ... <end_chan_data>		

timers before the experiments to properly record times and short descriptions of each experiment (see II-C). The second source of data was a video recording of the experiments with a timestamp of the recording embedded in each frame. We did not want to rely on any of those sources solely. The reason was that if something went wrong with one of them the experimental data would lose most of it's value without a way of identifying its portions corresponding to experiment versus the ones corresponding to faultless state of the feeder. Luckily we ended up having two good sources of that data, nevertheless we are convinced that having redundant sources of information is the right approach if possible.

It is worth mentioning that the manual way of recording experiments turned out to be surprisingly accurate. It also

Figure 4. Current and voltage waveforms recorded on Phase B at stations 101, 102, 104 and 104 respectively (top to bottom).

could not have been eliminated completely as we needed not only times but also descriptions of experiments.

III. AFTER THE EXPERIMENTS

A. Experimental data

A primary database of labeled waveforms was created, organized into 4 main folders corresponding to 4 recording stations. It contained over 200 files. A consistent naming convention for the files was used and they were arranged by phase, type (Voltage/Current) and time.

A secondary database of labeled waveforms was made of 1720 wavefiles in 261 subfolders. Files in .wav format were accompanied by configuration files containing metadata.

A list of experiment descriptions (from handwritten notes) was used to generate DataStream objects. The format has been defined that can be used as an input by the code to populate data structures appropriately, namely .cfg files for storing metadata of the analytics/development modules allowing the access to multiple wavefiles as a continuous data stream (compare II-D).

Over 12 Gigabytes of data have been collected corresponding to over 3.5 hours of experiments.

B. ...and what we did with it

With the amount of data we were facing standard tools for manipulating and visualizing time series were inadequate (Compare lesson eleven in IV). Envisioning upcoming paradigm of Smart Grid and related challenges we have developed a platform called Time Series Analytics Workspace (TSAW).

TSAW is a software environment for working with multiple large-size time series. It combines various visualization tools (see Fig.s 4, 6), manipulation utilities allowing various

 ISBN: 978-1-61208-136-6

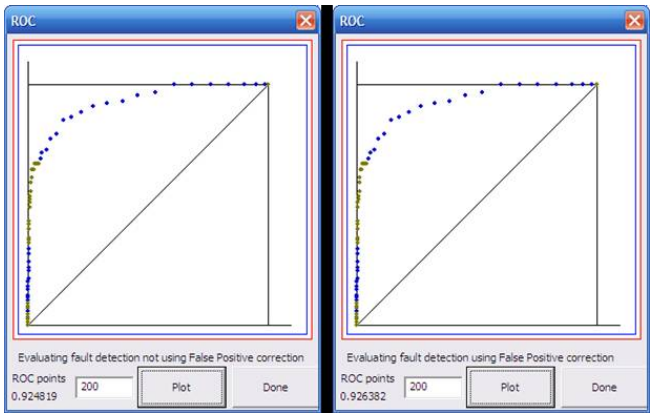

Figure 5. ROCs obtained on the experimental data using novel algorithms.

ways of working with the data and powerful analytics inbuilt. TSAW has been designed and built with broad array of applications in Smart Grid related projects in mind, not limited to the scope of HIF detection.

Thanks to working with the data using TSAW numerous properties of HIFs were understood. 6 new invention disclosures (see [4], [5]) were filed related to the work done and innovative algorithms were created based on the knowledge acquired. The performance of the algorithms was evaluated using the standard metric - AuC (see for example [11]). Performance efficiency yielding AuC of 0.924 has been achieved using anomaly detection combined with false positive elimination algorithm. (see Fig. 5).

IV. Lessons learnt

The first lesson learnt would be the confirmation of how great the importance of real experiments is. This was very much expected, but we still find this insight to be of an extreme value.

The second lesson we learnt was that the choice of recording data format was not the best possible. In one of the files one of the AD converter drivers inserted one 0 sample at the beginning of data. As the data was recorded in an interleaved fashion this lead to shifting of channels - the first channel became the second etc., so for example current of phase A was being recorded where the data for voltage of phase B should have been. This was discovered when gluing waveforms coming from different files showed discontinuity. Enhancing the recording format with markers containing the information about the data being recorded inside the channel and/or writing each channel to a different file might be a good idea to be considered.

Third lesson learnt was that data recording can be more efficient and economic if a remote communication was available between the test site and all RTU data recording station. The total time of data recording time for the experiment lasted about 4-5 hours, while each experiment conducted was only lasted about 5-10 minutes. Most of data recorded was within non-experiment time window and was irrelevant to the later data analysis and wasted storage space. The non-experimental data also added additional work to the post experimental work since experimental data need to be allocated by time filtering out these non-experiment-data. All these disadvantages can be resolved if a remote communication to each RTU was available from the test site so that each experiment can recorded separately with different time reference point. It is with pointing out though that some amount of non-experimental data is as important and the experimental data, as it allows to train models properly providing a baseline for true negatives.

Lesson four - installation of physical RTU units should meet following requirements:

a) Security: the unit should be sealed with a secure lock and installed at certain height to prevent any theft and unwanted access. The installation height should be also convenient enough so that unit could be physically reached by the experimenter for different purposes such as physical repair or removal if the USB data storage after experiments.
b) Weather proof: one of RTU was damaged due to leakage of rain after the experiment and this can be prevented if enclosure is well sealed.

Lesson five - the cost of installation of sensor and RTU can be high. With a crew of 2 workers, it took 1.5 full days to install and test 4 units of RTU and wire them to the pre-installed sensors.

Lesson six - our experiments confirmed that real (not only simulated) experimental data is essential to progress in physics in general and to get an understanding of the nature of HIFs in particular. Smart Grid and access to the readouts of meters capturing what phenomena accompany real events will provide whole new universe of knowledge that will clarify many unknowns and misconceptions about HIFs. Thanks to the access to the real data we were able to determine that on a contrary to a common belief that phase shifts should accompany HIFs it is not the case. We have established that not only this is not true in most cases, but also that the occurrence of phase shift provides an excellent tool for eliminating false positives [5].

Lesson seven - if we knew the exact setup of experiments ahead of time we could have attached a device to the switch starting/ending each trial (see II-A to increase the accuracy of recording experiments beginnings/endings (as compared to the handwatch we used).

Lesson eight - even best experiments are still only experiments (compare II-A) and need to be treated as such. They cannot either replace or be replace by a real data from the Smart Grid. The benefit of experimental data is having the full information of what happened and exact timestamps of

 ISBN: 978-1-61208-136-6

what happened. The drawback is that experiments cannot be 100% realistic for numerous reasons such as for example the fact that due to related hazard it would not be feasible to break a wire and make it fall on the ground, which is one very common scenario of HIF occurring. Such data will become available once Smart Grid starts becoming a reality. Also, equipment used during experiments (like the switch) generates a signal of its own that is not present in a real life scenario. All those aspects have to be taken under consideration while working with the data and building models.

Lesson nine - it would have been of a great value to have had a sensor station installed also on the lateral and closer to the experiment site. It was not possible during our experiments due to technical reasons and we had at out disposal only the HIF-generated signal mixed with a strong signal on the main feeder. Once Smart Grid becomes a reality such data will become available and we are very thrilled about the prospect of working with it.

Lesson ten - our experiments show consistency with the results of a paper [1] about determining the direction to a flicker source. At the Fig. 6 the first two rows are current and voltage at phase B recorded at station 101 which was located downstream from the experiments. Both current and voltage change in the same direction when the fault is generated. The last two rows are current and voltage at phase B recorded at station 102 which was located upstream from the experiments. Their perturbations have different directions, as described in [1].

Lesson eleven - tools for visualization of the data need to be be developed. With numerous sensors generating streams of data the need for an ability to display the readouts in a human-readable manner becomes essential. The challenge is to develop means of efficiently visualizing enormous amounts of data, orders of magnitude above what a typical software is able to handle effectively. TSAW (see III-B) is an example of such tool that allowed us to work effectively with the data.

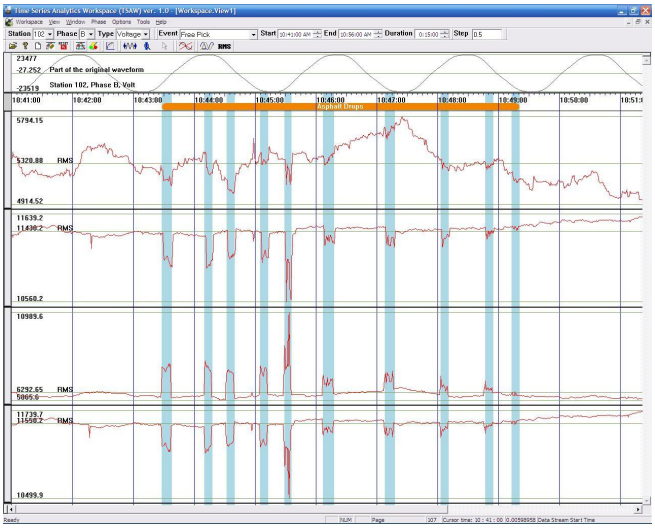

Figure 6. Effect of direction to the source on current and voltage - top to bottom: I at 101, V at 101 (downstream), I at 102, V at 102 (upstream).

ACKNOWLEDGMENT

The authors would like to thank Ron Ambrosio, Charlie Arteaga and members of the crew at the experiments site for their work and help with this project.

REFERENCES

[1] P. G. H. Axelberg and M. H. J. Bollen, *An Algorithm for Determining the Direction to a Flicker Source*, IEEE Transactions on Power Delivery, Vol.21, NO. 2, April 2006.

[2] C. Benner and P. Carswell and B. Don Russell, *Improved algorithm for detecting arcing faults using random fault behavior*. Electric Power Systems Research **17**.1, 49 — 56, (1989)

[3] T. M. Lai and L. A. Snider and E. Lo *Wavelet transform based relay algorithm for the detection of stochastic high impedance faults*. Electric Power Systems Research, **76**.8, 626 — 633, (2006)

[4] T. Nowicki and G. Swirszcz, *A Method for Detecting High Impedance Faults on Distribution Systems using Method of Deviation from a Local Model*, preprint 2010.

[5] T. Nowicki and G. Swirszcz, *Detecting and Eliminating False Positives in High Impedance Fault Detection on Distribution Systems*, preprint 2010.

[6] R. Patterson, *Signatures and software find high impedance faults*. IEEE Computer Applications in Power, **8**.3, 12—15 (1995) (updated 2002)

[7] B. D. Russell, *Computer relaying and expert systems: New tools for detecting high impedance faults* Electric Power Systems Research, **20**.1, 31—37, (1990)

[8] A. R. Sedighi and M. R. Haghifam and O. P. Malik and M. H. Ghassemian *High impedance fault detection based on wavelet transform and statistical pattern recognition* IEEE Transactions on Power Delivery, **20**.4, 2414—2421, (2005)

[9] A. R. Sedighi and M. R. Haghifam and O. P. Malik, *Soft computing applications in high impedance fault detection in distribution systems*. Electric Power Systems Research **76**.1-3, 136—144, (2005),

[10] J. Tengdin et. al.,High Impedance Fault Detection Technology Report of PSRC Working Group D15, http://grouper.ieee.org/groups/td/dist/documents/highz.pdf

[11] http://en.wikipedia.org/wiki/Receiver_operating_characteristic

 ISBN: 978-1-61208-136-6

Sensors and IEDs Required by Smart Distribution Applications

Smart Grid and Distribution Automation

Francisc Zavoda
Electric Equipment Expertise (EEE)
Research Institute of HQ (IREQ)
Varennes, Canada
e-mail: zavoda.francisc@ireq.ca

***Abstract*—In order to meet the electric energy needs at the beginning of this new millennium, utilities need to provide high quality power over a reliable grid, to satisfy customer's growing service quality expectations and to support, as well, a wide array of additional new services. One of the solutions is a successful power grid management activity such as "Smart Distribution" (SD) or Distribution Automation (DA), which hinges on the information collected from the grid itself using an integrated monitoring system that enables real-time monitoring of grid conditions for distribution system operators. It allows automatic reconfiguration of the grid to optimize the power delivery efficiency and/or reduce the impact and duration of outages. The foundation of the monitoring system infrastructure is based on transducers, sensors and Intelligent Electronic Devices (IEDs) collecting information throughout the distribution system. Hydro-Québec (HQ) is showing leadership in this field, conducting several projects related to Smart Distribution such as Volt&VAR Control (VVC), Fault Location (FL), Power Quality Monitoring (PQM) and evaluation of the metering potential of major distribution equipment controls, which collect raw data from the grid, treat it locally and transfer it to system control centers or elsewhere. There, the information is used for real time treatment or non real time post treatment. This paper discusses the structure and the accuracy of an integrated monitoring system based on sensors and IEDs and reports on some of the results and conclusions of Hydro-Québec's projects related to Smart Grid applications and technologies.**

Keywords-Smart Grid; DA (Distribution Automation); VVC (Volt & VAR Control); FL (Fault Location); PQ (Power Quality); monitoring; intelligent meters, control; accuracy;

I. INTRODUCTION

Electric utilities needs are becoming increasingly difficult to meet in the face of an emerging "digital society", with its highly automated and complex industry, computerized commercial business processes, changing nature of residential loads and a regulatory environment. All of that requires more reliable communication facilities and is becoming increasingly sensitive to reliability and quality of electrical supply. Momentary supply interruptions or severe voltage sags of prolonged duration can cause disruptions with significant economic consequences.

These requirements and constraints have caused the utilities to rethink their distribution system in terms of distribution automation, sensors, intelligent equipment and smart power system functions, in order to achieve its goals.

With the introduction of new IEDs/controls, classical disciplines in distribution like protection, control, metering, power quality evaluation and additional automation functionalities will come under one responsibility [1].

Some intelligent elements already exist in most distribution grids and this is the reason that the actual distribution system infrastructure (especially sensors, transducers and IEDs/controls) should be used to gather as much information as possible related to network, equipment and product (i.e., power quality) to improve the distribution system overall performance.

Nowadays, several manufacturers offer performing sensors and IEDs or intelligent controls to improve network performance.

II. SMART GRID AND SMART DISTRIBUTION

Growing service quality expectations make SD processes increasingly imperative for the power utilities and trigger the next major step in the evolution of distribution systems towards a Smart Grid.

At the beginning, the foundation of the Smart Grid concept was based only on applications with smart meters affecting the customer side. Then gradually, several DA applications, involving new technologies, have been implemented through the years and now Smart Grid is what its name really means.

In the past DA consisted mainly in automatic operations, conducted by autonomous IEDs/controls, such as fault location, isolation and service restoration and voltage regulation. Today, advances and falling prices of the communication and control technologies, which can be embedded in the distribution grid and used for monitoring and remote control of various major distribution equipment, such as switches, capacitors banks, reclosers and voltage regulators, bring along a list of new automated SD applications.

According to the IEEE PES Smart Distribution Working Group (SDWG) the following applications can generally be identified to SD [2]:

- Remote controlling of feeder reclosers and switches,

 ISBN: 978-1-61208-136-6

- Automatic feeder reconfiguration based on remote control of reclosers and switches (includes fault detection),
- Fault detection (distribution feeder devices),
- Fault location (accurate) based on waveform analysis,
- Capacitor bank control,
- Volt & VAR control using sensors on the feeder,
- Power Quality measurements (harmonic content),
- Distribution overhead grid monitoring (power measurements),
- Distribution underground grid monitoring and control.

The existing DA deployments and the AMI penetration are complimentary technologies, and they will ensure the achievement of Smart Grid initiatives taken by utilities showing leadership.

The Figure 1 illustrates the flow of information in a fully integrated distribution system.

A better knowledge of what is happening in the power system is needed for an improved management of distribution grid. New technologies (sensors, IEDs, software, telecommunication) can provide data required by smart applications to improve the system efficiency through utility's business needs. It is a necessary feedback loop to improve the distribution system performance. The choice of applications and technologies could differ from a utility to another, depending on each one's priorities (power reliability, PQ, customer satisfaction, environment, etc.) and business drivers should decide what applications, what type of data and finally what technologies are needed.

Regardless the path each utility may take to reach the intelligent or smart level of distribution system, reducing the overall cost is an important utility target and achieving it depends a lot on distribution equipment features like interoperability or interchangeability.

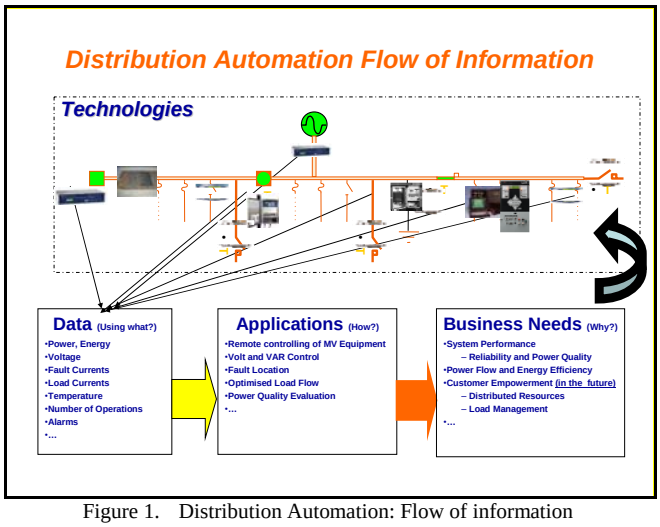

Figure 1. Distribution Automation: Flow of information

A successful implementation of SD applications requires three sets of standards, one for substations, a second one for feeders and the third one for customers. Then, is a need for coordination between these different standards.

The new way of thinking and operating the Smart Grid created the premises for an integrated distribution monitoring system, based on sensors and IEDs capable of providing the data required by latest smart distribution applications formely known as Advanced Distribution Automation (ADA) applications. Some of these devices are already in place in substations and along the feeders.

III. SENSORS AND IEDS

In the early microprocessor based IEDs, metering features such as voltage and current rms-values, power values, were just simple additional features. Today's IEDs have features, which go far beyond these basic functions including frequency, voltage and current harmonic content, symmetrical sequences, waveform capture, etc.

For Smart Grid and SD medium voltage applications, manufacturers propose new "Smart Sensors", which can work either autonomously, when equipped with a communication interface, or in combination with IEDs. Optical current and voltage sensors offer a number of major advantages, but because of a price yet high, it will take a while before a large number will be integrated to the grid. Until then, sensors present at this time on the grid, can be used successfully for monitoring purposes in combination with major distribution equipment controls (see Figure 2) [3].

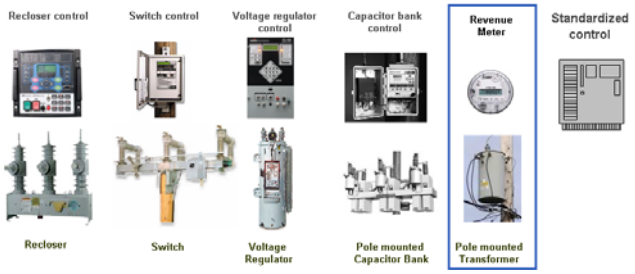

Figure 2. Exemples of major distribution equipments and their controls

IV. HYDRO-QUÉBEC AND SMART DISTRIBUTION APPLICATIONS

Hydro-Québec is showing leadership in this field with its proposed road map towards a smart grid, which should include (see Figure 3):

- Grid monitoring (to improve reliability).
- Equipment monitoring (to improve maintenance).
- Product monitoring (to improve PQ).

To achieve its ambitious programs on energy efficiency and outage duration reduction, Hydro-Québec has focused on three targets:

- Capacitor banks installation.
- Volt control.
- Accurate fault location.

Pilot projects have proven the efficiency and economic feasibility of two SD systems, VVC and FL.

 ISBN: 978-1-61208-136-6

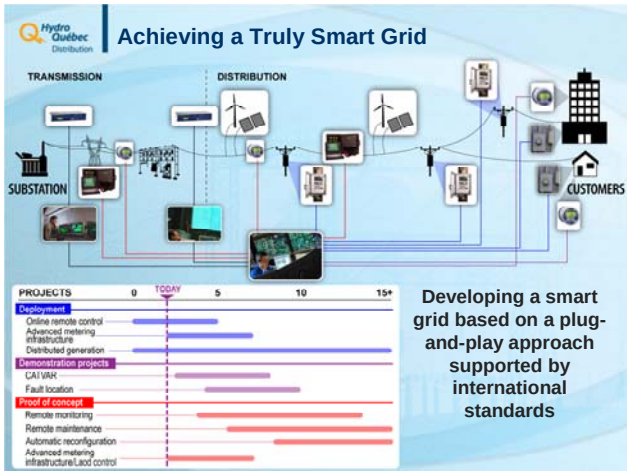

Figure 3. Hydro-Québec roadmap to achieve a truly Smart Grid

Another research program targeted the non-revenue metering potential of distribution medium voltage sensors and IEDs/controls and data integration from these devices. Features such as voltage and current measurement accuracy, linearity, remote control, communication, data transfer, etc., have been evaluated using IREQ's test facilities. Some results and conclusions from previous tests were presented in [4]. Results from latest tests are presented further down.

V. IREQ'S TEST FACILITIES

Besides a large number of laboratories, IREQ has an overhead distribution test line allowing research and development activities for distribution system, namely validation and certification of different distribution equipments (see Figure 4). It includes two feeders and different models of sensors, instrument transformers and pole-mounted major distribution equipments, which can be remotely controlled using available phone, Internet and WiMax communication links. The main switchboard for network and telecommunications is located in the control room.

The line is mainly used to facilitate tests related to SD applications, namely to verify new equipment functionality, metering and communications capabilities, remote control and command.

Figure 4. IREQ's test facilities (control room and feeders)

VI. TEST RESULTS

The research project conducted in 2010 included voltage and current measurement accuracy tests on medium voltage sensors/transducers along with different controls (recloser, switch, voltage regulator) present on Hydro-Québec's distribution grid to evaluate the error deadband. The evaluation tests were performed on the chain composed by two devices, the sensor and the control, and not separately on each of them.

Some tests were performed in laboratory using a system composed of one FLUKE 6100A master unit and two 6101A slave units. The calibrator provided 60 Hz current sine wave to feed standalone sensors (CVMI Lindsey 9660) and recloser external current transducers belonging to reclosers from different manufacturers (Cooper-VWVE, Cooper-Nova, Joslyn-TryMod 300).

Two setups were constructed; one to measure the accuracy of the chain ABB-OVR integral current transducers and PCD2000 control and a second one for voltage measurement accuracy with power distribution transformers (ABB 3 kVA and 10 kVA) and different IEDs/controls.

The last test evaluated the potential of a voltage regulator control (Cooper CL-6A) to measure voltage and current using reversible voltage regulator's integrated PTs and CT.

A. Current Measurement

The sensor-IED/control chains submitted to current measurement tests are illustrated in Table I.

The evaluation process was based on average rms-values over 5 or 15 minutes, depending on the type of control. SEL-651R and PCD2000 measured average rms-values over 5 minutes and S&C M series did it over 15 minutes.

TABLE I EXAMPLES OF SENSOR – IED/CONTROL CHAINS SUBMITTED TO TESTS

Chain sensor/transducer - control		
Type of measurement	***Distribution Device and Transducer/Sensor***	***Control***
Current	CVMI Lindsey-9660	SEL-651R
	CVMI Lindsey-9660	S&C M series
	ABB-OVR	PCD2000
	Cooper-VWVE	SEL-651R
	Cooper-Nova	SEL-651R
	Joslyn-TryMod 300	SEL-651R
Voltage	ABB MicroPole 3 kVA	SEL-651R
	ABB ONAN 10 kVA	S&C M series
Voltage and current	McGraw Edison/VR-32 50A	CL-6A

1) Recloser with standalone current sensors

The statistical results for the chain CVMI Lindsey-9660-SEL-651R are graphically presented in Figure 5.

This control is provided with an adjustable calibration factor (same for all three phases) for current and voltage and uses float values for doing calculations.

The current measurement error, for a load current superior to 120 A, meets the value (0.3 %) given in the sensor's data sheet.

 ISBN: 978-1-61208-136-6

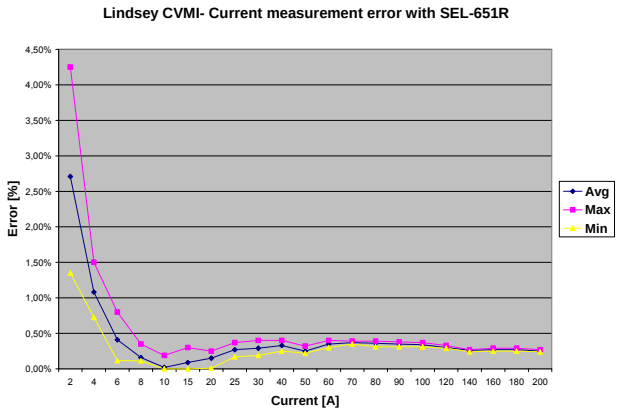

Figure 5. Current measurement error with CVMI Lindsey current sensors and SEL-651R control.

2) Recloser with integral current transducers

For this category, the test was performed on the chain composed by integral current transducers of an ABB-OVR recloser and its control PCD2000.

The three-phase recloser poles were connected in series and the current transducers were supposed to read the same current magnitude.

The level of current reading error of this chain, for a load range from 75 A to 400 A, was inferior to 1 %, which corresponds to the current measurement error value provided by the manufacturer. The error-load chart for three-phase recloser transducers and for currents from 10 A to 400 A is illustrated in Figure 6.

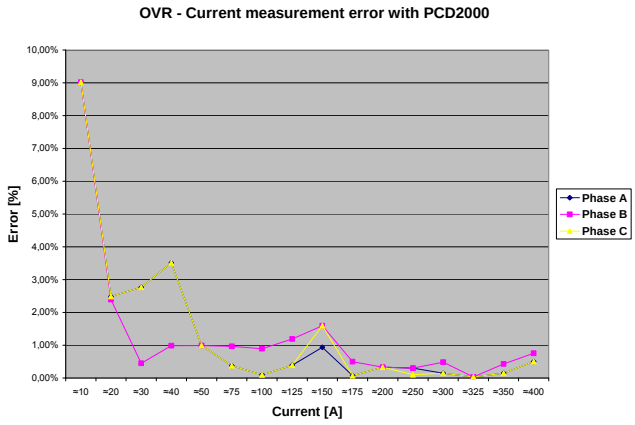

Figure 6: Current measurement error with OVR integrated current transducers and PCD2000 control.

3) Recloser with external current transducers

This test was carried out on a TriMod 300 recloser external current transducer connected to a SEL-651R control and the test results are presented in Figure 7.

The error chart shows an error level decreasing constantly from 1 % to 0.20 % and then becoming steady for currents higher than 100 A.

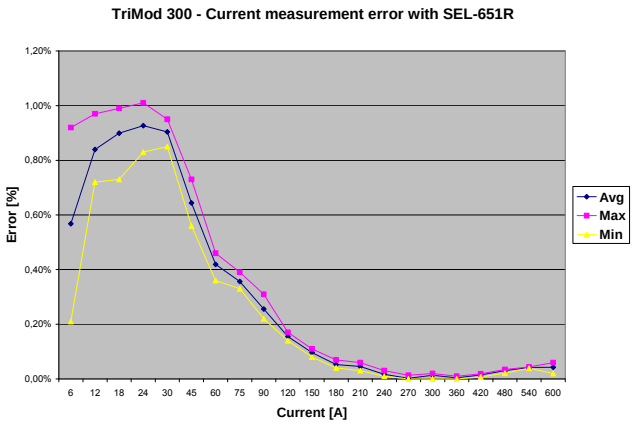

Figure 7. Current measurement error with TriMod external current transducers and SEL-651R control.

4) Switch with standalone current sensors

The test on CVMI Lindsey-9660 was repeated with an S&C M series control doing the current average rms value acquisition.

The chart of the current reading error, using this sensor-control chain, is presented in Figure 8.

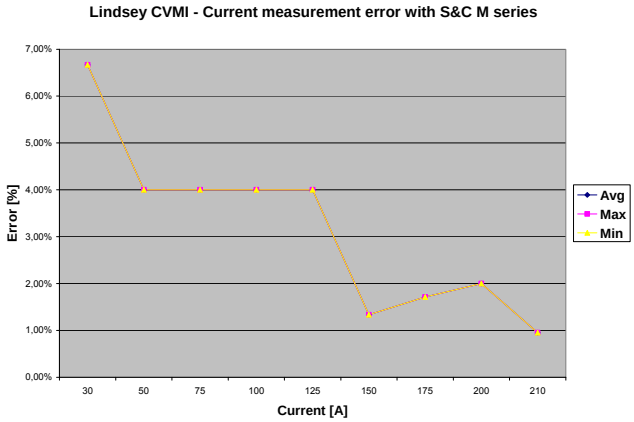

Figure 8. Current measurement error with CVMI Lindsey current sensors and S&C M series control.

The current measurement error is significantly higher comparing to the case 0 because of a pre-set fixed current calibration factor (adjustable factor unavailable) and an rms value calculation algorithm, based on integers instead of float values. Fortunately, most recent controls are provided with an adjustable calibration factor and unfortunately, it is the same for all three phases instead of one for each phase. The sensors are not identical and separate phase calibration factors would allow readings that are more accurate, either for current or for voltage.

B. Voltage Measurement

The tests on voltage measurement error tried to evaluate the level of error introduced by power distribution transformers used along with controls of major distribution equipments for voltage readings at MV (medium voltage)

level. The following combinations were used for voltage signal acquisition:

a) ABB-MicroPole 3 kVA with S&C M series.
b) ABB-MicroPole 3 kVA with SEL-651R.
c) ABB-ONAN 10 kVA with SEL-651R.

All the tests corresponding to this category were no-load tests and the voltage range was 12.4 kV to 15.6 kV.

The graphical representation of the measurement error for combinations a) and b) is shown in Figure 9. The average error for both combinations is inferior to the threshold 0.5 % suggested by the standard IEEE Std C57.12.00™-2006 « Standard General Requirements for Liquid-Immersed Distribution, Power, and Regulating Transformers ».

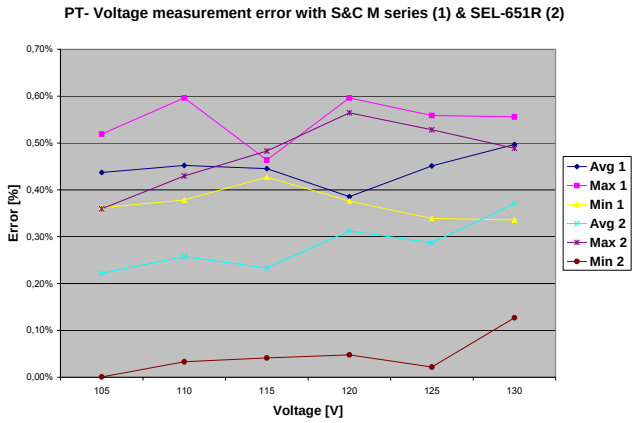

Figure 9. Voltage measurement error with 3 kVA MicroPole distribution transformer and S&C M series and SEL-651R controls:

C. Voltage and current

The last test, performed on a reversible voltage regulator PTs and CT and its control, is not yet totally concluded. So far, only the metering and communicating potential of the control (CL-6A) was evaluated. The IED/control was configured to save average current and voltage rms-values over one minute period, which are usually required by a VVC application. The remote data transfer from three CL-6A controls through a SMP4 gateway and over a FO (Fiber Optic) link was successful but the reliability, when using the same gateway and a phone line, was questionable.

D. Measurement error with the chain sensor-IED

The voltage and current measurement accuracy of the chain sensor-IED is generally acceptable for statistical grid evaluation, despite the fact that this hardware combination introduces a reading error higher than 0.1 %, value defined by IEC 61000-4-30 for class A devices. However, the continuous evolution of sensor and IED technologies and a better sensor calibration are potential factors contributing to the improvement of the chain accuracy in the next future.

VII. THE IED OF THE FUTURE

Smart distribution applications, based on information from IEDs and smart sensors, improve the efficiency of distribution grid management. Power engineers learnt from experience that operating at the same time an increasing number of different IED models, integrated to the distribution grid, causes stress on network operating personnel for several reasons:

- Different control hardware, firmware and communication software when different manufacturers.
- Data format not always compatible with standard formats.
- IEDs with lack of interoperability or low degree of interoperability.
- Not “plug and play” design yet.

To reduce cost and reach the “plug and play” design (see Figure 10), the development of distribution system technologies, including both aspects hardware and software, must be coordinated trough appropriate standards.

To be proactive, IREQ and its Strategic Platform initiated the project DACCORD, which proposes a new strategy for conception, integration, deployment and utilization of a generic modular IED/control for smart distribution systems, complying with future standards, in three stages:

1) New concept of IED/control.
2) Strategy for device integration, deployment and operation compatible with the Smart Grid architecture (new feature: plug and play (P&P) (interoperability included)).
3) New strategy of how to use IEDs/controls advanced complementary functions developed for SD applications.

The first stage is focused on developing a generic specification for a modular distribution equipment control, which will cover three aspects:

1) Hardware (modular):
a) Main board with CPU,
b) Front panel (including touch screen),
c) Communication interface,
d) Signal (voltage and current) interface,
e) Electronic interface (required for voltage and current sensors),
f) N/O and N/C contact blocs.
2) Software:
d) Firmware multi platform (CIM) including advanced functionalities such as:
- *Main function (protection, voltage regulation, VAR control, feeder reconfiguration,…).*
- *Remote metering.*
- *Remote-predictive maintenance or JIT (Just In Time) for distribution equipment.*
- *PQ.*
- *Security.*

e) Communication software and protocols:
- *IEC 61850 version for distribution feeders.*
- *IEC 61870.…..*
- *DNP 3.0.*

3) Backup power supply.

The data provided by such IEDs will fall into both real-time and non real-time categories. In the real-time category, distributed sensing provides increased power grid monitoring

for grid state estimators, device status and health, fault detection and location, PQ, safety and security. Advanced functioning will include demand distribution for load balancing; transformer, circuit breaker and tap changer monitoring; detection of energized downed lines, high impedance faults and faults in underground cables.

The bulk data download (waveforms) will be a feasible characteristic of the evolving telecommunication structure.

The lifespan of the backup power supply battery will be increased to 7 to 10 years by using new long life battery technology, remote maintenance and reducing IED energy consumption with efficient IED management.

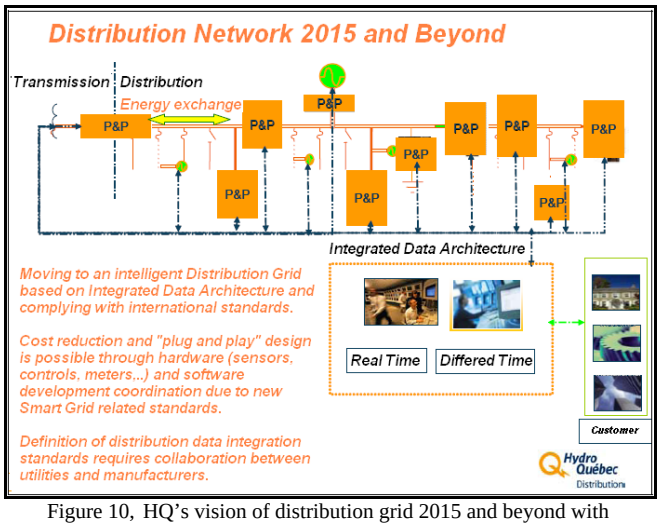

Figure 10, HQ's vision of distribution grid 2015 and beyond with integrated data architecture complaying with international standards

By this project IREQ (Hydro-Québec) tries to:

- Initiate a debate, within Smart Distribution related national and international Working Groups (CEATI, IEEE, CIGRE/CIRED, ...).
- Influence those WGs to start working on definitions for modular hardware and software of standardized IEDs in order to make possible the edition of future related standards.
- Kick off collaborations with other utilities, manufacturers and organizations.
- Influence distribution equipment manufacturers to develop and build standardized models.

VIII. CONCLUSIONS

The IEDs with very high functionality will lead to significant cost savings and offer new problem solving capabilities. With these changes, utility personnel will need extensive training on the new practices, and a close partnership between vendors and utility customers will be necessary.

Sensors and communication technology fields are evolving quickly. IED manufacturers are taking advantage of performance of new technologies, upgrading their devices to be compatible with smart sensors. The best example is the new generation of reclosers, with integral voltage and current sensors.

Smart grid integrated monitoring devices rise the potential for implementing DA applications like VVC, FL, PQM and open the gate for new ones. Old and new applications will share the same resources.

Due to extensive implementation of SCADA and AMI systems, the infrastructure required by DA applications mentioned above is often already in place.

HQ's projects resulted in the acquisition of knowledge about present distribution equipment performance and improvements needed in the future (technologies, sensors, IEDs, standards…) in order to integrate data acquisition.

The accuracy of data acquisition process is an important factor, critically affecting the efficiency and reliability of DA systems and furthermore the efficiency and reliability of the power distribution system.

The accuracy of the chain sensor-IED is generally acceptable. However, the controls under testing do not qualify for class A devices, as defined by IEC 61000-4-30.

The frequency response of smart sensors doesn't reach yet the level of accuracy that PQ experts would like. This feature should be improved in the next future to allow the implementation of smart applications based on discrimination of grid polluters.

Using IEDs/controls for grid monitoring is an inspired decision based on following advantages [5]:

- Presence of AMI in Smart Grids.
- Connection of IEDs to the MV side of the grid.
- Continuous evolution of IEDs and sensors.

There is a trend in controls evolution to follow up the path taken by intelligent meters a decade or more ago, and that is very encouraging.

ACKNOWLEDGMENT

This paper was sponsored by IREQ (Research Institute of Hydro-Québec) and by its Strategic Platform, a body that supports strategic initiatives, related to the power industry, and developments of new concepts for the power systems of the future.

REFERENCES

[1] T. Sezi and B.K. Duncan "New intelligent electronic devices change the structure of power distribution systems" IEEE IAC Phoenix, USA, October 1999.

[2] G. Simard, L. Clark, and B. Uluski, "Contribution from IEEE PES Distribution Automation Working Group", NIST interim smart grid standards interoperability roadmap workshop, Reston/Virginia, USA, April 2009.

[3] F. Zavoda, "The key role of Intelligent Electronic Devices (IED) in Advanced Distribution Automation (ADA)", CICED 2008, Guangzhou, China, December 2008.

[4] F. Zavoda and G. Simard, "Performance of Today's Intelligent Controllers and Meters, Elements of an Integrated Monitoring System for ADA", IEEE PES GM, Pittsburg, USA, July 2008.

[5] F. Zavoda, "Advanced Distribution Automation (ADA) Applications and Power Quality in Smart Grids", CICED 2010, Nanjing, China, September 2010.

 ISBN: 978-1-61208-136-6

BER Performance of Binary Transmitted Signal for Power Line Communication under Nakagami-like Background Noise

Youngsun Kim, Yong-Hwa Kim, Hui-Myoung Oh, and Sungsoo Choi
Power Telecommunication Research Center
Korea Electrotechnology Research Institute (KERI)
Ansan-city, Gyeonggi-do, Republic of Korea
Email: yskim, yongkim, hmoh, sschoi@keri.re.kr,

***Abstract*—Power line communication is an emerging communication technology for the home area network of Smart Grid. To evaluate the performance of power line communication, in our previous work, we derived the closed-form probability density function for the real part of amplitude distribution of Nakagami-like background noise. With this result, in this paper, we investigated the bit error rate performance of binary modulated signal with a single channel transmission. We derived an expression of bit error rate performance and verified its validity through simulations.**

***Keywords*-Power Line Communication; Background Noise; Nakagami Distribution; Bit Error Rate Performance.**

I. INTRODUCTION

Smart Grid becomes the focus of public attention as a next-generation energy efficiency optimization. In Smart Grid, various communication technologies enable a two-way exchange of energy consumption and control data via wired/wireless medium. Power line communication (PLC) has been adopted as a communication technology for the automatic meter reading (AMR) [1] and, recently, massively deployed in Korea. Now, PLC is a candidate technology for Smart Grid as a home area network (HAN) communication infrastructure.

To adopt the PLC technology effectively, there is a need for the channel modeling of background noise, impulsive noise, etc. [2], [3]. The channel modeling for the power-line channel has been extensively analyzed and simulated by many researchers. They tried to find the exact (or approximated) channel parameters such as noise, impedance, and attenuation. Among the various parameters for channel modeling, noise is important to evaluate the performance of PLC system. However, due to the nature of power-line channel such as various topologies, connected electrical appliances, types of electrical loads, etc. , the noise modeling could not be easily described as a mathematical expression.

Recently, it was proposed that the amplitude of background noise in power-line channel follows the Nakagami-m distribution [4] [5]. The bit error rate (BER) performance of the PLC system was also evaluated for both single and multi-channel transmission. In [5], however, the BER performances are not expressed as a closed-form mathematical expression, there is thus work to be done yet. We briefly review the previous work in Section II and derive the BER performance in Section III. The mathematical expression gives the system designer a better understanding of the system design and a performance prediction for his system.

II. PDF OF BACKGROUND NOISE FOR PLC CHANNEL

We derived the closed-form probability density function (PDF) of the real part noise, y, for power-line channel [6],

$$\begin{aligned} f(y) \quad &= \frac{1}{\sqrt{\pi}\Gamma(m)}\sqrt{\frac{m}{\Omega}}e^{-\frac{my^2}{\Omega}}\left\{\frac{\Gamma(\frac{1}{2}-m)}{\Gamma(1-m)}\left(\frac{my^2}{\Omega}\right)^{m-\frac{1}{2}}\right. \\ &\quad \times {}_1F_1\left(\tfrac{1}{2},\tfrac{1}{2}+m,\tfrac{my^2}{\Omega}\right)+\frac{\Gamma(m-\frac{1}{2})}{\sqrt{\pi}} \\ &\quad \left.\times {}_1F_1\left(1-m,\tfrac{3}{2}-m,\tfrac{my^2}{\Omega}\right)\right\}, \end{aligned} \tag{1}$$

for $0 < m < 1$ and $m \neq \frac{1}{2}$, where $\Gamma(\cdot)$ is the Gamma function, m and Ω are parameters defined as $\Omega = E[\alpha^2] = \overline{\alpha^2}$, $E[x] = \overline{x}$ denoting the expected value of x and $m = \frac{\left(\overline{\alpha^2}\right)^2}{(\alpha^2-\overline{\alpha^2})^2} > 0$, which comes from the amplitude PDF of a power-line background noise characterized by Nakagami-m distribution:

$$f(\alpha) = \frac{2m^m\alpha^{2m-1}}{\Gamma(m)\Omega^m}e^{-(m/\Omega)\alpha^2}, \qquad \alpha \geq 0. \tag{2}$$

Ω denotes the power of the amplitude, α. Originally, the Nakagami-m distribution represents the fading amplitude of wireless communication channel. It spans the one-sided Gaussian, Rayleigh, Hoyt, Rice and non-fading channel as m varies [7]. Furthermore, the confluent hypergeometric function of the first kind, ${}_1F_1$, as [8, Chap. 9.2] :

$${}_1F_1(a,b,z) = 1+\frac{a}{b}\frac{z}{1!}+\frac{a(a+1)}{b(b+1)}\frac{z^2}{2!}+\frac{a(a+1)(a+2)}{b(b+1)(b+2)}\frac{z^3}{3!}\cdots \tag{3}$$

is used for (1). For special case of $m = \frac{1}{2}$, we get

$$f(y) = \frac{1}{\pi}\sqrt{\frac{1}{2\Omega\pi}}e^{-\frac{y^2}{4\Omega}}K_0\left(\frac{y^2}{4\Omega}\right), \tag{4}$$

where $K_0(z)$ is the modified Bessel function of the second kind of order 0. The accuracy of the analyzed closed-form expression in (1) has been verified in [6]. Eqn. (1) shows

 ISBN: 978-1-61208-136-6

well evaluation of the noise modeling for Nakagmi-like background noise.

III. Derivation of the BER performance

In this section, we derive the BER performance of binary data transmission with the noise as described in section II. Fig. 1 demonstrates the system model for binary transmission. A transmitter sends binary data, A or $-A$, then, the decision metric at the receiver, r, is defined as

$$r = \pm A + y, \tag{5}$$

which is added by Nakagami-like background power-line noise, y. We assumed the perfect time and carrier synchronization in demodulation for the ease of analysis.

Then, the average bit error rate (BER), P_e, can be expressed as

$$P_e = p(A)P(E|s=A) + p(-A)P(E|s=-A) \tag{6}$$

where $p(A)$ is the probability that the transmitter sends data A, and $P(E|s=A)$ is the probability of error decision at the receiver when data A is transmitted. With equal probability of transmitting A and $-A$, Eqn. (6) is represented as

$$P_e = \frac{1}{2}P(E|s=A) + \frac{1}{2}P(E|s=-A). \tag{7}$$

Since the noise PDF, $p(y)$, is symmetric about $y=0$, we get

$$P_e = P(E|s=A) = P(E|s=-A) = \int_A^\infty f(y)dy. \tag{8}$$

By substituting Eqn.(1) into Eqn. (8), we obtain

$$\begin{aligned} P_e &= \textstyle\int_A^\infty f(y)dy \\ &= \textstyle\int_A^\infty \frac{1}{\sqrt{\pi}\Gamma(m)}\sqrt{\frac{m}{\Omega}}e^{-\frac{my^2}{\Omega}}\left\{\frac{\Gamma(\frac{1}{2}-m)}{\Gamma(1-m)}\left(\frac{my^2}{\Omega}\right)^{m-\frac{1}{2}}\right. \\ &\quad \times {}_1F_1\left(\tfrac{1}{2},\tfrac{1}{2}+m,\tfrac{my^2}{\Omega}\right) + \frac{\Gamma(m-\frac{1}{2})}{\sqrt{\pi}} \\ &\quad \left.\times {}_1F_1\left(1-m,\tfrac{3}{2}-m,\tfrac{my^2}{\Omega}\right)\right\}dy \\ &= \textstyle\frac{1}{\sqrt{\pi}\Gamma(m)}\sqrt{\frac{m}{\Omega}}\frac{\Gamma(\frac{1}{2}-m)}{\Gamma(1-m)}\int_A^\infty e^{-\frac{my^2}{\Omega}}\left(\frac{my^2}{\Omega}\right)^{m-\frac{1}{2}} \\ &\quad \times {}_1F_1\left(\tfrac{1}{2},\tfrac{1}{2}+m,\tfrac{my^2}{\Omega}\right)dy + \frac{1}{\sqrt{\pi}\Gamma(m)}\sqrt{\frac{m}{\Omega}}\frac{\Gamma(m-\frac{1}{2})}{\sqrt{\pi}} \\ &\quad \times \textstyle\int_A^\infty e^{-\frac{my^2}{\Omega}}{}_1F_1\left(1-m,\tfrac{3}{2}-m,\tfrac{my^2}{\Omega}\right)dy. \end{aligned} \tag{9}$$

Letting $\sqrt{\frac{m}{\Omega}}y = x$ gives $\sqrt{\frac{m}{\Omega}}dy = dx$, then, Eqn. (27) is

$$\begin{aligned} P_e &= \textstyle\frac{1}{\sqrt{\pi}\Gamma(m)}\frac{\Gamma(\frac{1}{2}-m)}{\Gamma(1-m)}\int_{\sqrt{\frac{m}{\Omega}}A}^\infty e^{-x^2}x^{2m-1} \\ &\quad \times {}_1F_1\left(\tfrac{1}{2},\tfrac{1}{2}+m,x^2\right)dx + \frac{1}{\sqrt{\pi}\Gamma(m)}\frac{\Gamma(m-\frac{1}{2})}{\sqrt{\pi}} \\ &\quad \times \textstyle\int_{\sqrt{\frac{m}{\Omega}}A}^\infty e^{-x^2}{}_1F_1\left(1-m,\tfrac{3}{2}-m,x^2\right)dx. \end{aligned} \tag{10}$$

Applying Kummer Transform [8, (13.1.27)],

$${}_1F_1(a,b,z) = e^z {}_1F_1(b-a,b,-z), \tag{11}$$

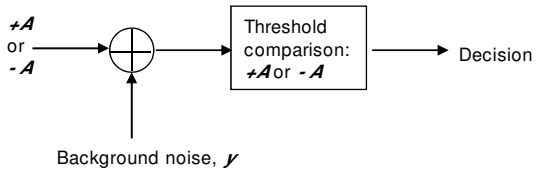

Figure 1. System model for binary transmission

to Eqn. (28) gives

$$\begin{aligned} P_e = \textstyle\frac{\Gamma(\frac{1}{2}-m)}{\sqrt{\pi}\Gamma(m)\Gamma(1-m)}\int_{\sqrt{\frac{m}{\Omega}}A}^\infty x^{2m-1}{}_1F_1\left(m,\frac{1}{2}+m,-x^2\right)dx \\ + \textstyle\frac{\Gamma(m-\frac{1}{2})}{\pi\Gamma(m)}\int_{\sqrt{\frac{m}{\Omega}}A}^\infty {}_1F_1\left(\frac{1}{2},\frac{3}{2}-m,-x^2\right)dx. \end{aligned} \tag{12}$$

In Eqn.(31), the first term in the integration is

$$\int_{\sqrt{\frac{m}{\Omega}}A}^\infty x^{2m-1}{}_1F_1\left(m,\frac{1}{2}+m,-x^2\right)dx. \tag{13}$$

By substituting Eqn.(3), Eqn.(13) is represented as

$$\int_{\sqrt{\frac{m}{\Omega}}A}^\infty x^{2m-1}\sum_{n=0}^\infty \frac{(m)_n}{(\frac{1}{2}+m)_n}\frac{(-x^2)^n}{n!}dx, \tag{14}$$

where $(m)_n$ is the Pochhammer symbol [9, (6.1.22)], which is defined as

$$\begin{aligned} (m)_n &= \frac{\Gamma(m+n)}{\Gamma(m)} \\ &= m(m+1)\cdots(m+n-1). \end{aligned} \tag{15}$$

Then, Eqn.(14) is represented as

$$\begin{aligned} &\sum_{n=0}^\infty \frac{(m)_n}{(\frac{1}{2}+m)_n}\frac{1}{n!}\int_{\sqrt{\frac{m}{\Omega}}A}^\infty x^{2m-1}(-x^2)^n dx \\ &= \sum_{n=0}^\infty \frac{(m)_n}{(\frac{1}{2}+m)_n}\frac{(-1)^n}{n!}\int_{\sqrt{\frac{m}{\Omega}}A}^\infty x^{2n+2m-1}dx \\ &= \sum_{n=0}^\infty \frac{(m)_n}{(\frac{1}{2}+m)_n}\frac{(-1)^n}{n!}\left[\frac{1}{2(n+m)}x^{2(n+m)}\right]_{x=\sqrt{\frac{m}{\Omega}}A}^\infty \\ &= \left[\sum_{n=0}^\infty \frac{(m)_n}{(\frac{1}{2}+m)_n}\frac{(-1)^n}{n!}\frac{1}{2(n+m)}x^{2(n+m)}\right]_{x=\sqrt{\frac{m}{\Omega}}A}^\infty \\ &= \left[\frac{x^{2m}}{2}\sum_{n=0}^\infty \frac{(m)_n}{(\frac{1}{2}+m)_n}\frac{1}{n+m}\frac{(-x^2)^n}{n!}\right]_{x=\sqrt{\frac{m}{\Omega}}A}^\infty. \end{aligned} \tag{16}$$

Since we can replace $\frac{1}{n+m}$ as

$$\begin{aligned} \frac{1}{n+m} &= \frac{m(m+1)\cdots(m+n-1)}{m(m+1)\cdots(m+n-1)(m+n)} \\ &= \frac{1}{m}\frac{m_n}{(m+1)_n}, \end{aligned} \tag{17}$$

$$P_e = \frac{\Gamma(\frac{1}{2}-m)}{2m\sqrt{\pi}\Gamma(m)\Gamma(1-m)}\left[x^{2m}\,{}_2F_2\left(m,m;\frac{1}{2}+m,m+1;-x^2\right)\right]_{x=\sqrt{\frac{m}{\Omega}}A}^{\infty} + \frac{\Gamma(m-\frac{1}{2})}{\sqrt{\pi}\Gamma(m)}\left[x\,{}_2F_2\left(\frac{1}{2},\frac{1}{2};\frac{3}{2}-m,\frac{3}{2};-x^2\right)\right]_{x=\sqrt{\frac{m}{\Omega}}A}^{\infty}. \quad (26)$$

the Eqn. (16) can be written as

$$\begin{aligned}&\left[\frac{x^{2m}}{2}\sum_{n=0}^{\infty}\frac{(m)_n}{(\frac{1}{2}+m)_n}\frac{1}{m}\frac{m_n}{(m+1)_n}\frac{(-x^2)^n}{n!}\right]_{x=\sqrt{\frac{m}{\Omega}}A}^{\infty}\\ &=\left[\frac{x^{2m}}{2m}\sum_{n=0}^{\infty}\frac{(m)_n}{(\frac{1}{2}+m)_n}\frac{m_n}{(m+1)_n}\frac{(-x^2)^n}{n!}\right]_{x=\sqrt{\frac{m}{\Omega}}A}^{\infty}\\ &=\left[\frac{x^{2m}}{2m}\,{}_2F_2\left(m,m;\frac{1}{2}+m,m+1;-x^2\right)\right]_{x=\sqrt{\frac{m}{\Omega}}A}^{\infty}\end{aligned} \quad (18)$$

where

$${}_2F_2(a_1,a_2;b_1,b_2;z) = 1+\frac{a_1}{b_1}\frac{a_2}{b_2}\frac{z}{1!}+\frac{a_1(a_1+1)}{b_1(b_1+1)}\frac{a_2(a_2+1)}{b_2(b_2+1)}\frac{z^2}{2!}+\cdots. \quad (19)$$

Now, we treat the integration of the second term in Eqn.(31),

$$\int_{\sqrt{\frac{m}{\Omega}}A}^{\infty}{}_1F_1\left(\frac{1}{2},\frac{3}{2}-m,-x^2\right)dx. \quad (20)$$

By substituting Eqn.(3) into Eqn.(20), we obtain

$$\int_{\sqrt{\frac{m}{\Omega}}A}^{\infty}\sum_{n=0}^{\infty}\frac{(\frac{1}{2})_n}{(\frac{3}{2}-m)_n}\frac{(-x^2)^n}{n!}dx. \quad (21)$$

Eqn. (21) is represented as

$$\begin{aligned}&\sum_{n=0}^{\infty}\frac{(\frac{1}{2})_n}{(\frac{3}{2}-m)_n}\frac{(-1)^n}{n!}\int_{\sqrt{\frac{m}{\Omega}}A}^{\infty}x^{2n}dx\\ &=\sum_{n=0}^{\infty}\frac{(\frac{1}{2})_n}{(\frac{3}{2}-m)_n}\frac{(-1)^n}{n!}\left[\frac{1}{2n+1}x^{2n+1}\right]_{x=\sqrt{\frac{m}{\Omega}}A}^{\infty}\\ &=\left[x\sum_{n=0}^{\infty}\frac{(\frac{1}{2})_n}{(\frac{3}{2}-m)_n}\frac{(-1)^n}{n!}\frac{x^{2n}}{2n+1}\right]_{x=\sqrt{\frac{m}{\Omega}}A}^{\infty}\\ &=\left[x\sum_{n=0}^{\infty}\frac{(\frac{1}{2})_n}{(\frac{3}{2}-m)_n}\frac{1}{2n+1}\frac{(-x^2)^n}{n!}\right]_{x=\sqrt{\frac{m}{\Omega}}A}^{\infty}.\end{aligned} \quad (22)$$

Since we can replace $\frac{1}{2n+1}$ as

$$\begin{aligned}\frac{1}{2n+1} &= \frac{1}{2}\frac{1}{\frac{1}{2}+n}\\ &= \frac{\frac{1}{2}(\frac{1}{2}+1)\cdots(\frac{1}{2}+n-1)}{\frac{3}{2}(\frac{3}{2}+1)\cdots(\frac{3}{2}+n-2)(\frac{3}{2}+n-1)}\\ &= \frac{(\frac{1}{2})_n}{(\frac{3}{2})_n},\end{aligned} \quad (23)$$

the Eqn. (22) can be written as

$$\begin{aligned}&\left[x\sum_{n=0}^{\infty}\frac{(\frac{1}{2})_n}{(\frac{3}{2}-m)_n}\frac{(\frac{1}{2})_n}{(\frac{3}{2})_n}\frac{(-x^2)^n}{n!}\right]_{x=\sqrt{\frac{m}{\Omega}}A}^{\infty}\\ &=\left[x\,{}_2F_2\left(\tfrac{1}{2},\tfrac{1}{2};\tfrac{3}{2}-m,\tfrac{3}{2};-x^2\right)\right]_{x=\sqrt{\frac{m}{\Omega}}A}^{\infty}.\end{aligned} \quad (24)$$

Using the relation,

$$\int z^{\alpha-1}{}_1F_1(a,b,cz)\,dz = \frac{z^{\alpha}{}_2F_2(a,\alpha;b,\alpha+1;cz)}{a}, \quad (25)$$

and substituting Eqns.(16) and (24) into Eqn. (31) gives Eqn. (26). Eqn. (26) represents the BER performance of binary transmitted signal without integration for the Nakagami-like power-line background noise.

Now, we derive the BER performance for $m=\frac{1}{2}$ as a special case. By substituting Eqn.(4) into Eqn. (8), we obtain

$$\begin{aligned}P_e &= \int_A^{\infty}f(y)dy\\ &= \int_A^{\infty}\frac{1}{\pi}\sqrt{\frac{1}{2\Omega\pi}}e^{-\frac{y^2}{4\Omega}}K_0\left(\frac{y^2}{4\Omega}\right)dy\\ &= \frac{1}{\pi}\sqrt{\frac{1}{2\Omega\pi}}\int_A^{\infty}e^{-\frac{y^2}{4\Omega}}K_0\left(\frac{y^2}{4\Omega}\right)dy.\end{aligned} \quad (27)$$

Letting $\frac{y^2}{4\Omega}=x$ gives $\frac{y}{2\Omega}dy=dx$, then, Eqn. (27) is

$$\begin{aligned}Pe &= \frac{1}{\pi}\sqrt{\frac{1}{2\Omega\pi}}\int_{\frac{A^2}{4\Omega}}^{\infty}2\Omega y^{-1}e^{-x}K_0(x)\,dx\\ &= \frac{1}{\pi}\sqrt{\frac{1}{2\Omega\pi}}\int_{\frac{A^2}{4\Omega}}^{\infty}\sqrt{\Omega}x^{-1}e^{-x}K_0(x)\,dx\\ &= \frac{1}{\pi}\sqrt{\frac{1}{2\pi}}\int_{\frac{A^2}{4\Omega}}^{\infty}x^{-1}e^{-x}K_0(x)\,dx.\end{aligned} \quad (28)$$

Eqn. (28) can be divided into two terms;

$$\begin{aligned}P_e &= \frac{1}{\pi}\sqrt{\frac{1}{2\pi}}\int_0^{\infty}x^{-1}e^{-x}K_0(x)\,dx\\ &\quad -\frac{1}{\pi}\sqrt{\frac{1}{2\pi}}\int_0^{\frac{A^2}{4\Omega}}x^{-1}e^{-x}K_0(x)\,dx.\end{aligned} \quad (29)$$

Then, applying [9, (6.621.4)],

$$\begin{aligned}&\int_0^{\infty}x^{\mu-1}e^{-\alpha x}K_{\nu}(\beta x)dx\\ &\quad=\frac{\sqrt{\pi}(2\beta)^{\nu}}{(\alpha+\beta)^{\mu+\nu}}\frac{\Gamma(\mu+\nu)\Gamma(\mu-\nu)}{\Gamma(\mu+\frac{1}{2})}\\ &\quad\times F\left(\mu+\nu,\nu+\tfrac{1}{2};\mu+\tfrac{1}{2};\tfrac{\alpha-\beta}{\alpha+\beta}\right),\end{aligned} \quad (30)$$

 ISBN: 978-1-61208-136-6

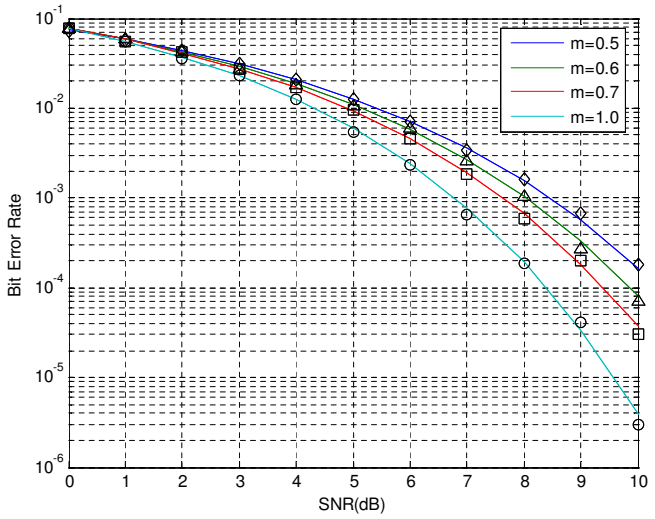

Figure 2. Simulated and analyzed BER performance under Nakagami-like background noise with $m = 0.5, 0.6, 0.7, 1.0$

where Re $\mu >$ | Re ν|, Re $(\alpha + \beta) > 0$ for $\mu = \frac{1}{2}$, $\nu = 0$, $\alpha = 1$, $\beta = 1$, to Eqn. (29) gives

$$\begin{aligned} P_e &= \frac{1}{\pi}\sqrt{\frac{1}{2\pi}}\left(\pi\sqrt{\frac{\pi}{2}} - \int_0^{\frac{A^2}{4\Omega}} x^{-1}e^{-x}K_0(x)\,dx\right) \\ &= \frac{1}{2} - \frac{1}{\pi}\sqrt{\frac{1}{2\pi}}\int_0^{\frac{A^2}{4\Omega}} x^{-1}e^{-x}K_0(x)\,dx. \end{aligned} \tag{31}$$

Eqn. (31) represents the BER performance of binary transmitted signal with Nakagami-like power-line background noise for $m = \frac{1}{2}$.

IV. Numerical Results

Numerical examples for the BER performance of binary modulated receiver under Nakagami-like background noise are presented through both analysis and simulation. The analyzed BER performance is obtained using Eqn.(26). For the ease of analysis, we assumed the transmitted data $A = 1$. The simulated performances are obtained by using the Monte Carlo method with 10^7 binary transmitted data. Fig. 2 compares the simulated and analyzed BER performance with $m = 0.5, 0.6, 0.7$ and 1. As m increases, the BER performance improves since the Nakagami-like background noise, y, has the shape of PDF close to Gaussian PDF, with a result similar to [5]. Thus, the signal-to-noise ratio increases as m increases. Simulation results with various m values show good agreement between simulations and analysis up to the SNR of 10 dB.

V. Conclusion

In this paper, the BER performance of binary transmitted signal under Nakagami-like background noise was presented. We derived the BER performance with conventional functions such as the hypergeometric function and the Gamma function. Simulated results show the validity of the derived BER performances. With these results, a PLC system designer can easily predict and analyze the performance of HAN system. The BER performance with impulsive noise and the transmission of multi-channel modulated signal would be the focus of the future work.

References

[1] Y. Zhang and S. Cheng, "Power Line Communications," IEEE Potentials, vol. 23, no. 4, pp. 4-8, Oct.-Nov. 2004.

[2] M. Zimmermann and K. Dostert, "A multipath model for the powerline channel," IEEE Trans. Commun., vol. 50, no. 4, pp. 553-559, April 2002.

[3] M. Zimmermann and K. Dostert, "Analysis and modeling of impulsive noise in broadband powerline communications," IEEE Trans. Electromagn. Compat., vol. 44, no. 1, pp. 249-258, Feb. 2002.

[4] M. Nakagami, "The m-distribution - A general formula of intensity distribution of rapid fading," in Statistical Methods in Radio Wave Propagation, pp. 3-36, Pergamon Press, Oxford, U.K, 1960.

[5] H. Meng, Y. L. Guan and S. Chen, "Modeling and analysis for noise effects on broadband power-line communications," IEEE Trans. Power Del., vol. 20, no. 2, pp. 630-637, April 2005.

[6] Y. Kim, H-M. Oh and S. Choi, "Closed-form expression of Nakagami-like background noise in power-line channel," IEEE Trans. Power Del., vol. 23, no. 3, pp. 1410-1412, Oct. 2008.

[7] M. K. Simon and M.-S. Alouini, Digital Communications Over Generalized Fading Channels : A Unified Approach to Performance Analysis, New York: Wiley, 2000.

[8] I. S. Gradshteyn and I. M. Ryzhik, Table of Integrals, Series, and Products, 6th ed., San Diego, CA: Academic, 2000.

[9] M. Abromowitz and I. A. Stegun, Handbook of Mathematical Functions with Formulas, Graphs, and Mathematical Tables, Dover Publications, New York, 1970.

 ISBN: 978-1-61208-136-6

A Systems Approach to the Smart Grid

Saraansh Dave*, Mahesh Sooriyabandara*, Mike Yearworth†
*Telecommunications Research Lab
Toshiba Research Europe Limited, Bristol, UK
Email: saraansh.dave@toshiba-trel.com; mahesh.sooriyabandara@toshiba-trel.com
†Systems Centre, Faculty of Engineering, University of Bristol, UK
Email: mike.yearworth@bristol.ac.uk

***Abstract*—This paper presents the case for using a systems approach to analyse the requirements and behaviours of the Smart Grid as well as designing relevant solutions. By linking systems thinking to agent-based modelling, we discuss how a Smart Grid can be modelled as Multi-Agent Systems by reviewing some related state-of-the-art research. This paper goes on to outline two research areas that we are developing, namely, demand response using dynamic pricing and emergent behaviours of a Smart Grid.**

***Index Terms*—Systems Thinking; Agent-Based Modelling; Smart Grids;**

I. Introduction

As the world pushes towards a more sustainable and resilient electrical supply there is a shift towards smart technology to revolutionise the electricity market. In Europe, one target of the Strategic Energy Technology (SET) Plan [1] states that by 2020 the grid should be able to integrate up to 35% renewable electricity effectively matching the demand to the supply. The European Technology Platforms Strategic Deployment Document for Europe's Electricity Network of the Future [2] quotes the International Energy Agency in approximating that EUR 500 billion will be invested by 2030 in electric grids. Without the use of smart technology this expenditure will not be used to move away from conventional centralised generation and distribution that is characteristic of todays electricity market. The smart technology in this context includes but is not limited to smart-meters, electric-vehicles, distributed storage, micro-generation, and bidirectional communications networks. Also, a shift towards distributed generation and grid optimisation is necessary to combat an increase in energy consumption and alternative energy sources. Clearly this advancement of distribution and generation will make the Smart Grid system and energy industry more complex. Complexity of Smart Grid could be defined as consisting of components which are distributed and interconnected with bidirectional flow of both energy and information. For instance, as the grid gains autonomous behaviour of its components, it will lead to 2-way communication between appliances, households, neighbourhoods, utilities, substations etc. As a complex socio-technical system the Smart Grid is likely to exhibit emergent behaviours suggesting the need for sophisticated theoretical studies now and mitigating strategies during build out.

The concepts of Systems Engineering are well adapted to approaching complex problems and could be beneficial in Smart Grid environments. Further, an agent-based modelling approach, which is a tool in control systems and simulations, is one method of estimating or observing any emergent behaviour. In this paper, we discuss how system thinking and agent-based modelling approaches can be used when tackling the problems of analysing Smart Grid systems, understanding potential emergent behaviours and developing Smart Grid functionalities involving multiple agents.

The paper is organized as follows: Section 2 and Section 3 will discuss the systems thinking approach using relevant concepts of systems engineering, methods and limitations of agent-based modelling. Several examples of applications of agent-based modelling approaches to Smart Grid are discussed in Section 4. Section 5 identifies key research areas for applying the systems thinking and finally formulates the technological problem surrounding demand response and emergent properties.

II. Systems Thinking for a Smart Grid

Acknowledging the electricity sector as being complex leads us to treat it as a 'wicked' problem as defined by Rittel and Webber [3]. Conklin's adaptation [4] of wicked problem characteristics is a useful standpoint from which to view Smart Grid development. Conklin argues that solutions are unique and must be approached that way; Smart Grid solutions may vary by country or even by region.

In this context the design and deployment of the Smart Grid is arguably a wicked problem as a whole and even the Smart Grid sub-systems can be regarded as wicked due to their interactive nature. Conklin goes on to say that while understanding and learning about the problem environment is important and natural it alone does not lead to a satisfactory or timely solution. Alongside study and understanding, experimentation and pilot programmes such as those undertaken by the European Union are necessary. Another way of coping with the complex problem of a Smart Grid is to simplify or tame the situation [4]. This approach leads to a solution more quickly but the conclusion/implementation is short lived as the wicked problem re-emerges. Even if the technology exists for some or all of the Smart Grid (e.g., technical architecture as described in Deployment Priority 1 of the Strategic Deployment Document [2]) the challenge of integrating it as well as understanding the consumers' requirements still remains.

In an early paper, Doyle [5] expresses the lack of controlled research on the effectiveness of systems thinking. He also

 ISBN: 978-1-61208-136-6

explains that such research would involve aspects of cognitive psychology which would be complicated and time consuming. However such a study would be necessary to determine or quantify the effect of such an approach. In a more recent paper, Maani and Maharaj [6] present an experiment they conducted to determine a relationship between systems thinking and complex decision making. Whilst the study was small in scale and could be viewed as subjective, the results showed that the relationship between systems thinking and complex decision making is not obvious. Its evidence supported the view that certain types of systems thinking may be more suited to improving performance. The authors noted that another evident reason for better performance was the approach taken to a problem; understanding the system structure and relationships (e.g., feedback) as well as observing outcomes of decisions led to better performance.

Taking a systems view encourages a complete solution which would include aspects such as user requirements and cross-system integration.

III. Modelling Smart Grid as a Multi-Agent System

There are various enablers to make the transition from systems thinking to systems modelling whereby quantitative and qualitative understanding can improve. Simple tools such as rich pictures (see Fig. 1) and system maps are used to understand the constituents of the system. A picture can be taken to another level of analysis using a system map which allows boundaries to be defined and system elements to be placed in the correct domains. More formal tools such as Unified Modeling Language (UML) can be useful in describing systems using standardised structure which can be easily understood.

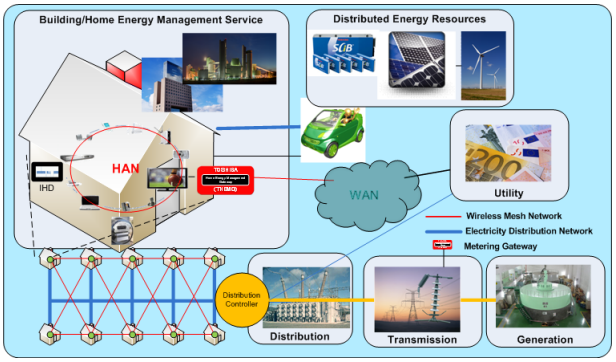

Fig. 1. Component view of a Smart Grid

Agent-based modelling (ABM) can also describe a system by allowing the user to define discrete 'agents' by their characteristics and behaviours. Nwana [7] describes agents as having a combination of the following three characteristics; ability to cooperate, act autonomously and the ability to learn. The specific combinations of these characteristics depends on the function of the agent. The contextual environment for the agents to act in can also be defined. Setting up a simulation in this style is a bottom-up approach as the constituent elements have defined behaviours whilst the system behaviour emerges from the interactions of the constituent agents. This allows emergent properties of a system to become apparent which may or may not have been intuitive.

Whilst ABM creates a useful framework for development of constitutive system elements it is through Multi-Agent Systems (MAS) that agent interactions can be focused on. It is due to these interactions that emergent behaviour arises. Gabbai et al. [8] give a good definition for MAS: *"a collection of autonomous, social actors where, through local interaction and social communication, emergent global behaviour occurs."*

Even agents with simple functions can elicit complex emergent behaviour through their interactions [9]. Albiero et al. [10] apply simple behavioural rules to multiple agents to create collective behaviour which would be difficult to produce using an algorithmic approach. Researchers in various fields have used ABM as a means to simulate intelligence with relative success. This paper suggests MAS as an appropriate agent approach for describing and investigating the Smart Grid domain.

There is a wide variety of software and tools to create ABMs and the remainder of this section contains a brief overview of some popular platforms (NetLogo, MATLAB, SWARM, MASON, JADE).

For small scale ABMs the most suitable platforms include MATLAB [11] and NetLogo [12]. Railsback et al. [13] recommend NetLogo as a user-friendly tool with a large amount of documentation and examples for beginners. Their study [13] shows that even though NetLogo is simple to program and run it can be applied to create sophisticated simulations for a range of domains (see the NetLogo website for examples [12]). However its lack of access to algorithms used by its commands makes reproducibility difficult which can deter some users.

For larger and possibly collaborative simulations it is advisable to use a lower-language simulation tool for example, SWARM, MASON and JADE. SWARM [14] has an active user group and comes in JAVA and Objective-C based platforms. Railsback et al. [13] appreciate its well organised structure but point out that it can be a challenging environment for beginners.

MASON [15] is comparable to SWARM in terms of scale and was written with specific requirements in mind. Luke et al. [15] explain that they required an environment which was able to; run on different operating systems, stop mid-run, have a separate visualization interface and be easily embedded into larger libraries.

The Java Agent Development Framework (JADE) [16] is a popular tool within research carried out in the Smart Grid domain as it is compliant with the standards set by the Foundation for Intelligent Physical Agents (FIPA). FIPA (http://www.fipa.org/) was created as the eleventh standards committee for the IEEE in 2005 and seeks to promote interoperations of agents and their services.

The decision on which platform to use for ABM or MAS

 ISBN: 978-1-61208-136-6

modelling is dependent on several factors including; programming experience of the user, complexity of the model required, portability and the need for collaborative working. For smaller models where a concept is being trialled or a quick prototype is required, NetLogo would be most suited for all types of users. If creating larger, more complex models then a low language platform like JADE might be more appropriate. As JADE has been used in various research papers and is FIPA compliant it is the most appropriate for MAS within the Smart Grid.

IV. Applications of Agents in the Smart Grid

A Smart Grid can be viewed as a system containing various agents. The actual agents used and their characteristics can vary depending on what area is being researched or analysed. The National Institute of Standards and Technology (NIST) has written a report entitled 'NIST Framework and Roadmap for Smart Grid Interoperability Standards, Release 1.0' [17] which has a useful picture depicting the actors and domains in a smart grid as shown in Fig. 2. This is an overview of domains that could exist in a smart grid and is a good starting point to understand the various stakeholders that exist in this environment.

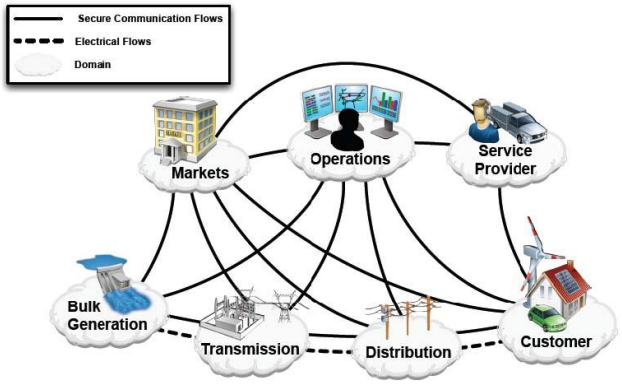

Fig. 2. NIST domains and actors for a Smart Grid [17]

Agent-based designs for Smart Grids have been implemented with Ghosn et al. [18] simulating a self-healing network using JADE. In this example, six agent types were used:

1) Device Agents
2) Distributed Energy Resource (DER) Agents
3) Consumer Agents
4) Intelligent Prevention Control Agents
5) Intelligent Response Control Agents
6) GUI Agents

These agents were chosen as the authors were primarily concerned with self-healing problems associated with an intelligent grid.

Pipattanasomporn et al. [19] discuss a simulation using four agents (listed below) as they focus on controlling a distributed grid as opposed to solely analysing fault finding/fixing:

1) Control Agent
2) DER Agent
3) User Agent
4) Database Agent

The paper focuses on the responsibilities of the control, user and database agents. As well as discussing the theory behind agent functions, they go on to develop a simulation environment to test the agent-based system. The MATLAB/Simulink environment was used to create a simulated circuit which interfaces via Transmission Control Protocol (TCP) connections to the multi-agent system. This demonstrates the capability that exists whereby novel agent-control models can be simulated in a circuit under various conditions (e.g., islanding).

Karnouskos and Holanda [20] give their appliance agents consumption profiles that are based on a survey done by the US Department of Energy. This allows simulation to be based on known consumption patterns to test validity of agent-based control systems. This type of analysis is non-trivial and pivotal to increase confidence in new control philosophies that are required for the future. As the authors state, their agent data is not sensitive enough to differentiate between demand changes through the year, which could be dependent on weather, holidays etc. Enhancements of these simulations can be used to predict possible emergent behaviours that could arise as the grid modernises.

A futuristic paper by Galus and Andersson [21] develops the idea of energy hubs [22] by specifically looking at the recharging of Plug-In Hybrid Electric Vehicles (PHEV). The problem space consists of consumers driving to a workplace and plugging their cars in for charging. Obviously without any control this would lead to a surge in power demand. The authors suggest using a customer preference value (which is unique for each consumer) to indicate how much consumers are willing to pay for electricity. The customer preference value allows the agent to establish the individuals' perceived benefit of energy and so will start to buy energy only when this is reflected in the price.

The European Union and various partners are involved in a number of field trials in different countries. Each trial has a set objective and timeline associated with it. The aim of running field trials is to develop and test capability that can be used in the Smart Grid. Results are then analysed and published by the partners. Two such trials are discussed; the SmartHouse/SmartGrid (SHSG) project and the Active Distribution networks with full integration of Demand and distributed energy Resources (ADDRESS) project.

The European Union SHSG Field Trials were held in three different countries (http://www.smarthouse-smartgrid.eu/index.php?id=43) and focused on different challenges:

1) *The Netherlands (Hoogkerk)*-This trial has twenty-five interconnected houses which together create a virtual power plant through various devices including smart meters, heat pumps, hybrid vehicles and photo-voltaics. The trial uses agent-based control software to negotiate cheaper power and maximise benefits for the consumers. A major objective of this trial is matching demand and supply from various resources on a mass-scale.

 ISBN: 978-1-61208-136-6

2) *Germany (Mannheim)*-This trial is focused on flexible electricity prices where customers can specify their requirements for device operation through a customer portal.
3) *Greece (Meltemi)*-This trial involves ten cottages in the Meltemi Camp which are predominantly used in the summer. Critical grid operations like islanding and load shedding are being trialled at this small scale.

Agent-based controllers were utilised in Hoogkerk and Meltemi to provide the microgrid with intelligence.

ADDRESS is a project that is founded by the European Commission under the 7th Framework Programme. ADDRESS (http://www.addressfp7.org) focuses on developing and validating solutions to enable active demand. The project started in June 2008 and is planned to continue for four years until 2012. It aims to develop technical solutions at the consumer and power system level to enable active demand. The first project results from 2009 focus on country-specific surveys, scenario (or use case) approaches and conceptual architecture for a smart grid [23]. The survey found the following:

1) The rise in Renewable Energy Sources (RES) is expected to increase the need for Active Demand (AD) services.
2) Energy retailers will be the key agents to deploy AD. The retail market is still linked to the distribution business but there are no significant barriers to decoupling these two functions.
3) Smart meters will be a key enabler for AD development. Individual country approaches to smart meters broadly fall into three categories; one where the regulator has defined standards, one where the private sector has been left to incentivize smart meters, and one where no decision has been made.
4) The low level voltage networks in most European countries have the ability to accommodate the ADDRESS concepts.

The first conceptual architecture to emerge from ADDRESS [23] consists of four main sections as shown in Fig. 3:

1) Aggregators
2) Energy Box - interface between aggregator and the consumer
3) Distribution System Operators
4) Markets and Contracts

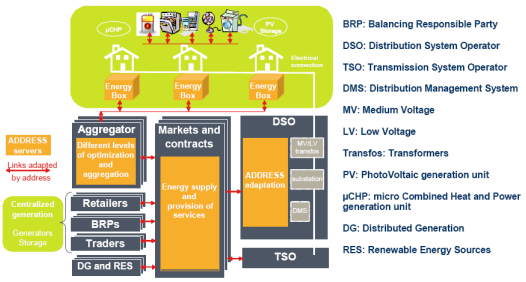

Fig. 3. ADDRESS conceptual architecture [23]

Within this architecture, the aggregators perform an important function as the negotiator between the other sections. The aggregator will collect signals from the market and power suppliers and compare it to data from consumers. Real time price signals and optimisation techniques will be used to meet consumer demand. Clearly an agent-based approach following principles as described by a number of research papers for example Dimeas and Hatziargyriou [24] and Rahman et al. [25] would be suited to this function.

These examples show a variety of agents that can be used to simulate or portray the research challenge from various perspectives. As current trials are utilising aspects of agent-based methods this should aid in increasing confidence of such systems within industry.

V. Research Areas

Agent-based methods can be used to create specific technical solutions as well as understand the interactions of various elements. The authors are currently working on two areas:

Specific Agent Based Solutions: Various Smart Grid researchers and organisations are using agents to create solutions for specific Smart Grid applications. The authors are currently developing agent methods to address demand response using dynamic pricing. Game theory will be used as the basis to achieve desired response patterns, for example; a group of households collaborating to reduce their collective peak to average ratio and hence gain a favourable tariff.

Emergent Properties of the Smart Grid: A Smart Grid can be viewed as a system of systems where each system is comprised of a diverse set of passive and active system components; belonging to various stakeholders, that interact with each other to provide a type of service or function. On the distribution side, the low voltage electricity system (from super grid side), energy management systems (e.g. home, building, factory etc), billing systems, micro generation systems and electric vehicle charging systems could be some examples of such systems. Fig. 4 shows the Smart Grid comprising of four systems; Generation, Distribution, Transmission and Consumer. The consumer system is then broken down into a further 5 constituent systems.

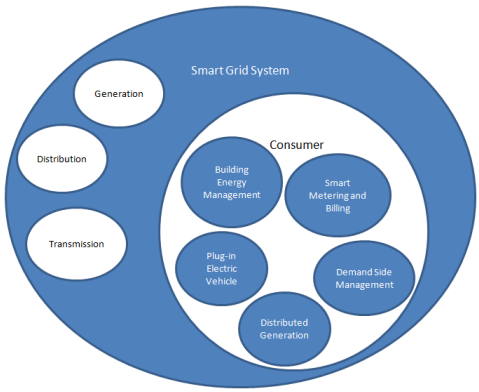

Fig. 4. A system view of the Smart Grid with the Consumer sub-system.

 ISBN: 978-1-61208-136-6

The design of such systems is an unprecedented task which presents many challenging research and engineering questions. Continuing with the idea of systems within systems, emergent properties resulting from the interaction of such components have not been investigated. The authors propose to undertake research whereby the Smart Grid is analysed from a top-down as well as socio-technical perspective with the aim of discovering emergent behaviour.

VI. Conclusion

Systems thinking helps to increase the understanding of interfaces and challenges in developing a resilient Smart Grid. Complex problems have been addressed using this framework in a variety of fields however there has been no explicit application to Smart Grids. As discussed, the use of agent-based models is suited to both analyses of the system as well as a tool to create practical solutions. Understanding the constituents of this complex system and simulating their collective presence will allow for the design of a Smart Grid with desirable emergent properties. From a commercial perspective this will also provide a rational focus on creating new products and services. Other future research work to be carried out by the authors will be to focus on using dynamic pricing as a tool for demand management. The aim is to model households and the utilities as agents with underlying game-theoretic behaviour. The results will determine the market conditions required and behaviour expectancy of households to produce effective demand management.

VII. Acknowledgments

This work is supported by the EPSRC funded IDC in Systems (EP/G037353/1) and Toshiba Research Europe Limited.

References

[1] European Commission, "A Technology Road Map for the Communication on Investing in the Development of Low Carbon Technologies (SET-Plan)," 2009.

[2] European Commission, "European Technolgy Platform: Strategic Deployment Document for Europe's Electricity Networks of the Future," 2010.

[3] H. W. J. Rittel and M. M. Webber, "Dilemmas in a general theory of planning," *Policy Sciences*, vol. 4, pp. 155–169, June 1973.

[4] J. Conklin, *Dialogue Mapping: Building Shared Understanding of Wicked Problems*, ch. 1. John Wiley & Sons, 2001.

[5] J. K. Doyle, "The cognitive psychology of systems thinking," *System Dynamics Review*, vol. 13, no. 3, pp. 253–265, 1997.

[6] K. E. Maani and V. Maharaj, "Links between systems thinking and complex decision making," *System Dynamics Review*, vol. 20, no. 1, pp. 21–48, 2004.

[7] H. S. Nwana, "Software agents : an overview," *The Knowledge Engineering Review*, vol. 11:3, pp. 205–244, 1996.

[8] J. M. E. Gabbai, H. Yin, W. A. Wright, and N. M. Allinson, "Self-Organization, Emergence and Multi-Agent Systems," in *2005 IEEE International Conference on Neural Networks and Brain*, pp. 1858–1863, 2005.

[9] C. M. Macal and M. J. North, "Tutorial on Agent-Based Modeling and Simulation," in *2005 Winter Simulation Conference* (M. E. Kuhl, N. M. Steiger, F. B. Armstrong, and J. A. Joines, eds.), (Orlando), pp. 2–15, 2005.

[10] F. H. P. Fitzek, M. D. Katz, F. Albiero, F. Fitzek, and M. Katz, *Introduction to NetLogo*, pp. 579–602. Dordrecht: Springer Netherlands, 2007.

[11] "Matlab at http://www.mathworks.co.uk/,"

[12] U. Wilensky, "Netlogo. http://ccl.northwestern.edu/netlogo/," 1999.

[13] S. F. Railsback, S. L. Lytinen, and S. K. Jackson, "Agent-based Simulation Platforms: Review and Development Recommendations," *Simulation*, vol. 82, pp. 609–623, Sept. 2006.

[14] P. Johnson and A. Lancester, "Swarm user guide: Swarm development group," 2000.

[15] S. Luke, C. Cioffi-Revilla, L. Panait, K. Sullivan, and G. Balan, "MASON: A Multiagent Simulation Environment," *Simulation*, vol. 81, pp. 517–527, July 2005.

[16] "Java agent development framework (jade) at http://jade.tilab.com/,"

[17] "NIST Framework and Roadmap for Smart Grid Interoperability Standards , Release 1.0. United States National Institute of Standards and Technology," 2010.

[18] S. B. Ghosn, P. Ranganathan, S. Salem, J. Tang, D. Loegering, and K. E, "Agent-oriented Designs for a Self Healing Smart Grid," *IEEE*, pp. 461–466, 2010.

[19] M. Pipattanasomporn, H. Feroze, and S. Rahman, "Multi-agent systems in a distributed smart grid: Design and implementation," *2009 IEEE/PES Power Systems Conference and Exposition*, pp. 1–8, Mar. 2009.

[20] S. Karnouskos and T. N. D. Holanda, "Simulation of a Smart Grid City with Software Agents," *2009 Third UKSim European Symposium on Computer Modeling and Simulation*, pp. 424–429, 2009.

[21] M. D. Galus and G. Andersson, "Demand Management of Grid Connected Plug-In Hybrid Electric Vehicles (PHEV)," in *IEEE Energy 2030*, (Atlanta), 2008.

[22] M. Geidl, G. Koeppel, P. Favre-Perrod, B. Klockl, G. Andersson, and K. Frohlich, "Energy Hubs for the Future," *IEEE Power & Energy Magazine*, no. January/February, pp. 24–30, 2007.

[23] E. Peeters, R. Belhomme, C. Batlle, F. Bouffard, S. Karkkainen, D. Six, and M. Hommelberg, "ADDRESS: scenarios and architecture for active demand development in the smart grids of the future," in *20th International Conference on Electricity Distribution*, no. 0406, (Prague), pp. 406–406, CIRED, 2009.

[24] A. Dimeas and N. Hatziargyriou, "A MAS Architecture for Microgrids Control," *Proceedings of the 13th International Conference on, Intelligent Systems Application to Power Systems*, pp. 402–406, 2005.

[25] S. Rahman, M. Pipattanasomporn, and Y. Teklu, "Intelligent Distributed Autonomous Power Systems (IDAPS)," *2007 IEEE Power Engineering Society General Meeting*, pp. 1–8, June 2007.

 ISBN: 978-1-61208-136-6

MAC Performance Evaluation in Low Voltage PLC Networks

Mehdi Korki†, Hai L. Vu*, Chuan Heng Foh‡, Xiao Lu‡, and Nasser Hosseinzadeh†
* Centre for Advanced Internet Architectures, Faculty of ICT, Swinburne Univ. of Technology
† Faculty of EIS, Swinburne Univ. of Technology, Melbourne, VIC 3122, Australia
‡ School of Computer Engineering, Nanyang Technological University, Singapore
{mkorki, hvu, nhosseinzadeh}@swin.edu.au; {aschfoh, luxi0007}@ntu.edu.sg

***Abstract*— Power line communication (PLC) system refers to the use of power distribution networks for communication purposes. In this paper, we investigate the performance of the low voltage (LV) power lines for smart grid applications involving data transfer in a specific narrow, low frequency band. We propose an analytical approach to obtain the line's transfer function and conduct simulation to determine the performance of the LV PLC system in terms of bit error rate. We then evaluate the performance of the medium access control protocol (MAC) for the LV PLC network taking into account its physical characteristic and performance limitation. We show by simulation that packet loss in this network can be significant even with a light traffic condition due to the noisy channel, and the goodput declines sharply once the individual transmission rate is high enough to congest the network. We also show that the channel errors can be reduced by adjusting the MAC parameters to allow the retransmissions recouping losses.**

Keywords-**Low voltage power line communication; medium access control protocol; performance evaluation; orthogonal frequency division multiplexing**

I. INTRODUCTION

The efficiency, safety and reliability of the electricity transmission and distribution system can be much improved by transforming the current electricity grids into an interactive (customers/operators) service network or *smart grid*. Furthermore, smart grid aims to take advantage of the existing power distribution networks to provide value-added services such as network management and control, broadband Internet access or intelligent home where devices are communicating via the electricity wires.

The electrical power system network is comprised of high voltage (HV), medium voltage (MV) and low voltage (LV) transmissions lines. The different transmission lines carry different power levels over different distances using various gauge aluminium conductors steel reinforced cables for electric distribution. The power transmission lines are known to be non-ideal for communication purpose due to noise and unpredictable impedance and attenuation, which vary with time, frequency and location. Despite that fact, power line communication (PLC) has been using in the past to send control signals within the electricity grid [1]. Recent development of more sophisticated modulation (e.g. spread spectrum or multiple carrier modulation) and stronger error correction schemes has overcome earlier obstacles and enabled PLC at speeds comparable to other wired communication mediums. Due to its pervasive nature, PLC now becomes a real contender for an alternative infrastructure in providing services that require data communication.

In particular, advanced metering infrastructure (AMI) is one of the smart grid applications that recently attracts considerable interest from both industry and the research community. It is because AMI provides consumers with the ability to use electricity more efficiently and at the same time enables utilities to monitor and repair their network in real time. Early version of AMI has already been implemented (e.g. in part of Victoria, Australia [2]) using wireless technologies to collect meter readings remotely and automatically. In this paper, we investigate the use of LV transmission line as a medium for data communication between electric meters and the substation as a data concentrator point located on different parts of the distribution network. The recommended frequency band for communication in the AMI application is a narrow, low frequency band between 9 and 490 kHz [3]. Although the choice of LV line for AMI communication is natural as it connects pole-mounted transformers to individual homes associating with the electric meter, its characteristic and network performance from the medium access control point of view are not well understood in the literature. It is because the majority of the work in this area was focusing on indoor PLC network and at the high frequency band applicable for high-speed broadband access [4]. Note that if the PLC is to be extended beyond substation transformers to the MV network, data transmission should then bypass those transformers that have a great impact on PLC in the frequency range of interest.

To this end, our contributions is twofold. We first describe in this paper an analytical model that enables us to obtain the transfer function of the LV PLC lines at the above specified frequency band for generic distribution networks (i.e., including outdoor transmission lines). Based on the obtained transfer function, we then investigate the performance of the LV PLC network as a data communication medium via simulation in terms of bit error rate (BER) versus the signal to noise ratio (SNR). Another major contribution of this paper is the evaluation of a medium access control (MAC) protocol for the LV PLC network based on our understanding of its physical characteristic and performance limitation. Both contributions are useful in designing and optimizing the PLC performance

 ISBN: 978-1-61208-136-6

under different load conditions and network configurations.

The rest of the paper is organized as follows. In Section II, we describe the low-voltage power line system and study its physical layer characteristics as well as its communication performance. In Section III, we introduce the MAC protocol for the considered LV PLC system, and conduct simulation experiments to evaluate its performance in Section IV. Finally, some important conclusions are drawn in Section V.

II. Low-voltage (LV) power line

In this section, we first outline our approach to study the characteristic of the LV power lines via its transfer function. We then study the performance of the PLC system in terms of bit error rate (BER) and their resistance to noise using the proposed transfer function and existing known noise models. Results obtained in this section are essential for the design of the medium access control (MAC) protocol of the PLC system. The proposed MAC and its performance will be discussed in later sections.

A. LV line characteristic

Data transmission over power lines suffers from various frequency-dependent reflections and attenuation caused by the cable material and network branching, and is getting worst as the length of the lines increases. There have been several techniques in the literature to model the power lines in attempt to describe the channel behaviour either in time or frequency domains.

Typical time-domain model such as a multipath propagation model is based on superposition of reflected signal on different paths within a PLC network. Model parameters of this multipath propagation approach can be calculated using a so-called echo model [1] that assumes the backward reflection from impedance discontinuity is negligible. Moreover, the model becomes intractable when there are multi branches connecting to the same joint. Alternatively, the parameters can be retrieved from measurements of the network in question, which requires little computation and is easy to implement. The latter, however, is not flexible as measurements must be carried out for every networks and configurations.

In the frequency-domain the transfer function of the PLC system is modeled as a product of simpler transfer functions from several cascading blocks constituting the network. In particular, a so-called transmission matrix or scattering matrix of the building block (e.g. two-wire transmission line block) is computed before its transfer function is determined. The transmission matrix describes the relationship between the voltage (V) and current (I), while the scattering matrix gives that of the incident and reflected waves. As a result, both incident and reflected waves will contribute in the transfer function obtained from transmission matrix. This model is scalable as the network complexity increases and can better describe the network behaviour as a function of physical parameters. The model parameters can again be obtained from the actual measurements, but can also be derived from eigen analysis of network matrices or the lumped-element circuit transmission line model [4]. In this paper, we will utilize the approach of the transmission matrix where the model parameters are determined based on the lumped-element circuit transmission line model. It is because the lumped-element circuit is accurate in the 9-490 kHz frequency range recommended for the AMI application where its length is much smaller than the circuit's operating wavelength [5].

To this end, two line parameters, i.e., the propagation constant γ and the characteristic impedance Z_0 of the lumped-element circuit model, can be given as

$$\gamma = \sqrt{(R + j\varpi L)(G + j\varpi C)}, \quad (1)$$

$$Z_0 = \sqrt{\frac{R + j\varpi L}{G + j\varpi C}}, \quad (2)$$

where ϖ is the angular frequency, R, L, C, G are resistance, inductance, shunt capacitance, and shunt conductance of a unit length (m) of the transmission line. The same method as in [4] can be used to determine R, L, C, G physical parameters.

A typical topology of the residential power lines is shown in Fig. 1, which can be considered as a composition of many suitable simpler networks (building blocks) as depicted in the same figure.

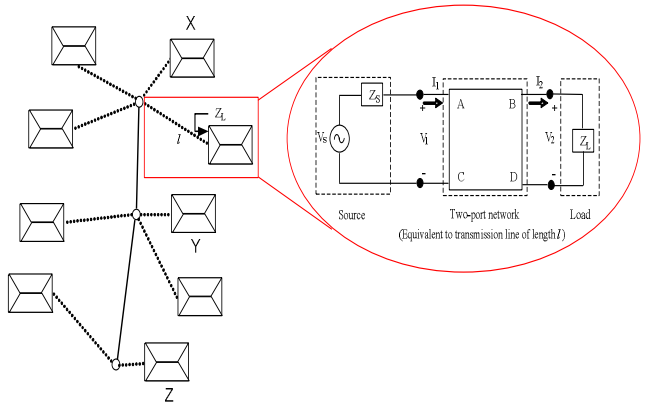

Fig. 1. Illustration of a PLC system.

In Fig. 1, the relation between the sending-end quantities (V_1 and I_1) and receiving-end quantities (V_2 and I_2) is written as

$$\begin{bmatrix} V_1 \\ I_1 \end{bmatrix} = \begin{bmatrix} A & B \\ C & D \end{bmatrix} \begin{bmatrix} V_2 \\ I_2 \end{bmatrix} = \begin{bmatrix} cosh(\gamma l) & Z_0 sinh(\gamma l) \\ \frac{1}{Z_0} sinh(\gamma l) & cosh(\gamma l) \end{bmatrix} \begin{bmatrix} V_2 \\ I_2 \end{bmatrix} \quad (3)$$

where l is the length of the transmission line. The 2×2 transmission matrix in (3) is called the ABCD matrix from which the transfer function (H) can be derived

$$H = \frac{Z_L}{AZ_L + B + CZ_L Z_S + DZ_S}, \quad (4)$$

where Z_L, Z_S are load and source impedances of the single-branch transmission line, respectively.

The overall ABCD matrix of the network shown in Fig. 1 consisting of multiple single-branch transmission lines, each

 ISBN: 978-1-61208-136-6

has different cable length and cable type and is described by the i^{th} ABCD matrix, is then given as

$$\begin{bmatrix} A & B \\ C & D \end{bmatrix} = \prod_i \begin{bmatrix} A_i & B_i \\ C_i & D_i \end{bmatrix}. \quad (5)$$

The overall transfer function is then obtained as in (4) where Z_L, Z_S are load and source impedances of the PLC network.

Based on a typical single-phase low voltage power line in Australia [2], the solid lines in Fig. 1 represent single-phase bare overhead aluminium conductor steel reinforced (ACSR) cables with the length of approximately 100 meters between two power poles. The dashed lines represent the branch copper cables with PVC insulations. The ACSR cables have a 431.2 mm^2 cross-sectional area and the copper cables have a 10 mm^2 cross-sectional area. As a result, the transfer functions of the power line channel over 9 kHz $\sim$ 490 kHz for the transmission pairs (X to Y and X to Z in Fig. 1) are depicted in Fig. 2. Here we set $Z_s = 50$ Ohm and Z_L is modeled as in [6].

It can be seen that the derived transfer functions do not have significant multipath effects as we expect in this band of frequency. The strong attenuation notches at about 124 kHz are mainly caused by the impedances of the branch loads inside the residential properties.

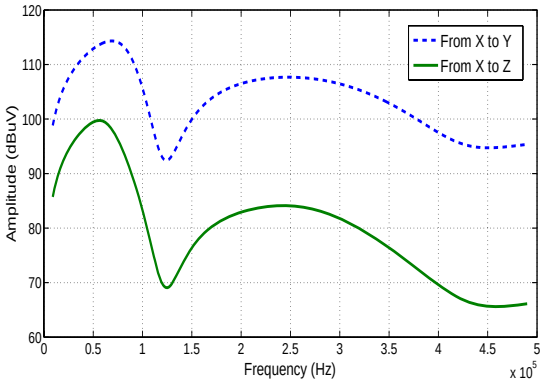

Fig. 2. Transfer function of the LV lines.

B. LV PLC System Performance

Having derived the transfer function, herein we study the performance of the single-phase LV PLC network in terms of BER using multicarrier simulation. In particular, OFDM (orthogonal frequency division multiplexing) modulation scheme is used in our simulation to investigate the BER that can be achieved via this system. Table I shows the parameters used in the simulation. To simulate a realistic PLC network, both white Gaussian noise (AWGN) and impulsive noise [7] are used in the simulation. The impulsive noise is the Middleton's class A and is characterized by the impulsive index α and the ratio Γ between the background noise power and impulsive noise power. In our simulation we chose $\alpha = 0.1$ and $\Gamma = 0.1$. The performance results are shown in Fig. 3 for both AWGN and impulsive noises, respectively.

TABLE I
PLC PHY PARAMETERS

Parameter	Value
Modulations for carriers	DQPSK
Total raw data rate	42.9 kbps
Coding scheme	1/2 rate convolutional code
Number of data subcarriers	96

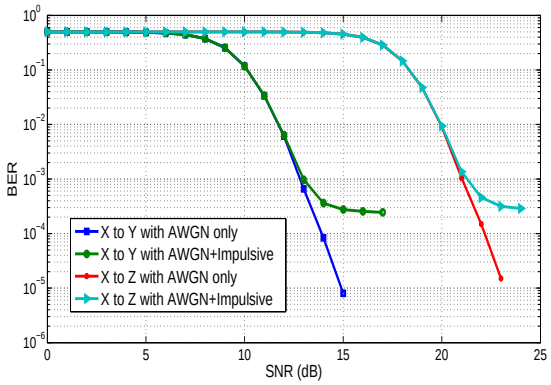

Fig. 3. BER vs. SNR for LV PLC system.

It can be seen in Fig. 3 that the BER is acceptable between point X and Y given the signal to noise ratio (SNR) is above 13 dB as recommended in [8] even in the presence of the AWGN or impulsive noises. For the SNR above the 15 dB, however, the BER is not improved when the impulsive noise is present. More importantly, at the same SNR (i.e. around 13 dB) the BER between point X and Z is very high suggesting that direct communication between them is not feasible.

III. The MAC protocol for LV PLC networks

Given the uniqueness in the physical layer of the LV PLC system, a new data link solution for reliable data exchanges in LV PLC network is necessary. There has been a number of research in the literature dealing with design of a MAC protocol for a PLC system [9]. Majority of the research work focuses on indoor PLC and the carrier sense multiple access with collision avoidance (CSMA/CA) protocol is the most popular choice for networking in the PLC environment. For example, Lee *et al.* in [11] presented an analytical work where the CSMA/CA protocol is used for an indoor PLC home network. Kim *et al.* in [10] later proposed a multihop PLC MAC protocol called Korea Standard power line MAC protocol (KS-MAC). The protocol KS-MAC standard uses the CSMA/CA protocol and considers multihop relaying operation again in an indoor PLC home network.

An outdoor PLC network has obvious differences in physical layer characteristics, and hence it warrants an investigation on the design of a MAC protocol and its performance. A popular solution has been proposed for the outdoor LV PLC environment by the PRIME Alliance Technical Working Group [12]. In this environment, the CSMA/CA protocol is

 ISBN: 978-1-61208-136-6

used in the MAC sublayer for the access of the common broadcast channel, and switching nodes are introduced to perform packet forwarding for different subnetworks.

Given the popularity of the CSMA/CA protocol for PLC networks, in this paper, we also consider use of CSMA/CA MAC protocol with layer-2 switching for our proposed LV PLC system. Similar to the common CSMA/CA channel access strategy, whenever an AMI station[1] is ready for transmissions, it first senses the medium to ensure that the channel is idle. If the channel is sensed idle for a guard period known as distributed interframe space (DIFS), then it transmits its packet. Otherwise, it performs a backoff which reschedules the transmission at a later time.

Herein the common binary exponential backoff (BEB) is adopted for our protocol design. During the backoff process, a discrete backoff counter is chosen uniformly in the range $[0, CW-1]$, where CW is called the contention window. The backoff counter is decremented by one for every fixed time period called a slot where the channel remains idle. It is frozen when a packet transmission is detected on the channel, and reactivated after the channel is sensed idle again for a guard period. The guard period is equal to a DIFS if the packet was received error-free, and equal to the extended interframe space (EIFS) if an error occurred. A station performs its transmission when its backoff counter reaches zero.

When a packet transmission is performed, the sender is expected an immediate positive acknowledgement (ACK) replied by the receiver. The sender may wait for a predefined short interframe space (SIFS) time period for the ACK to arrive. If such an ACK is received within the EIFS period, the packet is said to be transmitted successfully. Otherwise, the transmission is unsuccessful and another backoff for this packet transmission is initiated. For each packet the CW is initialized to CW_{min} and doubles after each unsuccessful transmission until it reaches CW_{max}, after which it remains constant until the packet is either successfully received or a retry limit is exceeded and the packet is dropped.

Since we have established in Sec. II that a transmission can only reach its one-hop neighbours in this network, any end-to-end transmission beyond one hop relies on intermediate stations to forward packets. We propose the use of layer-2 switching approach where any end-to-end transmission is performed within the data link layer. In particular, a station whose transmission is addressing to its intended receiver outside of its one hop range must explicitly select one of its neighbours to forward the packet. If there are two or more neighbours that can reach the intended receiver, the sender may randomly select one per packet basis. The one hop transmission for the packet sending/forwarding is performed using the CSMA/CA mechanism with BEB as described above. Given that the targeted communication network is a tree-like topology where the substation is the headend, our packet forwarding solution assumes that each station has knowledge about its neighbours.

[1]In this paper, the AMI station refers to a device consisting of a smart meter and a transceiver that enables communication between stations and with the headend substation.

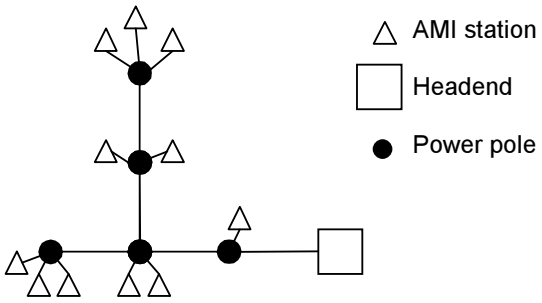

Fig. 4. The considered topology.

This information can be established during a network initialization procedure. For example, a particular broadcast-tree construction may be used for this purpose.

Specifically, in the initialization procedure, the headend first broadcasts an INIT control message to its immediate neighbours. Each neighbour station then rebroadcasts the message after a backoff. Each station also associates the source of the received INIT message as its upstream neighbour and exchange the neighbour list with them. The initialization procedure completes when the INIT messages propagate to the farthest station from the headend. To achieve convergence, neighbour lists are periodically exchanged between neighbours. As the topology change in the PLC network is infrequent, the impact of the time required for the initialization procedure on the overall performance of the operation is negligible. Finally, a similar operation is used for joining of a newly activated station by broadcasting a JOIN message.

IV. MAC Performance Evaluation and Discussion

In this section, we present simulation results of the proposed LV PLC network. For our experiments we use the ns-2 simulator [13] with appropriate modifications to the MAC module enabling the broadcast in PLC networks. Table II presents the system parameters used in the network and Fig. 4 depicts our considered topology. Each AMI station is attached to a power pole, and each power pole is 100 meters away from its neighbouring power pole. We consider a smart grid scenario where sensing data from each AMI station transmits to the headend. The sensing data may include information of the meter reading and projected power usage. The headend may also broadcast some small amount of information such as utility rates to all stations. The BER of the LV PLC channel is set to be 10^{-4} in our simulation. The parameter settings of our proposed MAC protocol are given in Table II.

In our simulation experiments, we consider that each AMI station generates a Poisson traffic with a particular arrival rate where the destination is the headend. The signals generated by each transceiver are broadcast on the common power line. However, these signals have limited traveling range. They can only reach AMI stations connected to the neighbouring power poles. Beyond this range, the signals appear as AWGN noise and cannot be detected properly as indicated in Sec II.

We first focus on the uplink transmission potential of the

 ISBN: 978-1-61208-136-6

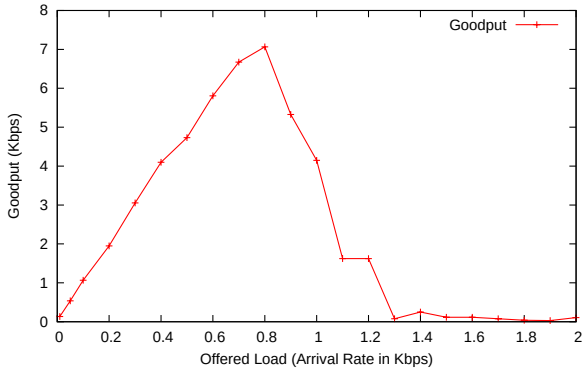

Fig. 5. Illustration of system goodput versus arrival rate.

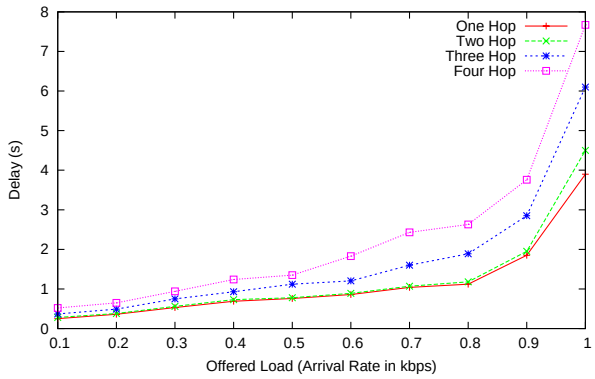

Fig. 6. Illustration of end-to-end transmission delay versus arrival rate for $CW_{min} = 32$.

system. In this setup, all stations except the headend generate a Poisson traffic stream addressing to the headend. We measure the goodput of the system, which describes the rate of useful information successfully received at the headend. We present the goodput performance of the system for a range of source arrival rates. As illustrated in Fig. 4, given a total of 11 AMI stations in the network, the total amount of generated traffic is 11 times the source arrival rates.

In Fig. 5, we present the system goodput for a range of offered load measured by the arrival rates. As observed from the results, the system offers transmission capability up to 7 kbps. This peak performance occurs when each station generates 0.8 kbps of traffic volume. With 11 stations, the total amount of traffic generated is 8.8 kbps and around 1.8 kbps of traffic suffers loss. This represents a delivery ratio of around 79.5%. These packet losses are mainly due to the noisy channel even with a retry limit of 7. When the arrival rate increases beyond 0.8 kbps, network congestion occurs where system goodput declines significantly. This is because with more traffic, transmission collisions intensify which leads to more packet losses.

We further investigate the end-to-end packet transmission delay in this setup. This measure provides critical information for the quality of service (QoS) design of the smart grid application. In Fig. 6, we depict the end-to-end packet transmission delay as a function of the arrival rate representing the load of the network. We show separately the transmission delay for different numbers of hops. As can be seen, the stations that are farther away from the headend incurs relay and thus

TABLE II
PLC MAC PARAMETERS

Parameter	Value
MAC Header size	26 bytes
Payload size	100 bytes
Slot	20μs
SIFS	10μs
DIFS	50μs
Retry Limit	7

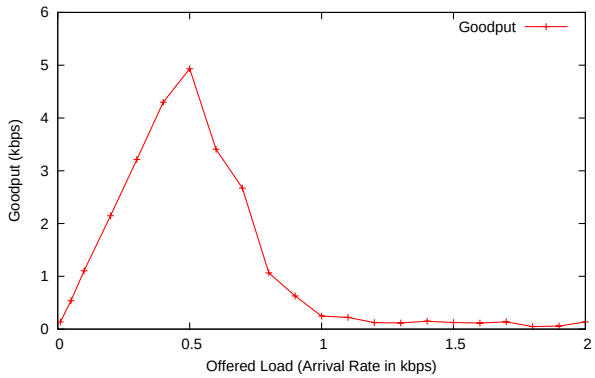

Fig. 7. Illustration of system goodput versus arrival rate with presence of downlink broadcast traffic.

the delay is higher. The transmission delay turns large at around 0.8 kbps of arrival rate indicating reaching of network congestion. Besides, due to the relatively low physical data rate and multihop transmission requirement, the end-to-end transmission delay for stations farther away from the headend exceeds 1 second, which indicates that the system may not be able to support delay sensitive applications.

In the next experiment, we include the downlink transmission and measure the uplink and downlink throughput. In this setup, the headend broadcasts a Poisson traffic stream to all AMI stations in the network. The packet arrival rate of the headend is the same as that of an individual AMI station. For the downlink broadcast traffic, it is considered successful and contributes to the goodput measure when all stations have received the packet. The system goodput results are shown in Fig. 7. We first observe the drop in the maximum goodput from just over 7 kbps to around 5 kbps for the cases without and with downlink broadcast traffic, respectively. With the presence of the downlink traffic, the network congestion appears when each AMI station generates Poisson traffic beyond 0.5 kbps. This indicates the high impact of downlink broadcast traffic.

 ISBN: 978-1-61208-136-6

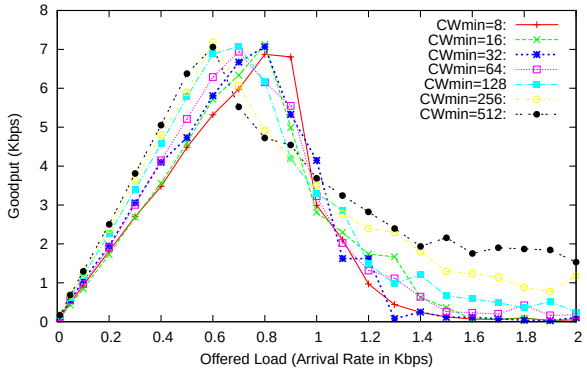

Fig. 8. Illustration of the influence of CW_{min} parameters on the system goodput.

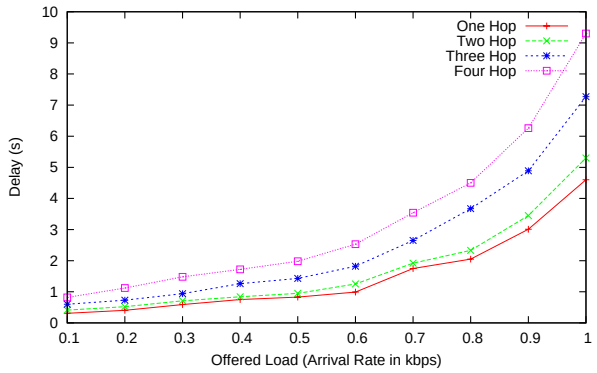

Fig. 9. Illustration of end-to-end transmission delay versus arrival rate for $CW_{min} = 512$.

In the final experiment, we study the influence of CW_{min} parameters on the system goodput. In Fig. 8, we show the system goodput performance versus arrival rate for a range of CW_{min} values while CW_{max} is maintained at 1024. As can be seen, with a larger CW_{min} value which indicates a less aggressive backoff, a lower packet loss rate is observed. This can be determined by slopes of the goodput curves in their increasing region. The extreme setting of $CW_{min} = 512$ achieves 7 kbps when the individual arrival rate is just above 0.6 kbps representing almost 100% of delivery ratio or no packet loss. Conversely, the setting of $CW_{min} = 32$ achieves 7 kbps when the individual arrival rate is 0.8 kbps representing around 79.5% of delivery ratio. However, a large setting of CW_{min} which combats packet loss effectively introduces longer retransmission delay and thus lengthens the end-to-end transmission delay. This is illustrated in Fig. 9 where the end-to-end transmission delay is longer than that reported in Fig. 6 for the setting of $CW_{min} = 32$.

V. Conclusion

In this paper, we have proposed an analytical model to obtain the transfer function of a low voltage power line and conducted simulation to determine the performance of the LV PLC system in terms of bit error rate. We found that there is no significant multipath effects in the band of frequency specified for AMI applications. This suggests that the popular multipath propagation model may not be suitable for modeling LV lines. Furthermore, we have observed that the BER is acceptable for communication between adjacent AMI stations as long as the SNR is above 13 dB, but that can not be carried out to stations that are further away in the network.

We have also designed the MAC protocol that is suitable for communication required for the smart grid applications in LV PLC networks such as AMI application. Via simulation, we have shown that packet loss in the LV PLC network can be significant even with a light traffic condition due to the noisy channel, and the goodput declines sharply once the individual transmission rate is high enough to congest the network. We have demonstrated that the channel errors can be reduced by adjusting the MAC parameters (i.e. CW_{min}) to allow the retransmissions recouping losses.

References

[1] M. Gotz, M. Rapp, and K. Dostert, “Power Line Channel Characteristics and Their Effect on Communication System Design,” *IEEE Communications Magazine*, pp.78-86, Apr. 2004.

[2] S. Bannister and P. Beckett, “Enhancing Powerline Communications in the ‘Smart Grid’ using OFDMA,” *Proc. of Australasian Universities Power Engineering Conference*, 2009.

[3] J. Bausch, T. Kistner, M. Babic, and K. Dostert, “Characteristics of Indoor Power Line Channels in the Frequency Range 50-500 kHz,” *Proc. of IEEE International Symposium on Power Line communications and Its applications*, pp. 86-91, 2006.

[4] H. Meng, S. Chen,Y.L Guan, C. L. Law, P. L. So, E. Gunawan, and T. T. Lie, “Modeling of Transfer Characteristics for the Broadband Power Line Communication Channel,” *IEEE Trans. Power Delivery*, vol. 19, no. 3, pp.1057-1064, 2004.

[5] D. M. Pozer, *Microwave Engineering*, Third Edition, New York, Wiley, 2005.

[6] G. Marubayashi, S. Tachikawa, “Spread Spectrum Transmission on Residential Power Line,” *Proc. IEEE International Symposium on Spread Spectrum Techniques and Applications*, vol.3, pp.1082-1086, 1996.

[7] N. Andreadou and F. N. Pavlidou, “Modeling the Noise on the OFDM Power-Line Communications System,” *IEEE Trans. Power Delivery*, vol. 25, no. 1, pp.150-157, Jan 2010.

[8] D. Cooper, and T. Jeans, “Narrowband, Low Data Rate Communications on the Low-Voltage Mains in the CENELEC Frequencies-Part I: Noise and Attenuation,” *IEEE Trans. Power Delivery*, vol. 17, no. 3, pp.718-723, July 2002.

[9] S. Galli and O. Logvinov, “Recent Developments in the Standardization of Power Line Communications within the IEEE,” *IEEE Communications Magazine*, vol. 46, no. 7, pp. 64-71, July 2008.

[10] M.-S. Kim, D.-M. Son, Y.-B. Ko, and Y.-H. Kim, “A simulation study of the PLC-MAC performance using network simulator-2,” *Proc. IEEE International Symposium on Power Line Communications and Its Applications*, pp. 99-104, 2008.

[11] K.-R. Lee, J.-M. Lee, W.-H. Kwon, B.-S. Ko, and Y.-M. Kim, “Performance evaluation of CSMA/CA MAC protocol in low-speed PLC environments,” *Proc. IEEE International Symposium on Power Line Communications and Its Applications*, pp. 179-184, 2003.

[12] The PoweRline Intelligent Metering Evolution (PRIME) ALLIANCE, Jan. 2011, http://www.prime-alliance.org/

[13] The network simulator ns-2, Jan. 2011, http://www.isi.edu/nsnam/ns/

 ISBN: 978-1-61208-136-6

Degrees of Freedom in Information Sharing on a Greener and Smarter Grid

Kristian Helmholt,
Department: Business Information Services
TNO
Groningen, The Netherlands
Kristian.Helmholt@tno.nl

Gerben Broenink,
Department: Security
TNO
Groningen, The Netherlands
Gerben.Broenink@tno.nl

ABSTRACT - Providing warmth, food, housing, and other necessities of life require the use of energy, which causes it to play a pivotal role in society. Changes in the production, distribution and consumption of energy (carriers) impact everyone. Next to well known (expected) changes in the area of renewable energy sources, we foresee the possibility of major changes in the way society shares information about production, distribution and consumption of energy (carriers). This is caused by the expected societal benefits of exchanging more information between parties connected on the energy grid: more efficiency though balancing of supply and demand, which in turn makes energy less scarce and avoids unnecessary 'heat pollution'. However, the sharing of information could introduce imbalances in 'societal' power between governments, companies and consumers. We argue that all parties involved should consciously decide – on a well informed basis - on what information they want to share. In this paper, we provide an overview of the degrees of freedom in information sharing on the green & smart energy grid of tomorrow.

Keywords – Smart grid; information sharing; privacy.

I. INTRODUCTION: RISE OF THE 'ENERGY INTERNET' DEMANDS INFORMATION SHARING

In the coming years, we expect a further development of the 'Energy Internet'. Classic energy grids (electricity, gas, heat, etc.) will evolve into an even larger combined world wide network which will be used by millions of parties to exchange both energy itself as well as information about the production and consumption of energy carriers (oil, gas, electricity, etc.). The Energy Internet is the next step in evolution of the classic 'Energy Grid', which today consists of electricity cables, transformers, pressurizing stations, gas pipes, etc. and is often characterized by a unidirectional flow. Electricity and gas flow from central power plants and gas production facilities, towards companies and consumer houses. The rise of decentralized production of energy carriers – for example: solar panels, windmills, biogas installations, etc. – will result in a more bidirectional flow of energy carriers. Consumers' houses and other decentralized facilities like farms will not only consume energy carriers but will sometimes also produce energy carriers to such an extent it is economically or environmentally interesting to transport the energy to other sites. In the Netherlands, for example, this is already the case in the 'green house industry'. The production of heat from gas is often combined with the simultaneous production of electricity. 'Surplus energy' from green houses is carried – using electricity - across the classic energy grid by so called 'Network Administrator' companies to other parties that have a need for this energy.

Next to the physical evolution, on top of the classic grid a new information sharing network will evolve. This network will be used to exchange information on many aspects of the (expected) production, storage, transportation and consumption of energy carriers (see [8], [9] and [11] for examples of information services and architectures). Another advanced example is the application of automated (i.e., computerized) trading agents that use real-time information to buy and sell energy according to a buy/sell strategy of their owners/parties they represent. To that, these agents could be equipped with the ability to switch energy carrier consuming equipment on or off, depending on the availability and price/costs of energy. Pricing strategies and regulations (set by governments) could influence buying and selling behaviour. This information exchange could take place on different levels: between individual houses in a residential area and factories, between groups of consumers and producers, etc. It is beyond the scope of this paper to describe the possible implementations of a more automated and dynamical market where real-time information is used to synchronize demand and supply. In this paper, we want to focus on how to categorize why, what kind of information and when it is exchanged. We have chosen to focus on exposure of behaviour and identity of parties on a Smart Grid. Also it is beyond scope to discuss the effects of local energy production and consumption on network stability.

In Section II, an overview of the related research is given. After that, our contribution and methodology is presented. In Section IV, we present the three degrees of freedom. Followed by, the consequences of the possible choices. In the end, we will present our conclusions.

II. RELATED RESEARCH

We found abundant research related to the concept of *using* information to create a greener and/or smarter energy grid. Potter [4], for example, recognizes the importance of information on the smart grid. He claims that the variation on renewable energy sources will be the largest variation on the smart grid. As a result – as we paraphrase it - better procedures are needed to forecast the weather in order to provide a better estimation the energy production from renewable energy sources. Potter focuses on the accuracy of the information on production of energy carriers from

 ISBN: 978-1-61208-136-6

renewable energy sources in order to optimize (smart) grid efficiency. Little attention is paid in this article to aspects of sharing information on energy usage between parties connected to the grid (e.g., factories, consumer households, etc.).

Another example of the usage of (extra) information for a smart grid was found in a pilot study called – 'PowerMatchingCity' [2] of the European 6th framework project INTEGRAL (Integrated ICT-platform based Distributed Control in Electricity Grids). In this pilot, the so called Powermatcher Smart Grid Technology [1] was used. It is built on a market based control concept in which each device attached to the grid produces bids on energy, and a central market where the offers and bids are matched to each other. Information between parties is exchanged as 'prices' and 'bids'. Suppliers offer 'energy' together with prices, while consumers bid on those offers. Through an auctioning mechanism the 'PowerMatching' system as a whole tries to find a market equilibrium where net balance is optimized [3]. A conceptually related example is Intelligent Metering/Trading/Billing System (ITMBS) as described in [10]

III. OUR CONTRIBUTION & METHODOLOGY

While we found an abundant research relating to the topic of using the information, research on the *type* of information and *reasons* or *objections* to share information on energy usage seems scarce [12]. We did find several projects and studies which developed their own information sharing model and we found it hard to compare the different models. Such a comparison is needed when a decision has to be made about an information sharing model; which has been the case in the Netherlands for example, where amongst others stakeholders politicians have been discussing the introduction of the Smart Meter. In that discussion questions arose like:

- What information should be shared?
- How much detail should be provided?
- Who can access the information?
- What is the impact of (not) sharing all information?

Our contribution is a structured model to compare information sharing on different (partial) Smart Grid designs and implementations, with a strong focus on the level of transparency (of behavior and identity) between parties on the Smart Grid. As a result, comparison should be less hard and more effective. This enables decision makers to come up with a substantiated choice more efficiently. We have named the proposed model 'Degrees Of Freedom in Information Sharing' (DOFIS) for Smart Grids (4SG), resulting in the DOFIS-4SG acronym.

The basic structure of the model is a set of axes, because we wanted to be able to carry out a comparison, between Smart Grid designs, in terms of different aspects. Each axis is a 'degree of freedom' and represents an aspect of information sharing with respect to *exposing* behavior or the identity of the owner or 'generator' of the information. This means not all aspects of information sharing are included. For example aspects like the size and structure of information are not included, since these aspects hardly reveal any information about the behavior of a party on the energy grid at all. The aspects of information sharing we did include are related to revealing behavior and identity. The basis for the included aspects was found in literature on Smart Grids and we tried to distill the greatest common denominators and make additions where they were necessary in order to provide for making comparisons. The process of distilling common denominators and making additions was supported by our experience with both information architectures for Smart Grids on which we are currently working and on our experience with information architectures in other domains where large scale information sharing takes place (telecommunications, healthcare, road pricing). This means that we did not mathematically derive these aspects, but carried out a selection process based on the criteria 1) 'relevant to exposing behavior and identity' and 2) the axes being 'orthogonal'. This means that the location on one axis cannot be derived from a combination of locations on the other axes. Compare this to a classic *x,y,z* 3D grid for describing the location of points in a 3D space: the *z* part of a coordinate cannot be deduced from the *x* and *y* part.

The process of distillation and selection above has resulted in what we call a 'space of comparison' which *currently* has three axes. Currently, we *suspect* that these axes and their subdivisions can be used to assess and compare all aspects of information sharing with respect to exposure of behavior and identity of parties on a Smart Grid. Providing proof for this should included in further research.

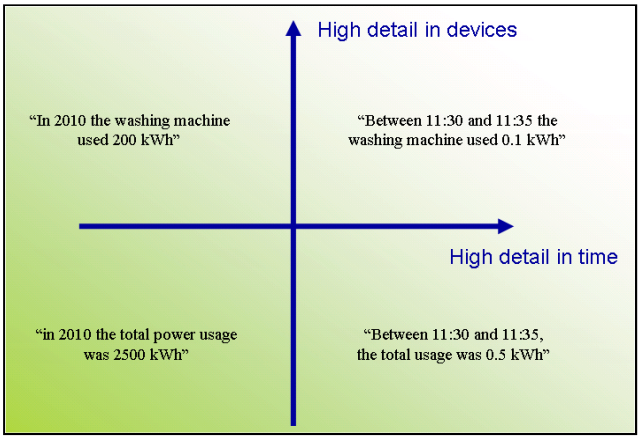

Figure 1. Different levels of detail in energy consumption information

Note that in this version of our model we use a simple view on energy systems/markets, where consumers are sharing information with each other, and with the producers of energy carriers. Business roles like retailers and distributors which are present in several market models are not mentioned explicitly. However, the sharing of

 ISBN: 978-1-61208-136-6

information between business roles like retailers and distributors can also be positioned using the DOFIS-4G model. Instead of consuming energy carriers directly, they consume energy carriers indirectly by reselling or distributing it to their customers.

IV. DEGREES OF FREEDOM

In this section we present the axes of our DOFIS-4SG model. All axes together constitute the model. In the next Section we will use this model to identify possible shifts in power (by information) between parties connected to (smart) energy grids.

A. *Level of Detail (LoD)*

The first axis we present is about the Level of Detail (LoD) of information. The LoD strongly influences what kind of market-models and types of energy matching & distribution are possible. For example, when a consumer shares its total usage of energy once a year, the receiving party can use this for constructing a yearly bill. However, when information is shared on an hourly basis, it becomes possible for the receiver to bill by the hour, and thus, it influences the consumption of energy by financial incentives. We identify two different types of LoD:

- **Devices.** To which extent is information shared about the energy usage of separate devices? For example, in the Netherlands in most houses only the total accumulated usage of electricity by all devices 'behind' the electricity meter is shared with the power supply company. However, information could also be shared on what device consume(s/d) the electricity. The energy supplier could use this information to understand which devices make up for what amount of the total power usage at a house.

- **Time.** To which extent is information shared about the energy usage over time. For example, instead of sharing information about the electricity use of once a year, it is also possible to share information more or less often.

In Figure 1, an overview is given of the two LoD types and how they congregate. Both axes represent one of the detail levels, and together they span a field of possible choices.

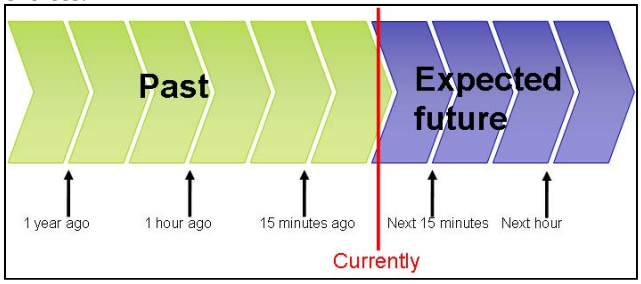

Figure 2. Information about the past, current and future

B. *Direction in Time (DiT)*

Next to the LoD, we consider the direction in time as another degree of freedom with respect to information sharing. There are three different points in time to share information:

- **Past.** Information on the usage of energy that has taken place in the past. Two examples about energy usage (e.g., power consumption) in the past that are often shared. The used amount of energy in a certain period (e.g., kWh) and the consumed amount of energy on a certain moment (e.g., Watt). In the current situation on the energy grid in the Netherlands, many consumers share their total power consumption in the past with their energy supplier once a year.

- **Current.** Information on the current speed at which energy is flowing. An example is the current power consumption (Watt). Note that it is theoretically impossible to share information about the absolute current use instantaneously.

- **Future.** Information on the estimated usage of energy that will take place in the future.

In Figure 2, a timeline is presented that shows the three points/periods in time.

C. *Recipients*

The third degree of freedom is about the amount and type of recipients of information on energy usage. For example, there is a huge difference between sending information to only one trusted party or to a group of parties which might send this information to even other parties.

In generally, the more recipients, the more the privacy of the consumer is violated. However, not only the amount of recipients is important, the type of recipient is important to. For example, there is a difference between sending information the energy supplier, or sending information to a neighbor.

V. CHOICES HAVE CONSEQUENCES

Now, as we have presented a model with (three) degrees of freedom, we can compare market models and energy systems with *respect to consequences*. In this Section, we will provide the reader with several examples in different areas that show the consequences of making different choices in information sharing. In other words: a different position in the DOFIS-4SG set of axes means different consequences. For example, certain services and market models preclude certain levels of privacy. We have identified four categories of consequences and we will use those to present the examples in a structured way. As an illustration of the consequences, we introduce two possible future energy systems/markets in which electrical energy will be exchanged/sold. Both energy systems are extreme, and it is not likely that only one of them will be put into practice. We

 ISBN: 978-1-61208-136-6

expect something in the middle. However, their location at opposite sides of the spectrum is useful to illustrate the consequences of information sharing decisions. The examples will show that choices (i.e., restrictions) on information sharing can enable or disable certain energy systems and markets. The two 'opposites' are:

- **"Massif Central".** In this scenario, governments and electricity supplying companies will invest their money in extra centralized energy production capacity. As a result the current energy grid will need to be scaled up, to be able to handle the peak loads in areas where electrification is increasing (in some areas of the Netherlands heating by gas is changing to heating by electricity using heat pumps). Thus, in the Massif Central scenario there seems to be little need for producers and consumers of energy carriers to share information. There is a relatively small need for 'real-time' control/coordination systems to manage the transport of energy (carriers), since there is relatively little to coordinate due to centralized power plants. This requires less agreement between parties on the Energy Internet. Thus far less information sharing is needed. Within the model it can be positioned as having A) a low Level of Detail with respect to time and devices, B) little to zero need for sharing information about the current and future and C) very few recipients (only electricity supplier) needed.

- **"Distributed Load".** This scenario is the opposite of the "Massif Central" scenario. Money is invested in a smart grid which will match production and consumption for efficiency and also to decrease peak loads on the network. Electricity from renewable sources (solar, wind) with a dynamical and relatively unpredictable behavior is allowed on a massive scale on the grid. To match production and consumption, there is functionality embedded in the Smart Grid to automatically switch devices like washing machines on and off, based on offerings of energy. As a result there is a greater need for producers and consumers of energy carriers to share information. Many different parties have to agree upon the amount of energy (carriers) that they will use at a certain time. Depending on the exact type of implementation, information about (household) appliances like washing machines might even be shared. Within the model this energy system/market can be positioned as having A) a high Level of Detail with respect to time and devices, B) need for sharing information about the current and future and C) a relatively larger group of recipients needed.

Note that the two example energy systems/markets are very roughly positioned. This is due to the fact that the two examples are roughly described because of reasons of space. The main purpose of these examples is to show that the model allows for comparison. Also note that we have not described all parties involved in detail.

With these two differently positioned example energy markets/systems in mind, we can provide the different categories.

A. Consequences for production, distribution and net-balance

The expected energy usage and production information is needed by intelligent distributed control algorithms to increase both efficiency and net-balance (e.g., see [13]). The overview in Table I shows that the choices with respect to the type and amount of information which is shared have consequences for the ability to arrive at one of the two energy systems described above. For example, without sharing any information on expected consumption, it is very difficult to arrive at a stable balance in a heavily distributed load situation with a significant amount of intermittent (renewable) energy sources.

TABLE I.
SHARING OF INFORMATION IN DIFFERENT SCENARIO'S

	"Massif Central"	**"Distributed Load"**
Level of detail of consuming devices	Information sharing is not necessary	Information sharing per device, in order to switch devices on/off, in order to balance the grid.
Level of detail in time	Information sharing is not necessary	High level of detail required, in order to switch devices on/off in real time.
Direction in time	Information sharing is not necessary	Information about the expected future needed, in order to optimize decisions about which device should be switched on/off
Recipients	Information sharing is not necessary	Information needs to be shared with several parties. Which ones, depends on where the intelligence is located within the Energy Internet.

B. Consequences for financial settlement

Financial settlement between consumers and producers of energy carriers requires information from a trustworthy source on the amount, date, time, etc. of energy (carriers) used, depending on the financial agreements between consumer and producer. For example, in the Netherlands, it is customary that consumers share information on their total energy carrier consumption (electricity and gas) each year with their power supplier. Since this is an accumulation – i.e., total kilowatt-hours of electricity and total cubic meters of gas – little can be deducted on the actual pattern of use of the consumer. Charging a customer for actual use at a daily

 ISBN: 978-1-61208-136-6

or monthly basis is not possible, due to the yearly accumulated exchange of information. Also, billing by the hour is not possible. If the producer would like to offer 'hourly prices', this means that there should be a log 'per hour'.

In one of our research projects at TNO, we are studying the necessity and effect of stimulating flexibility in energy usage by using financial incentives. For example, consumers could (indirectly) offer 'flextime' to producers. The idea here is that household appliances like washing machines are switched on if it is beneficial for the greener/smarter grid as a whole to do so. A consumer provides a 'flex offer' to the grid (how is beyond of the scope of this article) where it states that somewhere in next hours the washing machine should be turned on. The longer this period in time (i.e., the more flexibility), the higher the financial compensation the consumer gets, because the consumer is helping the greener/smarter grid to achieve its efficiency goals. This is only possible if the consumer is willing to share information with its energy supplier on when he/she expects or wants to use a certain amount of power. Note that it is also possible to share less detailed information with an energy supplier, by first accumulating that information in a group (e.g., a neighbourhood) and share the accumulated information. In this way, the producer has no information about the consumption of each separate home, but only the aggregate information of the entire neighbourhood. However, the financial compensation should probably go to this group. And within this group, the compensation should be divided again.

We do not elaborate on different financial compensation schemes in this article, neither do we elaborate on other possible incentives (e.g., see [7]): our point is that in order to provide a possible incentive, some degree of information sharing is required. We provide two example goals of a greener/smarter grid that might be achieved by using financial incentives. Those two examples are given in Table II. Note that these are 'imaginary' examples. Current legislation determines whether this is possible in today's energy market. Also note that the two example goals and incentives might also be used to improve network management (see next category of consequences), because their possible influence on the consumption of energy might result in less unwanted peaks for examples.

TABLE II.

CONSEQUENCES FOR BILLING

Goal	Required information level
Decrease total volume in a year	Relatively less detailed information is needed. Can be deduced from a meter with a 'running total', which is 'read' by a computer or humans once a year. No intermediate measurements are needed.
Decrease used volume in a certain period during a day	Relatively more detailed information might be needed. If periods are fixed (i.e., day and night) and energy prices remain the same during that period of the day for a year, then a meter with a 'running total' per period can be used; which are read at the end of each year. The more separate periods in a day, the more meters. If energy prices differ on a day to day basis, the meter should be read every day. If periods are not fixed, a meter with a running total per period does no longer suffice. Instead, the meter should be read at the beginning and the end of a period, and this information should be shared with the energy supplier.

Note that it is not (always) necessary to send measurement information to the transport or energy provider in order to provide the consumer with a bill. When information for 'pricing' is available 'on site' (i.e., next to the measurement device) the total amount of money to be paid in a certain period, could be calculated on site (in a special intelligent device next to the meter) at the consumer site. This requires that information on (actual) prices for energy (carriers) in a certain period needs to be sent to this device. Connectivity with energy transporting and measurement parties are needed. Note that in order for the total amount of money to be trusted by all parties, there are demands to the device carrying out the measurement and pricing, since the ability to change 'measurement data' or 'pricing information' on site within the device would enables the consumer to commit fraud. Vice versa, the consumer might not trust the provider/transporter of energy carriers if it cannot see measurement and pricing information. Measurement and pricing should therefore probably take place in a 'sealed environment' [6].

C. Consequences for network-management

Many different parties will connect to the Energy Internet of the future. This will be parties like: houses, factories, farms and hospitals. They use the energy infrastructure to receive energy carriers like electricity and gas. Also, in the future, they will send energy carriers. For example, houses with solar panels might produce electric power and farms might deliver biogas, just like green house companies with industrial strength Combined Heat & Power (CHP) equipment supply electric power. The classic asymmetry in power flow will disappear and more symmetry will evolve. Traditional models of the use of networks for energy carriers do no longer suffice. This impedes network management organizations in carrying out network capacity planning, maintenance, etc. In order to retain insight into the workings of the energy carrier transportation networks (as well as providing net balance, information about the (estimated) flow of energy carriers is needed. Currently, we suspect that more sharing of information between network management related parties on the grid is needed, but we cannot state yet which positions in the DOFIS-4SG preclude proper network management (in general) on a Smart Grid. The According to us, this is still a research topic.

 ISBN: 978-1-61208-136-6

D. Consequences for privacy and balance of power

Sharing information about energy (carrier) usage means sharing information about the behavior of (a collective of) machines (in houses/factories) and indirectly sharing information about company information (e.g., amount of products produced) or personal behavior. For example: a graph that shows the accumulated electrical power and/or gas consumption of a house through time – every minute - provides insight into activities of the residents; the presence of people is reflected in the usage of energy: with some basic knowledge of energy consumption patterns it is often possible to deduce the use of washing machines, televisions, etc. from such a graph [5]. If even more detailed information is shared – like a graph per household appliances– then very little knowledge is needed to deduce information about a person's life from his energy carrier consumption. For example, how early does a person get out of bed, when does he/she go to work, how often does he/she use the washing machine, etc. In short: sharing of information is a potential violation of privacy. In Table III, we show how the degrees of freedom are related to privacy.

TABLE III.
IMPACT ON PRIVACY

Degree of Freedom	Impact on privacy
More Level of Detail	An increase in the breakdown of accumulated information into detailed information (e.g., at the appliance level), means less privacy with respect to the consumer of energy carriers.
Direction in time	Information about the future provides insight into predicted or expected consumption of energy carriers and removes the ability for consuming parties to keep their future energy consumption private. The same applies to information about the current and the past. There is a potential privacy violation.
More Recipients	An increase in the amount of recipients means less privacy. Note that the type of recipients also matters. We expect that most consumers will not object to their energy provider receiving information, while most consumers will object to sending it to their next-door neighbors.

Closely related to the concept of privacy is the concept of the 'balance of power by information'. In general this concept is about the ability to exercise (a certain amount of) power by the recipient of energy usage information on the sender. For example, if information about predicted energy consumption somehow becomes available to criminals, they could decide to 'visit' a certain house when predicted energy consumption is at a minimum, since this is an indication of the inhabitants of the house be absent. Also, government agencies could decide to use that information for tracking down people involved in social security fraud. The amount of electricity used at a location provides information on whether or not – or how many - people actually inhabit a residence. This shifts the balance of power in the direction of the state and away from its citizens. Another example is the public availability of power consumption of factories: market analysts could use this information for estimates on production numbers. A final example is where (commercial) parties target certain consumers for new washing machine offers based on their power use signature.

In short: sharing information potentially shifts the balance of power by information. By sharing information with another party, that party is empowered in some way. More information could lead to more power (by information) and more power could mean the ability to collect even more information.

VI. CONCLUSIONS

In this paper, we have shown that the evolution of classic energy grids towards the future Energy Internet will have impact on information sharing between parties connected to the grids. In order to meet the growing demands for more sustainability (i.e., a greener grid) and more efficiency (i.e., a smarter grid) there is a need for change in information sharing. To evolve towards a greener grid, there seems to be a need for the increased use of decentralized intermittent energy sources (wind, waves, solar, etc.). This in turn seems to require more coordination between producing and consuming parties on the grid, just as is needed for a smarter grid. More coordination requires sharing more information, which in turn will have impact on privacy and balance of power. Also, the use of financial incentives to stimulate certain behavior with respect to energy carrier production and consumption (e.g., time and volume), will also require more information to be shared on the actual production and consumption patterns. Deciding upfront not to share this information because of privacy reasons means disabling several ways to evolve to a greener and smarter grid. This leads us to our final conclusion that for the evolution to a greener and smarter Energy Internet to take place it is important to put information sharing mechanisms into place, that stimulate sharing, provide as much privacy protection as possible and finally enable society to consciously decide on when and with whom information is shared. There should be a package of measures be put into place to impede an *automatic* ongoing concentration of power (by information). Especially because after a society has decided to share information at a certain Level of Detail, with a certain direction in time and with a certain number of recipients, we expect it will be difficult to turn back the clock. For example: government agencies that are used to having energy usage information at their disposal, will probably object to that stream of information being stopped, since this would mean a reduction of their abilities to carry out public tasks in the area of inspection and fraud detection. In other words: we think removing privacy is easier than reinstating it.

The DOFIS-4SG model we have presented enables policy and decision makers to compare different designs of energy systems and markets with respect to aspects of

 ISBN: 978-1-61208-136-6

exposing behavior and identity of parties Smart Grids. The comparison is not only with respect to aspects like 'level of detail' itself, but also with respect to the consequences of sharing information. We suspect that the model can be refined and extended and invite other researchers to do so. Currently, we are carrying out research on that refinement and in 2011 and beyond we hope to provide our research results.

ACKNOWLEDGMENT

We thank our fellow researchers at TNO for providing an environment where the issues in this paper could be discussed. Their active participation in Dutch and European research projects on Smart Grids provided us with a way to test out our ideas. We also thank those researchers who took the effort to describe what information is exchanged between parties in their energy-market model. This again enabled us to test out our ideas with respect to current research.

REFERENCES

[1] http://www.powermatcher.net/, last visit 15 march 2011.

[2] http://www.powermatchingcity.nl/, last visit 15 march 2011.

[3] K. Kok, Z. Derzsi, M. Hommelberg, C. Warmer, R. Kamphuis, and H. Akkermans, "Agent-Based Electricity Balancing with Distributed Energy Resources, A Multiperspective Case Study," *Hawaii International Conference on System Sciences, Proceedings of the 41st Annual* , pp. 173, 7-10 Jan. 2008

[4] C.W. Potter, A. Archambault, and K. Westrick, "Building a smarter smart grid through better renewable energy information", *200 IEEEPES Power Systems Conference and Exposition*, pp. 1-5, 2009

[5] C. Efthymiou, and G. Kalogridis, "Smart Grid Privacy via Anonymization of Smart Metering Data," *Smart Grid Communications (SmartGridComm), 2010 First IEEE International Conference on* , pp. 238-243, 4-6 Oct. 2010

[6] P. McDaniel, and S. McLaughlin, "Security and Privacy Challenges in the Smart Grid," *Security & Privacy, IEEE* , vol. 7, no..3, pp. 75-77, May-June 2009

[7] S. Caron, and G. Kesidis, "Incentive-Based Energy Consumption Scheduling Algorithms for the Smart Grid," Smart Grid Communications (SmartGridComm), *2010 First IEEE International Conference on* ,pp. 391-396, 4-6 Oct. 2010

[8] R.L. King, "Information services for smart grids," Power and Energy Society General Meeting - *Conversion and Delivery of Electrical Energy in the 21st Century, 2008 IEEE*, pp. 1-5, 20-24 July 2008

[9] M. McGranaghan, D. Von Dollen, P. Myrda, and E. Gunther, "Utility experience with developing a smart grid roadmap," Power and Energy Society General Meeting - *Conversion and Delivery of Electrical Energy in the 21st Century, 2008 IEEE* , pp. 1-5, 20-24 July 2008

[10] P. Wang, J.Y. Huang, Y. Ding, P. Loh, and L. Goel, "Demand Side Load Management of Smart Grids using intelligent trading/Metering/ Billing System," *Power and Energy Society General Meeting, 2010 IEEE* , pp. 1-6, 25-29 July 2010

[11] K. Young-Jin, M. Thottan, V. Kolesnikov, and L. Wonsuck, "A secure decentralized data-centric information infrastructure for smart grid," *Communications Magazine, IEEE* , vol. 48, no. 11, pp. 58-65, November 2010

[12] S. Rohjans, M. Uslar, R. Bleiker, J. González, M. Specht, T. Suding, and T. Weidelt, "Survey of Smart Grid Standardization Studies and Recommendations," *Smart Grid Communications (SmartGridComm), 2010 First IEEE International Conference on*, pp. 583-588, 4-6 Oct. 2010

[13] R.R. Negenborn, B. De Schutter, and H. Hellendoorn, "Multi-Agent Model Predictive Control of Transportation Networks," *Networking, Sensing and Control, 2006. ICNSC '06. Proceedings of the 2006 IEEE International Conference on*, pp. 296-301

 ISBN: 978-1-61208-136-6

Frequency response from electric vehicales

Jianzhing Wu, Janaka Ekanayake, Kamalanath Samarakoon
Institute of Energy
Cardiff School of Engineering
Cardiff, UK
e-mail:WuJ5@cf.ac.uk, EkanayakeJ@cf.ac.uk, kamalanath@ieee.org

Abstract—**The contribution of plug-in Electric Vehicles (EV) for frequency response was investigated. 24-hour EV load profiles obtained from a probabilistic approach was used. Three time dependent charging modes were considered. A single bus model of Great Britten power system was used for simulations. Simulations were carried out for a day with low demand. The simulation results shows that shedding EVs that are charging can reduce the frequency excursion significantly.**

Keywords - Frequency response, Electrical vehicles, Smart meter, Virtual power plant, Power system inertia

I. INTRODUCTION

A number of countries have taken specific policy initiatives to encourage renewable power generation and for introducing electric vehicles as they contribute to decarbonise their electrical energy and transport sectors. For example, in the UK, 15% of all energy is to be supplied by renewable energy by 2020. This translates into 30 - 40% of electrical energy being generated from renewable sources. It is anticipated that a large proportion of this power will come from wind power. Perhaps up to 40 GW of wind turbine generation on a Great Britain (GB) system with a total of around 100 GW of generating plant. The UK government also has plans to cut emissions from domestic transport by 14% on 2008 levels by 2020.

The uncertainty brought by variability of renewable energy generation will introduce a number of concerns over operation of the power system. A very high penetration of renewable energy sources demands considerable increase in frequency response and reserve that the system operator should maintain to ensure frequency performance within the control limits [1][2].

In this paper, the flexibility offered by plug-in electric vehicles (EV) by removing their charging load immediately after a frequency event is investigated. It is anticipated that this will enable operation of the future power system with current level of reserve margins.

The paper is organized as follows: initially the frequency control in the GB system is discussed; secondly integrating EVs for frequency studies is discussed; then modeling of the GB system with EV for frequency studies are discussed and finally results are presented.

II. FREQUENCY CONTROL IN THE GB SYSTEM

Frequency is determined and controlled by balancing system demand and total generation. The nominal frequency of the GB system is 50Hz. If the demand is greater than the generation, the frequency falls below 50Hz. Conversely, if the generation is greater than the demand, the frequency rises above 50Hz. In practice, the frequency varies around 50Hz by a small amount as the system demand continuously changes. When there is a significant power imbalance of the system, the frequency will show a large deviation.

The Electricity Supply Regulations require the system frequency to be maintained at 50Hz ±1% [1]. The Transmission License places an obligation on the National Grid Company (NGC) to plan and operate the system to ensure compliance with the Electricity Supply Regulations [2]. To meet these obligations the system is designed to accept the largest credible loss of 1320MW of generation (two of the largest generators, 2×660MW, on the system) and is operated to the following frequency containment policies:

- System frequency under normal operating conditions will be maintained within the operational limits of 50±0.2 Hz (NGC's current practice),
- For a sudden loss of generation or demand up to 300MW, the maximum frequency change will be limited to ±0.2Hz,
- For a sudden loss of generation or demand greater than 300MW and less than or equal to 1000MW, the maximum frequency change will be limited to ±0.5Hz,
- For a sudden loss of generation greater than 1000MW and less than or equal to 1320MW, the frequency change will be limited to –0.8Hz with frequency restored to 49.5Hz within 1 minute.

Any loss of generation greater than 1320MW will be treated as an emergency condition as it may cause the system frequency to fall below 49Hz. Automatic low frequency load shedding arrangements usually commence at 48.8Hz. In the event that the frequency is above 52Hz or below 47Hz, the independent protective actions are permitted to protect generators against danger to plant and/or for personnel safety.

A typical frequency transient for a generation loss of 1320MW is shown in Figure 1 [3][4].

 ISBN: 978-1-61208-136-6

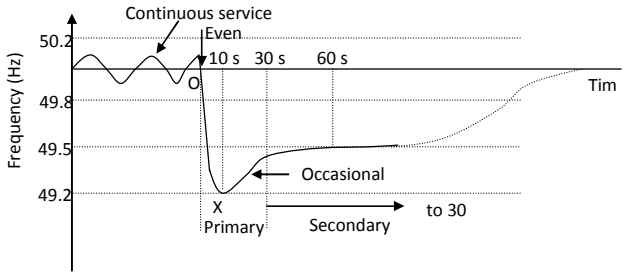

Figure 1. Typical frequency deviation following a loss of 1320MW generation [3]

Even though EVs are considered as an ideal choice for providing primary and secondary response, they have a negative effect during phase OX (see Figure 1). As modern wind turbine generators and EVs are connected to the grid through a power electronic interface, they will not contribute to the system inertia. This reduction in the overall system inertia and the increase of demand will lead to rapid change in frequency during phase OX.

III. INTEGRATING EVS FOR FREQUENCY SERVICES

An EV could participate in low frequency response services mainly in two ways. Easiest approach would be to switch off all EVs that are charging. This will introduce a proportional reduction in load, thus reducing the frequency excursion. In an event of a high frequency event all the plug-in EVs that are in stand-by mode with the state of charge of battery is less than 100% could be charged thus adding an additional load to the grid. EVs could also support the grid by acting as an energy store. For example during a low frequency event, EVs could discharge its stored energy thus acting as a distributed energy source. This paper concentrates on former aspect that is disconnecting a charging fleet of EVs during a frequency event.

The way EVs could participate for frequency services depends on the grid operator. For example, in the UK the frequency response services such as *Firm Frequency Response* (FFR) and *Frequency Control Demand Management* (FCDM) allow demand side participation in primary frequency control. The large-scale consumers are contracted in advance to switch OFF their loads (more than 10 MW and 3 MW in FFR and FCDM respectively) during a frequency excursion. In FFR and FCDM schemes, the contracted consumer should reduce load within 30 sec and 2 sec and maintain 10min and 30 min respectively.

A. *Individual EV on a frequency-responsive switch*

The demand side support for frequency reserve by controlling loads was proposed as early as in 1980 [5]. The paper proposed a frequency-responsive switch which controls significant energy consuming industrial or domestic loads. A similar switch could be utilized at each EV to switch them off when a frequency excursion occurs.

Recently, Smart Meter (SM) has drawn wide attention as a device which can help to save energy and to improve the efficiency of a power system. A number of initiatives that deploy smart meters are reported in [6]. The SM has a two-way communication between the supplier and also with domestic appliances including EVs connected to home area network (HAN). On the receipt of a signal from suppliers, the SMs could send signals to the control units to shed the EV immediately.

B. *EV as a virtual power plant (VPP)*

Several studies have identified the potential of EVs to participate in the electricity markets [7][8]. As power capabilities of an individual EV is rather small, their participation in the electricity markets will require a new entity: the EV Supplier/Aggregator (EVS/A). The EVS/A will serve as an intermediary between a large number of EVs and market players and/or system operators [9]. The role of the EVS/A is to cluster geographically dispersed EVs, and manage their generation and demand portfolios as a single entity.

The Virtual Power Plant (VPP) concept is an aggregation model which aims to overcome the challenges of Distributed Energy Resources' (DER) integration and enable their market participation. The VPP concept is considered as an ideal candidate for EVS/A. Figure 2 shows how the VPP interacts with the system operators (DSO and TSO). Upon recognizing a frequency excursion, the system operator could instruct the VPP to shed some or all of the charging EVs.

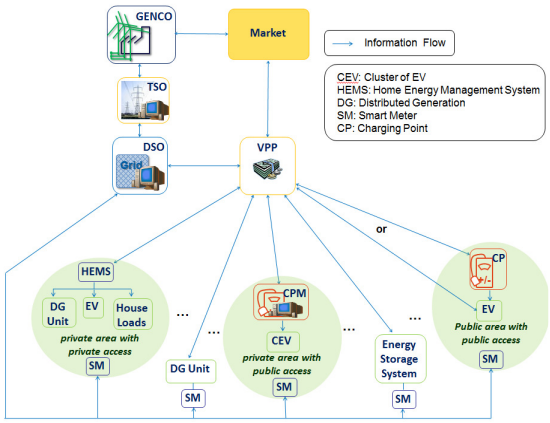

Figure 2. Integration between the VPP and grid operators [10]

IV. MODELLING OF POWER SYSTEM AND EVS FOR FREQUENCY STUDIES

A. *Power system representation*

Assuming a coherent response of all generators in the system to changes in the load, the power system can be represented by an equivalent generator [11]. The equivalent generator has an inertia constant H_{eq} and calculated using the following equation:

$$H_{eq} = \sum_{i=coal,gas,.....} H_i * \frac{S_i}{S_{sys}} \quad (1)$$

where H_i and S_i are the inertia constant and MVA rating of the individual power plant.

A simple model representing the inertia and damping of the GB system without the contribution due to governor action of synchronous generation is shown in Figure 3. In the model ΔPm refers to change in mechanical power of all the generators on the GB system and ΔPL is any change in total load. The damping providing by rotating loads is lumped into a single damping constant *D*.

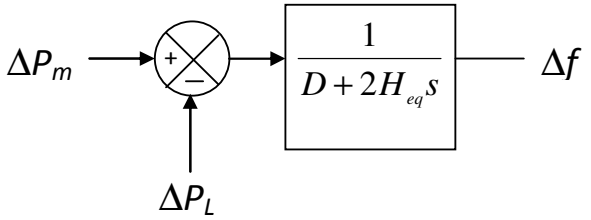

Figure 3. The system equivalent for frequency control analysis

B. *Turbine-governor model*

The composite power/frequency characteristic of the power system depends on the combined effect of the droops (R_1, R_2, ---, R_n) of all generator speed governors. It also depends on the frequency characteristics of all the loads in the system. For a system with the n generators and a composite load-damping constant of D, the steady-state frequency deviation Δf_{ss} following a load change ΔP_L is given by equation (2).

$$\Delta f_{ss} = \frac{-\Delta P_L}{(1/R_1 + 1/R_2 + \cdots + 1/R_n) + D} = \frac{-\Delta P_L}{1/R_{eq} + D} \quad (2)$$

where, the composite governor speed droop can be written as equation (3):

$$R_{eq} = \frac{1}{1/R_1 + 1/R_2 + \cdots 1/R_n} \quad (3)$$

The typical speed droop setting for both thermal and hydro generator governors is around 5% in per unit value. Thus, a system (as above) with a number of machines, each with a droop of 5%, will have a total system speed droop R_{eq} of 5%. However, the actual speed droop may range from 2% to 12%, depending on the different types of unit [11].

Taking account of the characteristics of steam and hydro turbines in the system, a system turbine-governor model shown in Figure 4 can be derived. The speed control of the turbine is provided by a droop governor with an equivalent gain value, R_{eq}. It operates on an input of the speed deviation formed between the reference speed and the actual speed. This changes the governor valve (steam turbine) or gate (hydro turbine) position. The typical governor actuator time constant, T_G, is 0.2 second. For a stable performance of the speed control, a transient-droop-compensation, which is a lead-lag transfer function with time constants T_1 and T_2, is introduced between governor and turbine. The turbine relates the response of mechanical power output following the governor action and is characterized by a time constant T_T which varies between 0.3 and 0.5 second.

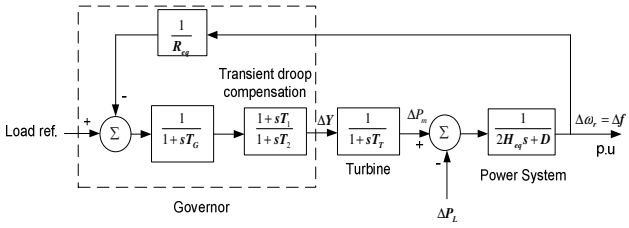

Figure 4. Block diagram of a system turbine-governor model

The parameter values of the single generator model shown in Figure 3, were obtained through parameter identification and model validation. A severe frequency event shown in Figure 5 which occurred in the UK on 27th May 2008 was used for validation.

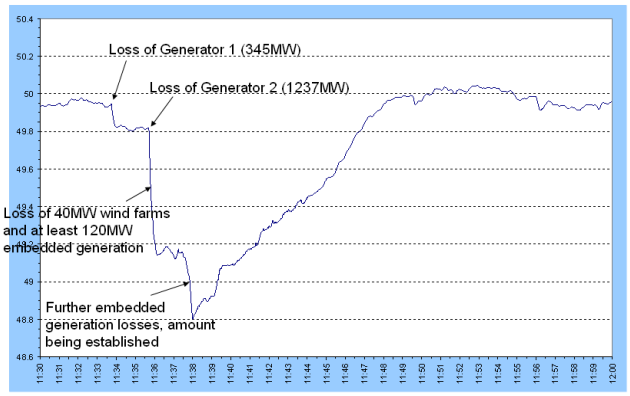

Figure 5. Frequency response on 27th May 2008 (http://www.nationalgrid.com/NR/rdonlyres/D680C70A-F73D-4484-BA54-95656534B52D/26917/PublicReportIssue1.pdf)

C. *EV representation*

To investigate the impact of the EV participation, a vital step is how to obtain realistic 24-hour EV load profiles. Different from conventional load forecasting, there is no historical EV use data available for reference. A feasible way is to generate the profiles via reasonable predictions and assumptions of EV market penetration, technical specifications, and use patterns (especially charging patterns), etc.

 ISBN: 978-1-61208-136-6

To determine regular EV charging profile a probabilistic approach was used. More details of this approach could be found in [12]. In this study three time dependent charging modes, namely, after-work charging, on-work and after-work charging and delayed night charging were considered. The EV power demand profiles for 2020 were obtained for three charging modes and shown in Figure 6. The information used in this study in mainly from reference [6].

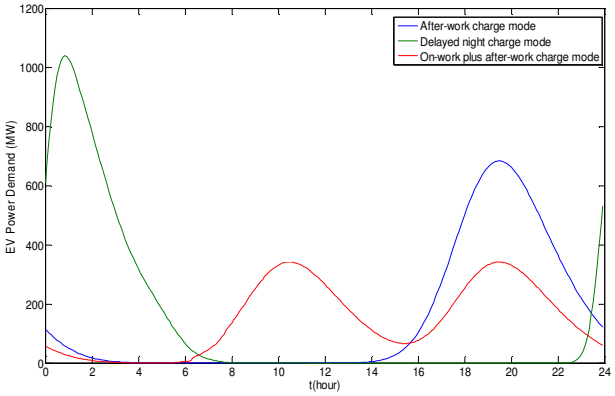

Figure 6. EV power demand profile for three charging modes considered

D. *The GB system model*

The model shown in Figure 4 was used to investigate the contribution of EV for the frequency response. H_{eq} was calculated for 2020 system assuming the generation schedule and inertia constants shown in Table 1.

TABLE I. OVERALL INERTIA CONSTANT OF THE GB SYSTEM

Generator type	Assumed Capacity GW	H_i	H_{eq}
New Coal	2.41	6.0	0.23
Coal	9.30	6.0	0.88
Gas	15.02	9.0	2.13
Nuclear	6.00	4.5	0.43
Interconnector	3.30	0.0	0.00
Other	4.76	6.0	0.45
Onshore wind	5.72	0.0	0.00
Offshore wind	13.68	0.0	0.00
Other renewables	3.36	6.0	0.32
Total	63.54		4.44

Figure 7 shows the model used to investigate the EV frequency response for the 2020 GB system. It was assumed that immediately after a frequency event is detected, EVs which are charging on the power system are disconnected using a frequency sensitive switch. This model was implemented in MATLAB/Simulink.

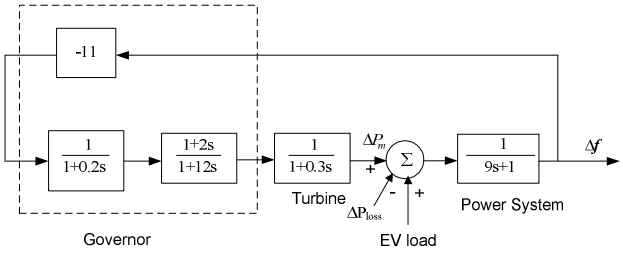

Figure 7. GB system model to investigate EV frequency response

V. RESULTS

Based on the obtained EV power demand profiles and the developed GB system model, the contribution from EVs for frequency response was studied. Figure 8 shows the EV contribution to the primary frequency response under different EV loads and low total demand condition. It is assumed that demand in 2020 is as same as in 2008 due to electricity network efficiency improvement activities in GB. The demand used in the simulations is the minimum summer GB demand in 2008 plus the three EV load profiles shown in Figure 6. It is assumed that the EV loads will be disconnected as soon as frequency starts to drop.

VI. CONCLUSIONS

The importance of frequency response from EV in a regime where there is a high penetration of renewable energy generation is demonstrated in this paper using computer simulations. A single bus GB system was used for simulations. The system inertia was determined to reflect the high penetration of renewable energy sources.

EVs were modeled using its demand curve over a day. Three charging modes namely, after-work, on-work and after-work, and delayed-night charging were used to construct the EV demand curves. During a low frequency event, the charging load was shed to provide frequency support. Simulations show that EV load has a significant contribution to reduce the frequency excursion. Highest effect was obtained with delayed nigh charging mode, if a frequency event occurs at mid night. At this time frequency drop can be reduced from 1.2% to 0.2%.

ACKNOWLEDGMENT

Authors wish to thank EU project MERGE for providing financial support for this work. Authors also wish to thanks Dr. X. Chu for providing EV load profiles for this study. J.B.E thanks the Low Carbon Research Institute for their support.

 ISBN: 978-1-61208-136-6

REFERENCES

[1] Strbac, G., Shakoor, A., Black, M., Pudjianto, D., and Boppc, T., "Impact of wind generation on the operation and development of the UK electricity systems", Electric Power Systems Research Vol. 77, 2007, pp. 1214-1227.

[2] Pearmine, R., Song, Y.H., and Chebbo, A., "Influence of wind turbine behaviour on the primary frequency control", IET Renewable Power Generation, 2007, Vol. 1, Issue 2, pp. 142-150.

[3] Erinmez, I.A., Bickers, D.O., Wood, G.F., and Hung, W.W., "NGC Experience with Frequency Control in England and Wales- Provision of Frequency Response by Generators", IEEE PES Winter Meeting, 31 January – 4 February, 1999, New York, USA.

[4] NGC, "Technical and Operational Characteristics of the Transmission System", April 2000;

[5] Fred C. Schweppe, Richard D. Tabores, James L. Kirtley, Hugh R. Outhred, Federick H. Pickle, and Alan J. Cox "Homeostatic Utility Control," IEEE Transactions on Power Apparatus and Systems, vol. PAS-99, no. 3, May/June 1980.

[6] K. Samarakoon, J. Ekanayake, and N. Jenkins "Development of Technical Concepts of DSP into smart meters," Centre for Distributed Generation and Sustainable Electrical Energy, Cardiff University, December 2008.

[7] Kempton, W., and Tomic, J., "Vehicle-to-grid power fundamentals: Calculating capacity and net revenue," Journal of Power Sources, 2005.

[8] Brooks, A., and Gage, T., "Integration of electric drive vehicles with the electric power grid—a new value stream", 18th International Electric Vehicle Symposium and Exhibition, Germany, 2001.

[9] Moreira, C. L., Rua, D., Karfopoulos, E., Zountouridou, E., Soares, F., Bourithi, I., Grau, I., Peças Lopes J. A., Cipcigan L.M., Seca, L., Moschakis M., Rocha Almeida P. M., Moutis P., Papadopoulos P., Rei R. J., Bessa R. J., and Skarvelis-Kazakos S. "Extend Concepts of MG by Identifying Several EV Smart Control Approaches to be Embedded in The Smartgrid Concept to Manage EV Individually or in Clusters", Mobile Energy Resources in Grids Of Electricity, Deliverable D1.2, September 2010.

[10] Deliverable D1.3, "Identifying EV smart control approaches under a VPP management", EU project on MERGE, http://www.ev-merge.eu/images/stories/uploads/MERGE_WP1_D1.3_Final.pdf, Access on 22 March 2011.

[11] Kundur P., "Power System Stability and Control, McGraw-Hill, Inc., 1994

[12] Draft of Deliverable D2.2, "Functional specification for tools to assess steady state and dynamic behaviour impacts, impact on electricity markets and impact of high penetration of EV on the reserve levels" EU project on MERGE, http://www.ev-merge.eu/index.php?option=com_content&view=category&layout=blog&id=64&Itemid=53, Access on 22 March 2011.

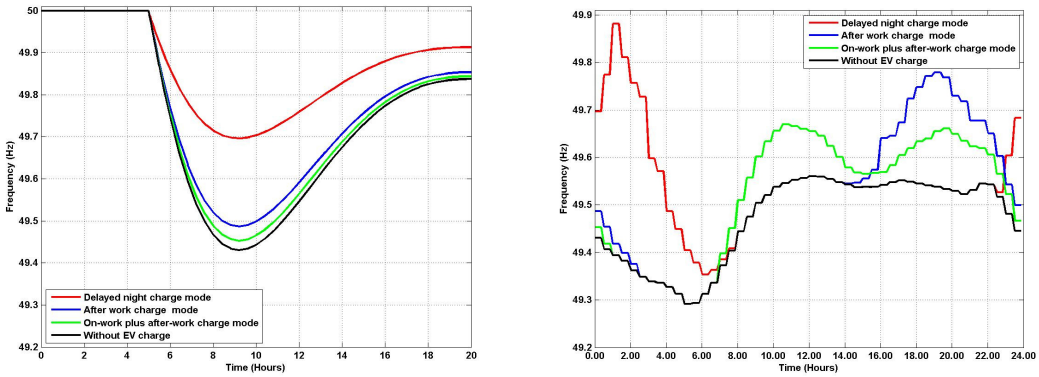

(a) Frequency drops at 00.00 hrs

(b) Maximum frequency drops at every 10 min during a day

Figure 8. The graphs when 1320 MW generation is lost in 2020 GB system (with minimum demand).

Privacy vs. Pricing for Smart Grids

Stojan Z. Denic, Georgios Kalogridis, and Zhong Fan
The Telecommunications Research Laboratory
Toshiba Research Europe Limited, Bristol, UK, BS1 4ND
e-mails: {stojan.denic, george, zhong.fan}@toshiba-trel.com

***Abstract*—In this paper, problems of privacy protection and power pricing for a new generation of electric power networks are addressed simultaneously. For an adopted electric power cost function, effects of the application of a privacy algorithm are studied. It is illustrated that a privacy algorithm can affect the price of the electric power by modulating the consumer's demand. It turns out that the effect is more pronounced for the networks with high uncertainty and inefficiency in power production.**

***Keywords*-Smart grid privacy; pricing**

I. INTRODUCTION

The smart grid is a recent paradigm representing a large number of different technologies aiming at revitalizing the electric power network. One of the goals of the smart grid is to bring intelligence into the existing aging network to improve its efficiency and robustness such that it will be more capable to respond to new higher consumption demands. (It is expected that the electric power consumption will be tripled worldwide by 2050 [1].) One way to achieve this is to employ communication networks which will enable the scanning of the power network state and carrying out appropriate actions to provide its stability and functionality.

Other factors that necessitate this metamorphosis is the introduction of renewable resources and electric vehicles into the network. The power production based on the renewable resources, such as solar and wind energy, may experience rapid changes due to weather conditions. This may cause large voltage variations which is not desirable from the point of view of the network stability. On the other hand, the electric vehicles represent a considerable new load, but in the same time they can serve as storage units for energy.

The new nature of the electric power network in terms of the production uncertainty and digitalization will affect overall network design including two network features, privacy and electric power price. The focus of this paper is an interplay between the consumer privacy protection and pricing of the electric power subject to the previous conditions which characterize the new electric power networks.

A. Contributions

To study the effect of privacy algorithms on the pricing of the electric power, we adopt the pricing model found in [2]. This model relates the price with the power consumer demand, and in the same time reflects the efficiency (or equivalently, uncertainty) of the power production. We employ the algorithm found in [3], and compute the price of the electric power for a given demand. This price is compared with the price when the algorithm is not used.

The results and contributions of this paper are the following:

- We use a Markov chain (which has already been tested in [4] for a single user power consumption modeling) to model a consumer group demand.
- The privacy algorithm is applied for different number of users, different sizes of batteries and for different levels of the network efficiency.
- Empirical cumulative distribution functions for the electric power demand and electric power price are computed for different model parameters.
- Relative changes in the power price which compare the case when the privacy algorithm is used and not used are computed for different battery sizes and different power production efficiencies.
- The effect of the new network architecture on the privacy algorithms applications is discussed.

The paper is organized as follows. Section II contains background material on the smart grid privacy and the pricing of the electric power. Section III gives the privacy system model. Section IV describes how the consumers' demand can be modeled by Markov chains. Section V introduces the electric power price model. In Section VI, the simulation results are provided accompanied with the result discussion. Section VII gives concluding remarks.

II. RELATED WORK

A. Consumer Privacy Protection

As mentioned above, the main assumption for the functioning of the smart grid is its ability to collect and store the information from the network continuously (such as power consumption) at even household level with increased granularity [5]. Although current policy regulations in the US and elsewhere are restrictive from the point of view of the collected data reuse [5], the storage of these data gives a possibility of their misemployment. If, in addition, the collected and stored data become available to other parties (besides utility companies) such as law enforcement agencies, marketing and malicious individuals, this could represent a privacy and security risk for consumers. A potential threat can be illustrated by the following example; the amount of information obtained from the household smart metering data may be demonstrated with the use of non-intrusive appliance load monitors (NALM), which analyze collected power consumption data to track appliance usage patterns [6], [7]. The

 ISBN: 978-1-61208-136-6

author of [8] argues that frequently collected metering data, e.g. at 15 minute intervals, may provide a window into the activities within homes, exposing a wealth of private activities to anyone with access to energy usage information.

To protect privacy, Kalogridis et al. [3] proposed a simple home power load management scheme. The power flow within a home may be controlled by running a portion of a consumption demand off a rechargeable battery, rather than directly off the grid. That is, smart metering data privacy can be protected by using a battery to mask power usage profiles.

B. Pricing of Electric Power and Privacy

As shown in [3], a consequence of the privacy algorithm usage is that it modifies the probability distribution of a power consumption (demand) as seen by the utility company. Because the electric power production cost depends on the demand [2], this means that the price of the electric power production can be different comparing to the case when the privacy algorithms are not used. Even more, in the smart grid, other factors to influence the probability distribution of the demand are the renewable resources and the battery storage implying that the privacy algorithms are only one part of this price equation.

That is why the goal of this paper is to explore to what extent the privacy protection can modulate the consumers' demand and the price of the electric power.

III. Smart Grid Privacy System Model

A. Appliance load signature masking

In this section we give a brief overview of the privacy protection scheme introduced in [3]. The system assumes the existence of 1) An energy storage facility, such as Electric Vehicle (EV), and 2) An 'electrical power routing' mechanism, where this term is taken to mean the selective control and power mixing of a number of electricity sources to cover consumption demands [9]. The system may be implemented with a rechargeable battery and a bidirectional inverter to optimize the flow and storage of electricity. Optionally, the system may also control energy generated locally from photovoltaic (PV) panels or wind turbines.

An overview of the privacy system can be seen in Fig. 1, comprising the following sub-systems.

- *Metering mechanism*: is used to obtain a set of electricity measurements from the smart meter or from smart appliances.
- *Event detection*: analyzes metering data in order to detect an occurring, or predict an imminent, event that may contain 'privacy information'. For example, this may be a power trigger generated by a particular event, such as a change in power consumption (e.g. appliance switch-on/off event).
- *Privacy protection algorithm*: configures power routing to mask a detected consumption event. Different protection settings may be edited with the help of an *in-home display* (IHD).

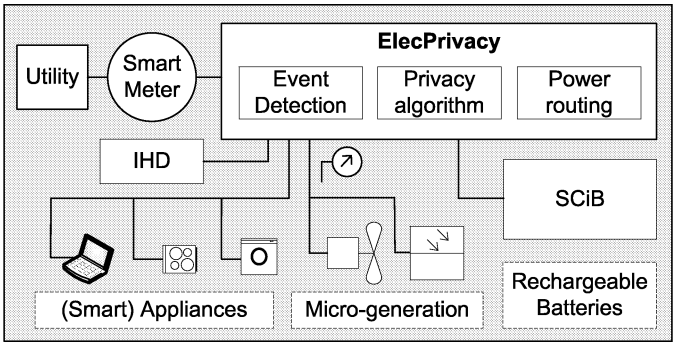

Fig. 1. Privacy protection system overview.

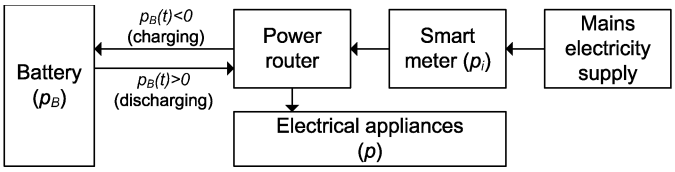

Fig. 2. Battery power mixing moderation model.

- *Power routing*: mixes a private (i.e. non-utility) energy resource (e.g. rechargeable battery) with utility energy to meet appliance demands.

The main objective is to 'detect a privacy threat' and respond by 'configuring power routing' in order to mask appliance load signatures. For simplicity, we assume that the system can perform such tasks in real-time.

B. Privacy protection water-filling algorithm

We consider the simple case where a battery is discharged or recharged with a $p_B(t)$ average power over a Δt metering interval in order to 'disguise' a given consumption load $p(t)$. With the use of battery power mixing, the home power trace becomes $p_i = p - p_B - p_L$, where $p_L(t)$ is the (average) battery power loss due to charging/discharging during $(t-\Delta t, t)$; this model is illustrated in Fig. 2. (In this paper the assumption is that a battery can fully discharge/recharge without any losses, i.e. $p_L = 0$.) We say that p_i is introduced by a transformation $\mathcal{G}$ on the (real-time) load demand p such that $p_i = \mathcal{G}p$. We then refer to $\mathcal{G}$ as privacy (protection) algorithm.

In our experiments we use the privacy algorithm in [3], which simulates water-filling [10], as outlined in Table I. Energy $e(t)$ denotes the (cumulative) energy consumed up to time t, with $e(0) = 0$, and $p(t) = \frac{e(t)-e(t-\Delta t)}{\Delta t}$.

Suppose that the battery has a finite capacity E_C, and a maximum discharge and recharge power of P_D and P_R, $-P_R \leq p_B(t) \leq P_D$, for all t. The proposed algorithm uses the battery in order to resist against power load changes. That is, the algorithm will force the battery to either discharge or recharge when the required load $p(t)$ is either larger or smaller (respectively) than the previously metered load $p_i(t - \Delta t)$. The power and duration of battery charging/discharging are configured to equal the power differences, unless battery bounds are reached.

 ISBN: 978-1-61208-136-6

TABLE I
BATTERY WATER-FILLING ALGORITHM.

Current battery charge level: $p_B(t) = e_i(t) - e(t - \Delta t) + p(t)\Delta t$
if $D(t) = p(t) - p_i(t - \Delta t) > 0$ (discharging case) **then**
  if There is enough battery energy/power to provide $D(t)$ for Δt **then**
    Mix in battery power so that $p_i(t) = p_i(t - \Delta t)$
  else
    Use maximum battery power while $B(t) > 0$
  end if
end if
if $C(t) = p_i(t - \Delta t) - p(t) > 0$ (charging case) **then**
  if Enough battery 'emptiness' to absorb $C(t)$ for Δt **then**
    Recharge battery so that $p_i(t) = p_i(t - \Delta t)$
  else
    Fully recharge battery
  end if
end if

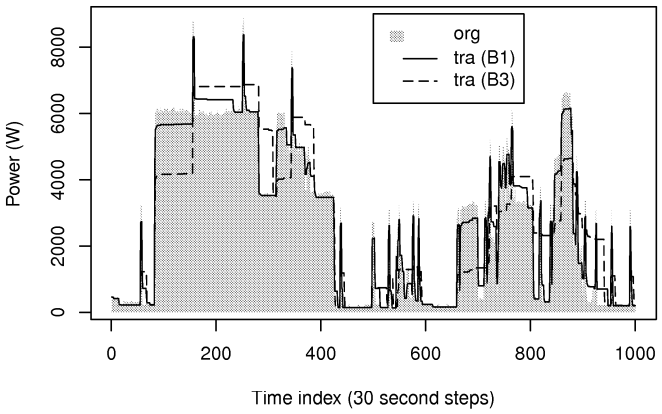

Fig. 3. Load signatures before and after the water-filling algorithm using different batteries: a) $B_1 = 500$W/1kWh and b) $B_3 = 2$kW/4kWh.

The effect of the water-filling algorithm can be seen in Fig. 3: the bigger the battery size, the more p is masked. In Fig. 3, it is assumed that $P_R = P_D$, and the battery is denoted by $B = P_D/E_C$.

IV. POWER CONSUMPTION MODELING

In [4], we demonstrated how a simple Markov chain model could be applied in representing the power consumption within a household. This representation relies on the clustering analysis of the measured data obtained from the measurement campaign performed during 30 days in several apartments [4]. Denote the Markov chain representation by the sequence of Markov chain states $X := \{X(k)\}_{k\geq 0}$, where the state $X(k) \in \{x_1, \ldots, x_N\}$. The Markov chain X is completely defined by the transition probability matrix $\mathbf{A}(k)$ and the vector of state probabilities $\mathbf{P}(k) := [\Pr\{X(k) = x_1\}, \ldots, \Pr\{X(k) = x_N\}]^T$, where T denotes the transpose of the vector. The transition probability matrix $\mathbf{A}$ contains conditional probabilities $a_{ij} := \Pr\{X(k+1) = x_i | X(k) = x_j\}$. Under the assumption that the power consumption can be described by a stationary process, the evolution of the state probability vector is given by

$$\mathbf{P}(k+1) = \mathbf{A}\mathbf{P}(k), \tag{1}$$

when $\mathbf{P}(0)$ is known.

It is shown in [4] that an accurate prediction of the power consumption can be carried out via its Markov chain representation. The Markov model is used in Section VI to describe the electric power demand of large number of consumers.

V. ELECTRIC POWER PRICE MODEL

The price model adopted in this paper had already been used in the smart grid literature [11], [12], to adapt power consumption demand in order to optimize its utility function. Next, this model will be briefly described, and for more details, readers are referred to [2].

The price model assumes that there are N_p power producers, which use the same technology to produce the power. Between the power producers and the consumers, there are several retailing companies which buy the power from the producers and sell it to final consumers. Both, the producers and the retailers can sell the power at a current moment or in forward market (in future). When the physical production of the producers is equated to the total retailer demand (which depends on the consumer demand), profit-maximizing price of each producer is given by

$$P_W = a\Big(\frac{Q}{N_p}\Big)^{c-1}. \tag{2}$$

Here, Q is the total retailer demand, a is a proportionality constant, and $c \geq 2$ is a constant which is related to the energy production efficiency. The expression given by (2) reflects a few important characteristics of the power production. First, the price is an increasing function of the demand Q, which captures the fact that the electric power comes from a variety of different sources such as hydro, nuclear, oil and coal plants each having a different cost of production. Second, when the power comes from inefficient resources, the constant c is chosen to be larger than 2 which implies an increasing price rate vs demand Q. In current systems, c can take value up to 5 [2].

VI. SIMULATION RESULTS ANALYSIS

To study the influence of the privacy algorithm on the price of the electrical power production, we assume that the number of homes (consumers) within one area is 300. According to Section IV, each consumer's power demand is modeled by a Markov chain with appropriately chosen transition probability matrix $\mathbf{A}$. Here, the consumers are considered to have a similar pattern of consumption, and the matrix $\mathbf{A}$ is taken from [4].

It is assumed that each house will apply the same algorithm and a battery of the same size to protect its privacy. The algorithm will be tested for three battery sizes, $B_1 = 500$W/1kWh $B_2 = 1$kW/2kWh and $B_3 = 2$kW/4kWh. It is interesting to note that charging rates for EVs could be from 7kW to 10kW leaving opportunity for usage of larger batteries if needed.

 ISBN: 978-1-61208-136-6

The results are generated in the following way. First, the power demands of all 300 consumers obtained when the privacy algorithm is not applied are summed up, generating the overall cumulative power demand for one area. Thereafter, the price of the electrical power production is obtained from (2) 'on an hourly' (OAH) basis; the time axis of 30 days is divided into the hour intervals, and the value of the cumulative energy demand for each hour interval is replaced in (2). The same procedure is repeated when the privacy algorithm is applied to modulate the demand of each of all 300 consumers. This OAH approach is in line with [2], since the most active electric power markets are for the next-hour and next-day delivery.

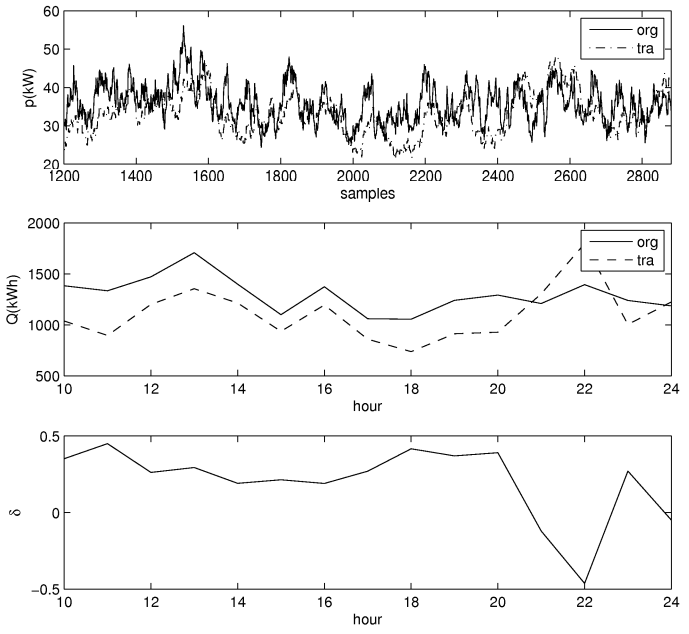

Fig. 4. From top to bottom: 1) The instantaneous power demand for 300 consumers, original and transformed ($p_{\text{org}}(t)$ and $p_{\text{tra}}(t)$), 2) Energy demand, original and transformed ($Q_{\text{org}}(t)$ and $Q_{\text{tra}}(t)$), computed on an hourly basis, 3) The OAH relative price difference between the original and transformed demand $\delta(t)$. The battery size is $B_2 = 1$kW/2kWh.

Fig. 4 shows the instantaneous power demands ($p_{\text{org}}(t)$ and $p_{\text{tra}}(t)$), the energy demands ($Q_{\text{org}}(t)$ and $Q_{\text{tra}}(t)$), and the OAH relative price difference

$$\delta(t) = (P_{W,\text{org}}(t) - P_{W,\text{tra}}(t))/P_{W,\text{org}}(t) \quad (3)$$

for 300 users for a fraction of time measured (14 hours) out of 30 days. The battery size is $B_2 = 1$kW/2kWh. The figure compares two cases, when the privacy algorithm is not used (original demand giving rise to the subscript 'org'), and when the privacy algorithm is used (transformed demand giving rise to the subscript 'tra'). It can be seen that due to the application of the privacy algorithm, the OAH price $P_{W,\text{tra}}(t)$ may vary by even 50% ($\delta(t) = \pm 0.5$) as compared to $P_{W,\text{org}}(t)$. Here, the parameter $c = 4$ implying high uncertainty of the electric power production. That the cumulative distribution (cdf) of the transformed demand $f_{Q,\text{tra}}$ is indeed changed as compared to the cdf of the original demand $f_{Q,\text{org}}$ is depicted in Fig. 5 and 6.

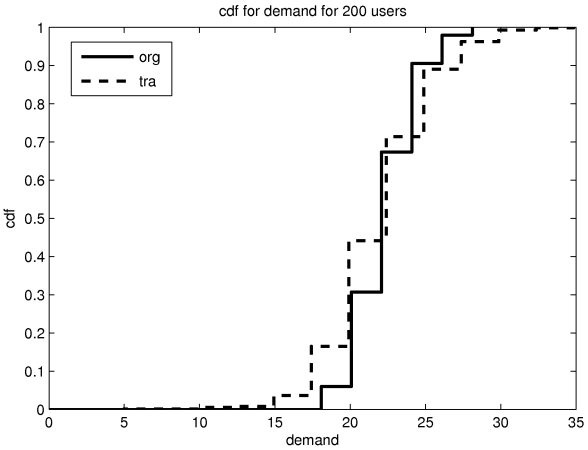

Fig. 5. The cdfs of the demand $f_{Q,\text{org}}$ and $f_{Q,\text{tra}}$ for the 200 consumers.

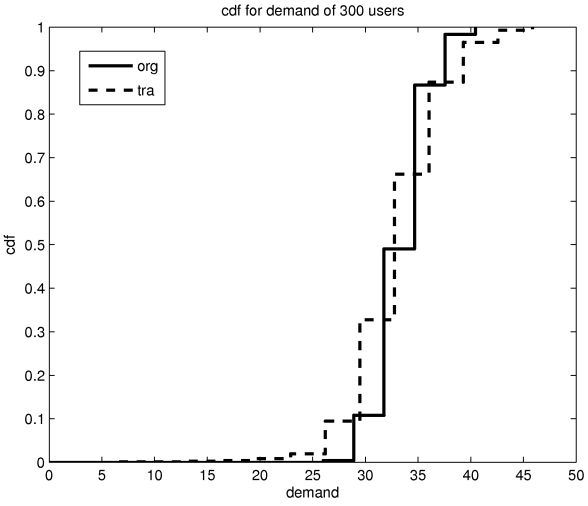

Fig. 6. The cdfs of the demand $f_{Q,\text{org}}$ and $f_{Q,\text{tra}}$ for the 300 consumers.

In addition, the cdfs of the prices $f_{P,\text{org}}$ and $f_{P,\text{tra}}$ are shown in Fig. 7 and 8. For a smaller value of c ($c = 2$ meaning smaller production uncertainty), the difference in the cdf of the original $f_{P,\text{org}}$ and transformed demand $f_{P,\text{tra}}$ is not so obvious. However, when $c = 4$ (meaning larger production uncertainty), the difference between cdfs is obvious as well as the difference between the cases of $c = 2$ and $c = 4$.

The tables II, III and IV contain the relative price differences

$$\delta_m = (P^m_{W,\text{org}} - P^m_{W,\text{tra}})/P^m_{W,\text{org}} \quad (4)$$

of cumulative (30 days) prices between the original and transformed demands for different numbers of the consumers and for 3 different battery sizes. $P^m_{W,\text{org}}$ and $P^m_{W,\text{tra}}$ are the cumulative 30 day prices of the original and transformed demand, respectively. The results suggest that: 1) For larger uncertainty in the electric power production ($c = 4$ or $c = 5$),

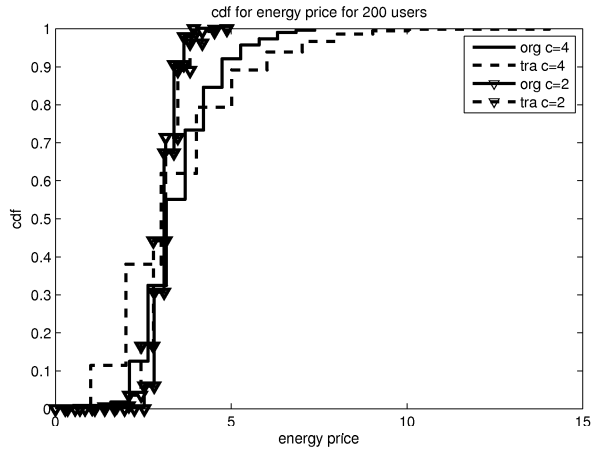

Fig. 7. The cdfs of the price $f_{P,\text{org}}$ and $f_{P,\text{tra}}$ for the 200 consumers.

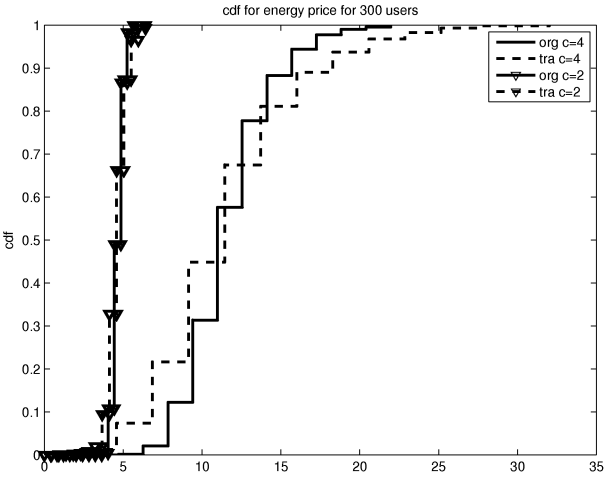

Fig. 8. The cdfs of the price $f_{P,\text{org}}$ and $f_{P,\text{tra}}$ for the 300 consumers.

the relative price difference is susceptible to the value of the consumer number, and it gets smaller as the number of consumers grows, 2) For smaller uncertainty in the production, the relative price difference is small, 3) At least for this example, the price of the transformed demand $P^m_{W,\text{tra}}$ is larger than the price of the original demand $P^m_{W,\text{org}}$ for larger uncertainty ($c = 4$ or $c = 5$) for all three batteries.

TABLE II
CUMULATIVE PRICE RELATIVE DIFFERENCE FOR $B_1 = 500$W/1KWH

Consumer #	100	150	200	250	300
$\delta_m(\%)$ for $c = 2$	0.24	0.26	0.24	0.24	0.23
$\delta_m(\%)$ for $c = 4$	-2.58	-1.65	-1.29	-0.84	-0.61
$\delta_m(\%)$ for $c = 5$	-5.42	-3.68	-2.96	-2.08	-1.62

Hence, we next discuss the influence of two parameters on the price, the number of consumers and the production uncertainty as described by c. The results suggest that if the same pricing model is applied for large number of consumers, the cumulative price for longer time period will be similar regardless of the application of the privacy algorithm. However, it is an open question if this will remain the same when dynamic pricing models (demand-response) are applied per consumer and not to one large group of consumers. From the point of view of the production uncertainty, it could be expected that, due to the presence of the electric vehicles and new sources of the electric power, the parameter c might be larger. Therefore, the effect of the application of privacy algorithms on pricing could be more pronounced.

TABLE III
CUMULATIVE PRICE RELATIVE DIFFERENCE FOR $B_2 = 1$KW/2KWH

Consumer #	100	150	200	250	300
$\delta_m(\%)$ for $c = 2$	0.56	0.62	0.62	0.6	0.6
$\delta_m(\%)$ for $c = 4$	-6.42	-3.82	-2.66	-1.87	-1.25
$\delta_m(\%)$ for $c = 5$	-14.06	-8.8	-6.46	-4.81	-3.54

TABLE IV
CUMULATIVE PRICE RELATIVE DIFFERENCE FOR $B_3 = 2$KW/4KWH

Consumer #	100	150	200	250	300
$\delta_m(\%)$ for $c = 2$	0.68	0.69	0.69	0.66	0.64
$\delta_m(\%)$ for $c = 4$	-3.7	-1.69	-1.05	-0.46	-0.29
$\delta_m(\%)$ for $c = 5$	-8.52	-4.5	-3.32	-2.07	-1.66

Although, the cumulative price relative difference δ_m is small for long time interval, it is interesting to notice that OAH relative price difference $\delta(t)$ can be large. For three different battery sizes discussed earlier and $c = 4$, $\delta(t) \in [-0.56, 0.89]$ for B_1, $\delta(t) \in [-1.35, 0.97]$ for B_2 and $\delta(t) \in [-1.48, 0.98]$ for B_3. Therefore, it seems that this interval size increases as the battery size increases. This instantaneous difference could be important for the electric power producers and retailers when they negotiate the deal between themselves.

VII. CONCLUSION

The smart grid should transform existing electric power network into very efficient, robust and flexible network which will use some of the latest achievements in the communication and control engineering and computational science. This paper considers the interaction between two important problems related to the design of the smart grid, privacy and pricing. We show by means of simulations that privacy algorithms affect the cdf of consumers' demand, and in that way can change the price of the electric power production. The level of influence depends on: 1) The size of the network, 2) The efficiency of the power production (through the parameter c) and 3) The length of the observation interval. This could be of interest to electrical power producers, retailers and designers.

ACKNOWLEDGMENT

The authors would like to thank the Directors of the Toshiba Telecommunications Research Laboratory for their support.

REFERENCES

[1] K. Kowalenko, "The smart grid: a primer," *IEEE The Institute Newsletter*, vol. 34, no. 4, page 5, Dec. 2010.

[2] H Bessembinder and M. Lemmon, "Equilibrium pricing and optimal hedging in electricity forward markets," *Journal of Finance,* pp. 1347–1382, Jun. 2002.

 ISBN: 978-1-61208-136-6

[3] G. Kalogridis, C. Efthymiou, S. Z. Denic, T. A. Lewis, and R. Cepeda, "Privacy for smart meters: towards undetectable appliance load signatures," *Proceedings of the First IEEE International Conference on Smart Grid Communications (SmartGridComm10)*, Maryland, USA, Oct. 4-6 2010, pp. 232–237.

[4] G. Kalogridis, S. Z. Denic, T. Lewis, and R. Cepeda, "Privacy protection system and metrics for hiding electrical events," *Int. J. Security and Networks*, vol. 6, no. 1, 2011, in press.

[5] M. Lisovich, D. K. Mulligan, and S. B. Wicker, "Inferring personal information from demand-response systems," *IEEE Security Privacy*, vol. 8, no. 1, pp. 11-20, Jan. 2010.

[6] C. Laughman, D. Lee, R. Cox, S. Shaw, S. B. Leeb, L. K. Norford, and P. Armstrong, "Advanced nonintrusive monitoring of electric loads," *IEEE Power Energy Mag.*, pp. 56-63, 2003.

[7] H. Y. Lam, G. S. K. Fung, and W. K. Lee, "A novel method to construct taxonomy electrical appliances based on load signatures," *IEEE Trans. on Consum. Electron.*, vol. 53, no. 2, pp. 653-660, 2007.

[8] E. L. Quinn, "Privacy and the New Energy Infrastructure," Feb 2009. [Online]. Available: http://papers.ssrn.com/sol3/papers.cfm?abstract\id=1370731

[9] N. V. Nedap, "The power router," Sep 2010. [Online]. Available: http://www.powerrouter.com

[10] T. M. Cover and J. A. Thomas, *Elements of information theory*. John Wiley & Sons, Inc. New York, NY, USA, 2006.

[11] Z. Fan, "Distributed demand response and user adaptation in smart grids," to appear in the *12th IFIP/IEEE International Symposium on Integrated Network Management (IM'11)*, Dublin, Ireland, May 2011, in press.

[12] C. Wang and M. de Groot, "Managing end-user preferences in the smart grid," *Proceedings of the First International Conference on Energy-Efficient Computing and Networking (e-Energy10)*, 2010, pp. 105–114.

 ISBN: 978-1-61208-136-6

Optimal Control of Residential Energy Storage Under Price Fluctuations

Peter van de ven
Department of Mathematics & Computer Science
Eindhoven University of Technology
P.O. Box 513, 5600 MB Eindhoven, The Netherlands
p.m.v.d.ven@tue.nl

Nidhi Hegde, Laurent Massoulié and Theodoros Salonidis
Technicolor Paris Research Lab
Technicolor
75015 Paris, France
{nidhi.hegde,laurent.massoulie,theodoros.salonidis}@technicolor.com

***Abstract*—An increasing number of retail energy markets exhibit price fluctuations and provide home users the opportunity to buy energy at lower than average prices. However, such cost savings are hard to realize in practice because they require human users to observe the price fluctuations and shift their electricity demand to low price periods. We propose to temporarily store energy of low price periods in a home battery and use it later to satisfy user demand when energy prices are high. This enables home users to save on their electricity bill by exploiting price variability without changing their consumption habits. We formulate the problem of minimizing the cost of energy storage purchases subject to both user demands and prices as a Markov Decision Process and show that the optimal policy has a threshold structure. We also use a numerical example to show that this policy can lead to significant cost savings, and we offer various directions for future research.**

***Index Terms*—Battery storage, dynamic pricing, dynamic programming, energy storage, threshold policy.**

I. Introduction

Wholesale energy prices exhibit significant fluctuations during each day due to variations in demand and generator capacity. Home users are traditionally not exposed to these fluctuations but pay a fixed retail energy price, as shown in Figure 1(a). Economists have long argued to remove the fixed retail prices in favor of prices that change during the day. Such *dynamic pricing* reflects the prices of the wholesale market and has been predicted to lead to lower demand peaks and lower average level and volatility of the wholesale price [5].

Dynamic pricing has been enabled by recent smart-grid technologies such as smart meters. A first example of dynamic pricing that is being increasingly adopted is time-of-use pricing (Figure 1(b)). Such schemes typically provide two or three price levels (e.g., 'off-peak', 'mid-peak' and 'on-peak') where the level is determined by the time of day. The price levels are determined well in advance and are typically not changed more than once or twice per year. A second example of dynamic pricing is real-time pricing (Figure 1(c)) where the retail energy price changes hourly or half-hourly to reflect the price on the wholesale energy market.

Dynamic pricing creates an opportunity for users to reduce energy costs by exploiting the price fluctuations. However, in practice users show only a minor shift in their demand to match the energy prices [2]–[4], [8]. A possible remedy is to equip homes with a battery that can be used for home energy storage. This battery can be charged when the energy price is low and the stored energy can then be used to protect against high prices. This allows users to benefit from the varying energy price without having to adjust their usage patterns accordingly. Energy can be stored both by a dedicated battery, or by using the battery pack of an electric car [9]. In the past such setup was not economically viable due to the high cost of batteries, but current developments have brought storage applications within reach.

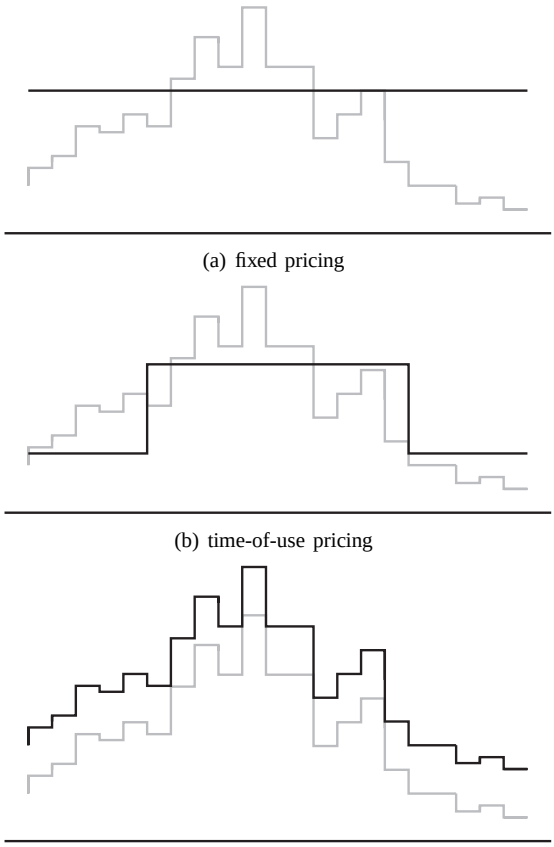

(a) fixed pricing

(b) time-of-use pricing

(c) real-time pricing

Figure 1. The wholesale energy price (gray) and various approaches to retail pricing (black).

 ISBN: 978-1-61208-136-6

In this paper, we address the problem of organizing home energy storage purchases to minimize long term energy costs under variable demands and prices. This problem involves deciding whether to satisfy demand directly from the grid or from the battery, as well as up to what level to charge or discharge the battery. The resulting optimization problem is difficult to handle due to the stochastic nature of price and demand and due to the fact that we aim to minimize the long-term costs. In our approach, we model the problem as a Markov Decision Process and we show that there exists a threshold-based stationary cost-minimizing policy. When the battery level is below this threshold, the battery is charged up to it, while the battery is discharged when above the threshold. By comparing the costs incurred under this policy with the cost of satisfying the demand directly from the grid, we can show that energy storage may lead to significant cost savings. In the current paper we provide an outline of this approach, which will be discussed in more detail in a follow-up paper.

To the best of our knowledge, previous work on home energy storage is limited and does not propose optimal control solutions subject to stochastic price and demand fluctuations. Home energy storage has been studied for the case of *arbitrage* i.e., buying energy when it is inexpensive, and selling it later to the grid for a higher price [6]. This problem has been studied assuming no demands and that prices are known in advance in a finite horizon setting. These assumptions allow deterministic optimization problem formulations which can be solved using linear programming techniques [1], [7]. However, these formulations do not take into account the stochasticity in prices and demands and do not allow for long-term cost optimization. Our approach can be readily adapted to an arbitrage problem in an infinite-horizon setting, where the behavior of the price process may be stochastic. A similar threshold-based optimal policy can be shown to hold in this case.

We also recently became aware of a parallel work that uses a model similar to ours to investigate control of energy storage in the context of *data centers* [10]. The model in [10] assumes that the battery is fully efficient and the proposed scheduling algorithm is a sub-optimal heuristic, whose gap from optimality increases as storage size decreases. In contrast, our model incorporates battery inefficiencies and we show that the optimal scheduling policy is threshold-based.

The rest of the paper is structured as follows. In Section II we introduce the model and describe the various decision variables. In Section III we propose an optimal policy and apply this policy to a numerical example. Section IV gives some concluding remarks and directions for future research.

II. Model outline

Consider a residential user with certain energy requirements and a battery that can be used for energy storage. Time is slotted, and we denote by $B(t)$ the buffer level (i.e., the state of charge) of the battery at time t, $t = 0, 1, \ldots$. Let $\bar{B}$ represent the maximum buffer level, so $B(t) \in [0, \bar{B}]$. In each time slot t, some demand $D(t)$ arises, and we may purchase energy at a price of $P(t)$ per unit. The demand has finite support $D(t) \in [0, \bar{D}]$, as does the price $P(t) \in [0, \bar{P}]$.

Denote by $\Omega = [0, \bar{D}] \times [0, \bar{P}]$ the set of possible realizations of demand and price, and for any $\boldsymbol{x} \in \Omega$, denote by $d(\boldsymbol{x})$ and $p(\boldsymbol{x})$ the corresponding price and demand, respectively. We assume that the demand and price level may be correlated, and evolve according to some stationary process. Specifically, we denote by $f_{\boldsymbol{x}}(\boldsymbol{y})$ the probability density function of moving from state $\boldsymbol{x}$ to state $\boldsymbol{y}$ in the next slot, for any $\boldsymbol{x}, \boldsymbol{y} \in \Omega$.

The battery may not be completely efficient, and its performance is affected by the charging efficiency $\eta_c \in (0, 1]$ and discharging efficiency $\eta_d \in (0, 1]$. Energy purchased to charge the battery is reduced by a factor η_c, and only a fraction η_d of the discharged energy is converted into electricity. In addition to satisfying the demand from the battery, we also allow demand to be met directly from the grid, bypassing the battery.

Let $A_1(t)$ denote the amount of energy purchased directly from the grid in slot t, $A_2(t)$ the amount of energy bought to charge the battery, and $A_3(t)$ the energy from the battery used towards satisfying demand , see Figure 2.

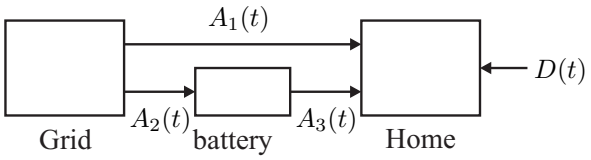

Figure 2. A graphical representation of the model.

We assume $A_1(t), A_2(t), A_3(t) \geq 0$, and since all demand must be met, we require that

$$D(t) = A_1(t) + \eta_d A_3(t).$$

The battery has a finite charging rate, so the amount of energy that can be used for charging the battery is bounded as $A_2(t) \leq \bar{A}$, for some $\bar{A} \in [0, \bar{B}]$.

The buffer level of the battery evolves according to

$$B(t+1) = B(t) + A_2(t)\eta_c - A_3(t),$$

and the energy costs in slot t is given by

$$g(t) = (A_1(t) + A_2(t))P(t).$$

Our goal is to choose in each slot $A_1(t)$, $A_2(t)$ and $A_3(t)$ as to minimize the total discounted cost

$$g = \sum_{t=0}^{\infty} g(t)\alpha^t, \tag{1}$$

with $0 < \alpha < 1$ the discount factor. Note that the total discounted cost is finite, since the per-slot costs are bounded.

Before we consider in more detail the infinite-horizon problem (1), we first note that it is never optimal to charge and discharge the battery in the same slot, i.e., we have $A_2(t)A_3(t) = 0$, $t = 0, 1, \ldots$. This is intuitively clear, because charging and discharging the battery in the same slot

 ISBN: 978-1-61208-136-6

corresponds to routing $\min\{A_2(t), \eta_d A_3(t)\}$ energy from the grid to the user, through the battery. Because of the battery inefficiency it is beneficial to instead circumvent the battery, and satisfy the demand directly from the grid.

This observation simplifies the minimization problem significantly, by reducing the number of decision variables. Specifically, denote by $\Delta(t)$ the buffer level difference between slot t and $t+1$, i.e.,

$$B(t+1) = B(t) + \Delta(t).$$

Then, in view of the restriction on simultaneous charging and discharging:

$$\begin{aligned} A_1(t) &= D(t) + \Delta(t)\eta_d \mathbf{1}_{\{\Delta(t)<0\}}, \\ A_2(t) &= \Delta(t)\eta_c^{-1}\mathbf{1}_{\{\Delta(t)>0\}}, \\ A_3(t) &= -\Delta(t)\eta_d \mathbf{1}_{\{\Delta(t)<0\}}. \end{aligned}$$

Thus, the choice for $\Delta(t)$ fixes $A_1(t)$, $A_2(t)$ and $A_3(t)$, and the model reduces to a single-variable decision problem. The per-slot costs may be rewritten in terms of $\Delta(t)$ as

$$g(t) = (D(t) + (\Delta(t))^+\eta_c^{-1} + (\Delta(t))^-\eta_d)P(t),$$

with $x^+ = \max\{x, 0\}$ and $x^- = -\max\{-x, 0\}$.

III. The optimal policy

In this section, we discuss how to choose in each slot the $\Delta(t)$ that minimizes the total discounted costs. To this end, we rewrite our model as a Markov decision process. We denote by $J_{\boldsymbol{x}}(b)$ the minimal total discounted costs, starting from state $\boldsymbol{x} \in \Omega$, and buffer level $b \in [0, \bar{B}]$. The cost function satisfies the Bellman equation

$$J_{\boldsymbol{x}}(b) = \inf_{\delta \in U_{\boldsymbol{x}}(b)} \{\gamma_{\boldsymbol{x}}(\delta) + \alpha G_{\boldsymbol{x}}(b+\delta)\},$$

with $\gamma_{\boldsymbol{x}}(\delta) = (d(\boldsymbol{x}) + \delta^+\eta_c^{-1} + \delta^-\eta_d)p(\boldsymbol{x})$ the immediate costs, $G_{\boldsymbol{x}}(b') = \int_{\boldsymbol{y}\in\Omega} f_{\boldsymbol{x}}(\boldsymbol{y}) J_{\boldsymbol{y}}(b')\mathrm{d}\boldsymbol{y}$, and $U_{\boldsymbol{x}}$ the control set that contains all allowed decisions for the difference in buffer level. It is readily seen that

$$U_{\boldsymbol{x}}(b) = [U_{\boldsymbol{x}}^-(b), U_{\boldsymbol{x}}^+(b)],$$

where $U_{\boldsymbol{x}}^-(b) = -\min\{b, d(\boldsymbol{x})\}$ and $U_{\boldsymbol{x}}^+(b) = \min\{\bar{B}-b, \bar{A}\}$.

In the remainder we restrict ourselves to the case $\eta_c = \eta_d = 1$, although the optimal policy for the more general case is similar to the policy described below for the completely efficient scenario.

The optimal policy specifies for each price $p = p(\boldsymbol{x})$ a buffer threshold $\beta(p) \in [0, \bar{B}]$. If $b \le \beta(p)$, then the optimal policy is to charge the buffer as close to $\beta(p)$ as the control set allows. If $b \ge \beta(p)$, the battery should be discharged up to $\beta(p)$ within the boundaries of the control set. Formally stated, the cost-minimizing choice for the buffer difference $\Delta_{\boldsymbol{x}}^*(b)$ is given by

$$\Delta_{\boldsymbol{x}}^*(b) = \begin{cases} \min\{\beta(p) - b, U_{\boldsymbol{x}}^+(b)\}, & b \le \beta(p), \\ \max\{\beta(p) - b, U_{\boldsymbol{x}}^-(b)\}, & b \ge \beta(p). \end{cases} \quad (2)$$

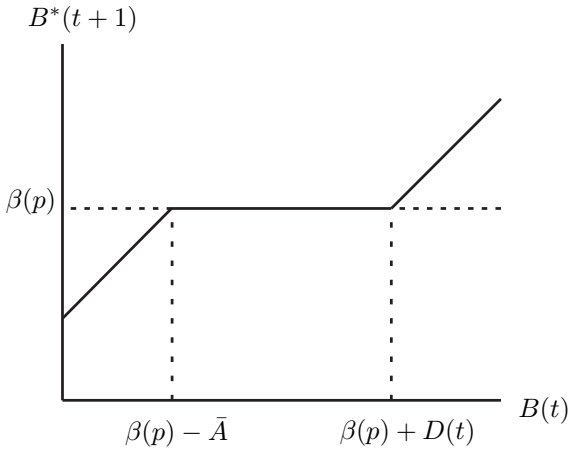

Figure 3. The structure of the optimal policy as a function of $B(t)$.

This policy is illustrated in Figure 3, which shows $B^*(t+1) = B(t) + \Delta_{\boldsymbol{x}}^*(b)$ plotted against $B(t)$, for some price level p.

According to (2), when $B(t) \ge \beta(p)$, the battery will be charged, and all demand will be met from the grid, so $A_1(t) = D(t)$. Conversely, when $B(t) > \beta(p)$ the demand is (partially) met from the battery, and we have $A_1(t) = (D(t) - (B(t) - \beta(p)))^+$ and $A_3(t) = \min\{D(t), B(t) - \beta(p)\}$.

The full analysis of the optimal policy (2) will appear in a subsequent paper.

A. A numerical example

We now present an example of energy storage under time-of-use pricing. We numerically determine the thresholds $\beta(p)$ through policy iteration, and use these to study the cost savings obtained from energy storage. The example below makes various simplifying assumptions on the demand and price processes. However, it clearly demonstrates the functionality of the optimal storage policy and the gains obtained from using energy storage.

Each day is divided into three periods of equal length, with corresponding prices (in Euro/kWh) $p_1 = 0.04$, $p_2 = 0.06$ and $p_3 = 0.07$. The demands (in kWh) are i.i.d. (independent and identically distributed), with the demand in period i, D_i having the distribution $D_i = (d_i + X)^+$, $i = 1, 2, 3$, with $d_1 = 5$, $d_2 = 6$, $d_3 = 7$ and $X \sim \mathcal{N}(0, 1)$. We assume that $\bar{A} = \bar{B}$, so there are no restrictions on charging the battery, and we set $\alpha = 0.99$. We discretize the state space into sections of 0.5 kWh, and use policy iteration to compute the thresholds β_1, β_2 and β_3. Figure 4 shows these thresholds plotted against $\bar{B}$. Note that $\beta_3 = 0$, as is to be expected for the threshold corresponding to the highest price.

We then simulate the demand process for 10^5 slots, and compute the total discounted costs over this period, both with and without battery storage. Figure 5 shows relative cost savings up to 40% obtained from energy storage, plotted against $\bar{B}$. We see that the cost savings initially increase with $\bar{B}$, but converge when the thresholds stabilize.

 ISBN: 978-1-61208-136-6

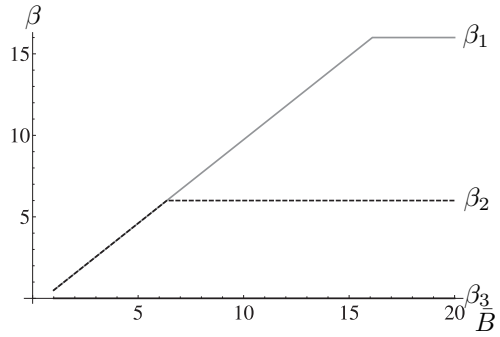

Figure 4. The optimal thresholds as a function of $\bar{B}$.

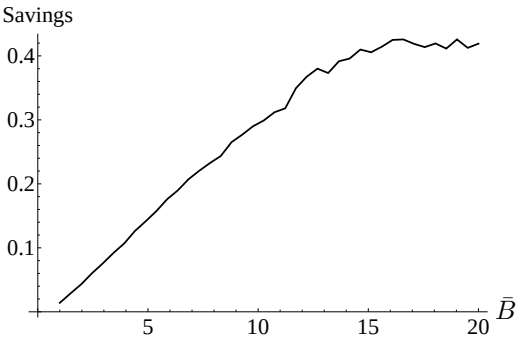

Figure 5. The cost savings as a function of $\bar{B}$.

IV. Conclusions and Outlook

We studied the control of residential energy storage under price fluctuations. We introduced a model for the battery operation and argued that the cost-minimizing storage policy is threshold-based. We showed by means of a small numerical example that residential energy storage can lead to significant savings in electricity cost.

We believe that this work opens up several avenues for future research. First, it is necessary to analytically show the existence of optimal threshold policies. Second, the computation of the optimal thresholds for more complex scenarios is challenging. Analytic expressions may be hard to derive and the large state space may make policy iteration computationally infeasible. Thus, it might be necessary to use approximations and bounds for the optimal threshold levels or use simple heuristics that provide reasonable performance.

It would also be interesting to incorporate in the model the battery lifetime and the costs of buying and replacing the battery. Battery lifetime benefits from longer sustained periods of charging and discharging. On one hand, this may complicate analysis because the optimal policy may depend on whether the battery was charged or discharged in previous slots. On the other hand, it may give rise to simple heuristics where the battery is alternatively fully charged and discharged. Taking into account the costs for buying and replacing the battery introduces the problem of battery dimensioning. Smaller batteries are cheaper but may provide less opportunity to exploit price fluctuations.

Finally, we may ask ourselves what will happen to the energy market when a significant fraction of users adopt energy storage. A possible outcome is that the resulting steady demand process will cause convergence of the energy market resulting in smaller price variations. While this is good from the perspective of both energy producers and users without energy storage, a less volatile price process will decrease the possibilities for exploiting price fluctuations for users with storage capacities. Consequently, the cost savings obtained from energy storage may decrease beyond the break-even point. The interplay between energy storage and the energy market is an interesting topic for future research.

References

[1] K. Ahlert and C. Van Dinther. Sensitivity analysis of the economic benefits from electricity storage at the end consumer level. In *Proc. of IEEE Bucharest Power Tech Conference*, Bucharest, Romania, June 28–July 2 2009.

[2] M.H. Albadi and E.F. El-Saadany. A summary of demand response in electricity markets. *Electric Power Systems Research*, 78(11):1989–1996, 2008.

[3] H. Allcott. Rethingking real time electricity pricing. Technical Report http://web.mit.edu/allcott/www/papers.html, MIT, Cambridge, MA, 2010.

[4] G. Barbose and C. Goldman. A survey of utility experience with real time pricing. Technical Report LBNL-54238, Berkeley National Laboratory, 2004.

[5] S. Borenstein. The long-run efficiency of real-time electricity pricing. *The Energy Journal*, 26(3):93–116, 2005.

[6] F. Graves, T. Jenkins, and D. Murphy. Opportunities for electricity storage in deregulating markets. *The Electricity Journal*, 12(8):46–56, 1999.

[7] W. Hu, Z. Chen, and B. Bak-Jensen. Optimal operation strategy of battery energy storage system to real-time electricity price in Denmark. In *Proc. of IEEE Power and Energy Society General Meeting*, Minneapolis, MN, July 25–29 2010.

[8] M.G. Lijesen. The real-time price elasticity of electricity. *Energy Economics*, 29(2):249–258, 2007.

[9] S.B. Peterson, J.F. Whitacre, and J. Apt. The economics of using plug-in hybrid electric battery packes for grid storage. *Journal of Power Sources*, 195(8):2377–2384, 2010.

[10] R. Urgaonkar, B. Urgaonkar, M.J. Neely, and A. Sivasubramanian. Optimal power cost management using stored energy in data centers. Technical Report https://www.cse.psu.edu/research/publications/tech-reports/2010/CSE-10-008.pdf, Penn State, 2011.

 ISBN: 978-1-61208-136-6

Satisfiability of Elastic Demand in the Smart Grid

Jean-Yves Le Boudec
EPFL
Lausanne, Switzerland
Email: jean-yves.leboudec@epfl.ch

Dan-Cristian Tomozei
EPFL
Lausanne, Switzerland
Email: dan-cristian.tomozei@epfl.ch

***Abstract*—We study a stochastic model of electricity production and consumption where appliances are adaptive and adjust their consumption to the available production, by delaying their demand and possibly using batteries. The model incorporates production volatility due to renewables, ramp-up and ramp-down time, uncertainty about actual demand versus planned production, delayed and evaporated demand due to adaptation to insufficient supply. We study whether threshold policies stabilize the system. The proofs use Markov chain theory on general state space.**

***Keywords*-Dynamical Systems, Smart Grids, Elastic Demand, Macroscopic Model, Stability**

I. INTRODUCTION

Recent results on modelling the future electricity markets [11] suggest that they may lead to highly undesirable equilibria for consumers, producers or both. A central reason for such an outcome might be the combination of volatility in supply and demand, the delays required for any unplanned capacity increase, and the inflexibility of demand which leads to high dis-utility costs of blackouts. Further, the use of renewable energy sources such as wind and solar increases volatility and worsens these effects [8].

Flexible load is advocated in [6] as a mechanism to reduce ramp-up requirements and adapt to the volatility of electricity supply that is typical of renewable sources. A deployments report [4] shows the feasibility of delaying air conditioners using signals from the distributor. Adaptive appliances combined with simple, distributed adaptation algorithms were advocated in [5], [7]; they are assumed to reduce, or delay, their demand when the grid is not able to satisfy them. Some examples might be: e-cars, which may have some flexibility regarding the time and the rate at which their batteries can be loaded; heating systems or air conditioners, which can delay their demand if instructed to; hybrid appliances which use alternative sources in replacement for the energy that the grid cannot supply. If the alternative energy source is a battery, then it will need to be replenished at a later point in time, which will eventually lead to later demand.

The presence of adaptive appliances may help address the volatility of renewable energy supply, however, backlogged demand is likely to be merely delayed, rather than canceled; this introduces a feedback loop into the global system of consumers and producers. Potentially, one might increase the backlogged demand to a point where future demand becomes excessive. In other words, one key question is whether it is possible to stabilize the system. This is the question we address in this paper.

To address this fundamental question, we consider a macroscopic model, inspired by the model in [8]. We assume that electricity supply follows a two-step allocation process: first, in a forecast step (*day ahead market*) demand and renewable supply are forecast, and the total supply is planned; second, (*real time market*) the actual, volatile demand and renewable supply are matched as possible. We assume that the rate at which supply can be varied in the real time step is subject to ramp-up and ramp-down constraints. Indeed, it is shown in [3] that it is an essential feature of the real time market. We modify the model in [8] and assume that the whole demand is adaptive. While this is clearly an exaggerate assumption, we do it for simplicity and as a first step, leaving the combination of adaptive and non-adaptive demand to a later research. We are interested in simple, distributed algorithms, as suggested in [5], therefore, we assume that the suppliers cannot directly observe the backlogged demand; in contrast, they see only the effective instantaneous demand; at any point in time where the supply cannot match the effective demand, the backlogged demand increases.

Our model is macroscopic, so we do not model in detail the mechanism by which appliances adapt to the available capacity; several possible directions for achieving this are described in [5]. However we do consider two essential parameters of the adaptation process. First, the *delay* $1/\lambda$ is the average delay after which frustrated demand is expressed again. Second, the *evaporation* μ is the fraction of backlogged demand that disappears and will not be resubmitted per time unit. The inverse delay λ is clearly positive; in contrast, as discussed in Section II, it is reasonable to assume that some adaptive appliances naturally lead to a positive evaporation (this is the case for a simple model of heating systems), but it is not excluded that inefficiencies in some appliances lead to negative evaporation.

Within these modelling assumptions, the electricity suppliers are confronted with a scheduling issue: how much capacity should be bought in the real time market to match

 ISBN: 978-1-61208-136-6

the adaptive demand. The effect of adaptation is to increase the latent demand, due to backlogged demand returning into the system. This is the mechanism by which the system might become unstable. We consider a threshold based mechanism as in [8]. It consists in targeting some fixed supply reserve at any point in time; the target reserve might not be met, due to volatility of renewable supply and of demand, and due to the ramp-up and ramp-down constraints.

Our contribution is to show that if evaporation is positive, then any such threshold policy does stabilize the system. In contrast, if evaporation is negative, then there exists no threshold policy which stabilizes the system. The case where evaporation is exactly equal to 0 remains unsolved.

Thus, our results suggest that evaporation plays a central role. Simple adaptation mechanisms as described in this paper might work if evaporation is positive (as one may perhaps generally expect), but will not work if evaporation is negative, i.e. if the fact that demand is backlogged implies that a higher fraction of demand returns into the system. This suggests that future research be done in order to gain a deeper understanding of evaporation, whether it can truly be assumed to be positive, and if not, how to control it.

We use discrete time, for tractability. We use the theory of Markov chains on general state spaces in [9]. In Section II we describe the assumptions and the model, and relate our model to prior work. In Section III we study the stability of the system under threshold policies. We conclude in Section IV.

II. Model and Assumptions

A. Assumptions and Notation

We use a discrete model, where $t \in \mathbb{N}$ represents the time elapsed since the beginning of this day. The time unit represents the time scale at which scheduling decisions are done, and is of the order of the second.

The supply is made of two parts: the planned supply $G^f(t)$, forecast in the day-ahead market, and the actual supply $G^a(t)$, which may differ, due to two causes. First, the forecasted supply may not be met, due to fluctuations, for example in wind and sunshine. Second, the suppliers attempt to match the demand by adding (or subtracting) some supply, bought in the real time market. We assume that this latter term is limited by ramp-up and ramp-down constraints. We model the actual supply as

$$G^a(t) = G(t-1) + G^f(t) + M(t), \tag{1}$$

where $M(t)$ is the random deviation from the planned supply due to renewables, $G(t-1)$ is the supply decision in the real time market. We view $G^a(t)$ as deterministic and given(it was computed yesterday in the day-ahead market), $M(t)$ as an exogenous stochastic process, imposed by nature, and $G(t-1)$ as a control variable.

We call $D^a(t)$ the "natural" demand. It is the total electricity demand that would exist if the supply would be sufficient. In addition, there is, at every time t, the *backlogged demand* $B(t)$, which results from adaptation: $B(t)$ is the demand that is expressed at time t due to a previous demand being backlogged. The total effective demand, or expressed demand, is

$$E^a(t) = D^a(t) + B(t). \tag{2}$$

We model the effect of demand adaptation as follows.

$$B(t) = \lambda Z(t), \tag{3}$$

$$Z(t+1) = Z(t) - B(t) - \mu Z(t) + F(t), \tag{4}$$

$$F(t) = [E^a(t) - G^a(t)]^+. \tag{5}$$

We used the convenient notation $(a)^+ := \max(0, a)$.

In the above equations, $F(t)$ is the *frustrated* demand, i.e. the denied satisfaction at time t. Eq. (5) expresses that, through adaptation, the demand that is served is equal to the minimum of the actual demand and the supply. The variable $Z(t)$ is the *latent backlogged* demand; it is the demand that was delayed, and might later be expressed. It is incremented by the frustrated demand.

The frustrated demand is expressed with some delay; we model this with Eq. (3), where λ^{-1} is the average delay, in time slots.

The evolution of latent backlogged demand is expressed by Eq. (4). The expressed demand $B(t)$ is removed from the backlog (some of it may return to the backlog, by means of Eq. (5) at some later time). The remaining backlog may evaporate at a rate μ, which captures the effect on total demand of delaying some demand. Delaying a demand may indeed result in a decreased backlogged demand, in which case the evaporation factor is positive. For example this occurs if we delay heating in a building with a heating system that has a constant energy efficiency; such a heating system will request more energy in the future, but the integral of the energy consumed over time is less whenever some heating requests are delayed. In this case, positive evaporation comes at the expense of a (hopefully slight) decrease in comfort (measured by room temperature). In other cases, though, we may not exclude that evaporation be negative. This may occur for example with heat pumps [1].

As in [8], we assume that the natural demand can be forecast with some error, so that

$$D^a(t) = D(t) + D^f(t), \tag{6}$$

where the forecasted demand $D^f(t)$ is deterministic and $D(t)$, the deviation from the forecast, is modelled as an exogenous stochastic process. We assume that the day ahead forecast is done with some fixed safety margin r_0, so that

$$G^f(t) = D^f(t) + r_0. \tag{7}$$

 ISBN: 978-1-61208-136-6

B. The Stochastic Model

We model the fluctuations in demand $D(t)$ and renewable supply $M(t)$ as stochastic processes such that their difference $M(t) - D(t)$ is an ARIMA$(0, 1, 0)$ Gaussian process, i.e.

$$(M(t+1) - D(t+1)) - (M(t) - D(t)) = N(t+1) \quad (8)$$

where $N(t)$ is white Gaussian noise, with variance σ^2. This is the discrete time equivalent of Brownian motion, as in [8].

Let $R(t)$ be the reserve, i.e the difference between the actual production and the expressed demand, defined by

$$R(t) = G^a(t) - E^a(t) = G(t-1) - \lambda Z(t) + r_0 + M(t) - D(t), \quad (9)$$

and let $H(t)$ be the increment in supply bought on the real time market, i.e.

$$H(t) = G(t) - G(t-1). \quad (10)$$

Putting all the above equations together, we obtain the system equations:

$$R(t+1) = R(t) + H(t) + N(t+1) - \lambda\left(Z(t+1) - Z(t)\right),$$
$$Z(t+1) = (1 - \lambda - \mu)Z(t) + \mathbb{1}_{\{R(t)<0\}}|R(t)|,$$

Thus we can describe our system by a two-dimensional stochastic process $X(t) = (R(t), Z(t))$, with $t \in \mathbb{N}$.

The sequence $H(t)$ is the control sequence. It is constrained by the *ramp-up and ramp-down constraints*:

$$-\xi \leq H(t) \leq \zeta, \quad (11)$$

where $\xi > 0$ and $\zeta > 0$ are some positive constants.

We assume a simple, threshold based control, which attempts to make the reserve equal to some threshold value $r^* > \zeta$; therefore

$$H(t) = \max\left(-\xi, \min\left(\zeta, r^* - R(t)\right)\right). \quad (12)$$

In summary, we have as model the stochastic sequence $X = (X(t))_{t\in\mathbb{N}}$ defined by

$$R(t+1) = R(t) - \lambda \mathbb{1}_{\{R(t)<0\}}|R(t)| + \lambda(\lambda+\mu)Z(t) + \left(\zeta \wedge (r^* - R(t))\right) \vee (-\xi) + N(t+1), \quad (13)$$

$$Z(t+1) = \mathbb{1}_{\{R(t)<0\}}|R(t)| + (1 - \lambda - \mu)Z(t), \quad (14)$$

where N is an iid white Gaussian noise sequence of variance σ^2. Note that X is a Markov chain on the state space $\mathsf{S} = \mathbb{R} \times \mathbb{R}^+$.

C. Related Models

Let us now discuss some similar models which have been considered in the literature.

In [9], the authors consider the so-called Linear State Space model (LSS), which introduces an n-dimensional stochastic process $X = \{X_k\}_k$, with $X_k \in \mathbb{R}^n$. For matrices $F \in \mathbb{R}^{n\times n}$, $G \in \mathbb{R}^{n\times p}$, and for a sequence of i.i.d. random variables of finite mean taking values in $\mathbb{R}^p$, the process evolves as

$$X_k = FX_{k-1} + GW_k, \ k \geq 1. \quad (15)$$

Our model (13)-(14) is in fact a superposition of three such LSS models, depending on the current state of the Markov chain. The challenge of showing that our model is stable comes from the fact that in the part of the state space in which $R(t) < 0$, the corresponding LSS does not satisfy the stability condition (LSS5) of [9] (which requires that the eigenvalues of F be contained in the open unit disk of $\mathbb{C}$).

In [10] a slightly different model for capturing elasticity of demand is proposed. More specifically, the authors consider a scenario in which a deterministically *bounded* amount of demand arrives at each time step, while the supplier decides whether to buy an additional amount of energy from an external source at a certain cost. Unsatisfied demand is backlogged. A threshold policy is analyzed and found to be stable (the size of the backlog is found to be deterministically bounded) and optimal. Pricing decisions are also explored. The main differences with the present work are the following:

- Additional parameters which model delay and loss of backlogged demand (i.e. λ and μ) enrich our model's expressivity.
- We consider potentially unbounded demand, modeled as a 0-mean Gaussian random variable, which makes proving stability more challenging.
- No results on pricing and cost-optimality are included in the present work.

The continuous time model used in [2] seeks to capture the presence of two types of energy sources, primary and ancillary, the latter being less desirable (i.e. more costly) than the former, both subject to (different) ramp-up constraints. A threshold policy is again discussed in the context of rigid demand, which is simply dropped if not enough energy is available. The analyzed Markov chain is a two-dimensional process having on the first coordinate the quantity of energy used from the ancillary source in order to satisfy as much demand as possible, and on the second coordinate the reserve (i.e. energy surplus).

III. System Stability under a Threshold Policy

For presentation ease, we consider like in [8] the case $\xi = \infty$. In other words, we relax the ramp-down constraint, i.e. the surplus energy can be disposed of easily. In the extended version of the paper [1] we show that a finite value of ξ does not alter the results. Thus, (11) becomes:

$$H(t) \leq \zeta, \quad (16)$$

and the threshold policy (12) writes as

$$H(t) = \min\left(\zeta, r^* - R(t)\right). \quad (17)$$

 ISBN: 978-1-61208-136-6

Let us study how the system stability of (13)-(14) depends on the evaporation parameter μ.

Define the following three domains:

$$D_1 = (-\infty, 0) \times \mathbb{R}_+,$$
$$D_2 = [0, r^* - \zeta) \times \mathbb{R}_+,$$
$$D_3 = [r^* - \zeta, +\infty) \times \mathbb{R}_+.$$

Then, denoting

$$X(t) = \begin{bmatrix} R(t) \\ Z(t) \end{bmatrix}, N_0(t) = \begin{bmatrix} N(t) \\ 0 \end{bmatrix}, \zeta_0 = \begin{bmatrix} \zeta \\ 0 \end{bmatrix},$$
$$r_0^* = \begin{bmatrix} r^* \\ 0 \end{bmatrix}, A_1 = \begin{bmatrix} 1+\lambda & \lambda(\lambda+\mu) \\ -1 & 1-\lambda-\mu \end{bmatrix},$$
$$A_2 = \begin{bmatrix} 1 & \lambda(\lambda+\mu) \\ 0 & 1-\lambda-\mu \end{bmatrix}, A_3 = \begin{bmatrix} 0 & \lambda(\lambda+\mu) \\ 0 & 1-\lambda-\mu \end{bmatrix},$$

the process (13)-(14) rewrites in matrix form:

$$X(t+1) = N_0(t+1) + \begin{cases} A_1 X(t) + \zeta_0, & X(t) \in D_1, \\ A_2 X(t) + \zeta_0, & X(t) \in D_2, \\ A_3 X(t) + r_0^*, & X(t) \in D_3. \end{cases} \quad (18)$$

The main reason for which the analysis of system stability is challenging is the fact that both A_1 and A_2 admit 1 as an eigenvalue.

The first result of this section can be stated in the form of the following

Theorem 1. *If $\mu > 0$, the Markov chain* (13),(14) *is positive Harris and ergodic. For any initial distribution ρ, the chain converges to its unique invariant probability measure π in total variation norm, i.e. denoting the transition probability by $\mathbb{P}$,*

$$\| \int_{\mathsf{S}} \rho(dx) \mathbb{P}^n(x, \cdot) - \pi(\cdot) \| \to_{n \to \infty} 0.$$

Recall that the total variation norm of a signed measure ν is defined as

$$\|\nu\| := \sup_{f : |f| \leq 1} |\nu(f)|.$$

The proof uses the theory of general state space Markov chains. The following lemmas are instrumental in proving the result. For brevity, we only provide proof outlines, while the complete proofs can be found in the extended version [1].

Lemma 1. *If $1 - \lambda - \mu < 1$, then there exists a measure φ on S such that the Markov chain* (13),(14) *is φ-irreducible.*

Proof: (Outline) Fix some finite closed interval I and some $a > 0$, and consider the set $E = I \times [0, a]$.

Consider the measure φ_E defined as follows: for any Borel set A, $\varphi_E(A) := \nu(A \cap E)$, where ν denotes the Lebesgue measure on $\mathbb{R}^2$.

We show that our chain is φ_E-irreducible, that is, if $A \subset \mathsf{S}$ is such that $\varphi_E(A) > 0$, then for all $x \in \mathsf{S}$, there is a strictly positive probability that the time τ_A of return in A is finite: $L(x, A) = \mathbb{P}(\tau_A < +\infty) > 0$.

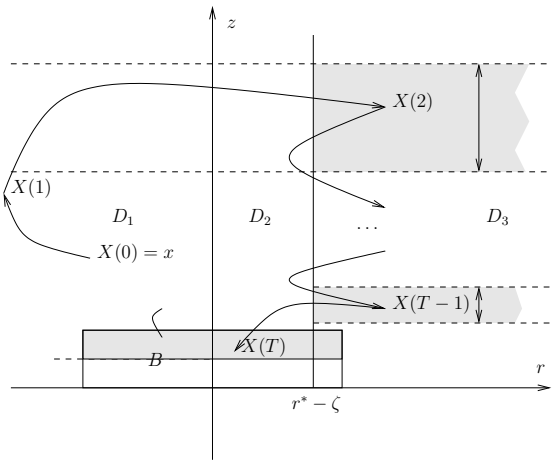

Figure 1. Typical trajectory

We consider any measurable set $B \subset E$. By Proposition 4.2.1 (ii) from [9], it suffices to show that there exists a finite $T > 0$, such that the probability of hitting B in T steps starting from any point $x \in \mathsf{S}$ is lower-bounded by a factor $\alpha(B, T, x) > 0$ (which might depend on B, T and x) times the irreducibility measure φ_E of B:

$$\mathbb{P}^T(x, B) \geq \alpha \varphi_E(B).$$

Indeed, if $\varphi_E(B) > 0$, then necessarily $\mathbb{P}^T(x, B) > 0$, and hence, $L(x, B) > 0$, since T is finite.

The key element in the proof is the observation that, at each time step, the R coordinate positions the Markov chain in region D_3 with a strictly positive probability due to the Gaussian sequence $(N(t))_t$. Furthermore, in this region the Z coordinate decreases geometrically at rate $1 - \lambda - \mu$. This property enables us to exhibit trajectories having a finite number of steps and leading from any point x to the set B. Such a trajectory is shown in Figure 1. ■

Lemma 1 shows that for any compact set of strictly positive Borel measure of the state space, its hitting time starting from any point is finite with strictly positive probability.

A set C is said to be *ν_T-small* for some non-trivial measure ν_T and a positive integer T, if for all $x \in C$, the probability of reaching any measurable B in T steps is lower-bounded as $\mathbb{P}^T(x, B) \geq \nu_T(B)$.

Furthermore, a set C is *petite* if there exists a distribution h on the positive integers and a non-trivial measure ν_h, such that for any $x \in C$, and for any Borel set B, the transition kernel of the *sampled chain* has the following property:

$$K_h(x, B) := \sum_{t \geq 0} h(t) \mathbb{P}^t(x, B) > \nu_h(B).$$

A ν_T-small set is implicitly δ_T-petite, where δ_T is the Dirac distribution.

 ISBN: 978-1-61208-136-6

Lemma 2. *For any set $C = J \times [0, b]$, with J a finite closed interval and $b > 0$, there exists $T_0 > 0$ and non-trivial measures $(\nu_T)_{T \geq T_0}$ such that C is ν_T-small for all $T \geq T_0$.*

Proof: (Outline) In Lemma 1 we essentially proved that we can reach any bounded Lebesgue-measurable set B of positive measure from any state x in a finite number of steps. In order to give an upper bound on the required number of steps, we defined the set $E = I \times [0, a]$ and we introduced the measure φ_E, which is defined as the Lebesgue measure of the set obtained via intersection with E.

In order to prove smallness, we need to eliminate the dependence of the number of steps T on the specific starting point $x \in C$ and on the destination B. Since we rely on the deterministic geometric decrease of the coordinate Z in region D_3, a choice for B which is such that all the points in $B \cap E$ have a Z-coordinate less than a certain δ, automatically leads to a logarithmic number of steps in δ (thus, arbitrarily large, for δ close to 0).

Instead, we pick a finite closed interval I and constants $\Delta > \delta > 0$, and we define the set $A := I \times [\delta, \Delta]$. Then it can be shown that there exists a minimum number of steps T_0 depending on A and C, and an $\alpha(T) > 0$ which does *not* depend on B, or the starting point x, but which does depend on T, such that for measures

$$\nu_T := \alpha(T)\varphi_A,$$

the set C is ν_T-small, for all $T \geq T_0$. ■

We give two direct consequences of the two above lemmas.

Since any set $C = J \times [0, b]$ is both ν_T- and ν_{T+1}-small for some $T > T_0$, it follows that

Corollary 1. *The Markov chain* (13),(14) *is aperiodic.*

Additionally,

Corollary 2. *Any compact subset of the state space is petite.*

We are now ready to give the following

Proof: (of Theorem 1)

We prove that the function $H : \mathbb{R} \times \mathbb{R}_+ \to \mathbb{R}_+$,

$$x = \begin{bmatrix} r \\ z \end{bmatrix} \mapsto H(x) = (r + \lambda z)^2 + (r + (\lambda + \mu)z)^2 \quad (19)$$

is a Lyapunov function for the system (13)-(14). It can be shown that H is *unbounded off petite sets*, that is for any $n < \infty$ the sublevel set $C_H(n) := \{y : H(y) \leq n\}$ is small. Furthermore, there exist constants $a, b, c > 0$ and a set $C = [-a, a] \times [0, b]$ such that the drift

$$\mathcal{D}H(x) := \mathbb{E}_x H(X(1)) - H(x)$$

satisfies

$$\mathcal{D}H(x) \leq -1 + c\mathbb{1}_C.$$

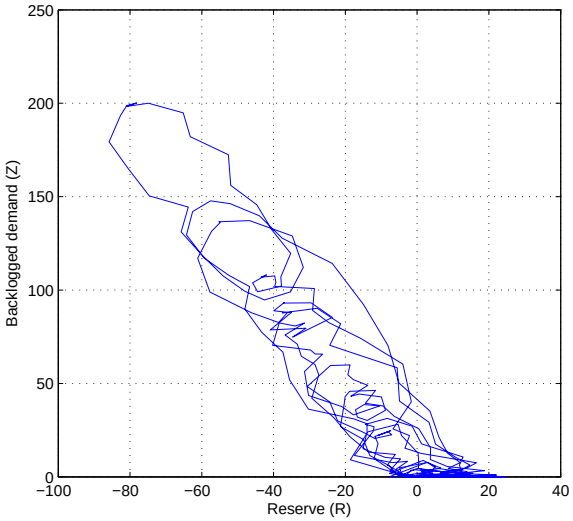

Figure 2. 500 iterations of the Markov process (13)-(14) for $\zeta = 1, r^* = 10, \sigma = 5, \lambda = 0.3, \mu = 0.1$

Separate cases need to be considered for each of the three regions D_1, D_2 and D_3.

A consequence of this result is that, by Theorem 9.1.8 of [9] and by Corollary 2, which shows that the set C is small, the chain is Harris recurrent. Furthermore, by Theorem 10.0.1 of [9], it admits a unique invariant measure π. Finally, by Theorem 13.0.1 of [9] and by Corollary 1, we get the finiteness of π and we conclude. ■

This first result signifies that for positive evaporation $\mu > 0$, the simple threshold policy (17) stabilizes the system. A typical simulated trajectory is shown in Figure 2. Most points are found around the state $(r^*, 0)$, with some excursions in domain D_1 due to the variability of the demand.

The second result of this section concerns the case for which we have negative evaporation $\mu < 0$. It is stated as the following

Theorem 2. *If $\mu < 0$, the Markov chain* (13)-(14) *is non-positive.*

Proof: (Outline) Notice that if $\mu \leq -\lambda$, then the Z coordinate of the Markov chain cannot decrease. Hence the chain is trivially unstable (it is not even φ-irreducible).

In the case $-\lambda < \mu < 0$, we turn again to [9] for proving the claim. In this case the Markov chain (13)-(14) is φ-irreducible. We need to find a function H which satisfies the hypothesis of Theorem 11.5.2 from [9] to show non-positivity.

 ISBN: 978-1-61208-136-6

Define $H : \mathbb{R} \times \mathbb{R}_+ \to \mathbb{R}_+$,

$$H(r,z) = \begin{cases} \log\left(\frac{r+(\lambda+\mu)z}{\mu}\right) & \text{if } r+(\lambda+\mu)z \le \mu, \\ 0 & \text{otherwise.} \end{cases} \tag{20}$$

Then, it can be shown that H has finite increments in any point of the state space, namely that

$$\sup_{x\in\mathsf{S}} \mathbb{E}_x|H(X(1)) - H(x)| < +\infty. \tag{21}$$

In order to show this property of H, we need to consider points x in all three domains D_1, D_2 and D_3, while distinguishing between the points $x = (r,z)$ in D_1 for which $r+(\lambda+\mu)z \le \mu$ holds, and those for which it does not.

Moreover, it can be shown that there exists a constant $v_0 > 1$ which is such that for all $x = (r,z) \in \mathsf{S}$ satisfying $r+(\lambda+\mu)z \le \mu v_0$, the drift of H evaluated in such points is positive:

$$\mathcal{D}H(x) := \mathbb{E}_x H(X(1)) - H(x) > 0. \tag{22}$$

Define the set $C := \{x = (r,z) : r+(\lambda+\mu)z \ge \mu v_0\} \cap \mathsf{S}$. Then any x in the complementary $\bar{C} := C^c \cap \mathsf{S}$ is such that $H(x) > \sup_{x_1\in C} H(x_1)$ and $\mathcal{D}H(x) > 0$. Using (21) and (22) we can apply Theorem 11.5.2 from [9] and conclude. ■

Let us sum up these results. We have shown that:

- If a positive fraction of latent jobs disappear during each time slot ($\mu > 0$), then *any* threshold policy stabilizes the system.
- On the other hand, if delaying any job results in an increase of its requirement/workload by a positive fraction ($\mu < 0$), then *there exists no threshold policy* that stabilizes the system.

The critical case for which $\mu = 0$ remains to be analyzed.

IV. Conclusion

In this paper, we considered a macroscopic model for electricity production and consumption. We assumed that the allocation process is done in two steps: a first step, in which demand and renewable supply are forecast (the day-ahead market) and a second step, in which real-time demand and real-time supply are matched as closely as possible (the real-time market), under ramp-up and ramp-down constraints regarding the rate at which real-time supply can be varied. We further assumed that all demand is adaptive and that backlogged demand cannot be observed by the supplier.

We introduced two parameters:

- the average delay $1/\lambda$ after which frustrated demand is expressed again, and
- the evaporation μ, the fraction of backlogged demand that dissappears.

We showed that, if the evaporation μ is positive, then a threshold policy, targeting a fixed supply reserve r^* at any time (under the ramp-up and ramp-down constraints), manages to stabilize the system for *any* value of r^*.

We also showed that, in case of negative evaporation μ, there exists no threshold policy which stabilizes the system.

Further research is needed to understand and control the phenomenon of negative evaporation.

References

[1] J.-Y. L. Boudec and D.-C. Tomozei. Satisfiability of elastic demand in the smart grid. *CoRR*, abs/1011.5606, 2010.

[2] I.-K. Cho and S. P. Meyn. Optimization and the price of anarchy in a dynamic newsboy model. In *Stochastic Networks, invited session at the INFORMS Annual Meeting*, pages 13–16, 2005.

[3] I.-K. Cho and S. P. Meyn. Efficiency and marginal cost pricing in dynamic competitive markets. To appear in *J. Theo. Economics*, 2006.

[4] J. Eto, J. Nelson-Hoffman, C. Torres, S. Hirth, B. Yinger, J. Kueck, B. Kirby, C. Bernier, R. Wright, A. Barat, et al. Demand response spinning reserve demonstration. 2007.

[5] S. Keshav and C. Rosenberg. How Internet Concepts and Technologies Can Help Green and Smarten the Electrical Grid. In *Proc. ACM SIGCOMM Green Networking Workshop*, August 2010.

[6] J. Kueck, B. Kirby, T. Laughner, and K. Morris. Spinning Reserve from Responsive Load. Technical report, Oak Ridge National Laboratory (ORNL), 2009.

[7] N. F. Maxemchuk. Communicating appliances. 2nd IMDEA Networks Annual International Workshop Energy Efficiency and Networking (Madrid), May-June 2010.

[8] S. Meyn, M. Negrete-Pincetic, G. Wang, A. Kowli, and E. Shafieepoorfard. The value of volatile resources in electricity markets. Submitted to the *49th Conf. on Dec. and Control*, 2010.

[9] S. P. Meyn and R. L. Tweedie. *Markov Chains and Stochastic Stability (2nd edition)*. Cambridge University Press, 2009.

[10] M. J. Neely, A. S. Tehrani, and A. G. Dimakis. Efficient algorithms for renewable energy allocation to delay tolerant consumers. Technical Report arXiv:1006.4649, Jun 2010.

[11] G. Wang, A. Kowli, M. Negrete-Pincetic, E. Shafieepoorfard, and S. Meyn. A control theorist's perspective on dynamic competitive equilibria in electricity markets. In *Proc. 18th World Congress of the International Federation of Automatic Control (IFAC)*, Milano, Italy, 2011.

 ISBN: 978-1-61208-136-6

Energy-aware Data Stream Management

Maik Thiele and Wolfgang Lehner
Technische Universität Dresden
Database Technology Group
Dresden, Germany
{maik.thiele, wolfgang.lehner}@tu-dresden.de

***Abstract*—With the increasing use of data stream management systems (DSMS's) in energy-critical areas the energy consumption of the DSMS itself is gaining growing importance. However, processing data streams in an energy-aware manner is still an open research question. In this paper, we propose a very first concept for a DSMS architecture which treats the energy consumption as a first-class-citizen. Therefore, we rely on data synopses and anytime algorithms in order to minimize the data quantity and the number of iteration which minimizes the overall energy consumption.**

Keywords – Data stream management; Energy-awareness, Synopses, Anytime Algorithm

I. INTRODUCTION

Currently, there is a severe lack of infrastructures allowing us to monitor and control the energy consumption of a given system under observation (SUO) from the software level. This results in the need for a monitoring component to observe, analyze and predict the amount of consumed energy resources. Such a component would acquire the input for its energy calculations from a mass of information; these typically arrive in the form of continuous data streams and originate from various sensors spread across the whole SUO. The use of continuous data streams necessitates suitable techniques to handle the information flow and associated service level agreements. Therefore, we intend to build a data stream management system (DSMS) to analyze the energy-behavior of a SUO and which itself is 1) energy-adaptive and 2) minimal-intrusive in term of energy consumption.

Regarding energy-efficiency we want to refer to the so-called "need-to-know" principle as the opposite of the "ubiquity" principle. The "need-to-know" principle only provides as much information as needed by the application in only the quality that is required by the application. In contrast, traditional data management systems follow the "ubiquity" principle by always presenting an up-to-date and consistent database even if no one is currently accessing the database. Through the consistent application of the "need-to-know" design principle to the data processing, we can minimize the quantity and granularity of the data in question and we can prematurely abort the execution of operations as soon as a defined quality has been reached. Both optimization criteria directly contribute to the minimization of the system's energy requirements.

In this paper, we will describe the architecture and design principles of a DSMS based on data synopses and anytime algorithms which are both ideally suited for an energy-aware data stream processing.

II. ENERGY-AWARE DATA MANAGEMENT

Despite the increasing research efforts in power management techniques, there has been little work to date on energy efficiency from a pure data management perspective. A recent study [1] has shown that, contrary to what previous work has suggested [2, 3, 4], within a single node intended for use in shared-nothing architectures, the most energy-efficient configuration is typically the one with the highest performance. In the few cases where this correlation does not hold, the improvements in energy efficiency are less than 10%, mainly due to the large up-front power costs in current server components. A major reason for this effect is given by the lack of so-called energy-proportional hardware [5], which only uses power in constant proportion to its performance. However, there have been some recent developments in this regard (e.g. PCRAM, finer CPU power states, SSDs, etc.) which will soon allow the energy-proportional operation of the hardware as a base of an energy-efficient operation.

But hardware-only approaches are just one part of the solution, and data management and analytics infrastructures will play a key role in optimizing for energy efficiency. In [1], the authors found that common database operations can exploit the full power range of a server and further detected that the CPU power consumption of different operators, for the same CPU utilization, can differ by as much as 60%. The authors stated that the most promising software knobs are the ones that can directly trade CPU cycles for disk access time, since these are two resources with significantly different power-usage profiles. Such trade-offs exist in access methods, compression techniques, and join algorithms. Given the increase in hardware heterogeneity in combination with energy proportionality, we can expect further opportunities here to identify optimal configurations; those should be exploited via specialized data management operators. For this purpose, we need an energy model that describes the different hardware resources with their interdependencies on the one hand and that comprises the

 ISBN: 978-1-61208-136-6

resource allocation of the different algorithms and methods on the other hand. First approaches in this regard with a focus on flash memory can be found in [6].

III. DSMS'S IN THE CONTEXT OF ENERGY ADAPTATION

A variety of research activities have already been directed towards different aspects of managing data streams: DSMS like Aurora [7], STREAM [8], PIPES [9], Gigascope [10], TelegraphCQ [11] and NiagaraCQ [12] represent major examples developed over the last years. Furthermore, there exists our QStream DSMS [13] where we already investigated quality-aware data streams using a hard real-time processing model. This model should be extended by an additional energy quality dimension.

The main characteristics of data streams normally do not allow the persistent storage and the subsequent time-consuming processing within a traditional data management system. Instead, the goal is a data-driven processing of the potentially unlimited data streams, where systems should behave adaptively, e.g., with regard to the current data arrival rates. That means, data must be provided as quickly as possible, in the sense of a data stream system and on the other hand, complex analyses are required, which necessitates storing large amounts of data. To materialize stream data, synopses are typically used, which will be briefly discussed in the next paragraph.

IV. ENERGY-AWARE DATA SYNOPSES

Gibbons et al. defined the term synopsis in [14] as a "random data structure" that is substantially smaller than the base data. Due to their small size, synopses come with various benefits: they can be managed in main memory, which decreases query processing time, and they can be transferred quickly within a storage hierarchy or via a network. Since synopses only represent a subset of the underlying data, query results often come with errors accordingly. However, it is possible to define exact bounds for these errors. All these features make synopses ideally suited for data analysis tasks in a DSMS. With constant synopsis size (footprint), it is thus possible to monitor data over a longer time period with little accuracy or to monitor them during short time intervals with high accuracy. In previous work [15, 16], the design of synopses was restricted to the preservation of certain memory sizes and error bounds. In our DSMS to be developed, we will consider the energy consumption as another optimization criterion when designing synopses. In this context, the energy consumption has to be considered from two perspectives: for storing and maintaining the synopses as well as for the query processing based on synopses. Furthermore, it will be decisive how many synopses have to be created and maintained for a certain workload. From the energy consumption point of view, we need to decide whether to create a few general or many specialized synopses.

V. ANYTIME ALGORITHMS

The synopses serve to buffer the stream of data and to represent it in a compact but lossy form. This allows speeding up the algorithms based on this data and to make their processing more energy-efficient. Another option to support energy efficiency is to leave out some iterations or computations within the data stream operators itself. This is possible with so-called anytime-algorithms, which trade computational resources for solution quality, i.e. the quality of the result improves with execution time. This requires a well-defined quality measure which allows to monitor the progress in problem solving and to allocate computational resources accordingly. Given this measure, it is possible to suspend the processing after a certain time period and to peek results which may not be in their final state (see Figure 1). Further it must be possible to resume the algorithm with minimal overhead.

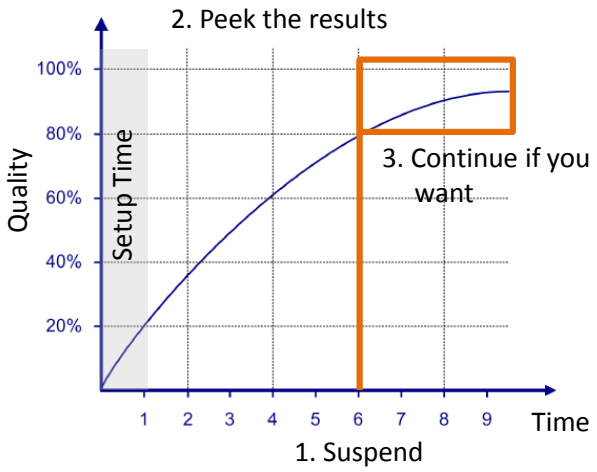

Figure 1. Anytime Processing Model

This characteristic makes them a perfect fit for an energy-efficient processing following the "need to know" principle. In particular, we will focus on anytime-data-mining algorithms, some of which have been documented in [17, 18], and on anytime-forecast algorithms. Obviously, the research work in both fields is very sparse, which implies that many algorithms need to be designed from scratch. For this purpose, we can rely on existing classifications and programming tools [19, 20] that provide an environment to support anytime-computation. This includes tools for the automatic construction of performance profiles (to quantify the performance improvement over time) as well as tools for composition, activation, and monitoring.

VI. RESEARCH GOALS

The broad range of software sensor data leads to many data streams that are pre-filtered through a set of sampling steps. The synopses are found on top of this sampling layer; they buffer and pre-aggregate data for detailed analyses. When doing so, a synopsis is always fed by one or multiple

 ISBN: 978-1-61208-136-6

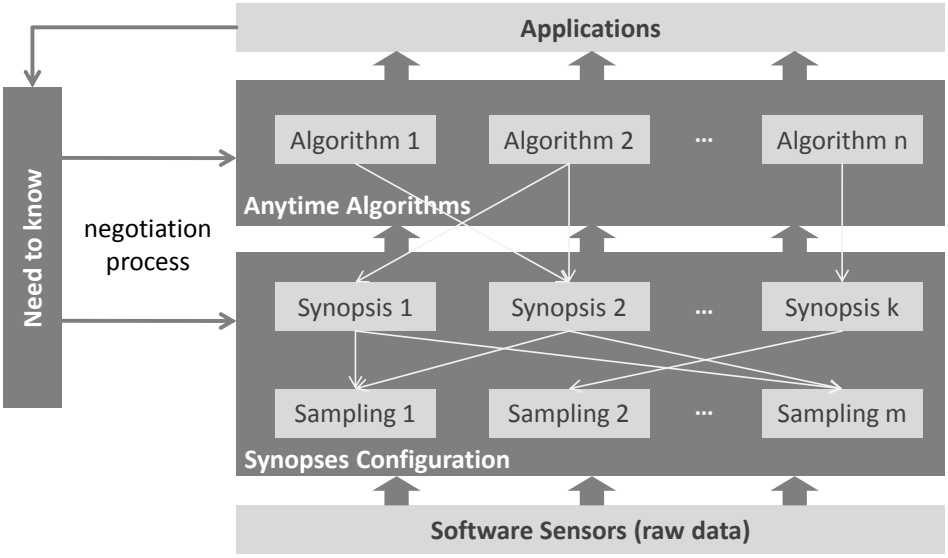

Figure 2. Data monitoring and processing following the "need-to-know"principle

sampling operators. In analogy to this, anytime-operators get their data from one or multiple synopses. All three layers are configured and controlled by the same "need-to-know" principles. In the following, we will present these ideas in detail.

A. *Formalization of the "need to know" principle as an enabler for energy-awareness*

The goal of this work package is to formalize the above mentioned "need-to-know" principle in order to specify the data quality constraints of the application layer. These constraints provide valuable help to optimize 1) the sampling preprocessing step, 2) the number, size and structure of the synopses, and the 3) algorithmic computation based on these synopses. Typical quality measures in a DSMS can be classified into time- and content-based metrics. The former indicates the DSMS's ability to adapt to the push-based data delivery and to the processing speed of the DSMS, e.g., throughput (or data rate) and the latency of the result. The latter focuses on problems caused by the handling of infinite streams or high input volumes. Content-based metrics that can be applied in this context are sampling rates, quality guarantees or error bounds. All these measures need to be reviewed and integrated into a common constraint model. Therefore, we need to check the interdependencies between these constraints and provide a declarative language that allows to express the specific requirements of the data consumers.

B. *Need-to-know" negotiation process*

In order to guarantee the "need-to-know" constraints a negotiation process is required that mediates between the application, the operation, and the synopsis layer (see Figure 2). In the first step, the capability for fulfilling the constraints need to be calculated locally on each layer and globally for the whole system. Therefore, we need to rely on data stream statistics that have to be collected during the runtime of the system. In a second step, the required resources (processing time at the operational level, space and I/O for the synopses, bandwidth for the sampling step, etc.) have to be reserved. If the statistics of the data stream do not change in any unforeseen manner, the required "need-to-know" constraints can be guaranteed. Otherwise, the negotiation process needs to be repeated.

C. *Data Stream Sampling*

The continuous data flow which need to be monitored calls for data stream sampling schemes as a pre-processing step (see Figure 2) to reduce or bound resource consumption. Although many techniques for maintaining database samples can also be used for data streams, there are problems that are unique to data stream sampling. The main difference in data stream sampling is that samples are often biased towards more recent items because recent items are considered more important by applications. Such a notion of recency does not exist in traditional database sampling and calls for novel sampling schemes. Additionally, since a data stream is changing continuously, efficient sample maintenance strategies must be developed as well.

D. *Synopsis Design and Configuration*

Synopses are necessary to materialize data stream content, which allows to apply a wide range of analytical operations such as outlier and trend detection, clustering, forecasts, and so on. Given a specific memory bound (footprint) and a set of "need-to-know" constraints, we want to derive the optimal synopsis configuration regarding energy-consumption. Since there is a many-to-many relationship between operations and synopses, we have to decide between general-purpose synopses, which may serve

 ISBN: 978-1-61208-136-6

a wide range of applications, and synopses designed for a very specific purpose. The design of the synopses must be coordinated with the previous sampling step, i.e. it has to be decided which data items will be pruned at the first level and which data items are considered to derive groups and aggregates at the second level. Another problem arises from the synopsis computation effort, which increases exponentially with the input parameters such as the number of relations or the number of grouping attributes. In order to keep the system load (and thus the energy consumption) for the computation and maintenance of synopses as low as possible, we will thus have to develop appropriate heuristics and greedy approaches.

E. Anytime-Algorithms

Whereas synopses restricted the storage consumption of the data, we also need new algorithmic approaches that make it possible to abort computations as early as possible. For this purpose, we want to look at the discipline of anytime-algorithms and transfer our findings to the "need-to-know" concept. That means that the underlying algorithms are not executed until they converge, but they are stopped as soon as the intermediate result fulfills the "need-to-know" constraints. These kind of algorithms, which continuously generate intermediate results, need to be developed for a broad range of application areas. Therefore, we have to perform research on algorithms whose runtime is not determined in advance but can be interrupted at any time during execution and return a result. Further, we have to work on performance profiles, which returns result quality (defined by the "need-to-know" negotiation process) as a function of time. As a starting point, we focus on clustering operations and, more precisely, on the k-means algorithm, which is widely used and well understood in the research community. In particular, there already exists a wavelet-based anytime-algorithm, which should be reviewed for its applicability [17]. This will give us first insights on how the "need-to-know" principle may interplay with the idea of anytime-algorithms.

Furthermore, we have to find the optimal configuration of the sampling steps (load shedding), the synopses (pre-aggregation), and the variety of analysis algorithms and operators.

VII. CONCLUSION

In this paper, we presented the concept of an energy-aware data stream management system. Therefore, we introduced the overall “need-to-know” principle which should be applied to each layer of the DSMS architecture. At the data layer we will use synopses to minimize the quantity and granularity of data. At the process level we will apply anytime operators which will allow us to prematurely abort the execution of operations as soon as a defined quality has been reached. Both concepts give us additional flexibility to build an adaptive and most of all an energy-aware DSMS.

REFERENCES

[1] Dimitris Tsirogiannis, Stavros Harizopoulos, and Mehul A. Shah. “Analyzing the energy efficiency of a database server,” In SIGMOD’10, pages 231–242, New York, NY, USA, 2010. ACM.

[2] Justin Meza, Mehul A. Shah, Parthasarathy Ranganathan, Mike Fitzner, and Judson Veazey. “Tracking the power in an enterprise decision support system,” In ISLPED’09, pages 261–266, New York, NY, USA, 2009. ACM.

[3] Willis Lang and Jignesh M. Patel. “Towards eco-friendly database management systems,” In CIDR, 2009.

[4] Zichen Xu. “Building a power-aware database management system,” In IDAR’10, pages 1–6, New York, NY, USA, 2010. ACM.

[5] Luiz André Barroso and Urs Hölzle. “The case for energy-proportional computing. Computer,” 40(12):33–37, 2007.

[6] Theo Härder, Karsten Schmidt, Yi Ou, and Sebastian Bächle. ”Towards Flash disk use in databases - keeping performance while saving energy?,” In BTW’09, pages 167–186, 2009.

[7] Nesime Tatbul, Ugur Çetintemel, Stan Zdonik, Mitch Cherniack, and Michael Stonebraker. “Load shedding in a data stream manager,” In VLDB’03, pages 309–320. VLDB Endowment, 2003.

[8] Brian Babcock, Mayur Datar, and Rajeev Motwani. “Load shedding for aggregation queries over data streams,” In ICDE’04, page 350, Washington, DC, USA, 2004. IEEE Computer Society.

[9] Jürgen Krämer and Bernhard Seeger. ”Pipes: a public infrastructure for processing and exploring streams,” In SIGMOD’04, pages 925–926, New York, NY, USA, 2004. ACM.

[10] Chuck Cranor, Theodore Johnson, Oliver Spataschek, and Vladislav Shkapenyuk. “Gigascope: a stream database for network applications,” In SIGMOD’03, pages 647–651, New York, NY, USA, 2003. ACM.

[11] Sirish Chandrasekaran, Owen Cooper, Amol Deshpande, Michael J. Franklin, Joseph M. Hellerstein, Wei Hong, Sailesh Krishnamurthy, Samuel R. Madden, Fred Reiss, and Mehul A. Shah. “Telegraphcq: continuous dataflow processing,” In SIGMOD’03, pages 668–668, New York, NY, USA, 2003. ACM.

[12] Jianjun Chen, David J. DeWitt, Feng Tian, and Yuan Wang. “Niagaracq: a scalable continuous query system for internet databases,” In SIGMOD’00, pages 379–390, New York, NY, USA, 2000. ACM.

[13] Sven Schmidt, Thomas Legler, Sebastian Schär, and Wolfgang Lehner. ”Robust real-time query processing with QStream,” In VLDB ’05, pages 1299–1301. VLDB Endowment, 2005.

[14] Phillip B. Gibbons and Yossi Matias. “Synopsis data structures for massive data sets,” In SODA ’99, pages 909–910, Philadelphia, PA, USA, 1999. Society for Industrial and Applied Mathematics.

[15] Rainer Gemulla, Wolfgang Lehner, and Peter J. Haas. ”A Dip in the Reservoir: Maintaining Sample Synopses of Evolving Datasets,” In VLDB’06, pages 595–606, 2006.

[16] Rainer Gemulla and Wolfgang Lehner. ”Sampling time-based sliding windows in bounded space,” In SIGMOD ’08, pages 379–392, New York, NY, USA, 2008. ACM.

[17] Michail Vlachos, Jessica Lin, Eamonn Keogh, and Dimitrios Gunopulos. “A wavelet-based anytime algorithm for k-means clustering of time series,” In In Proc. Workshop on Clustering High Dimensionality Data and Its Applications, pages 23–30, 2003.

[18] Philipp Kranen, Ira Assent, Corinna Baldauf, and Thomas Seidl. “Self-adaptive anytime stream clustering,” In Wei Wang, Hillol Kargupta, Sanjay Ranka, Philip S. Yu, and Xindong Wu, editors, ICDM’09, pages 249–258. IEEE Computer Society, 2009.

[19] Bei Hui, Ying Yang, and GeoUrey I. Webb. “Anytime classification for a pool of instances,” Mach. Learn., 77(1):61–102, 2009.

[20] Joshua Grass and Shlomo Zilberstein. “Anytime algorithm development tools,” SIGART Bull., 7(2):20–27, 1996.

 ISBN: 978-1-61208-136-6

Ubiquitous Smart Grid Control Solution based on a Next Generation Network as Integration Platform

Robin Acker, Nicolas Buchmann, Thorsten Fugmann, Christopher Knöll, Maximilian Porzelt and Michael Massoth
Department of Computer Science
Hochschule Darmstadt University of Applied Sciences
Darmstadt, Germany
e-mail*: nextfactor@h-da.de, michael.massoth@h-da.de*

Abstract—**This paper describes the architecture of an ubiquitous control solution for smart grids, distributed process control nodes, home automation and wide-area measurement systems. The proposed architecture is based on a next generation network as control and integration platform. Every network entity, like sensors, actors or process control nodes, has a Session Initiation Protocol Uniform Resource Identifier and presence status. The real-time, two-way information and process control communication between the network entities on the one side, and the grid and process control network operators or facility manager and house owners on the other side, will be realized via the Session Initiation Protocol and Presence Service. The main achievement of this paper is a detailed system design with a description of the used components and a first prototype implementation.**

Keywords - KNX; Home Automation; Next Generation Network; Presence Service; SIP.

I. INTRODUCTION

The current mega trend leads to smart cities and a more intelligent way of energy management. Every part of those cities, such as traffic control or smart grids is connected with each other and can be controlled from central points. Smart grids are intelligent electricity networks where suppliers and consumers are connected via a digital bidirectional communication. As a part of smart cities, smart buildings (facilities or houses) play an important role in this intelligent city management. The facility manager or owner can remotely monitor and control his house or facility where-ever and whenever he or she likes. A Smart Home should enable interaction with its owner, including the ability to monitor the status and control of home appliances and devices remotely from anywhere in the world. Such devices may consists of alarm systems, keyless access control, smoke detectors, light, heat, water or other energy management systems, medical devices, and all types of sensors, e.g., room, door, window or security surveillance, monitoring and control, statistics and remote metering to every automated system and appliance in the home.

A. Requirements

Smart grids, distributed process control networks, home automation and wide-area measurement systems should be able to identify and respond to man-made or natural disruptions. Grid and process control network operators should be able to isolate affected areas and redirect electric power flows around the damaged facilities. Facility manager and house owners should be able to react on abnormal energy consumption.

One of the most important issues is smart state monitoring of the power grids, which is basis of control and management of smart grids and distributed process control networks in order to avoid or mitigate the system-wide disruptions like blackouts. A real-time, two-way information and process control communication is essential key.

B. Purpose and Relevance

The purpose of this paper is to sketch a new approach and draft of a mobile ubiquitous home and facility control solution based on the Session Initiation Protocol (SIP) and Presence Service, to realize a near-real-time push solution. The described draft uses the advantages of the IP Multimedia Subsystem (IMS) to remotely monitor and control Home Automation Systems via a mobile device using open source licensed software. The IMS is standardized next generation network architecture to deliver IP-based multimedia (voice, video, and data) services across fixed and mobile networks.

According to Infonetics Research, the worldwide IMS equipment vendor revenue has reached US$ 426 million in 2009. The IMS equipment market, including IMS core and IMS application servers, continues to grow strong and healthy to US$ 1.44 billion in 2014 [11]. This promising forecast shows the business opportunity and relevance of the proposed draft for ubiquitous home control service.

C. Structure of the Paper

Following this introduction, Section 2 describes related work and further interesting projects suitable for this concept. In Section 3 and 4, an overview of the general approach is given. The components of a possible system design are discussed in Section 5. Section 6 details the system design. A view over the possible security functions is given in Section 7. Section 8 concludes the paper and gives an outlook of future work.

II. RELATED WORK

Smart Home Control is, of course, not such a new topic. Many companies and institutions are working on solutions for energy efficient management for buildings. But there are only a few who try to build a complete concept with open standards. Most systems focus on the inside or outside system of the building only. This means that the goal is to build a solution either for the management of actors and sensors, or to develop a good communication solution for existing bus systems.

 ISBN: 978-1-61208-136-6

The new idea is to connect the technology of Next Generation Networks (NGN) with Smart Home Control. The next step is to use SIP, with all its benefits, as the main communication protocol and connect it with a bus system standard (like KNX [15]) for the sensors and actors. Some approaches to this topic already exist.

For example, Schulzrinne et al. described how ubiquitous computing could be integrated into home networks [12]. For his approach he prefers SIP. Another approach was done by an IETF Working Group. The idea is based on the assumption that in the future every building is equipped with a full featured IP network. Therefore, SIP will be used for home control [8].

Another approach was made by the HomeSip project team [7][13][14]. Its goal is to create a SIP-based Home Control System. The important parts of the system are the SIP proxy and the SIP sensor network gateways. The SIP proxy is the central part for communication. The sensor network gateways are embedded Linux systems which are used to control the sensor networks and connect them with the SIP proxy. So, SIP should be used for communication between the sensor networks, the SIP proxy and the mobile controlling devices, like mobile phones or smartphones. All information from and to the sensor networks are transported via SIP.

III. CONCEPT

The big advantage and unique selling point of the IMS is the Presence Service which enables the control and integration platform to accept, store and distribute presence information about SIP identities. With this feature every sensor and actor, connected to the KNX bus which is described in Subsection 5.C., gets its own address (i.e., SIP URI) to log on to the service. After the registration the device can set its own current status, like “deactivated” or “active”. The sent KNX telegram is mapped to a SIP request and sent to the Presence Server. Now the user can monitor and even change the current settings on his mobile device.

IV. OVERALL SYSTEM DESIGN

The advantages of Next Generation Networks are used to build a communication platform between mobile devices and an intelligent building with a Home Automation solution. As depicted in Figure 1, a so-called “Gateway” interconnects the NGN core network and the Smart Home.

With the used standards a full near-real-time push solution for Home Automations status messages should be realized.

To interconnect the two architectures a special gateway (Bridge) is needed. The gateway manages connections between the SIP-based NGN and the single appliances of the Home Automation System. One significant function of the IP Multimedia Subsystem is the Presence Server, throughout it is possible to represent different Home Automation appliances as “users” to the Presence Server. Each “user” can set its own current status. Thus it is possible to register a mobile device at the SIP network, and in this way at the Presence Server. Hence, the status information of the different Home Automation appliances (i.e., the users) can be viewed on a mobile device.

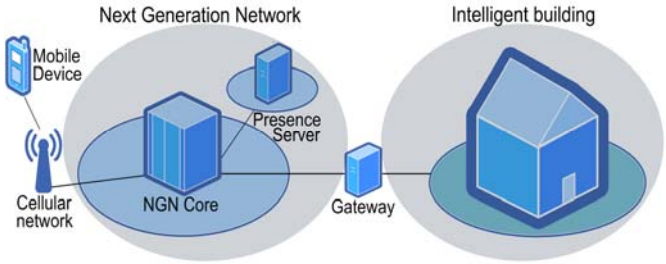

Figure 1: Overall system design (high level)

The gateway is responsible for updating the status information at the Presence Server. For example, any time a sensor in the Home Automation System changes its status, an update has to be sent by the gateway.

In order to control appliances in the Smart Home, such as switching lights on or off, a message must be sent by the mobile device to the specific Home Automation component. Therefore, a SIP message is generated and sent to the gateway, which forwards the information to the Home Automation System.

V. COMPONENTS

The following section introduces the components which are needed for the proposed concept.

A. Next Generation Network Core

To set up the NGN Core networks, we evaluated two Solutions to guarantee, that the Signaling Gateway is able to work with different NGN platforms.

The IP Multimedia Subsystem (IMS) [1] is a control architecture based on the standardized SIP [2] designed by the wireless standards body 3rd Generation Partnership Project (3GPP). It aims to standardize access to different networks. Therefore, all communication is based on the Internet Protocol (IP).

As lightweight solution to realize the NGN Core, a SIP Server with a Registrar and a Presence Service could be used. A common SIP server can also provide all the functionality which are needed to set up a SIP-based communication platform.

SIP is a signaling protocol for controlling multimedia communication. It can be used to create, modify, or terminate a multimedia session which can exist between two (unicast) or multiple parties (multicast).

With the Session Description Protocol (SDP) [3] properties of multimedia streams are described. SDP is used by SIP for negotiation regarding media codecs, transport protocols, and transport addresses.

SIP for Instant Messaging and Presence Leveraging Extensions (SIMPLE) [4] describes a presence and instant messaging protocol suite based on SIP.

Instant messaging enables users to communicate in near-real-time by text. For the Presence Service, a User Agent (UA) has to register at a Presence Server. The server acts as a Presence Agent. It stores the status of the UA. Other users

 ISBN: 978-1-61208-136-6

(subscribers) can subscribe to the UA's presence information. Every time when the UA changes its status, the subscribers will be notified near-real-time by the Presence Agent.

B. Sipdroid

Sipdroid 2.0 [5] is a VoIP client for the mobile operating system Android. The program is capable of establishing VoIP calls and sending messages over the network. The Protocol used is SIP.

C. KNX

KNX [9] is an open standard for Home Automation in intelligent buildings. In December 2003 KNX became European standard (CENELEC EN 50090, CEN EN 13321-1 and 13321-2). At the end of 2004 it was decided that the "European Norm" (EN 50090) should become international standard. In November 2006 the KNX protocol became ISO/IEC standard (ISO/IEC14543-3). The high interest in China led to adoption of the ISO/IEC 14543 standard to the Chinese norm (GB/Z 20965). Additionally for the US market there is the US standard (ANSI/ASHRAE 135).

KNX is the only open, internationally acknowledged standard for Home Automation and Intelligent Building Control.

The KNX standard is administrated by the KNX Association and supports the following communication media: Twisted pair wiring, powerline networking, radio, infrared and Ethernet (EIBnet/IP or KNXnet/IP).

KNX was invented in response to the following shortcomings: In conventional home installations, the control line and the powerline are not detachable. For example, normal lights are controlled by giving them energy or turning the energy off. Complex control mechanisms are hard to implement.

One of KNX's main features is that it detaches the control line from the power line. KNX is a dedicated control bus over which every connected device can exchange information with other devices. Devices of different manufacturers can communicate with each other if they fulfill the KNX standard and are certified by the KNX Association.

KNX devices are divided into "actors" and "sensors". An actor can be, for example, a device which can open or close a window or a device which controls the sunblind. Sensors can be polled for physical status information. For example a window's status can be open or closed, or a sensor for outdoor temperature can report back the temperature.

Many complex scenarios are possible. For example, with the help of an outdoor temperature sensor and sunlight intensity sensor a sunblind actor could control the sunblind depending on the data which the sensors deliver. Another scenario would be an actor for controlling an awning, combined with a wind strength sensor which would pull up the awning if the wind is to strong.

How the actors and sensors communicate with each other is specified in the KNX standard.

The KNX bus works with a 9.6 kbit/s transfer rate which is enough for more than 60,000 connected devices to the KNX bus.

Every device connected to the KNX network can be addressed with a unique 16-bit address, depicted in Figure 3. A KNX bus can theoretically have a maximum of 65,536 devices.

The topology of the KNX bus is based on lines. [10] In Figure 2 there is only one single Backbone Line. Up to 15 Main Lines can be connected to the Backbone Line, which are numbered from 1 to 15. The Backbone Line is Main Line 0. Main Lines are connected to the Backbone Line via Backbone Couplers. The Backbone Couplers belong to the Main Lines and not to the Backbone Line. A Backbone Coupler always has the Device-number 0.

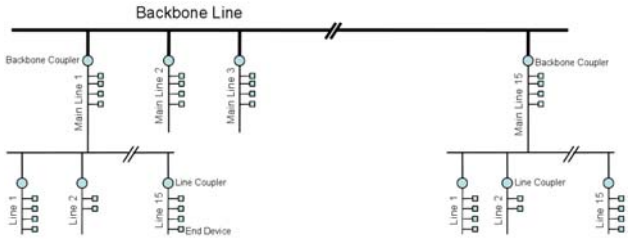

Figure 2: KNX bus topology

The hierarchical subordinates to the Main Lines are the lines. Every Main Line can have up to 15 lines which are numbered like the Main Lines from 1 to 15. A Main Line always has the line number 0. Just as Main Lines are connected with Backbone Couplers to the Backbone Line, Lines are connected to the Main Lines via Line Couplers.
A Line Coupler has the device number 0.

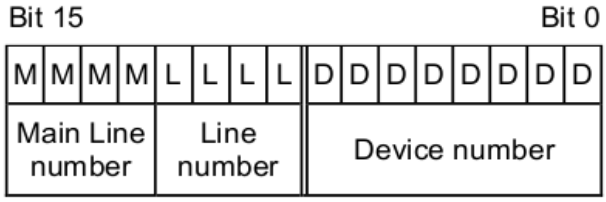

Figure 3: KNX address scheme

As depicted in Figure 3 the 16-bit Address is divided into 3 different fields: 4 Bits for addressing the Main Line, 4 Bits for addressing the appropriate line and 8 Bits for addressing the specific device. For example 3.8.10 addresses the 10th device connected to line number 8 at Main Line 3. Accordingly 0.0.4 addresses the 4th device directly connected to the Backbone Line. Consequently 4.0.10 addresses the 10th device connected to the 4th Main Line.

In conclusion, every line can have up to 255 devices, because device 0 is always the coupler. As seen in Figure 2, not only the lines are able to have connected devices, the Main Lines and the Backbone Line can respectively have up to 255 connected devices. By subtracting the reserved coupler addresses from the theoretical maximum of 65,536 devices, a maximum of 61,455 end devices are possible, which can be connected to a single KNX bus installation.

D. Calimero

Calimero 2.0 is a collection of Java APIs that form a high level framework for communication with a KNX/EIB

 ISBN: 978-1-61208-136-6

installation with the use of KNXnet/IP. The framework helps build high level applications which need to communicate with the KNX bus systems for remote access and control. It can receive/decode KNX messages and send/encode its own KNX messages.

E. Signaling Gateway

The signaling gateway, depicted in Figure 4, is the main part in this concept. This software service connects the KNX bus to the IMS network.

As already mentioned, with a KNXnet/IP device, KNX telegrams could be transferred to the IP network. The whole telegram is packed into the payload of an UDP packet and is sent over the network. Thus, one function of the signaling gateway is to receive these IP packets sent by the KNXnet/IP device. Further, the information contained in the telegram has to be extracted. This could consist of sensor values or other status messages of different Home Automation appliances.

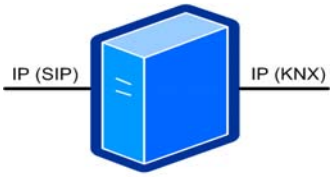

Figure 4: Connection interfaces of the signaling gateway

The KNXnet/IP device is also able to receive IP packets sent via the IMS from the IP network and forward the containing telegram to the KNX bus. Thus, in order to control appliances which are associated with the bus installation the signaling gateway has to have the ability to generate KNX telegrams.

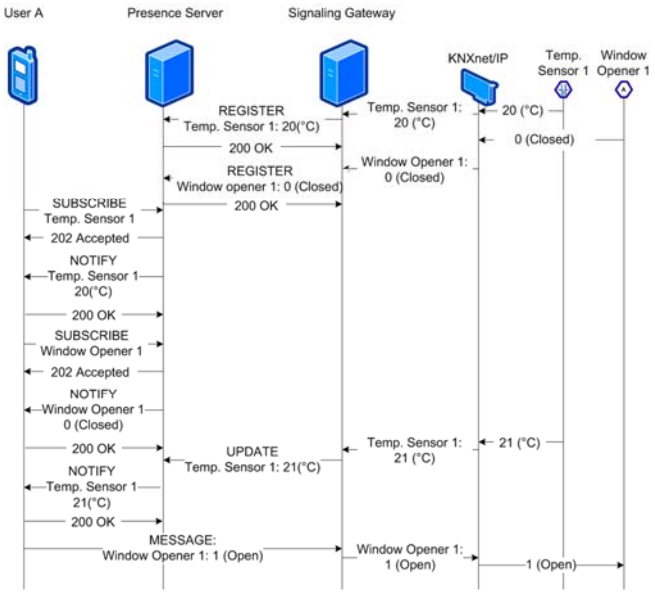

Figure 5: Message flow

With the open source Java Framework Calimero, it is possible to parse and generate KNX telegrams. This framework will be used in the signaling gateway to handle communication with the KNX bus.

Once the information of the telegram is filtered, the status change must be transmitted to the Presence Server located in the IMS. This brings out the second main function of the signaling gateway: The connection to the IMS. The signaling gateway registers every appliance of the KNX bus installation as a "user" at the Presence Server. To set the status of a user, a SIP message must be sent through the IMS network. This message flow is depicted in Figure 5. To view the current status of a part of the Home Automation System the mobile device just has to subscribe to the Presence Server.

If a user wants to control an appliance of the Home Automation System, a SIP message is sent from the mobile device to the signaling gateway. Further, the information in the SIP message body, depicted in Figure 6, must be mapped into a KNX telegram. This body is optional and can include e.g. SDP, SOAP, XML or ASCI.

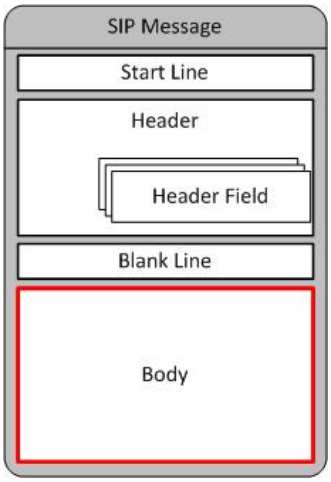

Figure 6: SIP message structure

VI. TECHNICAL FEASIBILITY

The intention of this concept is to use the advantages of the IP Multimedia Subsystem (IMS) and Presence Service in order to control Home Automation Systems, like the KNX bus installation, with a mobile device. KNX was chosen because it is the only open, internationally acknowledged standard for Home Automation and Intelligent Building Control.

A. Requirements

First of all, the IMS network infrastructure is needed, including the IMS core and application servers, as shown in Figure 7. The IMS core has the main functions of the IP Multimedia Subsystem like proxies and a user registration server. The application server in this case provides a Presence Service. The so called Presence Server handles a list of “users” and their own current statuses. Further, a mobile handset is needed that is capable of communicating with the IMS. To accomplish this, a special SIP User Agent

 ISBN: 978-1-61208-136-6

is required. In the next step a Home Automation System must be installed. In this concept the KNX automation system is used, also depicted in Figure 7. With this internationally standardized bus installation, it is possible to build up huge and powerful automation systems to control and monitor many different components in a building. With KNXnet/IP devices, status and control messages (telegrams) of the KNX bus can be transferred to IP networks. The most important part of this concept is the signaling gateway between the IMS network and the KNX bus installation

This software service provides the main functions for the communication between a mobile device and the Home Automation appliances.

B. *Overview*

The KNX bus installation implements the network connections and the addressing scheme for the different actors and sensors. Actors are appliances which can perform different actions, for example switching lights on or off. They provide a switching state and can receive telegrams from physical switches, sensors or software tools. Sensors are appliances which can detect different conditions like temperature or brightness. They are capable of sending telegrams to specific actors or software tools.

With the functions of the Presence Service of the IMS every sensor and actor of the KNX bus can be built up into a single “user” (entry in the Presence Service list). Therefore, each sensor or actor gets its own SIP address (URI) to register at the Presence Server. Every device which is registered to this service can set its own current status. Mainly this function is used to realize a service of messenger applications to set their own status in the contact list to “Not Available”, for example. In this concept we use the Presence Service to provide a list of all sensors and actors connected to the Home Automation System. Thus, every appliance sets its own status. For example the status of the temperature sensor may be 20.0°C.

Now it is possible for the user to get a list of his appliances displayed on his mobile device. For this purpose an SIP client is needed. Every SIP client also has a SIP URI to be identifiable in the IMS network. Making it possible to register to the Presence Server in order to view the list of appliances connected to the KNX bus installation.

With this system design a full push solution can be realized. The list of Home Automation appliances is updated automatically in real time. So there is no need to update the status of every single device manually.

This feature enables the ability to use the mobile device as a full alarm and critical state indicator. Thus, a push solution in mobile home control would give some whole new ways to use it.

The second step is to control different actors of the Home Automation System. To do this the user has to choose the specific actor and the operation which should be performed on the mobile device. The information is packed into a SIP message and sent through the IMS to the signaling gateway. The signaling gateway runs a user authentication to ensure the message was sent by an authorized mobile device. As shown in Figure 8, the information of the actor and the specific action of the SIP message is packed into a UDP packet and sent to the KNXnet/IP. Further, the KNXnet/IP device generates KNX telegram out of the UDP packet information and passes it to the bus installation. When the actor has performed the switching operation, the new status is sent to the Presence Server.

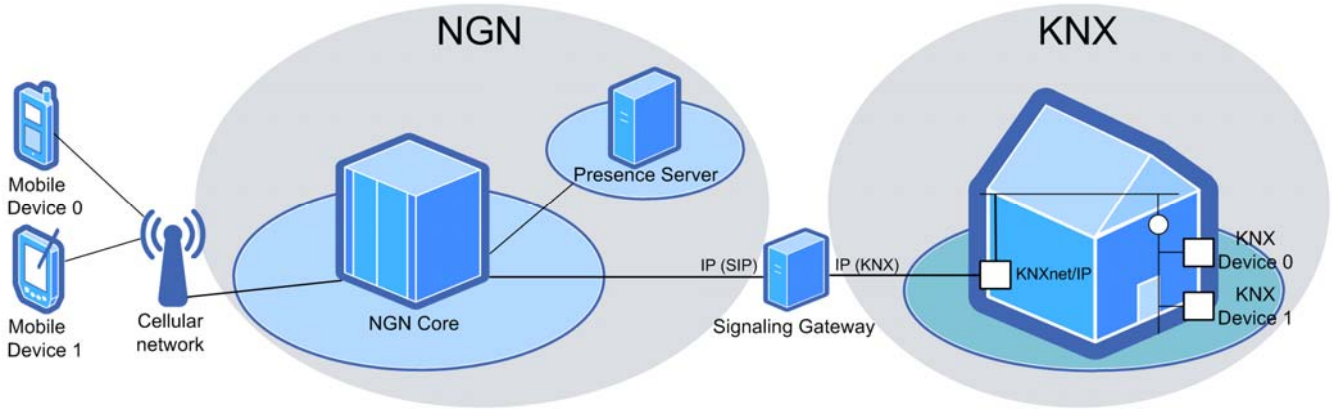

Figure 7: Detailed system design of the ubiquitous smart grid (home) control and integration platform prototype

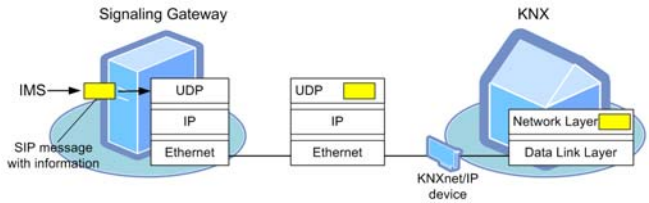

Figure 8: KNX telegram flow

VII. SECURITY

For a concept like this where communication over untrusted networks takes place, a strong security concept is important. To find a solution, the focus must set on two problems: The first is, of course, a secure connection

 ISBN: 978-1-61208-136-6

between the components. But on the other hand we have to think of the bandwidth usage and the computational workload. This is very important for mobile devices.

Therefore, one possible solution would be Multimedia Internet Keying (MIKEY) [6]. MIKEY is a key management solution for multimedia scenarios (e.g., SIP). The benefits are the simplicity, the low extra bandwidth consumption, the low computational workload and the time efficiency. So it is a well matching enhancement for the proposed concept to ensure an acceptable security level.

On the other hand KNX telegram security is also a must, due to local attacks on the KNX Bus. EIBsec is the common security extension for KNX [16]. The main goal of EIBsec is to protect the control network against local attacks. Services for providing a secure data transmission and authentication are included. The authentication mechanism allows verifying the identities of the involved communication partners including all sensors and actors. After proving the identities of the involved devices, the data are transmitted through a secure channel which guaranteed data confidentiality, integrity and freshness. The main advantage of EIBsec is that management services as well as the exchange of group messages can be secured. Another important feature of EIBsec is the compatibility to standard KNX protocol.

VIII. Actual Status of the Prototype

The actual prototype consists of a full addressed and configured KNX bus system with different kinds of sensors and actors like weather station, dimmers and digital/analog switches for lighting and power outlets. To communicate with the Signaling Gateway a KNX Net/IP device is also part of the KNX bus system. The Signaling Gateway is implemented as a converged application for a Glassfish Server. The application is based on the Sailfin (CAFE) extension and the Calimero 2.0 KNX-API, which provides functions to interact with the KNX bus. Sailfin offers the basis of a full featured Presence Service and SIP Call Control Functions. It is possible to connect the Signaling Gateway with an NGN core (e.g. Open IMS core) as an application server. With a standard SIP user agent for mobile devices (e.g. Sipdroid) it is possible to communicate with the Signaling Gateway to get status information of the KNX devices.

IX. Conclusion and Future Work

This paper presents a full concept of a ubiquitous home control solution, using the advantages of the IP Multimedia Subsystem, to realize a near-real-time push solution.

Our approach to the topic of Smart Home Automation is a different one. Instead of developing new commands for SIP or evolving a new kind of appliance, our approach only uses standards.

The achieved advantages are enormous. Many buildings all over the world already have a system to manage their buildings. Furthermore, an increasing amount of companies convert their network infrastructure to SIP (mostly because of VoIP). With our approach these two technologies can easily work together. The economical and ecological advantages are obvious: The system of the building can be managed remotely. A facility manager is able to manage more buildings, because he or she does not need to be at a single building most of the time. The ecological aspect of a smart home consists of enormous amounts of saved energy.

In future work, the first point is to create an own client for remote building control. It has to be platform independent, so it could be used on every mobile platform.

Next thing is to look at other bus-systems which are available. Maybe it is possible that the approach shown in this paper could also be used for other bus-systems.

Finally, new approaches to remote building control have to be checked. For example SIP extensions for communicating with networked appliances [8].

Acknowledgment

This work has been performed within the “Smart Home Control und Sensornetzwerke” project, which is partly funded by the “Zentrum für Forschung und Entwicklung” (ZFE) at the Hochschule Darmstadt - University of Applied Sciences, Darmstadt. Additionally the authors would like to acknowledge the support of the Albrecht JUNG GmbH & Co. KG by their contribution of KNX actors, sensors and other KNX home automation devices.

References

[1] J. Soininen (Ed.), “Transition scenarios for 3gpp networks,” IETF, RFC 3574, Aug. 2003.

[2] J. Rosenberg, H. Schulzrinne, G.Camarillo, A. Johnston, J. Peterson, R. Sparks, M. Handley and E. Schooler, “SIP: session initiation protocol,” IETF, RFC 3261, Jun. 2002.

[3] M. Handley, V. Jacobson, and C. Perkins, “SDP: session description protocol,” IETF, RFC 4566, Jul. 2006.

[4] SIP for Instant Messaging and Presence Leveraging Extensions (SIMPLE). IETF Working Group.

[5] sipdroid, http://sipdroid.org 10.12.2010.

[6] J. Arkko, E. Carrara, F. Lindholm, M. Naslund, and K. Norrman, “MIKey: multimedia internet keying,” IETF, RFC 3830, Aug. 2004.

[7] HomeSIP Project, http://www.enseirb.fr/cosynux/HomeSIP/ 10.12.2010.

[8] S. Moyer, D. Marples, S. Tsang, J. Katz, P. Gurung, T. Cheng, A. Dutta, H. Schulzrinne, and Roychowdhury, “Framework draft for networked appliances using the session initiation protocol,” IETF, Internet Draft, expired Dec. 2001.

[9] KNX Association, “KNX logical topology faq,” 2005.

[10] KNX Association, “KNX system specifications,” 2009.

[11] Infonetics Research, “IMS equipment and subscribers report”, Mar. 2010.

[12] H. Schulzrinne, X. Wu, and S. Sidiroglou, and S. Berger, “Ubiquitous computing in home networks,” IEEE Communications Magazine, vol. 41, Nov. 2003, pp. 128-135, doi: 10.1109/MCOM.2003.1244933.

[13] B, Bertran, C. Consel, P. Kadionik, and B. Lamer, “A sip-based Home Automation platform: an experimental study,” Proc. 13th International Conference on Intelligence in Next Generation Networks, 2009 (ICIN 2009), IEEE Press, Oct. 2009, pp. 1-6, doi: 10.1109/ICIN.2009.5357075.

[14] C. Bertran, C. Consel, W. Jouve, H. Guan, and P. Kadionik, “SIP as a universal communication bus: a methodology and an experimental study,” Proc. 2010 IEEE International Conference on In Communications (ICC 10), IEEE Press, Jul. 2010, pp. 1-5, doi: 10.1109/ICC.2010.5502591.

[15] KNX Association , http://www.knx.org/knx-standard/standardisation/ 10.12.2011.

[16] Granzer, Kastner, Neugschwandtner “EIBsec: A Security Extension to KNX” KNX Scientific Conference 2006

 ISBN: 978-1-61208-136-6

Controlling a group of microCHPs: planning and realization

Maurice G.C. Bosman, Vincent Bakker, Albert Molderink, Johann L. Hurink, Gerard J.M. Smit

Department of Electrical Engineering, Mathematics and Computer Science
University of Twente
P.O. Box 217, 7500 AE, Enschede, The Netherlands
{m.g.c.bosman,v.bakker,a.molderink,j.l.hurink,g.j.m.smit}@utwente.nl

***Abstract*—This paper discusses the planning problem of a group of domestic Combined Heat and Power (microCHP) appliances, which together form a Virtual Power Plant (VPP). To act on an electricity trading market, this VPP has to specify a production plan for electricity for given times of the day to offer to this market. These amounts have to be delivered exactly when these times arrive; moreover, deviations from these contracts are penalized for. We focus on the planning of individual microCHPs for one day ahead, given that the aggregated output of the group should fulfill a desired production pattern that the VPP wants to offer on the market. The contribution in this context is twofold. Firstly, we present a planning approach based on column generation which calculates for all individual appliances production patterns. The production patterns are calculated such that the deviation of the agregated pattern of all appliances from a prespecified pattern is minimized. Secondly, we investigate how a desired pattern for the group can be specified based on global parameters and which patterns can be realized afterwards by the developed planning approach. In this way we get insight what kind of pattern may be offered on the market. The presented results show that we can find near optimal solutions using a column generation technique and that we can offer patterns with large variation on the market, as long as the running average does not deviate too much from the possible production.**

Keywords - ***column generation; scheduling***

I. INTRODUCTION

During the last years the electricity supply chain (the production, consumption, distribution, storage and load management of electricity) has changed. Important aspects in this change are the increase of the availability of renewable energy sources, the development of distributed electricity generators and the demand for more energy efficient appliances [1].

A specific type of upcoming distributed electricity generators is microCHP (Combined Heat and Power on a domestic scale). When running, a microCHP produces both heat and electricity for household usage at the kW level. The produced electricity can be delivered back to the electricity grid or consumed locally. The control of the microCHP is heat led, meaning that the heat demand of the building defines the possible production of heat and, simultaneously, the possible electricity output. Combined with a heat buffer, the production of heat and electricity can be decoupled to some extent and an operator has flexibility in the times that the microCHP is producing, which creates a certain degree of freedom in electricity production. This freedom of electricity production may be used to increase stability in the grid, on a large scale it may allow to replace a conventional power plant, and more. To effect these possibilities the individual microCHPs need to be controlled, as standalone devices, but also in cooperation with other microCHPs or generators in a so-called Virtual Power Plant (VPP) (see for a German example [2]). For possible methodologies of the control of a VPP we refer to [3], [4] and [5].

The production of a VPP can be traded on different markets, from which the day-ahead electricity trading market is one option. To act on this market, the VPP has to provide an offer a day ahead and has to matched this offer in real-time by the group of generators the next day. In this paper we investigate for a fleet of microCHPs how to 1) use a good day ahead planning to provide and afterwards match an offered production and 2) derive a simple guideline on how such an offer could look like.

The paper is organized as follows. In Section II, an introduction on the electricity trading market and on column generation is given. Section III gives a more detailed formulation of the considered problem, the way column generation is applied to it and a derivation of a lower bound on the quality of the achieved solutions. In Section IV, a scenario is proposed; results are given in Section V. The paper ends with some conclusions and future work.

II. RESEARCH FOCUS

The research in this paper focuses on the application of a column generation technique to find a planning for a group of microCHPs to reach a prespecified production pattern on the electricity trading market. To understand the idea of the planning problem, first a short introduction of the relevant electricity market is given. Then the general idea of the column generation approach is explained.

A. Electricity trading market

For electricity trading many different type of markets exist around the world, ranging from long term trading up to real-time balancing. For the setting considered in this paper, mainly the day ahead markets are of interest, i.e. the markets where electricity is traded for one day ahead, e.g., [6], [7]. In this market electricity is traded on an hourly basis, whereas on

 ISBN: 978-1-61208-136-6

intraday (balancing) markets trade is on a 15 minute basis [6]. Bids can be made for specific hours and on blocks of consecutive hours. The electricity is traded in multiples of 100 kWh. When the market is cleared, the blocks that were traded need to be generated on the next day as specified in the contracts. Penalty costs are incurred when the contracts cannot be supplied.

B. Column generation

In this paper we apply a general method called column generation to find a good solution for our specific optimization problem in reasonable computation time. The idea of column generation is to divide the given problem in two parts: a main problem and (a) sub problem(s). The main problem consists in principle of the original problem but reduced to a small part of the solution space, indicated by a set of solution vectors, the so-called 'columns'. Based on the solution for this (restricted) main problem, new columns are added to the solution space, as long as they improve the objective value of the main problem. In the sub problem(s) the new columns are found, by optimizing on the added value of the new columns, taking into account the current solution of the main problem.

Column generation is widely applied in practice. An example of the use of this technique is given in [8], where it is applied to solve the Cutting Stock Problem. It has also been used to solve the Vehicle Routing Problem, as in [9].

III. Approach

The planning problem for a group of microCHPs on the one hand focuses on the individual control of the microCHPs, installed in (small) buildings, satisfying the local (household) constraints, but on the other hand aims at achieving an aggregated electricity output of the group which can be traded on a day ahead market and, thus, has to fulfill specified requirements. In general, this problem is NP-complete in the strong sense [10].

A concrete formulation of the problem is given in Section III-A. Next, a column generation technique is explained in Section III-B, which is a heuristic method that is used to solve the problem in reasonable computation time. Finally, in Section III-C lower bounds are derived for the problem, to analyze the quality of the developed heuristic method and to analyze the impact of choices for a specific offer on the electricity trading market.

A. Problem formulation

The main objective for a VPP, when acting on a market, is to maximize its profit (or revenue). For this, the VPP has to decide on which times of the day it wants to produce how much electricity. The overall amount of electricity a VPP consisting of a group of microCHPs can offer to the market is limited by the individual production capacities of the microCHPs. These can be calculated based on predictions of the local heat demand. However, for trading, not only the overall capacity of the VPP but it's deviation over the time periods of a day needs to be specified to be able to act on the day ahead market. For this, a planning of the production of all individual microCHP's is needed. This planning may be steered by bounds on the overall production profile, whereby these bounds result from possible ways to act on the market.

A feasible planning of a microCHP naturally should respect the individual heat demand within the building where the microCHP has been installed. In addition, the total electricity production should be within the given bounds resulting from possible actions on the market. The goal of the planning problem in this paper is to find such a feasible planning, in contrast to a planning with the objective of maximizing profit in the market.

Let microCHPs $i = 1, \ldots, N$ be given and let the time horizon of 24 hours be discretized in time intervals $j = 1, \ldots, N_T$. Furthermore, let P be the set of possible binary production patterns for the type of microCHP that is used. These patterns do not take into account heat demand requirements or total desired electricity production, but include the (technical) restrictions of the microCHP. Note that the set P can be extremely large.

In general, the offered bounds on the market (i.e., the desired production pattern) are represented by upper and lower bound vectors $P^{upper} = (P_1^{upper}, \ldots, P_{N_T}^{upper})$ and $P^{lower} = (P_1^{lower}, \ldots, P_{N_T}^{lower})$. These vectors specify per time period a lower and upper bound on the total production of the microCHPs that should be generated during that time period. A pattern $p \in P$ for a microCHP is defined as a binary vector $p = (p_1, \ldots, p_{N_T})$ where $p_j \in \{0, 1\}$ specifies whether the microCHP is on or off. The problem is to pick exactly one pattern for each microCHP, such that the sum of all production patterns falls between the lower and upper bound of the desired production pattern in all time intervals. For this, let $F_i \subset P$ be a subset of all possible production patterns that takes the local heat demand into account of the building where microCHP i is installed, in case that a heat buffer is used. Thus, this set specifies the locally feasible patterns for microCHP i. The choice for using this set is explained in Section III-B, where we restrict ourselves to solving the problem by only using those production patterns that can supply the heat demand.

The planning problem for the VPP now can be formulated by the following Integer Linear Program (ILP):

$$\min \sum_{j=1}^{N_T} (sl_j + ex_j) \tag{1}$$

$$\sum_{i=1}^{N} \sum_{p \in F_i} p_j y_{ip} + sl_j \geq P_j^{lower} \quad j = 1, \ldots, N_T \tag{2}$$

$$\sum_{i=1}^{N} \sum_{p \in F_i} p_j y_{ip} - ex_j \leq P_j^{upper} \quad j = 1, \ldots, N_T \tag{3}$$

$$\sum_{p \in P} y_{ip} = 1 \qquad i = 1, \ldots, N \tag{4}$$

$$sl_j, ex_j \geq 0 \qquad j = 1, \ldots, N_T \tag{5}$$

$$y_{ip} \in \{0, 1\}, \tag{6}$$

where y_{ip} is a binary decision variable indicating whether pattern $p \in P$ is chosen for generator i (in this case $y_{ip} = 1$)

or not ($y_{ip} = 0$). In Equations (2) and (3) slack and excess variables sl_j and ex_j are introduced to calculate the deviation from the desired (and predefined) production pattern (P^{upper}, P^{lower}). The sum of slack and excess variables is minimized in Equation (1). Finally, Equation (4) requires that exactly one pattern is chosen for each generator.

A feasible planning is achieved when the sum of slack and excess variables equals 0. If no feasible planning can be found, the objective value is a measure of the deviation from the desired production pattern.

B. Column generation

The problem formulated by equations (1)-(6) takes into account locally feasible production patterns from the sets F_i. These sets however are still very large and, therefore, it is already difficult to solve the problem for instances with 10 microCHPs if all possible patterns are added to the sets F_i [11]. For this reason a column generation technique is applied.

The column generation technique starts with a relatively small set of feasible patterns $S_i \subset F_i$ for each microCHP i. By looking at only a small set of patterns the problem can be solved relatively fast. However, this comes with a possible loss of patterns that are necessary for a high quality solution. The VPP might perform better, when some feasible production patterns from F_i not in S_i would be added to the set S_i. Unfortunately, we do not know on beforehand which patterns are useful in the final solution. Therefore it is the idea of the column generation technique to improve the current solution step by step, by searching for those patterns which promise to improve the current solution, and by adding these patterns to the (small) feasible pattern sets S_i of the corresponding microCHPs. We have chosen to expand the pattern set S_i by at most one pattern per iteration as the heuristic evolves.

The column generation technique uses a main problem and sub problems as indicated in Algorithm 1. The main problem is similar to equations (1)-(6), with the only difference that the set F_i is replaced by S_i:

$$\min \sum_{j=1}^{N_T} (sl_j + ex_j) \tag{7}$$

$$\sum_{i=1}^{N} \sum_{p \in S_i} p_j y_{ip} + sl_j \geq P_j^{lower} \quad j = 1, \ldots, N_T \tag{8}$$

$$\sum_{i=1}^{N} \sum_{p \in S_i} p_j y_{ip} - ex_j \leq P_j^{upper} \quad j = 1, \ldots, N_T \tag{9}$$

$$\sum_{p \in P} y_{ip} = 1 \qquad i = 1, \ldots, N \tag{10}$$

$$sl_j, ex_j \geq 0 \qquad j = 1, \ldots, N_T \tag{11}$$

$$y_{ip} \in \{0, 1\}. \tag{12}$$

The second phase of the column generation technique consists of creating new patterns that can be added to the current pattern sets S_i for each microCHP in the main problem. These new patterns should contribute to the existing sets in the sense that they must give possibilities to decrease the objective value in the first phase (i.e., the sum of slack and excess). A new pattern p is only added to S_i if it 1) promises to improves the existing solution and 2) is a locally feasible pattern ($p \in F_i$).

Let λ_j represent the shadow prices for equations (8) and (9), obtained from the optimal dual solution of the linear relaxation of (7)-(12). A pattern p only may improve the existing relaxed solution if:

$$\sum_{j=1}^{N_T} \lambda_j p_j > 1. \tag{13}$$

However, this does not necessarily mean that this pattern can be automatically selected in the new solution of the main problem, since newly added patterns of other microCHPs (by solving these sub problems) can lead to different choices for this specific microCHP. As a consequence, the main problem has to be solved for the new sets S_i completely in each iteration.

The second requirement (p is locally feasible) has not been formalized yet. The reason for this is that the constraints that we use for forcing this requirement are only used in the sub problem of the column generation technique. For the main problem it suffices to know that the patterns have been checked for feasibility before; these feasible patterns are given input data for the main problem. The feasibility check is controlled by using two parameter sets, specifying in each interval j the minimum production the microCHP generator i should have generated ($MinOn_{ij}$) and the maximum production the generator could have generated ($MaxOn_{ij}$) up to and including the current interval. These parameters $MinOn_{i,j}$ and $MaxOn_{i,j}$ are fixed in such a way that they fulfill technical runtime/off-time constraints of the microCHP and the heat demand requirements of the building (for details see [10]). Startup and shutdown phases are neglected.

Summarizing, the sub problems of the column generation are given by the following ILP formulation for all microCHPs i:

$$\max \sum_{j=1}^{N_T} \lambda_j p_j \tag{14}$$

$$\sum_{k=1}^{j} p_k \leq MaxOn_{ij} \quad j = 1, \ldots, N_T \tag{15}$$

$$\sum_{k=1}^{j} p_k \geq MinOn_{ij} \quad j = 1, \ldots, N_T \tag{16}$$

$$p_j \in \{0, 1\} \qquad j = 1, \ldots, N_T, \tag{17}$$

where from all locally feasible patterns the one is chosen that maximizes the added value to the main problem. If constraint (13) is satisfied, the pattern p is added to the set S_i.

To summarize, the solution method is given in Algorithm 1. In each iteration, the main problem is solved first, after which for each microCHP the sub problem is solved and new feasible and improving patterns are added. If at least one sub problem leads to an improvement, the routine is repeated.

C. Lower bound of the objective

The lower and upper bounds P^{lower} and P^{upper} (representing the desired production pattern) and the possible production bounds $MaxOn_i$ and $MinOn_i$ form the basic input

 ISBN: 978-1-61208-136-6

Algorithm 1 Column generation

```
init S_i for all i; finished ← false
while not finished do
  finished ← true
  solve main problem
  for all i do
    p ← optimal solution of sub problem i
    if Σ_{j=1}^{N_T} λ_j p_j > 1 then
      S_i ← S_i ∪ p;
      finished ← false
    end if
  end for
end while
```

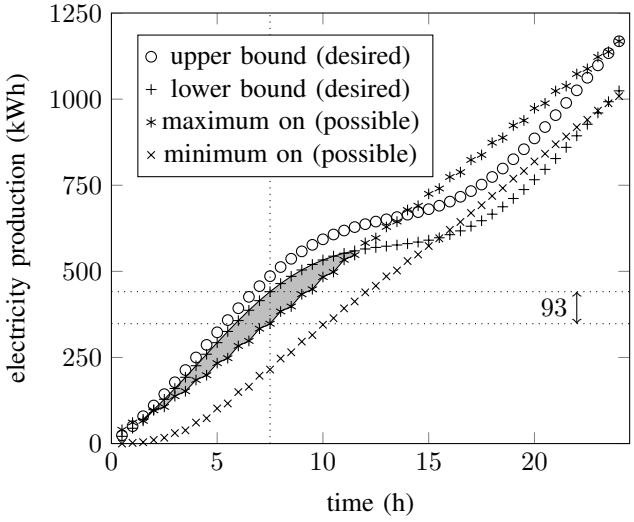

(a) The total desired production and the total possible production result in a first phase lower bound

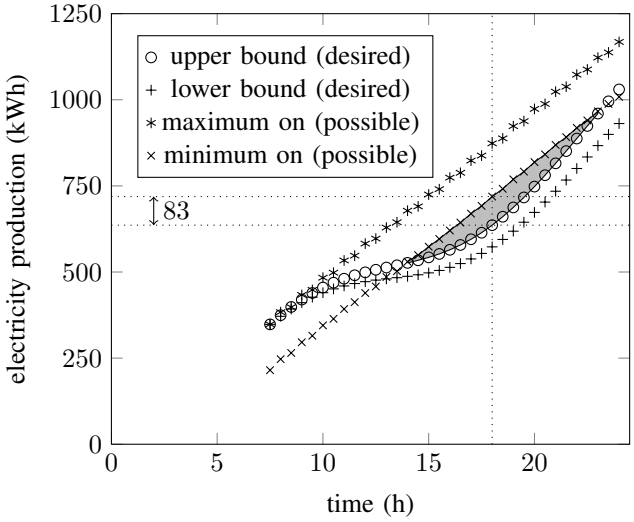

(b) The second phase of the lower bound calculation and the resulting lower bound improvement

Fig. 1. The calculation of the lower bound of the group planning problem

parameters of a problem instance. To derive a lower bound z_{LB} for the objective of the main problem, we concentrate on these parameters. Since we have a minimization problem and the sum of slack and excess variables cannot be negative, the theoretical lower bound z_{LB} is at least 0.

The calculation of the lower bound works in phases. In each phase a minimal guaranteed mismatch (slack or excess) z_{LB}^{extra} is found and added to the current lower bound.

In the first phase, the additional value of the lower bound z_{LB}^{extra} equals:

$$z_{LB}^{extra} = \max_j \begin{cases} \sum_{k=1}^{j} P_k^{lower} - \sum_i MaxOn_{ij} \\ \sum_i MinOn_{i,j} - \sum_{k=1}^{j} P_k^{upper} \\ 0. \end{cases} \quad (18)$$

This value equals the maximum deviation of the aggregated possible production from the aggregated desired production pattern. An example of this phase is shown in Figure 1(a), where the aggregated minimal mismatch per time interval is given by the gray area. In this example, the maximum difference between the maximal possible production and the minimal desired production is found at time 7.5, with a value of 93. So, in this example, the lower bound has now improved from 0 to 93.

The first value of j for which z_{LB}^{extra} is found is the starting point r for the calculation of the next phase. This starting point is important in two ways. First, the mismatch in previous intervals cannot be undone, if we only look at intervals $j > r$. Secondly, the starting point r offers a natural reset point; the sum of desired maximum (minimum) production upto and including interval r can be replaced by the maximum (minimum) possible production upto and including interval r. Other reset values either are not allowed (these total productions are not possible at r) or would increase the value of z_{LB}^{extra}. Considering the second option, these values do not represent the lower bound, since the chosen reset values are reachable (at least in the lower bound calculation) and give a smaller mismatch. So, $\sum_{k=1}^{j} P_k^{lower}$ is replaced by $\sum_i MinOn_{i,r} + \sum_{k=r+1}^{j} P_k^{lower}$ and $\sum_{k=1}^{j} P_k^{upper}$ by $\sum_i MaxOn_{i,r} + \sum_{k=r+1}^{j} P_k^{upper}$, and we look for mismatch in the future (time intervals $j > r$):

$$z_{LB}^{extra} = \max_{j>r} \begin{cases} (\sum_i MinOn_{ir} + \sum_{k=r+1}^{j} P_k^{lower}) - \sum_i MaxOn_{ij} \\ \sum_i MinOn_{ij} - (\sum_i MaxOn_{ir} + \sum_{k=r+1}^{j} P_k^{upper}) \\ 0. \end{cases} \quad (19)$$

In the example, the second phase calculation is shown in Figure 1(b), where an additional lower bound z_{LB}^{extra} of 83 is found. The lower bound is now: $z_{LB} = 93 + 83 = 176$.

 ISBN: 978-1-61208-136-6

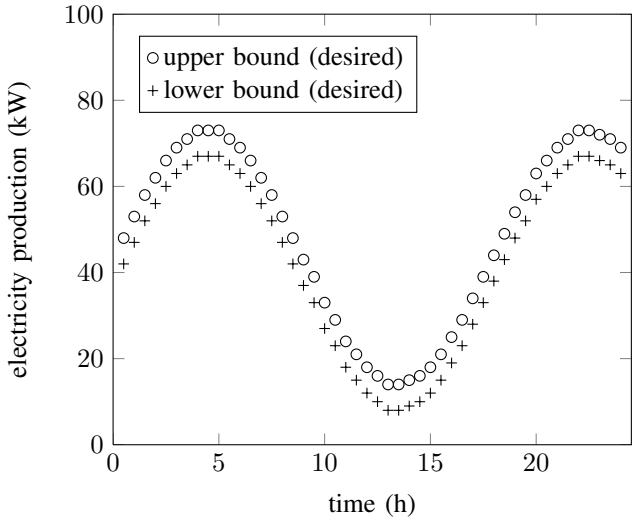

Fig. 2. An example of a desired production pattern; a sine with amplitude 30 and period 18

IV. SCENARIO

In this section, some computational results achieved with the presented approach are given. For this, a scenario is set up to answer two kinds of problems. First, the defined instances should provide a framework to test the quality of the column generation technique. Secondly, the instances should give an indication of the type of pattern that qualifies for being offered on the electricity trading market.

To support both questions, we focus on variation in the offered/desired patterns and keep the possible total production constant. The variation is created by adding a sine function to a constaint profile, where we vary both amplitude and period of the sine function, i.e. the sine function characterizes the variation of the profile.

The instances consist of a group of 100 microCHPs and a discretization of the one day time horizon into 48 time intervals. Although this group size is too small to be able to act on the electricity market at the moment (microCHPs generates at the 1 kW level), this size already gives a good indication of the possibilities of the planning method. Decisions are made on an half an hour basis. The discretization in half hour periods is more fine grained than required, since the day ahead electricity market works on an hourly basis, however, for this granulation the planning problem gets more realistic (and more difficult). If needed, the production patterns can be simply converted to hourly blocks.

The maximum and minimum possible production $MaxOn_i$ and $MinOn_i$ are chosen to differ per microCHP, i.e. the heat demand differs per building. The aggregated values of all microCHPs are already given in Figure 1.

The initial patterns in the sets S_i are derived from the parameters $MaxOn_i$ and $MinOn_i$. Each microCHP sub problem starts with two patterns, one resulting from the earliest possible time intervals that the microCHP can be switched on, and one resulting from the latest possible time intervals that the microCHP has to be switched on.

Upper and lower bounds of the desired production are defined as follows. The upper bound P^{upper} is derived from the highest integer value of μ^{upper} for which a given amplitude amp and period per result in a total desired production that is still feasible, when only looking at the total possible production:

$$\max \mu^{upper} \tag{20}$$

$$\sum_j P_j^{upper} \leq \sum_i MaxOn_{i,N_T} \tag{21}$$

$$P_j^{upper} = rnd(amp \times \sin(f(per) \times j)) + \mu^{upper} \forall j, \tag{22}$$

where $f(per)$ is the frequency corresponding to the given period per and $rnd()$ is a rounding function. Likewise, the lower bound P^{lower} results from the lowest sine curve fitting in the possible minimum production:

$$\min \mu^{lower} \tag{23}$$

$$\sum_j P_j^{lower} \geq \sum_i MinOn_{i,N_T} \tag{24}$$

$$P_j^{lower} = rnd(amp \times \sin(f(per) \times j)) + \mu^{lower} \forall j. \tag{25}$$

Looking at the final time interval in Figure 1(a), we can conclude that the lower and upper bound of the example fit within the possible total production domain. Figure 2 gives the corresponding resulting individual values.

Based on the above, an instance is defined as a pair $I(amp, per)$ and a solution can be characterized by a tuple $(I(amp, per), z_{LB}, z_{found})$. For this paper, we choose $amp \in \{0, 1, \ldots, 40\}$ and $per \in \{2, 3, \ldots, 24\}$.

V. RESULTS

Figure 3 shows the lower bound and the best found solutions for the defined instances. The lower bound is plotted as a surface plot, whereas the found solutions are given as dots in the figure. For the example used throughout this paper, the found optimization value is 176.5, whereas the lower bound is 176, close to the lower bound.

In general, the column generation technique finds solutions, which are close to the derived lower bounds of the objective value. This means that when the total production capacity of the microCHPs is known and the variations on the average production per time interval is not to extreme, the column generation technique can find actual assignments of individual patterns to match the pattern. However, for small amplitudes the difference between the lower bound and the found value can be relatively large. The inability to find better patterns for these instances is probably due to the simple choice for the initial patterns in the sets S_i.

Regarding the quality of the eventual production pattern, Figure 3 shows that the period has the most influence on the deviation from the desired pattern. For small periods, the mismatch stays relatively low, even for large values of the amplitude. This indicates that we may use large variation in our market offer, as long as the sum of positive and negative deviations from the possible production is close to zero.

 ISBN: 978-1-61208-136-6

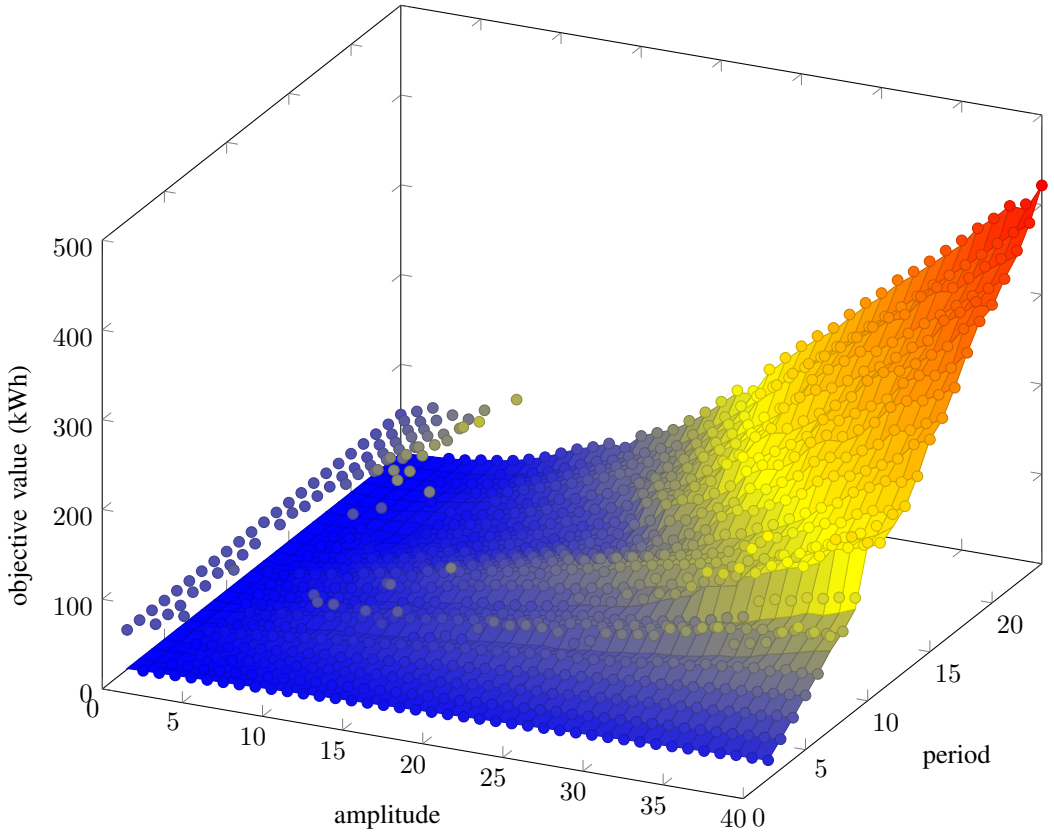

Fig. 3. Calculated lower bounds and solutions derived from the column generation technique, for sines with varying amplitude and period

VI. Concluding Remarks and Recommendations

In this paper, we have presented an application of the column generation technique to the planning problem of a group of microCHPs. This technique finds near optimal solutions for a large fraction of the defined instances. It is possible to specify in advance a desired output pattern, which is calculated based only on global parameters, and afterwards create individual patterns which combine to an output of the whole group, which is close to the desired output. This enables the group to act on the electricity trading market by only using global information.

As a guideline to what kind of production pattern the group should offer on the market, we can state the following: large variations may occur, as long as they are 'corrected' in close-by intervals. In other words, we can offer patterns with large variation on the market, as long as the running average does not deviate too much from the possible production.

Future work - In future work, the influence of the initial pattern set on the resulting quality of the overall solution should be investigated. We believe that by a better choice the results also for small amplitudes improve.

In the current implementation of the column generation technique we neglected startup and shutdown times, opposite to the work in [11]. It is of interest to see the impact of adding these requirements, which results in a more accurate modeling of the electricity production.

Finally, to be able to trade on a real market, the group size has to increase. It has to be validated if the proposed planning method also works for these larger groups.

VII. Acknowledgements

This research is conducted within the SFEER project (07937) supported by STW, Essent and GasTerra.

References

[1] J. Scott and F. Vaessen, P. andVerheij, "Reflections on smart grids for the future," in *KEMA consultancy document for the Dutch Ministry of Economic Affairs*, 2008.

[2] Lichtblick, "Zuhausekraftwerk: die intelligenz des schwarms." Lichtblick ZuhauseKraftwerk GmbH, 2009.

[3] H. Hassenmueller, "Power in numbers," in *Pictures of the Future, the Magazine for Research and Innovation*. Siemens, 2009, pp. 40–42.

[4] J. K. Kok, C. J. Warmer, and I. G. Kamphuis, "Powermatcher: multiagent control in the electricity infrastructure," in *AAMAS '05: Proceedings of the fourth international joint conference on Autonomous Agents and MultiAgent Systems*. New York, NY, USA: ACM, 2005, pp. 75–82.

[5] A. Molderink, V. Bakker, M. G. C. Bosman, J. L. Hurink, and G. J. M. Smit, "Management and control of domestic smart grid technology," *IEEE Transactions on Smart Grid*, vol. 1, no. 2, pp. 109–119, 2010.

[6] http://www.apxendex.com, visited 20-01-2011.

[7] http://www.epexspot.com/en/, visited 20-01-2011.

[8] P. C. Gilmore and R. E. Gomory, "A linear programming approach to the cutting-stock problem," *Operations Research*, vol. 9, no. 6, pp. 849–859, 1961.

[9] R. A. Skitt and R. R. Levary, "Vehicle routing via column generation," *European Journal of Operational Research*, no. 21, pp. 65–76, 1985.

[10] M. G. C. Bosman, V. Bakker, A. Molderink, J. L. Hurink, and G. J. M. Smit, "On the microchp scheduling problem," in *Proceedings of the Third Global Conference on Power Control and Optimization (PCO)*, 2010, p. 8.

[11] ——, "Planning the production of a fleet of domestic combined heat and power generators," *European Journal of Operational Research (submitted)*, p. 16, 2010.

 ISBN: 978-1-61208-136-6

Stability Analysis for Multiple Voltage Source Converters Connected at a Bus

Arindam Ghosh, Gerard Ledwich and Firuz Zare
School of Engineering System
Queensland University of Technology
Brisbane, Australia
a.ghosh@qut.edu.au, g.ledwich@qut.edu.au and
f.zare@qut.edu.au

Ritwik Majumder
Power Technology Group
ABB Corporate Research
Vasteras, Sweden
ritwik.majumder@se.abb.com

Abstract— This paper develops a tool for the stability analysis when multiple voltage controlled converters are connected to a distribution bus. In particular, the analysis is applicable to voltage source converters (VSCs) and has been extended to consider current control as well as voltage control. It is assumed that each VSC is controlled by a state feedback linear quadratic regulator (LQR) based switching design. A suitable model of the converter is first developed by including the state feedback gains. The model is then extended to incorporate parallel operation of two VSCs, connected to a bus. To consider autonomous operation, the power sharing arrangements without any explicit communication, i.e., droop controllers are incorporated in the model. Finally, a linearized model of the system is developed for Eigen analysis. It has been shown that the system response predicted by the developed model matches PSCAD simulation results very closely, thus confirming that the model developed can be used as an analytical tool.

Keywords- Voltage source converters, autonomous operation, linear quadratic control, stability analysis.

I. INTRODUCTION

In the past few decades, the use of power converters has become more common in uninterrupted power supply (UPS) application as well as in interfacing the micro sources in a distributed generation (DG) system. In a UPS application, the parallel operation of the converters can provide solution to improve capability, reliability and redundancy. In a distributed generation system, the micro sources, especially the intermittent types (like wind and solar), are interfaced through voltage source converters (VSCs) to the network [1].The converter can be used to maximize the energy yield from the micro source, control of output power and to improve power quality. The parallel connected converters control the power flow and quality by controlling the power conversion between the dc bus and the available grid [2].

Current regulator instability in parallel VSCs has been discussed in [3], in which a simple method of paralleling structures with carrier-based PWM current regulators to independently regulate each inverter's current is employed. The instability between the parallel inverters and the common motor can result in large uncontrolled currents, when the current regulators enter PWM over modulation region, resulting in a loss of current control.

However a current/load sharing mechanism has to be employed to avoid the overloading of any converters, especially when multiple converters are operating in an autonomous mode. Control of output power using output feedback is commonly used. Since the output currents of the converters are regulated at every switching instant, even with the harmonics in the output current, converters can share the current as desired.

The load sharing or the real and reactive power sharing can be achieved by controlling two independent quantities – frequency and the fundamental voltage magnitude [4, 5]. In [4], a control method for a converter feeding real and reactive power into a stiff system with a defined voltage is proposed, while [5] proposes a control scheme to improve the system transient stability. Both the paper uses frequency droop characteristics. In this paper however an angle droop is used as the power sharing mechanism [6].

A multi-converter system with instantaneous power sharing control is effectively a high order multi variable system. The VSCs should be controlled in such a manner that ensures a stable operation of the system. The system stability during load sharing has been further explored in [7-10]. Transient stability of a power system with high penetration level of power electronics interfaced (converter connected) distributed generation is explored in [7]. In [8], small-signal stability analysis of the combined droop and average power method for load sharing control of multiple distributed generation systems (DGs) in a stand-alone ac supply mode is discussed. The overall dynamics of the regulated converter is described in [9], where the characterization of regulated converters is addressed to enable the assessment of the stability, performance, supply and load interactions as well as transient responses. The stability analysis in autonomous operation is shown in [10]

 ISBN: 978-1-61208-136-6

in a hybrid system, where a wind-PV-battery system is feeding an isolated single-phase load.

In this paper, a model of a VSC that is operating in a closed-loop state feedback control is developed. The model is then extended to incorporate parallel operation of two VSCs. To consider autonomous operation, the power sharing arrangements through droop controllers, are incorporated in the model. Finally a linearized model of the system is developed for eigen analysis. Eigenvalues studies are performed with the mathematical expressions of the model using MATLAB. Also, all the results are verified through simulation studies using PSCAD. It is shown that the system response predicted by the model developed matches the PSCAD simulation results very closely.

A converter with its associate control affects the stability of a system that includes multiple VSCs. The main contribution of this paper is to demonstrate how the stability of such a system can be analyzed. This can be used as a screening tool before installing multiple parallel connected VSCs and choosing droop control parameters.

II. CONVERTER STRUCTURE AND CONTROL

All the DGs are assumed to consist of ideal dc voltage source supplying a voltage of V_{dc} to a VSC. The structure of the VSC is shown in Fig. 1. The VSC contains three H-bridges that are supplied from the common dc bus. The outputs of the H-bridges are connected to three single-phase transformers that are connected in wye for required isolation and voltage boosting [11]. The resistance R_T represents the switching and transformer losses, while the inductance L_T represents the leakage reactance of the transformers. The filter capacitor C_f is connected to the output of the transformers to bypass switching harmonics, while L_f represents an added output inductance of the DG system. Together L_T, C_f and L_f form an LCL or T-filter.

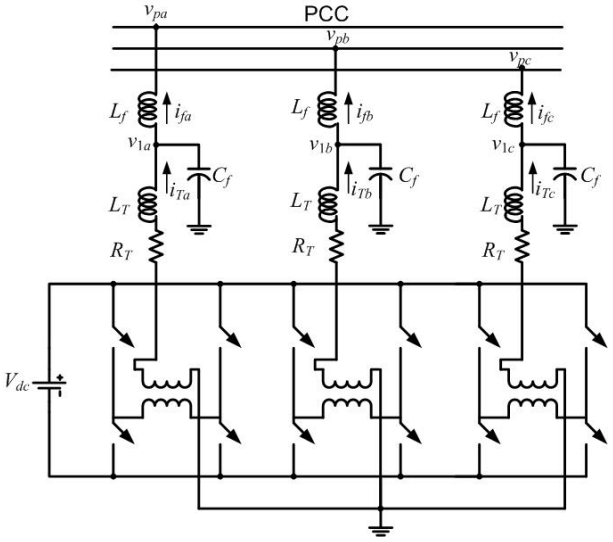

Figure 1. Converter structure.

The equivalent circuit of one phase of the converter is shown in Fig. 2. In this, $u \cdot V_{dc}$ represents the converter output voltage, where u is the switching function and is given by $u = \pm 1$. The main aim of the converter control is to generate u. From the circuit of Fig. 2, the following state vector is chosen

$$z^T = \begin{bmatrix} i_T & i_f & v_c \end{bmatrix} \tag{1}$$

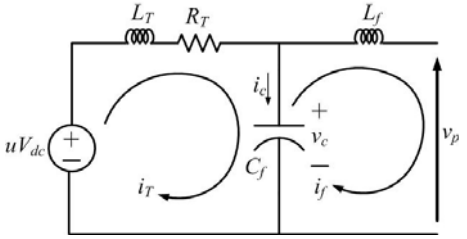

Figure 2. Single-phase equivalent circuit of VSC.

Then the state space equation of the system can be written as

$$\dot{z} = Az + Bu_c + Cv_p \tag{2}$$

where u_c is the continuous time approximation of the switching function u. and

$$A = \begin{bmatrix} -R_T/L_T & 0 & -1/L_T \\ 0 & 0 & 1/L_f \\ 1/C_f & -1/C_f & 0 \end{bmatrix}, B = \begin{bmatrix} V_{dc}/L_T \\ 0 \\ 0 \end{bmatrix}, C = \begin{bmatrix} 0 \\ -1/L_f \\ 0 \end{bmatrix}$$

The main aim of the converter control is to generate u_c from a suitable state feedback control law such that the output voltage and current are tracked properly according to their references. It is easy to generate references for the output voltage v_c and current i_f from power flow condition. However, the same cannot be said about the reference for the current i_T. On the other hand, once the reference for v_c is obtained, it is easy to calculate a reference for the current i_c through the filter capacitor (see Fig. 2).

To facilitate this, we define a new set of state vectors as

$$x^T = \begin{bmatrix} i_c & i_f & v_c \end{bmatrix} \tag{3}$$

We then have the following state transformation matrix

$$x = \begin{bmatrix} 1 & -1 & 0 \\ 0 & 1 & 0 \\ 0 & 0 & 1 \end{bmatrix} z = C_P z \tag{4}$$

The transformed state space equation is then given by combining (2) and (4) as

$$\dot{x} = C_p A C_p^{-1} x + C_p B u_c + C_p C v_p \tag{5}$$

If the system of (5) is sampled with a sampling time of ΔT, then its discrete-time description can be written in the form

$$x(k+1) = Fx(k) + Gu_c(k) + Hv_p(k) \tag{6}$$

To control the converter, we shall employ a discrete time line quadratic regulator which has the form

$$\begin{aligned} u_c(k) &= -K\left[x(k) - x_{ref}(k)\right] \\ &= \begin{bmatrix} k_1 & k_2 & k_3 \end{bmatrix}\left[x_{ref}(k) - x(k)\right] \\ &= k_1\left(i_{cref} - i_c\right) + k_2\left(i_{fref} - i_f\right) + k_3\left(v_{cref} - v_c\right) \end{aligned} \tag{7}$$

where x_{ref} is the reference vector and K is the feedback gain matrix obtained using discrete time linear quadratic regulator (LQR) with a state weighting matrix of Q and a control penalty of r. From $u_c(k)$, the switching function is generated as

$$\begin{aligned} &\text{If } u_c(k) > h \text{ then } u = +1 \\ &\text{elseif } u_c(k) < -h \text{ then } u = -1 \end{aligned} \tag{8}$$

where h is a small number. We shall now demonstrate the effectiveness of the control through the following example.

A Linear Quadratic Regulator is shown to produce an infinite gain margin and a phase margin of at least 60° [12]. Another important aspect of the LQR is that it is tolerant of input nonlinearities. The LQR design is stable provided that the effective gain of the input nonlinearity is constrained in the sector between ½ and 2 [12]. When the errors are large, and the control is bounded between + 1 and – 1 the elements of the gain matrix K must be small. For a set of decreasing values of r, we get a corresponding set of increasing values of K. Thus there always exists a value of r such that Kx is bounded appropriately. If we start from a finite set of state errors, there will be a K such that $K(x - x_{ref})$ will satisfy the upper sector bound, and since the system is open loop stable, the lower bound is not essential.

Example 1: In this example, let us assume that the VSC of Fig. 1 is connected to an infinite bus at the PCC. The system parameters considered for the study are given in Table I. To design the discrete-time controller, we have chosen a diagonal state weighting matrix as Q = diag(1 1000 10) and the control weighting as 0.01. This choice of Q emphasizes a maximum tracking effort on i_f and a minimum on i_c. The sampling time is chosen as 10 μs. The resultant gain matrix is K = [0.4338 8.3977 0.8405].

The desired converter output voltage is 11 kV (L-L, rms) with a phase angle of 30° (which translates into an instantaneous phase voltage of 8.98 kV peak). This sets the references of the currents from simple circuit laws. The peak of i_f reference is 59.195 A with an angle of 15°, while the peak of i_c reference is $\omega C_f 9.98\times10^3$ A and its phase angle 60°, i.e., leading v_c by 30°. The nine instantaneous reference quantities (3 for each phase are formed) and are tracked using the control law given in (7) and (8).

TABLE I. : SYSTEM PARAMETERS FOR EXAMPLE 1.

System Quantities	Values
Systems frequency	50 Hz
PCC voltage V_p	11 kV (L-L, rms)
PCC voltage phase	0° (Reference)
DC voltage V_{dc}	3.0 kV
Single-phase transformers	3//11 kV, with 10% leakage reactance (L_T = 31.8 mH)
Transformer losses R_T	0.1 Ω
Filter capacitor C_f	50 μF
Filter inductance L_f	250 mH

The results are shown in Fig. 3. The converter output voltages and the injected currents (i_f) and their references (dotted lines) are shown in this figure. It can be seen that the transients die out within 2½ cycles (0.05 s) and the converter tracks the reference quantities.

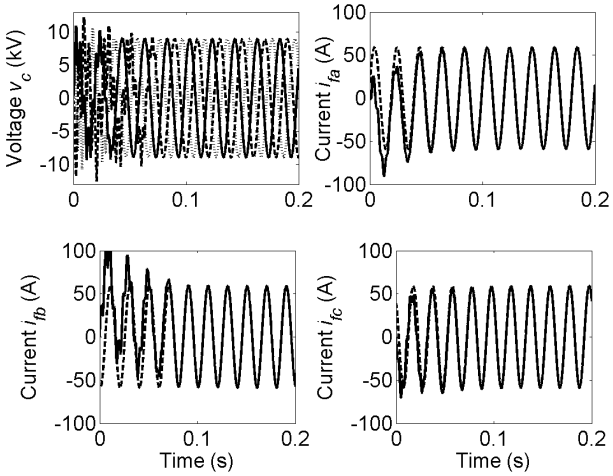

Figure 3. Voltage and current tracking in Example 1.

III. MATHEMATICAL MODEL OF VSC

In this section, a composite model of the converter in the d-q domain is developed, which includes the controller as well. Traditional sliding mode design consider a function S and control such that $S\dot{S} \le 0$. Then the system will approach $S = 0$, which is called the sliding line [13, 14]. When a finite switch rate constraint is applied, the system will chatter around $S = 0$, at the switching frequency. For switching at ± 1, the magnitudes of the switch frequency terms are all less than 1. When the system gain, at switch frequency and above, is less than α, then the system response at switch frequency is less than α. Thus when the system has sufficient lowpass filtering, its dynamics will follow the switching line with a negligible error. Since the VSC has an LCL filter to bypass the switch frequency harmonics, we can model the

system as if it is on the sliding line. It is however to be noted that this model reduction will fail if there is a system resonance near the switch frequency. Therefore the choice of the filter parameters is critical.

A. Converter Model

From equivalent circuit shown in Fig. 2, the following equations are obtained for each of the phases of the three-phase system

$$\frac{di_T}{dt} = -\frac{R_T}{L_T} i_T + \frac{\left(-v_c + u_c.V_{dc}\right)}{L_T} \tag{9}$$

$$\frac{dv_c}{dt} = \frac{\left(i_T - i_f\right)}{C_f} \tag{10}$$

$$v_c - v_p = L_f \frac{di_f}{dt} \tag{11}$$

Equations (9-11) are transformed into a *d-q* reference frame of converter output voltages, rotating at system frequency ω, where *a-b-c* to *d-q* transformation matrix P is given by

$$P = \frac{2}{3}\begin{bmatrix} \cos(\omega t) & \cos\left(\omega t - \frac{2\pi}{3}\right) & \cos\left(\omega t + \frac{2\pi}{3}\right) \\ -\sin(\omega t) & -\sin\left(\omega t - \frac{2\pi}{3}\right) & -\sin\left(\omega t + \frac{2\pi}{3}\right) \\ \frac{1}{2} & \frac{1}{2} & \frac{1}{2} \end{bmatrix}$$

Defining a state vector as

$$x_i = [i_{Td} \quad i_{Tq} \quad i_{fd} \quad i_{fq} \quad v_{cd} \quad v_{cq}]^T \tag{13}$$

the state equation in the *d-q* frame is given by

$$\dot{x}_i = A_i x_i + B_i u_{cdq} + C_i v_{pdq} \tag{14}$$

where u_{cdq} and v_{tdq} are two vectors containing the d and q axis components of u_c and v_t and

$$A_i = \begin{bmatrix} -R_T/L_T & \omega & 0 & 0 & -1/L_T & 0 \\ -\omega & -R_T/L_T & 0 & 0 & 0 & -1/L_T \\ 0 & 0 & 0 & \omega & 1/L_f & 0 \\ 0 & 0 & -\omega & 0 & 0 & 1/L_f \\ 1/C_f & 0 & -1/C_f & 0 & 0 & \omega \\ 0 & 1/C_f & 0 & -1/C_f & -\omega & 0 \end{bmatrix}$$

$$B_i = \begin{bmatrix} V_{dc}/L_T & 0 \\ 0 & V_{dc}/L_T \\ 0 & 0 \\ 0 & 0 \\ 0 & 0 \\ 0 & \end{bmatrix} \quad \text{and} \quad C_i = \begin{bmatrix} 0 & 0 \\ 0 & 0 \\ -1/L_f & 0 \\ 0 & -1/L_f \\ 0 & 0 \\ 0 & 0 \end{bmatrix}$$

From (7) and (4), u_c can be expressed as

$$u_c = k_1\left(i_{cref} - i_T + i_f\right) + k_2\left(i_{fref} - i_f\right) + k_3\left(v_{cref} - v_c\right)$$

The above equation can be expressed as

$$u_c = -k_1 i_T + \left(k_1 - k_2\right) i_f - k_3 v_c + k_1 i_{cref} + k_2 i_{fref} + k_3 v_{cref} \tag{15}$$

From (15), the d and q components of u_c are given as

$$\begin{bmatrix} u_d \\ u_q \end{bmatrix} = G_i x_i + H_i x_{refdq} \tag{16}$$

where

$$G_i = \begin{bmatrix} -k_1 & 0 & \left(k_1 - k_2\right) & 0 & -k_3 & 0 \\ 0 & -k_1 & 0 & \left(k_1 - k_2\right) & 0 & -k_3 \end{bmatrix}$$

$$H_i = \begin{bmatrix} k_1 & 0 & k_2 & 0 & k_3 & 0 \\ 0 & k_1 & 0 & k_2 & 0 & k_3 \end{bmatrix}$$

$$x_{refdq} = [i_{cdref} \quad i_{cqref} \quad i_{fdref} \quad i_{fqref} \quad v_{cdref} \quad v_{cqref}]^T$$

Substituting (16) into (14) we get

$$\dot{x}_i = \left(A_i + B_i G_i\right) x_i + B_i H_i x_{refdq} + C_i v_{pdq} \tag{17}$$

B. Computation of References

To solve the state equation (17), the reference vector x_{refdq} is required as input. In this sub-section, we shall discuss how they can easily be written in terms of the known quantities. We must however remember that all the d-q quantities are expressed in the reference frame of the converter output

voltages. Let us define the three-phase instantaneous reference converter output voltages as

$$v_{caref} = V_{cm}\sin(\omega t), \quad v_{cbref} = V_{cm}\sin(\omega t - 120°),$$
$$v_{ccref} = V_{cm}\sin(\omega t + 120°)$$

Then the transformation (19) will result in

$$\begin{bmatrix} v_{cdref} \\ v_{cqref} \end{bmatrix} = \begin{bmatrix} 0 \\ -V_{cm} \end{bmatrix} \tag{18}$$

Consequently, the reference for the capacitor currents that are leading the corresponding voltages by 90° are given as

$$\begin{bmatrix} i_{cdref} \\ i_{cqref} \end{bmatrix} = \begin{bmatrix} V_{cm}\omega C_f \\ 0 \end{bmatrix} \tag{19}$$

Now the expression for the power and reactive power are given by

$$P = \frac{3}{2}\left(v_d i_d + v_q i_q\right) \tag{20}$$

$$Q = \frac{3}{2}\left(v_q i_d - v_d i_q\right) \tag{21}$$

Let the real and reactive power that are desired to be injected to the PCC by the converter be denoted respectively P_{ref} and Q_{ref}. Then from (18), (20) and (21) we can write

$$\begin{bmatrix} i_{fdref} \\ i_{fqref} \end{bmatrix} = -\frac{2}{3V_{cm}}\begin{bmatrix} Q_{ref} \\ P_{ref} \end{bmatrix} \tag{22}$$

Combining (18), (19) and (22) we form the reference vectors in terms of V_{cm}, P_{ref} and Q_{ref}.

C. Transformation into a Common Reference Frame

The reference quantities are defined in terms of the reference frame of the converter output voltage. These need to be converted into a common reference frame. Let us choose the PCC voltage as the reference frame D-Q. Let also the angle between the PCC voltage and the converter voltage be δ. Then the relation between these two frames is shown in Fig. 4. From these figure we can write

$$\begin{bmatrix} f_D \\ f_Q \end{bmatrix} = \begin{bmatrix} \cos\delta & -\sin\delta \\ \sin\delta & \cos\delta \end{bmatrix}\begin{bmatrix} f_d \\ f_q \end{bmatrix} = T\begin{bmatrix} f_d \\ f_q \end{bmatrix} \tag{23}$$

All the reference d-q quantities are pre-multiplied by T to transform them in D-Q frame. The converter equation (17) can then be re-written as

$$\dot{x}_i = \left(A_i + B_i G_i\right)x_i + B_i H_i x_{refDQ} + C_i v_{pDQ} \tag{24}$$

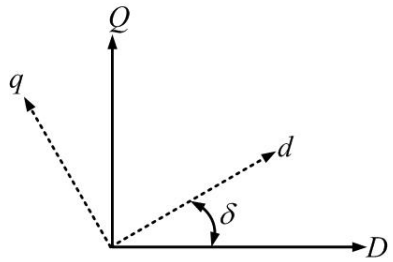

Figure 4. Relation between d-q and D-Q frames.

Example 2: In this example, we shall investigate the converter model developed in (24) and compare the results obtained with those of Example 1. Therefore the system parameters that are chosen are the same as those given in Example 1. For this case, the real and reactive power injected by the converter are 770.3 kW and 206.4 kVAr respectively. The state equations are solved in MATLAB. The three-phase converter output voltage and injected current are shown in Fig. 5. It can be seen that the steady state response of these quantities are almost identical to those of Fig. 3.

Comparing the responses in Figs. 3 and 5, it can be seen that they differ in the initial starting period. During this period, the system is trying to reach the sliding line. Once the system is on this line, the two responses are nearly identical. This is illustrated in this above example. Once the system is on the sliding line, it is robust to perturbations to system operating conditions, as will be illustrated in some of the subsequent examples. Therefore the model presented can be used for eigenvalue analysis and system response prediction

IV. Mathematical Model of Two VSCs Operating in Parallel

In this section, we develop the model when two VSCs are operating in parallel. The single-line diagram of the system considered is shown in Fig. 6. In this, the PCC is connected to an infinite bus with a voltage of v_s. A load, with an impedance of $R_L + j\omega L_L$ is connected to the PCC. The load current is denoted by i_L. The system parameters and quantities of the two VSCs are denoted by subscripts 1 and 2.

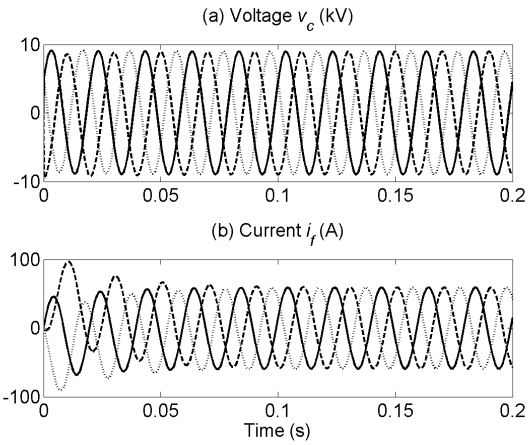

Figure 5. Output voltage and injected current for Example 2.

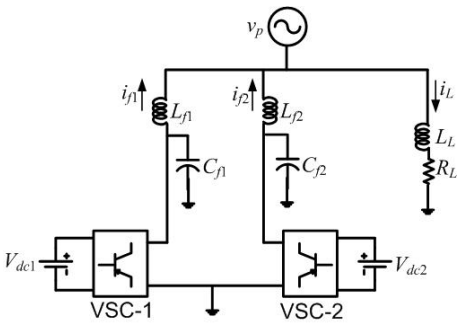

Figure 6. Single-line diagram of parallel operation of two VSCs.

The state equations of the VSCs can be written in the form (24) as

$$\dot{x}_{i1} = \left(A_{i1} + B_{i1}G_{i1}\right)x_{i1} + B_{i1}H_{i1}x_{ref1DQ} + C_{i1}v_{pDQ} \tag{25}$$

$$\dot{x}_{i2} = \left(A_{i2} + B_{i2}G_{i2}\right)x_{i2} + B_{i2}H_{i2}x_{ref2DQ} + C_{i2}v_{pDQ} \tag{26}$$

Furthermore, the load current in D-Q component is given as

$$\frac{d}{dt}\begin{bmatrix} i_{LD} \\ i_{LQ} \end{bmatrix} = \begin{bmatrix} -R_L/L_L & \omega \\ -\omega & -R_L/L_L \end{bmatrix}\begin{bmatrix} i_{LD} \\ i_{LQ} \end{bmatrix} + \begin{bmatrix} 1/L_L & 0 \\ 0 & 1/L_L \end{bmatrix}\begin{bmatrix} v_{pD} \\ v_{PQ} \end{bmatrix} \tag{27}$$

Therefore defining a composite state vector as

$$x_t^T = \begin{bmatrix} x_{i1}^T & x_{i2}^T & i_{LD} & i_{LQ} \end{bmatrix}$$

we can combine (25)-(27) to form the overall state space equation of the system.

Example 3: Let us consider the system shown in Fig. 6. Both the VSCs have the same parameters and the PCC voltage the same as discussed in Examples 1 and 2. The load resistance is 48.2 Ω and the inductance is 0.3 H. At the beginning, the following are assumed

$$V_{c1ref} = \left|\frac{11}{\sqrt{3}}\right| \angle 30° \text{ kV and } V_{c2ref} = \left|\frac{11}{\sqrt{3}}\right| \angle 20° \text{ kV}$$

This implies that P_{1ref} and Q_{1ref} are the same as those given in Example 2, while P_{2ref} = 526.9 kW and Q_{2ref} = 92.9 kVAr. With the system operating in steady state with these values, the reference for VSC-2 is suddenly changed at 0.05 s. The peak of the voltage is reduced to 95% of the nominal value, while its phase angle is changed to 30°. The reference powers are P_{2ref} = 731.79 kW and Q_{2ref} = 122.9 kVAr. The system responses for VSC-2 are shown in Figs. 7 and 8, where the solid lines depict the MATLAB results and the dotted lines depict the PSCAD outputs. In Fig. 7, the converter output voltages (v_{c2}) are shown. It can be seen that the PSCAD results are almost identical to those of MATLAB. The injected currents (i_{f2}) are shown in Fig. 8. It can be seen that the difference between the PSCAD simulation results and the predicted behaviors using MATLAB are very small and they match exactly in the steady state.

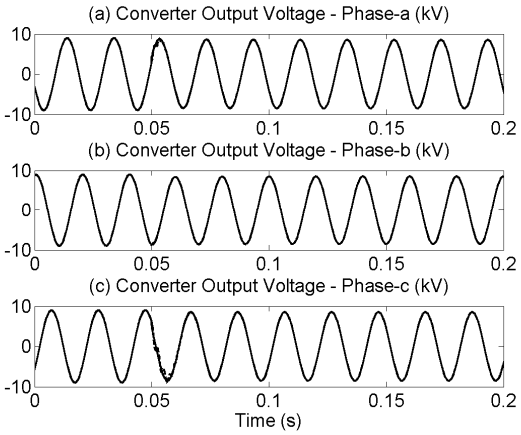

Figure 7. Simulated and predicted output voltages of VSC-2.

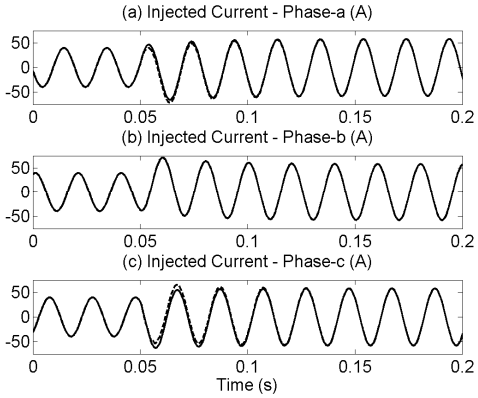

Figure 8. Simulated and predicted injected current by VSC-2.

V. MATHEMATICAL MODEL FOR AUTONOMOUS OPERATION

For this case, we assume that the PCC is a floating source, i.e., the voltage source v_p in Fig. 6 is absent and the two converters operate in parallel to share the load through droop characteristics. In this paper, we use an angle droop based on the active power [6] and a voltage magnitude droop based on reactive power. These are given by

$$\begin{aligned} \delta &= \delta_{rated} - m \times (P - P_{rated}) \\ V_{cm} &= V_{cm-rated} - n \times (Q - Q_{rated}) \end{aligned} \tag{28}$$

where $V_{cm\text{-}rated}$ and δ_{rated} are the rated voltage magnitude and angle respectively of a VSC when it is supplying the load to its rated power levels of P_{rated} and Q_{rated}.

Calculating real and power from instantaneous measurements can often lead to ripple in these quantities that will cause ripple in the converter references. To avoid this, the real and reactive power are passed through low pass filters before they are used in the droop equations. These low pass filters are given by

$$\begin{aligned} P_e &= \frac{\omega_c}{s + \omega_c} P \\ Q_e &= \frac{\omega_c}{s + \omega_c} Q \end{aligned} \tag{29}$$

where P and Q are instantaneous measured values and P_e and Q_e are their respective filtered outputs. We now substitute these values and δ and V_{cm} in (18), (19) and (22)

Since the PCC is not connected to an infinite bus, we have to eliminate the vector v_{pDQ} from the state equation. From (27), we can write

$$\begin{bmatrix} v_{pD} \\ v_{PQ} \end{bmatrix} = L_L \frac{d}{dt} \begin{bmatrix} i_{LD} \\ i_{LQ} \end{bmatrix} - L_L \begin{bmatrix} -R_L/L_L & \omega \\ -\omega & -R_L/L_L \end{bmatrix} \begin{bmatrix} i_{LD} \\ i_{LQ} \end{bmatrix} \tag{30}$$

Again, using Kirchoff's current law (KCL) at PCC, we get

$$i_{LD} = i_{f1D} + i_{f2D} \text{ and } i_{LQ} = i_{f1Q} + i_{f2Q} \tag{31}$$

Let us now define a new set of state vectors that contain only the state equations of the two converters. This is given by

$$x_c^T = \begin{bmatrix} x_{i1}^T & x_{i2}^T \end{bmatrix}$$

We can then express (30) in terms of the above state vector and its derivative as

$$\begin{bmatrix} v_{pD} \\ v_{PQ} \end{bmatrix} = A_P \dot{x}_c + B_P x_c$$

where the matrices A_p and B_p both have dimensions (12×2) and are computed from (30) and (31). From (24) and (32), we get the state space for the autonomous operation of the two VSCs as

$$\begin{aligned} \dot{x}_c = &\begin{bmatrix} A_{i1} + B_{i1}G_{i1} & \\ & A_{i2} + B_{i2}G_{i2} \end{bmatrix} x_c \\ &+ \begin{bmatrix} B_{i1}H_{i1} & \\ & B_{i2}H_{i2} \end{bmatrix} x_{crefDQ} + \begin{bmatrix} C_{i1} \\ C_{i2} \end{bmatrix} \left(A_P \dot{x}_c + B_P x_c \right) \end{aligned} \tag{33}$$

The above equation can be regrouped to form the state space equations for the autonomous operation of the VSCs as

$$\dot{x}_c = A_c x_c + B_c x_{crefDQ} \tag{34}$$

where

$$E = I_{12} - \begin{bmatrix} C_{i1} \\ C_{i2} \end{bmatrix} A_P$$

$$A_c = E^{-1} \left(\begin{bmatrix} A_{i1} + B_{i1}G_{i1} & \\ & A_{i2} + B_{i2}G_{i2} \end{bmatrix} + \begin{bmatrix} C_{i1} \\ C_{i2} \end{bmatrix} B_P \right)$$

$$B_c = E^{-1} \begin{bmatrix} B_{i1}H_{i1} & \\ & B_{i2}H_{i2} \end{bmatrix}$$

and I_{12} is a (12×12) identity matrix.

Example 4: Let us consider the same system discussed in Example 3, except the voltage source v_{ps}, which is removed. Also the filter inductance of VSC-2 has been changed to 0.3125 H. The droop coefficients from (28) are chosen as

$m_1 = 0.1$ rad/MW and $m_2 = 0.125$ rad/MW

$n_1 = 0.01$ kV/MVAr and $n_2 = 0.0125$ kV/MVAr

The cutoff frequency for the low pass filters are chosen as ω_c = 31.4 rad/s. The results are shown in Figs. 9 to 12. In all these figures, the MATLAB model and PSCAD simulation results are shown in sub-figures (a) and (b) and the errors between them are shown in (c). Fig. 9, the output voltage for phase-a of VSC-2 is shown. It can be seen that the maximum error between the MATLAB prediction and PSCAD simulation are less than 30 V, while the peak of the phase voltage is nearly 9 kV. This implies that the error is less than 0.33%. Similarly From the converter output (injected) current of VSC-2, shown in Fig. 10, it can be seen that the error is less than 0.2 A (0.4%). The output powers of the two converters are shown in Fig. 11. The errors are less than 0.5%. Similarly, from the reactive power plot shown in Fig. 12, it can be seen that the errors are less than 0.1 %. We can then surmise that the prediction model can predict the system behavior fairly accurately.

 ISBN: 978-1-61208-136-6

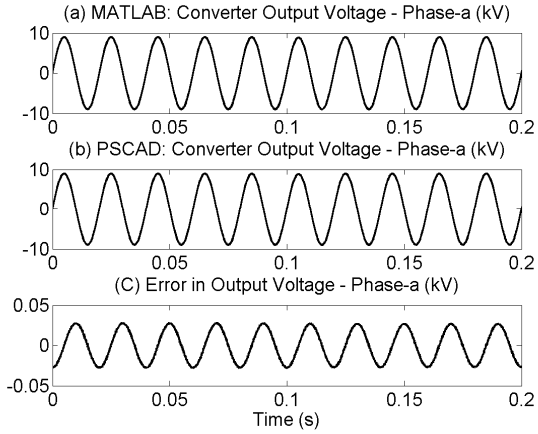

Figure 9. VSC-2 output voltage of phase-a and its error.

VI. SMALL SIGNAL MODEL FOR EIGEN ANALYSIS

Since the system response obtained by the mathematical model closely matches that of the PSCAD simulation, the VSC model developed in the previous sections can be used to find an autonomous small signal model of the system discussed in the previous section. To facilitate this, we must eliminate the reference vector (34).

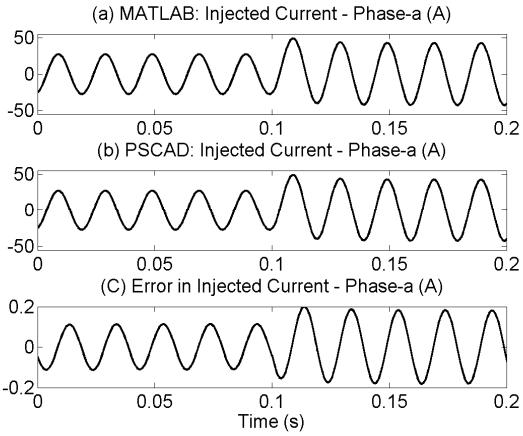

Figure 10. VSC-2 output current of phase-a and its error.

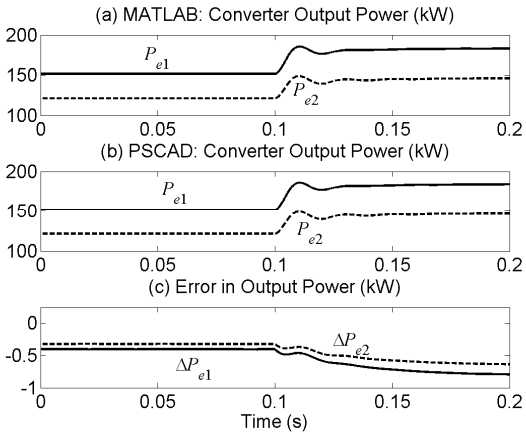

Figure 11. Output active power of the converters and their error.

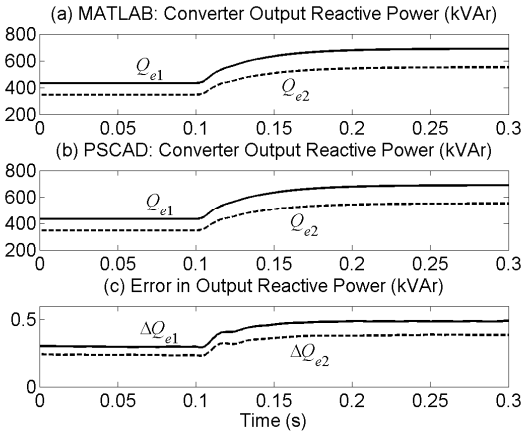

Figure 12. Output reactive power of the converters and their error.

From (29), (20) and (21), we can write

$$\dot{P}_e = -\omega_c P_e + \frac{3\omega_c}{2}\left(v_{cd} i_{fd} + v_{cq} i_{fq}\right)$$
$$\dot{Q}_e = -\omega_c Q_e + \frac{3\omega_c}{2}\left(v_{cq} i_{fd} - v_{cd} i_{fq}\right) \quad (35)$$

Linearizing the above equations around an operating point, we obtain

$$\Delta\dot{P}_e = -\omega_c \Delta P_e + \frac{3\omega_c}{2}\left(v_{cd0}\Delta i_{fd} + i_{fd0}\Delta v_{cd} + v_{cq0}\Delta i_{fq} + i_{fq0}\Delta v_{cq}\right)$$
$$\Delta\dot{Q}_e = -\omega_c \Delta Q_e + \frac{3\omega_c}{2}\left(v_{cq0}\Delta i_{fd} + i_{fd0}\Delta v_{cq} - v_{cd0}\Delta i_{fq} - i_{fq0}\Delta v_{dq}\right) \quad (36)$$

where the suffix Δ defines a perturbed quantity and subscript 0 signifies the nominal values. Defining a vector of active and reactive powers as

$$x_{pq} = \begin{bmatrix} P_{e1} & Q_{e1} & P_{e2} & Q_{e2} \end{bmatrix}^T$$

equation (26) can be written as

$$\Delta\dot{x}_{pq} = A_{pq}\Delta x_{pq} + B_{pq}\Delta x_c \quad (37)$$

where A_{pq} = diag($-\omega_c$ $-\omega_c$ $-\omega_c$ $-\omega_c$) and B_{pq} can be derived from (36).

We shall now replace the reference quantities by ΔP_e and ΔQ_e. To do that, we first linearize the droop equations (28) to obtain

$$\Delta\delta = -m \times \Delta P_e$$
$$\Delta V_{cm} = -n \times \Delta Q_e \quad (38)$$

Then from (18) and (23) we get

$$\begin{bmatrix} v_{cDref} \\ v_{cQref} \end{bmatrix} = \begin{bmatrix} \cos\delta & -\sin\delta \\ \sin\delta & \cos\delta \end{bmatrix} \begin{bmatrix} 0 \\ -V_{cm} \end{bmatrix}$$

Linearizing the above equation and substituting (38), we get

$$\begin{bmatrix} \Delta v_{cDref} \\ \Delta v_{cQref} \end{bmatrix} = \begin{bmatrix} -mV_{cmo}\cos\delta_0 & -n\sin\delta_0 \\ -mV_{cm0}\sin\delta_0 & n\cos\delta_0 \end{bmatrix} \begin{bmatrix} \Delta P_e \\ \Delta Q_e \end{bmatrix} \quad (39)$$

In a similar way, we find the references for the capacitor current are given as

$$\begin{bmatrix} \Delta i_{cDref} \\ \Delta i_{cQref} \end{bmatrix} = \begin{bmatrix} \lambda_1\sin\delta_0 & -\lambda_2\cos\delta_0 \\ -\lambda_1\cos\delta_0 & -\lambda_2\sin\delta_0 \end{bmatrix} \begin{bmatrix} \Delta P_e \\ \Delta Q_e \end{bmatrix} \quad (40)$$

where $\lambda_1 = m\omega C_f V_{cm0}$ and $\lambda_2 = n\omega C_f$. Finally replacing P_{ref} and Q_{ref} by P_e and Q_e respectively in (22), we get the linearized expressions for the injected currents as

$$\begin{bmatrix} \Delta i_{fDref} \\ \Delta i_{fQref} \end{bmatrix} = \frac{1}{V_{cm0}} \begin{bmatrix} \beta_{11} & \beta_{12} \\ \beta_{21} & \beta_{22} \end{bmatrix} \begin{bmatrix} \Delta P_e \\ \Delta Q_e \end{bmatrix} \quad (41)$$

where

$$\beta_{11} = -(2/3)(mQ_{e0}\sin\delta_0 + mP_{e0}\cos\delta_0 - \sin\delta_0)$$
$$\beta_{12} = -(2/3)\cos\delta_0 + ni_{fD0}$$
$$\beta_{21} = -(2/3)(mP_{e0}\sin\delta_0 + \cos\delta_0 - mQ_{e0}\cos\delta_0)$$
$$\beta_{22} = -(2/3)\sin\delta_0 + ni_{fQ0}$$

We can then write the reference vector in (34) as

$$\Delta x_{crefDQ} = M_c \Delta x_{pq} \quad (42)$$

where the elements of M_c are obtained from (39)-(41). Combing (34), (37) and (42), we get a homogeneous state space description of the complete system as

$$\begin{bmatrix} \Delta\dot{x}_c \\ \Delta\dot{x}_{pq} \end{bmatrix} = \begin{bmatrix} A_c & B_c M_c \\ B_{pq} & A_{pq} \end{bmatrix} \begin{bmatrix} \Delta x_c \\ \Delta x_{pq} \end{bmatrix} \quad (43)$$

This homogenous model can now be used for eigenvalue analysis.

Example 5: Let us consider the system discussed in Example 4. For eigenvalue analysis we vary a parameter m from 0.01×10^{-6} rad/W to 1.8×10^{-6} rad/W. Furthermore we choose the angle droop gains as $m_1 = m$ and $m_2 = 1.25\times m$. The plots of the dominant eigenvalues are shown in Fig. 13. It can be seen that for $m = 1.4785\times10^{-6}$ rad/W, the dominant eigenvalues cross the imaginary axis. Also the oscillation frequency of the dominant eigenvalues is roughly 314 rad/s (50 Hz). From eigenvectors it has been determined that these eigenvalues are associated with real and reactive power supplied by the VSCs.

To validate the eigenvalue results, PSCAD simulations studies are carried out for the same system. With the system operating at steady state with the nominal values of droop gains given in example, the value of m is changed suddenly at 0.1 s. Fig. 14 shows the plots of the real power output of VSC-2 for three different values of m. Fig. 14 (a) shows a damped oscillation for $m = 1.3\times10^{-6}$ rad/W, for which all the eigenvalues are not the left half s-plane. Fig. 14 (b) shows sustained oscillation for $m = 1.4785\times10^{-6}$ rad/W, for which the dominant eigenvalues are on the imaginary axis. The unstable case for which the dominant eigenvalues are on the right half s-plane are shown in Fig. 14 (c) for $m = 1.8\times10^{-6}$ rad/W. Also notice that there are five peaks and five troughs in each 0.1 s, indicating that the oscillation frequency is 50 Hz. This fundamental frequency oscillation is also predicted by the eigenvalues.

It is to be noted that n_1 and n_2 do not have a significant influence on the eigenvalues. However, if they are chosen arbitrarily large, the voltage regulation will fail and the converter output voltage will collapse leading to an instability in which no power can be transferred.

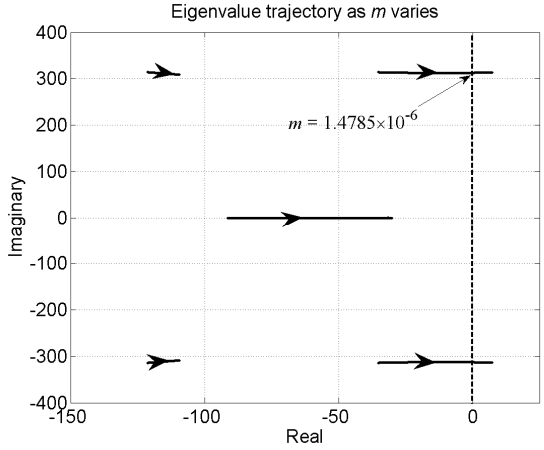

Figure 13. Eigenvalues plots from stability analysis.

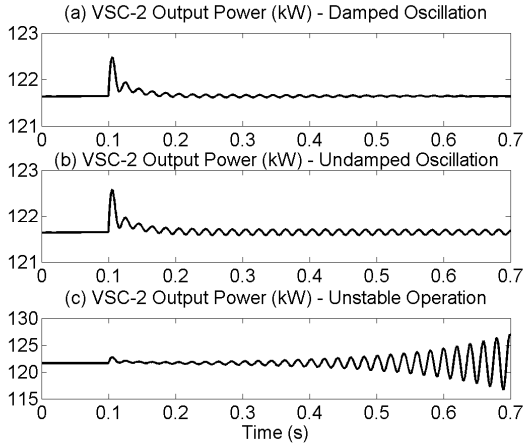

Figure 14. VSC-2 output power showing stable, undamped and unstable

VII. CONCLUSIONS

This paper proposes a method for developing a model for multiple VSCs operating in parallel in an autonomous mode. Each VSC is equipped with a T-filter and is assumed to operating in a full state feedback control of output voltage and current. The feedback gains are derived using LQR equations. Eigen value analysis and simulation studies are carried out in parallel. It has been shown that the system response predicted by the mathematical model matches the simulation results accurately, especially along the sliding line. Therefore the proposed model, with minor modification to include network, can be used for studying large systems when multiple converters operating in parallel to share loads.

ACKNOWLEDGMENT

The authors thank ABB Corporate Research, Sweden and Queensland University of Technology, Australia.

REFERENCES

[1] M. Reza, D. Sudarmadi, F. A. Viawan, W. L. Kling, and L. Van Der Sluis, "Dynamic Stability of Power Systems with Power Electronic Interfaced DG," Power Systems Conference and Exposition, PSCE'06, pp. 1423-1428, 2006.

[2] G. Ledwich and A. Ghosh. "Flexible DSTATCOM operating in voltage or current control mode," Generation, Transmission and Distribution, IEE Proceedings-Vol. 149, No. 2, pp. 215-224, 2002.

[3] J. Thunes, R. Kerkman, D. Schlegel, and T. Rowan, "Current regulator instabilities on parallel voltage-source inverters," IEEE Trans. Industry Applications, Vol. 35, No. 1, pp. 70-77, 1999.

[4] M. C. Chandorkar, D. M. Divan, and R. Adapa, "Control of parallel connected inverters in standalone ac supply systems," IEEE Trans. Industry Applications, Vol. 29, No. 1, pp. 136-143, 1993.

[5] J. M. Guerrero, L. G. de Vicuna, J. Matas, M. Castilla, and J. Miret, "A wireless controller to enhance dynamic performance of parallel inverters in distributed generation systems," IEEE Trans. Power Electronics, Vol. 19, No. 5, pp. 1205-1213, 2004.

[6] R. Majumder, A. Ghosh, G. Ledwich, and F. Zare, "Load sharing and power quality enhanced operation of a distributed microgrid," Accepted to appear in IET Renewable Power Generation, Vol. 3 , No. 2, pp. 109-119, 2008

[7] J. G. Slootweg and W. L. Kling, "Impacts of distributed generation on power system transient stability," Power Engineering Society Summer Meeting, 2002 IEEE Vol. 2, No. , pp. 862-867, 2002.

[8] M. N. Marwali, M. Dai, and A. Keyhani, "Stability Analysis of Load Sharing Control for Distributed Generation Systems," IEEE Trans. Energy Conversion, Vol. 22, No. 3, pp. 737-745, 2007.

[9] T. Suntio, M. Hankaniemi, and M. Karppanen, "Analysing the dynamics of regulated converters," Proc. IEE Electric Power Applications, Vol. 153, No. 6, pp. 905-910, 2006

[10] W. Li and L. Tsung-Jen, "Stability and Performance of an Autonomous Hybrid Wind-PV-Battery System," International Conference on Intelligent Systems Applications to Power Systems, pp. 1-6, 2007.

[11] A. Ghosh and A. Joshi, "A new approach to load balancing and power factor correction in power distribution system," IEEE Trans. Power Delivery, Vol. 15, No. 1, pp. 417-422, 2000.

[12] B. D. O. Anderson and J. B. Moore, Linear Optimal Control, Prentice-Hall, Englewood Cliffs, N.J., 1971.

[13] J. J. E. Slotine and W. Li, Applied Nonlinear Control, Prentice-hall, Englewood Cliffs, N.J., 1991.

[14] H. K. Khalil, Nonlinear Systems, 3rd Ed., Prentice-Hall, Upper Saddle River, N.J., 2002.

 ISBN: 978-1-61208-136-6